ON THE ELECTRONIC AND GEOMETRIC STRUCTURE PROPERTIES OF SILICON-GERMANIUM NANOCLUSTERS: A HYBRID DENSITY FUNCTIONAL THEORETIC STUDY

by

SARAH ELIZABETH DUESMAN

Presented to the Faculty of the Graduate School of
The University of Texas at Arlington in Partial Fulfillment
of the Requirements
for the Degree of

MASTER OF SCIENCE IN PHYSICS

THE UNIVERSITY OF TEXAS AT ARLINGTON
DECEMBER 2011

ACKNOWLEDGEMENTS

I wish to thank the many people who have made this thesis possible. First and foremost, I am indebted to Dr. Ray for accepting me into his research group, for instigating this project, and for providing guidance and advice while I completed this work. Next, I wish to thank my parents, Leo and Karen, and my fiancé, Robert Guess. When numbers, equations, and clusters left my thoughts chaotic and disordered, especially this past summer, their patient, peaceful spirits have lent me a calm and tranquil strength. My committee members, Dr. Cuntz and Dr. Koh, who have willingly taken time from their own research to look over my thesis and hear my defense also deserve special mention. Finally I wish to thank the friends and colleagues I have met while in this department, including the members of Dr. Ray's group over the past year and a half: Kapil, Haoliang, Kinjal, Sarah, Megan, Jianguang, Li, Dayla, and Prabath.

August 12, 2011

ABSTRACT

ON THE ELECTRONIC AND GEOMETRIC STRUCTURE PROPERTIES

OF SILICON-GERMANIUM NANOCLUSTERS:

A HYBRID DENSITY FUNCTIONAL

THEORETIC STUDY*

Sarah Elizabeth Duesman, M.S.

The University of Texas at Arlington, 2011

Supervising Professor: Asok Ray

Hybrid density functional theory has been used to study the electronic and geometric structure properties of silicon-germanium nanoclusters containing up to eight atoms. The hybrid functional used is Becke's three-parameter exchange functional with the exchange-correlation functional of Lee, Yang, and Parr (B3LYP). A large 6-311G(3df,3pd) basis set as implemented in the suite of software Gaussian 03/09 has been used for accurate determinations of all properties of the Si_mGe_n ($m + n \leq 8$) nanoclusters. For each cluster, various different isomers have been studied to arrive at a global minimum energy structure, and for each of these isomers we report our results on bond lengths, symmetry group, electronic state, binding energy per atom, HOMO-LUMO gap, and dipole moment. We also report results on vertical ionization

* Work partially supported by the Welch Foundation, Houston, Texas (Grant No. Y-1525) and the GAAN program.

potential, adiabatic ionization potential, vertical electron affinity, and adiabatic electron affinity. Results have been compared with available experimental results. Finally, for the lowest energy isomers, harmonic frequencies, fragmentation energies, average coordination numbers, and Mulliken atomic charges have been calculated.

TABLE OF CONTENTS

LIST OF ILLUSTRATIONS

Figure Page

LIST OF TABLES

CHAPTER 1

INTRODUCTION

1.1 Homo-nuclear Nanoclusters

In the past computational studies of semiconducting nanoclusters of only two to eight atoms have focused on single elements. Previous theoretical work on silicon clusters [1-18] and germanium clusters [19-25], the two elements that we will be studying, forms a background for understanding the clusters that we predict. The research on pure silicon nanoclusters suggests that clusters with 4, 6, 7, or 10 atoms are particularly stable [4]. Germanium favors 7- or 10- atom clusters [23]. The accuracy of the theoretical methods have held up against comparison to experiment [26-32]. More recent work studies the properties of clusters formed from a combination of different elements [33-34]. In our group we have already conducted a thorough investigation of the SiC nanoclusters, both neutral [35] and cationic [36]. With a similar treatment we are now turning our attention to nanoclusters of Si and Ge.

1.2 Previous Research on Silicon and Germanium Hetero-nuclear Nanoclusters

In his 2003 paper on *ab initio* calculations, S. Ogut [37], commented that structures composed solely of silicon have the same atomic arrangements (but with different bond lengths) as those that are solely germanium. The geometries of small homo-nuclear nanoclusters of group IV elements have been well established [38-40]. For silicon and germanium, it appears that the considerable differences are only apparent in medium and large clusters of thirteen or more atoms [41]. It is natural to consider what form molecules combining these atoms will take. Some research exists on SiGe alloys [42-46], but these focus on clusters of 50 to hundreds of atoms. We are concerned with only small silicon and germanium clusters.

A few papers have looked at these clusters, in varying levels of depth. Five groups have published results that can be readily compared to ours. The first three groups reported data for the neutral clusters only, the fourth group looked at neutral and cationic clusters, and the fifth group looked at neutral, cationic, and anionic nanoclusters. A. N. Andriotis, M. Menon, and G. E. Froudakis [47] looked at four clusters to evaluate different computational theories. We compare their bond lengths for the SiGe dimer, two isomers of Si_2Ge_2 tetramers, and a Si_2Ge_4 rhombic bipyramid to our values. S.-D. Li *et al.* [48] also made DFT calculations on small clusters of silicon and germanium, reporting bond lengths, symmetry groups, electronic states, HOMO-LUMO gaps, and frequencies. In 2007, L. R. Marim and collaborators [49] used DFT to find the geometry of the most stable trimers, tetramers, two isomers of the pentamers, and septamers. They also reported a cohesive energy per atom that compares with our binding energy per atom. P. Wielgus *et al.* [50] reported their *ab initio* calculations of geometries, symmetry groups, electronic states, and frequencies for the neutral and cationic SiGe dimer, L-shaped and triangular trimers, planar tetragonal tetramers, and trigonal bipyramid pentamers.

Earlier this year, the fifth group, Y.-S. Wang and S. D. Chao [51], published a detailed study of the neutral and ionic clusters. They included figures of the most stable neutral, cationic, and anionic trimer through hexamer nanoclusters. Bond lengths were labeled on the trimer clusters. They used density functional theory to find these optimized geometries. Then, for the neutral clusters (dimers through septamers), they used the coupled cluster method to determine the electronic state, dissociation energies, and HOMO-LUMO gaps. For each neutral cluster, they reported two dissociation energies: one calculated and one estimated. When divided by the number of atoms, the magnitudes of these can be compared to our binding energies per atom. While there have been previous studies of silicon-germanium nanoclusters, our work builds on them, reporting more theoretical predictions for a wider range of isomers of neutral, cationic, and anionic silicon-germanium dimers, trimers, tetramers, pentamers, hexamers, and septamers.

1.3 Nanocluster Features Investigated in This Work

To better understand the characteristics of semiconductors at the atomic level, we have used *ab initio* calculations to investigate the behavior of small molecules made of two semiconductors – silicon and germanium. We studied nanoclusters of two to seven atoms formed from the combination of these two elements. Here we report our findings for the neutral, cationic, and anionic nanoclusters these elements are most likely to form. Using density functional theory (DFT) to predict the energies of these molecules, we optimized both their geometrical structures and their spins. For each of these molecules, we report the bond length, symmetry group, dipole moment and the following electronic characteristics: electronic state, binding energy per atom, HOMO-LUMO gap, vertical and adiabatic ionization potential, and vertical and adiabatic electron affinity. For the most stable isomers of each combination of silicon and germanium atoms, we include frequencies, atomic charges, illustrations of the HOMO and LUMO, and fragmentation energies. We summarize our findings with plots of the binding energy per atom versus the number of atoms.

CHAPTER 2

THEORY

2.1 Density Functional Theory

There are two approaches to solving a many-electron problem: the Hartree-Fock theory and the density functional theory. Both of these theories simplify the full problem to that of many electrons moving in an external potential field. In the case of the Hartree-Fock formalism, the solution to the many-body Schrodinger equation is written in the form of a Slater determinant. The resulting HF equations depend on the occupied electron orbitals, which enter the HF equations in a nonlocal way. Because the nonlocal potential of the Hartree-Fock theory method is difficult to apply to extended systems, most of the electronic structure calculations for solids are based on density functional theory (DFT), which results from work of Hohenberg, Kohn and Sham [52-59]. We have used density functional theory in our research.

The basic understanding in quantum mechanics is that a system's wave function Ψ contains all information we can possibly have about the system. Thus, most problems related to electronic structures can be studied by the time-independent Schrödinger equation. For an isolated system with N electrons in the Born-Oppenheimer nonrelativistic approximation, this is given by

$$H\Psi = E\Psi \tag{2.1}$$

In equation (2.1), E is the electronic energy, $\Psi = \Psi(x_i, x_2, ..., x_n)$ is the many-electron wave function, where x_i denote the particle coordinates and spins, and H is the Hamiltonian in atomic units:

$$H = \sum_{i=1}^{N}(-\frac{1}{2}\nabla_i^2) + \sum_{i=1}^{N} v(r_i) + \sum_{i<j}^{N} \frac{1}{r_{ij}} \tag{2.2}$$

in which the first term is the kinetic energy term for each electron, the second term is

$$v(r) = -\sum_{\alpha} \frac{Z_\alpha}{|\, r_i - R_\alpha \,|} \tag{2.3}$$

the "external" potential due to nuclei of charges Z_α acting on the i^{th} electron, and the third term is the electron-electron potential energy term.

It has been an important goal of physics to solve this many particle problem. In the Hartree approximation [60], the many-electron wave function is constructed from the product of single particle functions,

$$\Psi(x_i, x_2, ..., x_n) = \Psi_1(x_1)\Psi_2(x_2)...\Psi_n(x_n) \tag{2.4}$$

Each of the functions $\Psi_1(x_1)$ satisfies a one-electron Schrödinger equation, with an additional potential term, which arises from the average field of the other electrons. The Schrödinger equation for a single electron can be written as

$$\left[-\frac{h^2}{2m}\nabla^2 + V_{ext} + \Phi_i\right]\Psi_i(x) = \varepsilon_i \Psi_i(x) \tag{2.5}$$

where the Coulomb potential Φ_i is given by Poisson's equation

$$\nabla^2 \Phi_i = 4\pi\, e^2 \sum_{j=1, i\neq j}^{N} \left|\Psi_j\right|^2 \tag{2.6}$$

and V_{ext} is the potential due to the nuclei. Considering the Pauli exclusion principle, the simple product wave function can be replaced by a single determinantal function, which leads to the Hartree-Fock approximation [61, 62]. The inclusion of Fermi statistics, which introduces an additional, nonlocal exchange term in the Schrödinger equation, improves the total energy calculation, but the single particle picture, with the wave function described in terms of orbitals

with particular spins and occupation numbers, is unchanged. C. Coulson noted that a single configuration (Slater determinant) wave function must inevitably lead to a poor energy since the lowest-lying configuration is generally only one of very many with comparable energies [63]. He suggested that a better approximation would result from taking a linear combination. This approach known as "configuration interaction" (CI) improves the correlation effects beyond Hartree-Fock approximation by including the many-particle wave functions. In principle, CI provides an exact solution of the many-electron problems. In practice, however, the explosive increase in the number of configurations with increasing electron number limits its application to only small systems with relatively few electrons. Furthermore, the complexity of the resulting solutions means that a simple interpretation of the results is often difficult.

An alternative approach, which originated from the Thomas-Fermi model [64, 65], is based on the density of electrons in the system, n(r),

$$n(r) = N\int dr_2 ... \int dr_n \Psi^*(r_1, r_2, ..., r_n)\Psi(r_1, r_2, ..., r_n). \quad (2.7)$$

The Thomas-Fermi model assumes that the motions of the electrons are uncorrelated and that the corresponding kinetic energy can be described by a local approximation based on the results for uniform electron gas, $\left[n(r)\right]^{5/3}$. Furthermore, Dirac [66] proposed that exchange effects can be included by incorporating a term derived from the exchange energy density in a homogenous system. The exchange potential in a system of variable density could be approximated by a term with a local dependence ~ $\left[n(r)\right]^{1/3}$ on electron density. In fact, this dependence on the density is a consequence of the concept of the "exchange" or "Fermi" hole, i.e., the region near an electron is avoided by electrons of the same spin, and not included in the exchange potential of a homogenous system. The Thomas-Fermi model provided a prototype for modern density functional theory.

Hohenberg and Kohn used built on the Thomas-Fermi model, using it in conjunction with their two theorems [67]. Note that the Hamiltonian in (2.2) contains the number of

electrons N and the external potential $v(r)$. Hence, N and $v(r)$ will determine all properties for the ground state. In place of N and $v(r)$, the first Hohenberg-Kohn theorem legitimizes the use of electron density $n(r)$ as the basic variable. It states that the external potential $v(r)$ is determined, within a trivial additive constant, by the electron density $n(r)$.

Hohenberg and Kohn proved this theorem by the *reductio ad absurdum* method. First consider the electron density $n(r)$ for the nondegenerate ground state of a N-electron system. Then the number of electrons is determined by

$$\int n(r)dr = N . \tag{2.8}$$

If $n(r)$ also determines $v(r)$, it follows that $n(r)$ determines the ground-state wave function Ψ (and all other electronic properties of the system). Suppose that there are two different external potentials v and v_1 that give the same $n(r)$ for their ground state. Then there would be two Hamiltonians, H and H_1, whose ground-state densities were the same although the normalized wave functions Ψ and Ψ_1 would be different. Each of these Hamiltonians and its corresponding wave function would satisfy Schrodinger's equation:

$$H\Psi = E\Psi \tag{2.9}$$

$$H_1\Psi_1 = E_1\Psi_1 \tag{2.10}$$

E and E_1 are the ground-state energies for H and H_1 respectively. Therefore, the expectation value of H in Ψ_1 has to be greater than E because it would be in a higher state:

$$\begin{aligned} E < \langle \Psi_1 \mid H \mid \Psi_1 \rangle &= \langle \Psi_1 \mid H + H_1 - H_1 \mid \Psi_1 \rangle \\ &= \langle \Psi_1 \mid H_1 \mid \Psi_1 \rangle + \langle \Psi_1 \mid H - H_1 \mid \Psi_1 \rangle \\ &= E_1 + \int n(r)[v(r) - v_1(r)]dr \end{aligned} \tag{2.11}$$

Similarly, the expectation value of H_1 in Ψ would be greater than E_1,

$$E_1 < \langle \Psi \mid H_1 \mid \Psi \rangle = \langle \Psi \mid H_1 + H - H \mid \Psi \rangle$$

$$= \langle \Psi \mid H \mid \Psi \rangle + \langle \Psi \mid H - H_1 \mid \Psi \rangle \tag{2.12}$$

$$= E + \int n(r)[v(r) - v_1(r)]dr$$

Adding (2.11) and (2.12) leads to

$$E + E_1 < E_1 + E \tag{2.13}$$

This is a contradiction, so there cannot be two different external potentials that give the same ground-state densities.

With proof that $n(r)$ determines N, v, and all properties of the ground state, the total ground state energy can be written as a functional of the electron density:

$$E[n] = T[n] + V_{ne}[n] + V_{ee}[n] \tag{2.14}$$

where $T[n]$ is the kinetic energy, $V_{ne}[n]$ is the nuclei-electron interaction energy and $V_{ee}[n]$ is the electron-electron Coulomb interaction energy. The nuclei-electron interaction is considered an external potential, and it has already been proved that an external potential $v(r)$ can be expressed as

$$V_{ne}[n] = \int n(r)v(r)dr \tag{2.15}$$

Hohenberg and Kohn also grouped the other two energy terms into a single functional $F_{HK}[n]$. So the energy is written as

$$E[n] = \int n(r)v(r)dr + F_{HK}[n] \tag{2.16}$$

where

$$F_{HK}[n] = T[n] + V_{ee}[n] \tag{2.17}$$

The second Hohenberg-Kohn theorem states that for a trial density, $n_1(r)$, such that $n_1(r) \geq 0$ and $\int n_1(r)dr = N$,

$$E_0 \leq E[n_1] \tag{2.18}$$

where $E[n_1]$ is the energy functional from equation (2.14). This theorem gives the energy is a application of the variational principle, in which the ground-state electron density is considered to be the density that minimizes $E[n]$.

The proof of this second theorem begins by considering that there must be a ground state density function $n(r)$ with a corresponding external potential, v, Hamiltonian, H, and wave function, Ψ. This ground state density function is not known exactly, but a trial density function $n_1(r)$ can be used as a starting point:

$$\langle \Psi_1 \mid H \mid \Psi_1 \rangle = \int n_1(r)v(r)dr + F_{HK}[n_1] \tag{2.19}$$

Furthermore, the energy associated with the trial function must be greater than the ground state energy:

$$E[n_1] \geq E[n]. \tag{2.20}$$

The variational principle (2.16) requires that the ground-state density minimizes equation (2.19):

$$\frac{\delta E[n]}{\delta n(r)} = 0 \tag{2.21}$$

Using the constraint that

$$\int n(r)dr = N \tag{2.22}$$

and the chemical potential, μ, as a Lagrange multiplier gives the Euler-Lagrange equation

$$\mu = v(r) + \frac{\delta F_{HK}[n]}{\delta n(r)} \tag{2.23}$$

This equation is the basis of density functional theory. Unfortunately, (2.23) cannot be solved exactly because $F_{HK}[n]$ is not explicitly known. To proceed, some satisfactory approximation for this term must be utilized.

The form of DFT used in this work follows from the theories of Kohn and Sham [54]. First, they rearrange the unknown $F_{HK}[n]$ term. They assume that the kinetic energy term has a component that is independent of the electron-electron interaction $T_S[n]$ and that the electron-electron potential term has a component that is described as a classical Coulomb potential $J[n]$. Then, the unknown term can be written as

$$F_{HK}[n] = T_S[n] + J[n] + E_{xc}[n] \tag{2.24}$$

where

$$E_{xc}[n] = T[n] - T_s[n] + V_{ee}[n] - J[n]. \tag{2.25}$$

This exchange term includes all the terms that involve electron-electron interaction.

Rather than working strictly in terms of density functionals, Kohn and Sham write the ground state wave function as a combination of N orbitals $\Psi_i(r,s)$

$$\Psi_s = \frac{1}{\sqrt{N!}} \det[\Psi_1 \Psi_2 ... \Psi_n]. \tag{2.26}$$

This makes the Sham kinetic energy term

$$T_s[n] = \sum_{i=1}^{N} \left\langle \Psi_i \left| -\frac{1}{2}\nabla^2 \right| \Psi_i \right\rangle. \tag{2.27}$$

Kohn and Sham keep the Coulomb potential term as a functional of density, though

$$J[n] = \frac{1}{2}\int \frac{n(r)n(r')}{|r-r'|} dr dr'. \tag{2.28}$$

Also, the density can be redefined in terms of the orbitals:

$$n(r) = \sum_{i}^{N} \sum_{s} \left| \Psi_i (r, s) \right|^2 . \tag{2.29}$$

As before, the variational principle involves minimizing the energy expression. This time it is minimized with the constraint that the orbitals are orthonormal

$$\int \Psi_i^* \Psi_j \, dx = \delta_{ij} \tag{2.30}$$

and introducing ε_{ij} terms as the Lagrange multipliers. After applying the variational principle, Kohn and Sham found that for a single orbital

$$\left(-\frac{1}{2} \nabla^2 + v_{eff} \right) \Psi_i = \varepsilon_i \Psi_i \tag{2.31}$$

where the background effective potential is

$$v_{eff} = v(r) + \int \frac{n(r')}{|r - r'|} dr' + v_{xc}(r) \tag{2.32}$$

and the exchange potential is

$$v_{xc}(r) = \frac{\delta E_{xc}[n]}{\delta n(r)} . \tag{2.33}$$

These three equations (2.31 – 2.33) and the definition of the density in terms of orbitals (2.29) are the four essential Kohn-Sham equations.

Figure 2.1 illustrates the method in which the Kohn-Sham equations can be applied to find the energy of a system. The process begins with a trial density function, $n_0(r)$. This initial density is inserted into equations (2.32) and (2.33) to solve for v_{eff}. Then the effective potential is inserted into equations (2.29) and (2.31) to find a new density function, $n(r)$. The process is subject to a convergence requirement ε_r. If the difference between $n_0(r)$ and $n(r)$ is less than this requirement, the density is used in equation (2.16) to find the ground state energy. If

the convergence criteria is not met, then $n(r)$ becomes a new trial density and the loop starts again until the convergence criteria is satisfied.

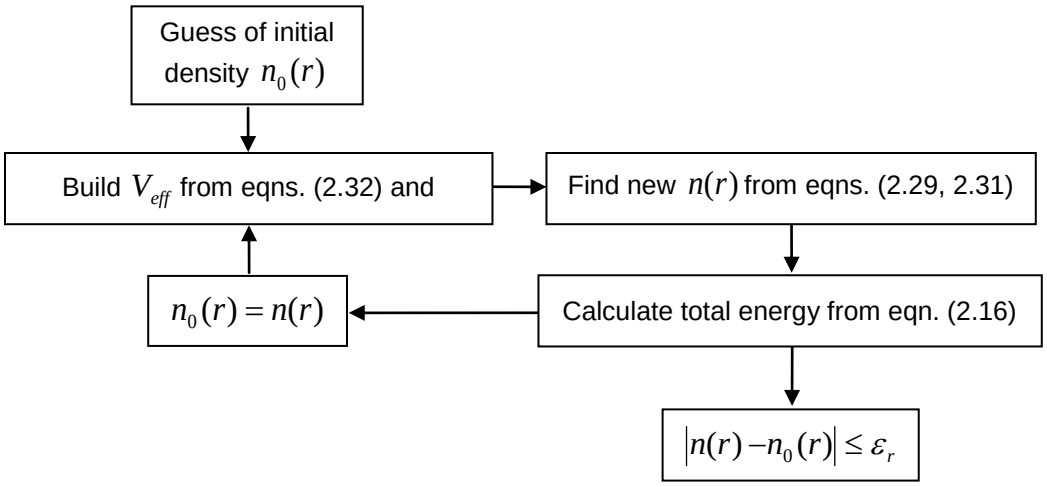

Figure 2.1 Flowchart for DFT calculations

The Kohn-Sham scheme provides a simple but rigorous way to compute the electronic properties within density functional theory. In principle, the Kohn-Sham equations will yield exact ground state properties if an exact exchange correlation potential is given. However, the Kohn-Sham scheme does not provide methods to obtain the explicit exchange and correlation functionals and therefore, approximations have to be considered.

2.2 Models of Exchange and Correlation Functionals

There are basically three distinct approximations in DFT to the exchange correlation functional: the local density approximation (LDA), the generalized gradient approximation (GGA) and the hybrid approximation.

2.2.1. Local Density Approximation

This local density approximation was proposed by Kohn and Sham. They showed that it could be applied to the limiting case of a slowly varying density [54].

$$E_{xc}^{LDA}[n] = \int n(r)\varepsilon_{xc}(n)dr \tag{2.34}$$

where $\varepsilon_{xc}(n)$ is the exchange and correlation energy per particle of a uniform electron gas of density $n(r)$. The functional derivative of $E_{xc}^{LDA}[n]$ gives the local approximation to the Kohn-Sham exchange-correlation potential

$$v_{xc}^{LDA}(r) = \frac{\delta E_{xc}^{LDA}}{\delta n(r)} = \varepsilon_{xc}(n(r)) = n(r)\frac{\delta \varepsilon_{xc}(n)}{\delta n} \tag{2.35}$$

The Kohn-Sham equation becomes

$$\left[-\frac{1}{2}\nabla^2 + v(r) + \int \frac{n(r')}{|r-r'|}dr' + v_{xc}^{LDA}(r)\right]\Psi_1 = \varepsilon_i \Psi_i \tag{2.36}$$

$$\varepsilon_{xc}(n) = \varepsilon_x(n) + \varepsilon_c(n) \tag{2.37}$$

where $\varepsilon_x(n)$ is the exchange energy per particle of a homogenous electron gas,

$$\varepsilon_{xc}(n) = -\frac{3}{4}\left(\frac{3}{\pi}\right)^{1/3} n(r)^{1/3} = -\frac{0.4582}{r_s} \tag{2.38}$$

and $\varepsilon_c(n)$ is the correlation energy per particle of a homogenous electron gas,

$$\varepsilon_c(n) = \frac{1}{2}\left(\frac{g_0}{r_s} + \frac{g_1}{r_s^{3/2}} + \frac{g_2}{r_s^{2}} + \ldots\right) \qquad \text{for } r_s >> 1 \tag{2.39}$$

Here r_s is the Wigner-Seitz radius,

$$\frac{4}{3}\pi r_s^3 = \frac{1}{n} \tag{2.40}$$

The Kohn-Sham-LDA is further extended to the spin dependent case by replacing the scalar external potential $v(r)$ by a spin dependent potential $v_{\alpha\beta}(r)$ and replacing the charge density $n(r)$ by the density matrix $n_{\alpha\beta}(r)$ [68-70]. The electron densities with spin projection up $n_{\alpha}(r)$ and down $n_{\beta}(r)$ are treated separately. Similarly, one can deal with $n(r) = n_{\alpha}(r) + n_{\beta}(r)$ and the polarization $\zeta(r) = \left[n_{\alpha}(r) - n_{\beta}(r)\right] / n(r)$. ζ takes values between -1 (fully polarized downwards) and +1 (fully polarized upwards). The spin-up and spin-down densities are generated from the spin-up and spin-down Kohn-Sham wave functions. This so-called local spin density (LSD) approximation improved LDA for atomic and molecular systems with unpaired spins.

LDA and its spin generalization LSD allow one to use the knowledge of the uniform electron gas to predict properties of the in homogenous electron gases occurring in atoms, molecules and solids. LSD usually has moderate accuracy for most systems of interest, making errors of order 5-10%. Its most remarkable feature is its reliability, making the same kinds of errors on every system it's applied to. The success of LDA and LSD is attributed to the fact that the exchange-correlation hole $n_{xc}^{LDA}(r_1, r_2)$ is spherically symmetric and it obeys the sum rule. In other words, if an electron has been found at r_1 there is one less electron left to find elsewhere

$$\int n_{xc}^{LDA}(r_1, r_2) dr_2 = -1 \tag{2.41}$$

where the exchange-correlation hole $n_{xc}^{LDA}(r_1, r_2)$ is defined by

$$V_{ee} = \iint \frac{1}{r_{12}} n_2(r_1, r_2) dr_1 dr_2 = J[n] + \frac{1}{2} \iint \frac{1}{r_{12}} n(r_1) n_{xc}^{LDA}(r_1, r_2) dr_1 dr_2 \tag{2.42}$$

with $J[n]$ being the classical Coulomb interaction. This is true because for every r_1, $n_{xc}^{LDA}(r_1, r_2)$ is the exact exchange-correlation hole of a homogenous electron gas with density $n(r_1)$. Hence, the LDA and LSD describe the total charge of $n_{xc}^{LDA}(r_1, r_2)$ correctly.

2.2.2. Generalized Gradient Approximation

Since the LDA formula for E_{xc} is formally justified for systems with slow varying densities, it seemed natural to seek gradient corrections to E_{xc}^{LDA} by the gradient expansion approximation (GGA), which expands the functional in a Taylor series in gradients of the density [71],

$$E_{xc}^{GEA}[n_\alpha, n_\beta] = E_{xc}^{LSD}[n_\alpha, n_\beta] + \sum_{\alpha\beta}\int C_{\alpha\beta}(n_\alpha(r), n_\beta(r))\frac{\nabla n_\alpha(r)}{n_\alpha^{2/3}}.\frac{\nabla n_\beta(r)}{n_\beta^{2/3}}d^3r \quad (2.43)$$

However, GGA does not give better energy than LDA for systems such as atoms and molecules. There are two reasons for this. First, the GGA exchange-correlation hole improves the LDA hole only at short separations, but is poorly damped and oscillatory at large separations, and secondly GGA violates the sum rule of the exchange-correlation hole. Accordingly, Perdew and others introduced the so-called generalized gradient approximation [72-77] such that the exchange correlation energy can be written as a functional of both the density and its gradient:

$$E_{xc}^{GGA}[n_\alpha, n_\beta] = \int d^3r f(n_\alpha(r), n_\beta(r), \nabla n_\alpha(r), \nabla n_\beta(r)) \quad (2.44)$$

The first modern GGA was that of Langreth and Mehl [78], who proposed the idea of truncating the gradient expansion for the exchange-correlation hole. Considering the problems encountered by GGA, Perdew *et al*. [76, 77] proposed several versions of GGA functional by introducing the real-space cutoff procedure on the hole, which restores the sum rule or the normalization and negativity conditions on the GGA hole and generates a short-ranged hole whose angular and system average was much closer to the true hole. The Perdew-Wang 1991

(PW91) GGA functional [78] incorporates no free parameters and is entirely determined from uniform electron gas properties and extract constraints. The Perdew-Burke-Ernzerhof [76] functional is a simplified and refined version of the PW91 functional. Becke [73] derived an exchange functional known as B88 incorporating the known behavior of the exchange hole at large distances outside a finite system. Lee, Yang and Parr [74] obtained the correlation energy as an explicit functional of the density and it's gradient and Laplacian, now generally known as the "LYP" functional.

The well-known GGA functionals systematically improve the LDA and, in some calculations, approach the accuracy of traditional quantum chemical (e.g, Configuration Interaction) methods, at much less computational cost. However, because of the quasilocal nature of GGA, the dispersion or long-ranged van der Waals interaction arising from long-ranged correlated electronic density fluctuations in the weak bonding systems such as noble gas dimmers could not be accurately described by either LDA or GGA. On the other hand, similar to LDA, GGA has the difficulty to describe the hole centered for from the electron causing the hole.

2.2.3. Hybrid Density Functional Method

Considering the local or semi local nature of LDA and GGA, Becke proposed the so-called Hybrid Density Functional method which incorporates the exact treatment of exchange by Hartree-Fock theory with DFT approximations for dynamical correlation. This idea was motivated by re-examination of the adiabatic connection,

$$H_\lambda = T + \lambda V_{ee} + \sum_i v_\lambda(r_i) \tag{2.45}$$

where λ is an inter-electronic coupling-strength parameter that "switches on" the $1/r_{12}$ Coulomb repulsion between electrons. $\lambda = 0$ corresponds to the non-interacting Kohn-Sham reference

system, while $\lambda = 1$ corresponds to the fully interacting real system, with $n(r)$ being fixed as the exact ground state density of H_λ. The $E_{xc}[n]$ can be written as

$$E_{xc}[n] = \int_0^1 d\lambda U_{xc}^{\lambda}[n] \tag{2.46}$$

where

$$U_{xc}^{\lambda}[n] = \left\langle \Psi_n^{\lambda} \mid V_{ee} \mid \Psi_n^{\lambda} \right\rangle - J[n]. \tag{2.47}$$

The obvious first approximation for the λ dependence of the integrated in equation (2.46) is a linear interpolation, resulting in the Becke's half-and-half functional:

$$E_{xc}^{h\&h}[n] = \frac{1}{2}\left(U_{xc}^{0} + U_{xc}^{1}\right) \tag{2.48}$$

where U_{xc}^{o} is the exact exchange energy of the KS determinant and U_{xc}^{1} is the potential energy contribution to the exchange-correlation energy of the fully interacting system. This half and half functional has the merit of having a finite slope as $\lambda \to 0$, and it becomes exact if $E_{xc,\lambda=1}^{DFT}$ is exact and the system has high density. However, it does not provide a good quality of the total energy and the uniform gas limit is not obtained. Due to this Becke proposed the semi-empirical generalization of 3-parameter hybrid exchange-correlation functional

$$E_{xc}^{B3} = E_{xc}^{LSDA} + a_o(E_x^{exact} - E_x^{LSDA}) + a_x \Delta E_x^{GGA} + a_c \Delta E_c^{GGA} \tag{2.49}$$

where a_o, a_x and a_c are semiempirical coefficients to be determined by an appropriate fit to experimental data. E_x^{exact} is the exchange energy of the Slater determinant of the Kohn-Sham orbitals. ΔE_x^{GGA} is the gradient correction for the exchange, and ΔE_c^{GGA} is the gradient correction for the correlation. Equation (2.49) describes the Becke, three-parameter, Lee-Yang-Parr (B3LYP) that we used in our calculations.

CHAPTER 3

COMPUTATIONAL DETAILS

3.1 Choice of Basis Set

For our computational analysis of SiGe nanoclusters, we chose to use B3LYP-DFT [79, 80]. To apply this theory, we used GAUSSIAN'03 [81] and, when it became available to us, GAUSSIAN'09 [82]. Before beginning our in-depth study, we looked at single silicon and germanium atoms and silicon and germanium dimers with the purpose of determining a basis set. Our main concern was to compare computation times for each of the three basis sets to see if the additional time taken by the larger sets was justified by the extra precision they granted. We tried three basis sets: LANL2DZ, 3-21G**, and 6-311G(3df,3pd) (in order of increasing complexity) [83]. Table 3.1 compares our computational data with the known experimental data, from a chemistry and physics handbook [84]. What we found, though, was that with one- and two-atom systems the difference in computation time is negligible. The difference between basis sets is most clearly seen in the adiabatic electron affinities (the next section includes a discussion of how the AEA are calculated), which increase towards the experimental value with the larger basis set. Because of this and because the larger basis sets more closely approach the experimental values without using significantly more computing time, we chose to continue with a fairly large basis set, 6-311G(3df,3pd), speculating that even as the number of atoms under consideration increased, the computation time would not become unmanageable.

Table 3.1 Comparison of the Results from Three Different Basis Sets to Experimental Values

	Si Atom		Ge Atom	
Basis Set	IP (eV)	EA (eV)	IP (eV)	EA (eV)
LANL2DZ	8.47	0.90	8.01	0.84
3-21G**	8.14	0.80	7.89	0.81
6-311G(3df,3pd)	8.11	1.10	7.90	1.14
Experimental	8.15	1.39	7.90	1.23

As Hehre, Radom, Schleyer, and Pople [83] explain, a basis set, $\varphi_\mu(r)$, is formed from a summation of primitive Gaussian functions:

$$\varphi_\mu(r) = \sum_{i=1}^{N} d_{i\mu} \exp\left(-\alpha_{i\mu} f_\mu^2 r^2\right) \tag{3.1}$$

where N is the number of primitive functions, $d_{i\mu}$ is the contraction coefficient, $\alpha_{i\mu}$ is the exponential coefficient, and $f_\mu$is a scaling factor that is set to one in our calculations. The coefficients of for each term in each function [85] are given in table 3.2 for silicon and table 3.3 for germanium.

Table 3.2 The 6-311G(3df,3pd) Basis Set for Silicon

Function(s)	Orbital	$\alpha_{i\mu}$	$d_{i\mu}$
1	s	69379.23000	0.0007570004081
		10354.94000	0.005932003198
		2333.879600	0.03108801676
		657.1429500	0.1249670674
		214.3011300	0.3868972086
		77.62916800	0.5548882991
2	s	77.62916800	0.1778809451
		30.63080700	0.6277648062
		12.80129500	0.2476229236
3	s	3.926866000	1.000000000
4	s	1.452343000	1.000000000
5	s	0.2562340000	1.000000000
6	s	0.09427900000	1.000000000
7-9	p	335.4831900	0.008865998148
		78.90036600	0.06829898573
		24.98815000	0.2909579392
		9.219711000	0.7321168470
10-12	p	3.621140000	0.6198794404
		1.451310000	0.4391483120
13-15	p	0.5049770000	1.000000000
16-18	p	0.1863170000	1.000000000
19-21	p	0.06543200000	1.000000000
22-26	d	1.800000000	1.000000000
27-31	d	0.4500000000	1.000000000
32-36	d	0.1125000000	1.000000000
37-43	f	0.3200000000	1.000000000

Table 3.3 The 6-311G(3df,3pd) Basis Set for Germanium

Function(s)	Orbital	$\alpha_{i\mu}$	$d_{i\mu}$
1	s	357500.0000	0.0008389874508
		53670.00000	0.006263555625
		12300.00000	0.03203628451
		3512.000000	0.1275111324
		1161.000000	0.3916534782
		428.0000000	0.5452848425
2	s	428.0000000	0.1815987853
		170.0000000	0.6224758362
		72.06000000	0.2487183363
3	s	26.69000000	1.000000000
4	s	11.50000000	1.000000000
5	s	3.742000000	1.000000000
6	s	1.499000000	1.000000000
7	s	0.2292000000	1.000000000
8	s	0.08675000000	1000000000
9-11	p	2345.000000	0.02251405162
		554.2000000	0.1833504204
		177.3000000	0.8600319719
12-14	p	66.13000000	0.3430582877
		26.90000000	0.5065174718
		11.26000000	0.2614086952
15-17	p	11.26000000	0.06724631043
		6.116000000	0.3723817190
		2.819000000	0.6176328512
18-20	p	1.211000000	1.000000000
21-23	p	0.3568000000	1.000000000
24-26	p	0.1621000000	1.000000000
27-29	p	0.06084000000	1.000000000

Table 3.3 – *Continued*

Function(s)	Orbital	$\alpha_{i\mu}$	$d_{i\mu}$
30-34	d	74.84000000	0.03038992138
		21.23000000	0.1731895519
		7.297000000	0.4408988594
		2.549000000	0.5653185375
35-39	d	0.8165000000	1.000000000
40-44	d	0.6840000000	1.000000000
45-49	d	0.2280000000	1.000000000
50-54	d	0.07600000000	1.000000000
55-61	f	0.3500000000	1.000000000

3.2 Comparative Energies

In the tables that follow, we calculated five different values relating the energies of our various structures. The first, binding energy per atom (Binding E / Atom) compares the energy of a cluster to the energy of the dissociated atoms using the following equation:

$$\text{Binding E / Atom} = [\ (mE_{Si} + nE_{Ge}) - (E_{Si_mGe_n})\ ] / (m + n) \qquad (3.2)$$

where E_{Si} (E_{Ge}) is the energy of a single Si (Ge) atom as calculated with the 6-311G(3df,3pd) basis set, m is the number of Si atoms, n is the number of Ge atoms, and $E_{Si_mGe_n}$ is the energy of the particular system under consideration.

Similar to the binding energy, the fragmentation energy (Fragmentation E) relates the energy of a cluster to the energy of smaller clusters. For each molecule, except the dimer, there are several different fragmentation energies because they could conceivably fragment into different combinations of smaller clusters. For example, Si_2Ge can break up along three channels:

$Si_2Ge \rightarrow Si_2 + Ge$

$Si_2Ge \rightarrow SiGe + Si$

$Si_2Ge \rightarrow Si + Si + Ge$

The equation for fragmentation energy depends on the channel. In general, it is calculated by:

$$\text{Fragmentation E} = (\Sigma\, E_{\text{fragment}}) - (E_{\text{Si}_m\text{Ge}_n}) \quad (3.3)$$

where E_{fragment} is the energy of a fragmented cluster and $E_{\text{Si}_m\text{Ge}_n}$ is the energy of the original molecule.

Additionally we considered the vertical ionization potential (VIP), the adiabatic ionization potential (AIP), the vertical electron affinity (VEA), and the adiabatic electron affinity (AEA). We consider the ionization potentials to be the energy needed to release an electron from the molecule, and we calculated them with:

$$\text{VIP (or AIP)} = E_{(\text{Si}_m\text{Ge}_n)^+} - E_{\text{Si}_m\text{Ge}_n} \quad (3.4)$$

As before, $E_{\text{Si}_m\text{Ge}_n}$ is the energy of the neutral cluster under consideration, and $E_{(\text{Si}_m\text{Ge}_n)^+}$ is the energy of the cation of the cluster. For the VIP this cation has the same geometry as the neutral cluster. To calculate the AIP, the cation does not have exactly the same structure as the neutral. We used the optimized neutral geometry as the input for the cations. We included a positive charge equal to one electron and re-optimized the clusters to find the most stable cation molecules. In the end, the AIP compares a neutral and a cationic cluster that have similar structures (including similar symmetry groups) but slightly different bond lengths and angles. (Compare the neutral figures with the cation figures.) In a few cases, two neutrals have the same corresponding cation. This occurs when two neutrals optimized to the same cationic cluster. To avoid confusion, we have indicated in the tables exactly which figures we compared when calculating the AIP.

The complement of ionization potential, electron affinity, or the energy involved when an electron joins the cluster, comes from the following formula:

$$\text{VEA (or AEA)} = E_{\text{Si}_m\text{Ge}_n} - E_{(\text{Si}_m\text{Ge}_n)^-} \quad (3.5)$$

In this case, $E_{(\text{Si}_m\text{Ge}_n)^-}$ is the energy of the anion of the cluster. Just as with the ionization potential, we report both the vertical electron affinity to compare exactly the same geometries

and the adiabatic electron affinity to compare geometries that have been optimized with and without an additional electron.

3.3 Additional Properties

Finally, we have calculated one more quantity, the HOMO-LUMO gap. This value gives a relative indication of the conductivity of a material since the HOMO-LUMO gap is the energy involved when an electron shifts from the highest occupied molecular orbital (HOMO) to the lowest unoccupied one (LUMO). This calculation differs from the previous four because we calculated it not with the energy of an entire cluster, but with the energies of the LUMO (E_{LUMO}) and of the HOMO (E_{HOMO}):

$$\text{HOMO-LUMO gap} = E_{LUMO} - E_{HOMO} \qquad (3.6)$$

In some of our clusters, the HOMO and LUMO do not have the same spin. In this case, the HOMO-LUMO gap includes the energy that would be required to flip the spin. The values we reported that involve this issue are clearly marked in the tables.

Our final table lists the average coordination number for each of the most stable isomers. This value is simply the average number of bonds per atom for each cluster. All the other quantities presented in the tables came directly from our analysis using the Gaussian programs.

CHAPTER 4

RESULTS

For each of the molecules studied, we have included an illustration of the optimized geometry, which includes all bond lengths. For symmetrical molecules, we omitted labels for the redundant bond lengths. Also for each molecule, significant properties are listed in the tables. In the figures and the tables, the clusters are listed in order of increasing total energy. So, the ground state cluster in each category is always listed first. Additional figures for the most stable isomers only include the Mulliken atomic charge on each atom, illustrations of the HOMO's and LUMO's, and plots of binding energy per atom, fragmentation energy, and the second order difference in energies versus number of atoms. Also for these most stable isomers we list the fragmentation energies, the frequencies, and the average coordination numbers.

4.1 SiGe Dimer

In the simplest system we studied, the silicon-germanium dimer, our results compare with those previously reported. Andriotis, Menon, and Froudakis [47] reported two values for bond length, 2.320 Å and 2.341 Å. Additionally they found the electronic state to be $^3\Sigma_g$. The SiGe dimer of Li *et al.* [48] has a bond length of 2.22 Å, $C_{\infty v}$ symmetry group, and triplet sigma state. Furthermore they calculated the HOMO-LUMO gap to be 1.36 eV and a frequency of 431 cm^{-1}. Wielgus *et al.* [50] also reported data on this dimer. They included two sets of data because they compared two different computational methods. For the neutrals, they found 2.233 Å and 2.329 Å bond lengths, triplet sigma and triplet pi states, and 403 cm^{-1} and 433 cm^{-1} frequency. For the cations, they reported three different clusters, with different electronic states.

The first had a $^4\Sigma$ electronic state, 2.340 Å or 2.360 Å bond lengths, 381 cm^{-1} or 361 cm^{-1} frequency, and 7.52 eV or 7.63 eV ionization energies. The second had a $^2\Pi$ electronic state, 2.538 Å or 2.554 Å bond lengths, 331 cm^{-1} or 307 cm^{-1} frequencies, and 8.17 eV or 8.12 eV ionization energies. Finally, the third had a $^2\Sigma$ electronic state, 2.368 Å or 2.377 Å bond lengths, 443 cm^{-1} or 351 cm^{-1} frequency, and 8.12 eV or 8.05 eV ionization energies. Wang and Chao [51] found two stable structures. The first has a triplet-sigma electronic state, a HOMO-LUMO gap of 3.40 eV, and a frequency of 396(SG). The second has a singlet-sigma electronic state, a HOMO-LUMO gap of 0.88 eV, and a frequency of 383(SG).

Our bond length of 2.34 Å most closely matches that of Andriotis, Menon, and Froudakis [47]. Like Li *et al.* [48], we found a $C_{\infty v}$ symmetry group and triplet sigma electronic state. We found a binding energy per atom of 1.531 eV and a HOMO-LUMO gap of 1.652. This gap is slightly larger than the 1.36 eV that Li *et al.* reported, but our frequency of 395.768 cm^{-1} is lower than theirs. This frequency matches that of Wang and Chao [51]. Also, we calculated a VIP of 7.740 eV and a VEA of 1.796 eV. When a SiGe molecule breaks down into a Si atom and a Ge atom, it has a fragmentation energy of 3.061. Figures 4.4 through 4.6 show the Mulliken atomic charge on each atom, while figures 4.7 through 4.15 illustrate the HOMO and LUMO of the molecule.

For a SiGe dimer that has lost an electron and become a cation, we found that the bond length increases to 2.37 Å. At the same time, the cation is more stable, with a binding energy per atom of 1.613 eV. Figure 4.5 shows that more charge remains on the germanium atom. Comparison of figures 4.7 through 4.12 shows that the neutral molecule has a HOMO with a Σ state while the LUMO has a Π state, but for the cations this is reversed and the HOMO has the Π state while the LUMO has the Σ state. The anion of the SiGe dimer has the smallest bond length of 2.249 Å, and the highest binding energy per atom of 1.884 eV.

Table 4.1 Properties of the SiGe Neutral Dimer

Figure	Symmetry Group	Electronic State	Binding E / Atom (eV)	HOMO-LUMO Gap (eV)	Dipole Moment (D)
4.1	$C_{\infty v}$	$^3\Sigma$	1.531	1.652	0.217

Table 4.2 Properties of the $(SiGe)^+$ Cationic Dimer

Figure	Symmetry Group	Electronic State	Binding E / Atom (eV)	HOMO-LUMO Gap (eV)	Dipole Moment (D)
4.2	$C_{\infty v}$	$^4\Sigma$	1.613	2.241[a]	1.955

[a] HOMO and LUMO have opposite spins; this value includes the energy required to flip the spin of the electron.

Table 4.3 Properties of the $(SiGe)^-$ Anionic Dimer

Figure	Symmetry Group	Electronic State	Binding E / Atom (eV)	HOMO-LUMO Gap (eV)	Dipole Moment (D)
4.3	$C_{\infty v}$	--	1.884	1.581	2.153

Table 4.4 Ionization Potentials and Electron Affinities of the SiGe Dimer

Neutral Figure	VIP (eV)	Cationic Figure	AIP (eV)	VEA (eV)	Anionic Figure	AEA (eV)
4.1	7.740	4.2	7.736	1.796	4.3	1.845

Table 4.5 Fragmentation Energy of the SiGe Neutral Dimer

Fragmented Clusters	Fragmentation Energy (eV)
Si + Ge	3.061

Table 4.6 Fragmentation Energy of the $(SiGe)^+$ Cationic Dimer

Fragmented Clusters	Fragmentation Energy (eV)
$Si + Ge^+$	3.226

Table 4.7 Fragmentation Energy of the $(SiGe)^-$ Anionic Dimer

Fragmented Clusters	Fragmentation Energy (eV)
$Si + Ge^-$	3.769

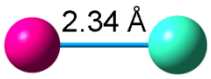

Figure 4.1 Geometry of the SiGe Neutral Dimer (The Silicon Atom is Pictured in Pink, and the Germanium Atom is Pictured in Green.)

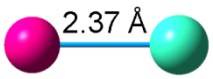

Figure 4.2 Geometry of the $(SiGe)^+$ Cationic Dimer

Figure 4.3 Geometry of the $(SiGe)^-$ Anionic Dimer

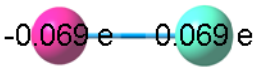

Figure 4.4 Atomic Charges of the SiGe Neutral Dimer

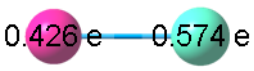

Figure 4.5 Atomic Charges of the $(SiGe)^+$ Cationic Dimer

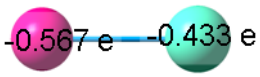

Figure 4.6 Atomic Charges of the $(SiGe)^-$ Anionic Dimer

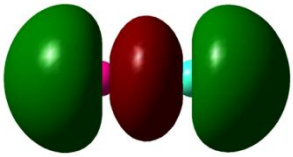

Figure 4.7 HOMO of the SiGe Neutral Dimer

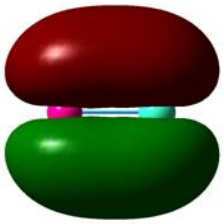

Figure 4.8 LUMO of the SiGe Neutral Dimer

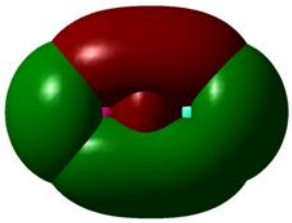

Figure 4.9 HOMO and LUMO of the SiGe Neutral Dimer

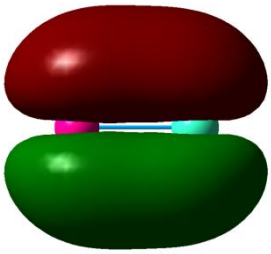

Figure 4.10 HOMO of the $(SiGe)^{+}$ Cationic Dimer

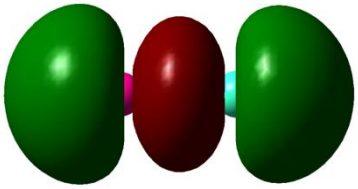

Figure 4.11 LUMO of the $(SiGe)^{+}$ Cationic Dimer

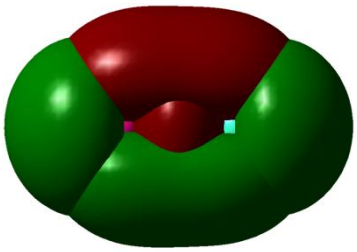

Figure 4.12 HOMO and LUMO of the $(SiGe)^{+}$ Cationic Dimer

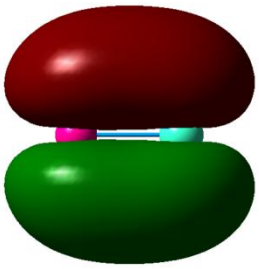

Figure 4.13 HOMO of the $(SiGe)^{-}$ Anionic Dimer

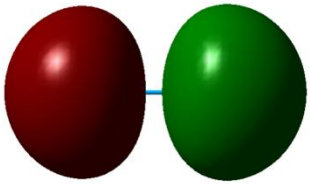

Figure 4.14 LUMO of the $(SiGe)^{-}$ Anionic Dimer

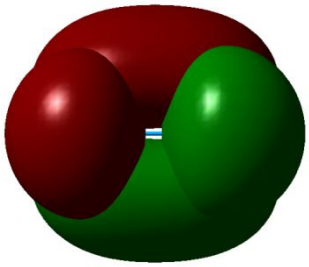

Figure 4.15 HOMO and LUMO of the $(SiGe)^{-}$ Anionic Dimer

4.2 Si_2Ge Trimers

For the Si_2Ge trimer, Li *et al.* [48] found a triangular structure with each atom bonding to the other two. Their SiGe bond length is 2.39 Å and their Si-Ge-Si angle is 57°. This structure falls in the C_{2v} symmetry group and has a $^3B_2$ electronic state. They calculated a HOMO-LUMO gap of 1.9 eV and the following frequencies: 274 cm^{-1} (B2), 440 cm^{-1} (A1), and 243 cm^{-1} (A1). Marim *et al.* [49] found a completely different structure, an asymmetrical L-shape, with a Ge-Si-Si angle of 83.16°. Their Si-Si bond length is 2.19 Å and only one of the Si atoms bonds to the Ge atom with a bond length of 2.25 Å. They calculated a cohesive energy per atom, by the same method that we calculated the binding energy per atom, giving them an energy of 2.23 eV per atom.

Wielgus *et al.* [50] found two neutral Si_2Ge isomers. Their ground state cluster, an L-shape comparable to that of Marim *et al.* has a Si-Si-Ge angle of 80.7° or 81.2°. (They used two different methods.) Irrespective of theory, they found a C_s group and a $^1A'$ state. Finally, they report frequencies of 158, 441, and 557 cm^{-1} or 146, 416, and 540 cm^{-1}. Their second structure is a triangle similar to Li *et al.* with a Si-Ge-Si angle of 55.9° or 56.7°. They report the same group and state as Li *et al.*, but their frequencies are 214, 308 and 449 cm^{-1} or 249, 278, or 449 cm^{-1}. Additionally, they found two cationic Si_2Ge isomers. The more stable was a triangle (C_{2v} symmetry) with a $^2A_1$ electronic state, a Si-Ge-Si angle of 51.2° or 51.0°, and the following frequencies: 59 cm^{-1} or i73 cm^{-1}, 517 cm^{-1} or 264 cm^{-1}, and 685 cm^{-1} or 530 cm^{-1}. The second isomer was L-shaped (C_s symmetry) with a $^2A''$ electronic state, a Si-Ge-Si angle of 88.6°, and the following frequencies: 126 cm^{-1}, 394 cm^{-1}, and 504 cm^{-1}.

Wang and Chao [51] found three stable Si_2Ge neutral trimers. The most stable is an L-shape with an Si-Ge bond of 2.249 Å, a Si-Si bond of 2.181 Å, and a Ge-Si-Si angle of 82.91°. This structure has an electronic state of $^1A'$, a dissociation energy of -6.5558 or -9.8755, a HOMO-LUMO gap of 2.38, and frequencies of 146(a'), 424(a'), and 523(a'). Their second structure is a triangle without a bond between the Si atoms. It has two Si-Ge bonds of 2.242 Å,

and a Si-Ge-Si angle of 80.10°. This structure has an electronic state of $^3B_2$, a dissociation energy of -6.1918 or -9.5970, a HOMO-LUMO gap of 3.58, and frequencies of 245(a1), 275(b2), and 440(a1). Their third neutral trimer is a triangle with two Si-Ge bonds of 2.386 Å and a Si-Ge-Si angle of 56.96°. They reported this structure to have $^3B_2$ symmetry, an electronic state of $^1A_1$, a dissociation energy of -6.8999, a HOMO-LUMO gap of 2.23, and frequencies of 148(a'), 426(a'), and 432(a'). Furthermore, they found cations with geometries similar to the first two neutral clusters. The first cation has a Si-Ge bond of 2.390 Å, a Si-Si bond of 2.169 Å, and Ge-Si-Si angle of 71.58°. The second cation has two Si-Ge bonds of 2.524 Å, and a Si-Ge-Si angle of 50.52°. Finally, they found a single anion with the same geometry as the most stable cation and neutral cluster. Its Si-Ge bond length is 2.358 Å, its Ge-Ge bond length is 2.240 Å, and its Ge-Si-Si angle is 66.17°.

We found four isomers for the Si_2Ge trimer. The most stable Si_2Ge cluster is the most stable trimer we studied. The first two clusters are symmetrical triangles and the last two are linear. Figure 4.16 illustrates the neutral geometries including bond lengths and angles. For our most stable isomer, the bond length, Si-Ge-Si angle, symmetry group, electronic state, HOMO-LUMO gap, and frequencies match those of Li *et al.* Additionally we calculated a binding energy of 2.250 eV (very close to the 2.23 found by Marim *et al.*), a VIP of 8.059 eV, and a VEA of 2.153 eV. From our fragmentation energy calculations, the Si_2Ge molecule is most likely to break up into a Si_2 dimer and a Ge atom.

In the case of the Si_2Ge cations, we found four isomers (figure 4.17). Comparing these with the neutral clusters we found that the triangular structures were again more stable than the linear ones. In the most stable cluster, the Si-Si bond shrank to 2.15 Å while the Si-Ge bond expanded to 2.39 Å. For the second triangular structure, the two silicon atoms became close enough (2.48 Å) for them to likely bond, unlike in the neutral trimer where they were separated. For the linear structures, all the bond lengths of the cations are larger than the corresponding bonds in the neutrals.

Moving away from structural properties, our computations showed that each of the cations have a slightly higher binding energy than the corresponding neutrals, suggesting that the cations are more stable. Investigations of the Mulliken atomic charges (figures 4.22 through 4.24) show that the germanium atom has more charge than the silicon atoms, just as in the SiGe dimer.

The Si_2Ge anion geometries follow the same patterns as the neutral and cation clusters. In general, the bond lengths lie somewhere between the neutral and cation bond lengths. Binding energies per atom are higher than those for the cations and anions in all cases.

Table 4.8 Properties of the Si_2Ge Trimers

Figure	Symmetry Group	Electronic State	Binding E / Atom (eV)	HOMO-LUMO Gap (eV)	Dipole Moment (D)
4.16 (a)	C_{2v}	$^3B_2$	2.250	1.904 [a]	0.203
4.16 (b)	C_{2v}	$^1A_1$	2.171	2.244	0.062
4.16 (c)	$C_{\infty v}$	$^1\sum$	2.065	2.245	0.504
4.16 (d)	$D_{\infty h}$	$^1\sum_g$	2.010	2.316	0.000

[a] HOMO and LUMO have opposite spins; this value includes the energy required to flip the spin of the electron.

Table 4.9 Properties of the $(Si_2Ge)^+$ Trimers

Figure	Symmetry Group	Electronic State	Binding E / Atom (eV)	HOMO-LUMO Gap (eV)	Dipole Moment (D)
4.17 (a)	C_{2v}	$^2A_1$	2.256	2.066 [a]	1.627
4.17 (b)	C_{2v}	$^2B_2$	2.189	2.072	1.693
4.17 (c)	$C_{\infty v}$	--	2.111	1.352	2.513
4.17 (d)	$D_{\infty h}$	--	2.034	1.317	0.000

[a] HOMO and LUMO have opposite spins; this value includes the energy required to flip the spin of the electron.

Table 4.10 Properties of the $(Si_2Ge)^-$ Trimers

Figure	Symmetry Group	Electronic State	Binding E / Atom (eV)	HOMO-LUMO Gap (eV)	Dipole Moment (D)
4.18 (a)	C_{2v}	$^2B_2$	2.597	1.654	2.034
4.18 (b)	C_{2v}	$^2A_1$	2.555	1.494	2.235
4.18 (c)	$C_{\infty v}$	--	2.338	1.171	3.363
4.18 (d)	$D_{\infty h}$	--	2.281	1.219	0.000

Table 4.11 Ionization Potentials and Electron Affinities of the Si_2Ge Trimer

Neutral Figure	VIP (eV)	Cationic Figure	AIP (eV)	VEA (eV)	Anionic Figure	AEA (eV)
4.16 (a)	8.059	4.17 (a)	7.882	2.153	4.18 (a)	2.179
4.16 (b)	8.026	4.17 (b)	7.846	1.859	4.18 (b)	2.289
4.16 (c)	7.886	4.17 (c)	7.762	1.956	4.18 (c)	1.957
4.16 (d)	7.958	4.17 (d)	7.829	1.946	4.18 (d)	1.951

Table 4.12 Fragmentation Energies of the Most Stable Si_2Ge Neutral Trimer

Fragmented Clusters	Fragmentation Energy (eV)
Si_2 + Ge	3.528
SiGe + Si	3.689
2Si + Ge	6.751

Table 4.13 Fragmentation Energies of the Most Stable $(Si_2Ge)^+$ Cationic Trimer

Fragmented Clusters	Fragmentation Energy (eV)
$(SiGe)^+$ + Si	3.543
Si_2 + Ge^+	3.546
Si +Si + Ge^+	6.769

Table 4.14 Fragmentation Energies of the Most Stable $(Si_2Ge)^-$ Anionic Trimer

Fragmented Clusters	Fragmentation Energy (eV)
$(SiGe)^-$ + Si	4.024
$Si_2 + Ge^-$	4.569
$2Si + Ge^-$	7.792

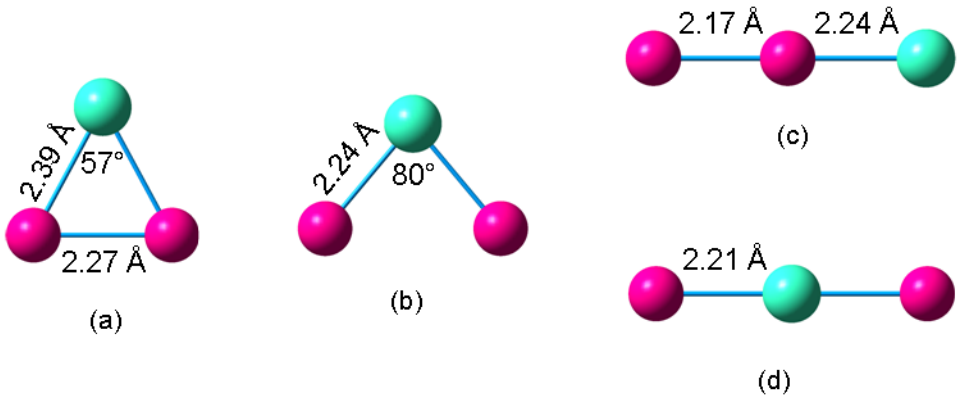

Figure 4.16 Geometries of the Si_2Ge Neutral Trimers from (a) Most Stable through (d) Least Stable

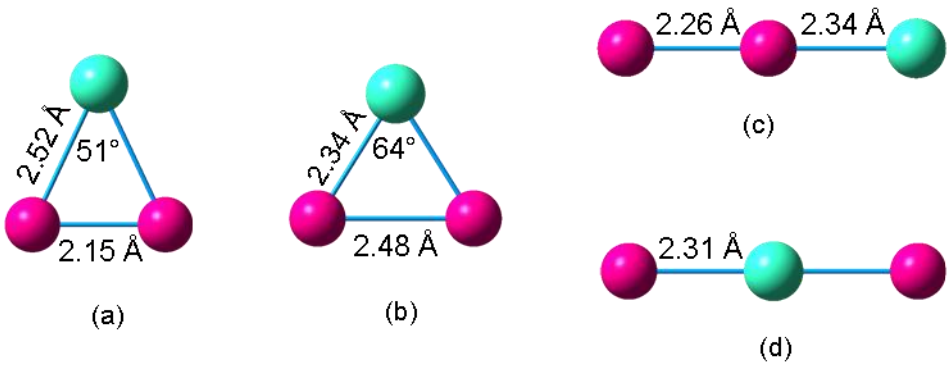

Figure 4.17 Geometries of the $(Si_2Ge)^+$ Cationic Trimers from (a) Most Stable through (d) Least Stable

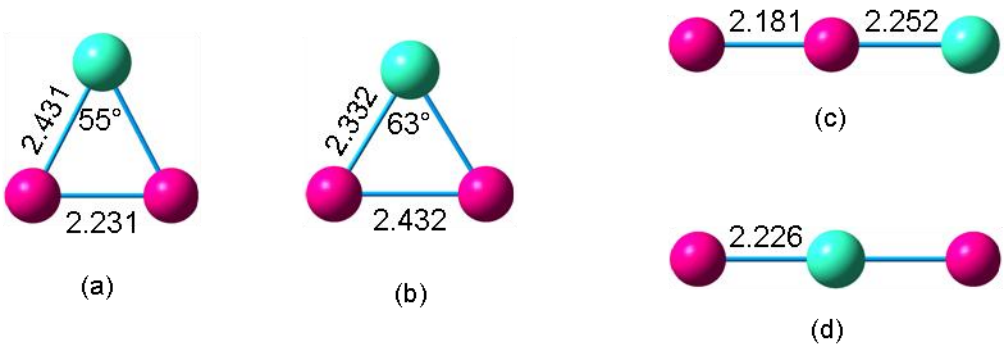

Figure 4.18 Geometries of the $(Si_2Ge)^-$ Anionic Trimers from (a) Most Stable through (d) Least Stable

4.3 $SiGe_2$ Trimers

Li *et al.* [48] also studied this molecule in depth. Their structure is again triangular, but the two Ge atoms do not bond, and their Si-Ge bond length is 2.25 Å while their Ge-Si-Ge angle is 85°. Their cluster has C_{2v} symmetry, a $^1A_1$ state, a 2.44 eV HOMO-LUMO gap, and 424 cm^{-1} (B_2), 427 cm^{-1} (A_1), and 112 cm^{-1} (A_1) frequencies. Marim *et al.* [49] found nearly this same molecule, with Si-Ge bonds of 2.26 Å, and a Ge-Si-Ge angle of 84.6°. They also calculated a cohesive energy of 2.19 eV per atom. However, Wielgus *et al.* [50] found three completely different geometries. Their ground state neutral molecule is L-shaped (the Si atom bonds with only one Ge atom) with a Ge-Ge-Si angle of 83.0° or 83.7°, C_{2v} symmetry, a $^1A_1$ state, and frequencies of 117, 432, and 441 or 110, 412, and 441 cm^{-1}. Their next isomer is a triangle, but each atom bonds with the other two. For this structure they found a Si-Ge-Si angle of 63°, C_{2v} symmetry, a $^3B_2$ state, and frequencies of 205, 249, and 377 or 198, 215, and 371 cm^{-1}. However, they only found two cation isomers, both L-shaped. The more stable had C_{2v} symmetry, a $^2B_1$ electronic state, Si-Ge bonds of 2.352 Å or 2.363 Å, an angle of 90.2° or 92.6°, and the following frequencies: 95 cm^{-1} or 83 cm^{-1}, 380 $cm^{-}1$ or 358 cm^{-1}, and 407 cm^{-1} or 379 cm^{-1}. The second cluster had C_s symmetry, a ^2A" electronic state, an angle of 86.2° or 88.9°, and the following frequencies: 113 cm^{-1}, 282 cm^{-1}, and 399 cm^{-1}.

Wang and Chao [51] found three neutral $SiGe_2$ clusters. The most stable is a triangle with two Si-Ge bonds of 2.250 Å and a Ge-Si-Ge angle of 84.52°. This cluster has an electronic state of ^{1}A1, a dissociation energy of -6.0898 or -10.0812, a HOMO-LUMO gap of 2.43, and frequencies of 111(a1), 423(b2), and 426(a1). Their second-most stable $SiGe_2$ trimer is an L-shape with Ge-Ge bond of 2.311 Å, Si-Ge bond 2.243 Å, and Ge-Ge-Si bond of 81.78°. For this structure they reported an electronic state of ^{1}A1, a dissociation energy of -5.8665 or -9.7762, a HOMO-LUMO gap of 3.53, and frequencies of 148(a'), 426(a'), and 423(a). Their last neutral cluster is a triangle with ^{3}B2 symmetry, Si-Ge bonds of 2.374 Å, and a Ge-Si-Ge angle of 62.83°. This cluster has an electronic state of ^{3}A2, a dissociation energy of -7.1596, a HOMO-LUMO gap of 2.23, and frequencies of 198(a1), 215(b2), and 370(a1). Their investigation of the cationic clusters resulted in two different geometries that resemble their two most stable neutral clusters. The first has Si-Ge bonds of length 2.309 Å and a Ge-Si-Ge angle of 74.96°. Their second cation has a Ge-Ge bond of 2.420 Å, a Si-Ge bond of 2.342 Å, and a Ge-Ge-Si angle of 92.23°. Finally, their anion cluster, which has a geometry similar to the most stable neutral and cation, has Si-Ge bonds of length 2.328 Å and a Ge-Si-Ge angle of 68.58°

Our calculations show a ground state trimer similar to that of Li *et al.* and Wang and Chao, and our second cluster is the same as Wang and Chao's third most stable cluster. We also find two linear structures. As with Si_2Ge, the triangular structures are more stable than the linear ones. Our most stable isomer has the same bond length, angle, symmetry group, electronic state, HOMO-LUMO gap, and frequencies as Li *et al* and Wang and Chao. Additionally we found the binding energy to be 2.217 eV, the VIP to be 8.025 eV and the VEA to be 1.697 eV. This molecule is most likely to fragment into the SiGe dimer and a Ge atom, with a fragmentation energy of 3.591. The second most stable structure, also triangular, but with a smaller Ge-Si-Ge bond of 63°, has the same symmetry group as the first, but a different electronic state ($^3B_2$), a binding energy of 2.155, a VIP of 8.045, and a VEA of 2.148.

For the $SiGe_2$ cations we found only three stable isomers (figure 4.20). This is because when we re-optimized the first and second neutral clusters with the a positive charge, they both optimized to the same triangular structure. This cluster was also reported by Wang and Chao to be the most stable $SiGe_2$ cation. Its Ge-Si-Ge angle is approximately halfway between the value for the two most stable neutral structures. As with the Si_2Ge trimers, the bond lengths of the linear structures are longer for the cations than for the neutrals. Furthermore, our calculations show that the HOMO-LUMO gaps of the cations (table 4.16) are consistently less than any gap value for the neutrals. Also, the Mulliken atomic charges on the germanium atoms are significantly higher than that on the silicon atom. This is a trend that holds for all the structures pictured in figure 65.

When we analyzed the $SiGe_2$ anions, we again found that optimization using the geometries of the two triangular neutral clusters led to the same triangular cluster (figure 4.21 (a)). This cluster matches the anion reported by Wang and Chao. We also list the linear anions. Their bond lengths are only slightly larger than the linear cations. For example, the Si-Ge bond in the most stable linear structure only increases from 2.24 Å to 2.25 Å

Table 4.15 Properties of the $SiGe_2$ Trimers

Figure	Symmetry Group	Electronic State	Binding E / Atom (eV)	HOMO-LUMO Gap (eV)	Dipole Moment (D)
4.19 (a)	C_{2v}	$^1A_1$	2.217	2.436	0.242
4.19 (b)	C_{2v}	$^3B_2$	2.155	1.892 [a]	0.232
4.19 (c)	$D_{\infty h}$	$^1\sum_g$	2.016	2.192	0.000
4.19 (d)	$C_{\infty v}$	$^1\sum$	1.965	2.247	0.522

[a] HOMO and LUMO have opposite spins; this value includes the energy required to flip the spin of the electron.

Table 4.16 Properties of the $(SiGe_2)^+$ Trimers

Figure	Symmetry Group	Electronic State	Binding E / Atom (eV)	HOMO-LUMO Gap (eV)	Dipole Moment (D)
4.20 (a)	C_{2v}	$^2B_2$	2.201	1.771	0.600
4.20 (b)	$D_{\infty h}$	--	2.101	1.312	0.000
4.20 (c)	$C_{\infty v}$	--	2.031	1.283	1.772

Table 4.17 Properties of the $(SiGe_2)^-$ Trimers

Figure	Symmetry Group	Electronic State	Binding E / Atom (eV)	HOMO-LUMO Gap (eV)	Dipole Moment (D)
4.21 (a)	C_{2v}	$^2A_1$	2.516	1.807	1.193
4.21 (b)	$D_{\infty h}$	--	2.277	1.285[a]	0.000
4.21 (c)	$C_{\infty v}$	--	2.225	1.162	2.679

[a] HOMO and LUMO have opposite spins; this value includes the energy required to flip the spin of the electron.

Table 4.18 Ionization Potentials and Electron Affinities of the $SiGe_2$ Trimers

Neutral Figure	VIP (eV)	Cationic Figure	AIP (eV)	VEA (eV)	Anionic Figure	AEA (eV)
4.19 (a)	8.025	4.20 (a)	7.949	1.697	4.21 (a)	2.033
4.19 (b)	8.045	4.20 (a)	7.762	2.148	4.21 (a)	2.220
4.19 (c)	7.769	4.20 (b)	7.645	1.921	4.21 (b)	1.921
4.19 (d)	7.828	4.20 (c)	7.701	1.914	4.21 (c)	1.918

Table 4.19 Fragmentation Energies of the Most Stable $SiGe_2$ Neutral Trimer

Fragmented Clusters	Fragmentation Energy (eV)
SiGe + Ge	3.591
Si + Ge_2	3.724
Si + 2Ge	6.652

Table 4.20 Fragmentation Energies of the Most Stable $(SiGe_2)^+$ Cationic Trimer

Fragmented Clusters	Fragmentation Energy (eV)
$(SiGe)^+ + Ge$	3.378
$Si + (Ge_2)^+$	3.395
$SiGe + Ge^+$	3.542
$Si + Ge + Ge^+$	6.604

Table 4.21 Fragmentation Energies of the Most Stable $(SiGe_2)^-$ Anionic Trimer

Fragmented Clusters	Fragmentation Energy (eV)
$(SiGe)^- + Ge$	3.779
$(Ge_2)^- + Si$	3.942
$SiGe + Ge^-$	4.486
$Si + Ge^- + Ge$	7.548

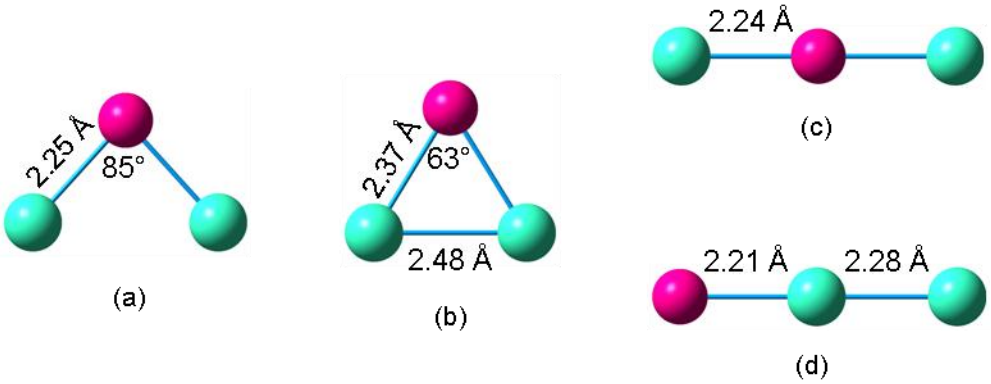

Figure 4.19 Geometries of the $SiGe_2$ Neutral Trimers from (a) Most Stable through (d) Least Stable

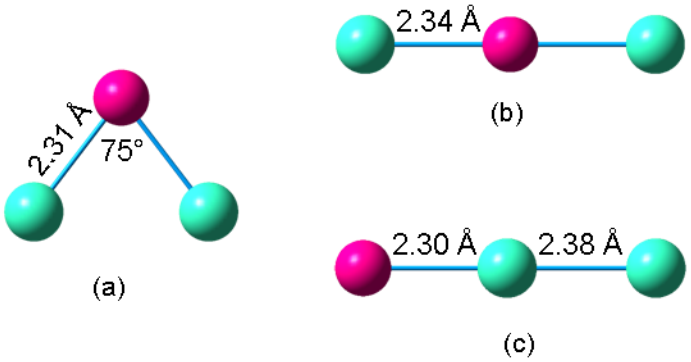

Figure 4.20 Geometries of the $(SiGe_2)^+$ Cationic Trimers from (a) Most Stable through (c) Least Stable

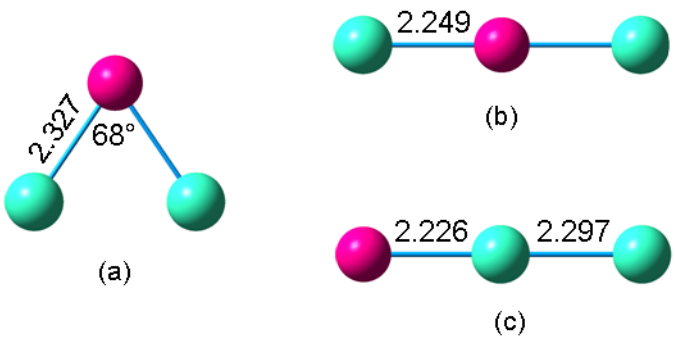

Figure 4.21 Geometries of the $(SiGe_2)^-$ Anionic Trimers from (a) Most Stable through (c) Least Stable

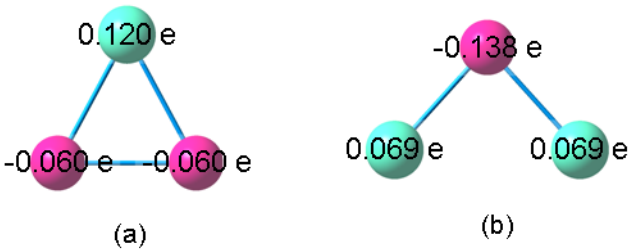

Figure 4.22 Atomic Charges of the Most Stable (a) Si_2Ge and (b) $SiGe_2$ Neutral Trimer

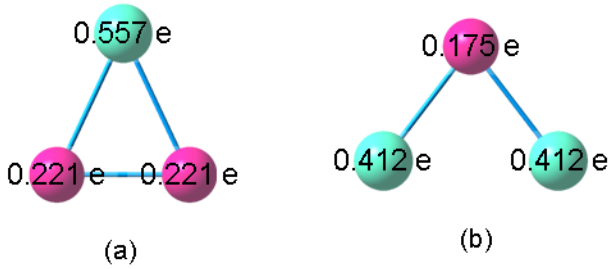

Figure 4.23 Atomic Charges of the Most Stable (a) $(Si_2Ge)^+$ and (b) $(SiGe_2)^+$ Cationic Trimer

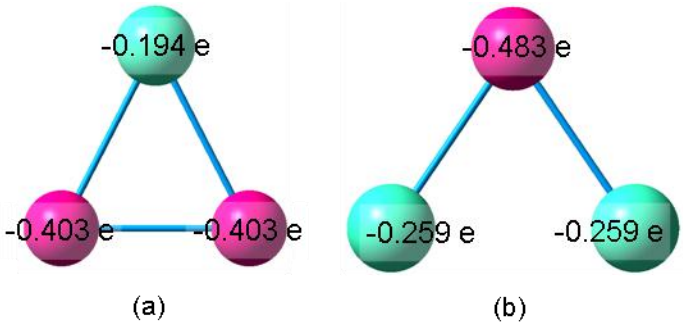

Figure 4.24 Atomic Charges of the Most Stable (a) $(Si_2Ge)^-$ and (b) $(SiGe_2)^-$ Anionic Trimer

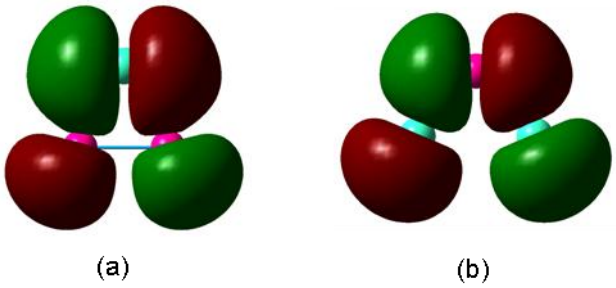

Figure 4.25 HOMO of the Most Stable (a) Si_2Ge and (b) $SiGe_2$ Neutral Trimer

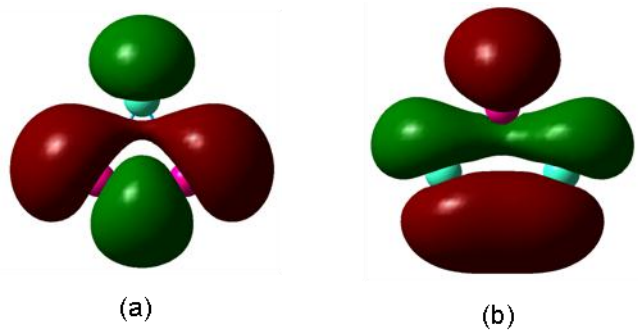

Figure 4.26 LUMO of the Most Stable (a) Si_2Ge and (b) $SiGe_2$ Neutral Trimer

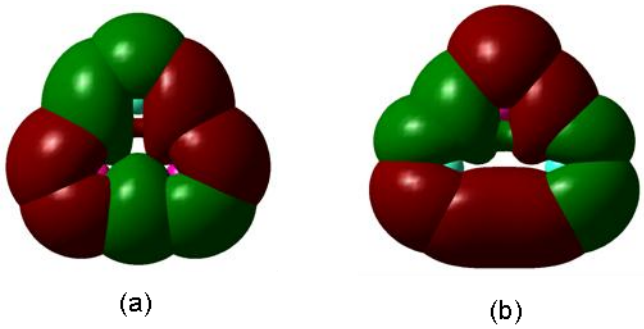

Figure 4.27 HOMO and LUMO of the Most Stable (a) Si_2Ge and (b) $SiGe_2$ Neutral Trimer

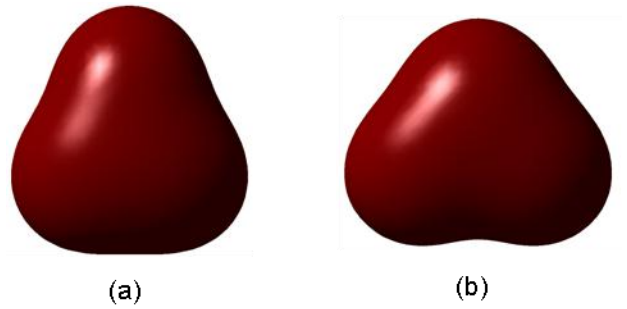

Figure 4.28 HOMO of the Most Stable (a) $(Si_2Ge)^+$ and (b) $(SiGe_2)^+$ Cationic Trimer

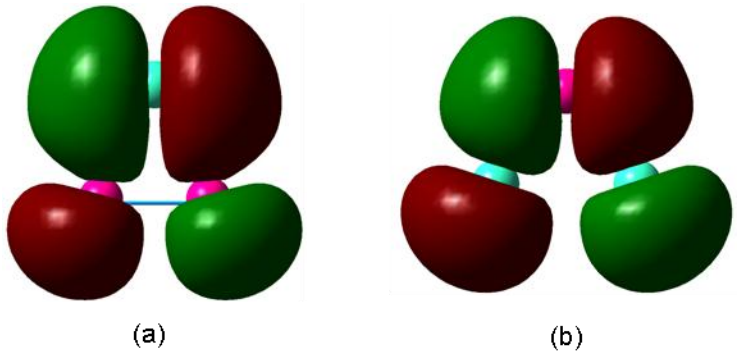

Figure 4.29 LUMO of the Most Stable (a) $(Si_2Ge)^+$ and (b) $(SiGe_2)^+$ Cationic Trimer

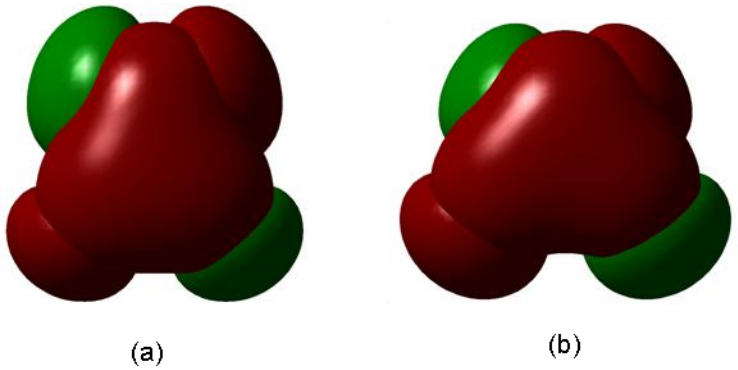

Figure 4.30 HOMO and LUMO of the Most Stable (a) $(Si_2Ge)^+$ and (b) $(SiGe_2)^+$ Cationic Trimer

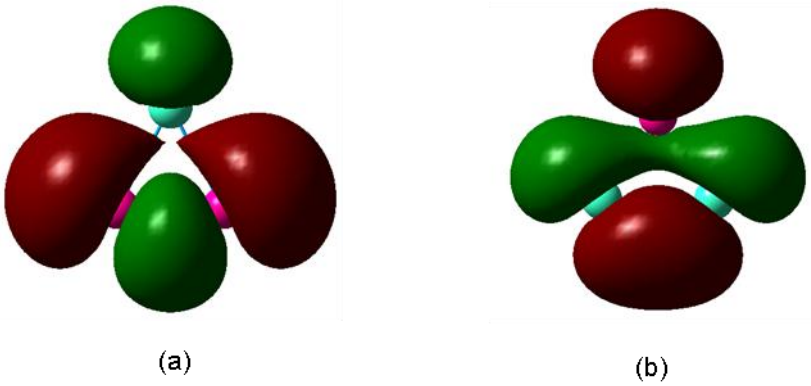

Figure 4.31 HOMO of the Most Stable (a) $(Si_2Ge)^-$ and (b) $(SiGe_2)^-$ Anionic Trimer

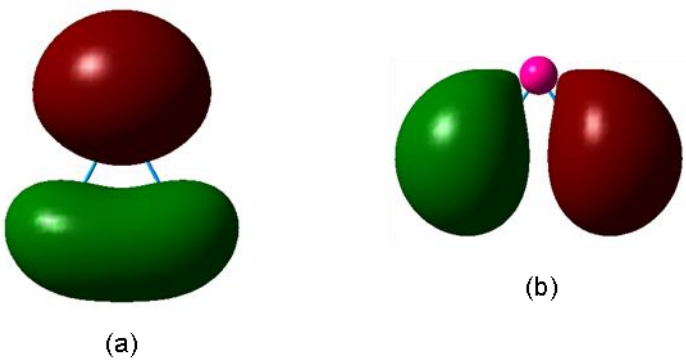

Figure 4.32 LUMO of the Most Stable (a) $(Si_2Ge)^-$ and (b) $(SiGe_2)^-$ Anionic Trimer

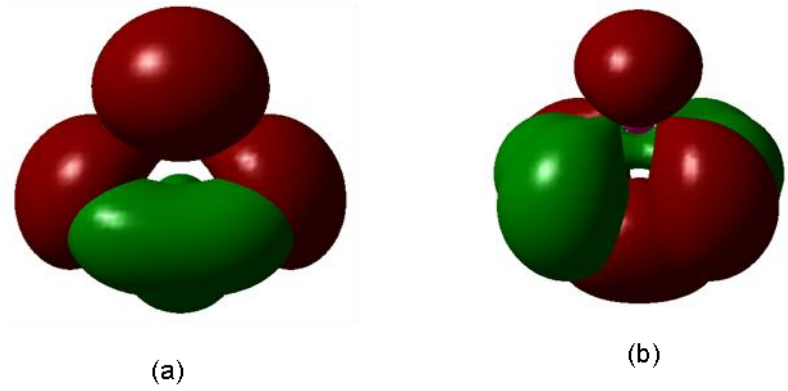

Figure 4.33 HOMO and LUMO of the Most Stable (a) $(Si_2Ge)^-$ and (b) $(SiGe_2)^-$ Anionic Trimer

4.4 Si_3Ge Tetramers

Three other sources have carried out calculations on the Si_3Ge tetramer. The first, Marim *et al.* [49] found a rhombus-shaped cluster with two Si atoms bonding across the middle. Their Si-Ge bond length is 2.40 Å, their middle Si-Si bond length is 2.45 Å, the other two Si-Si bonds lengths are 2.33 Å, and they calculated a cohesive energy of 2.70 eV per atom. The second source, Wielgus *et al.* [50] found two rhombus-shaped neutral isomers. The first is the same as that of Marim et al, with slightly different bond lengths. Wielgus *et al.* found a Si-Ge bond length of 2.415 Å, a middle Si-Si bond length of 2.438 Å, and two more Si-Si bonds with length 2.328 Å. They found this cluster to have C_{2v} symmetry and a $^1A_1$ electronic state. For this ground state cluster they also calculated a VIP of 8.19 eV. Their second cluster was again a rhombus, but the distance (3.520 Å) between the Si atom and the Ge atom across the middle is likely too large to form a bond. They found this cluster to belong to the same symmetry group and electronic state as their first one. Additionally, they reported two cationic rhombic isomers. The first had C_{2v} symmetry, a $^2A_1$ electronic state and the following bonds: Si-Ge bonds of 2.481 Å, Si-Si bonds of 2.369 Å, and a middle Si-Si bond of 2.303 Å. The second cluster had C_{2v} symmetry and a $^2B_2$ electronic state, and a 2.578 Å bond through the middle.

Wang and Chao [51] investigated two Si_3Ge geometries and found the values for the neutrals and ions of both. Both are rhombuses. The most stable for all three charges has a Si-Si bond through the middle, while the other has Si-Ge bond through its middle. The most stable neutral has an electronic state of ^{1}A1, a dissociation energy of -10.9645 or -14.7104, a HOMO-LUMO gap of 2.39, and frequencies of 479(a1), 413(a1), and 269(a1). The second neutral has an electronic state of ^{1}A', a dissociation energy of -9.6354 or -14.5790, a HOMO-LUMO gap of 2.34, and frequencies of 487(a'), 317(a'), and 81(a').

The first class of we tetramers studied, Si_3Ge molecules, shows four different kinds of geometries – rhombic, triangular with an extra atom attached to one of the vertices, trigonal and linear. The first cluster pictured in figure 4.34 (a) is our most stable tetramer structure. Our two

most stable Si_3Ge clusters are similar to those found by Wielgus *et al.*, but we also investigated five other stable clusters. Our most stable isomer, is also a rhombus with two Si atoms bonding (with length 2.43 Å) through the middle. On one side there is a triangle with Si-Ge-Si angle 61° and Si-Ge bonds of 2.40 Å, and on the other side there is a Si-Si-Si triangle. The angle formed by Si atoms 2-3-4 is 63° and the Si bonds between atoms 2-3 and 3-4 are both 2.32 Å long. In agreement with both sources previously discussed we found the symmetry group to be C_{2v} and the electronic state to be $^1A_1$. For this cluster, our binding energy per atom is 2.762 eV, and our HOMO-LUMO gap is 2.394 eV. We found a slightly lower VIP (8.003 eV) than Wielgus *et al.* and a VEA of 1.967 eV. Also, our calculations predict that with a fragmentation energy of 4.297 eV this cluster breaks into a Si_2Ge trimer and a Si atom.

The structures of the Si_3Ge cations closely match those of the neutrals, with one exception. We did not find there to be a stable trigonal cation molecule. For the rhombic structures, the central bonds stretched as much as 0.28 Å while the other bonds shrank by at most 0.04 Å. Regarding the binding energy per atom, each value for the cations is larger than that of the neutral molecule with the comparable structure. This trend continues, in general, for all the molecules studied.

Table 4.22 Properties of the Si_3Ge Tetramers

Figure	Symmetry Group	Electronic State	Binding E / Atom (eV)	HOMO-LUMO Gap (eV)	Dipole Moment (D)
4.34 (a)	C_{2v}	$^1A_1$	2.762	2.394	0.500
4.34 (b)	C_{2v}	$^1A_1$	2.727	2.343	0.051
4.34 (c)	C_{2v}	$^1A_1$	2.360	1.342	1.571
4.34 (d)	C_{2v}	$^1A_1$	2.274	1.408	0.997
4.34 (e)	$C_{\infty v}$	$^3\sum$	2.151	1.804[a]	0.568
4.34 (f)	$C_{\infty v}$	$^3\sum$	2.094	1.834[a]	0.184

[a] HOMO and LUMO have opposite spins; this value includes the energy required to flip the spin of the electron.

Table 4.23 Properties of the $(Si_3Ge)^+$ Tetramers

Figure	Symmetry Group	Electronic State	Binding E / Atom (eV)	HOMO-LUMO Gap (eV)	Dipole Moment (D)
4.35 (a)	C_{2v}	$^2A_1$	2.795	1.998 [a]	1.805
4.35 (b)	C_s	$^2A'$	2.787	2.044 [a]	1.542
4.35 (c)	C_{2v}	$^2A_1$	2.530	1.716	0.957
4.35 (d)	C_{2v}	$^2A_1$	2.427	1.727	0.842
4.35 (e)	$C_{\infty v}$	--	2.272	1.189	2.982
4.35 (f)	$C_{\infty v}$	--	2.199	1.225	0.971

[a] HOMO and LUMO have opposite spins; this value includes the energy required to flip the spin of the electron.

Table 4.24 Properties of the $(Si_3Ge)^-$ Tetramers

Figure	Symmetry Group	Electronic State	Binding E / Atom (eV)	HOMO-LUMO Gap (eV)	Dipole Moment (D)
4.36 (a)	C_{2v}	$^2B_1$	2.975	1.768[a]	2.472
4.36 (b)	C_s	$^2A''$	2.937	1.849[a]	1.558
4.36 (c)	C_{2v}	$^2B_1$	2.723	1.831[a]	2.877
4.36 (d)	C_{2v}	$^2B_1$	2.643	1.854[a]	0.113
4.36 (e)	$C_{\infty v}$	--	2.480	1.092	4.075
4.36 (f)	$C_{\infty v}$	--	2.433	1.113	1.431

[a] HOMO and LUMO have opposite spins; this value includes the energy required to flip the spin of the electron.

Table 4.25 Ionization Potentials and Electron Affinities of the Si_3Ge Tetramers

Neutral Figure	VIP (eV)	Cationic Figure	AIP (eV)	VEA (eV)	Anionic Figure	AEA (eV)
4.34 (a)	8.003	4.35 (a)	7.767	1.967	4.36 (a)	1.989
4.34 (b)	7.923	4.35 (b)	7.661	1.958	4.36 (b)	1.980
4.34 (c)	7.266	4.35 (c)	7.223	2.559	4.36 (c)	2.589
4.34 (d)	7.318	4.35 (d)	7.286	2.584	4.36 (d)	2.616
4.34 (e)	7.488	4.35 (e)	7.414	2.404	4.36 (e)	3.003
4.34 (f)	7.549	4.35 (f)	7.480	2.439	4.36 (f)	3.048

Table 4.26 Fragmentation Energies of the Most Stable Si_3Ge Neutral Tetramer

Fragmented Clusters	Fragmentation Energy (eV)
$Si_2Ge + Si$	4.297
$Si_2 + SiGe$	4.764
$Si_2 + Si + Ge$	7.825
$SiGe + 2Si$	7.987
$3Si + Ge$	11.048

Table 4.27 Fragmentation Energies of the Most Stable $(Si_3Ge)^+$ Cationic Tetramer

Fragmented Clusters	Fragmentation Energy (eV)
$(Si_2Ge)^+ + Si$	4.413
$Si_2 + (SiGe)^+$	4.733
$(SiGe)^+ + Si + Si$	7.955
$Si_2 + Si + Ge^+$	7.959
$Si + Si + Si + Ge^+$	11.181

Table 4.28 Fragmentation Energies of the Most Stable $(Si_3Ge)^-$ Anionic Tetramer

Fragmented Clusters	Fragmentation Energy (eV)
$(Si_2Ge)^- + Si$	4.107
$Si_2 + (SiGe)^-$	4.908
$(SiGe)^- + 2Si$	8.130
$Si_2 + Si + Ge^-$	8.676
$3Si + Ge^-$	11.899

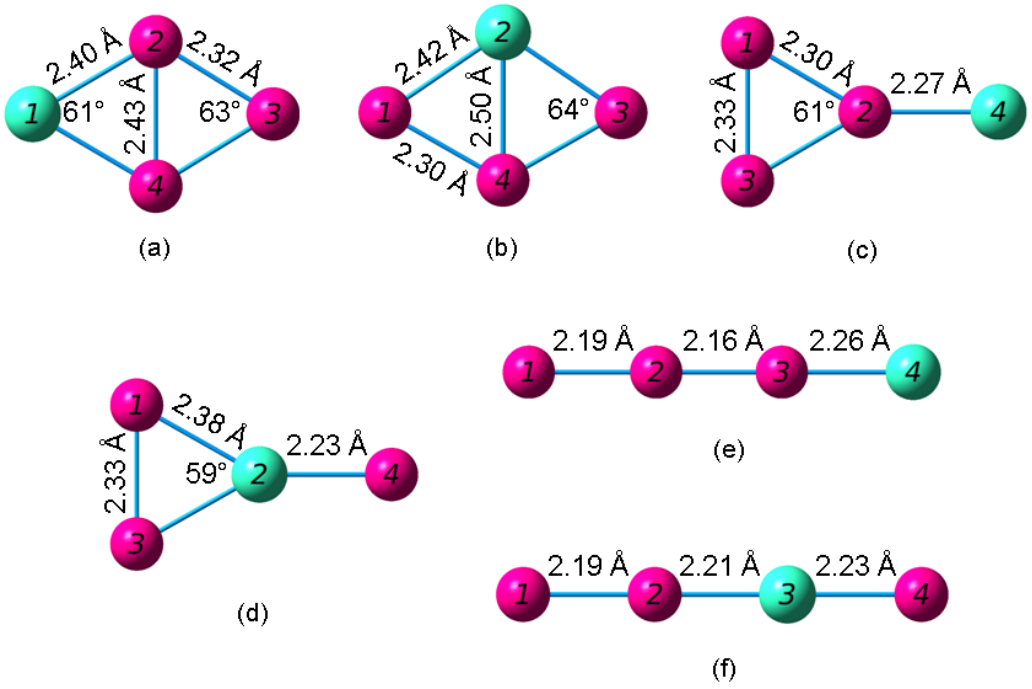

Figure 4.34 Geometries of the Si_3Ge Neutral Tetramers from (a) Most Stable through (f) Least Stable

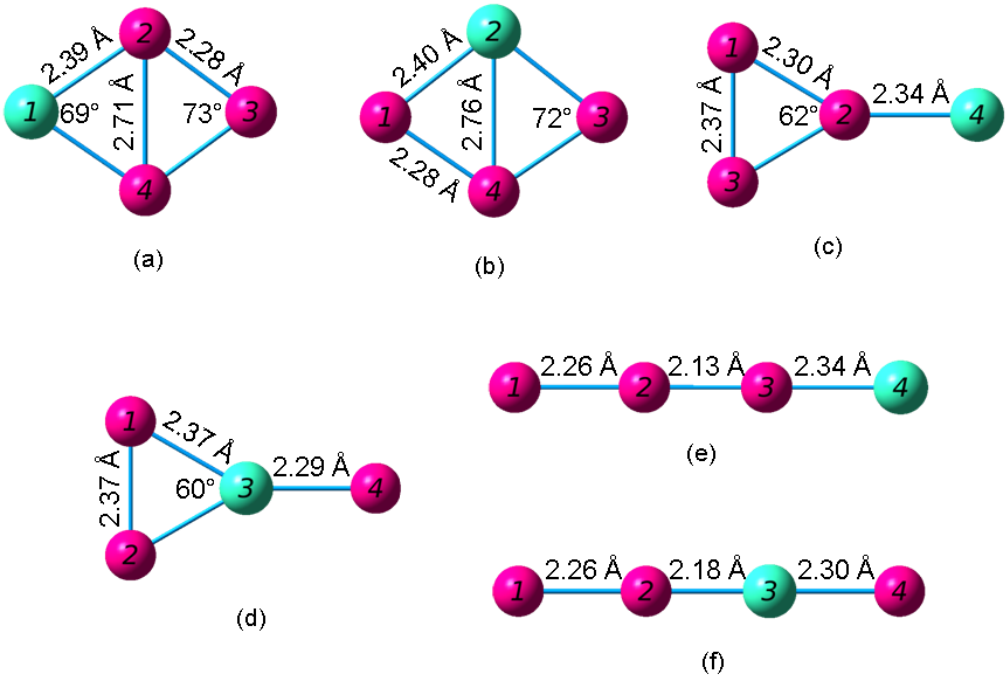

Figure 4.35 Geometries of the $(Si_3Ge)^+$ Cationic Tetramers from (a) Most Stable through (f) Least Stable

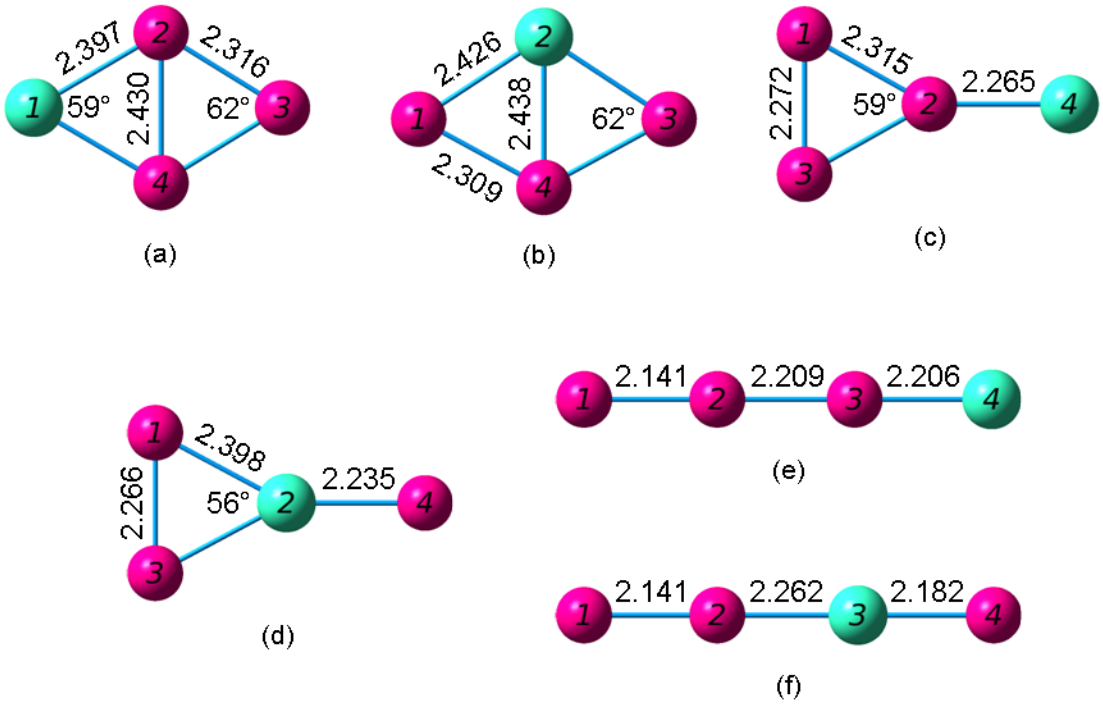

Figure 4.36 Geometries of the $(Si_3Ge)^-$ Anionic Tetramers from (a) Most Stable through (f) Least Stable

4.5 Si_2Ge_2 Tetramers

In the literature, the most calculations have been performed on the Si_2Ge_2 tetramer cluster. Andriotis, Menon, and Froudakis [47] found two isomers, both rhomboidal. The ground state has a Si-Si bond through the middle of length 2.497 Å or 2.44 Å. The other bonds are Si-Ge bonds of length 2.435 Å or 2.47 Å. The second structure has a Ge-Ge bond through the middle of length 2.616 Å or 2.60 Å and four Si-Ge bonds of length 2.453 Å or 2.41 Å. Each of these bonds has two possible lengths because the purpose of their paper was to show that their tight binding molecular dynamics method compared to established methods.

Totally, Li *et al.* [48] found 5 different isomers for this structure – four rhombuses with D_{2h} symmetry and one trigon with C_{2v} symmetry. The first two rhombuses have a Si-Si bond through the middle. The main difference between the two is that the first has a ^1A_g electronic state while the second has a $^3B_{3u}$ electronic state. The structure with single multiplicity has a Si-

Si bond length of 2.44 Å and four Si-Ge bonds of length 2.39 Å, a HOMO-LUMO gap of 2.46 eV, and the following frequencies: 396 cm^{-1} (B_{1u}), 180 cm^{-1} (B_{2u}), 67 cm^{-1} (B_{3u}). The corresponding isomer with triplet multiplicity has a Si-Si bond length of 2.59 Å and Si-Ge bonds lengths of 2.36 Å. They calculated that this structure has a gap energy of 0.47 eV and frequencies of 339 cm^{-1} (B_{1u}), 220 cm^{-1} (B_{2u}) and 133 cm^{-1} (B_{3u}). Similarly, they also found two rhombuses with a Ge-Ge bond through the middle – one in the ^1A_g state and another in the $^3B_{3u}$ state. For the singlet structure, the Ge-Ge bond length is 2.58 Å and the Si-Ge bond lengths are 2.40 Å while the gap energy is 2.29 eV and the frequencies are 386 cm^{-1} (B_{1u}), 77 cm^{-1} (B_{3u}), and 180 cm^{-1} (B_{2u}). For the triplet structure, the found the middle Ge-Ge bond to have a length of 2.71 Å, the Si-Ge bonds to have lengths of 2.36 Å, the HOMO-LUMO gap to have an energy of 0.77 eV, and frequencies of 221 cm^{-1} (B_{1u}) and 141 cm^{-1} (B_{3u}). Their final structure, a trigon with a Si-Si bond of length 2.49 Å, Si-Ge bonds with length 2.58 Å, and a Ge-Ge bond of length 2.67 Å, had a HOMO-LUMO gap of 1.49 eV and the following frequencies: 218 cm^{-1} (A'), 276 cm^{-1} (A"), and 228 cm^{-1} (A').

Marim *et al.* [49] reported only the ground state rhombus with a Si-Si bond (2.47 Å long) through the middle. The other four Si-Ge bonds are of length 2.40 Å. Additionally, they calculated a cohesive energy of 2.67 eV per atom. Wielgus *et al.* [50] reported three different rhomboidal structures. Just as the other sources found, the ground state was again the rhombus with a Si-Si bond through the middle (D_{2h} symmetry). Their ^1A_g electronic state agrees with the ground state of Li *et al.* and they calculated a VIP of 8.09 eV. They found two other neutral isomers. The second-most stable isomer has a Si-Ge bond through the middle, C_s symmetry, and a ^{1}A' electronic state. The final neutral isomer has a Ge-Ge bond through the middle, D_{2h} symmetry, a ^1A_g electronic state, and Si-Ge bonds of 2.415 Å. They also found three cationic clusters. The first had D_{2h} symmetry, and a ^2A_g electronic state, and Si-Ge bonds of 2.469 Å. The second had D_{2h} symmetry, a $^2B_{2u}$ electronic state, and Si-Ge bonds of 2.390 Å. Finally, the third had C_s symmetry and a ^{2}A' electronic state.

Wang and Chao [51] investigated three different rhombic geometries. For the neutral and anionic cases the bond through the middle is (in order of decreasing stability: Si-Si, Si-Ge and Ge-Ge. For the cation however, they found that the most stable cluster had a Si-Ge bond through the middle and the second most stable to have the Ge-Ge bond through the middle. (They only reported two cations). Additional properties for the first neutral cluster are: an electronic state of ^{1}Ag, a dissociation energy of -10.8263 or -15.1134, a HOMO-LUMO gap of 2.46, and frequencies of 395(b1g), 180(b2u), and 67(b3u). For the second cluster, they found an electronic state of ^{1}A', a dissociation energy of -10.4442 or -14.9898, a HOMO-LUMO gap of 2.35, and frequencies of 466(a'), 238(a'), and 300(a'). Finally, for the third cluster they foundan electronic state of ^{1}A1, a dissociation energy of -9.1905 or -14.8327, a HOMO-LUMO gap of 2.29, and frequencies of 386(a1), 77(a1), and 380(a1).

Our ground state Si_2Ge_2 tetramer has the same structure as that of Li *et al.* and we calculate the same HOMO-LUMO gap. Our binding energy per atom of 2.695 eV is the same as the cohesive energy of Marim *et al.* Additionally, our VIP of 8.059 eV is only slightly lower than that calculated by Wielgus *et al.* We also found a VEA of 1.948 eV and a fragmentation energy of 4.029 for decomposition into a Si_2Ge trimer and a Ge atom. We found two more rhomboidal isomers comparable to those seen in the literature. Beyond that, we found a nearly-square cluster with a Si-Si bond of length 2.31 Å, Si-Ge bonds of length 2.40 Å, and a Ge-Ge bond of length 2.49 Å. Our least stable isomers include two structures that look like a triangle with an extra atom attached and four linear structures (figure 4.37).

Careful consideration of the Si_2Ge_2 cations led us to describe seven stable isomers. We found only one rhomboidal cation although we found three different stable rhomboidal neutral clusters. As with the rhomboids in the Si_3Ge category, the middle bond of the most stable Si_2Ge_2 cation is longer than any of the middle bonds of the neutral rhomboids.

Table 4.29 Properties of the Si_2Ge_2 Tetramers

Figure	Symmetry Group	Electronic State	Binding E / Atom (eV)	HOMO-LUMO Gap (eV)	Dipole Moment (D)
4.37 (a)	D_{2h}	^1A_g	2.695	2.457	0.000
4.37 (b)	C_s	$^1A'$	2.669	2.347	0.493
4.37 (c)	C_{2v}	$^3B_2$	2.306	1.674	0.304
4.37 (d)	C_{2v}	$^1A_1$	2.266	1.334	0.462
4.37 (e)	C_{2v}	$^1A_1$	2.244	1.368	1.553
4.37 (f)	$D_{\infty h}$	$^3\sum_g$	2.112	1.747[a]	0.000
4.37 (g)	$C_{\infty v}$	$^3\sum$	2.061	1.775[a]	0.775
4.37 (h)	$C_{\infty v}$	$^3\sum$	2.056	1.775[a]	0.382
4.37 (i)	$D_{\infty h}$	$^3\sum_g$	2.002	1.802[a]	0.000

[a] HOMO and LUMO have opposite spins; this value includes the energy required to flip the spin of the electron.

Table 4.30 Properties of the $(Si_2Ge_2)^+$ Tetramers

Figure	Symmetry Group	Electronic State	Binding E / Atom (eV)	HOMO-LUMO Gap (eV)	Dipole Moment (D)
4.38 (a)	C_s	$^2A'$	2.732	1.965[a]	1.779
4.38 (b)	D_{2h}	$^2B_{1,u}$	2.723	1.909[a]	0.000
4.38 (c)	C_{2v}	$^2A_1$	2.564	1.348	1.769
4.38 (d)	C_{2v}	$^2A_1$	2.453	1.936	3.505
4.38 (e)	C_{2v}	$^4A_2$	2.336	0.972[a]	1.751
4.38 (f)	$D_{\infty h}$	--	2.262	1.141	0.000
4.38 (g)	$C_{\infty v}$	--	2.195	1.173	2.941
4.38 (h)	$C_{\infty v}$	--	2.190	1.174	1.499
4.38 (i)	$D_{\infty h}$	--	2.121	1.210	0.000

[a] HOMO and LUMO have opposite spins; this value includes the energy required to flip the spin of the electron.

Table 4.31 Properties of the $(Si_2Ge_2)^-$ Tetramers

Figure	Symmetry Group	Electronic State	Binding E / Atom (eV)	HOMO-LUMO Gap (eV)	Dipole Moment (D)
4.39 (a)	D_{2h}	$^2B_{2,g}$	2.902	1.703[a]	0.000
4.39 (b)	D_{2h}	$^2B_{2,g}$	2.830	1.855[a]	0.000
4.39 (c)	C_{2v}	$^2B_1$	2.620	1.819[a]	3.532
4.39 (d)	C_{2v}	$^2B_1$	2.601	1.781[a]	2.793
4.39 (e)	C_{2v}	$^4B_1$	2.462	1.408[a]	2.185
4.39 (f)	$D_{\infty h}$	--	2.431	1.054	0.000
4.39 (g)	$C_{\infty v}$	--	2.388	1.074	4.570
4.39 (h)	$C_{\infty v}$	--	2.384	1.073	2.159
4.39 (i)	$D_{\infty h}$	--	2.341	1.089	0.000

[a] HOMO and LUMO have opposite spins; this value includes the energy required to flip the spin of the electron.

Table 4.32 Ionization Potentials and Electron Affinities of the Si_2Ge_2 Tetramers

Neutral Figure	VIP (eV)	Cationic Figure	AIP (eV)	VEA (eV)	Anionic Figure	AEA (eV)
4.37 (a)	8.059	4.38 (b)	7.787	1.948	4.39 (a)	1.965
4.37 (b)	7.906	4.38 (a)	7.649	1.930	4.39 (b)	1.783
4.37 (c)	6.919	4.38 (c)	6.866	1.653	4.39 (e)	1.763
4.37 (d)	7.211	4.38 (d)	7.153	2.520	4.39 (c)	2.553
4.37 (e)	7.617	4.38 (e)	7.532	2.539	4.39 (d)	2.567
4.37 (f)	7.375	4.38 (f)	7.300	2.363	4.39 (f)	2.413
4.37 (g)	7.437	4.38 (g)	7.365	2.399	4.39 (g)	2.449
4.37 (h)	7.441	4.38 (h)	7.364	2.394	4.39 (h)	2.450
4.37 (i)	7.488	4.38 (i)	7.425	2.446	4.39 (i)	2.494

Table 4.33 Fragmentation Energies of the Most Stable Si_2Ge_2 Neutral Tetramer

Fragmented Clusters	Fragmentation Energy (eV)
$Si_2Ge + Ge$	4.029
$SiGe_2 + Si$	4.128
$Si_2 + Ge_2$	4.629
2SiGe	4.657
$Si_2 + 2Ge$	7.558
SiGe + Si + Ge	7.719
$Ge_2 + 2Si$	7.852
2Si + 2Ge	10.780

Table 4.34 Fragmentation Energies of the Most Stable $(Si_2Ge_2)^+$ Cationic Tetramer

Fragmented Clusters	Fragmentation Energy (eV)
$(Si_2Ge)^+ + Ge$	4.175
$Si_2Ge + Ge^+$	4.157
$(SiGe_2)^+ + Si$	4.322
$Si_2 + (Ge_2)^+$	4.495
$SiGe + (SiGe)^+$	4.639
$(SiGe)^+ + Si + Ge$	7.703
$Si_2 + Ge + Ge^+$	7.865
$(Ge_2)^+ + Si + Si$	7.700
$SiGe + Si + Ge^+$	7.717
$Si + Si + Ge + Ge^+$	10.926

Table 4.35 Fragmentation Energies of the Most Stable $(Si_2Ge_2)^-$ Anionic Tetramer

Fragmented Clusters	Fragmentation Energy (eV)
$(Si_2Ge)^-$ + Ge	3.816
$(SiGe_2)^-$ + Si	4.060
$(SiGe)^-$ + SiGe	4.778
Si_2 + $(Ge_2)^-$	4.779
Si_2Ge + Ge^-	4.857
$(SiGe)^-$ + Si + Ge	7.839
$(Ge_2)^-$ + 2Si	8.001
Si_2 + Ge^- + Ge	8.385
SiGe + Si + Ge^-	8.546
2Si + Ge^- + Ge	11.608

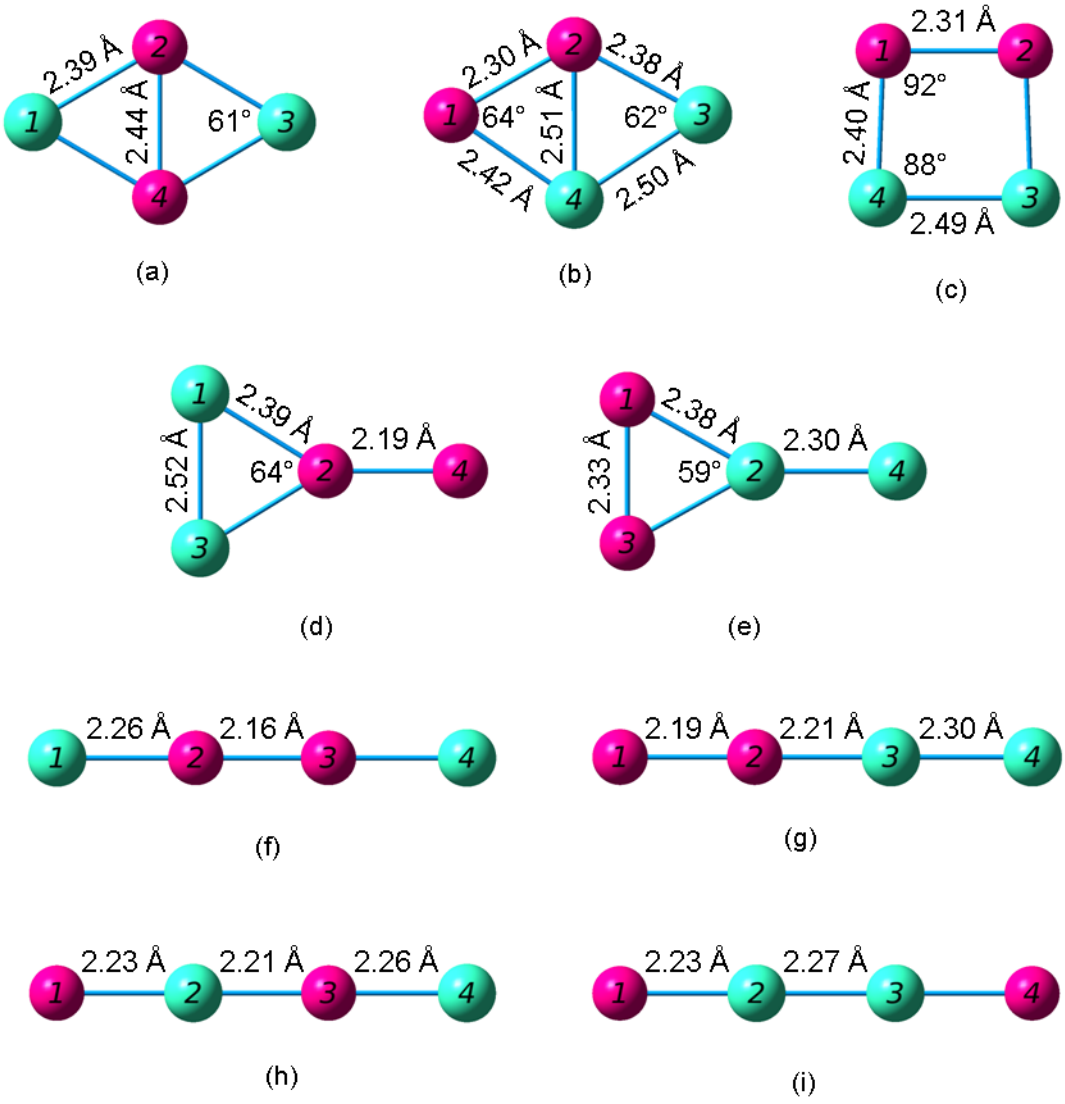

Figure 4.37 Geometries of the Si_2Ge_2 Neutral Tetramers from (a) Most Stable through (i) Least Stable

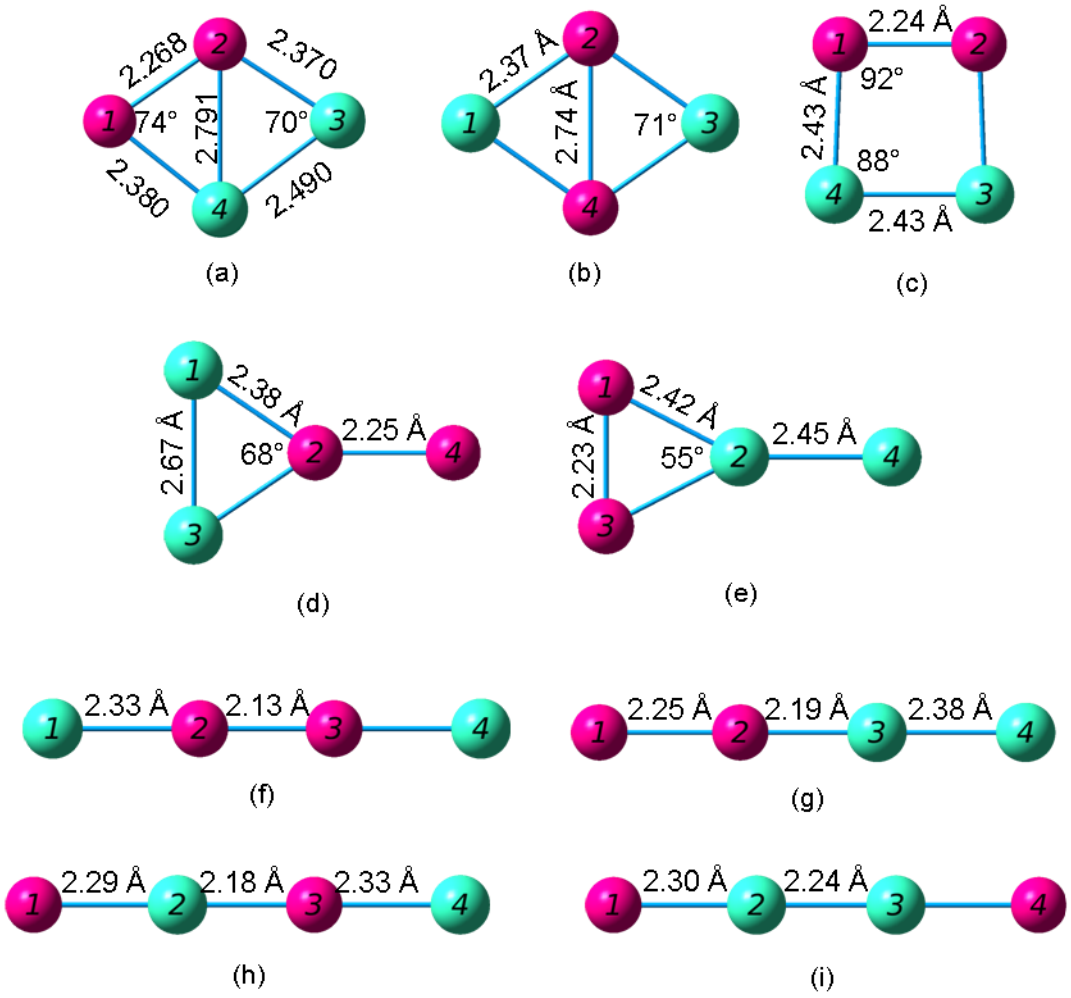

Figure 4.38 Geometries of the $(Si_2Ge_2)^+$ Cationic Tetramers from (a) Most Stable through (i) Least Stable

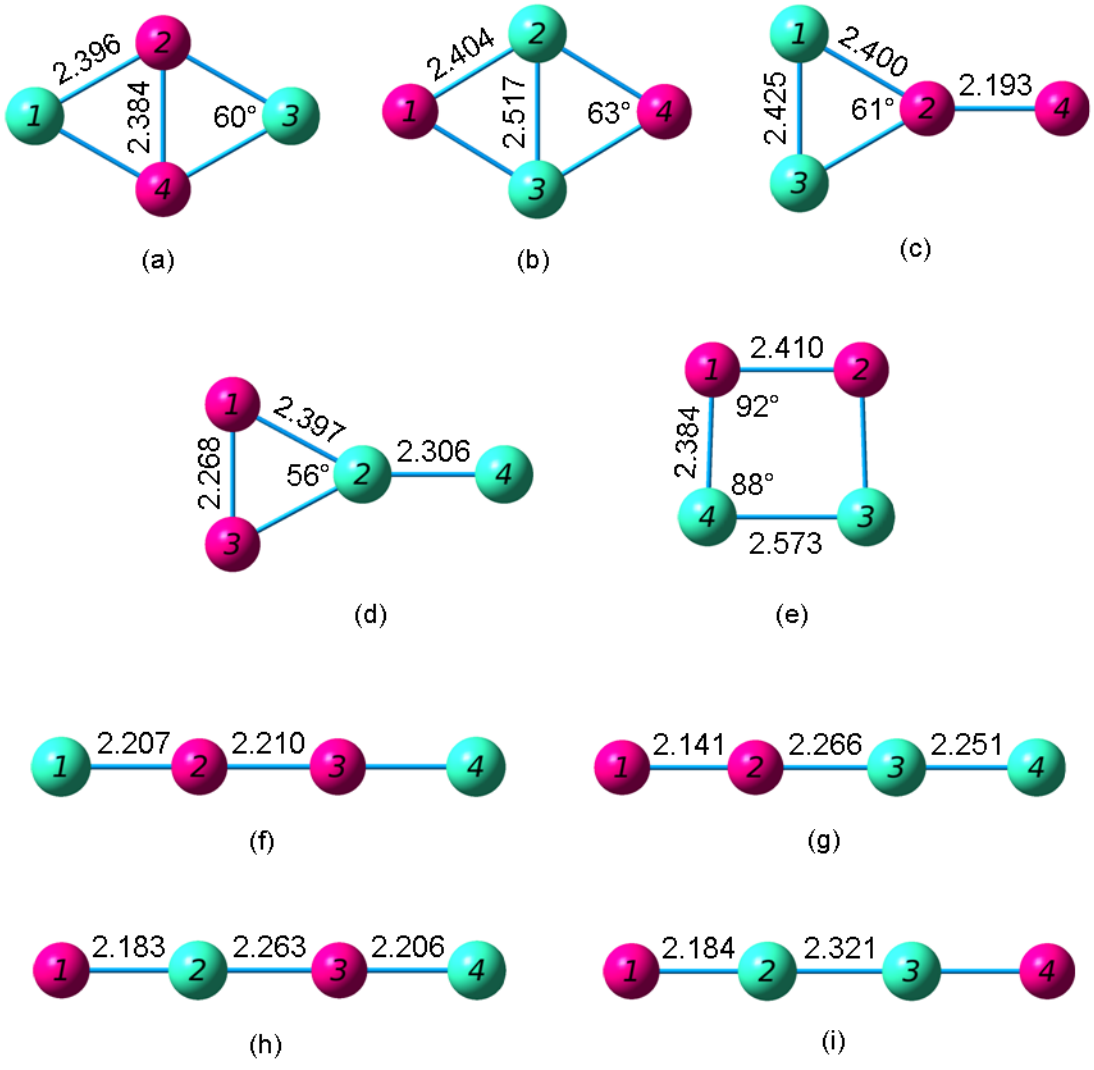

Figure 4.39 Geometries of the $(Si_2Ge_2)^-$ Anionic Tetramers from (a) Most Stable through (i) Least Stable

4.6 $SiGe_3$ Tetramers

In the literature and our work, the general consensus is that the most stable $SiGe_3$ tetramer is a rhombus (C_{2V} symmetry) with a Si-Ge bond through the middle. Li *et al.* [48] found this Si-Ge bond length to be 2.53 Å, while the other two Si-Ge bond lengths are 2.37 Å, and the Ge-Ge bond lengths are 2.49 Å. This structure has a $^1A_1$ electronic state, a gap energy of 2.39 eV, and the following frequencies: 403 cm^{-1} (B_2), 240 cm^{-1} (B_2), and 342 cm^{-1} (A_1). For this same structure Marim *et al.* [49] reported nearly the same bond lengths: a middle Si-Ge bond length of 2.54 Å, other Si-Ge bond lengths of 2.39 Å, and Ge-Ge bond lengths of 2.47 Å. Their cohesive energy came to 2.63 eV per atom.

Wielgus *et al.* [50] again found a neutral ground state structure with the same geometry and extremely close bond lengths. Their middle Si-Ge bond length is 2.538 Å, their other Si-Ge bond lengths are 2.399 Å, and their Ge-Ge bond lengths are 2.507 Å. They also found the same electronic state as Li *et al.*, and they calculated the VIP to be 8.07 eV. They found a second isomer, another rhombus (C_{2v} symmetry) with a Ge-Ge bond through the middle. For this structure, the middle Ge-Ge bond is 2.614 Å long, the other Ge-Ge bonds are 2.494 Å long, the Si-Ge bonds are 2.411 Å long, and the electronic state is again $^1A_1$. Additionally, they found two cationic isomers, both rhombic with C_{2v} symmetry and $^2A_1$ electronic states.

Wang and Chao [51] investigated two $SiGe_3$ geometries and found the values for the neutrals and ions of both. Both are rhombuses. The most stable for all three charges has a Si-Ge bond through the middle, while the other has no bond through its middle. The most stable neutral has middle Si-Ge bond length of 2.527 Å, an electronic state of ^{1}A', a dissociation energy of -10.3821 or -15.4092, a HOMO-LUMO gap of 2.39, and frequencies of 401(a'), 240(a'), and 341(a'). The second neutral has an electronic state of ^{1}A1, a dissociation energy of -10.0966 or -15.2617, a HOMO-LUMO gap of 2.30, and frequencies of 384(a1), 265(a1), and 210(a1). The most stable geometry has a middle Si-Ge bond length of 2.821 Å in the cation case, and 2.466 in the anion case.

Our calculations produce a ground state $SiGe_3$ tetramer that is consistent with published results. We found the same bond lengths and HOMO-LUMO gap as Li *et al.* Our binding energy of 2.609 eV per atom is only slightly less that the cohesive energy of Wielgus *et al.* and our VIP of 7.919 eV is comparable to that of Wielgus *et al.* Our second most stable structure is a rhombus comparable to the second most stable isomer of Wielgus *et al.* Isomers with less stability include two triangle structures with an extra atom, a trigon, and two linear structures (figure 4.40).

Figure 4.41 depicts the $SiGe_3$ cations we investigated. Although the neutral $SiGe_3$ isomers included a trigon, no such structure remained stable in our cation calculations. As with the other rhombuses in the tetramer cations we investigated, the bond through the middle expanded from the neutral to the cation cluster. In the case of the $SiGe_3$ rhombuses this bond extended beyond 2.8 Å, and we concluded that a bond would no longer be likely to exist.

Table 4.36 Properties of the $SiGe_3$ Tetramers

Figure	Symmetry Group	Electronic State	Binding E / Atom (eV)	HOMO-LUMO Gap (eV)	Dipole Moment (D)
4.40 (a)	C_{2v}	$^1A_1$	2.609	2.388	0.067
4.40 (b)	C_{2v}	$^1A_1$	2.576	2.303	0.484
4.40 (c)	C_{2v}	$^1A_1$	2.231	1.293	1.004
4.40 (d)	C_{2v}	$^1A_1$	2.157	1.359	0.389
4.40 (e)	$C_{\infty v}$	$^3\Sigma$	2.023	1.719[a]	0.202
4.40 (f)	$C_{\infty v}$	$^3\Sigma$	1.969	1.745[a]	0.595

[a] HOMO and LUMO have opposite spins; this value includes the energy required to flip the spin of the electron.

Table 4.37 Properties of the $(SiGe_3)^+$ Tetramers

Figure	Symmetry Group	Electronic State	Binding E / Atom (eV)	HOMO-LUMO Gap (eV)	Dipole Moment (D)
4.41 (a)	C_{2v}	$^2B_2$	2.668	1.871[a]	0.899
4.41 (b)	C_{2v}	$^2A_1$	2.664	1.938[a]	1.050
4.41 (c)	C_{2v}	$^2A_1$	2.443	1.890	1.758
4.41 (d)	C_{2v}	$^2A_1$	2.353	1.860	2.690
4.41 (e)	$C_{\infty v}$	--	2.185	1.127	0.570
4.41 (f)	$C_{\infty v}$	--	2.116	1.159	1.723

[a] HOMO and LUMO have opposite spins; this value includes the energy required to flip the spin of the electron.

Table 4.38 Properties of the $(SiGe_3)^-$ Tetramers

Figure	Symmetry Group	Electronic State	Binding E / Atom (eV)	HOMO-LUMO Gap (eV)	Dipole Moment (D)
4.42 (a)	C_{2v}	$^2A_2$	2.808	1.707[a]	1.003
4.42 (b)	C_{2v}	$^2B_1$	2.774	1.780[a]	1.687
4.42 (c)	C_{2v}	$^2B_1$	2.573	1.746[a]	0.739
4.42 (d)	C_{2v}	$^2B_1$	2.505	1.767[a]	2.784
4.42 (e)	$C_{\infty v}$	--	2.340	1.036	1.055
4.42 (f)	$C_{\infty v}$	--	2.296	1.051	2.911

[a] HOMO and LUMO have opposite spins; this value includes the energy required to flip the spin of the electron.

Table 4.39 Ionization Potentials and Electron Affinities of the $SiGe_3$ Tetramers

Neutral Figure	VIP (eV)	Cationic Figure	AIP (eV)	VEA (eV)	Anionic Figure	AEA (eV)
4.40 (a)	7.919	4.41 (a)	7.664	1.915	4.42 (a)	1.934
4.40 (b)	7.801	4.41 (b)	7.546	1.908	4.42 (b)	1.929
4.40 (c)	7.109	4.41 (c)	7.053	2.477	4.42 (c)	2.504
4.40 (d)	7.167	4.41 (d)	7.119	2.494	4.42 (d)	2.527
4.40 (e)	7.316	4.41 (e)	7.253	2.361	4.42 (e)	2.406
4.40 (f)	6.839	4.41 (f)	7.312	2.930	4.42 (f)	2.446

Table 4.40 Fragmentation Energies of the Most Stable $SiGe_3$ Neutral Tetramer

Fragmented Clusters	Fragmentation Energy (eV)
$SiGe_2 + Ge$	3.784
$SiGe + Ge_2$	4.446
$SiGe + 2Ge$	7.375
$Ge_2 + Si + Ge$	7.508
$Si + 3Ge$	10.436

Table 4.41 Fragmentation Energies of the Most Stable $(SiGe_3)^+$ Cationic Tetramer

Fragmented Clusters	Fragmentation Energy (eV)
$SiGe_2 + Ge^+$	4.021
$(SiGe_2)^+ + Ge$	4.069
$SiGe + (Ge_2)^+$	4.403
$(SiGe)^+ + Ge_2$	4.519
$SiGe + Ge + Ge^+$	7.612
$(SiGe)^+ + Ge + Ge$	7.447
$(Ge_2)^+ + Si + Ge$	7.464
$Ge_2 + Si + Ge^+$	7.744
$Si + Ge + Ge + Ge^+$	10.673

Table 4.42 Fragmentation Energies of the Most Stable $(SiGe_3)^-$ Anionic Tetramer

Fragmented Clusters	Fragmentation Energy (eV)
$(SiGe_2)^-$ + Ge	3.685
$(SiGe)^-$ + Ge_2	4.536
SiGe + $(Ge_2)^-$	4.565
$SiGe_2$ + Ge^-	4.580
$(SiGe)^-$ + 2Ge	7.464
$(Ge_2)^-$ + Si + Ge	7.626
SiGe + Ge^- + Ge	8.171
Ge_2 + Si + Ge^-	8.304
Si + Ge^- + 2Ge	11.233

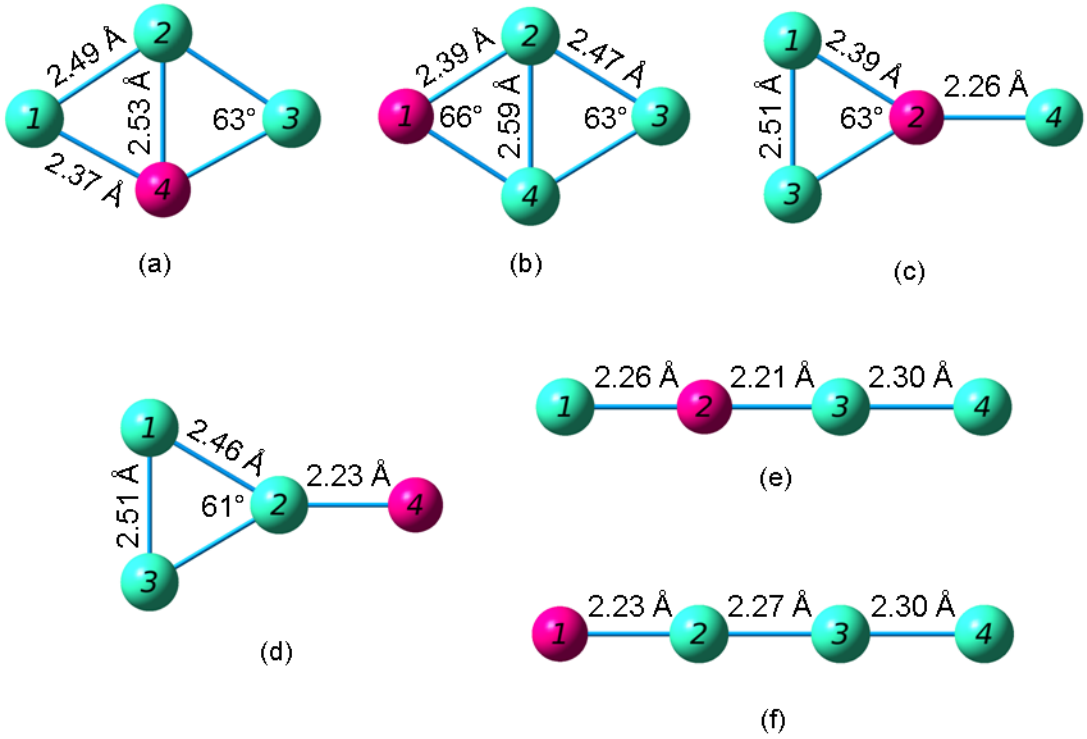

Figure 4.40 Geometries of the $SiGe_3$ Neutral Tetramers from (a) Most Stable through (f) Least Stable

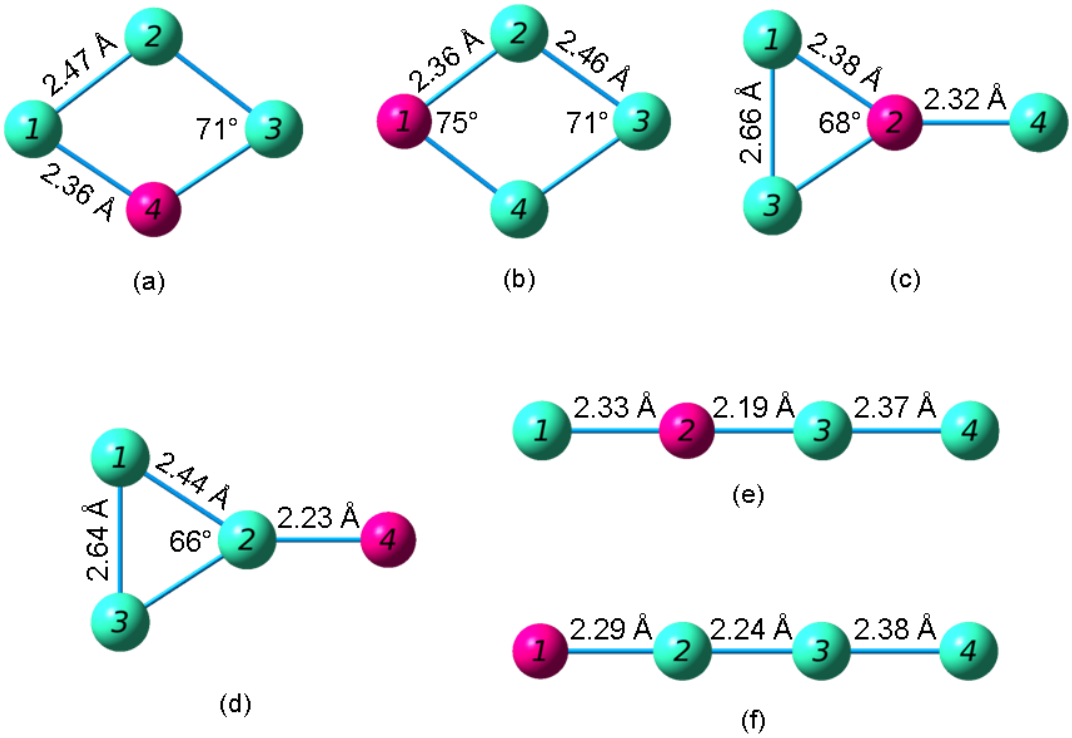

Figure 4.41 Geometries of the $(SiGe_3)^+$ Cationic Tetramers from (a) Most Stable through (f) Least Stable

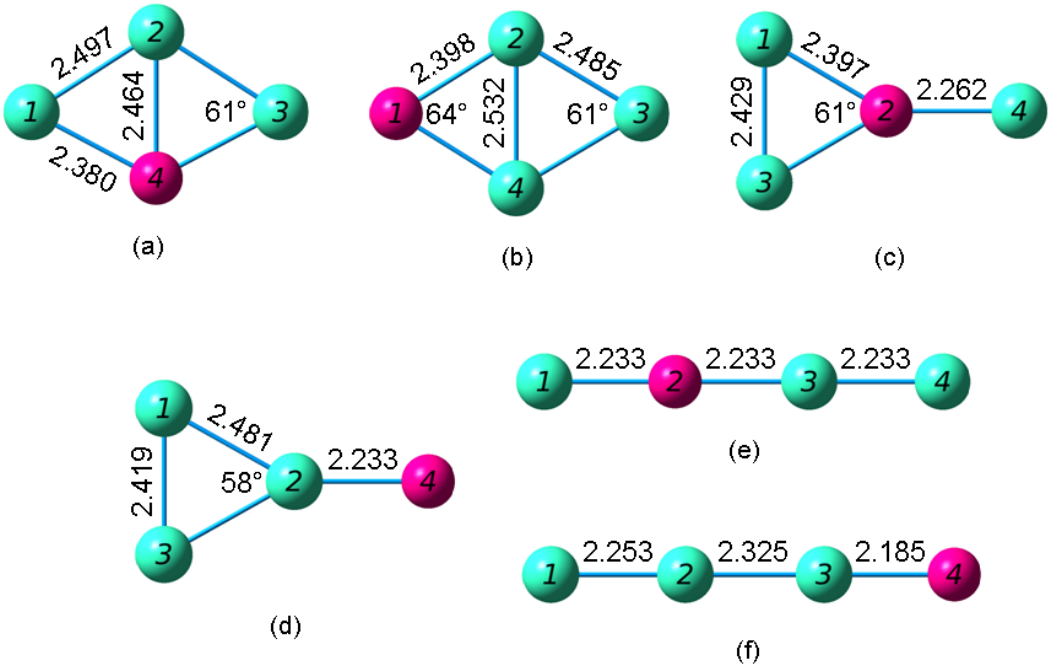

Figure 4.42 Geometries of the $(SiGe_3)^-$ Anionic Tetramers from (a) Most Stable through (f) Least Stable

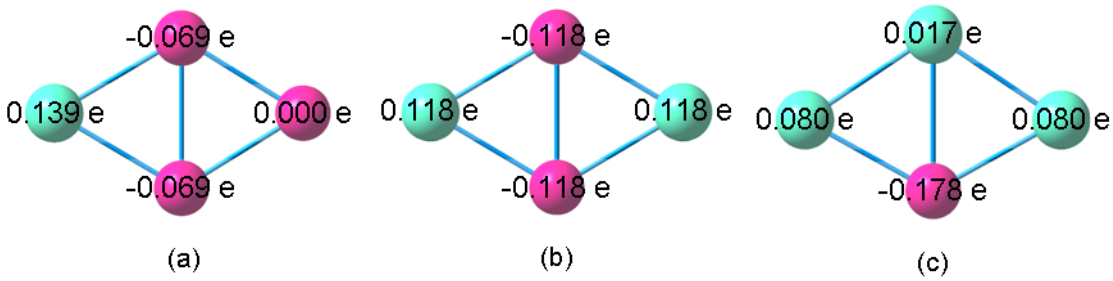

Figure 4.43 Atomic Charges of the Most Stable (a) Si_3Ge (b) Si_2Ge_2 and (c) $SiGe_3$ Neutral Tetramer

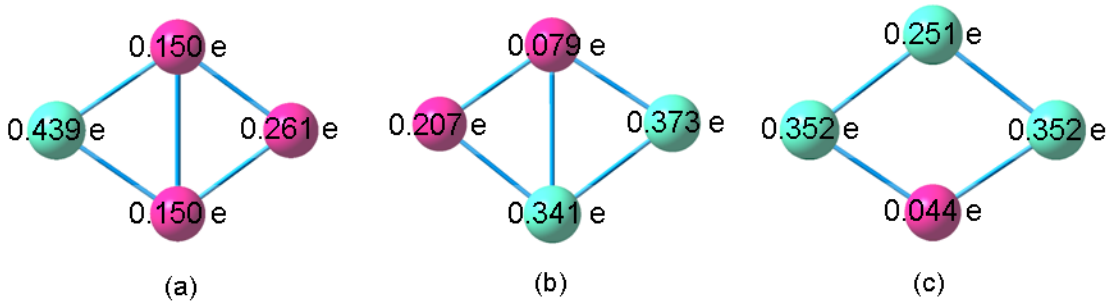

Figure 4.44 Atomic Charges of the Most Stable (a) $(Si_3Ge)^+$ (b) $(Si_2Ge_2)^+$ and (c) $(SiGe_3)^+$ Cationic Tetramer

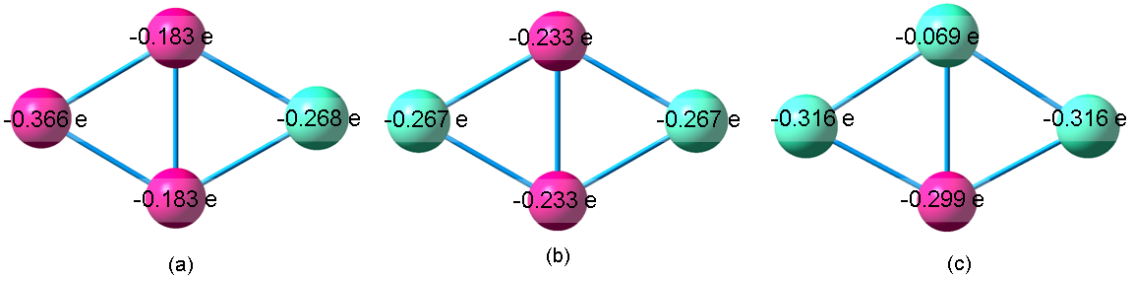

Figure 4.45 Atomic Charges of the Most Stable (a) $(Si_3Ge)^-$ (b) $(Si_2Ge_2)^-$ and (c) $(SiGe_3)^-$ Anionic Tetramer

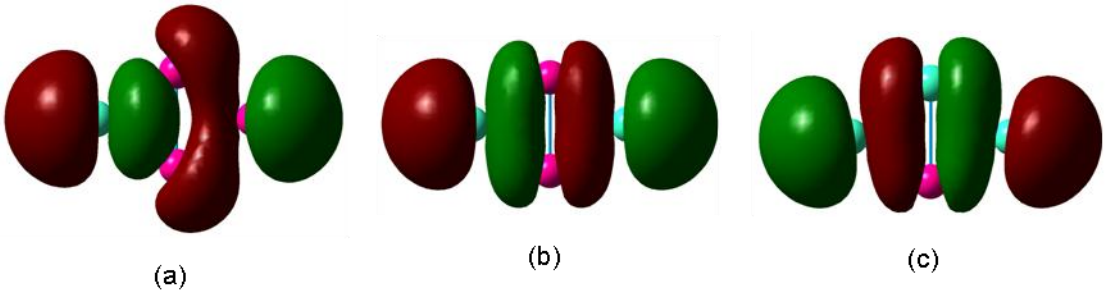

Figure 4.46HOMO of the Most Stable (a) Si_3Ge (b) Si_2Ge_2 and (c) $SiGe_3$ Neutral Tetramer

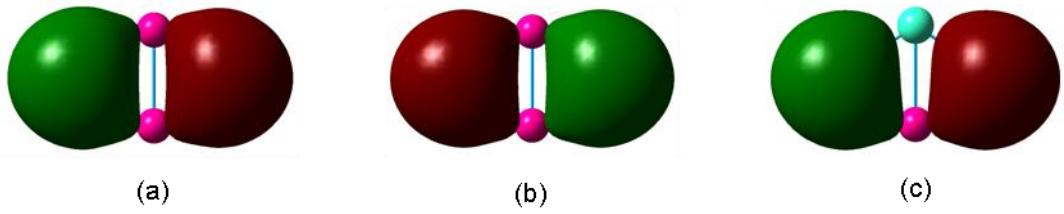

Figure 4.47 LUMO of the Most Stable (a) Si_3Ge (b) Si_2Ge_2 and (c) $SiGe_3$ Neutral Tetramer

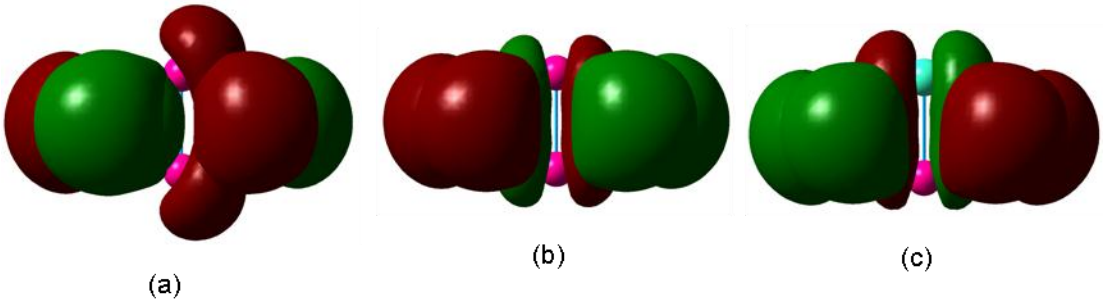

Figure 4.48 HOMO and LUMO of the Most Stable (a) Si_3Ge (b) Si_2Ge_2 and (c) $SiGe_3$ Neutral Tetramer

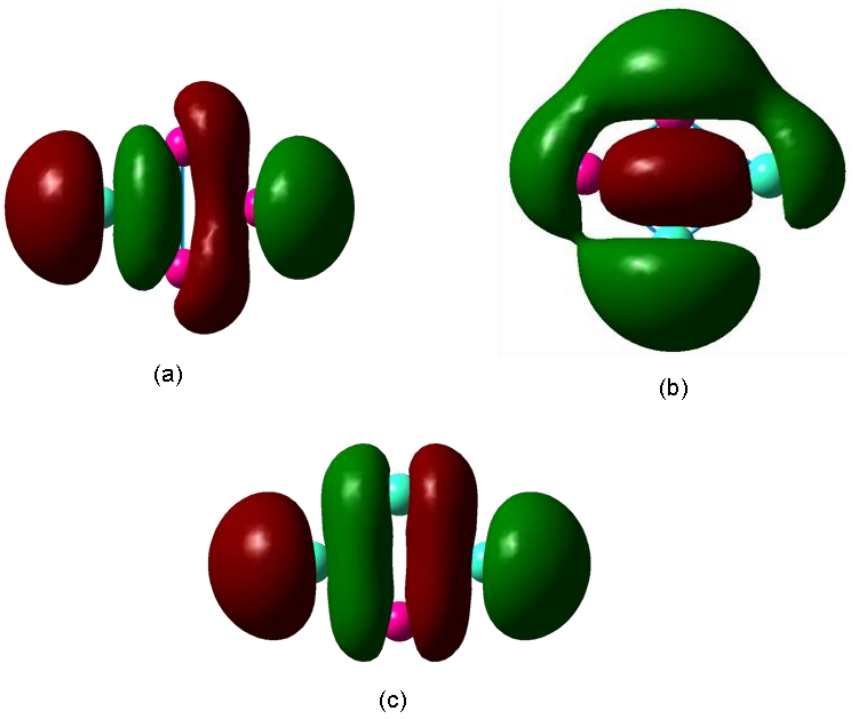

Figure 4.49 HOMO of the Most Stable (a) $(Si_3Ge)^+$ (b) $(Si_2Ge_2)^+$ and (c) $(SiGe_3)^+$ Cationic Tetramer

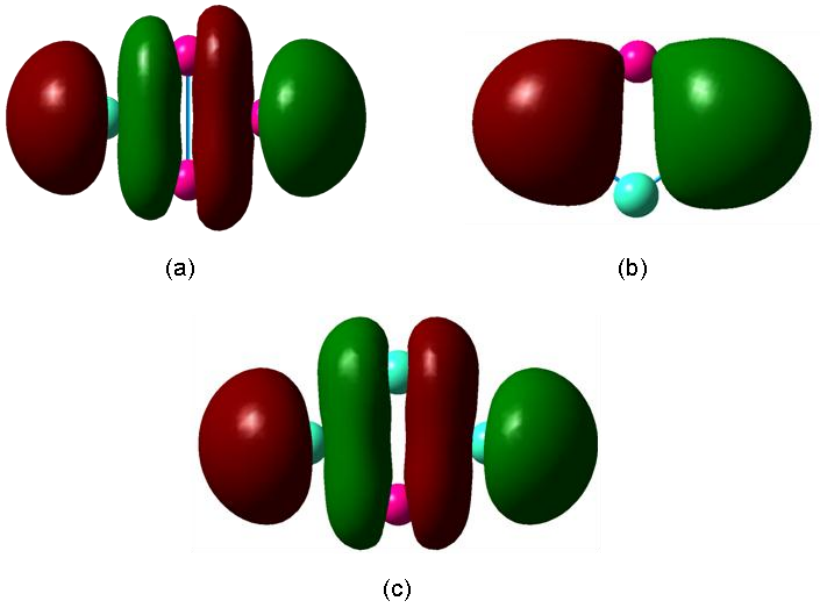

Figure 4.50 LUMO of the Most Stable (a) $(Si_3Ge)^+$ (b) $(Si_2Ge_2)^+$ and (c) $(SiGe_3)^+$ Cationic Tetramer

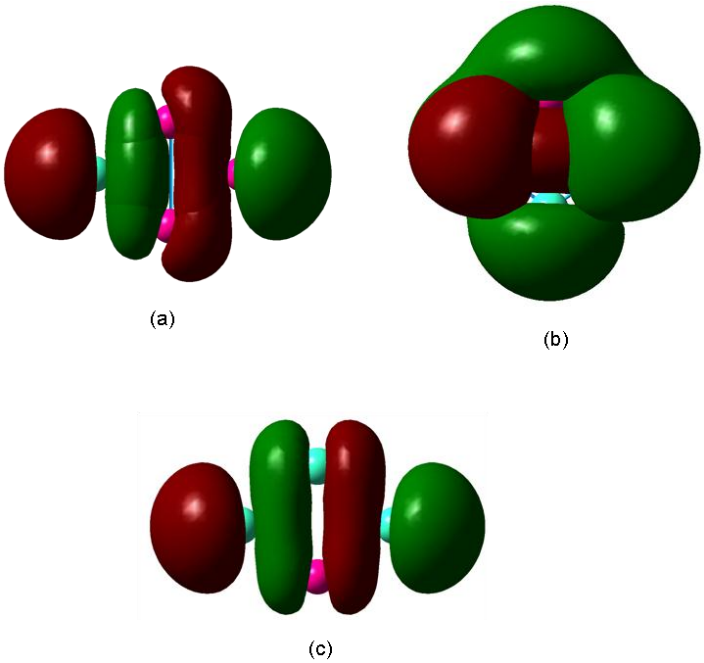

Figure 4.51 HOMO and LUMO of the Most Stable (a) $(Si_3Ge)^+$ (b) $(Si_2Ge_2)^+$ and (c) $(SiGe_3)^+$ Cationic Tetramer

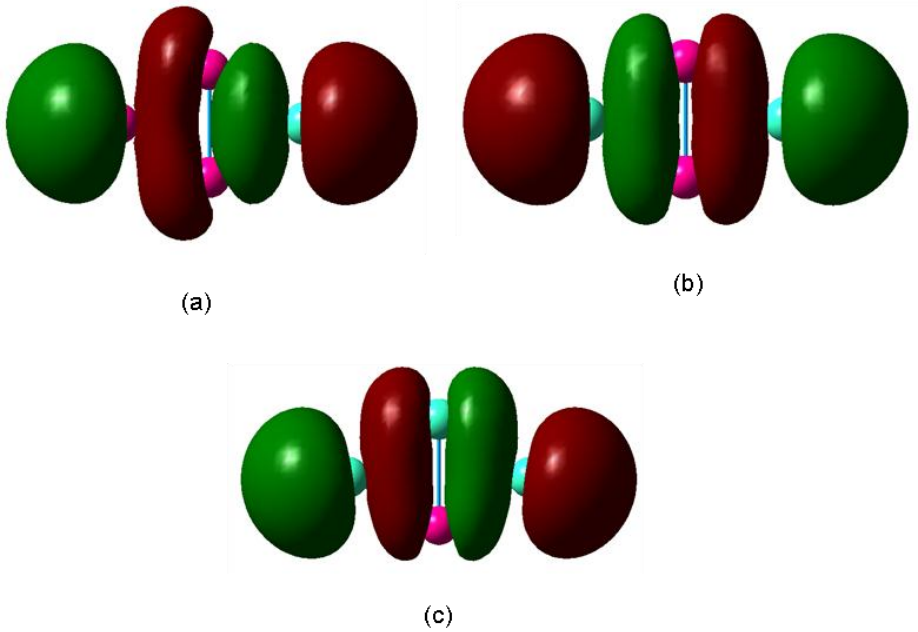

Figure 4.52 HOMO of the Most Stable (a) $(Si_3Ge)^-$ (b) $(Si_2Ge_2)^-$ and (c) $(SiGe_3)^-$ Anionic Tetramer

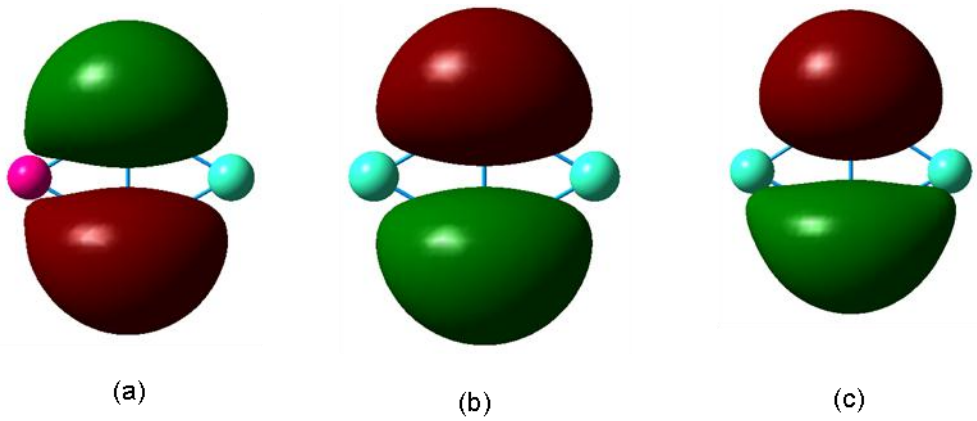

Figure 4.53 LUMO of the Most Stable (a) $(Si_3Ge)^-$ (b) $(Si_2Ge_2)^-$ and (c) $(SiGe_3)^-$ Anionic Tetramer

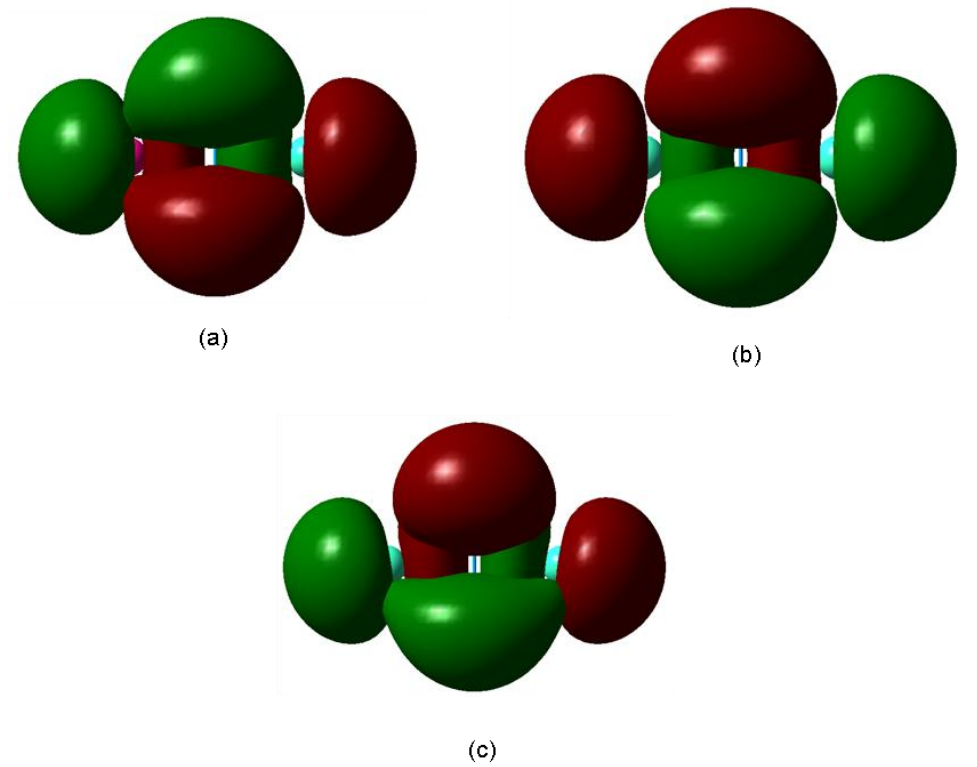

Figure 4.54 HOMO and LUMO of the Most Stable (a) $(Si_3Ge)^-$ (b) $(Si_2Ge_2)^-$ and (c) $(SiGe_3)^-$ Anionic Tetramer

4.7 Si_4Ge Pentamers

Beginning with the pentamers, the high stability of three-dimensional structures can be seen. Marim *et al.* [49] report data for two isomers of the Si_4Ge pentamer. Their cluster with a lower cohesive energy (2.85 eV per atom) is a trigonal bipyramid with the Ge atom shared between the two pyramids. Their Si-Si bond lengths are 2.33 Å, and their SiGe bond lengths are 2.40 Å. The second cluster is an asymmetrical structure formed from a Si_3Ge tetrahedral with an additional Si atom attached to the Ge atom and one other Si atom. Within the tetrahedral, Si-Si bond lengths range from 2.26 Å to 2.66 Å, and the bond length from the Ge atom to the attached Si atom is 2.46 Å. For this structure, they computed a cohesive energy of 2.74 eV per atom.

For the pentamers, Wielgus *et al.* [50] studied only trigonal bipyramids. For neutral Si_4Ge, they investigated to two possibilities: the Ge atom at a tip of the structure and in the pyramids' base. They found the case where the Ge is in the shared pyramid base to be the more stable structure. In this case there is a C_{2v} symmetry, the Si-Si bond lengths are 2.316 Å, and the Si-Ge bond lengths are 2.396 eV. The second kind of trigonal bipyramid (Ge at a tip) has C_{3v} symmetry, Si-Si bonds of 2.308 Å, and Si-Ge bonds of 2.400 Å. For cationic Si_4Ge they reported data for only one isomer geometrically similar to the most stable neutral (C_{2v} symmetry.) This cluster has Si-Si bonds of 2.300 Å and Si-Ge bonds of 2.510 Å. They found an ionization energy of 7.91 eV. Wang and Chao [51] give results for only one Si_4Ge cluster, a trigonal bipyramid with a Si-Ge-Si base. They found that the neutral, cation and anion clusters all have similar geometry. The neutral cluster has an electronic state of ^{1}A', a dissociation energy of -18.1169 or -20.0829, a HOMO-LUMO gap of 3.13, and frequencies of 375(a"), 435(a'), and 358(a').

From our research we determined that the most stable pentamer has a Si_4Ge stoichiometry. We found the same trigonal bipyramids as Wielgus *et al.* for our two most stable isomers. For the ground state, our Si-Si bond lengths are the same but our Si-Ge bond length

is greater at 2.49 Å. Our binding energy per atom is larger than that of Marim *et al.* at 2.927 eV. We also calculated a HOMO-LUMO gap of 3.099 eV, a VIP of 7.948 eV, and a VEA of 1.371 eV. Our second most stable structure is the same trigonal bipyramid with a Ge atom at a tip as found by Wielgus *et al.*, and our bond lengths are the same as theirs. Our next two most stable isomers are more trigonal bipyramids. These have the same arrangements of atoms as the first two, but they have a triplet electronic states (the first two were singlets) and they are stretched so that there is a greater distance between the tip atoms. The fifth isomer is a tetragonal pyramid with a four-atom base, and the sixth isomer is an asymmetric arrangement comparable to the second isomer of Marim *et al.*, but with different bond lengths. Other two-dimensional structures are a fan of silicon atoms around a germanium atom, a rhombus of silicon atoms with a germanium attached to one, a triangle with a chain of two extra atoms, and two linear structures.

Figure 4.56 illustrates the five stable Si_4Ge cations that we considered. As with the neutrals, the most stable structure is again a trigonal bipyramid. But with decreasing stability, the correspondence between the cation and neutral structures becomes mixed up. For the cations a couple of two-dimensional molecules (the fan shape and the rhombus with an extra atom) are more stable than the asymmetric three-dimensional molecule, whereas for the neutrals the three-dimensional arrangements were strictly more stable than the two-dimensional ones.

Table 4.43 Properties of the Si_4Ge Pentamers

Figure	Symmetry Group	Electronic State	Binding E / Atom (eV)	HOMO-LUMO Gap (eV)	Dipole Moment (D)
4.55 (a)	C_s	$^1A'$	2.927	3.099	0.335
4.55 (b)	C_{2v}	$^3A_2$	2.809	1.598[a]	0.023
4.55 (c)	C_s	$^1A'$	2.715	2.057	0.119
4.55 (d)	C_{2v}	$^1A_1$	2.668	1.739	0.419
4.55 (e)	C_{2v}	$^3A_2$	2.643	1.257[a]	0.242
4.55 (f)	$D_{\infty h}$	$^1\Sigma_g$	2.110	1.712	0.000

[a] HOMO and LUMO have opposite spins; this value includes the energy required to flip the spin of the electron.

Table 4.44 Properties of the $(Si_4Ge)^+$ Pentamers

Figure	Symmetry Group	Electronic State	Binding E / Atom (eV)	HOMO-LUMO Gap (eV)	Dipole Moment (D)
4.56 (a)	C_{2v}	$^2B_2$	2.951	1.773 [a]	1.517
4.56 (b)	C_{2v}	$^2A_2$	2.846	1.710 [a]	0.988
4.56 (c)	C_{2v}	$^2B_1$	2.837	1.668	0.440
4.56 (d)	C_s	$^2A'$	2.796	1.809	1.754
4.56 (e)	$D_{\infty h}$	--	2.252	1.157	0.000

[a] HOMO and LUMO have opposite spins; this value includes the energy required to flip the spin of the electron.

Table 4.45 Properties of the $(Si_4Ge)^-$ Pentamers

Figure	Symmetry Group	Electronic State	Binding E / Atom (eV)	HOMO-LUMO Gap (eV)	Dipole Moment (D)
4.57 (a)	C_{2v}	$^2B_1$	3.148	1.900[a]	1.768
4.57 (b)	C_s	$^2A''$	2.955	1.712[a]	1.244
4.57 (c)	C_{2v}	$^2B_2$	2.916	1.893[a]	1.323
4.57 (d)	C_{2v}	$^2B_2$	2.890	1.624[a]	0.621
4.57 (e)	$D_{\infty h}$	--	2.412	1.014	0.000

[a] HOMO and LUMO have opposite spins; this value includes the energy required to flip the spin of the electron.

Table 4.46 Ionization Potentials and Electron Affinities of the Si_4Ge Pentamers

Neutral Figure	VIP (eV)	Cationic Figure	AIP (eV)	VEA (eV)	Anionic Figure	AEA (eV)
4.55 (a)	7.948	4.56 (a)	7.781 [b]	1.371	4.57 (a)	2.242
4.55 (b)	7.827	4.56 (a)	7.191 [b]	2.685	4.57 (a)	2.832
4.55 (c)	7.527	4.56 (d)	7.495	2.075	4.57 (b)	2.339
4.55 (d)	7.100	4.56 (b)	7.011	2.021	4.57 (d)	2.247
4.55 (e)	6.982	4.56 (c)	6.933	2.144	4.57 (c)	2.503
4.55 (f)	7.241	4.56 (e)	7.188	2.646	4.57 (e)	2.647

Table 4.47 Fragmentation Energies of the Most Stable Si_4Ge Neutral Pentamer

Fragmented Clusters	Fragmentation Energy (eV)
$Si_3Ge + Si$	3.585
$Si_2Ge + Si_2$	4.660
$Si_2Ge + 2Si$	7.882
$2Si_2 + Si_2$	8.188
$Si_2 + SiGe + Si$	8.349
$Si_2 + 2Si + Ge$	11.410
$SiGe + 3Si$	11.572
$4Si + Ge$	14.633

Table 4.48 Fragmentation Energies of the Most Stable $(Si_4Ge)^+$ Cationic Pentamer

Fragmented Clusters	Fragmentation Energy (eV)
$(Si_3Ge)^+ + Si$	3.571
$(Si_2Ge)^+ + Si_2$	4.761
$(Si_2Ge)^+ + Si + Si$	7.984
$Si_2 + (SiGe)^+ + Si$	8.304
$Si_2 + Si_2 + Ge^+$	8.307
$(SiGe)^+ + Si + Si + Si$	11.527
$Si_2 + Si + Si + Ge^+$	11.530
$Si + Si + Si + Si + Ge^+$	14.753

Table 4.49 Fragmentation Energies of the Most Stable $(Si_4Ge)^-$ Anionic Pentamer

Fragmented Clusters	Fragmentation Energy (eV)
$(Si_3Ge)^- + Si$	3.838
$(Si_2Ge)^- + Si_2$	4.723
$(Si_2Ge)^- + 2Si$	7.945
$Si_2 + (SiGe)^- + Si$	8.746
$2Si_2 + Ge^-$	9.292
$(SiGe)^- + 3Si$	11.969
$Si_2 + 2Si + Ge^-$	12.515
$4Si + Ge^-$	15.738

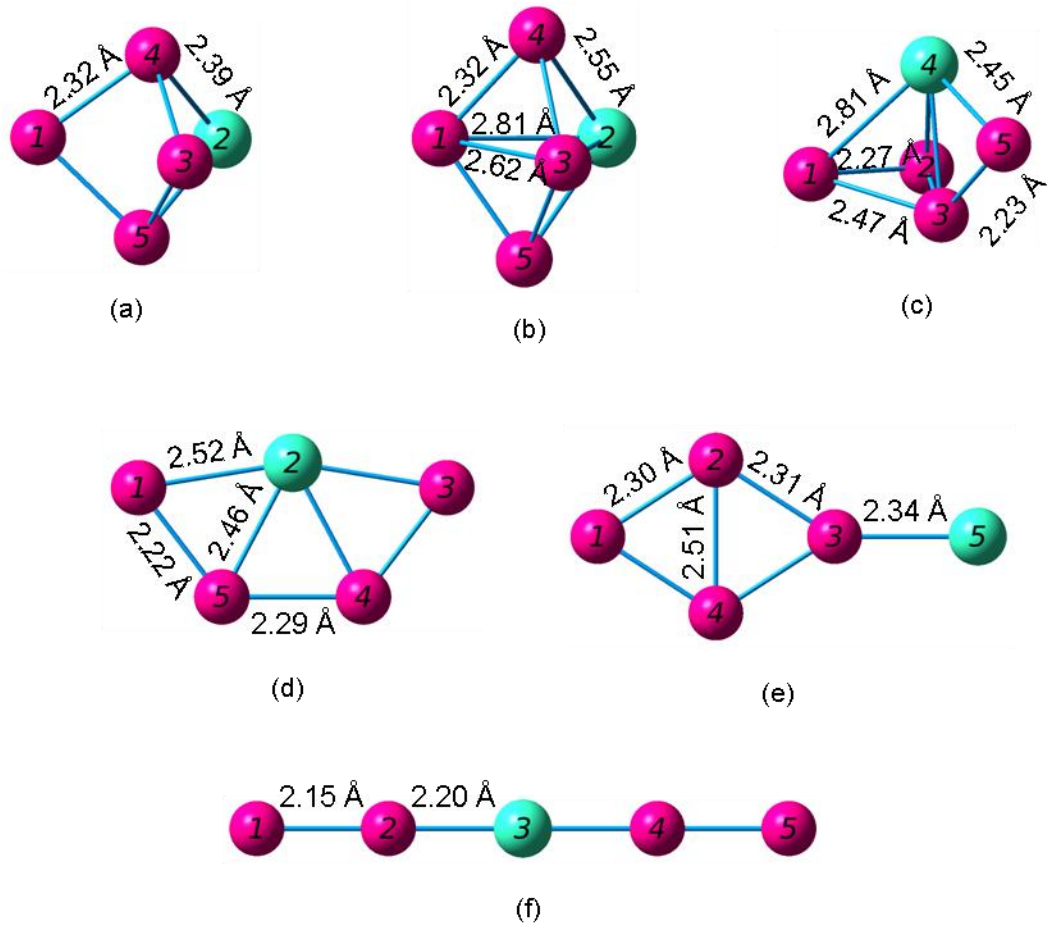

Figure 4.55 Geometries of the Si_4Ge Neutral Pentamers from (a) Most Stable through (f) Least Stable

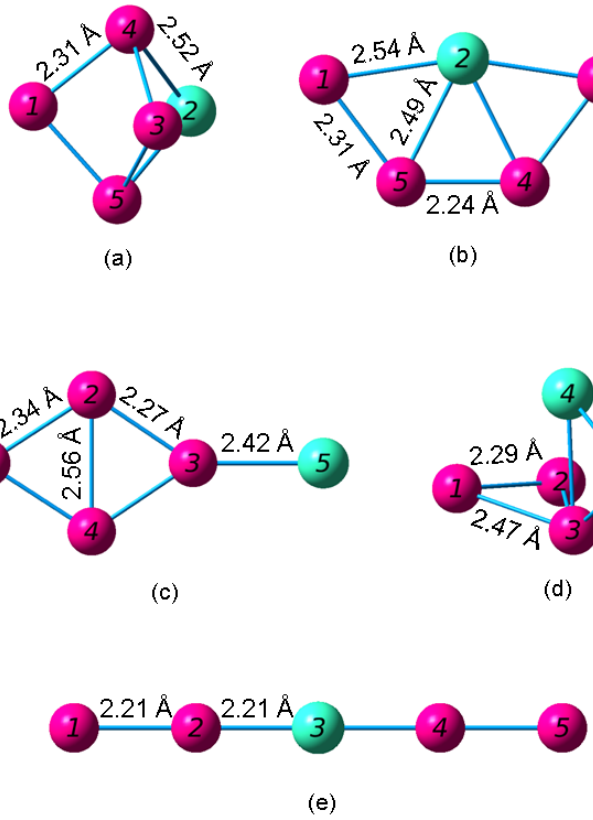

Figure 4.56 Geometries of the $(Si_4Ge)^+$ Cationic Pentamers from (a) Most Stable through (e) Least Stable

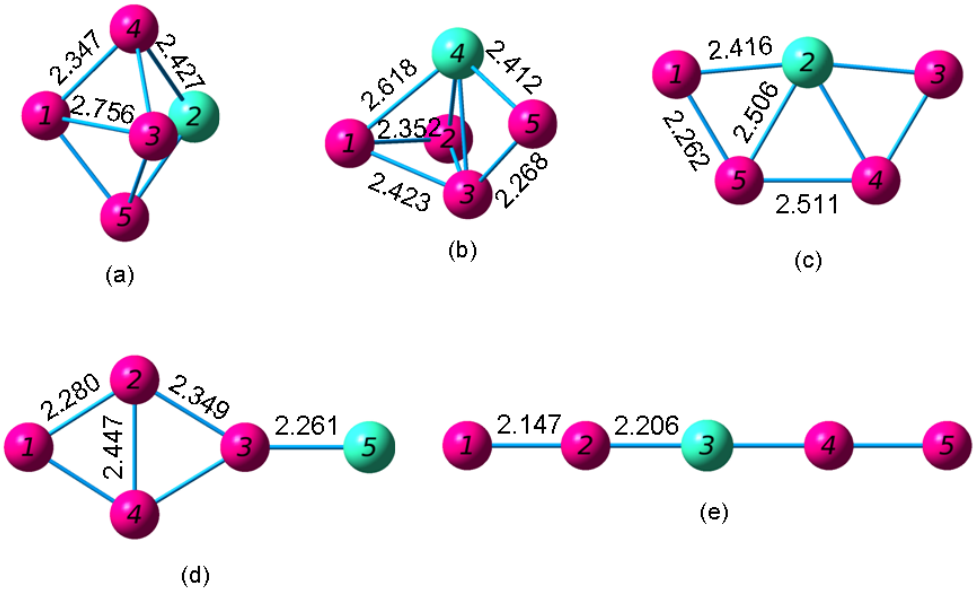

Figure 4.57 Geometries of the $(Si_4Ge)^-$ Anionic Pentamers from (a) Most Stable through (e) Least Stable

4.8 Si_3Ge_2 Pentamers

As with the Si_4Ge pentamers, the ground state of the Si_3Ge_2 pentamers is also a trigonal bipyramid. Li *et al.* [48] found this structure to have the two Ge atoms on either tip, giving the structure a D_{3h} symmetry. In this case all bonds are Si-Ge bonds of length 2.39 Å. They found the electronic state to be $^1A_1$, the HOMO-LUMO gap to be 3.00 eV, and the following frequencies: 361 cm^{-1} (E'), 289 cm^{-1} (A"$_2$), and 147 cm^{-1} (E').

Marim *et al.* [49] found this structure to have the two Ge atoms in the base shared between pyramids. Their Si-Si bond lengths are 2.34 Å, and their Si-Ge bond lengths are 2.40 Å. For this structure, they calculated a cohesive energy of 2.84 eV per atom. This group also found an additional asymmetric structure similar to their asymmetrical structure for Si_4Ge but with a Ge atom replacing one of the Si atoms in the tetragonal portion of the structure. Within the tetragonal portion of this Si_3Ge_2 structure, the Si-Si bond length is 2.25 Å, the Si-Ge bond lengths are 2.46 Å and 2.67 Å, and the Ge-Ge bond length is 2.51 Å. For the Si atom added to the side of the structure, the Si-Si bond is 2.25 Å and the Si-Ge bond is 2.46 Å. This structure has a cohesive energy of 2.72 eV.

Wielgus *et al.* [50] investigated the three possibilities for the neutral trigonal bipyramid structures. Their ground state had the two Ge atoms and one Si atom in the base shared between the pyramids (C_{2v} symmetry). For this structure, the Si-Si bond lengths are 2.318 Å and the Si-Ge bond lengths are 2.397 Å. Their next most stable isomer has one of the Ge atoms in the base and one at a tip, giving it a C_s symmetry. In this case, the Si-Si bond length is 2.309 Å, the Si-Ge bond lengths are 2.387 Å and 2.401 Å, and the Ge-Ge bond length is 2.478 Å. Their final isomer has one Ge atom at either tip and is comparable to the structure of Li *et al.* In this case they report the Si-Si bond lengths to be 2.392 Å. As with the Si_4Ge cluster, they only reported data for the cationic cluster with the same structure as the neutral (C_{2v} symmetry). This cluster has Si-Si bonds of 2.262 Å, Si-Ge bonds of 2.465 Å, and an ionization energy of 7.81 eV.

Wang and Chao [51] report only one Si_3Ge_2 cluster, a trigonal bipyramid with a Ge-Si-Ge base. They found that the neutral, cation and anion clusters all have similar geometry. The neutral cluster has an electronic state of $^1A'$, a dissociation energy of -17.8274 or -19.7928, a HOMO-LUMO gap of 3.14, and frequencies of 339(a'), 362(a"), and 290(a").

From our calculations, we find three most stable isomers of Si_3Ge_2 to be comparable to those of Wielgus *et al.* In fact our first structure has the same bond lengths as theirs. We also find a $^1A_1$ electronic state and a binding energy of 2.877 eV (only slightly larger than that of Marim *et al.*) Our HOMO-LUMO gap is rather large at 3.139 eV, but it is not much larger than Li *et al.* Our VIP comes to 7.922 eV and our VEA is 1.326 eV. Our second and third most stable structures also have the same geometry and bond lengths as the second and third structures of Wielgus *et al.* We find one more trigonal bipyramid, a stretched version of the second isomer with a triplet electronic state. Additionally, we investigated 7 two dimensional isomers.

The Si_3Ge_2 cations (figure 4.59 and table 4.51) again include a two-dimensional fan shape that is more stable than the three-dimensional structures. But as with all the molecules the linear structures and structures with a linear portion (such as the triangles with two linear atoms attached) remain the least stable isomers.

Table 4.50 Properties of the Si_3Ge_2 Pentamers

Figure	Symmetry Group	Electronic State	Binding E / Atom (eV)	HOMO-LUMO Gap (eV)	Dipole Moment (D)
4.58 (a)	C_{2v}	$^1A_1$	2.877	3.139	0.321
4.58 (b)	C_1	^1A	2.834	3.012	0.342
4.58 (c)	C_{2v}	$^1A_1$	2.775	2.995	0.002
4.58 (d)	C_s	$^3A"$	2.729	1.650[a]	0.066
4.58 (e)	C_{2v}	$^1A_1$	2.687	1.615	0.070
4.58 (f)	C_{2v}	$^3B_2$	2.338	1.133	0.701
4.58 (g)	C_{2v}	$^1A_1$	2.315	1.263	1.197
4.58 (h)	C_{2v}	$^1A_1$	2.265	1.284	0.905
4.58 (i)	$D_{\infty h}$	$^1\Sigma_g$	2.146	1.667	0.000

[a] HOMO and LUMO have opposite spins; this value includes the energy required to flip the spin of the electron.

Table 4.51 Properties of the $(Si_3Ge_2)^+$ Pentamers

Figure	Symmetry Group	Electronic State	Binding E / Atom (eV)	HOMO-LUMO Gap (eV)	Dipole Moment (D)
4.59 (a)	C_{2v}	$^2A_1$	2.914	1.792 [a]	1.249
4.59 (b)	C_{2v}	$^2A_2$	2.892	1.591 [a]	0.660
4.59 (c)	C_1	^2A	2.872	1.745 [a]	1.724
4.59 (d)	C_{2v}	$^2B_2$	2.796	1.613	0.055
4.59 (e)	C_{2v}	$^2B_1$	2.634	1.914	1.911
4.59 (f)	C_{2v}	$^4A_2$	2.471	1.355 [a]	2.152
4.59 (g)	C_{2v}	$^4A_2$	2.420	1.335 [a]	0.960
4.59 (h)	$D_{\infty h}$	--	2.314	1.091	0.000

[a] HOMO and LUMO have opposite spins; this value includes the energy required to flip the spin of the electron.

Table 4.52 Properties of the $(Si_3Ge_2)^-$ Pentamers

Figure	Symmetry Group	Electronic State	Binding E / Atom (eV)	HOMO-LUMO Gap (eV)	Dipole Moment (D)
4.60 (a)	C_{2v}	$^2B_2$	3.085	1.879[a]	1.470
4.60 (b)	C_1	^2A	3.061	1.830[a]	2.003
4.60 (c)	C_{2v}	$^2B_1$	3.020	1.764[a]	0.000
4.60 (d)	C_{2v}	$^2B_2$	2.896	1.525[a]	1.108
4.60 (e)	C_s	$^2A'$	2.818	1.592[a]	1.268
4.60 (f)	C_{2v}	$^2B_2$	2.680	1.479[a]	3.810
4.60 (g)	C_{2v}	$^2B_2$	2.628	1.482[a]	1.792
4.60 (h)	$D_{\infty h}$	--	2.433	0.978	0.000

[a] HOMO and LUMO have opposite spins; this value includes the energy required to flip the spin of the electron.

Table 4.53 Ionization Potentials and Electron Affinities of the Si_3Ge_2 Pentamers

Neutral Figure	VIP (eV)	Cationic Figure	AIP (eV)	VEA (eV)	Anionic Figure	AEA (eV)
4.58 (a)	7.922	4.59 (a)	7.717	1.326	4.60 (a)	2.179
4.58 (b)	7.889	4.59 (c)	7.714	1.399	4.60 (b)	2.272
4.58 (c)	7.851	4.59 (d)	7.795	1.487	4.60 (c)	2.362
4.58 (d)	7.820	4.59 (c)	7.187	2.654	4.60 (b)	2.799
4.58 (e)	6.968	4.59 (b)	6.872	2.008	4.60 (d)	2.186
4.58 (f)	6.457	4.59 (e)	6.417	2.161	4.60 (e)	3.541
4.58 (g)	7.224	4.59 (f)	7.119	2.940	4.60 (f)	2.966
4.58 (h)	7.209	4.59 (g)	7.127	2.929	4.60 (g)	2.952
4.58 (i)	7.117	4.59 (h)	7.060	2.568	4.60 (h)	2.571

Table 4.54 Fragmentation Energies of the Most Stable Si_3Ge_2 Neutral Pentamer

Fragmented Clusters	Fragmentation Energy (eV)
$Si_3Ge + Ge$	3.338
$Si_2Ge_2 + Si$	3.605
$SiGe_2 + Si_2$	4.511
$Si_2Ge + SiGe$	4.575
$Si_2Ge + Si + Ge$	7.635
$SiGe_2 + 2Si$	7.734
$Si_2 + SiGe + Ge$	8.102
$Si_2 + Ge_2 + Si$	8.235
$2SiGe + Si$	8.263
$Si_2 + Si + 2Ge$	11.163
$SiGe + 2Si + Ge$	11.324
$Ge_2 + 3Si$	11.457
$3Si + 2Ge$	14.386

Table 4.55 Fragmentation Energies of the Most Stable $(Si_3Ge_2)^+$ Cationic Pentamer

Fragmented Clusters	Fragmentation Energy (eV)
$(Si_3Ge)^+ + Ge$	3.388
$Si_3Ge + Ge^+$	3.521
$(Si_2Ge_2)^+ + Si$	3.675
$Si_2Ge + (SiGe)^+$	4.593
$(Si_2Ge)^+ + SiGe$	4.739
$(SiGe_2)^+ + Si_2$	4.743
$(Si_2Ge)^+ + Si + Ge$	7.800
$Si_2Ge + Si + Ge^+$	7.818
$(SiGe_2)^+ + Si + Si$	7.966
$Si_2 + (SiGe)^+ + Ge$	8.121
$Si_2 + (Ge_2)^+ + Si$	8.138
$SiGe + (SiGe)^+ + Si$	8.282
$Si_2 + SiGe + Ge^+$	8.285
$(SiGe)^+ + Si + Si + Ge$	11.343
$Si_2 + Si + Ge + Ge^+$	11.346
$(Ge_2)^+ + Si + Si + Si$	11.360
$SiGe + Si + Si + Ge^+$	11.508
$Si + Si + Si + Ge + Ge^+$	14.569

Table 4.56 Fragmentation Energies of the Most Stable $(Si_3Ge_2)^-$ Anionic Pentamer

Fragmented Clusters	Fragmentation Energy (eV)
$(Si_3Ge)^- + Ge$	3.528
$(Si_2Ge_2)^- + Si$	3.819
$Si_3Ge + Ge^-$	4.379
$(Si_2Ge)^- + SiGe$	4.573
$(SiGe_2)^- + Si_2$	4.656
$Si_2Ge + (SiGe)^-$	4.908
$(Si_2Ge)^- + Si + Ge$	7.635
$(SiGe_2)^- + 2Si$	7.879
$Si_2 + (SiGe)^- + Ge$	8.436
$(SiGe)^- + SiGe + Si$	8.597
$Si_2 + (Ge_2)^- + Si$	8.598
$Si_2Ge + Si + Ge^-$	8.676
$Si_2 + SiGe + Ge^-$	9.143
$(SiGe)^- + 2Si + Ge$	11.658
$(Ge_2)^- + 3Si$	11.821
$Si_2 + Si + Ge^- + Ge$	12.204
$SiGe + 2Si + Ge^-$	12.366
$3Si + Ge^- + Ge$	15.427

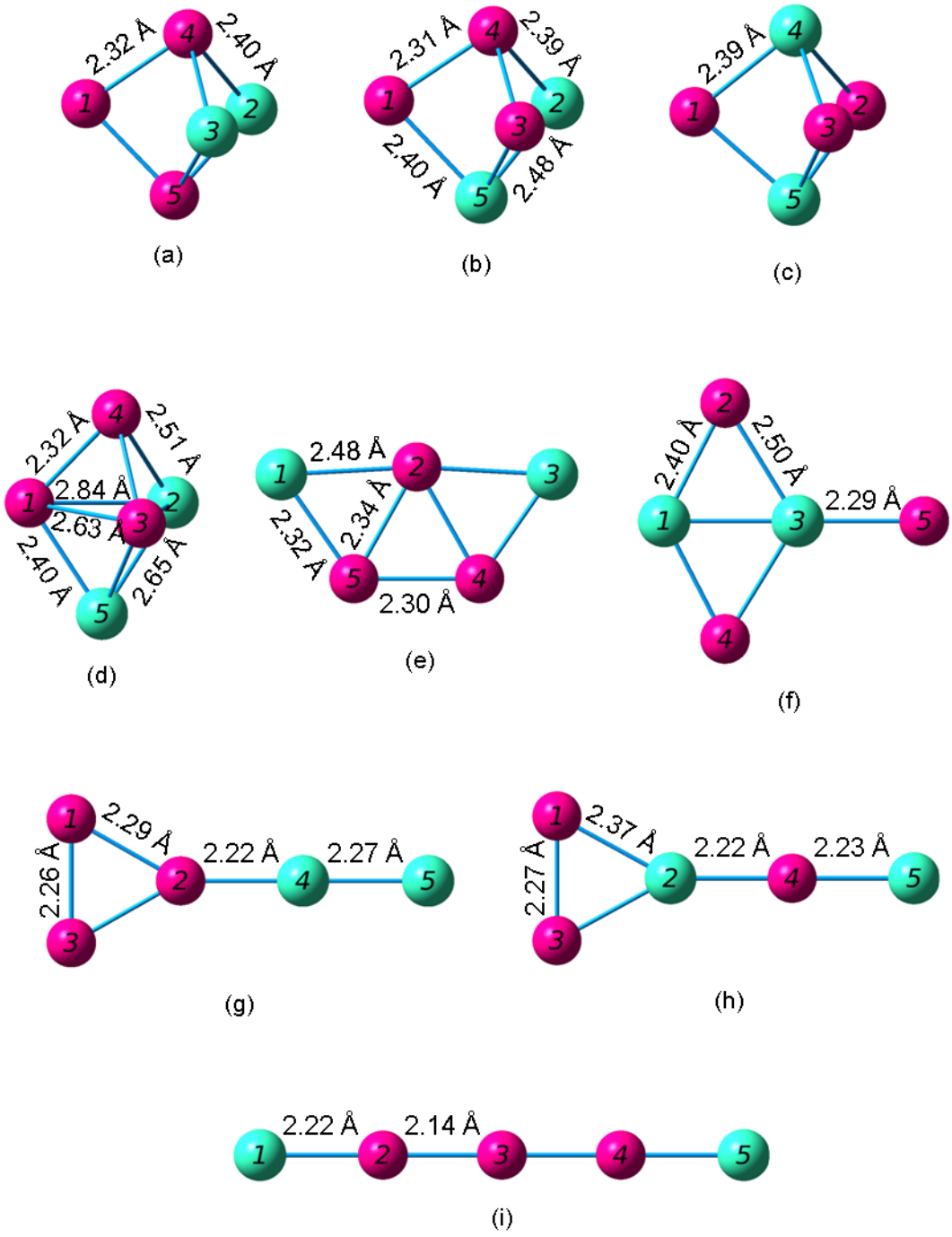

Figure 4.58 Geometries of the Si_3Ge_2 Neutral Pentamers from (a) Most Stable through (i) Least Stable

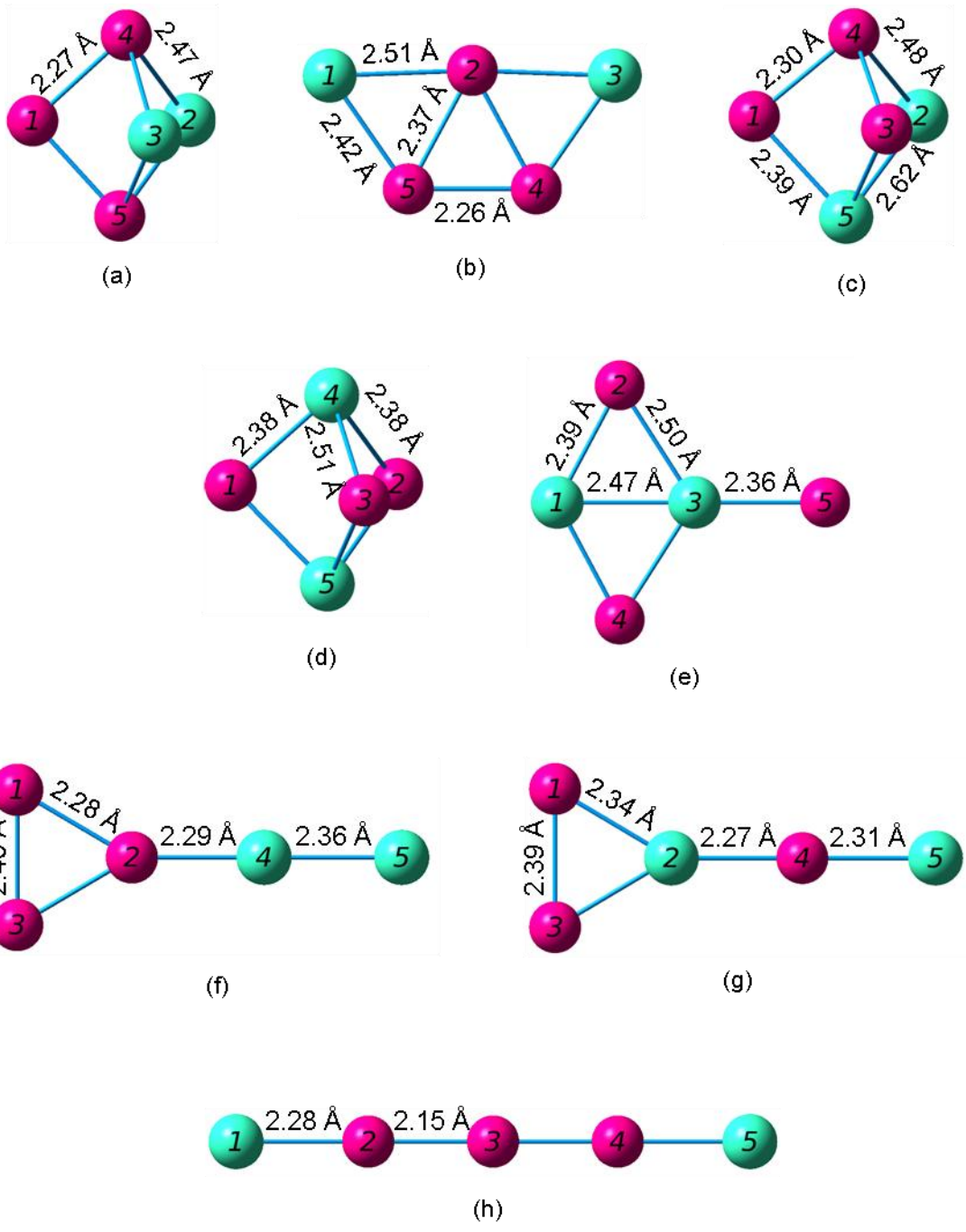

Figure 4.59 Geometries of the $(Si_3Ge_2)^+$ Cationic Pentamers from (a) Most Stable through (h) Least Stable

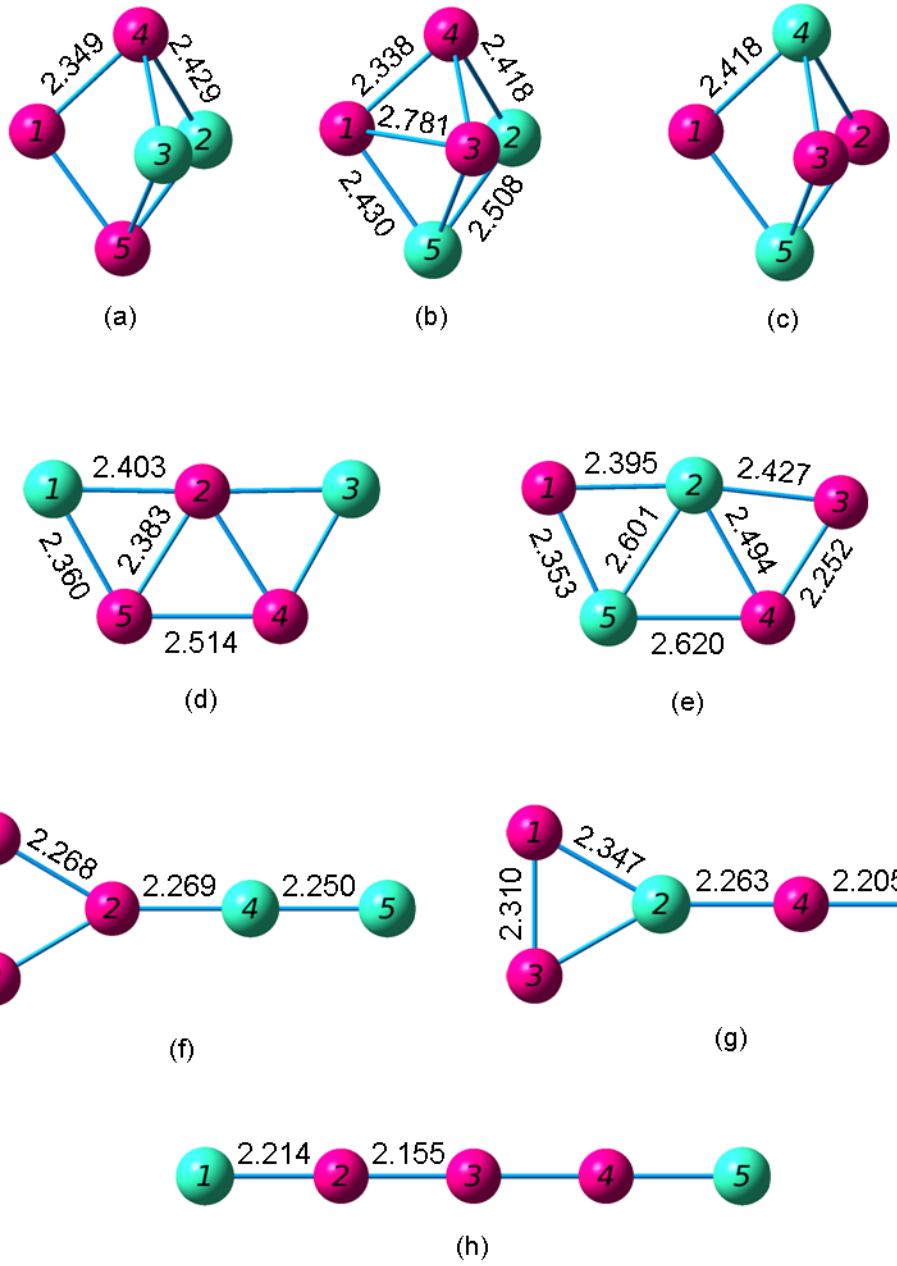

Figure 4.60 Geometries of the $(Si_3Ge_2)^-$ Anionic Pentamers from (a) Most Stable through (h) Least Stable

4.9. Si_2Ge_3 Pentamers

The ground state of the Si_2Ge_3 pentamers is again a trigonal bipyramid. Li *et al.* [48] found this structure to have the three Ge atoms on the base shared between the pyramids, giving the structure a D_{3h} symmetry. In this case all bonds are Si-Ge bonds of length 2.40 Å. They found the electronic state to be $^1A_1$, the HOMO-LUMO gap to be 3.27 eV, and the following frequencies: 337 cm^{-1} (E'), 311 cm^{-1} (A''_2), and 154 cm^{-1} (A'_1).

Marim *et al.* [49] also found this structure to have the three Ge atoms in the base shared between pyramids. Their Si-Ge bond lengths are nearly the same at 2.41 Å. For this structure, they calculated a cohesive energy of 2.82 eV per atom. This group also found an additional asymmetric structure similar to their asymmetrical structure for Si_3Ge_2 but with the third Ge atom replacing the Si atom that was attached to two atoms in the tetragon. Within the tetragonal portion of this Si_3Ge_2 structure, the Si-Si bond length is 2.25 Å, the Si-Ge bond lengths are 2.51 Å and 2.71 Å, and the Ge-Ge bond length is 2.51 Å. For the Ge atom added to the side of the structure, the Si-Ge bond is 2.32 Å and the Ge-Ge bond is 2.53 Å. This structure has a cohesive energy of 2.70 eV.

Wielgus *et al.* [50] investigated the three possibilities for the trigonal bipyramid structures. Their ground state had the three Ge atoms in the base shared between the pyramids (D_{3h} symmetry). For this structure, the Si-Ge bond lengths are 2.399 Å. Their next most stable isomer has two of the Ge atoms in the base and one at a tip, giving a C_s symmetry. In this case, the Si-Si bond length is 2.311 Å, the Si-Ge bond lengths are 2.390 Å and 2.402 Å, and the Ge-Ge bond length is 2.479 Å. Their final isomer has one Ge atom at either tip and one in the base. In this case they report the Si-Ge bond lengths to be 2.392 Å and the Ge-Ge bond lengths to be 2.469 Å. As with the other clusters, they only reported data for the cationic cluster with the same structure as the neutral (D_{2v} symmetry). This cluster has Si-Ge bonds of 2.44 Å and 2.346 Å and an ionization energy of 7.99 eV.

Wang and Chao [51] reported the most stable neutral and anion cluster to be a trigonal bipyramid with a Ge-Ge-Ge base. The most stable neutral cluster has an electronic state of ^{1}A', a dissociation energy of -17.4912 or -19.5004, a HOMO-LUMO gap of 3.27, and frequencies of 336(e'), 336(e'), and 310(a2"). For the most stable cation they found a trigonal bipyramid with a Ge-Si-Ge base.

We find the same three structures with the same bond lengths as Wielgus for our first three most stable isomers. The ground state (with the three Si atoms at either tip) has the same electronic state ($^1A_1$) and HOMO-LUMO gap (3.272 eV) as Li *et al.* found. Our binding energy of 2.827 eV per atom is basically the same as the cohesive energy found by Marim *et al.* We also found a VIP of 8.022 eV and a VEA of 1.30 eV. Our final three-dimensional isomer has not been previously reported. It is a structure similar to the third isomer but with more distance between tip atoms and a triplet electronic state. The two-dimensional structures have the same shapes as those with a Si_3Ge_2 composition, with the addition of one bow-tie shaped structure.

Our computations resulted in data for nine Si_2Ge_3 cations (figure 4.62 and table 4.58). As with the other pentamers, the fan-shaped structure is more stable than one of the three-dimensional structures, which contrasts with our findings for the neutrals, where all the trigonal bipyramids are more stable than any two-dimensional structure.

Table 4.57 Properties of the Si_2Ge_3 Pentamers

Figure	Symmetry Group	Electronic State	Binding E / Atom (eV)	HOMO-LUMO Gap (eV)	Dipole Moment (D)
4.61 (a)	C_{2v}	$^1A_1$	2.827	3.272	0.000
4.61 (b)	C_s	$^1A'$	2.791	3.030	0.331
4.61 (c)	C_l	^1A	2.738	2.927	0.340
4.61 (d)	C_{2v}	$^3A_2$	2.642	1.702[a]	0.063
4.61 (e)	C_{2v}	$^1A_1$	2.589	1.690	0.000
4.61 (f)	C_{2v}	$^3A_2$	2.435	1.343[a]	0.063
4.61 (g)	C_s	$^3A''$	2.339	1.344	0.796
4.61 (h)	C_{2v}	$^1A_1$	2.200	1.262	1.109
4.61 (i)	$D_{\infty h}$	$^1\Sigma_g$	2.055	1.649	0.000
4.61 (j)	$D_{\infty h}$	$^1\Sigma_g$	1.966	1.743	0.000

[a] HOMO and LUMO have opposite spins; this value includes the energy required to flip the spin of the electron.

Table 4.58 Properties of the $(Si_2Ge_3)^+$ Pentamers

Figure	Symmetry Group	Electronic State	Binding E / Atom (eV)	HOMO-LUMO Gap (eV)	Dipole Moment (D)
4.62 (a)	C_s	$^2A'$	2.841	1.757 [a]	1.455
4.62 (b)	C_{2v}	$^2A_1$	2.837	1.578	0.093
4.62 (c)	C_{2v}	$^2A_2$	2.805	1.599 [a]	1.073
4.62 (d)	C_{2v}	$^2B_2$	2.786	1.727 [a]	0.864
4.62 (e)	C_{2v}	$^2B_1$	2.625	1.672	3.370
4.62 (f)	C_s	$^2A''$	2.486	1.531 [a]	1.695
4.62 (g)	C_{2v}	$^4A_2$	2.355	1.313 [a]	1.395
4.62 (h)	$D_{\infty h}$	--	2.229	1.091	0.000
4.62 (i)	$D_{\infty h}$	--	2.123	1.099	0.000

[a] HOMO and LUMO have opposite spins; this value includes the energy required to flip the spin of the electron.

Table 4.59 Properties of the $(Si_2Ge_3)^-$ Pentamers

Figure	Symmetry Group	Electronic State	Binding E / Atom (eV)	HOMO-LUMO Gap (eV)	Dipole Moment (D)
4.63 (a)	C_{2v}	$^2B_2$	3.025	1.861[a]	0.000
4.63 (b)	C_s	$^2A'$	3.005	1.809[a]	1.701
4.63 (c)	C_1	^2A	2.969	1.724	1.284
4.63 (d)	C_{2v}	$^2B_2$	2.785	1.535[a]	1.508
4.63 (e)	C_{2v}	$^2B_2$	2.711	1.838	2.550
4.63 (f)	C_s	$^2A'$	2.662	1.212	3.250
4.63 (g)	C_{2v}	$^2B_2$	2.559	1.457[a]	2.725
4.63 (h)	$D_{\infty h}$	--	2.340	0.953	0.000
4.63 (i)	$D_{\infty h}$	--	2.255	1.004	0.000

[a] HOMO and LUMO have opposite spins; this value includes the energy required to flip the spin of the electron.

Table 4.60 Ionization Potentials and Electron Affinities of the Si_2Ge_3 Pentamers

Neutral Figure	VIP (eV)	Cationic Figure	AIP (eV)	VEA (eV)	Anionic Figure	AEA (eV)
4.61 (a)	8.022	4.62 (b)	7.852	1.300	4.63 (a)	2.126
4.61 (b)	7.847	4.62 (a)	7.649	1.378	4.63 (b)	2.210
4.61 (c)	7.821	4.62 (d)	7.661	1.435	4.63 (c)	2.296
4.61 (d)	7.829	4.62 (d)	7.181	2.629	4.63 (c)	2.777
4.61 (e)	6.906	4.62 (c)	6.817	1.913	4.63 (d)	2.119
4.61 (f)	6.998	4.62 (e)	6.950	2.444	4.63 (e)	2.516
4.61 (g)	7.520	4.62 (f)	7.166	2.681	4.63 (f)	2.752
4.61 (h)	7.191	4.62 (g)	7.091	2.909	4.63 (g)	2.933
4.61 (i)	7.085	4.62 (h)	7.029	2.564	4.63 (h)	2.566
4.61 (j)	7.170	4.62 (i)	7.117	2.576	4.63 (i)	2.580

Table 4.61 Fragmentation Energies of the Most Stable Si_2Ge_3 Neutral Pentamer

Fragmented Clusters	Fragmentation Energy (eV)
Si_2Ge_2 + Ge	3.356
$SiGe_3$ + Si	3.700
$SiGe_2$ + SiGe	4.423
Si_2Ge + Ge_2	4.457
Si_2Ge + 2Ge	7.386
$SiGe_2$ + Si + Ge	7.484
Si_2 + Ge_2 + Ge	7.985
2SiGe + Ge	8.014
SiGe + Ge_2 + Si	8.147
Si_2 + 3Ge	10.914
SiGe + Si + 2Ge	11.075
Ge_2 + 2Si + Ge	11.208
2Si + 3Ge	14.136

Table 4.62 Fragmentation Energies of the Most Stable $(Si_2Ge_3)^+$ Cationic Pentamer

Fragmented Clusters	Fragmentation Energy (eV)
$(Si_2Ge_2)^+ + Ge$	3.312
$Si_2Ge_2 + Ge^+$	3.425
$(SiGe_3)^+ + Si$	3.533
$Si_2Ge + (Ge_2)^+$	4.246
$SiGe_2 + (SiGe)^+$	4.328
$(Si_2Ge)^+ + Ge_2$	4.508
$(SiGe_2)^+ + SiGe$	4.540
$(Si_2Ge)^+ + Ge + Ge$	7.437
$Si_2Ge + Ge + Ge^+$	7.455
$SiGe_2 + Si + Ge^+$	7.553
$(SiGe_2)^+ + Si + Ge$	7.602
$Si_2 + (Ge_2)^+ + Ge$	7.774
$SiGe + (SiGe)^+ + Ge$	7.918
$SiGe + (Ge_2)^+ + Si$	7.935
$(SiGe)^+ + Ge_2 + Si$	8.051
$Si_2 + Ge_2 + Ge^+$	8.054
$SiGe + SiGe + Ge^+$	8.083
$(SiGe)^+ + Si + Ge + Ge$	10.980
$Si_2 + Ge + Ge + Ge^+$	10.983
$(Ge_2)^+ + Si + Si + Ge$	10.997
$SiGe + Si + Ge + Ge^+$	11.144
$Ge_2 + Si + Si + Ge^+$	11.277
$Si + Si + Ge + Ge + Ge^+$	14.206

Table 4.63 Fragmentation Energies of the Most Stable $(Si_2Ge_3)^-$ Anionic Pentamer

Fragmented Clusters	Fragmentation Energy (eV)
$(Si_2Ge_2)^- + Ge$	3.517
$(SiGe_3)^- + Si$	3.892
$Si_2Ge_2 + Ge^-$	4.344
$(Si_2Ge)^- + Ge_2$	4.404
$(SiGe_2)^- + SiGe$	4.515
$SiGe_2 + (SiGe)^-$	4.704
$Si_2Ge + (Ge_2)^-$	4.767
$(Si_2Ge)^- + 2Ge$	7.332
$(SiGe_2)^- + Si + Ge$	7.577
$(SiGe)^- + SiGe + Ge$	8.294
$Si_2 + (Ge_2)^- + Ge$	8.295
$Si_2Ge + Ge^- + Ge$	8.374
$(SiGe)^- + Ge_2 + Si$	8.427
$SiGe + (Ge_2)^- + Si$	8.457
$SiGe_2 + Si + Ge^-$	8.472
$Si_2 + Ge_2 + Ge^-$	8.973
$2SiGe + Ge^-$	9.002
$(SiGe)^- + Si + 2Ge$	11.356
$(Ge_2)^- + 2Si + Ge$	11.518
$Si_2 + 2Ge + Ge^-$	11.902
$SiGe + Si + Ge + Ge^-$	12.063
$Ge_2 + 2Si + Ge^-$	12.196
$2Si + Ge^- + 2Ge$	15.124

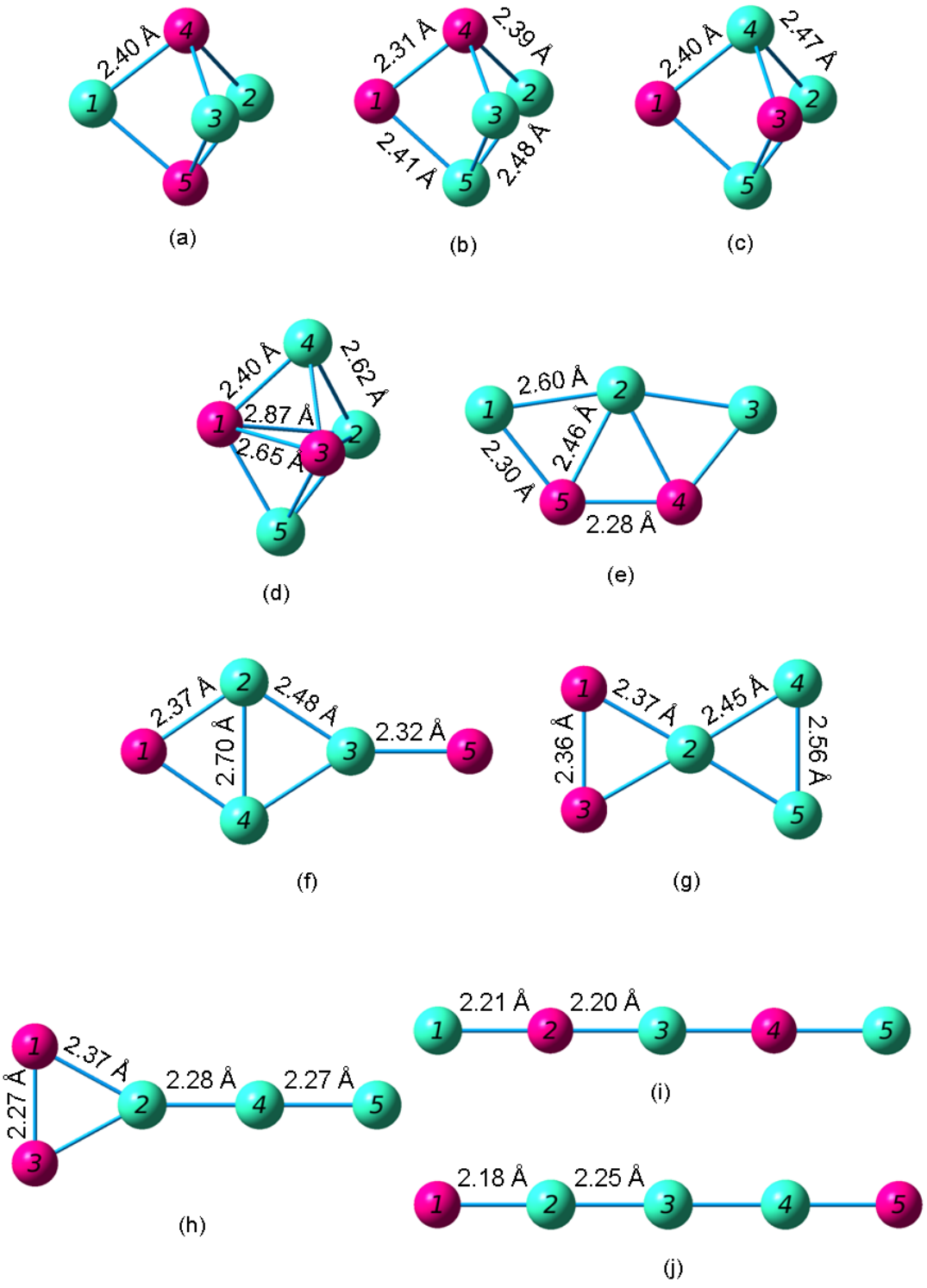

Figure 4.61 Geometries of the Si_2Ge_3 Neutral Pentamers from (a) Most Stable through (j) Least Stable

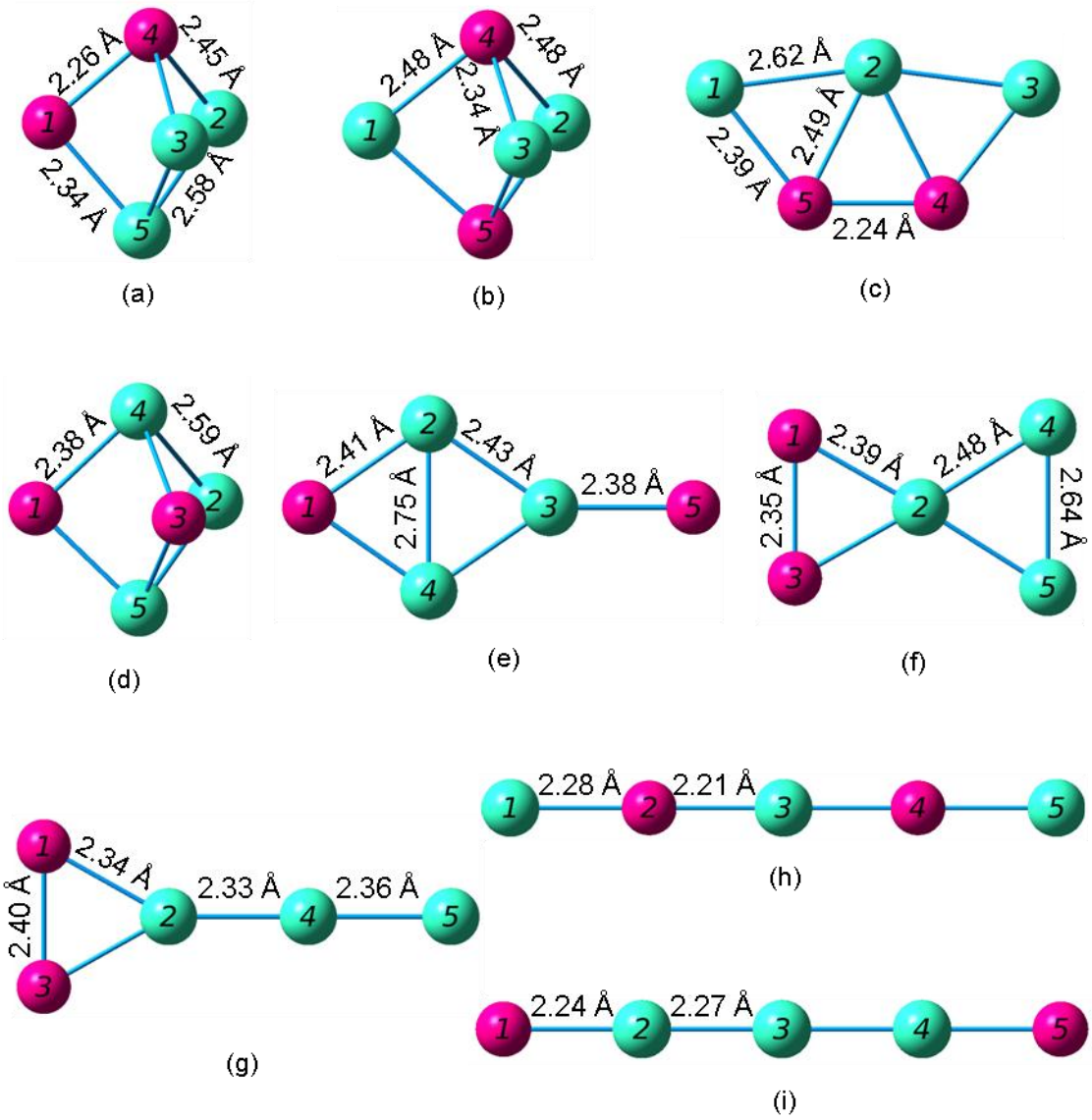

Figure 4.62 Geometries of the $(Si_2Ge_3)^+$ Cationic Pentamers from (a) Most Stable through (i) Least Stable

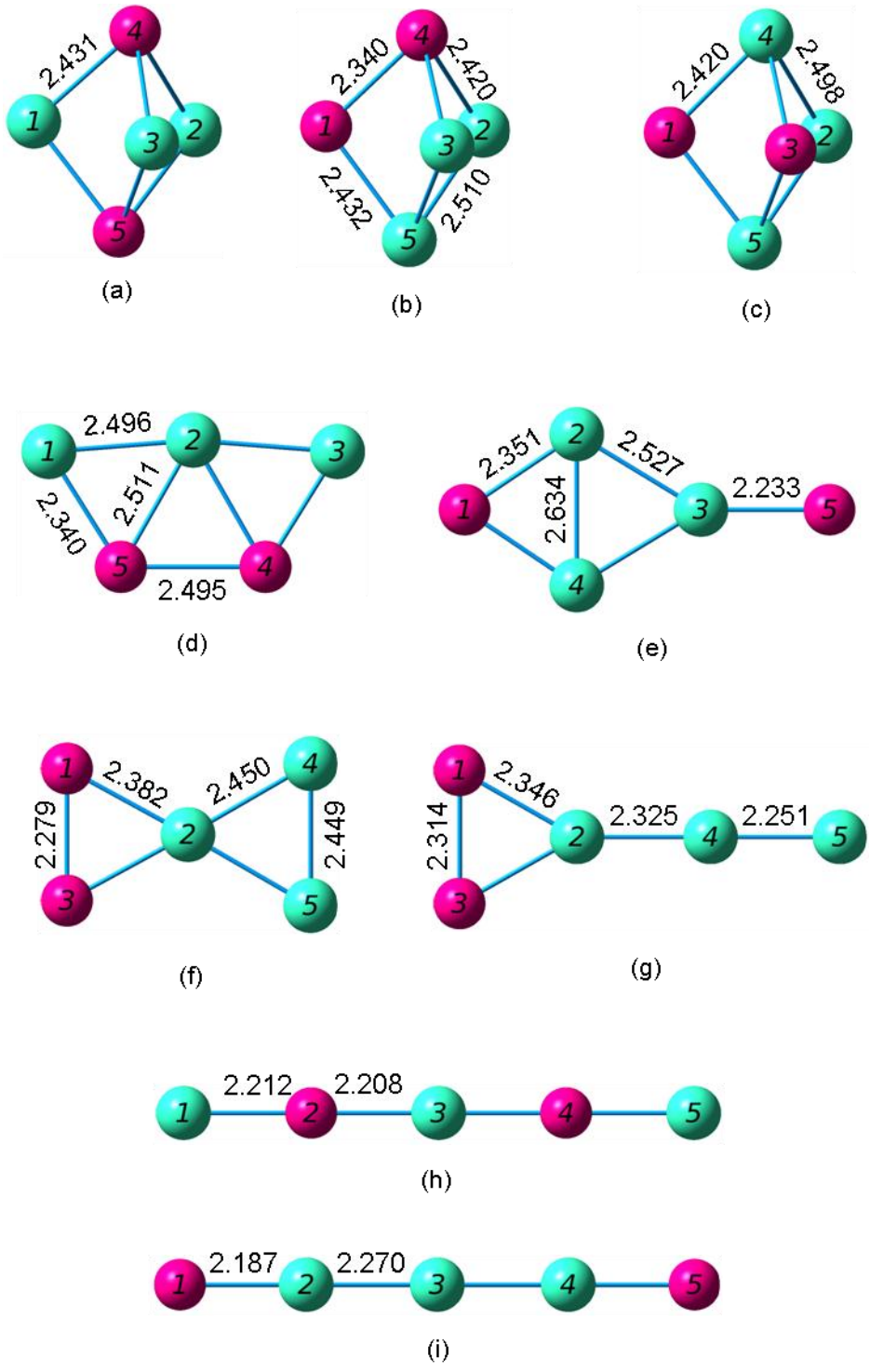

Figure 4.63 Geometries of the $(Si_2Ge_3)^-$ Anionic Pentamers from (a) Most Stable through (i) Least Stable

4.10. $SiGe_4$ Pentamers

Marim *et al.* [49] found one $SiGe_4$ trigonal bipyramid structure with the Si atom at one of the tips. In this case the Si-Ge bonds are 2.40 Å long and the Ge-Ge bonds are 2.47 Å long. For this structure, they calculated a cohesive energy of 2.78 eV per atom. Their other structure has the same asymmetrical structure as they found for the other pentamers. In this case, the Si atom is part of the tetragonal structure that the added Ge atom attaches to. The Si-Ge bond lengths are 2.31 Å and 2.70 Å and the Ge-Ge bonds lengths are 2.50 Å and 2.53 Å. This structure has a cohesion energy per atom of 2.67 eV per atom.

As with the other pentamers, Wielgus [50] *et al.* looked at the possible trigonal bipyramids. Their ground state has the Si atom at one of the tips and a C_{3v} symmetry. The Si-Ge bond lengths are 2.391 Å and the Ge-Ge bond lengths are 2.480 Å. Their other structure is again a trigonal bipyramid, but with the Si atom in the base between the two pyramids, putting it in the C_2v symmetry group. For this structure, the Si-Ge bond lengths are 2.394 Å and the Ge-Ge bond lengths are 2.470 Å. As with the other pentamer clusters, they only reported data for the cationic cluster with the same structure as the neutral cluster (C_{3v} symmetry). This cluster has Si-Ge bonds of 2.364 Å, Ge-Ge bonds of 2.453 Å, and an ionization energy of 7.87 eV.

Wang and Chao [51] report only one $SiGe_4$ cluster, a trigonal bipyramid with a Ge-Ge-Ge base. They found that the neutral, cation and anion clusters all have similar geometry. The neutral cluster has an electronic state of ^{1}A1, a dissociation energy of -16.9670 or -19.0726, a HOMO-LUMO gap of 3.15, and frequencies of 321(e), 321(e), and 357(a1).

Our first two isomers are comparable to those found by Wielgus *et al.*, and have the same bond lengths. The most stable structure has an electronic state of ^{1}A', a binding energy of 2.747 eV per atom (a little higher than the cohesion energy per atom found by Marim *et al.*), a HOMO-LUMO gap of 3.147 eV, a VIP of 7.940 eV, and a VEA of 1.352 eV. This structure is most likely to fragment into a $SiGe_3$ tetramer and a Ge atom with a fragmentation energy of 3.300 eV. The next most stable structure is similar to the second structure found by Wielgus,

with an electronic state of $^1A_1$. Our third structure is similar to the second structure of Marim *et al.*, but with slightly different bond lengths (figure 4.64). All our other structures are two dimensional. Two are rhombuses with an extra atom, the next two are triangles with two extra atoms, and the last is a linear structure.

We found seven cationic clusters of $SiGe_4$ (figure 4.65 and table 4.65). The two most stable cations have the same structure as the two most stable neutrals. As before, the binding energy per atom of the cations is larger than that of the neutral clusters.

Table 4.64 Properties of the $SiGe_4$ Pentamers

Figure	Symmetry Group	Electronic State	Binding E / Atom (eV)	HOMO-LUMO Gap (eV)	Dipole Moment (D)
4.64 (a)	C_s	$^1A'$	2.747	3.147	0.060
4.64 (b)	C_{2v}	$^1A_1$	2.700	2.676	0.330
4.64 (c)	C_{2v}	$^3A_2$	2.455	1.285[a]	0.337
4.64 (d)	C_{2v}	$^3A_2$	2.390	1.319[a]	0.396
4.64 (e)	D_{4h}	$^3A_{1,g}$	2.211	1.714[a]	0.562
4.64 (f)	C_{2v}	$^1A_1$	2.152	1.154	0.591
4.64 (g)	$C_{\infty v}$	$^1\Sigma$	1.942	1.704	0.780

[a] HOMO and LUMO have opposite spins; this value includes the energy required to flip the spin of the electron.

Table 4.65 Properties of the $(SiGe_4)^+$ Pentamers

Figure	Symmetry Group	Electronic State	Binding E / Atom (eV)	HOMO-LUMO Gap (eV)	Dipole Moment (D)
4.65 (a)	C_s	$^2A''$	2.772	1.505	0.925
4.65 (b)	C_{2v}	$^2A_1$	2.761	1.732[a]	0.782
4.65 (c)	C_{2v}	$^2B_1$	2.676	1.544	3.202
4.65 (d)	C_s	$^2A'$	2.660	1.691[a]	1.373
4.65 (e)	C_{2v}	$^2B_1$	2.597	1.631	4.207
4.65 (f)	C_{2v}	$^4A_2$	2.323	1.422[a]	2.081
4.65 (g)	$C_{\infty v}$	--	2.115	1.068	1.668

[a] HOMO and LUMO have opposite spins; this value does not include the energy required to flip the spin of the electron.

Table 4.66 Properties of the $(SiGe_4)^-$ Pentamers

Figure	Symmetry Group	Electronic State	Binding E / Atom (eV)	HOMO-LUMO Gap (eV)	Dipole Moment (D)
4.66 (a)	C_s	$^2A'$	2.951	1.791[a]	0.973
4.66 (b)	C_{2v}	$^2B_2$	2.920	1.719[a]	1.121
4.66 (c)	C_s	$^2A''$	2.879	1.300	1.395
4.66 (d)	C_{2v}	$^2B_2$	2.711	1.797	2.928
4.66 (e)	C_{2v}	$^2B_2$	2.657	1.809	4.361
4.66 (f)	C_{2v}	$^2B_2$	2.517	1.471[a]	2.173
4.66 (g)	$C_{\infty v}$	--	2.223	0.974	3.126

[a] HOMO and LUMO have opposite spins; this value includes the energy required to flip the spin of the electron.

Table 4.67 Ionization Potentials and Electron Affinities of the $SiGe_4$ Pentamers

Neutral Figure	VIP (eV)	Cationic Figure	AIP (eV)	VEA (eV)	Anionic Figure	AEA (eV)
4.64 (a)	7.940	4.65 (a)	7.778	1.352	4.66 (a)	2.156
4.64 (b)	7.792	4.65 (b)	7.598	1.406	4.66 (b)	2.235
4.64 (c)	6.852	4.65 (d)	7.232	2.351	4.66 (c)	2.901
4.64 (d)	6.911	4.65 (c)	6.798	2.405	4.66 (d)	2.418
4.64 (e)	6.536	4.65 (e)	6.865	1.648	4.66 (e)	2.476
4.64 (f)	7.016	4.65 (f)	6.875	2.940	4.66 (f)	2.965
4.64 (g)	7.087	4.65 (g)	7.035	2.537	4.66 (g)	2.541

Table 4.68 Fragmentation Energies of the Most Stable $SiGe_4$ Neutral Pentamer

Fragmented Clusters	Fragmentation Energy (eV)
$SiGe_3$ + Ge	3.300
$SiGe_2$ + Ge_2	4.156
$SiGe_2$ + 2Ge	7.084
SiGe + Ge_2 + Ge	7.747
2Ge_2 + Si	7.880
SiGe + 3Ge	10.675
Ge_2 + Si + 2Ge	10.808
Si + 4Ge	13.737

Table 4.69 Fragmentation Energies of the Most Stable $(SiGe_4)^+$ Cationic Pentamer

Fragmented Clusters	Fragmentation Energy (eV)
$(SiGe_3)^+ + Ge$	3.186
$SiGe_3 + Ge^+$	3.423
$SiGe_2 + (Ge_2)^+$	3.998
$(SiGe_2)^+ + Ge_2$	4.327
$SiGe_2 + Ge + Ge^+$	7.207
$(SiGe_2)^+ + Ge + Ge$	7.255
$SiGe + (Ge_2)^+ + Ge$	7.589
$(SiGe)^+ + Ge_2 + Ge$	7.705
$Ge_2 + (Ge_2)^+ + Si$	7.722
$SiGe + Ge_2 + Ge^+$	7.869
$(SiGe)^+ + Ge + Ge + Ge$	10.633
$(Ge_2)^+ + Si + Ge + Ge$	10.650
$SiGe + Ge + Ge + Ge^+$	10.798
$Ge_2 + Si + Ge + Ge^+$	10.931
$Si + Ge + Ge + Ge + Ge^+$	13.859

Table 4.70 Fragmentation Energies of the Most Stable $(SiGe_4)^-$ Anionic Pentamer

Fragmented Clusters	Fragmentation Energy (eV)
$(SiGe_3)^-$ + Ge	3.522
$(SiGe_2)^-$ + Ge_2	4.278
$SiGe_3$ + Ge^-	4.319
$SiGe_2$ + $(Ge_2)^-$	4.496
$(SiGe_2)^-$ + 2Ge	7.207
$(SiGe)^-$ + Ge_2 + Ge	8.058
SiGe + $(Ge_2)^-$ + Ge	8.087
$SiGe_2$ + Ge^- + Ge	8.103
$(Ge_2)^-$ + Ge_2 + Si	8.220
SiGe + Ge_2 + Ge^-	8.765
$(SiGe)^-$ + 3Ge	10.986
$(Ge_2)^-$ + Si + 2Ge	11.149
SiGe + Ge^- + 2Ge	11.693
Ge_2 + Si + Ge^- + Ge	11.826
Si + Ge^- + 3Ge	14.755

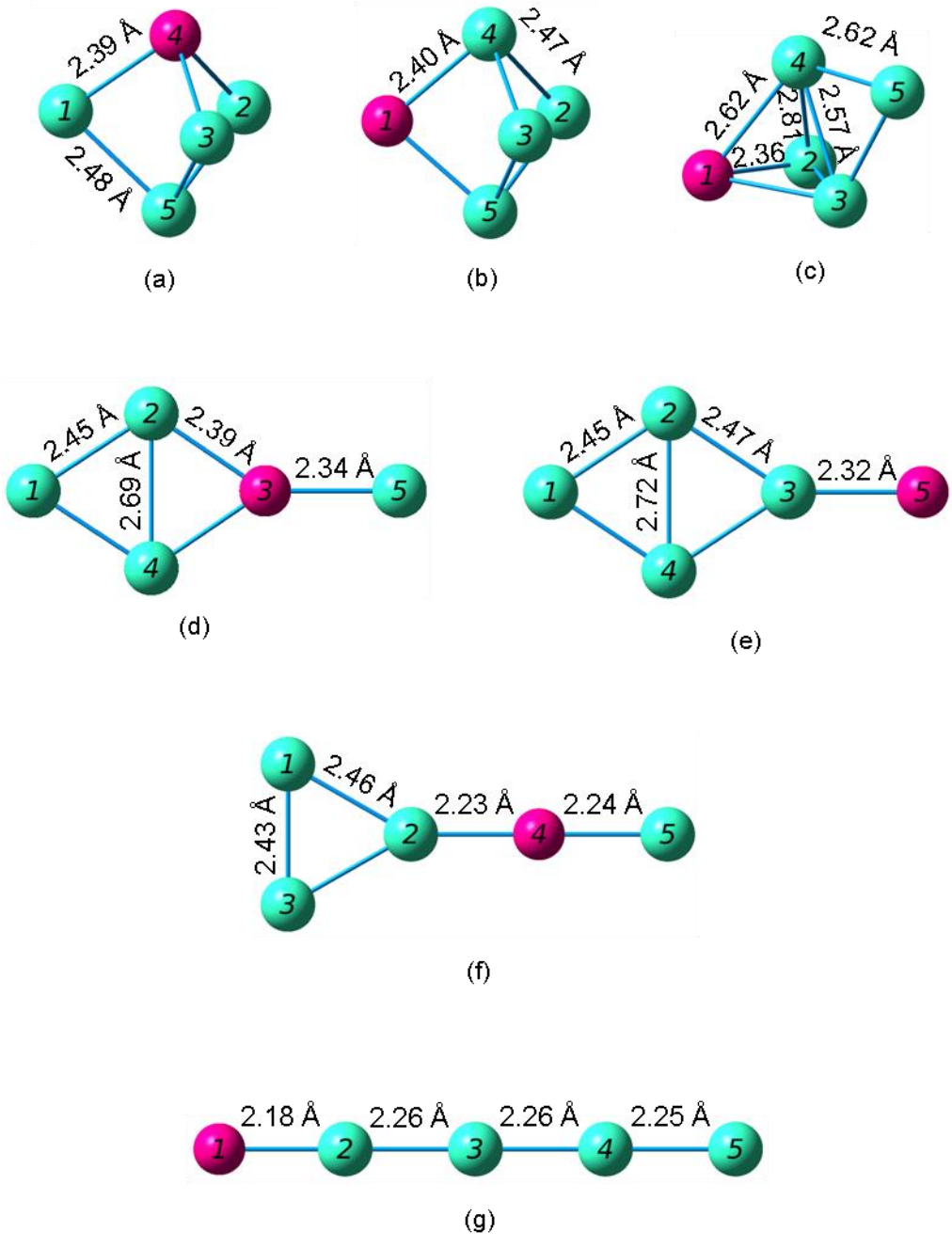

Figure 4.64 Geometries of the $SiGe_4$ Neutral Pentamers from (a) Most Stable through (g) Least Stable

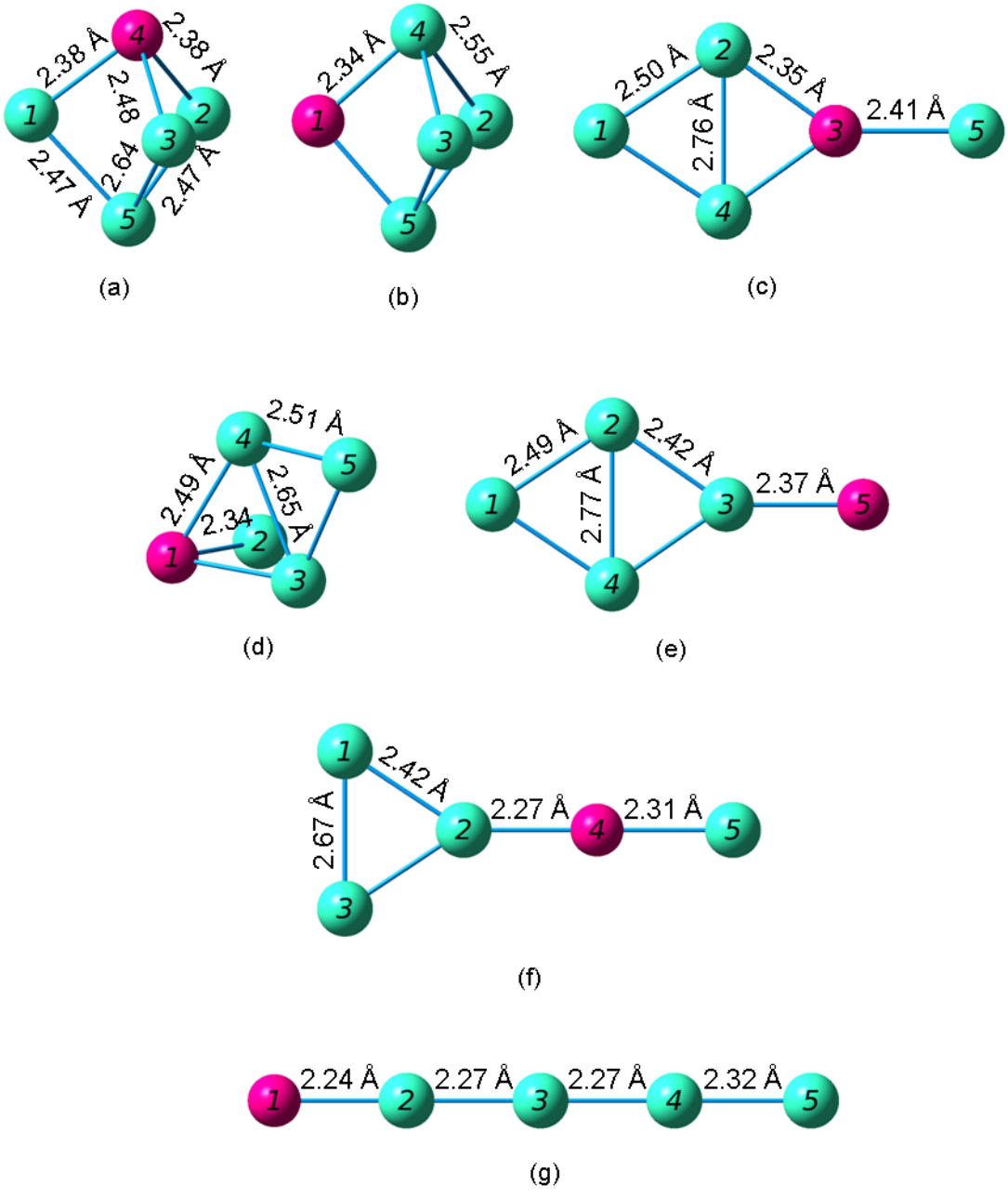

Figure 4.65 Geometries of the $(SiGe_4)^+$ Cationic Pentamers from (a) Most Stable through (g) Least Stable

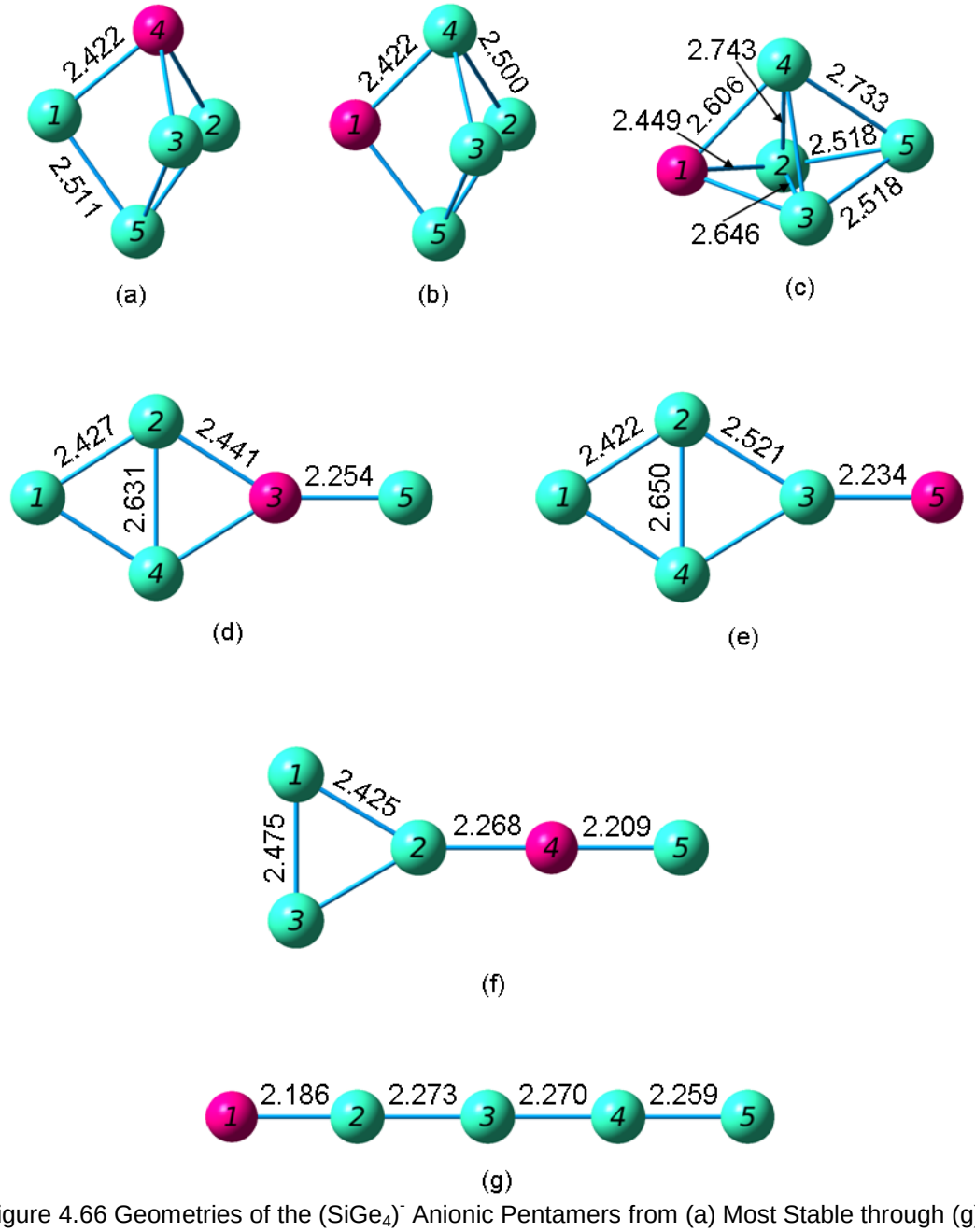

Figure 4.66 Geometries of the $(SiGe_4)^-$ Anionic Pentamers from (a) Most Stable through (g) Least Stable

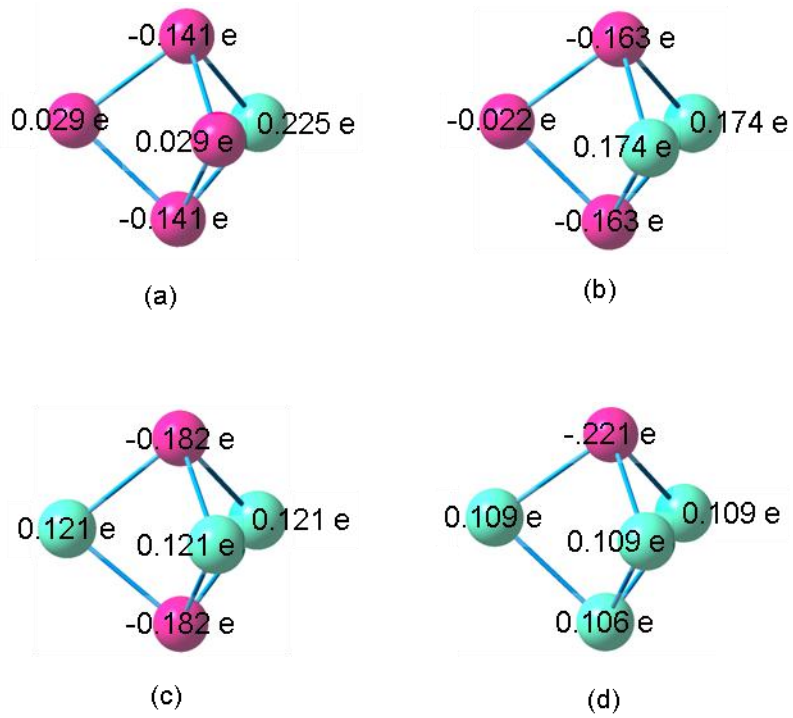

Figure 4.67 Atomic Charges of the Most Stable (a) Si_4Ge (b) Si_3Ge_2 (c) Si_2Ge_3 and (d) $SiGe_4$ Neutral Pentamer

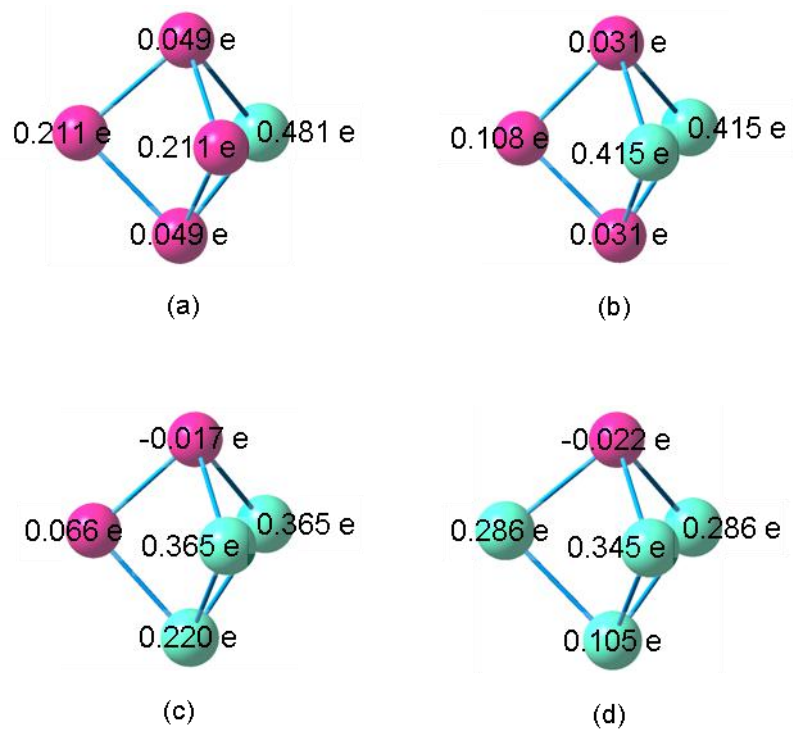

Figure 4.68 Atomic Charges of the Most Stable (a) $(Si_4Ge)^+$ (b) $(Si_3Ge_2)^+$ (c) $(Si_2Ge_3)^+$ and (d) $(SiGe_4)^+$ Cationic Pentamer

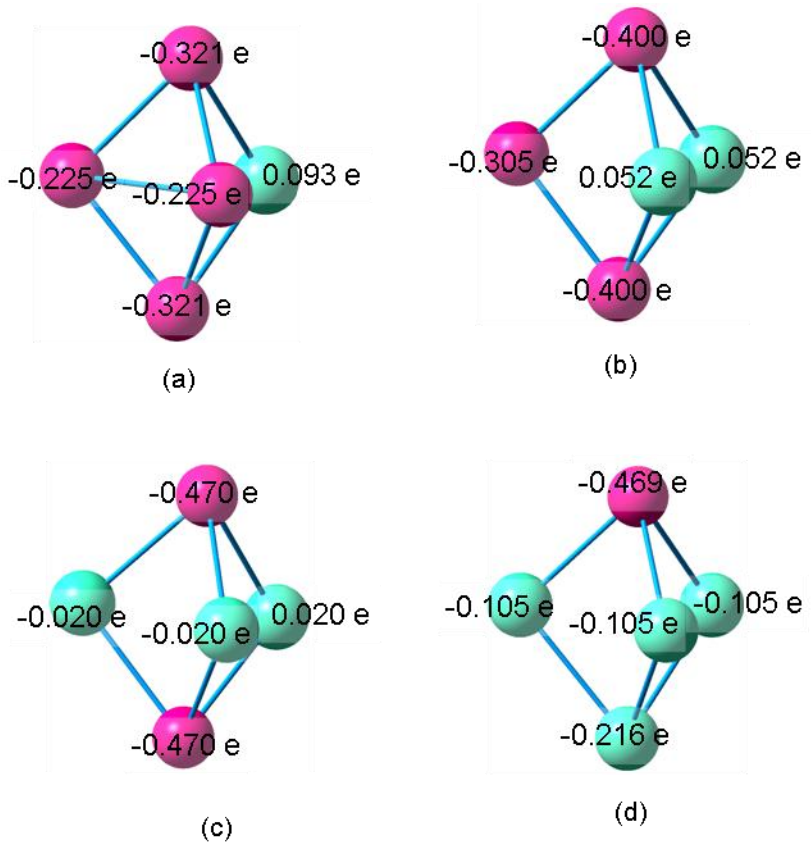

Figure 4.69 Atomic Charges of the Most Stable (a) $(Si_4Ge)^-$ (b) $(Si_3Ge_2)^-$ (c) $(Si_2Ge_3)^-$ and (d) $(SiGe_4)^-$ Anionic Pentamer

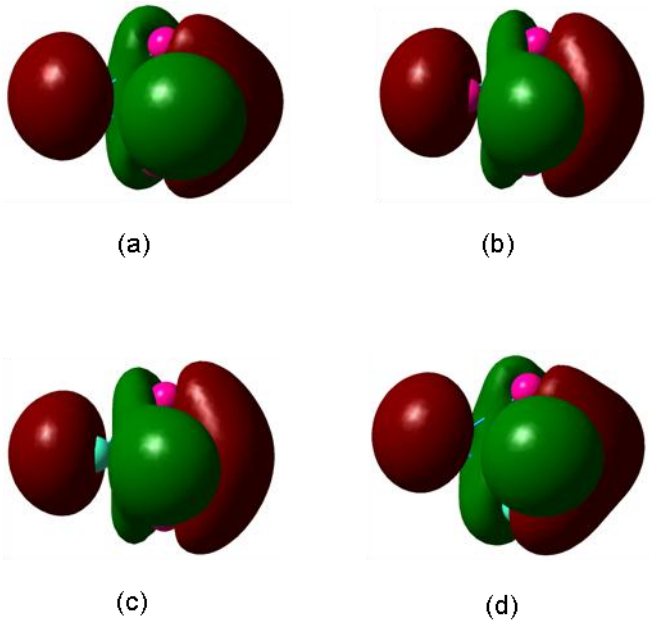

Figure 4.70 HOMO of the Most Stable (a) Si_4Ge (b) Si_3Ge_2 (c) Si_2Ge_3 and (d) $SiGe_4$ Neutral Pentamer

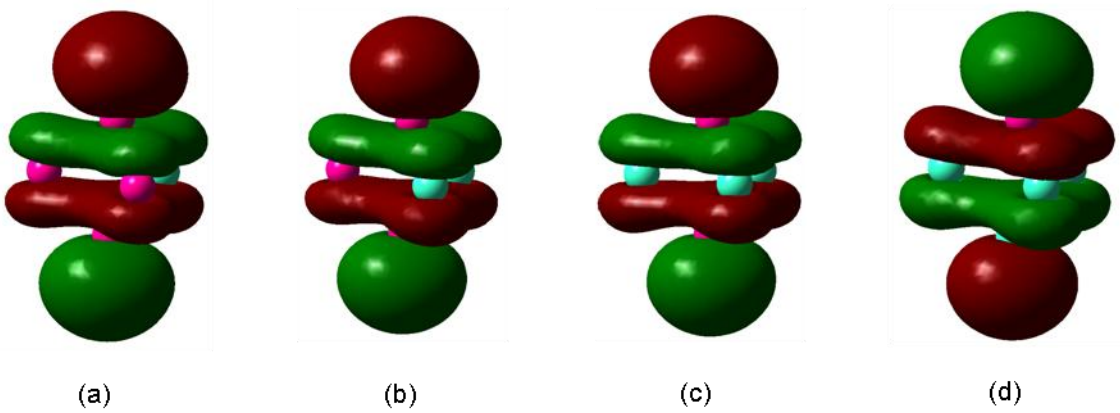

Figure 4.71 LUMO of the Most Stable (a) Si_4Ge (b) Si_3Ge_2 (c) Si_2Ge_3 and (d) $SiGe_4$ Neutral Pentamer

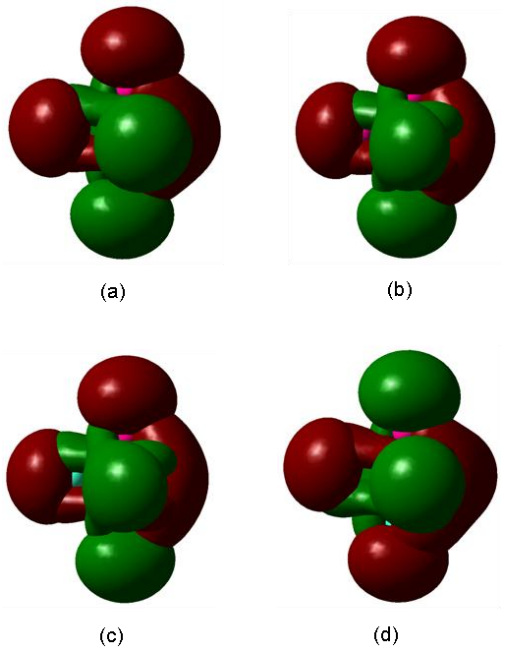

Figure 4.72 HOMO and LUMO of the Most Stable (a) Si_4Ge (b) Si_3Ge_2 (c) Si_2Ge_3 and (d) $SiGe_4$ Neutral Pentamer

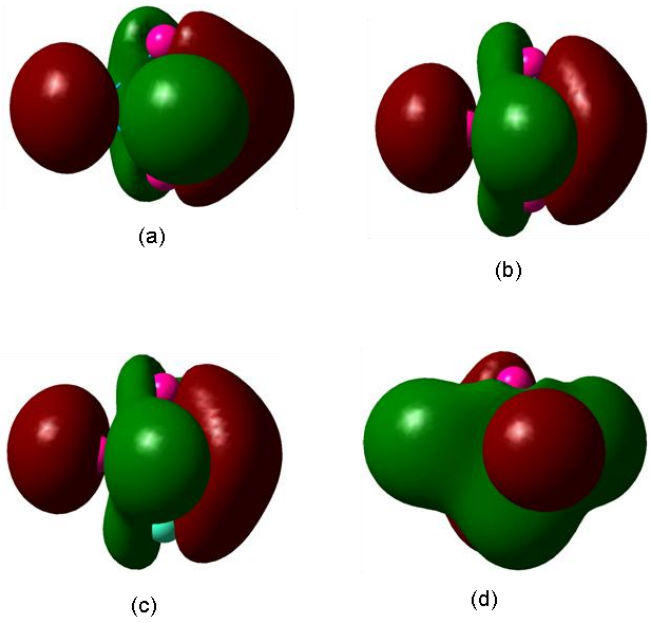

Figure 4.73 HOMO of the Most Stable (a) $(Si_4Ge)^+$ (b) $(Si_3Ge_2)^+$ (c) $(Si_2Ge_3)^+$ and (d) $(SiGe_4)^+$ Cationic Pentamer

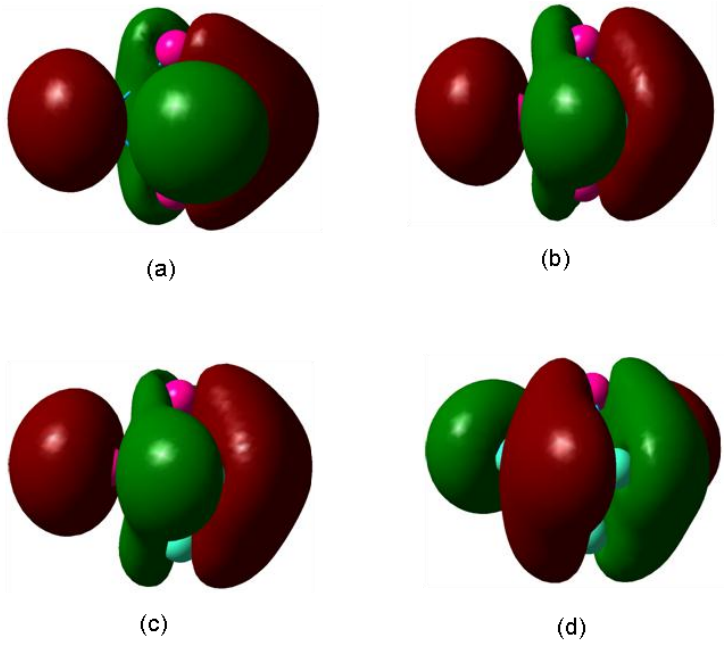

Figure 4.74 LUMO of the Most Stable (a) $(Si_4Ge)^+$ (b) $(Si_3Ge_2)^+$ (c) $(Si_2Ge_3)^+$ and (d) $(SiGe_4)^+$ Cationic Pentamer

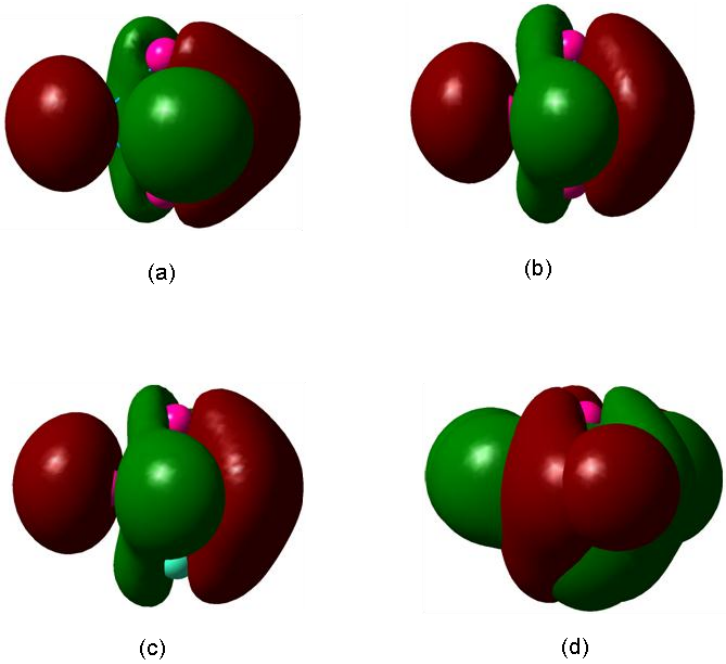

Figure 4.75 HOMO and LUMO of the Most Stable (a) $(Si_4Ge)^+$ (b) $(Si_3Ge_2)^+$ (c) $(Si_2Ge_3)^+$ and (d) $(SiGe_4)^+$ Cationic Pentamer

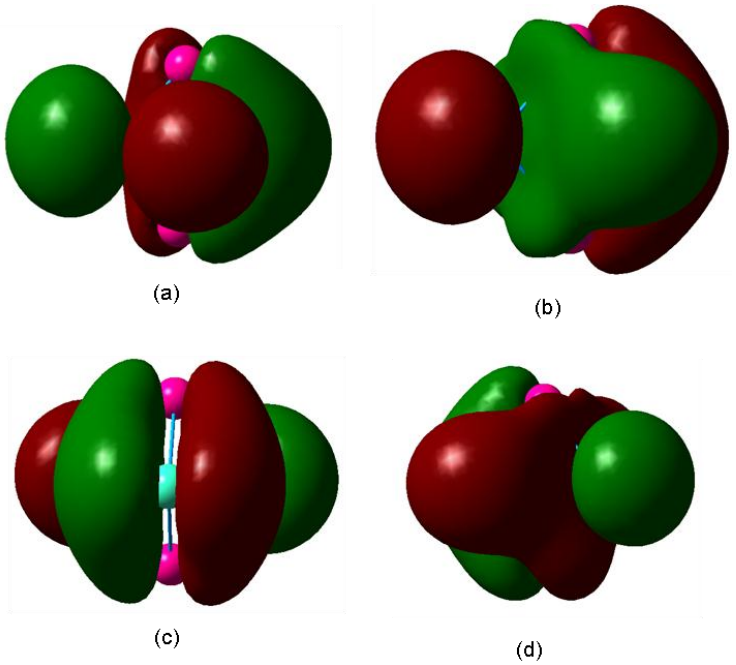

Figure 4.76 HOMO of the Most Stable (a) $(Si_4Ge)^-$ (b) $(Si_3Ge_2)^-$ (c) $(Si_2Ge_3)^-$ and (d) $(SiGe_4)^-$ Anionic Pentamer

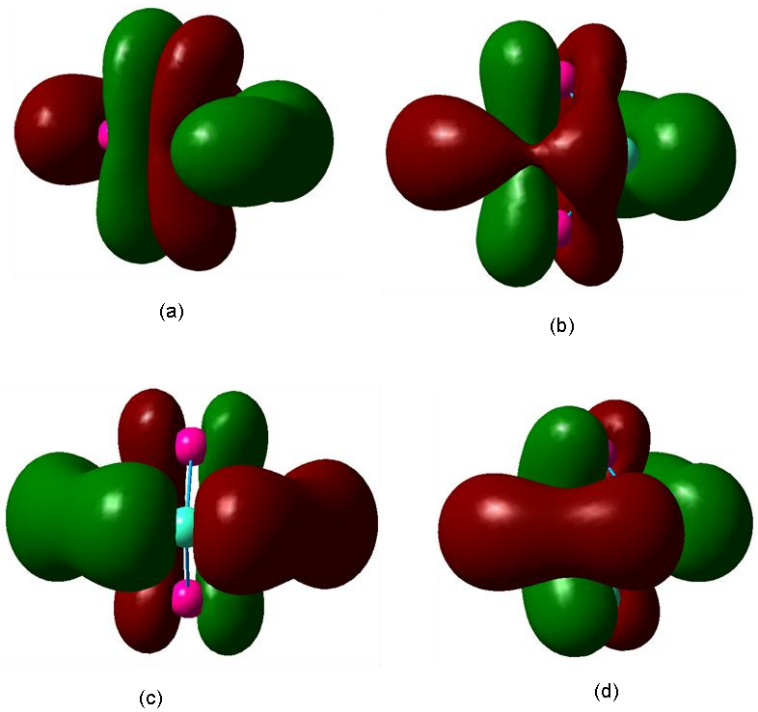

Figure 4.77 LUMO of the Most Stable (a) $(Si_4Ge)^-$ (b) $(Si_3Ge_2)^-$ (c) $(Si_2Ge_3)^-$ and (d) $(SiGe_4)^-$ Anionic Pentamer

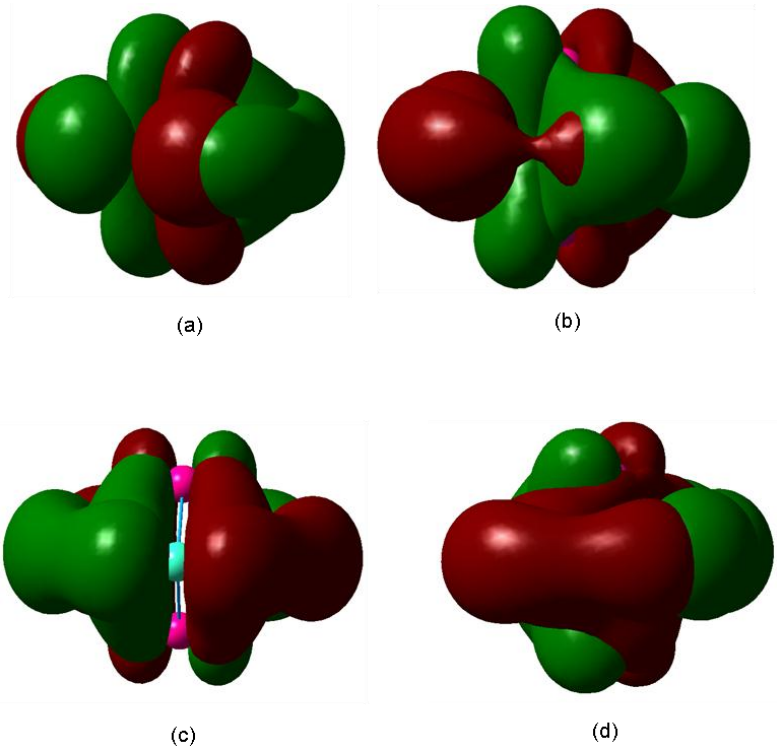

Figure 4.78 HOMO and LUMO of the Most Stable (a) $(Si_4Ge)^-$ (b) $(Si_3Ge_2)^-$ (c) $(Si_2Ge_3)^-$ and (d) $(SiGe_4)^-$ Anionic Pentamer

4.11 Si_5Ge Hexamers

Wang and Chao [51] provide the most complete study of the silicon-germanium hexamers. Their Si_5Ge cluster is a rhombic bipyramid. It has a ^1A electronic state, a dissociation energy of -24.5977 eV or -25.1265 eV, a HOMO-LUMO gap of 3.21 eV, and the following frequencies: 435(a), 400(a), and 439(a). They found a structure with similar geometry to be the most stable cation and anion.

For our most stable structure, we found the same rhombic bipyramid as Wang and Chao. We found that the second and third most stable clusters are also rhombic bipyramids with slightly different geometries. We provide data for eight different neutral and cation clusters and seven anions. In the case of the anions, both the second and third most stable neutral clusters optimized to the most stable anion cluster.

We took some of our input geometries from Raghavachari's work [1] on small pure silicon nanoclusters. The most stable rhombic bipyramids originated in this way. Other geometries came from adding an additional atom to a pentamer structure. We formed the geometry pictured in figures 4.79 (d), 4.80 (c), and 4.81 (e) by attaching a single germanium atom to two of the silicon atoms in a trigonal bipyramid. Attaching this single germanium atom to silicon atoms in the face of a trigonal bipyramid (such as attaching it to atoms 1 and 3 in figure 4.79 (d) led back to a rhombic bipyramid. The prism-shaped clusters in figures 4.79 (f), 4.79 (g), 4.80 (f), 4.80 (g), 4.81 (c), and 4.81 (d) were created by adding a single atom (atom 5) to one of the triangular faces of a tetragonal pyramid. The two-dimensional Si_5Ge cluster originated from adding a single germanium atom to a pentagon of silicon atoms. The optimized result was the triangular cluster pictured in figure 4.79 (h).

Table 4.71 Properties of the $Si_5GeHexamers$

Figure	Symmetry Group	Electronic State	Binding E / Atom (eV)	HOMO-LUMO Gap (eV)	Dipole Moment (D)
4.79 (a)	C_{2v}	$^1A_1$	3.097	3.217	0.681
4.79 (b)	C_s	$^1A'$	3.043	3.099	0.256
4.79 (c)	C_{4v}	$^1A_1$	3.035	3.043	0.063
4.79 (d)	C_s	$^1A'$	3.004	2.460	1.151
4.79 (e)	C_s	$^3A''$	2.991	2.007[a]	0.510
4.79 (f)	C_s	$^1A'$	2.977	2.100	0.716
4.79 (g)	C_s	$^1A'$	2.951	2.157	0.518
4.79 (h)	C_{2v}	$^1A_1$	2.755	0.976	0.797

[a] HOMO and LUMO have opposite spins; this value includes the energy required to flip the spin of the electron.

Table 4.72 Properties of the $(Si_5Ge)^+$ Hexamers

Figure	Symmetry Group	Electronic State	Binding E / Atom (eV)	HOMO-LUMO Gap (eV)	Dipole Moment (D)
4.80 (a)	C_{2v}	$^2A_1$	3.133	1.593	1.120
4.80 (b)	C_s	$^2A''$	3.129	2.029	1.234
4.80 (c)	C_s	$^2A'$	3.114	1.759	1.085
4.80 (d)	C_{2v}	$^2B_1$	3.104	1.814	1.214
4.80 (e)	C_s	$^4A''$	3.088	1.888	1.262
4.80 (f)	C_s	$^2A''$	3.086	1.662	1.718
4.80 (g)	C_s	$^2A''$	3.043	1.697	1.339
4.80 (h)	C_{2v}	$^2B_1$	2.923	1.091	2.527

[a] HOMO and LUMO have opposite spins; this value includes the energy required to flip the spin of the electron.

Table 4.73 Properties of the $(Si_5Ge)^-$ Hexamers

Figure	Symmetry Group	Electronic State	Binding E / Atom (eV)	HOMO-LUMO Gap (eV)	Dipole Moment (D)
4.81 (a)	C_s	$^2A'$	3.202	1.822	1.502
4.81 (b)	C_s	$^2A'$	3.183	1.080	1.973
4.81 (c)	C_s	$^2A'$	3.153	1.579	2.773
4.81 (d)	C_s	$^2A'$	3.141	1.585	1.483
4.81 (e)	C_s	$^2A'$	3.113	1.473	2.644
4.81 (f)	C_{2v}	$^2B_1$	3.082	0.900	2.053
4.81 (g)	C_{2v}	$^2A_2$	3.072	1.216	2.112

[a] HOMO and LUMO have opposite spins; this value includes the energy required to flip the spin of the electron.

Table 4.74 Ionization Potentials and Electron Affinities of the Si_5Ge Hexamers

Neutral Figure	VIP (eV)	Cationic Figure	AIP (eV)	VEA (eV)	Anionic Figure	AEA (eV)
4.79 (a)	8.047	4.80 (a)	7.686	0.852	4.81 (f)	1.045
4.79 (b)	7.779	4.80 (b)	7.386	1.344	4.81 (a)	2.087
4.79 (c)	7.844	4.80 (d)	7.486	1.443	4.81 (a)	2.137
4.79 (d)	7.453	4.80 (c)	7.240	1.469	4.81 (e)	1.792
4.79 (e)	7.482	4.80 (e)	7.316	2.165	4.81 (b)	2.289
4.79 (f)	7.470	4.80 (f)	7.247	2.088	4.81 (c)	2.190
4.79 (g)	7.574	4.80 (g)	7.348	2.128	4.81 (d)	2.278
4.79 (h)	7.037	4.80 (h)	6.896	2.948	4.81 (g)	3.038

Table 4.75 Fragmentation Energies of the Most Stable Si_5Ge Neutral Hexamer

Fragmented Clusters	Fragmentation Energy (eV)
$Si_4Ge + Si$	3.948
$Si_2 + Si_3Ge$	4.311
$Si_3Ge + 2Si$	7.533
$Si_2 + Si_2Ge + Si$	8.608
$2Si_2 + SiGe$	9.075
$Si_2Ge + 3Si$	11.831
$2Si_2 + Si + Ge$	12.136
$Si_2 + SiGe + 2Si$	12.297
$Si_2 + 3Si + Ge$	15.359
$SiGe + 4Si$	15.520
$5Si + Ge$	18.582

Table 4.76 Fragmentation Energies of the Most Stable $(Si_5Ge)^+$ Cationic Hexamer

Fragmented Clusters	Fragmentation Energy (eV)
$(Si_4Ge)^+ + Si$	4.043
$Si_2 + (Si_3Ge)^+$	4.392
$(Si_3Ge)^+ + Si + Si$	7.615
$Si_2 + (Si_2Ge)^+ + Si$	8.805
$Si_2 + Si_2 + (SiGe)^+$	9.125
$(Si_2Ge)^+ + Si + Si + Si$	12.027
$Si_2 + (SiGe)^+ + Si + Si$	12.348
$Si_2 + Si_2 + Si + Ge^+$	12.351
$(SiGe)^+ + Si + Si + Si + Si$	15.570
$Si_2 + Si + Si + Si + Ge^+$	15.573
$Si + Si + Si + Si + Si + Ge^+$	18.796

Table 4.77 Fragmentation Energies of the Most Stable $(Si_5Ge)^-$ Anionic Hexamer

Fragmented Clusters	Fragmentation Energy (eV)
$(Si_4Ge)^- + Si$	3.473
$(Si_3Ge)^- + Si_2$	4.088
$(Si_3Ge)^- + 2Si$	7.311
$(Si_2Ge)^- + Si_2 + Si$	8.195
$2Si_2 + (SiGe)^-$	8.996
$(Si_2Ge)^- + 3Si$	11.418
$Si_2 + (SiGe)^- + 2Si$	12.219
$2Si_2 + Si + Ge^-$	12.765
$(SiGe)^- + 4Si$	15.442
$Si_2 + 3Si + Ge^-$	15.987
$5Si + Ge^-$	19.210

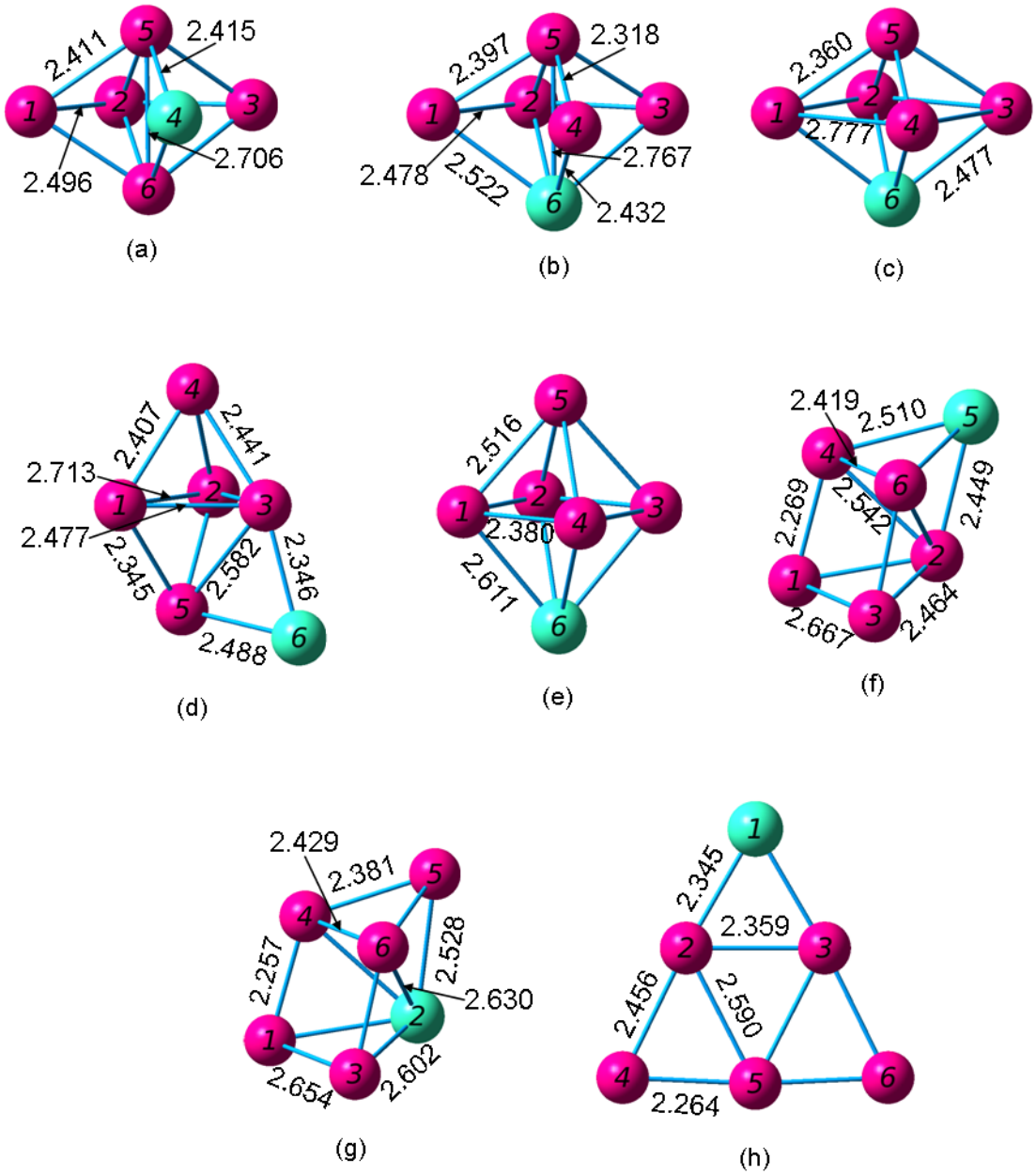

Figure 4.79 Geometries of the Si_5Ge Neutral Hexamers from (a) Most Stable through (h) Least Stable

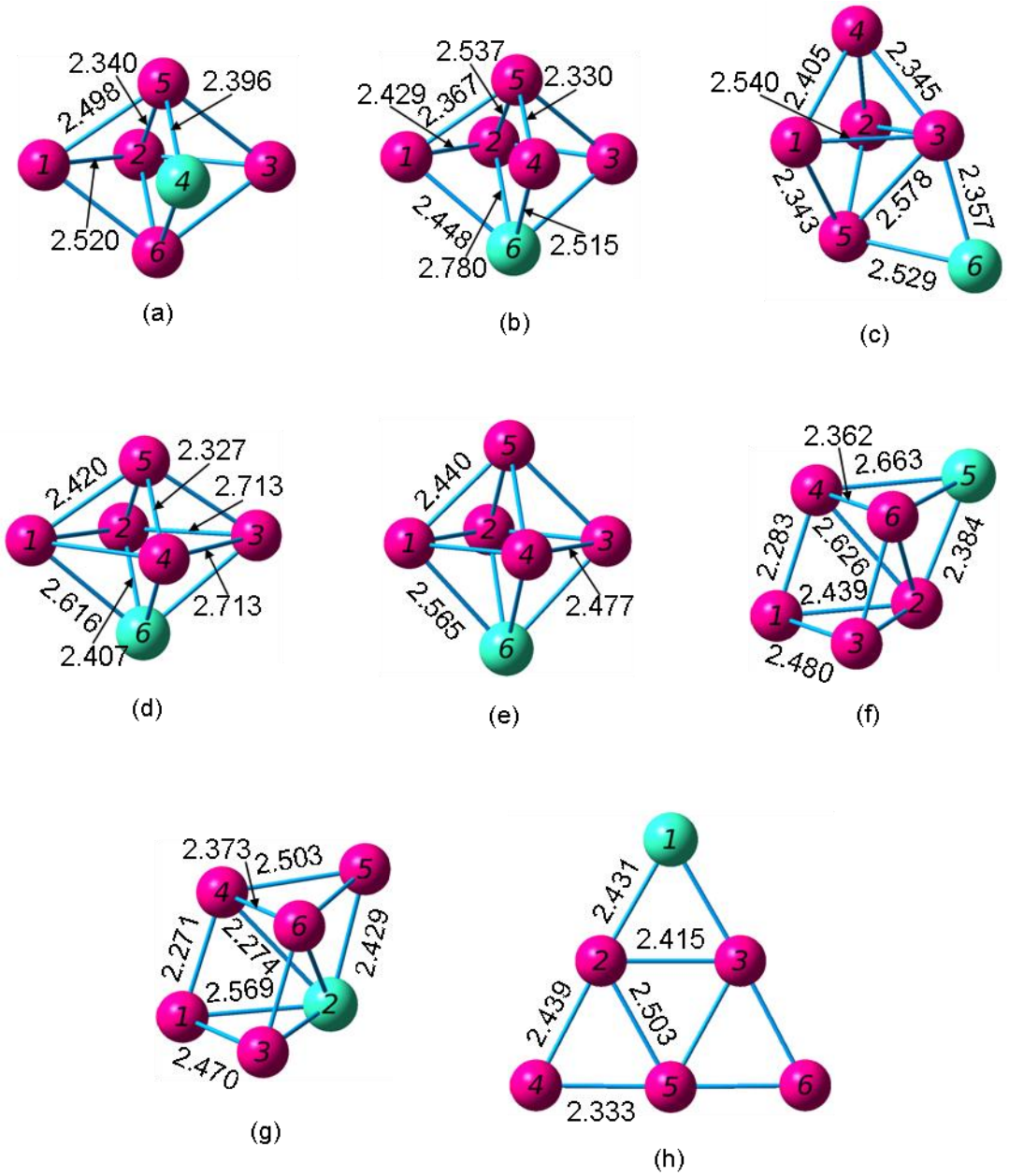

Figure 4.80 Geometries of the $(Si_5Ge)^+$ Cationic Hexamers from (a) Most Stable through (h) Least Stable

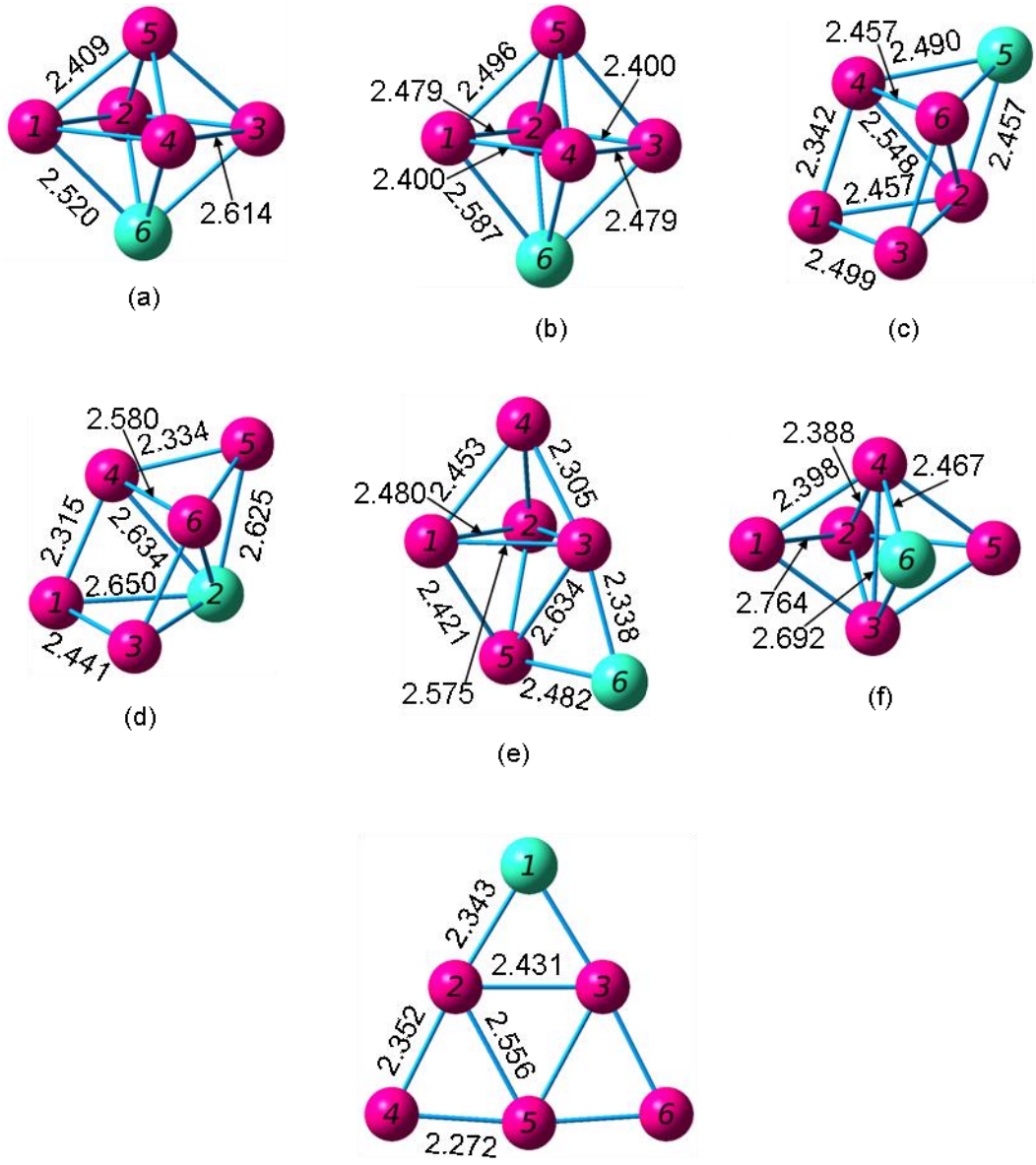

Figure 4.81 Geometries of the $(Si_5Ge)^-$ Anion Hexamers from (a) Most Stable through (g) Least Stable

4.12 Si_4Ge_2 Hexamers

For the Si_4Ge_2 hexamer, Wang and Chao [51] found one geometry for the neutral and anionic charges. It is a trapezoidal bipyramid with a symmetrical Si-Si-Ge-Ge base. In the neutral case, this cluster has a $^1A_1$ electronic state, a dissociation energy of -24.9140 eV or -24.8272 eV, a HOMO-LUMO gap of 3.38 eV, and the following frequencies: 401(a), 436(a), and 282(a). The cation cluster is a rhombic bipyramid, with a Si-Ge-Si-Ge base.

For our most stable structure, we found the same rhombic bipyramid as Wang and Chao. We found three more rhombic bipyramids with slightly different geometries and slightly higher energies. Totally, we investigated nineteen different neutral clusters and eighteen cations and anions. The neutral clusters pictured in figures 4.82 (f) and 4.82 (i) both optimized to a single cation (figure 4.83 (f)) and a single cation (figure 4.84 (g)) Even in the neutrals, these clusters are extremely similar; both are 2-d silicon squares with germanium-tipped triangles on opposite sides. The only difference is their bond lengths. The more stable (figure 4.82 (f)) originated with this geometry, but the other (figure 4.82 (i)) started out as a hexagonal structure. After optimization, the two clusters became similar.

Just as with the Si_5Ge clusters, the idea for rhombic bipyramids came from Raghavachari's work [1]. The two-dimensional structures are modifications of previous work from this group done by Pradhan and Ray [7] on silicon-carbon nanoclusters. We looked at their Si_2C_4 clusters and replaced the two silicon atoms with two germanium atoms and the four carbon atoms with four silicon atoms. After an extensive look into the two-dimensional Si_4Ge_2 clusters and Si_2Ge_4 clusters, we found that they consistently have higher energies than the bipyramid and prism-shaped clusters. As a result, our work with the other hexamers focuses on the three-dimensional clusters.

Table 4.78 Properties of the Si_4Ge_2 Hexamers

Figure	Symmetry Group	Electronic State	Binding E / Atom (eV)	HOMO-LUMO Gap (eV)	Dipole Moment (D)
4.82 (a)	C_s	$^1A'$	3.052	3.387	0.792
4.82 (b)	D_{2h}	^1A_g	3.040	3.163	0.000
4.82 (c)	C_s	$^1A'$	3.008	3.056	0.735
4.82 (d)	C_{2v}	$^1A_1$	2.944	2.929	0.304
4.82 (e)	C_{2v}	$^3B_2$	2.782	1.651[a]	0.512
4.82 (f)	D_{2h}	^1A_g	2.685	1.840	0.000
4.82 (g)	C_{2v}	$^1A_1$	2.680	1.026	0.623
4.82 (h)	C_{2v}	$^3A_2$	2.492	1.062	0.000
4.82 (i)	D_{2h}	$^3B_{1,g}$	2.439	0.103[a]	0.000
4.82 (j)	D_{2h}	$^3B_{1,g}$	2.424	1.133	0.000
4.82 (k)	C_{2v}	$^3A_2$	2.358	1.166	0.000
4.82 (l)	C_{2v}	$^1A_1$	2.282	1.357	2.052
4.82 (m)	C_{2v}	$^1A_1$	2.243	1.414	1.478
4.82 (n)	C_{2v}	$^1A_1$	2.235	1.390	1.231
4.82 (o)	$C_{\infty v}$	$^3\Sigma$	2.113	1.531[a]	1.120
4.82 (p)	$C_{\infty v}$	$^3\Sigma$	2.093	1.531[a]	0.835
4.82 (q)	$C_{\infty v}$	$^3\Sigma$	2.093	1.530[a]	0.717
4.82 (r)	$D_{\infty h}$	$^3\Sigma_g$	2.068	1.544[a]	0.000
4.82 (s)	$C_{\infty v}$	$^3\Sigma$	2.051	1.545[a]	0.248

[a] HOMO and LUMO have opposite spins; this value includes the energy required to flip the spin of the electron.

Table 4.79 Properties of the $(Si_4Ge_2)^+$ Hexamers

Figure	Symmetry Group	Electronic State	Binding E / Atom (eV)	HOMO-LUMO Gap (eV)	Dipole Moment (D)
4.83 (a)	D_{2h}	$^2B_{2,u}$	3.127	2.065[a]	0.000
4.83 (b)	C_s	$^2A'$	3.119	1.981[a]	1.161
4.83 (c)	C_s	$^2A''$	3.107	2.022[a]	1.280
4.83 (d)	C_{2v}	$^2B_2$	3.042	1.992[a]	0.051
4.83 (e)	C_{2v}	$^2B_1$	2.905	1.170	0.450
4.83 (f)	D_{2h}	$^2B_{1,u}$	2.888	1.692[a]	0.000
4.83 (g)	C_{2v}	$^2B_1$	2.847	1.096	1.077
4.83 (h)	C_{2v}	$^2B_2$	2.729	1.264	0.000
4.83 (i)	D_{2h}	$^2B_{2,u}$	2.654	1.516[a]	0.000
4.83 (j)	D_{2h}	$^2B_{2,u}$	2.587	1.448	0.000
4.83 (k)	C_{2v}	$^2B_2$	2.434	1.112	1.670
4.83 (l)	C_{2v}	$^2B_2$	2.386	1.116	2.546
4.83 (m)	C_{2v}	$^2B_2$	2.381	1.173	3.725
4.83 (n)	$C_{\infty v}$	--	2.265	0.997	4.600
4.83 (o)	$C_{\infty v}$	--	2.244	0.993	3.412
4.83 (p)	$C_{\infty v}$	--	2.244	0.993	2.036
4.83 (q)	$D_{\infty h}$	--	2.212	1.019	0.000
4.83 (r)	$C_{\infty v}$	--	2.194	1.013	1.203

[a] HOMO and LUMO have opposite spins; this value includes the energy required to flip the spin of the electron.

Table 4.80 Properties of the $(Si_4Ge_2)^-$ Hexamers

Figure	Symmetry Group	Electronic State	Binding E / Atom (eV)	HOMO-LUMO Gap (eV)	Dipole Moment (D)
4.84 (a)	C_s	^2A"	3.176	1.836[a]	2.388
4.84 (b)	D_{2h}	$^2B_{1,u}$	3.170	1.842[a]	0.000
4.84 (c)	C_s	^2A'	3.150	1.794[a]	2.185
4.84 (d)	C_{2v}	$^2B_1$	3.110	1.708[a]	0.002
4.84 (e)	C_{2v}	$^2A_2$	3.028	1.271	2.580
4.84 (f)	C_{2v}	$^2A_2$	2.992	1.263	0.746
4.84 (g)	D_{2h}	$^2B_{1,g}$	2.853	1.624[a]	0.000
4.84 (h)	C_{2v}	$^4B_1$	2.723	1.351[a]	0.000
4.84 (i)	D_{2h}	$^2B_{3,u}$	2.662	1.431[a]	0.000
4.84 (j)	D_{2h}	$^2B_{3,u}$	2.592	1.404[a]	0.000
4.84 (k)	C_{2v}	$^2B_1$	2.585	1.524	1.858
4.84 (l)	C_{2v}	$^2B_1$	2.548	1.550[a]	0.032
4.84 (m)	C_{2v}	$^2B_1$	2.542	1.522	1.734
4.84 (n)	$C_{\infty v}$	--	2.402	0.934	6.899
4.84 (o)	$C_{\infty v}$	--	2.382	0.930	5.033
4.84 (p)	$C_{\infty v}$	--	2.381	0.932	3.590
4.84 (q)	$D_{\infty h}$	--	2.364	0.945	0.000
4.84 (r)	$C_{\infty v}$	--	2.345	0.946	7.821

[a] HOMO and LUMO have opposite spins; this value includes the energy required to flip the spin of the electron.

Table 4.81 Ionization Potentials and Electron Affinities of the Si_4Ge_2 Hexamers

Neutral Figure	VIP (eV)	Cationic Figure	AIP (eV)	VEA (eV)	Anionic Figure	AEA (eV)
4.82 (a)	7.874	4.83 (b)	7.494	1.188	4.84 (a)	1.884
4.82 (b)	7.744	4.83 (a)	7.382	1.251	4.84 (b)	1.914
4.82 (c)	7.696	4.83 (c)	7.304	1.326	4.84 (c)	1.993
4.82 (d)	7.691	4.83 (d)	7.314	1.440	4.84 (d)	2.131
4.82 (e)	7.285	4.83 (e)	7.162	2.517	4.84 (e)	2.618
4.82 (f)	6.822	4.83 (f)	6.688	1.948	4.84 (g)	2.143
4.82 (g)	7.043	4.83 (g)	6.901	2.917	4.84 (f)	3.008
4.82 (h)	6.534	4.83 (h)	6.481	2.497	4.84 (h)	2.523
4.82 (i)	6.079	4.83 (f)	5.208	3.516	4.84 (g)	3.624
4.82 (j)	6.572	4.83 (i)	6.518	2.506	4.84 (i)	2.569
4.82 (k)	6.591	4.83 (j)	6.531	2.492	4.84 (j)	2.538
4.82 (l)	7.031	4.83 (k)	6.987	2.950	4.84 (k)	2.960
4.82 (m)	7.099	4.83 (l)	7.038	2.948	4.84 (l)	2.968
4.82 (n)	7.066	4.83 (m)	7.024	2.970	4.84 (m)	2.981
4.82 (o)	7.053	4.83 (n)	6.992	2.814	4.84 (n)	2.870
4.82 (p)	7.077	4.83 (o)	6.993	2.810	4.84 (o)	2.869
4.82 (q)	7.035	4.83 (p)	6.993	2.804	4.84 (p)	2.869
4.82 (r)	7.082	4.83 (q)	7.040	2.857	4.84 (q)	2.908
4.82 (s)	7.126	4.83 (r)	7.042	2.840	4.84 (r)	2.905

Table 4.82 Fragmentation Energies of the Most Stable Si_4Ge_2 Neutral Hexamer

Fragmented Clusters	Fragmentation Energy (eV)
$Si_4Ge + Ge$	3.676
$Si_3Ge_2 + Si$	3.923
$Si_3Ge + SiGe$	4.199
$Si_2Ge_2 + Si_2$	4.306
$2Si_2Ge$	4.807
$Si_3Ge + Si + Ge$	7.261
$Si_2Ge_2 + 2Si$	7.529
$Si_2Ge + Si_2 + Ge$	8.335
$SiGe_2 + Si_2 + Si$	8.434
$Si_2Ge + SiGe + Si$	8.497
$2Si_2 + Ge_2$	8.935
$2SiGe + Si_2$	8.963
$Si_2Ge + 2Si + Ge$	11.558
$SiGe_2 + 3Si$	11.657
$2Si_2 + 2Ge$	11.864
$SiGe + Si_2 + Si + Ge$	12.025
$Si_2 + Ge_2 + 2Si$	12.158
$2SiGe + 2Si$	12.186
$Si_2 + 2Si + 2Ge$	15.086
$SiGe + 3Si + Ge$	15.248
$4Si + 2Ge$	18.309

Table 4.83 Fragmentation Energies of the Most Stable $(Si_4Ge_2)^+$ Cationic Hexamer

Fragmented Clusters	Fragmentation Energy (eV)
$(Si_4Ge)^+ + Ge$	4.007
$Si_4Ge + Ge^+$	4.127
$(Si_3Ge_2)^+ + Si$	4.191
$Si_3Ge + (SiGe)^+$	4.486
$(Si_3Ge)^+ + SiGe$	4.517
$(Si_2Ge_2)^+ + Si_2$	4.644
$(Si_2Ge)^+ + Si_2Ge$	5.241
$(Si_3Ge)^+ + Si + Ge$	7.579
$Si_3Ge + Si + Ge^+$	7.712
$(Si_2Ge_2)^+ + Si + Si$	7.866
$(Si_2Ge)^+ + Si_2 + Ge$	8.769
$Si_2Ge + (SiGe)^+ + Si$	8.783
$Si_2Ge + Si_2 + Ge^+$	8.787
$(Si_2Ge)^+ + SiGe + Si$	8.930
$(SiGe_2)^+ + Si_2 + Si$	8.934
$Si_2 + Si_2 + (Ge_2)^+$	9.106
$(SiGe)^+ + Si_2 + SiGe$	9.250
$(Si_2Ge)^+ + Si + Si + Ge$	11.991
$Si_2Ge + Si + Si + Ge^+$	12.009
$(SiGe_2)^+ + Si + Si + Si$	12.156
$(SiGe)^+ + Si_2 + Si + Ge$	12.312
$Si_2 + Si_2 + Ge^+ + Ge$	12.315
$Si_2 + (Ge_2)^+ + Si + Si$	12.329
$(SiGe)^+ + SiGe + Si + Si$	12.473
$SiGe + Si_2 + Si + Ge^+$	12.476
$(SiGe)^+ + Si + Si + Si + Ge$	15.534
$Si_2 + Si + Si + Ge^+ + Ge$	15.537
$(Ge_2)^+ + Si + Si + Si + Si$	15.551
$SiGe + Si + Si + Si + Ge^+$	15.699
$Si + Si + Si + Si + Ge^+ + Ge$	18.760

Table 4.84 Fragmentation Energies of the Most Stable $(Si_4Ge_2)^-$ Anionic Hexamer

Fragmented Clusters	Fragmentation Energy (eV)
$(Si_4Ge)^- + Ge$	3.318
$(Si_3Ge_2)^- + Si$	3.628
$(Si_3Ge)^- + SiGe$	4.095
$(Si_2Ge_2)^- + Si_2$	4.225
$Si_3Ge + (SiGe)^-$	4.239
$Si_4Ge + Ge^-$	4.422
$(Si_2Ge)^- + Si_2Ge$	4.512
$(Si_3Ge)^- + Si + Ge$	7.156
$(Si_2Ge_2)^- + 2Si$	7.448
$Si_3Ge + Si + Ge^-$	8.007
$(Si_2Ge)^- + Si_2 + Ge$	8.041
$(Si_2Ge)^- + SiGe + Si$	8.202
$(SiGe_2)^- + Si_2 + Si$	8.285
$Si_2Ge + (SiGe)^- + Si$	8.536
$(SiGe)^- + Si_2 + SiGe$	9.003
$2Si_2 + (Ge_2)^-$	9.004
$Si_2Ge + Si_2 + Ge^-$	9.082
$(Si_2Ge)^- + 2Si + Ge$	11.263
$(SiGe_2)^- + 3Si$	11.508
$(SiGe)^- + Si_2 + Si + Ge$	12.064
$(SiGe)^- + SiGe + 2Si$	12.225
$Si_2 + (Ge_2)^- + 2Si$	12.226
$Si_2Ge + 2Si + Ge^-$	12.305
$2Si_2 + Ge^- + Ge$	12.610
$Si_2 + SiGe + Si + Ge^-$	12.771
$(SiGe)^- + 3Si + Ge$	15.287
$(Ge_2)^- + 4Si$	15.449
$Si_2 + 2Si + Ge^- + Ge$	15.833
$SiGe + 3Si + Ge^-$	15.994
$4Si + Ge^- + Ge$	19.055

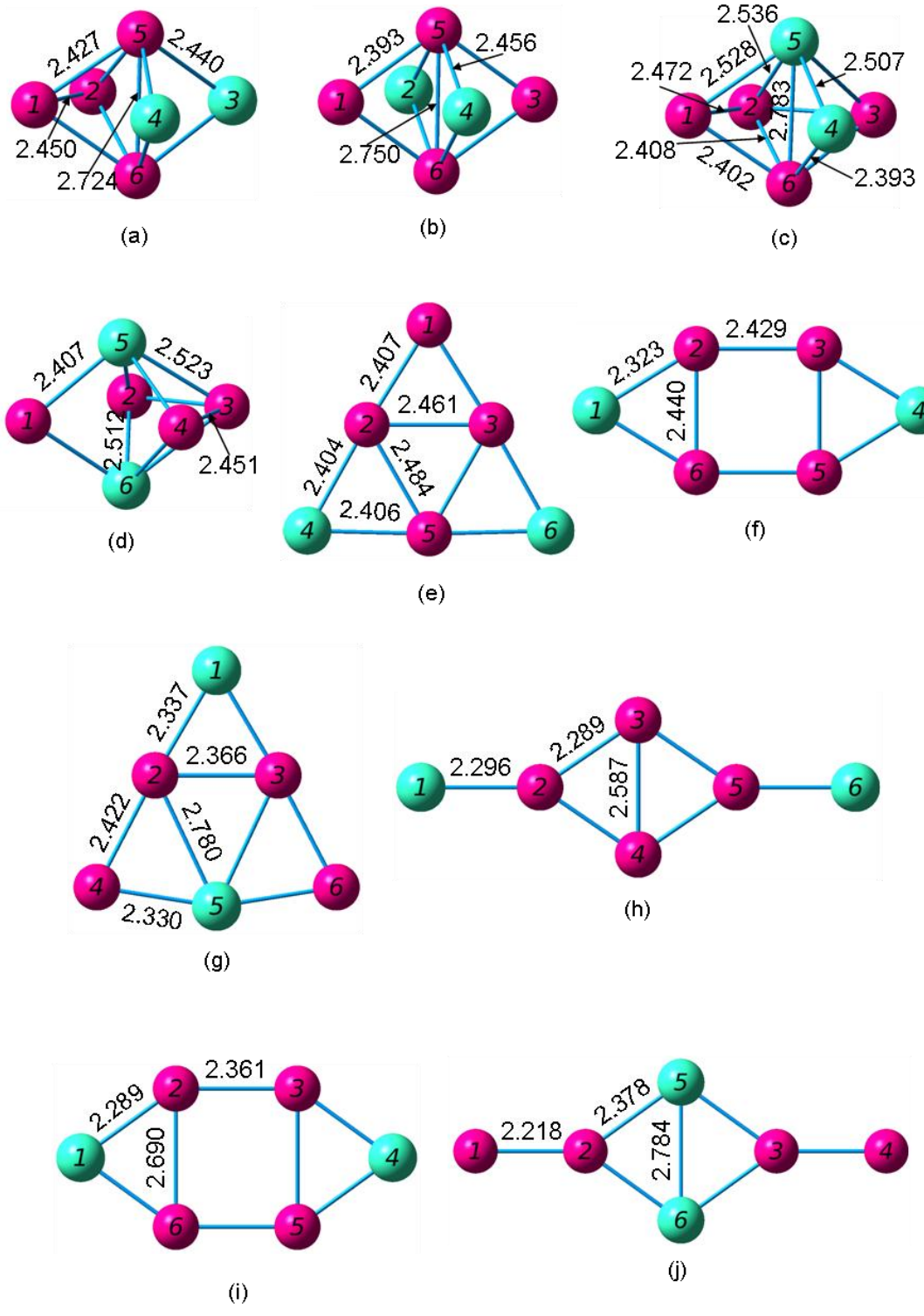

Figure 4.82 Geometries of the Si_4Ge_2 Neutral Hexamers from (a) Most Stable through (s) Least Stable

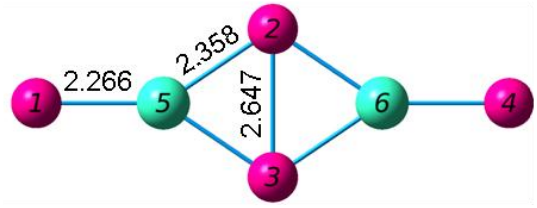

(k)

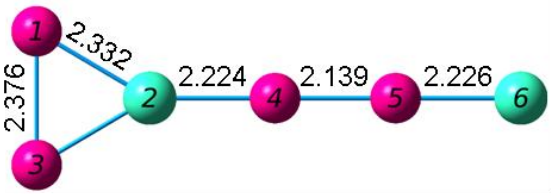

(l)

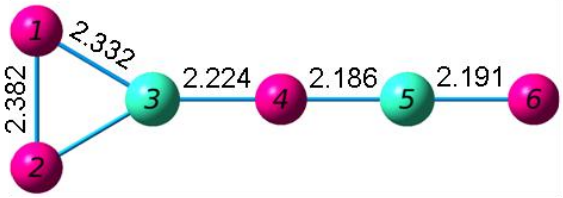

(m)

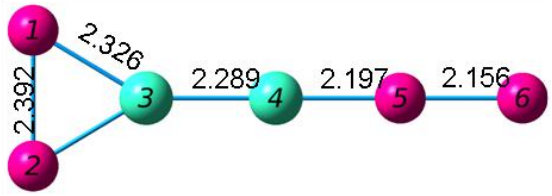

(n)

(o)

(p)

(q)

(r)

(s)

Figure 4.82 – *Continued*

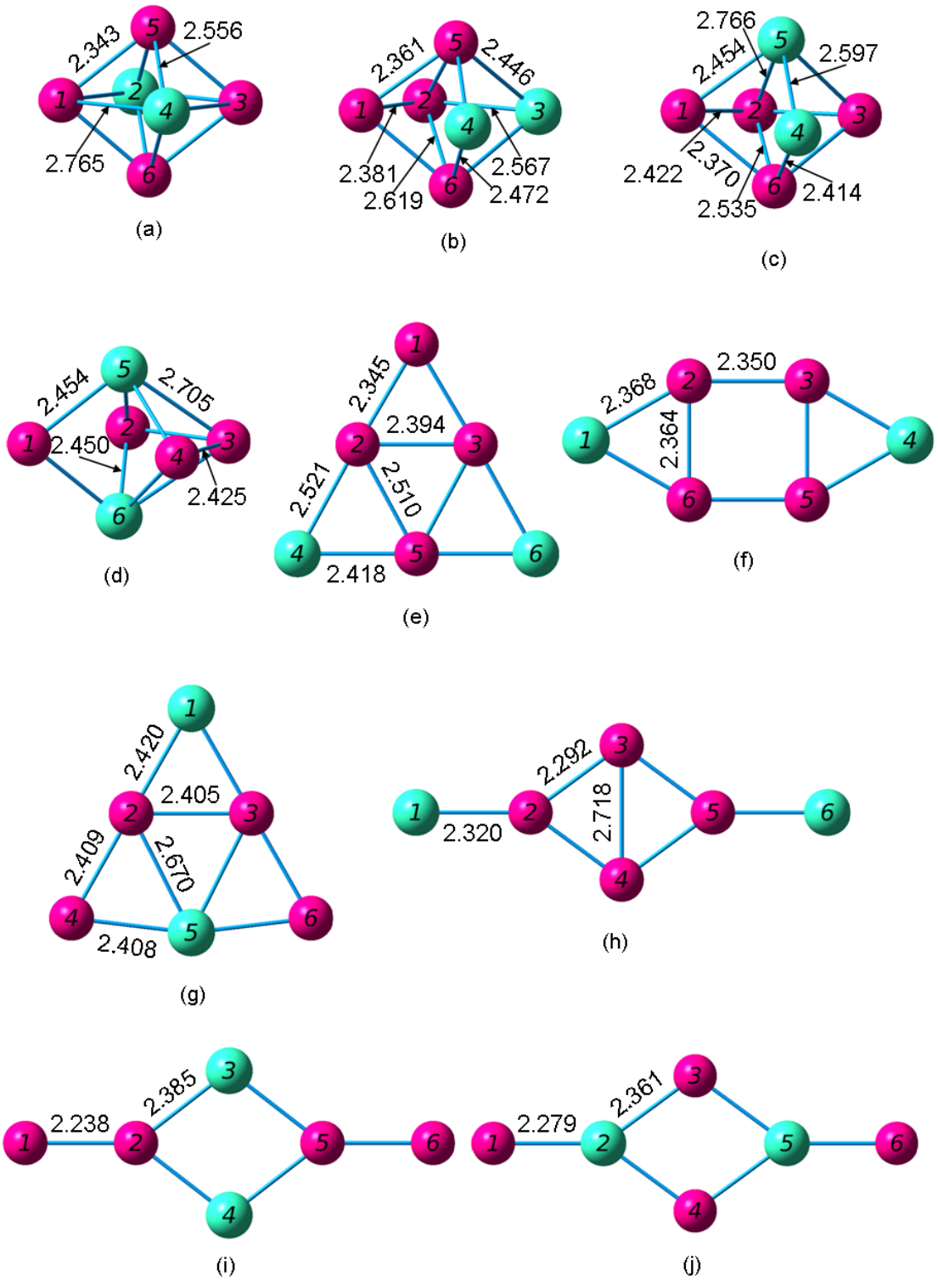

Figure 4.83 Geometries of the $(Si_4Ge_2)^+$ Cationic Hexamers from (a) Most Stable through (r) Least Stable

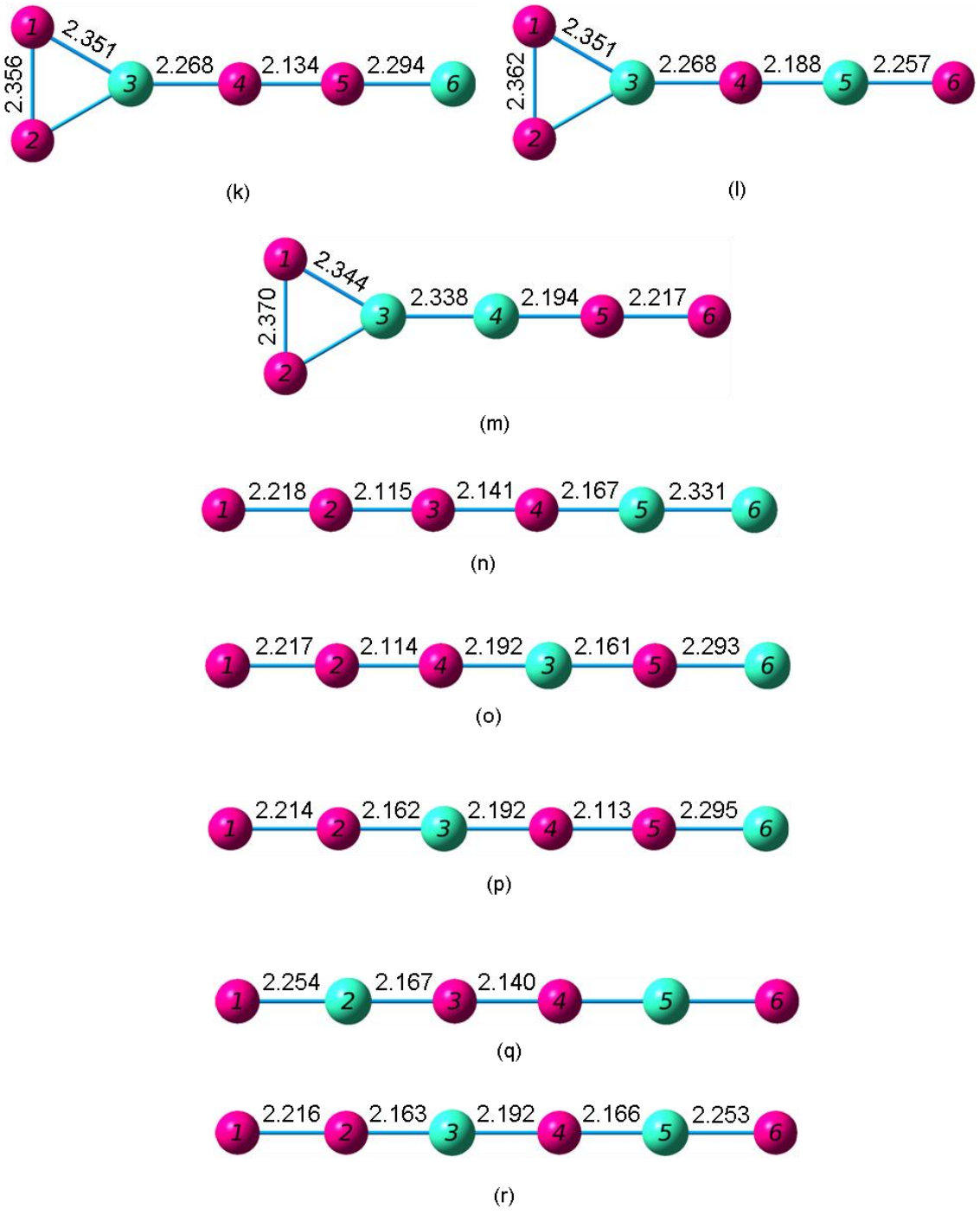

Figure 4.83 – *Continued*

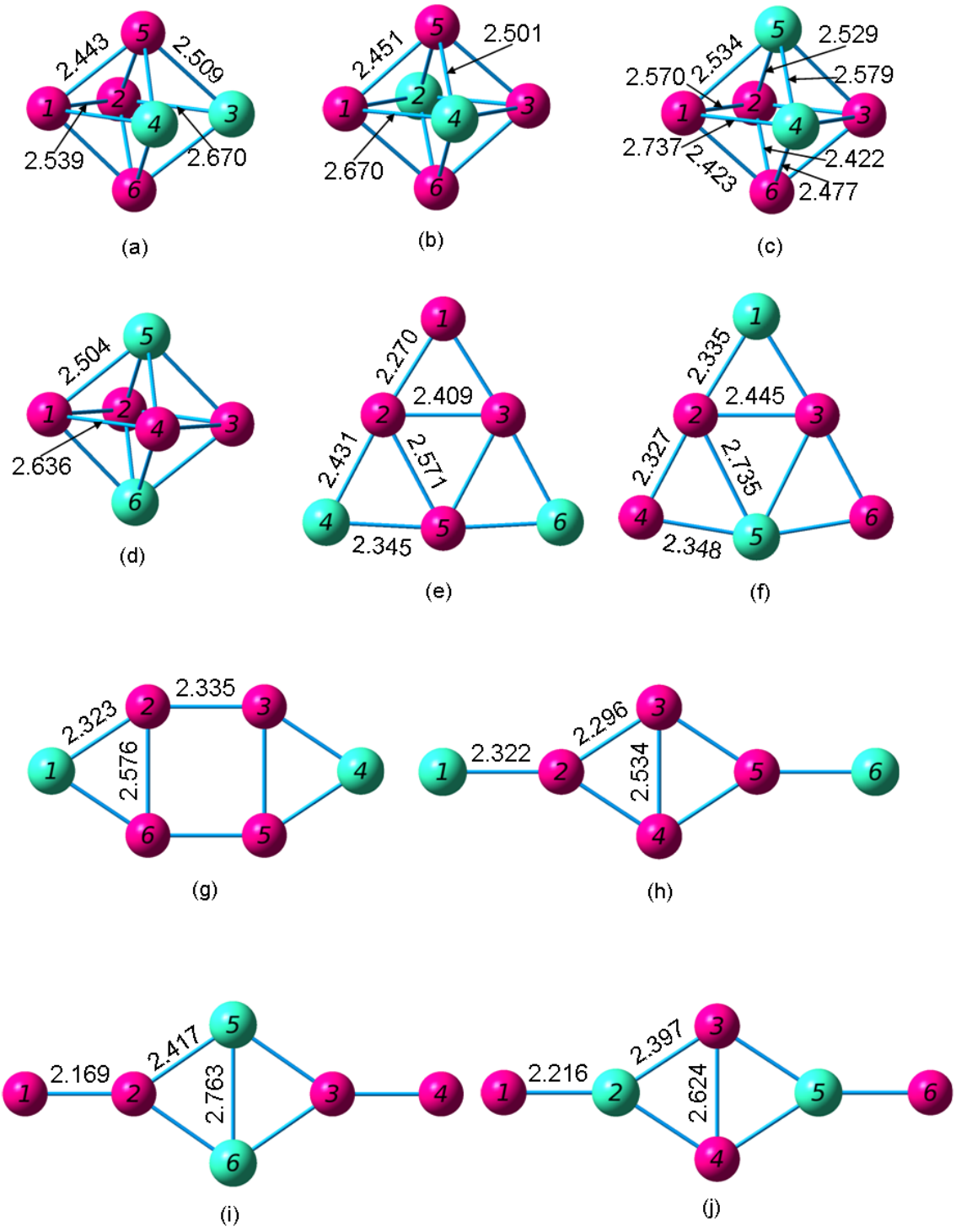

Figure 4.84 Geometries of the $(Si_4Ge_2)^-$ Anionic Hexamers from (a) Most Stable through (r) Least Stable

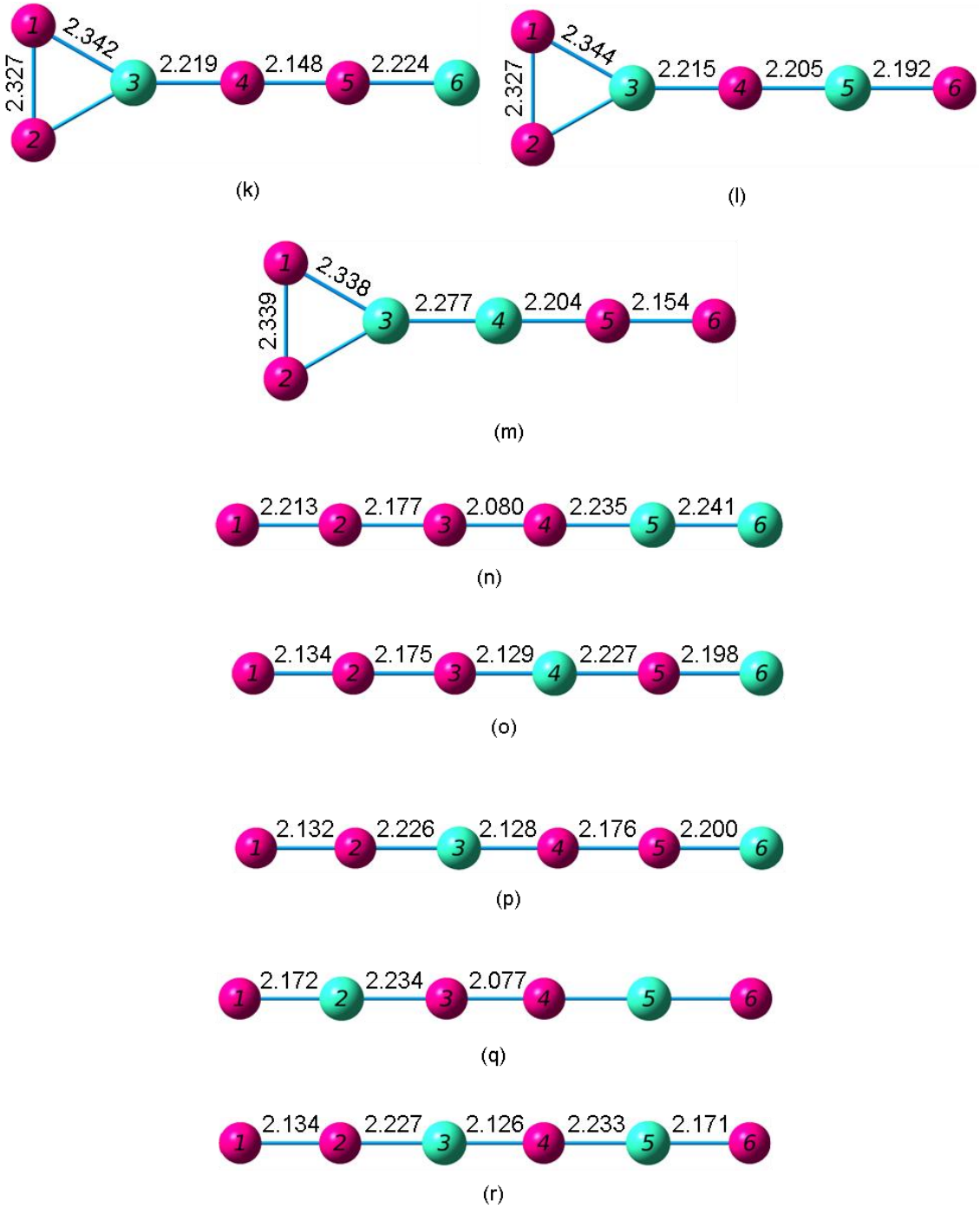

Figure 4.84 – *Continued*

4.13 Si_3Ge_3 Hexamers

Li *et al*. [48] reported a rhombic bipyramid with C_{2v} symmetry. Within this cluster there are two Si-Si bonds with lengths of 2.44 Å, two Si-Ge bonds with lengths of 2.61 Å, two Si-Ge bonds with lengths of 2.43 Å, and four Si-Ge bonds with lengths of 2.48 Å. This cluster has a $^1A_1$ electronic state, a 3.33 eV HOMO-LUMO gap, and 339(B_1), 408(A_1), and 376 (A_1) frequencies.

Wang and Chao [51] found a similar cluster for the ground state neutral, cationic, and anionic Si_3Ge_3 hexamer. In the neutral case, this cluster has a $^1A_1$ electronic state, a dissociation energy of -24.4130 eV or -24.4828 eV, a HOMO-LUMO gap of 3.33 eV, and the following frequencies: 338(a), 408(a), and 375(a).

For our most stable structure, we found the same rhombic bipyramid as Li *et al.* and Wang and Chao. We found four more rhombic bipyramids with slightly different geometries and one prism-shaped cluster. Totally, we investigated seven different neutral, cation, and anion clusters. Our input geometries came from the previous work on Si clusters, SiC clusters, and the SiGe pentamers as described in the previous sections about hexamers.

Table 4.85 Properties of the Si_3Ge_3 Hexamers

Figure	Symmetry Group	Electronic State	Binding E / Atom (eV)	HOMO-LUMO Gap (eV)	Dipole Moment (D)
4.85 (a)	C_{2v}	$^1A_1$	3.002	3.329	0.478
4.85 (b)	C_s	$^1A'$	2.966	3.155	0.861
4.85 (c)	C_s	$^1A'$	2.957	3.148	0.053
4.85 (d)	C_s	$^1A'$	2.952	2.977	0.057
4.85 (e)	C_s	$^1A'$	2.914	2.880	0.786
4.85 (f)	C_s	$^1A'$	2.867	2.299	0.091
4.85 (g)	$C_{\infty v}$	$^3\Sigma$	2.027	1.508[a]	0.521

[a] HOMO and LUMO have opposite spins; this value includes the energy required to flip the spin of the electron.

Table 4.86 Properties of the $(Si_3Ge_3)^+$ Hexamers

Figure	Symmetry Group	Electronic State	Binding E / Atom (eV)	HOMO-LUMO Gap (eV)	Dipole Moment (D)
4.86 (a)	C_{2v}	$^2A_1$	3.120	1.988[a]	0.679
4.86 (b)	C_s	^2A"	3.102	1.999[a]	0.849
4.86 (c)	C_s	^2A'	3.096	2.024[a]	0.834
4.86 (d)	C_s	^2A"	3.064	1.057	1.017
4.86 (e)	C_s	^2A'	3.041	1.583	0.704
4.86 (f)	C_s	^2A"	2.595	1.570[a]	1.418
4.86 (g)	$C_{\infty v}$	--	2.315	0.983	1.221

[a] HOMO and LUMO have opposite spins; this value includes the energy required to flip the spin of the electron.

Table 4.87 Properties of the $(Si_3Ge_3)^-$ Hexamers

Figure	Symmetry Group	Electronic State	Binding E / Atom (eV)	HOMO-LUMO Gap (eV)	Dipole Moment (D)
4.87 (a)	C_{2v}	$^2B_1$	3.074	1.814[a]	1.475
4.87 (b)	C_s	^2A'	3.066	1.768[a]	2.423
4.87 (c)	C_s	^2A'	3.052	1.774[a]	1.100
4.87 (d)	C_s	^2A"	3.010	1.681[a]	1.653
4.87 (e)	C_s	^2A'	2.975	1.529[a]	1.936
4.87 (f)	$C_{\infty v}$	--	2.185	0.919	2.185

[a] HOMO and LUMO have opposite spins; this value includes the energy required to flip the spin of the electron.

Table 4.88 Ionization Potentials and Electron Affinities of the Si_3Ge_3 Hexamers

Neutral Figure	VIP (eV)	Cationic Figure	AIP (eV)	VEA (eV)	Anionic Figure	AEA (eV)
4.85 (a)	7.833	4.86 (a)	7.468	1.197	4.87 (a)	1.847
4.85 (b)	7.781	4.86 (d)	7.640	1.259	4.87 (b)	1.950
4.85 (c)	7.712	4.86 (c)	7.329	1.288	4.87 (b)	1.970
4.85 (d)	7.643	4.86 (b)	7.217	1.363	4.87 (c)	2.001
4.85 (e)	7.867	4.86 (e)	7.532	1.425	4.87 (d)	2.041
4.85 (f)	7.609	4.86 (f)	7.388	2.022	4.87 (e)	2.184
4.85 (g)	6.996	4.86 (g)	6.956	2.803	4.87 (f)	2.865

Table 4.89 Fragmentation Energies of the Most Stable Si_3Ge_3 Neutral Hexamer

Fragmented Clusters	Fragmentation Energy (eV)
Si_3Ge_2 + Ge	3.625
Si_2Ge_3 + Si	3.875
Si_3Ge + Ge_2	4.034
Si_2Ge_2 + SiGe	4.169
$SiGe_3$ + Si_2	4.352
Si_2Ge + $SiGe_2$	4.608
Si_3Ge + 2Ge	6.963
Si_2Ge_2 + Si + Ge	7.231
$SiGe_3$ + 2Si	7.575
$SiGe_2$ + Si_2 + Ge	8.136
Si_2Ge + SiGe + Ge	8.199
$SiGe_2$ + SiGe + Si	8.297
Si_2Ge + Ge_2 + Si	8.332
Si_2 + SiGe + Ge_2	8.798
3SiGe	8.827
Si_2 + SiGe + 2Ge	11.727
Si_2 + Ge_2 + Si + Ge	11.860
2SiGe + Si + Ge	11.888
3Si + 3Ge	18.011

Table 4.90 Fragmentation Energies of the Most Stable $(Si_3Ge_3)^+$ Cationic Hexamer

Fragmented Clusters	Fragmentation Energy (eV)
$(Si_3Ge_2)^+ + Ge$	3.874
$Si_3Ge_2 + Ge^+$	4.057
$Si_3Ge + (Ge_2)^+$	4.186
$(Si_2Ge_3)^+ + Si$	4.237
$(Si_3Ge)^+ + Ge_2$	4.333
$Si_2Ge_2 + (SiGe)^+$	4.437
$(Si_2Ge_2)^+ + SiGe$	4.488
$(SiGe_3)^+ + Si_2$	4.547
$(Si_2Ge)^+ + SiGe_2$	5.022
$Si_2Ge + (SiGe_2)^+$	5.088
$(Si_3Ge)^+ + Ge + Ge$	7.262
$Si_3Ge + Ge^+ + Ge$	7.395
$(Si_2Ge_2)^+ + Si + Ge$	7.549
$Si_2Ge_2 + Si + Ge^+$	7.663
$(SiGe_3)^+ + Si + Si$	7.770
$Si_2Ge + (SiGe)^+ + Ge$	8.466
$Si_2Ge + (Ge_2)^+ + Si$	8.483
$SiGe_2 + (SiGe)^+ + Si$	8.565
$SiGe_2 + Si_2 + Ge^+$	8.568
$(Si_2Ge)^+ + SiGe + Ge$	8.613
$(SiGe_2)^+ + Si_2 + Ge$	8.617
$Si_2Ge + SiGe + Ge^+$	8.631
$(Si_2Ge)^+ + Ge_2 + Si$	8.746
$(SiGe_2)^+ + SiGe + Si$	8.778
$Si_2 + SiGe + (Ge_2)^+$	8.950
$Si_2 + (SiGe)^+ + Ge_2$	9.066
$(SiGe)^+ + SiGe + SiGe$	9.094
$Si_2 + (SiGe)^+ + Ge + Ge$	11.994
$Si_2 + (Ge_2)^+ + Si + Ge$	12.011
$(SiGe)^+ + SiGe + Si + Ge$	12.156
$Si_2 + SiGe + Ge^+ + Ge$	12.159
$Si_2 + Ge_2 + Si + Ge^+$	12.292
$SiGe + SiGe + Si + Ge^+$	12.320
$Si + Si + Si + Ge^+ + Ge + Ge$	18.443

Table 4.91 Fragmentation Energies of the Most Stable $(Si_3Ge_3)^-$ Anionic Hexamer

Fragmented Clusters	Fragmentation Energy (eV)
$(Si_3Ge_2)^- + Ge$	3.293
$(Si_2Ge_3)^- + Si$	3.596
$(Si_3Ge)^- + Ge_2$	3.893
$(Si_2Ge_2)^- + SiGe$	4.051
$Si_3Ge + (Ge_2)^-$	4.066
$Si_2Ge_2 + (SiGe)^-$	4.171
$(SiGe_3)^- + Si_2$	4.265
$(Si_2Ge)^- + SiGe_2$	4.276
$Si_3Ge_2 + Ge^-$	4.334
$Si_2Ge + (SiGe_2)^-$	4.421
$(Si_3Ge)^- + 2Ge$	6.821
$(Si_2Ge_2)^- + Si + Ge$	7.112
$(SiGe_3)^- + 2Si$	7.488
$Si_3Ge + Ge^- + Ge$	7.672
$(Si_2Ge)^- + SiGe + Ge$	7.867
$Si_2Ge_2 + Si + Ge^-$	7.940
$(SiGe_2)^- + Si_2 + Ge$	7.950
$(Si_2Ge)^- + Ge_2 + Si$	8.000
$(SiGe_2)^- + SiGe + Si$	8.111
$Si_2Ge + (SiGe)^- + Ge$	8.201
$SiGe_2 + (SiGe)^- + Si$	8.299
$Si_2Ge + (Ge_2)^- + Si$	8.363
$Si_2 + (SiGe)^- + Ge_2$	8.800
$(SiGe)^- + 2SiGe$	8.829
$Si_2 + SiGe + (Ge_2)^-$	8.830
$SiGe_2 + Si_2 + Ge^-$	8.845
$Si_2Ge + SiGe + Ge^-$	8.908
$Si_2 + (SiGe)^- + 2Ge$	11.729
$(SiGe)^- + SiGe + Si + Ge$	11.890
$Si_2 + (Ge_2)^- + Si + Ge$	11.891

Table 4.91 – *Continued*

Fragmented Clusters	Fragmentation Energy (eV)
Si_2 + SiGe + Ge^- + Ge	12.436
Si_2 + Ge_2 + Si + Ge^-	12.569
2SiGe + Si + Ge^-	12.597
3Si + Ge^- + 2Ge	18.720

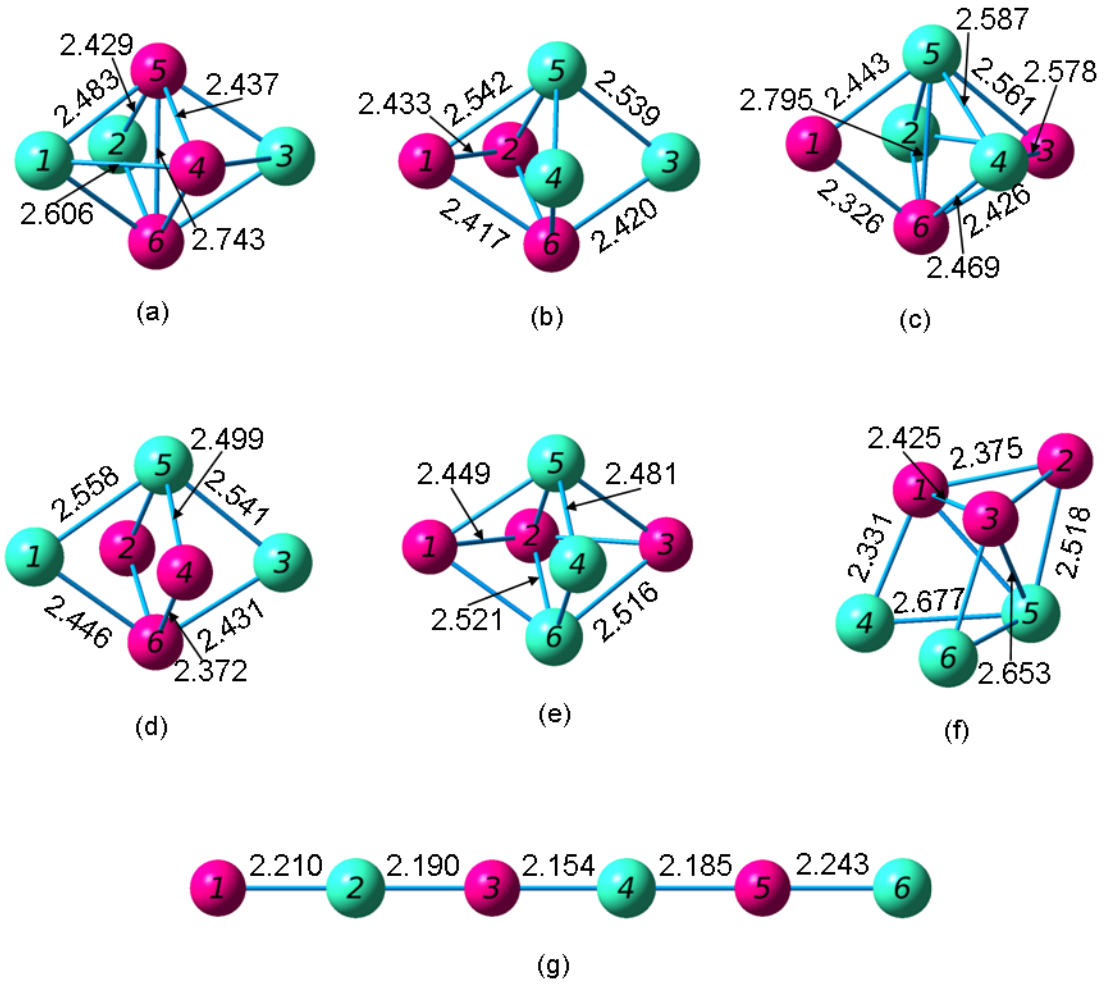

Figure 4.85 Geometries of the Si_3Ge_3 Neutral Hexamers from (a) Most Stable through (g) Least Stable

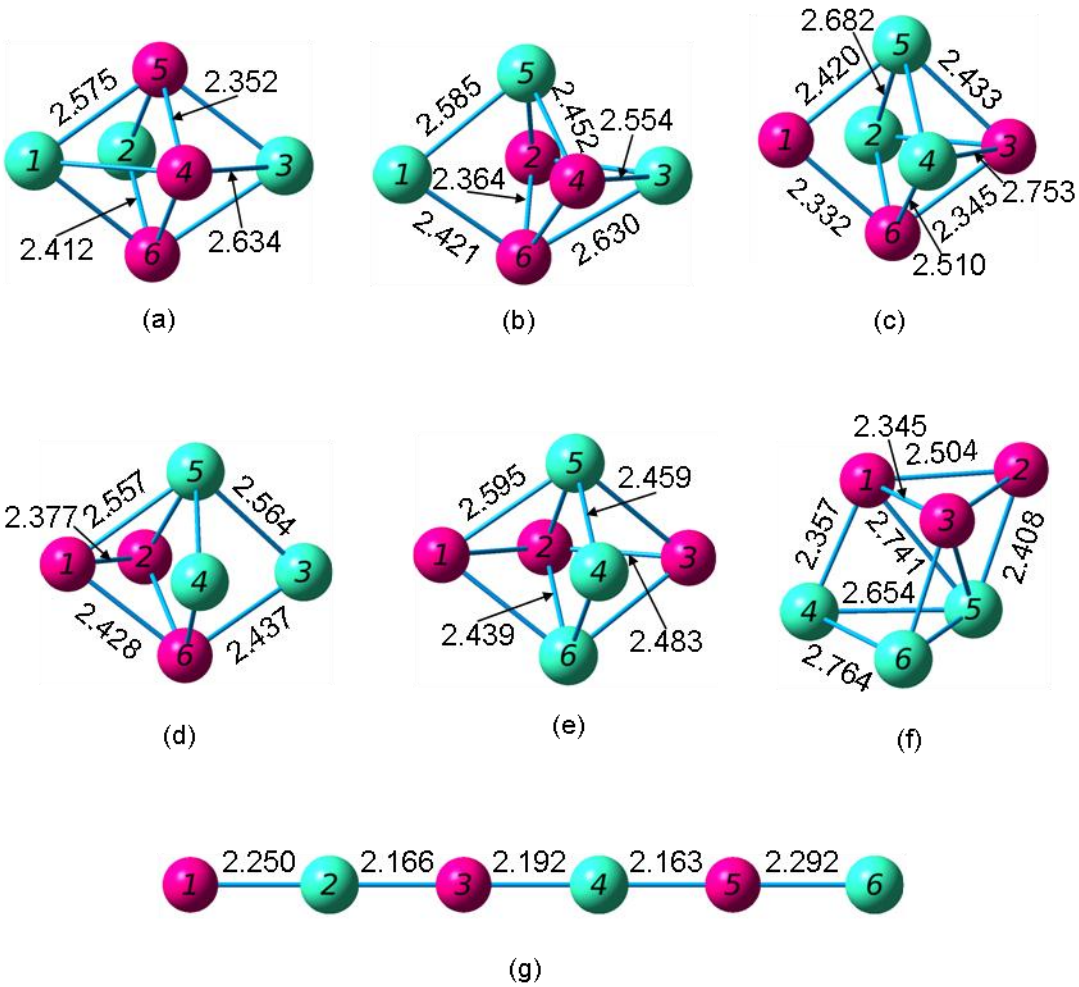

Figure 4.86 Geometries of the $(Si_3Ge_3)^+$ Cationic Hexamers from (a) Most Stable through (g) Least Stable

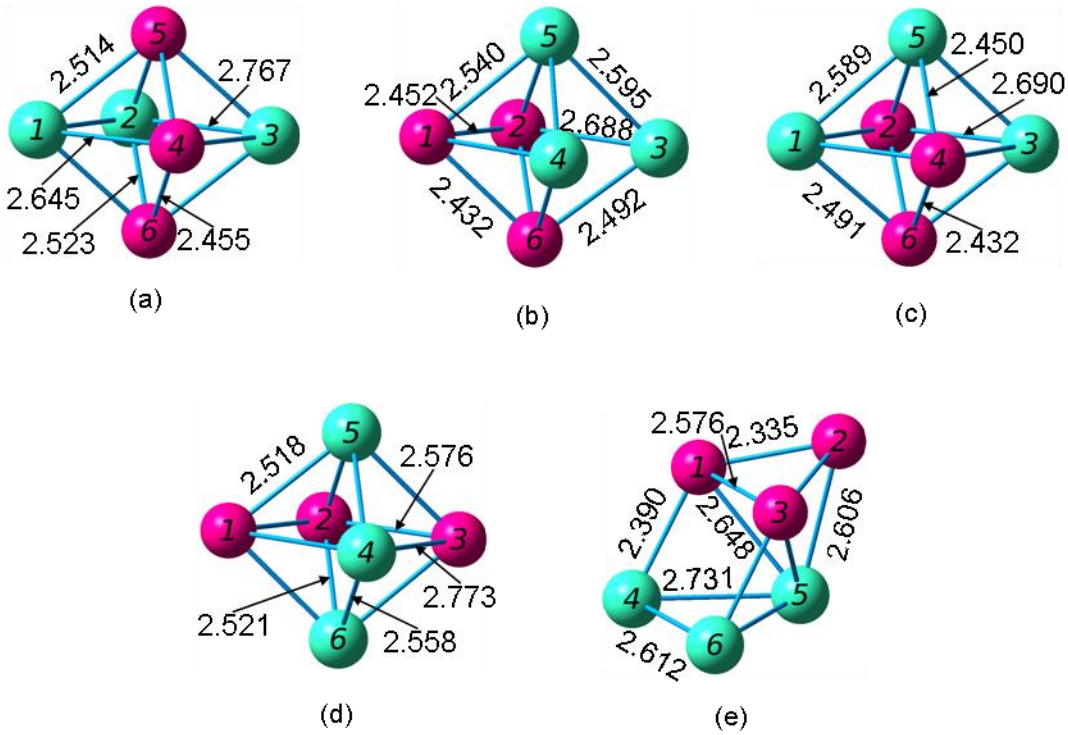

Figure 4.87 Geometries of the $(Si_3Ge_3)^-$ Anionic Hexamers from (a) Most Stable through (f) Least Stable

4.14 Si_2Ge_4 Hexamers

Adriotis, Menon, and Froudakis [47] reported results for only one hexamer, the Si_2Ge_4 rhombic bipyramid. The base of this pyramid is a Si2Ge2 rhombus (with a 2.933 Å or 2.76 Å Si-Si bond through the middle). The other bonds are Si-Ge with lengths 2.508 Å or 2.47 Å and Ge-Ge bonds with lengths 2.877 Å or 2.91 Å.

Wang and Chao [51] found a similar cluster for the ground state neutral and anionic Si_2Ge_4 hexamer. In the neutral case, this cluster has a ^1A electronic state, a dissociation energy of -24.3170 eV or -24.1520 eV, a HOMO-LUMO gap of 3.41 eV, and the following frequencies: 332(a), 332(a), and 249(a). The cation cluster is also a rhombic bipyramid, but it is asymmetrical, and the Si-Si bond is not through the middle.

For our most stable structure, we found the same rhombic bipyramid as Adriotis, Menon, and Froudakis and Wang and Chao. We found three more rhombic bipyramids with slightly different geometries, one prism-shaped cluster, and several two-dimensional clusters. Totally, we investigated eleven different neutral cation, and anion clusters.

Table 4.92 Properties of the Si_2Ge_4 Hexamers

Figure	Symmetry Group	Electronic State	Binding E / Atom (eV)	HOMO-LUMO Gap (eV)	Dipole Moment (D)
4.88 (a)	D_{4h}	$^1A_{1,g}$	2.954	3.408	0.000
4.88 (b)	C_s	$^1A'$	2.922	3.186	0.515
4.88 (c)	C_{2v}	$^1A_1$	2.876	2.911	0.957
4.88 (d)	D_{2h}	^1A_g	2.857	2.804	0.000
4.88 (e)	C_s	$^1A'$	2.814	2.242	0.273
4.88 (f)	C_{2h}	^1A_g	2.663	2.518	0.000
4.88 (g)	C_{2v}	$^1A_1$	2.403	1.405	0.443
4.88 (h)	D_{2h}	$^3B_{1,g}$	2.321	1.070	0.000
4.88 (i)	D_{2h}	^1A_g	2.276	1.210	0.000
4.88 (j)	C_{2v}	$^1A_1$	2.157	1.368	2.288
4.88 (k)	$D_{\infty h}$	$^3\Sigma_g$	2.026	1.474[a]	0.000

[a] HOMO and LUMO have opposite spins; this value includes the energy required to flip the spin of the electron.

Table 4.93 Properties of the $(Si_2Ge_4)^+$ Hexamers

Figure	Symmetry Group	Electronic State	Binding E / Atom (eV)	HOMO-LUMO Gap (eV)	Dipole Moment (D)
4.89 (a)	C_s	$^2A'$	3.007	1.952[a]	0.884
4.89 (b)	D_{2h}	$^2B_{2,u}$	3.006	1.780	0.000
4.89 (c)	C_{2v}	$^2B_2$	2.932	1.039	0.305
4.89 (d)	C_s	$^2A''$	2.917	1.551[a]	0.929
4.89 (e)	D_{2h}	$^2B_{3,u}$	2.904	1.395	0.000
4.89 (f)	C_{2h}	^2B_u	2.758	1.180	0.000
4.89 (g)	C_{2v}	$^2B_2$	2.599	1.496	1.121
4.89 (h)	D_{2h}	$^2B_{2,u}$	2.573	1.322	0.000
4.89 (i)	D_{2h}	$^2B_{2,u}$	2.514	1.448	0.000
4.89 (j)	C_{2v}	$^2B_2$	2.321	1.171	0.544
4.89 (k)	$D_{\infty h}$	--	2.197	0.958	0.000

[a] HOMO and LUMO have opposite spins; this value includes the energy required to flip the spin of the electron.

Table 4.94 Properties of the $(Si_2Ge_4)^-$ Hexamers

Figure	Symmetry Group	Electronic State	Binding E / Atom (eV)	HOMO-LUMO Gap (eV)	Dipole Moment (D)
4.90 (a)	D_{4h}	$^2A_{2,u}$	3.068	1.790[a]	0.000
4.90 (b)	C_s	$^2A'$	3.051	1.746[a]	1.653
4.90 (c)	C_{2v}	$^2B_2$	3.035	1.509[a]	1.979
4.90 (d)	D_{2h}	$^2B_{2,u}$	3.015	1.662[a]	0.000
4.90 (e)	C_s	$^2A'$	2.983	1.526[a]	0.940
4.90 (f)	C_{2h}	^2B_g	2.809	1.407[a]	0.000
4.90 (g)	C_{2v}	$^2B_1$	2.649	1.408[a]	1.630
4.90 (h)	D_{2h}	$^4B_{2,g}$	2.545	1.276[a]	0.000
4.90 (i)	D_{2h}	$^2B_{3,u}$	2.509	1.459	0.000
4.90 (j)	C_{2v}	$^2B_1$	2.451	1.477	3.384
4.90 (k)	$D_{\infty h}$	--	2.307	0.897	0.000

[a] HOMO and LUMO have opposite spins; this value includes the energy required to flip the spin of the electron.

Table 4.95 Ionization Potentials and Electron Affinities of the Si_2Ge_4 Hexamers

Neutral Figure	VIP (eV)	Cationic Figure	AIP (eV)	VEA (eV)	Anionic Figure	AEA (eV)
4.88 (a)	7.937	4.89 (b)	7.585	1.212	4.90 (a)	1.824
4.88 (b)	7.766	4.89 (a)	7.391	1.262	4.90 (b)	1.913
4.88 (c)	7.704	4.89 (c)	7.565	1.478	4.90 (c)	2.092
4.88 (d)	7.950	4.89 (e)	7.620	1.466	4.90 (d)	2.084
4.88 (e)	7.506	4.89 (d)	7.282	2.010	4.90 (e)	2.151
4.88 (f)	7.411	4.89 (f)	7.326	1.823	4.90 (f)	2.017
4.88 (g)	6.933	4.89 (g)	6.729	2.452	4.90 (g)	2.610
4.88 (h)	6.438	4.89 (h)	6.391	2.455	4.90 (h)	2.481
4.88 (i)	6.528	4.89 (i)	6.472	2.479	4.90 (i)	2.538
4.88 (j)	6.981	4.89 (j)	6.915	2.874	4.90 (j)	2.900
4.88 (k)	6.922	4.89 (k)	6.873	2.761	4.90 (k)	2.824

Table 4.96 Fragmentation Energies of the Most Stable Si_2Ge_4 Neutral Hexamer

Fragmented Clusters	Fragmentation Energy (eV)
$Si_2Ge_3 + Ge$	3.587
$SiGe_4 + Si$	3.986
$Si_2Ge_2 + Ge_2$	4.014
$SiGe_3 + SiGe$	4.225
$2SiGe_2$	4.419
$Si_2Ge_2 + 2Ge$	6.943
$SiGe_3 + Si + Ge$	7.287
$SiGe_2 + SiGe + Ge$	8.009
$Si_2Ge + Ge_2 + Ge$	8.044
$SiGe_2 + Ge_2 + Si$	8.142
$Si_2 + 2Ge_2$	8.643
$2SiGe + Ge_2$	8.672
$Si_2Ge + 3Ge$	10.972
$SiGe_2 + Si + 2Ge$	11.071
$Si_2 + Ge_2 + 2Ge$	11.572
$2SiGe + 2Ge$	11.600
$SiGe + Ge_2 + Si + Ge$	11.733
$2Ge_2 + 2Si$	11.866
$Si_2 + 4Ge$	14.500
$SiGe + Si + 3Ge$	14.662
$Ge_2 + 2Si + 2Ge$	14.795
$2Si + 4Ge$	17.723

Table 4.97 Fragmentation Energies of the Most Stable $(Si_2Ge_4)^+$ Cationic Hexamer

Fragmented Clusters	Fragmentation Energy (eV)
$(Si_2Ge_3)^+ + Ge$	3.836
$Si_2Ge_3 + Ge^+$	3.905
$Si_2Ge_2 + (Ge_2)^+$	4.053
$(SiGe_4)^+ + Si$	4.183
$(Si_2Ge_2)^+ + Ge_2$	4.220
$(SiGe_3)^+ + SiGe$	4.308
$SiGe_3 + (SiGe)^+$	4.380
$(SiGe_2)^+ + SiGe_2$	4.786
$(Si_2Ge_2)^+ + Ge + Ge$	7.148
$Si_2Ge_2 + Ge^+ + Ge$	7.262
$(SiGe_3)^+ + Si + Ge$	7.369
$SiGe_3 + Si + Ge^+$	7.606
$Si_2Ge + (Ge_2)^+ + Ge$	8.082
$SiGe_2 + (SiGe)^+ + Ge$	8.164
$SiGe_2 + (Ge_2)^+ + Si$	8.181
$SiGe_2 + SiGe + Ge^+$	8.328
$(Si_2Ge)^+ + Ge_2 + Ge$	8.345
$Si_2Ge + Ge_2 + Ge^+$	8.363
$(SiGe_2)^+ + SiGe + Ge$	8.377
$(SiGe_2)^+ + Ge_2 + Si$	8.510
$Si_2 + (Ge_2)^+ + Ge_2$	8.682
$SiGe + SiGe + (Ge_2)^+$	8.710
$(SiGe)^+ + SiGe + Ge_2$	8.826
$(Si_2Ge)^+ + Ge + Ge + Ge$	11.273
$Si_2Ge + Ge^+ + Ge + Ge$	11.291
$SiGe_2 + Si + Ge^+ + Ge$	11.390
$(SiGe_2)^+ + Si + Ge + Ge$	11.438
$Si_2 + (Ge_2)^+ + Ge + Ge$	11.610
$(SiGe)^+ + SiGe + Ge + Ge$	11.755
$SiGe + (Ge_2)^+ + Si + Ge$	11.772
$(SiGe)^+ + Ge_2 + Si + Ge$	11.888

Table 4.97 – *Continued*

Fragmented Clusters	Fragmentation Energy (eV)
$Si_2 + Ge_2 + Ge^+ + Ge$	11.891
$(Ge_2)^+ + Ge_2 + Si + Si$	11.905
$SiGe + SiGe + Ge^+ + Ge$	11.919
$SiGe + Ge_2 + Si + Ge^+$	12.052
$(SiGe)^+ + Si + Ge + Ge + Ge$	14.816
$Si_2 + Ge^+ + Ge + Ge + Ge$	14.819
$(Ge_2)^+ + Si + Si + Ge + Ge$	14.833
$SiGe + Si + Ge^+ + Ge + Ge$	14.981
$Ge_2 + Si + Si + Ge^+ + Ge$	15.113
$Si + Si + Ge^+ + Ge + Ge + Ge$	18.042

Table 4.98 Fragmentation Energies of the Most Stable $(Si_2Ge_4)^-$ Anionic Hexamer

Fragmented Clusters	Fragmentation Energy (eV)
$(Si_2Ge_3)^- + Ge$	3.285
$(SiGe_4)^- + Si$	3.655
$(Si_2Ge_2)^- + Ge_2$	3.873
$Si_2Ge_2 + (Ge_2)^-$	4.023
$(SiGe_3)^- + SiGe$	4.116
$SiGe_3 + (SiGe)^-$	4.205
$(SiGe_2)^- + SiGe_2$	4.210
$Si_2Ge_3 + Ge^-$	4.273
$(Si_2Ge_2)^- + 2Ge$	6.802
$(SiGe_3)^- + Si + Ge$	7.177
$Si_2Ge_2 + Ge^- + Ge$	7.629
$(Si_2Ge)^- + Ge_2 + Ge$	7.689
$(SiGe_2)^- + SiGe + Ge$	7.800
$(SiGe_2)^- + Ge_2 + Si$	7.933
$SiGe_3 + Si + Ge^-$	7.973
$SiGe_2 + (SiGe)^- + Ge$	7.989
$Si_2Ge + (Ge_2)^- + Ge$	8.053
$SiGe_2 + (Ge_2)^- + Si$	8.151
$(SiGe)^- + SiGe + Ge_2$	8.651
$Si_2 + (Ge_2)^- + Ge_2$	8.652
$2SiGe + (Ge_2)^-$	8.681
$SiGe_2 + SiGe + Ge^-$	8.696
$Si_2Ge + Ge_2 + Ge^-$	8.730
$(Si_2Ge)^- + 3Ge$	10.617
$(SiGe_2)^- + Si + 2Ge$	10.862
$(SiGe)^- + SiGe + 2Ge$	11.580
$Si_2 + (Ge_2)^- + 2Ge$	11.581
$Si_2Ge + Ge^- + 2Ge$	11.659
$(SiGe)^- + Ge_2 + Si + Ge$	11.713
$SiGe + (Ge_2)^- + Si + Ge$	11.742
$SiGe_2 + Si + Ge^- + Ge$	11.757

Table 4.98 – *Continued*

Fragmented Clusters	Fragmentation Energy (eV)
$(Ge_2)^- + Ge_2 + 2Si$	11.875
$Si_2 + Ge_2 + Ge^- + Ge$	12.258
$2SiGe + Ge^- + Ge$	12.287
$SiGe + Ge_2 + Si + Ge^-$	12.420
$(SiGe)^- + Si + 3Ge$	14.641
$(Ge_2)^- + 2Si + 2Ge$	14.803
$Si_2 + Ge^- + 3Ge$	15.187
$SiGe + Si + Ge^- + 2Ge$	15.348
$Ge_2 + 2Si + Ge^- + Ge$	15.481
$2Si + Ge^- + 3Ge$	18.410

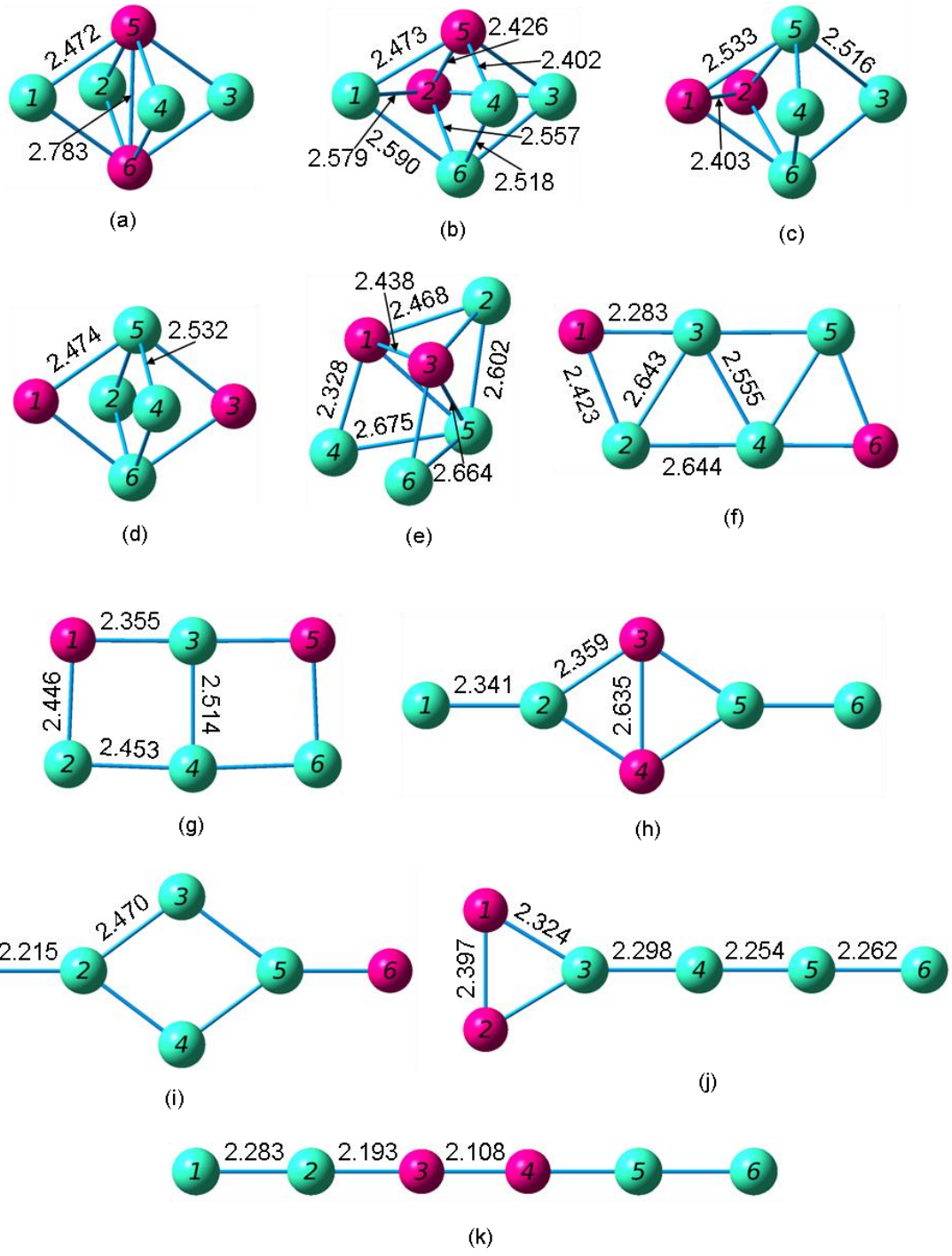

Figure 4.88 Geometries of the Si_2Ge_4 Neutral Hexamers from (a) Most Stable through (k) Least Stable

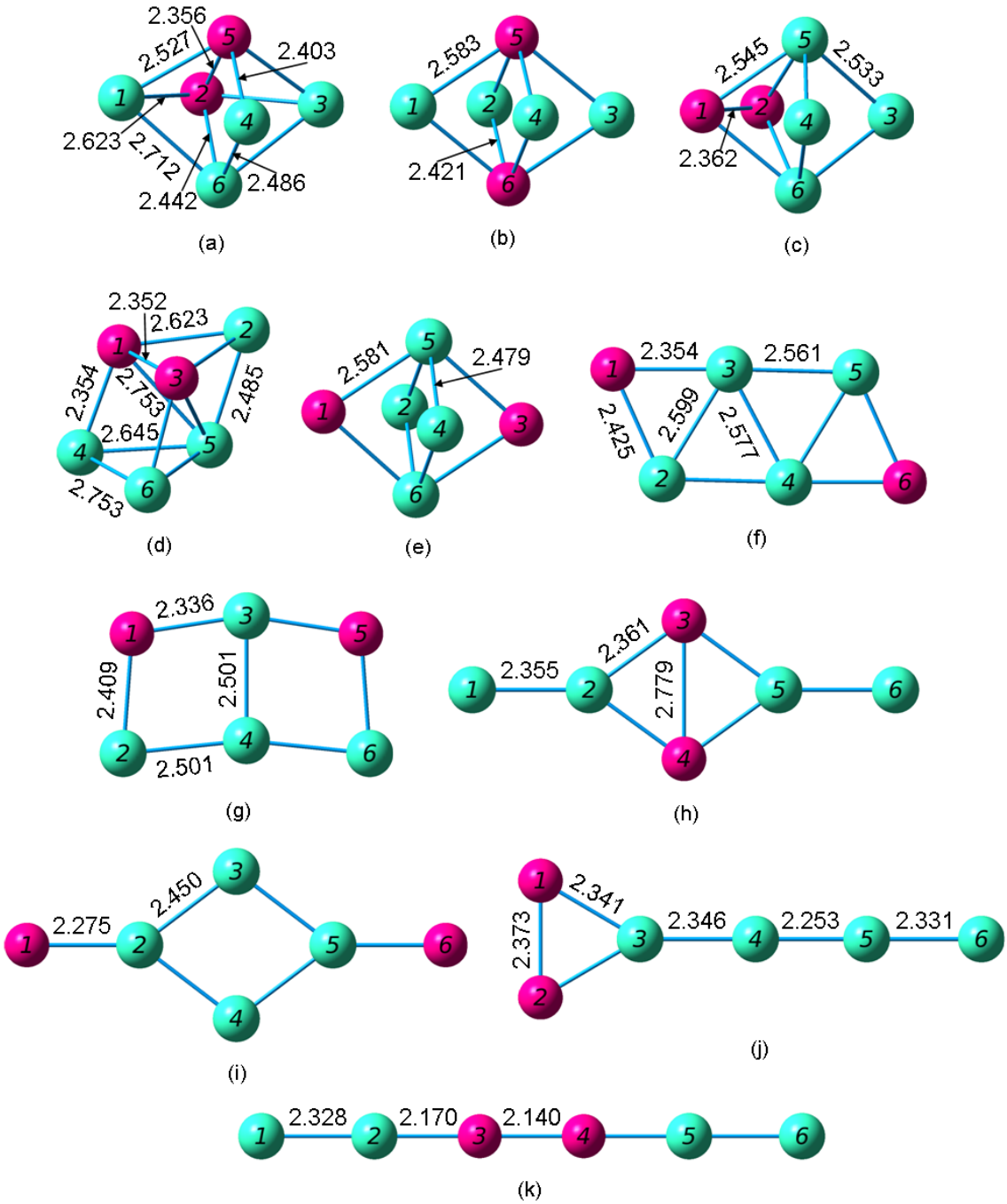

Figure 4.89 Geometries of the $(Si_2Ge_4)^+$ Cation Hexamers from (a) Most Stable through (k) Least Stable

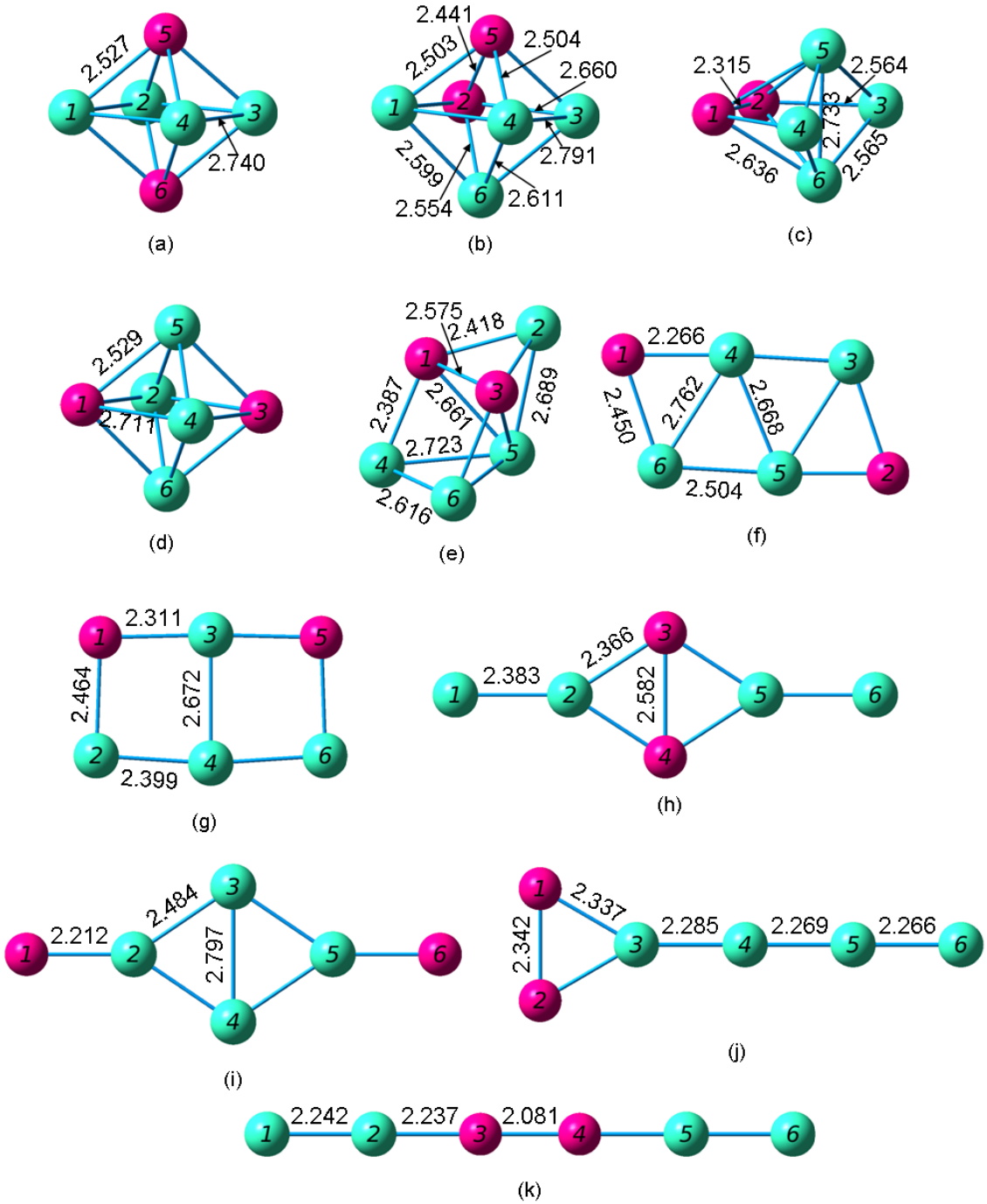

Figure 4.90 Geometries of the $(Si_2Ge_4)^-$ Anion Hexamers from (a) Most Stable through (k) Least Stable

4.15 $SiGe_5$ Hexamers

Only Wang and Chao [51] have previously studied the $SiGe_5$ hexamer. For the neutral cluster, they found two different bipyramids. The most stable is a square bipyramid with C_{4v} symmetry, a $^1A_1$ electronic state, a dissociation energy of -23.6127 eV or -23.6485 eV, a HOMO-LUMO gap of 3.22 eV, and the following frequencies: 339(a), 338(a), and 219(a). The other cluster is a rhombic bipyramid with C_{2v} symmetry, a $^1A_1$ electronic state, a dissociation energy of -22.4562 eV or -23.4307 eV, a HOMO-LUMO gap of 3.22 eV, and the following frequencies: 339(b1), 339(b2), 220(b2) and 220(b1). They also reported finding a cation and anion cluster with the same geometry as the most stable neutral cluster.

For our two most stable structures, we found the same rhombic bipyramids as Wang and Chao. We found four more three-dimensional clusters. Totally, we investigated six different neutral, cation, and anion clusters. Their input geometries came from the optimized Si5Ge clusters. We simply switched the replaced each silicon atom with a germanium atom and the germanium atom with a silicon atom and re-optimized them. Two input clusters led to the same output cluster, and the resulting geometries are pictured in figures 4.91, 4.92, 4.93.

Table 4.99 Properties of the $SiGe_5$ Hexamers

Figure	Symmetry Group	Electronic State	Binding E / Atom (eV)	HOMO-LUMO Gap (eV)	Dipole Moment (D)
4.91 (a)	C_s	$^1A'$	2.877	3.222	0.024
4.91 (b)	C_{2v}	$^1A_1$	2.838	3.032	0.559
4.91 (c)	C_s	$^1A'$	2.742	2.032	0.110
4.91 (d)	C_s	$^1A'$	2.737	2.570	0.264
4.91 (e)	C_s	$^1A'$	2.717	2.095	0.135
4.91 (f)	C_s	$^3A''$	2.715	1.758[a]	0.475

[a] HOMO and LUMO have opposite spins; this value includes the energy required to flip the spin of the electron.

Table 4.100 Properties of the $(SiGe_5)^+$ Hexamers

Figure	Symmetry Group	Electronic State	Binding E / Atom (eV)	HOMO-LUMO Gap (eV)	Dipole Moment (D)
4.92 (a)	C_s	^2A”	2.946	1.781	0.640
4.92 (b)	C_{2v}	$^2A_1$	2.932	1.926[a]	0.390
4.92 (c)	C_s	^2A”	2.872	1.507[a]	0.599
4.92 (d)	C_s	^2A’	2.863	1.555[a]	0.949
4.92 (e)	C_s	^2A”	2.829	1.527[a]	0.358
4.92 (f)	C_s	^4A”	2.822	1.725[a]	0.584

[a] HOMO and LUMO have opposite spins; this value includes the energy required to flip the spin of the electron.

Table 4.101 Properties of the $(SiGe_5)^-$ Hexamers

Figure	Symmetry Group	Electronic State	Binding E / Atom (eV)	HOMO-LUMO Gap (eV)	Dipole Moment (D)
4.93 (a)	C_s	^2A’	3.005	1.724[a]	0.846
4.93 (b)	C_{2v}	$^2B_1$	2.977	1.635[a]	1.255
4.93 (c)	C_s	^2A’	2.932	1.030	1.256
4.93 (d)	C_s	^2A’	2.915	1.450[a]	0.649
4.93 (e)	C_s	^2A’	2.907	1.443[a]	0.854
4.93 (f)	C_s	^2A”	2.842	1.472	2.475

[a] HOMO and LUMO have opposite spins; this value includes the energy required to flip the spin of the electron.

Table 4.102 Ionization Potentials and Electron Affinities of the $SiGe_5$ Hexamers

Neutral Figure	VIP (eV)	Cationic Figure	AIP (eV)	VEA (eV)	Anionic Figure	AEA (eV)
4.91 (a)	7.823	4.92 (a)	7.488	1.311	4.93 (a)	1.903
4.91 (b)	7.676	4.92 (b)	7.333	1.378	4.93 (b)	1.970
4.91 (c)	7.340	4.92 (c)	7.123	2.058	4.93 (d)	2.173
4.91 (d)	7.326	4.92 (d)	7.144	1.618	4.93 (f)	1.768
4.91 (e)	7.450	4.92 (e)	7.227	2.095	4.93 (e)	2.274
4.91 (f)	7.370	4.92 (f)	7.032	2.338	4.93 (c)	2.444

Table 4.103 Fragmentation Energies of the Most Stable $SiGe_5$ Neutral Hexamer

Fragmented Clusters	Fragmentation Energy (eV)
$SiGe_4 + Ge$	3.526
$SiGe_3 + Ge_2$	3.898
$SiGe_3 + 2Ge$	6.826
$SiGe_2 + Ge_2 + Ge$	7.682
$SiGe + 2Ge_2$	8.344
$SiGe_2 + 3Ge$	10.610
$SiGe + Ge_2 + 2Ge$	11.272
$2Ge_2 + Si + Ge$	11.405
$SiGe + 4Ge$	14.20
$Ge_2 + Si + 3Ge$	14.334
$Si + 5Ge$	17.262

Table 4.104 Fragmentation Energies of the Most Stable $(SiGe_5)^+$ Cationic Hexamer

Fragmented Clusters	Fragmentation Energy (eV)
$(SiGe_4)^+ + Ge$	3.815
$SiGe_4 + Ge^+$	3.938
$SiGe_3 + (Ge_2)^+$	4.029
$(SiGe_3)^+ + Ge_2$	4.073
$(SiGe_3)^+ + Ge + Ge$	7.001
$SiGe_3 + Ge^+ + Ge$	7.238
$SiGe_2 + (Ge_2)^+ + Ge$	7.813
$SiGe_2 + Ge_2 + Ge^+$	8.094
$(SiGe_2)^+ + Ge_2 + Ge$	8.142
$SiGe + (Ge_2)^+ + Ge_2$	8.476
$(SiGe)^+ + Ge_2 + Ge_2$	8.592
$SiGe_2 + Ge^+ + Ge + Ge$	11.022
$(SiGe_2)^+ + Ge + Ge + Ge$	11.071
$SiGe + (Ge_2)^+ + Ge + Ge$	11.404
$(SiGe)^+ + Ge_2 + Ge + Ge$	11.520
$(Ge_2)^+ + Ge_2 + Si + Ge$	11.537
$SiGe + Ge_2 + Ge^+ + Ge$	11.684
$Ge_2 + Ge_2 + Si + Ge^+$	11.817
$(SiGe)^+ + Ge + Ge + Ge + Ge$	14.448
$(Ge_2)^+ + Si + Ge + Ge + Ge$	14.465
$SiGe + Ge^+ + Ge + Ge + Ge$	14.613
$Ge_2 + Si + Ge^+ + Ge + Ge$	14.746
$Si + Ge^+ + Ge + Ge + Ge + Ge$	17.674

Table 4.105 Fragmentation Energies of the Most Stable $(SiGe_5)^-$ Anionic Hexamer

Fragmented Clusters	Fragmentation Energy (eV)
$(SiGe_4)^- + Ge$	3.273
$(SiGe_3)^- + Ge_2$	3.867
$SiGe_3 + (Ge_2)^-$	3.985
$SiGe_4 + Ge^-$	4.291
$(SiGe_3)^- + 2Ge$	6.795
$(SiGe_2)^- + Ge_2 + Ge$	7.552
$SiGe_3 + Ge^- + Ge$	7.592
$SiGe_2 + (Ge_2)^- + Ge$	7.769
$(SiGe)^- + 2Ge_2$	8.402
$SiGe + (Ge_2)^- + Ge_2$	8.432
$SiGe_2 + Ge_2 + Ge^-$	8.447
$(SiGe_2)^- + 3Ge$	10.480
$(SiGe)^- + Ge_2 + 2Ge$	11.331
$SiGe + (Ge_2)^- + 2Ge$	11.360
$SiGe_2 + Ge^- + 2Ge$	11.376
$(Ge_2)^- + Ge_2 + Si + Ge$	11.493
$SiGe + Ge_2 + Ge^- + Ge$	12.038
$2Ge_2 + Si + Ge^-$	12.171
$(SiGe)^- + 4Ge$	14.259
$(Ge_2)^- + Si + 3Ge$	14.422
$SiGe + Ge^- + 3Ge$	14.966
$Ge_2 + Si + Ge^- + 2Ge$	15.099
$Si + Ge^- + 4Ge$	18.028

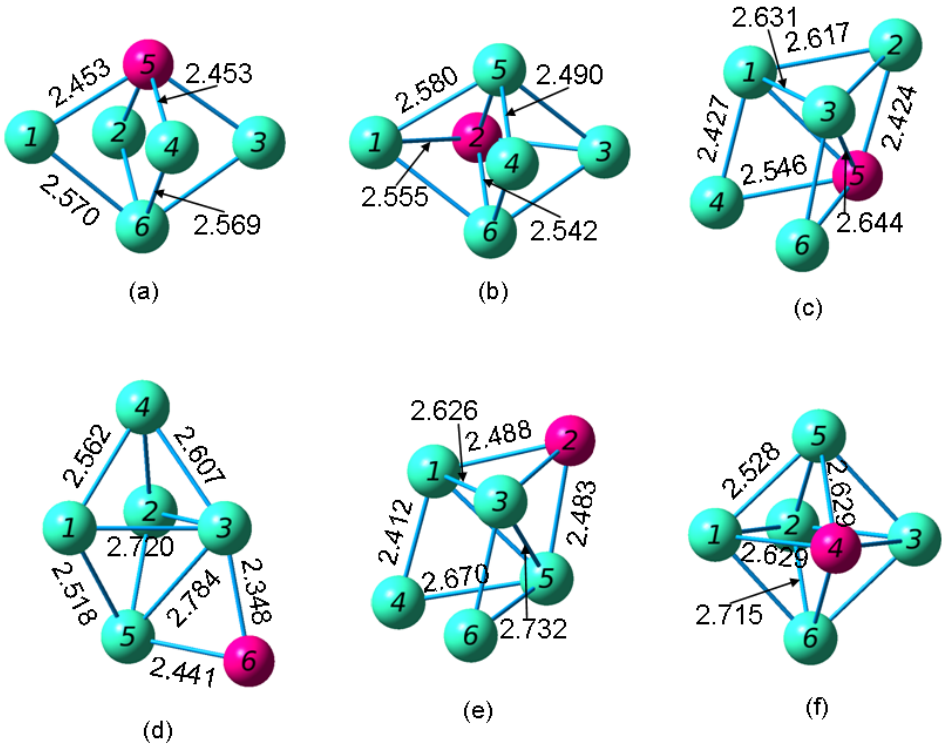

Figure 4.91 Geometries of the $SiGe_5$ Neutral Hexamers from (a) Most Stable through (f) Least Stable

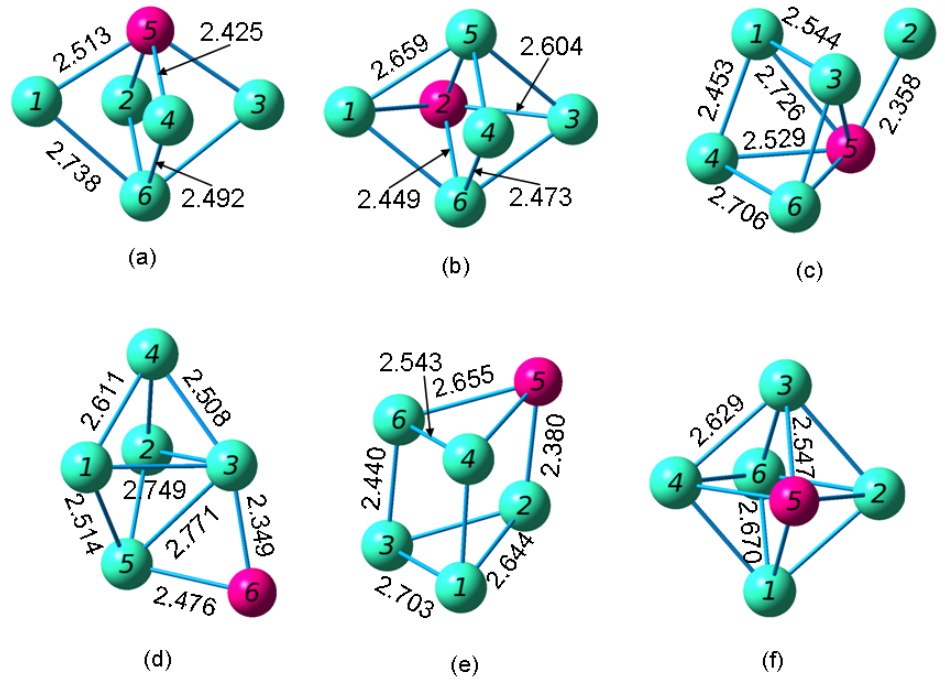

Figure 4.92 Geometries of the $(SiGe_5)^+$ Cation Hexamers from (a) Most Stable through (f) Least Stable

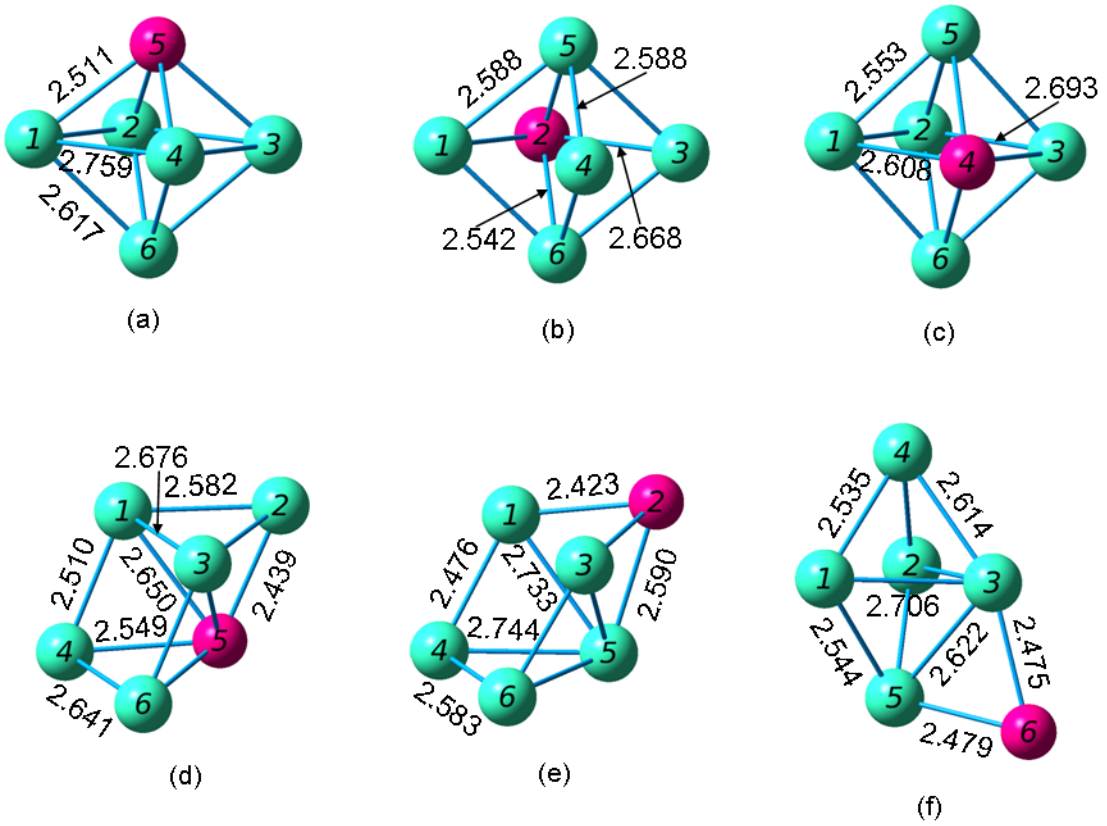

Figure 4.93 Geometries of the $(SiGe_5)^-$ Anion Hexamers from (a) Most Stable through (f) Least Stable

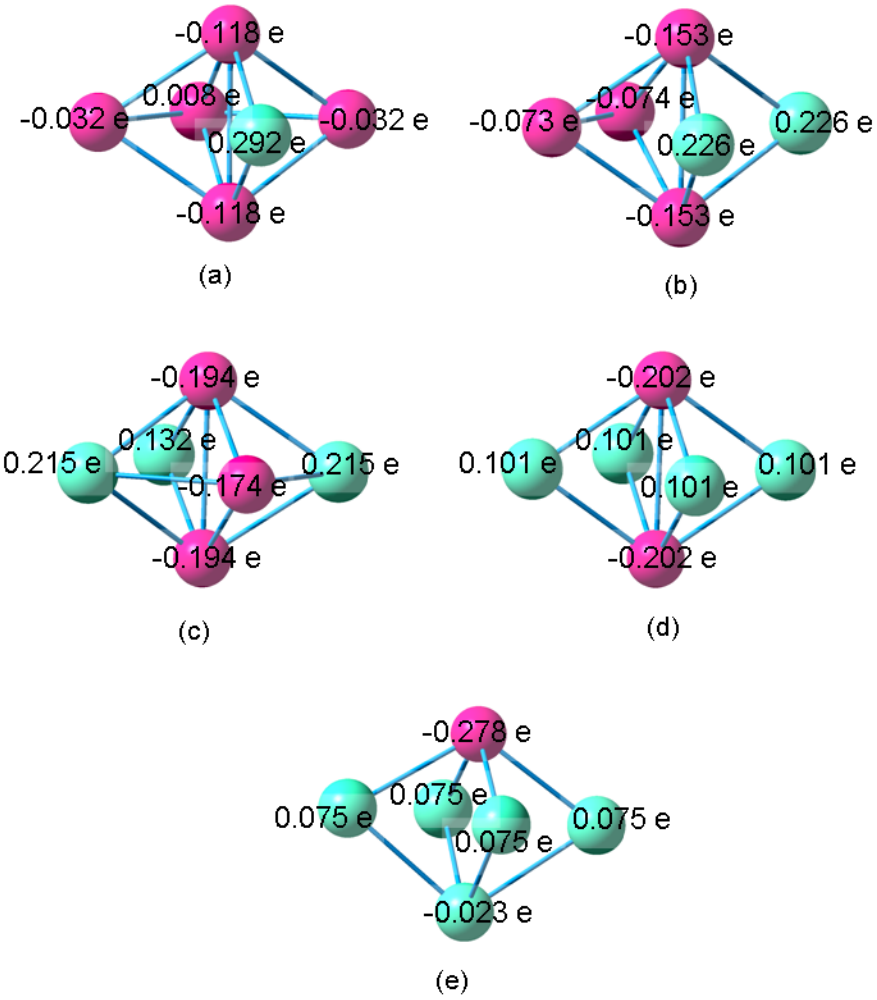

Figure 4.94 Atomic Charges of the Most Stable (a) Si_5Ge (b) Si_4Ge_2 (c) Si_3Ge_3 (d) Si_2Ge_4 and (e) $SiGe_5$ Neutral Hexamer

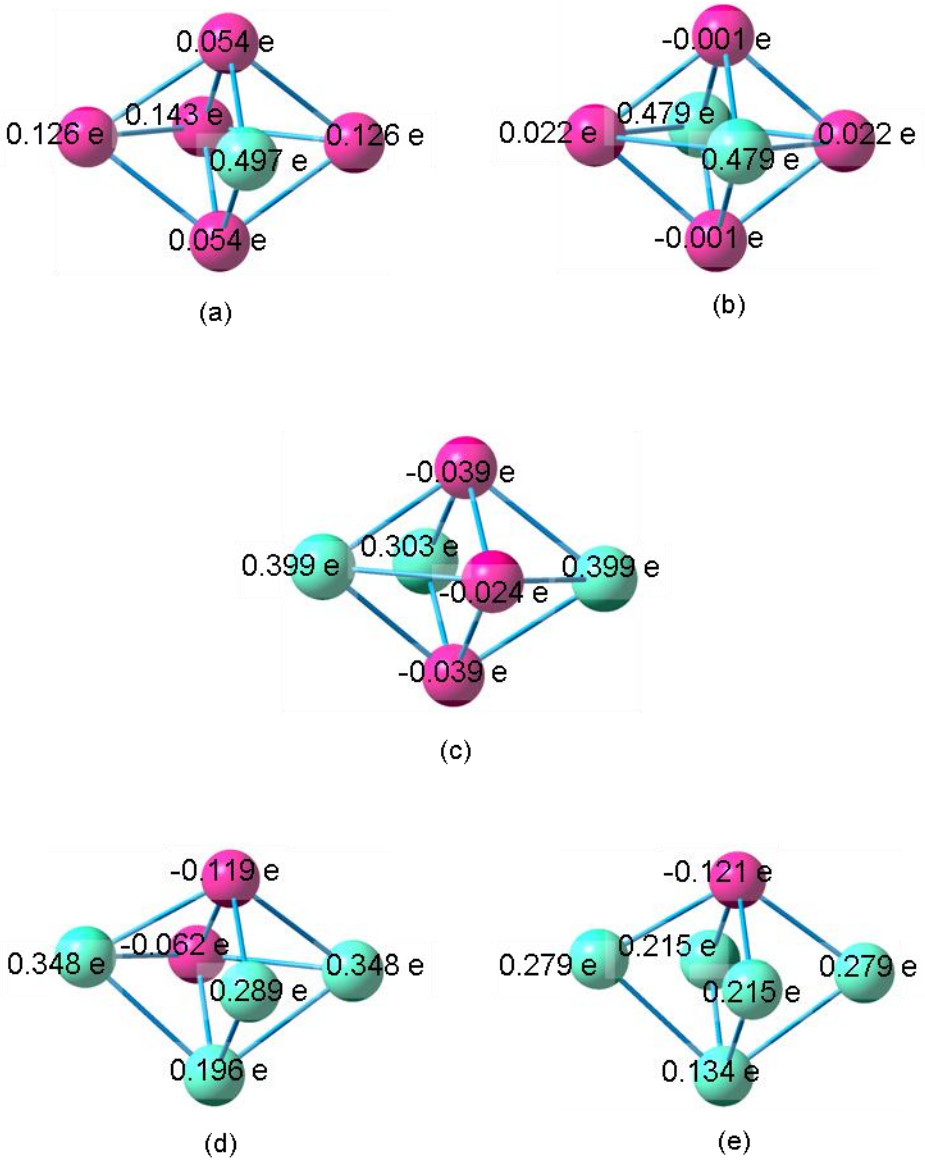

Figure 4.95 Atomic Charges of the Most Stable (a) $(Si_5Ge)^+$ (b) $(Si_4Ge_2)^+$ (c) $(Si_3Ge_3)^+$ (d) $(Si_2Ge_4)^+$ and (e) $(SiGe_5)^+$ Cationic Hexamer

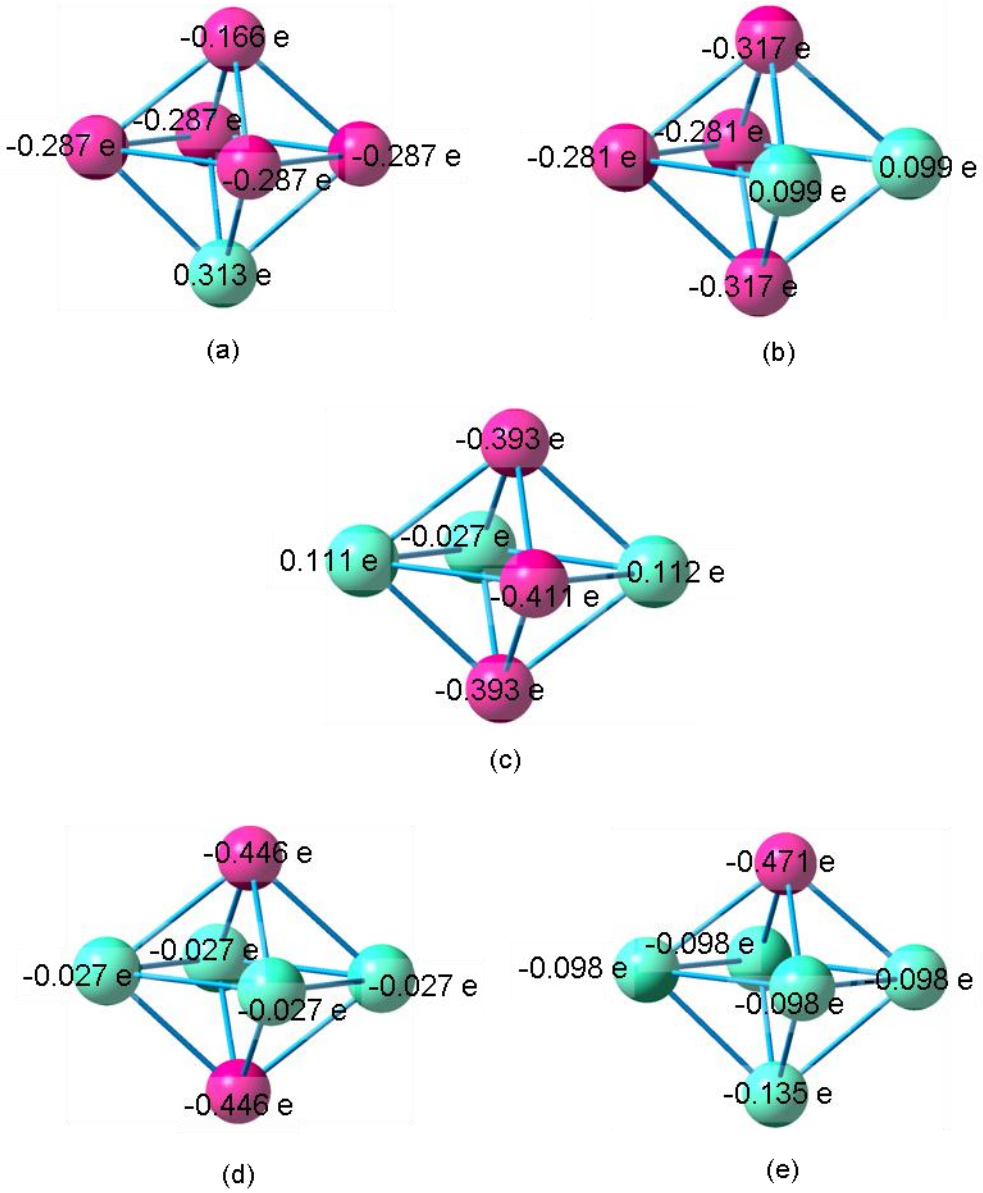

Figure 4.96 Atomic Charges of the Most Stable (a) $(Si_5Ge)^-$ (b) $(Si_4Ge_2)^-$ (c) $(Si_3Ge_3)^-$ (d) $(Si_2Ge_4)^-$ and (e) $(SiGe_5)^-$ Anionic Hexamer

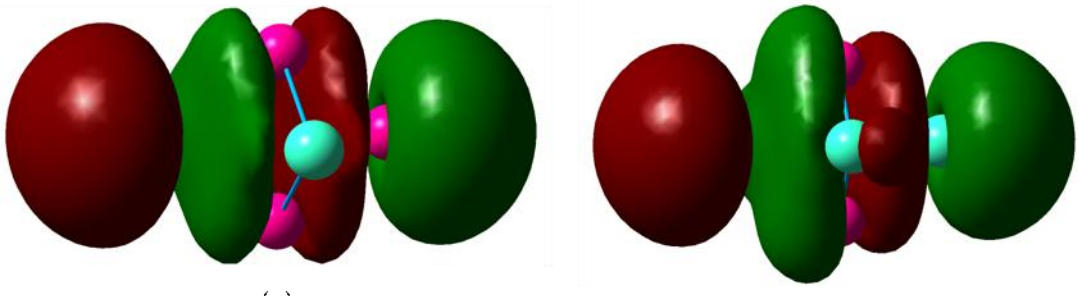

(a)

(b)

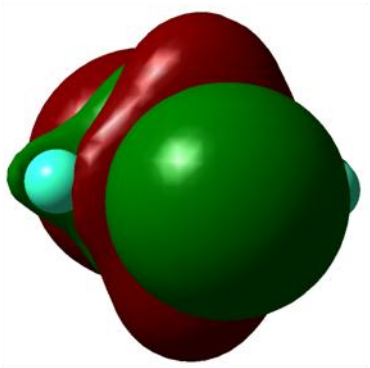

(c)

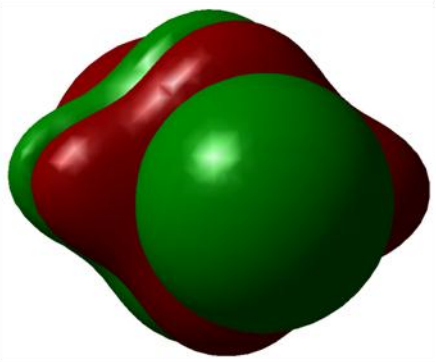

(d)

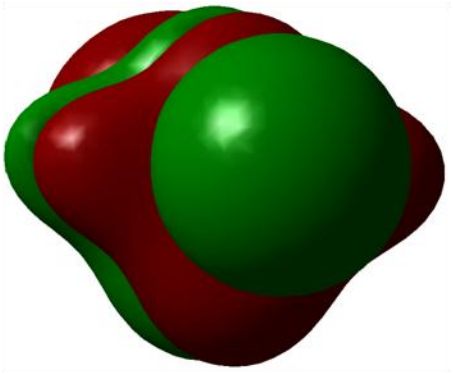

(e)

Figure 4.97 HOMO of the Most Stable (a) Si_5Ge (b) Si_4Ge_2 (c) Si_3Ge_3 (d) Si_2Ge_4 and (e) $SiGe_5$ Neutral Hexamer

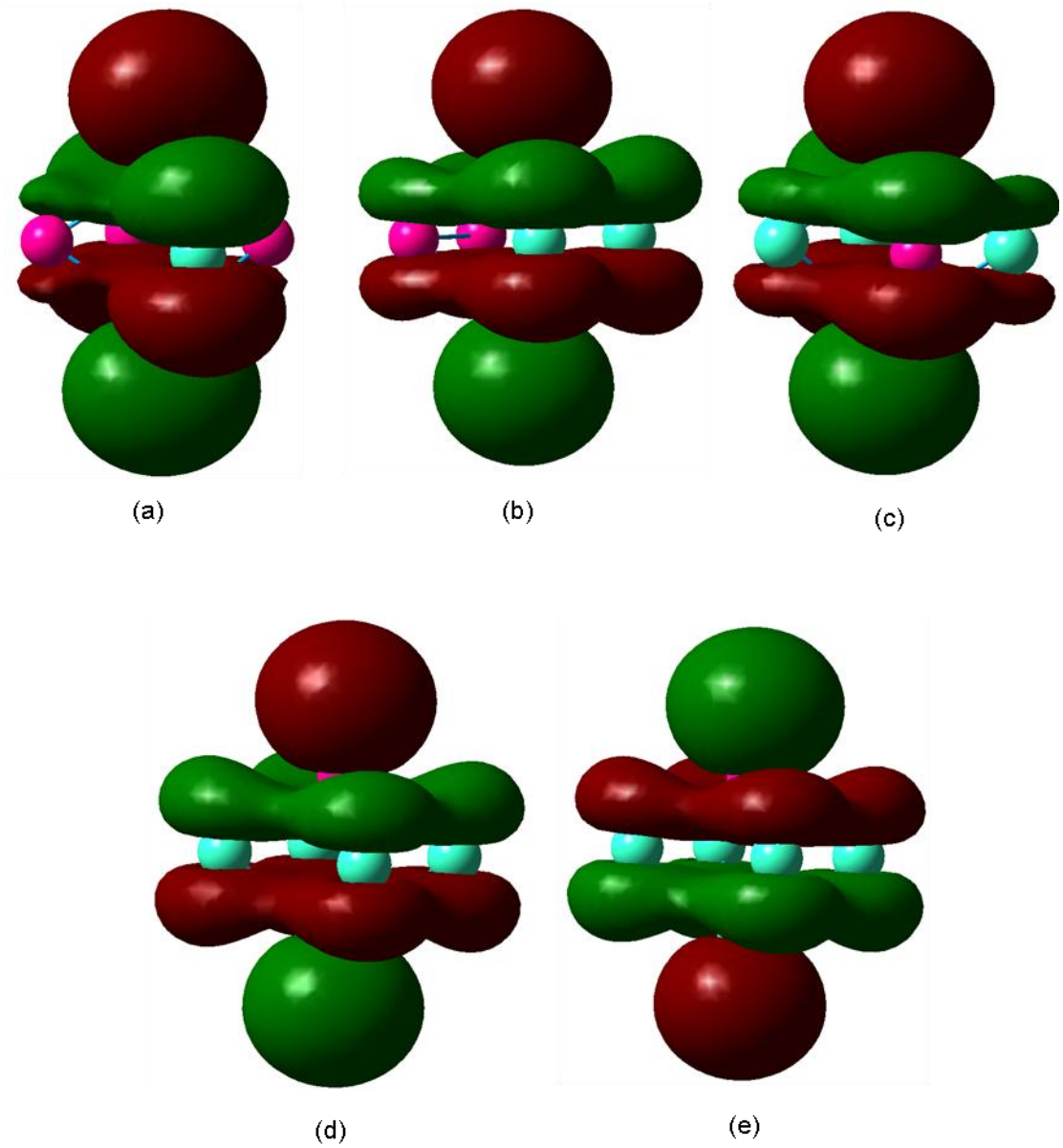

igure 4.98 LUMO of the Most Stable (a) Si_5Ge (b) Si_4Ge_2 (c) Si_3Ge_3 (d) Si_2Ge_4 and (e) $SiGe_5$ Neutral Hexamer

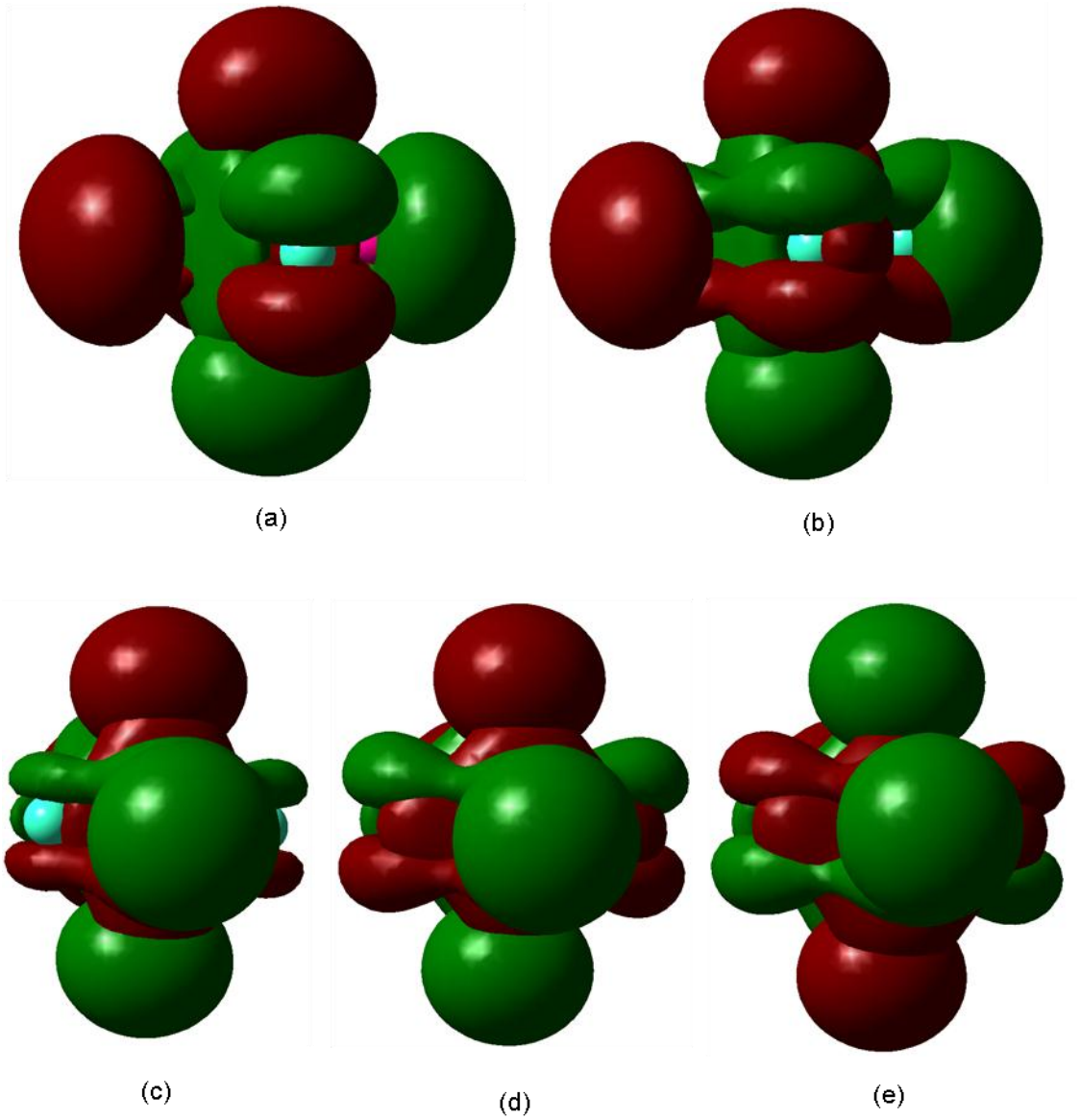

Figure 4.99 HOMO and LUMO of the Most Stable (a) Si_5Ge (b) Si_4Ge_2 (c) Si_3Ge_3 (d) Si_2Ge_4 and (e) $SiGe_5$ Neutral Hexamer

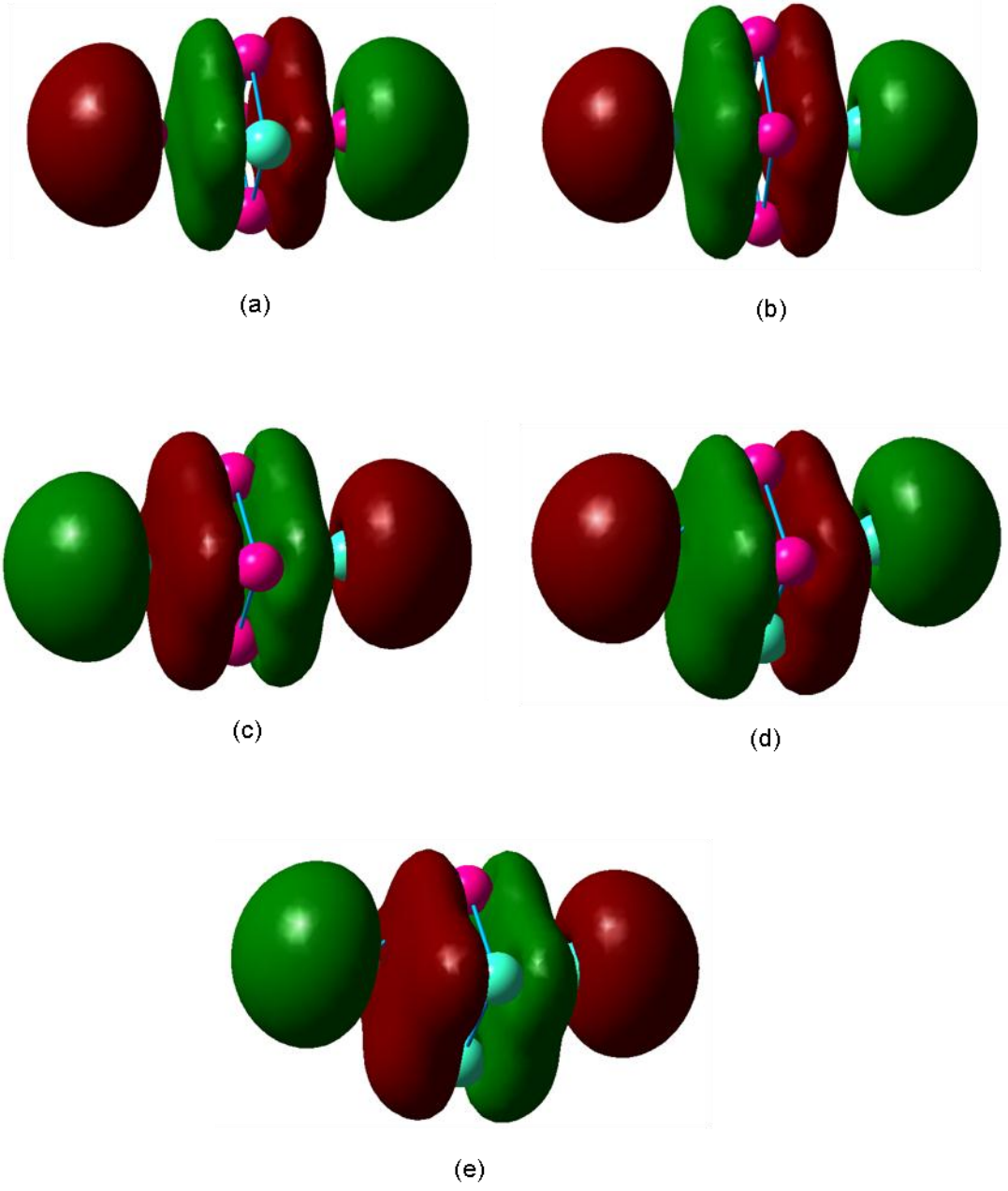

Figure 4.100 HOMO of the Most Stable (a) $(Si_5Ge)^+$ (b) $(Si_4Ge_2)^+$ (c) $(Si_3Ge_3)^+$ (d) $(Si_2Ge_4)^+$ and (e) $(SiGe_5)^+$ Cationic Hexamer

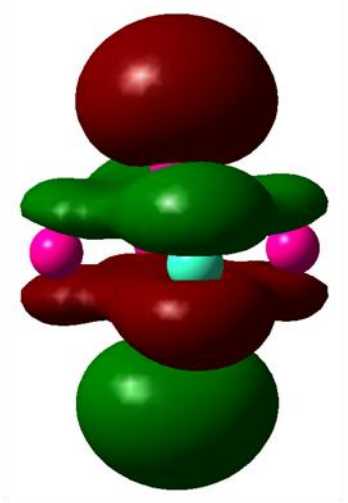

(a)

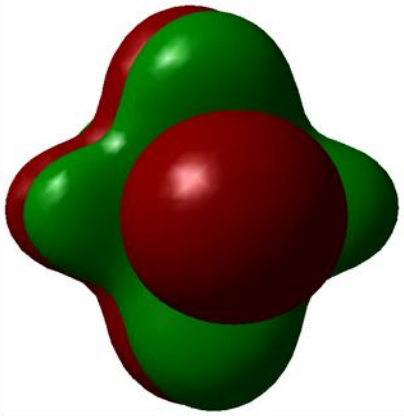

(b)

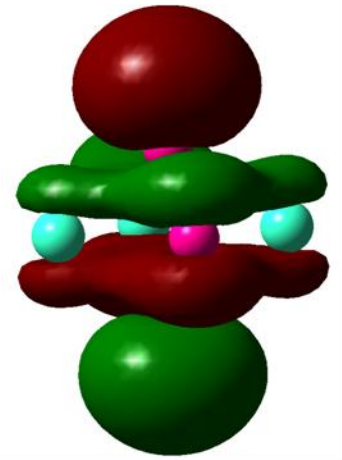

(c)

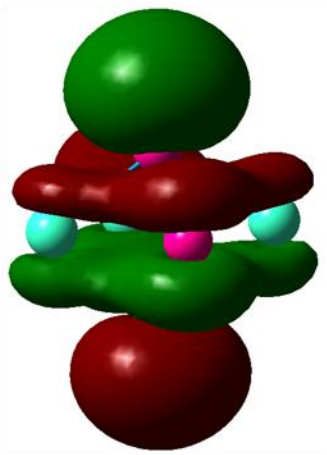

(d)

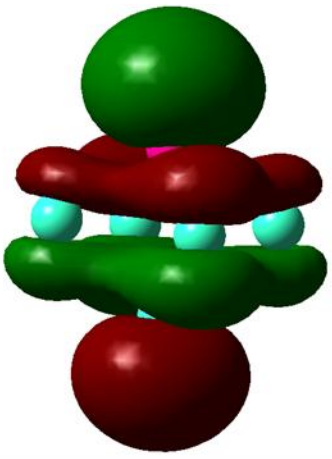

(e)

Figure 4.101 LUMO of the Most Stable (a) $(Si_5Ge)^+$ (b) $(Si_4Ge_2)^+$ (c) $(Si_3Ge_3)^+$ (d) $(Si_2Ge_4)^+$ and (e) $(SiGe_5)^+$ Cationic Hexamer

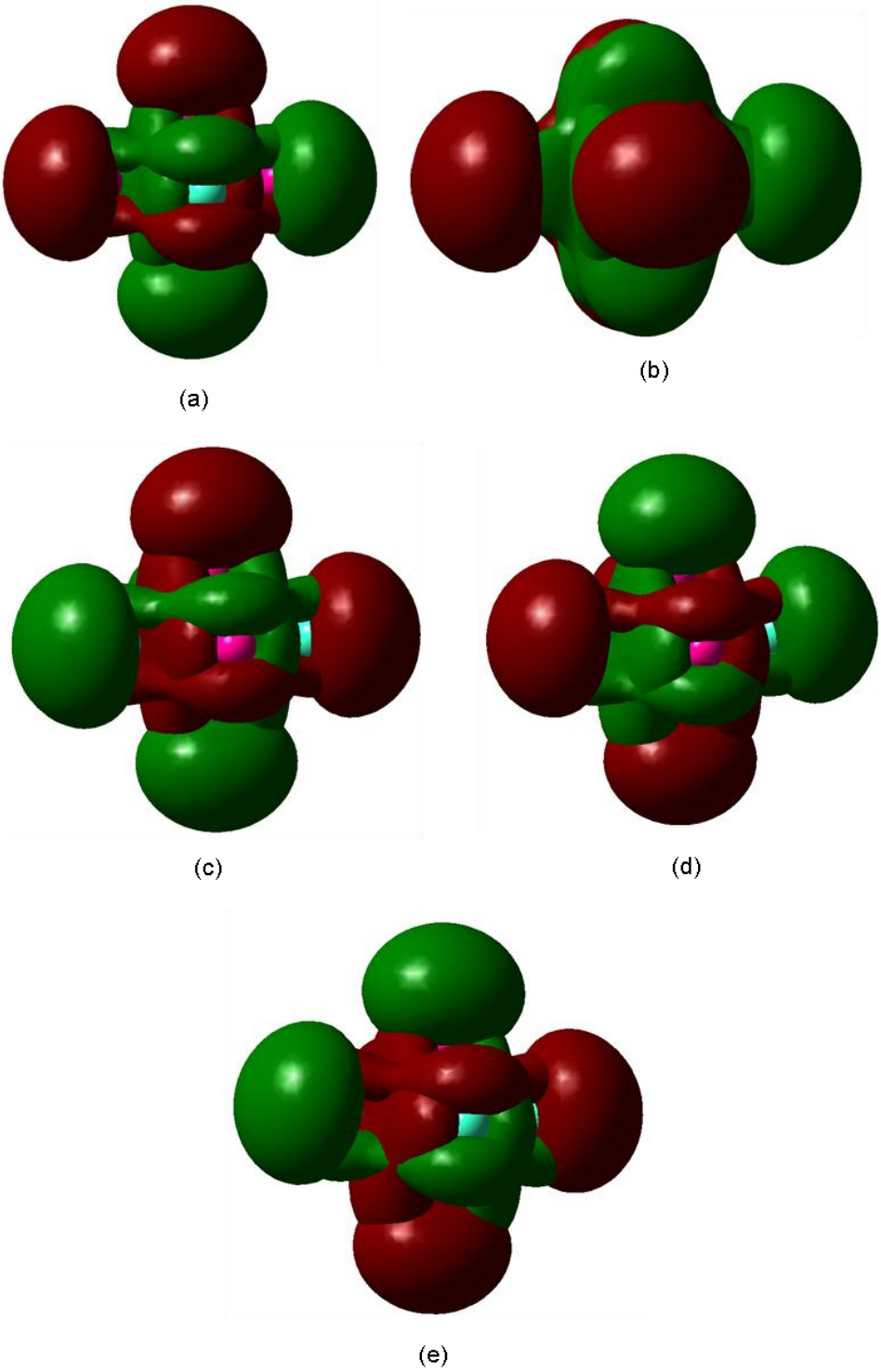

Figure 4.102 HOMO and LUMO of the Most Stable (a) $(Si_5Ge)^+$ (b) $(Si_4Ge_2)^+$ (c) $(Si_3Ge_3)^+$ (d) $(Si_2Ge_4)^+$ and (e) $(SiGe_5)^+$ Cationic Hexamer

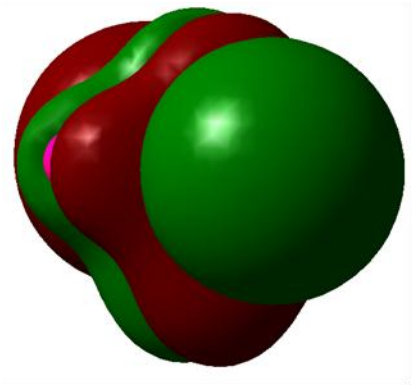

(a)

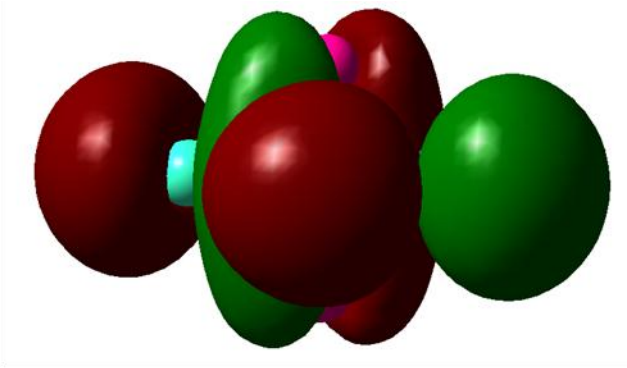

(b)

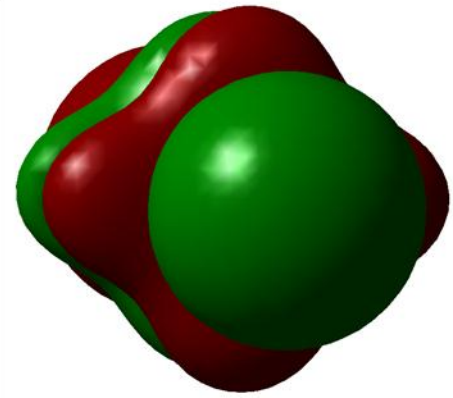

(c)

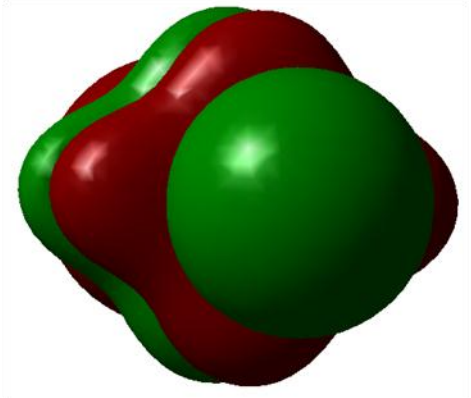

(d)

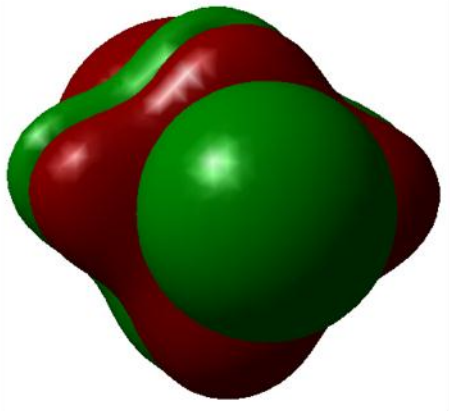

(e)

Figure 4.103 HOMO of the Most Stable (a) $(Si_5Ge)^-$ (b) $(Si_4Ge_2)^-$ (c) $(Si_3Ge_3)^-$ (d) $(Si_2Ge_4)^-$ and (e) $(SiGe_5)^-$ Anionic Hexamer

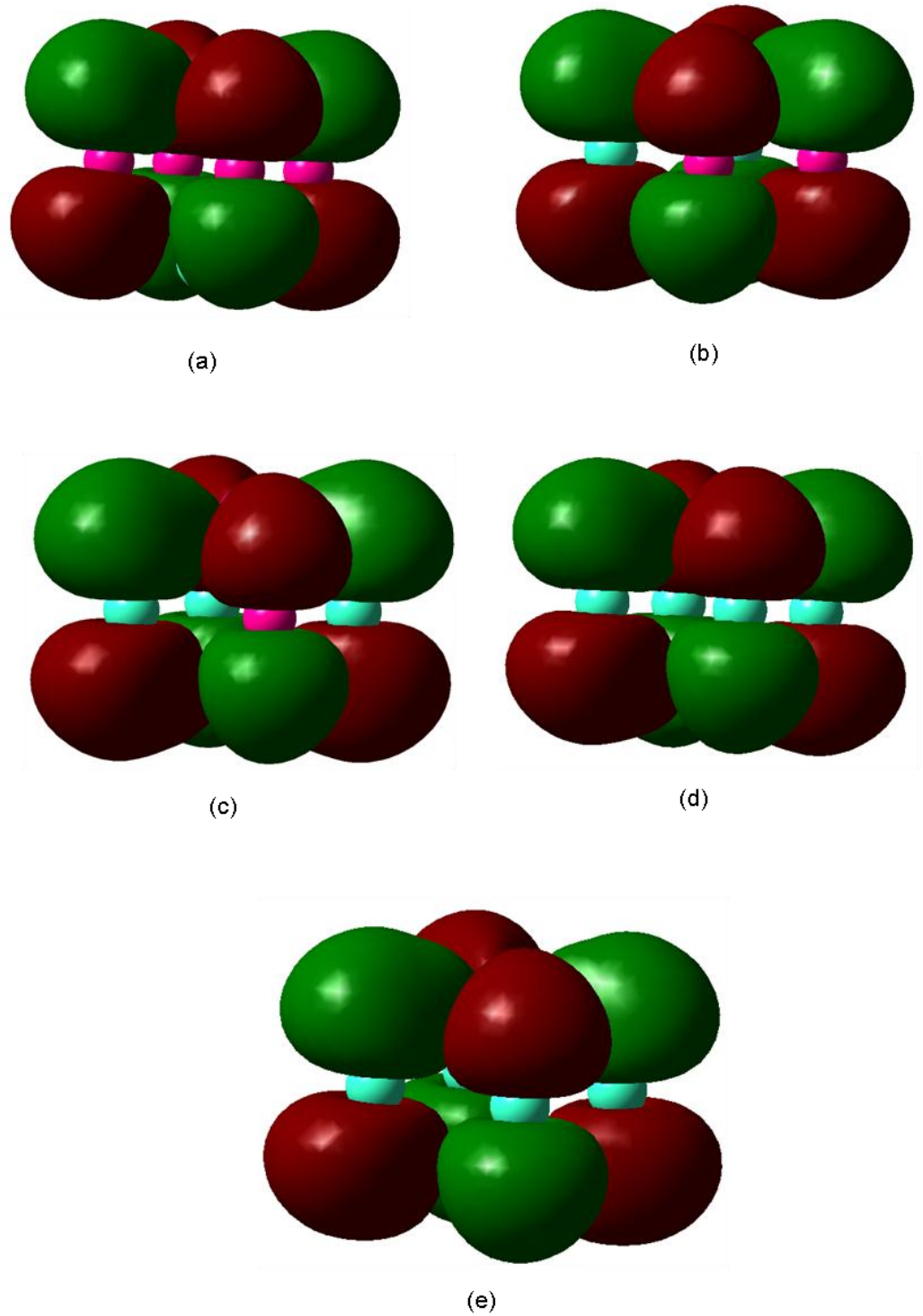

Figure 4.104 LUMO of the Most Stable (a) $(Si_5Ge)^-$ (b) $(Si_4Ge_2)^-$ (c) $(Si_3Ge_3)^-$ (d) $(Si_2Ge_4)^-$ and (e) $(SiGe_5)^-$ Anionic Hexamer

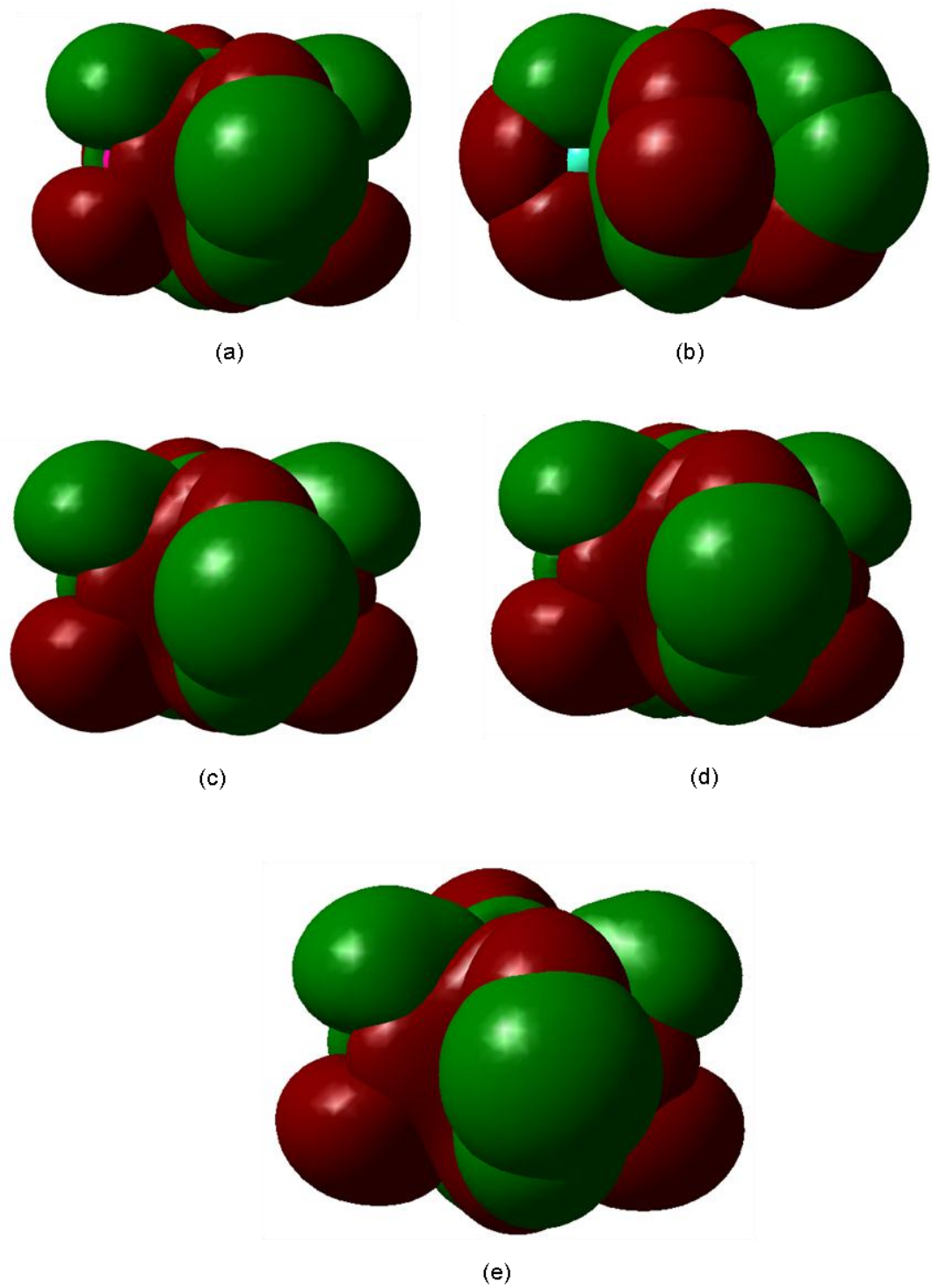

Figure 4.105 HOMO and LUMO of the Most Stable (a) $(Si_5Ge)^-$ (b) $(Si_4Ge_2)^-$ (c) $(Si_3Ge_3)^-$ (d) $(Si_2Ge_4)^-$ and (e) $(SiGe_5)^-$ Anionic Hexamer

4.16 Si_6Ge Septamers

Marim *et al.* [49] reported their ground state cluster to be a pentagonal bipyramid. The base has four Si atoms and one Ge atom. Within this base there are two Si-Ge bonds with lengths of 2.60 Å, 2 Si-Si bonds with lengths of 2.49 Å, and one Si-Si bond with a length of 2.50 Å. The bonds connecting the Ge atom to the Si tips are 2.58 Å. They calculated a cohesive energy of 3.10 eV/atom for this cluster. Wang and Chao [51] reported that the most stable Si_6Ge cluster has a ^1A electronic state, a dissociation energy of -26.8923 eV or -29.9587 eV, a HOMO-LUMO gap of 3.06 eV, and the following frequencies: 399(a), 381(a), and 417(a).

With the septamers we investigated even more clusters than we did for the smaller clusters because there are many more possible geometries and we wanted to make sure we found the most stable. The paper by Pradhan and Ray [6], which up to the pentamers and even into the hexamers had provided a basis for our input geometries, investigated only two kinds of septamers: Si_3C_4 and Si_4C_3. Also, we found beginning with the hexamers that our results started to deviate from this work because we needed to find and work with more three-dimensional clusters, especially bipyramids. In short, we had to turn to new sources to inspire our input geometries. To an even greater extent than with the hexamers, we scoured the literature for possibilities. We again found that a work by Raghavachari, this time working with C. Rohlfing [20] included geometries that we needed to try. Their paper discussed pure silicon nanoclusters including septamers. We borrowed their two most stable geometries and replaced one atom with a germanium atom. The first, a pentagonal bipyramid, turned out to be our most stable cluster as well (figure 4.106 (a)). Actually, for all the septamers a pentagonal bipyramid is the most stable. The next cluster is described by Raghavachari and Rohlfing as a bicapped tetrahedral with an additional cap on one of the middle triangular faces. It is also our second-most stable cluster (figure 4.106 (b)). Another, less stable variation of this geometry is pictured in figure 4.106 (g). In their paper, Raghavachari and Rohlfing discuss that they formed these clusters by taking a bicapped tetrahedral and adding an additional cluster at various points. We

extended this idea for the other clusters we investigated. To form the third, fourth, and sixth most stable clusters (figures 4.106 (c), 4.106 (d), and 4.106 (f)) we attached an extra germanium atom to atoms 3 and 4. We also tried capping one of the off-center triangular faces, resulting in the clusters pictured in figures 4.106 (e), 4.106 (h), 4.106 (i), and 4.106 (k). The least stable way to attach an extra atom is to atoms 2 and 3 in figures 4.106 (j), 4.106 (l), 4.106 (m), 4.106 (n), and 4.106 (o). Finally, our two least stable clusters consist of silicon rhombic bipyramids with a single germanium atom attached either to two atoms (figure 4.106 (p)) or to a single atom (figure 4.106 (q)).

Our results for the Si_6Ge septamers are summarized in tables 4.106 through 4.112 and figures 4.106 through 4.108. For each of our 17 neutral clusters, we found a corresponding cation and anion cluster.

Table 4.106 Properties of the Si_6Ge Neutral Septamers

Figure	Symmetry Group	Electronic State	Binding E / Atom (eV)	HOMO-LUMO Gap (eV)	Dipole Moment (D)
4.106 (a)	C_{2v}	$^1A_1$	3.186	3.065	0.465
4.106 (b)	C_1	^1A	3.097	2.988	0.871
4.106 (c)	C_{2v}	$^1A_1$	3.085	2.580	1.053
4.106 (d)	C_s	$^1A'$	3.077	2.669	0.461
4.106 (e)	C_1	^1A	3.067	2.442	0.830
4.106 (f)	C_s	$^1A'$	3.059	2.862	0.338
4.106 (g)	C_1	^1A	3.058	2.714	0.767
4.106 (h)	C_1	^1A	3.058	2.513	0.767
4.106 (i)	C_1	^1A	3.045	2.425	0.686
4.106 (j)	C_s	$^1A'$	3.035	1.586	2.045
4.106 (k)	C_1	^1A	3.035	2.410	0.745
4.106 (l)	C_s	$^1A'$	3.022	1.775	1.389
4.106 (m)	C_s	$^1A'$	3.019	1.628	0.951
4.106 (n)	C_s	$^1A'$	3.011	1.725	1.57
4.106 (o)	C_s	$^1A'$	2.973	1.665	1.535
4.106 (p)	C_{2v}	$^1A_1$	2.944	1.806	1.990
4.106 (q)	C_{2v}	$^1A_1$	2.841	1.069	0.808

Table 4.107 Properties of the $(Si_6Ge)^+$ Cationic Septamers

Figure	Symmetry Group	Electronic State	Binding E / Atom (eV)	HOMO-LUMO Gap (eV)	Dipole Moment (D)
4.107 (a)	C_{2v}	$^2B_2$	3.218	1.634[a]	1.347
4.107 (b)	C_1	^2A	3.189	1.600[a]	1.134
4.107 (c)	C_1	^2A	3.164	1.604[a]	1.225
4.107 (d)	C_s	$^2A'$	3.162	1.611[a]	0.572
4.107 (e)	C_1	^2A	3.161	1.554[a]	1.353
4.107 (f)	C_{2v}	$^2A_1$	3.153	1.556[a]	0.484
4.107 (g)	C_1	^2A	3.153	1.657[a]	1.357
4.107 (h)	C_1	^2A	3.146	1.636[a]	1.210
4.107 (i)	C_s	$^2A'$	3.145	1.601[a]	3.157
4.107 (j)	C_s	$^2A'$	3.142	1.537	2.139
4.107 (k)	C_1	^2A	3.135	1.488[a]	1.547
4.107 (l)	C_s	$^2A'$	3.122	1.567[a]	2.726
4.107 (m)	C_s	$^2A'$	3.114	1.537[a]	2.014
4.107 (n)	C_s	$^2A'$	3.110	1.541	0.630
4.107 (o)	C_{2v}	$^2A_1$	3.109	1.690[a]	0.152
4.107 (p)	C_s	$^2A'$	3.094	1.635[a]	1.537
4.107 (q)	C_{2v}	$^2B_1$	3.093	1.597	0.212

[a] HOMO and LUMO have opposite spins; this value includes the energy required to flip the spin of the electron.

Table 4.108 Properties of the $(Si_6Ge)^-$ Anionic Septamers

Figure	Symmetry Group	Electronic State	Binding E / Atom (eV)	HOMO-LUMO Gap (eV)	Dipole Moment (D)
4.108 (a)	C_{2v}	$^2B_1$	3.285	1.638[a]	1.876
4.108 (b)	C_s	^2A"	3.244	1.730[a]	1.917
4.108 (c)	C_s	^2A"	3.232	1.779[a]	2.311
4.108 (d)	C_s	^2A"	3.228	1.755[a]	2.765
4.108 (e)	C_s	^2A"	3.224	1.776[a]	1.383
4.108 (f)	C_1	^2A	3.219	1.739[a]	1.521
4.108 (g)	C_{2v}	$^2B_1$	3.204	1.761[a]	1.451
4.108 (h)	C_1	^2A	3.189	1.418	2.285
4.108 (i)	C_s	^2A"	3.188	1.786[a]	0.912
4.108 (j)	C_s	^2A"	3.187	1.706[a]	2.912
4.108 (k)	C_1	^2A	3.174	1.481[a]	1.519
4.108 (l)	C_1	^2A	3.167	1.418[a]	2.258
4.108 (m)	C_1	^2A	3.162	1.450[a]	1.396
4.108 (n)	C_s	^2A"	3.162	1.725	1.034
4.108 (o)	C_1	^2A	3.162	1.408[a]	1.739
4.108 (p)	C_{2v}	$^2B_1$	3.108	1.706	2.272
4.108 (q)	C_{2v}	$^4B_2$	3.080	1.329[a]	0.103

[a] HOMO and LUMO have opposite spins; this value includes the energy required to flip the spin of the electron.

Table 4.109 Ionization Potentials and Electron Affinities of the Si_6Ge Septamers

Neutral Figure	VIP (eV)	Cationic Figure	AIP (eV)	VEA (eV)	Anionic Figure	AEA (eV)
4.106 (a)	7.835	4.107 (a)	7.674	1.537	4.108 (a)	1.836
4.106 (b)	7.561	4.107 (e)	7.453	1.446	4.108 (h)	1.779
4.106 (c)	7.511	4.107 (f)	7.423	1.842	4.108 (g)	1.971
4.106 (d)	7.524	4.107 (j)	7.443	1.787	4.108 (j)	1.913
4.106 (e)	7.168	4.107 (b)	7.051	1.592	4.108 (l)	1.836
4.106 (f)	7.664	4.107 (n)	7.545	1.719	4.108 (n)	1.860
4.106 (g)	7.489	4.107 (k)	7.362	1.626	4.108 (k)	1.951
4.106 (h)	7.273	4.107 (c)	7.157	1.610	4.108 (o)	1.866
4.106 (i)	7.304	4.107 (g)	7.143	1.748	4.108 (f)	2.352
4.106 (j)	7.213	4.107 (d)	7.015	2.506	4.108 (b)	2.600
4.106 (k)	7.238	4.107 (h)	7.121	1.702	4.108 (m)	2.031
4.106 (l)	7.380	4.107 (l)	7.202	2.502	4.108 (c)	2.606
4.106 (m)	7.221	4.107 (i)	7.018	2.496	4.108 (d)	2.600
4.106 (n)	7.348	4.107 (m)	7.180	2.528	4.108 (e)	2.626
4.106 (o)	7.275	4.107 (p)	7.057	2.529	4.108 (i)	2.641
4.106 (p)	6.913	4.107 (o)	6.742	2.046	4.108 (q)	2.287
4.106 (q)	6.265	4.107 (q)	6.132	2.260	4.108 (p)	2.919

Table 4.110 Fragmentation Energies of the Most Stable Si_6Ge Neutral Septamer

Fragmented Clusters	Fragmentation Energy (eV)
$Si_5Ge + Si$	3.718
$Si_4Ge + Si_2$	4.444
$Si_4Ge + 2Si$	7.667
$Si_3Ge + Si_2 + Si$	8.029
$Si_2Ge + 2Si_2$	9.103
$Si_3Ge + 3Si$	11.251
$Si_2Ge + Si_2 + 2Si$	12.326
$3Si_2 + Ge$	12.631
$SiGe + 2Si_2 + Si$	12.793
$2Si_2 + SiGe + Si$	12.793
$Si_2Ge + 4Si$	15.549
$2Si_2 + 2Si + Ge$	15.854
$SiGe + Si_2 + 3Si$	16.016
$SiGe + 5Si$	19.238
$6Si + Ge$	22.300

Table 4.111 Fragmentation Energies of the Most Stable $(Si_6Ge)^+$ Cationic Septamer

Fragmented Clusters	Fragmentation Energy (eV)
$(Si_5Ge)^+ + Si$	3.730
$(Si_4Ge)^+ + Si_2$	4.551
$(Si_4Ge)^+ + Si + Si$	7.773
$(Si_3Ge)^+ + Si_2 + Si$	8.122
$(Si_2Ge)^+ + Si_2 + Si_2$	9.312
$(Si_3Ge)^+ + Si + Si + Si$	11.345
$(Si_2Ge)^+ + Si_2 + Si + Si$	12.534
$(SiGe)^+ + Si_2 + Si_2 + Si$	12.855
$Si_2 + Si_2 + (SiGe)^+ + Si$	12.855
$Si_2 + Si_2 + Si_2 + Ge^+$	12.858
$(Si_2Ge)^+ + Si + Si + Si + Si$	15.757
$Si_2 + Si + Si + (SiGe)^+ + Si$	16.077
$(SiGe)^+ + Si_2 + Si + Si + Si$	16.077
$Si_2 + Si_2 + Si + Si + Ge^+$	16.080
$(SiGe)^+ + Si + Si + Si + Si + Si$	19.300
$Si + Si + Si + Si + Si + Si + Ge^+$	22.526

Table 4.112 Fragmentation Energies of the Most Stable $(Si_6Ge)^-$ Anionic Septamer

Fragmented Clusters	Fragmentation Energy (eV)
$(Si_5Ge)^- + Si$	3.788
$(Si_4Ge)^- + Si_2$	4.038
$(Si_4Ge)^- + 2Si$	7.261
$(Si_3Ge)^- + Si_2 + Si$	7.876
$(Si_2Ge)^- + 2Si_2$	8.761
$(Si_3Ge)^- + 3Si$	11.099
$(Si_2Ge)^- + Si_2 + 2Si$	11.983
$(SiGe)^- + 2Si_2 + Si$	12.784
$2Si_2 + (SiGe)^- + Si$	12.784
$3Si_2 + Ge^-$	13.330
$(Si_2Ge)^- + 4Si$	15.206
$Si_2 + (SiGe)^- + 3Si$	16.007
$Si_2 + (SiGe)^- + 3Si$	16.007
$2Si_2 + 2Si + Ge^-$	16.553
$(SiGe)^- + 5Si$	19.230
$6Si + Ge^-$	22.998

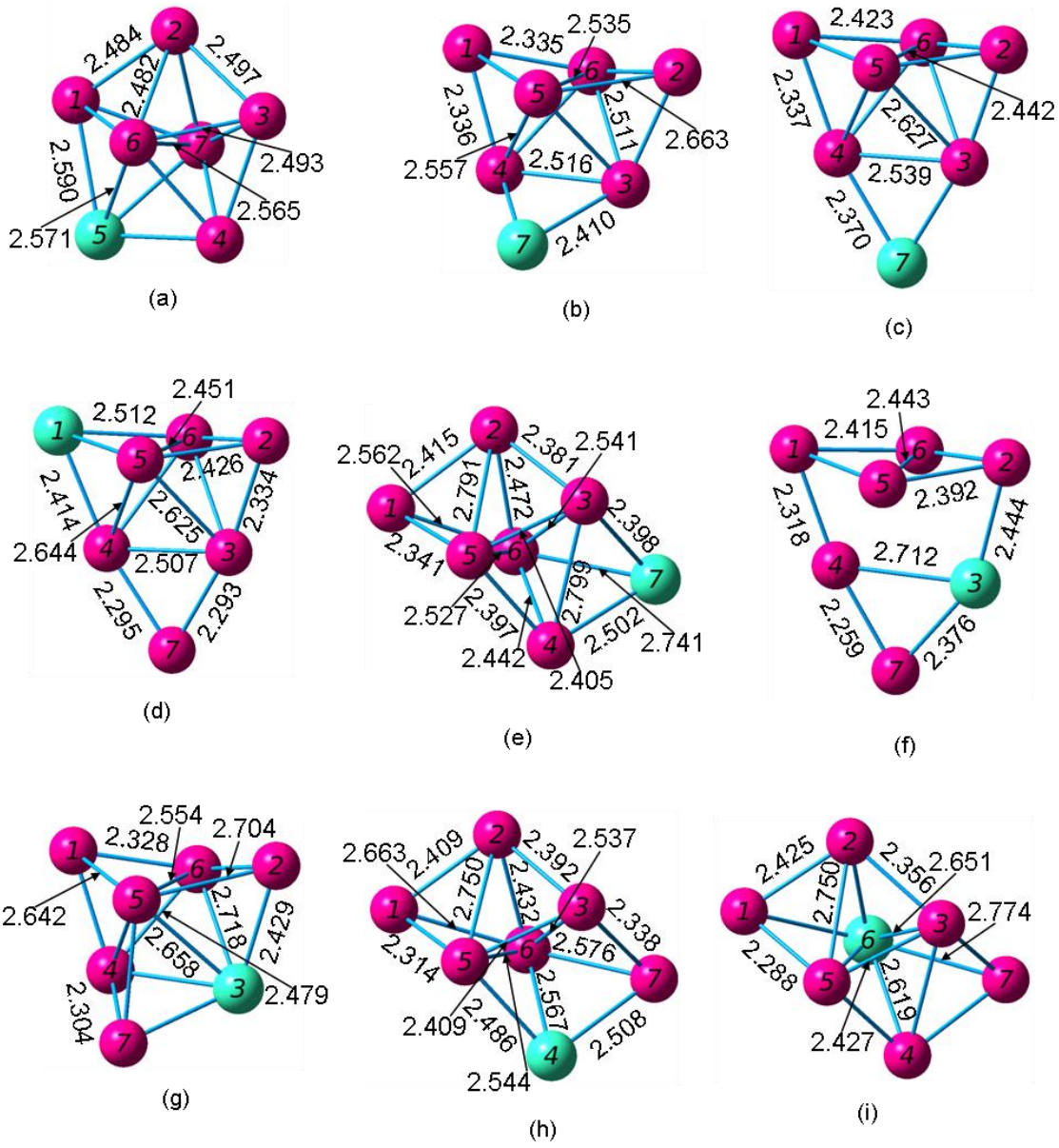

Figure 4.106 Geometries of the Si_6Ge Neutral Septamers from (a) Most Stable through (q) Least Stable

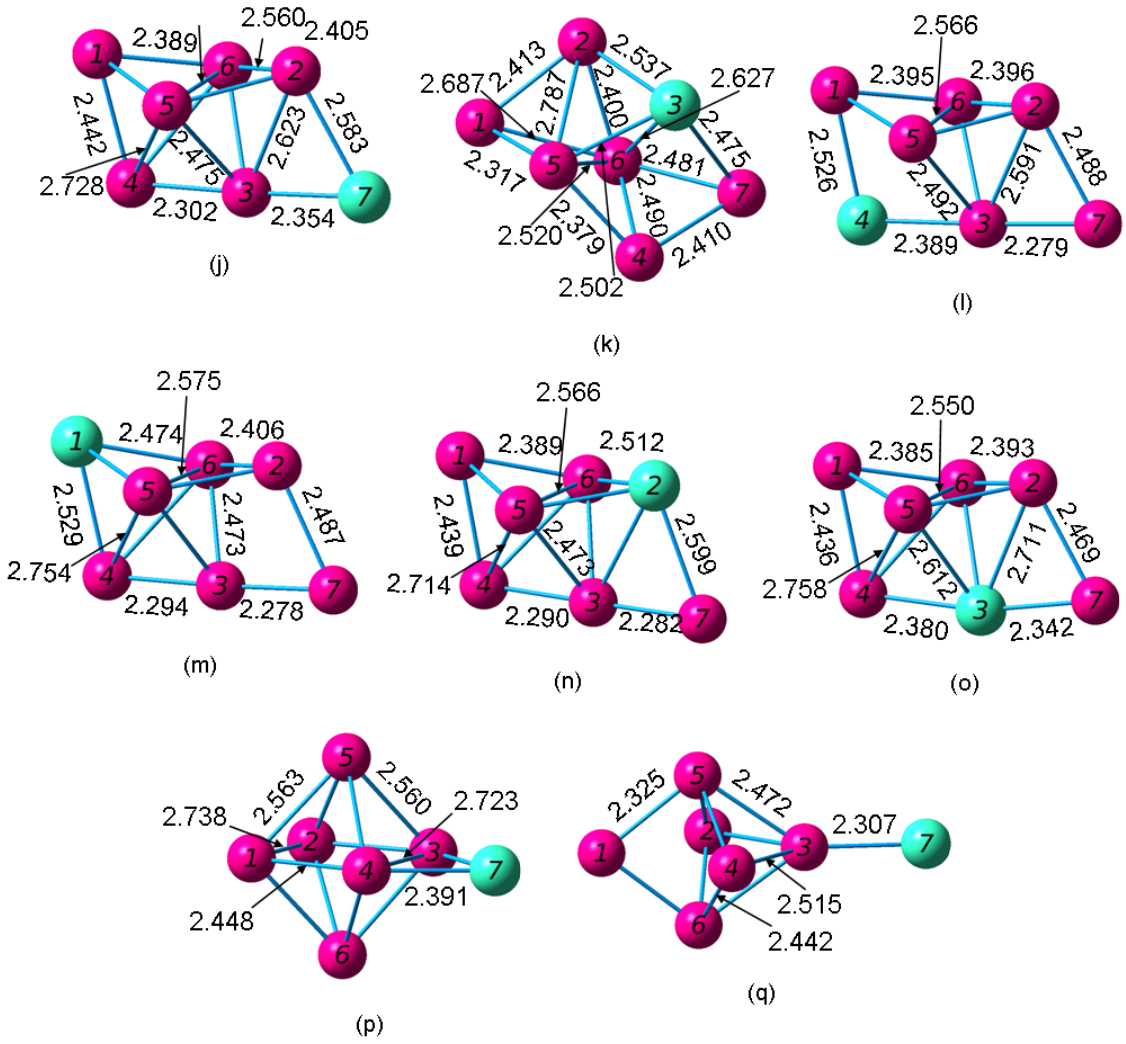

Figure 1.106 – *Continued*

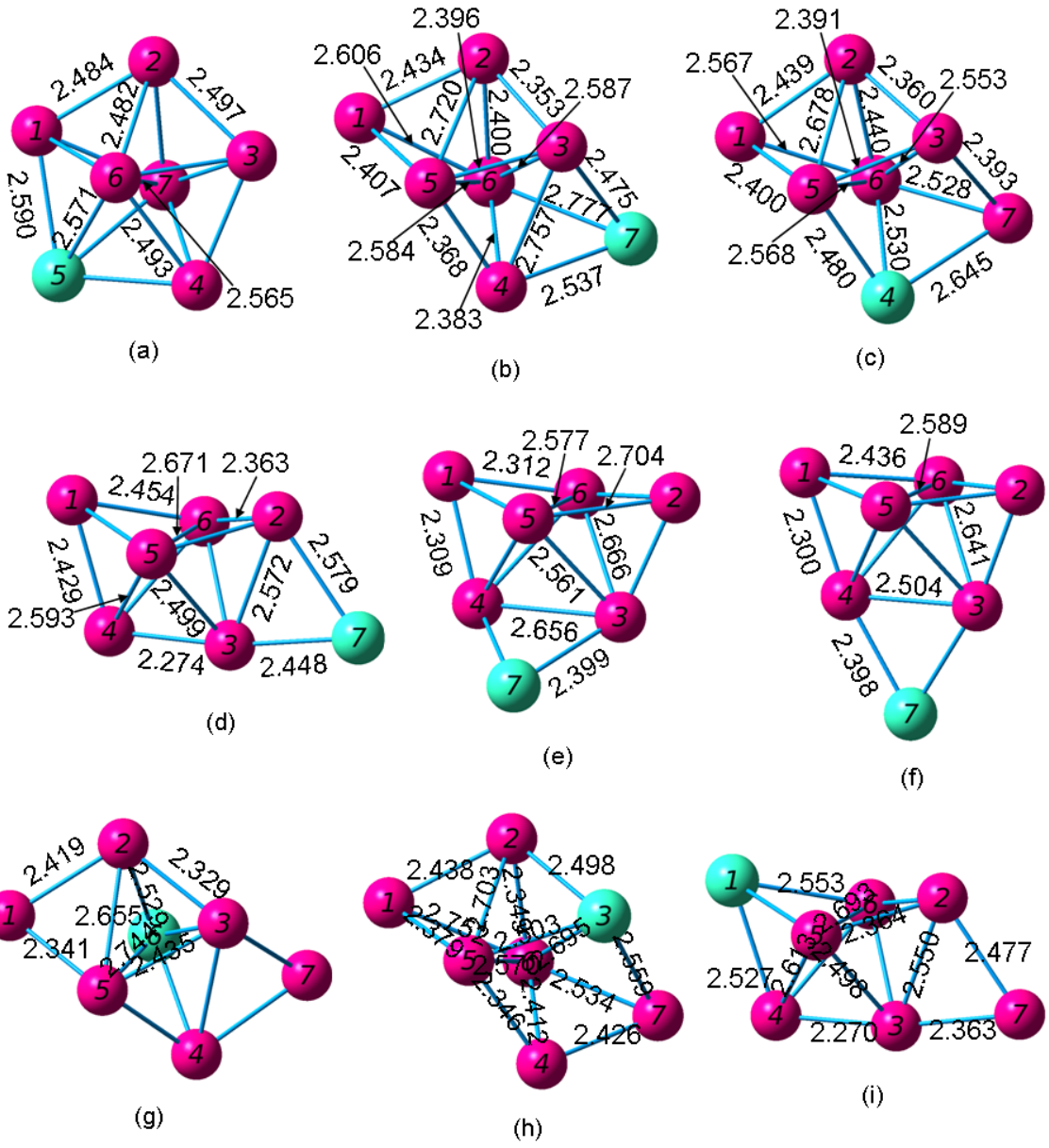

Figure 4.107 Geometries of the $(Si_6Ge)^+$ Cationic Septamers from (a) Most Stable through (q) Least Stable

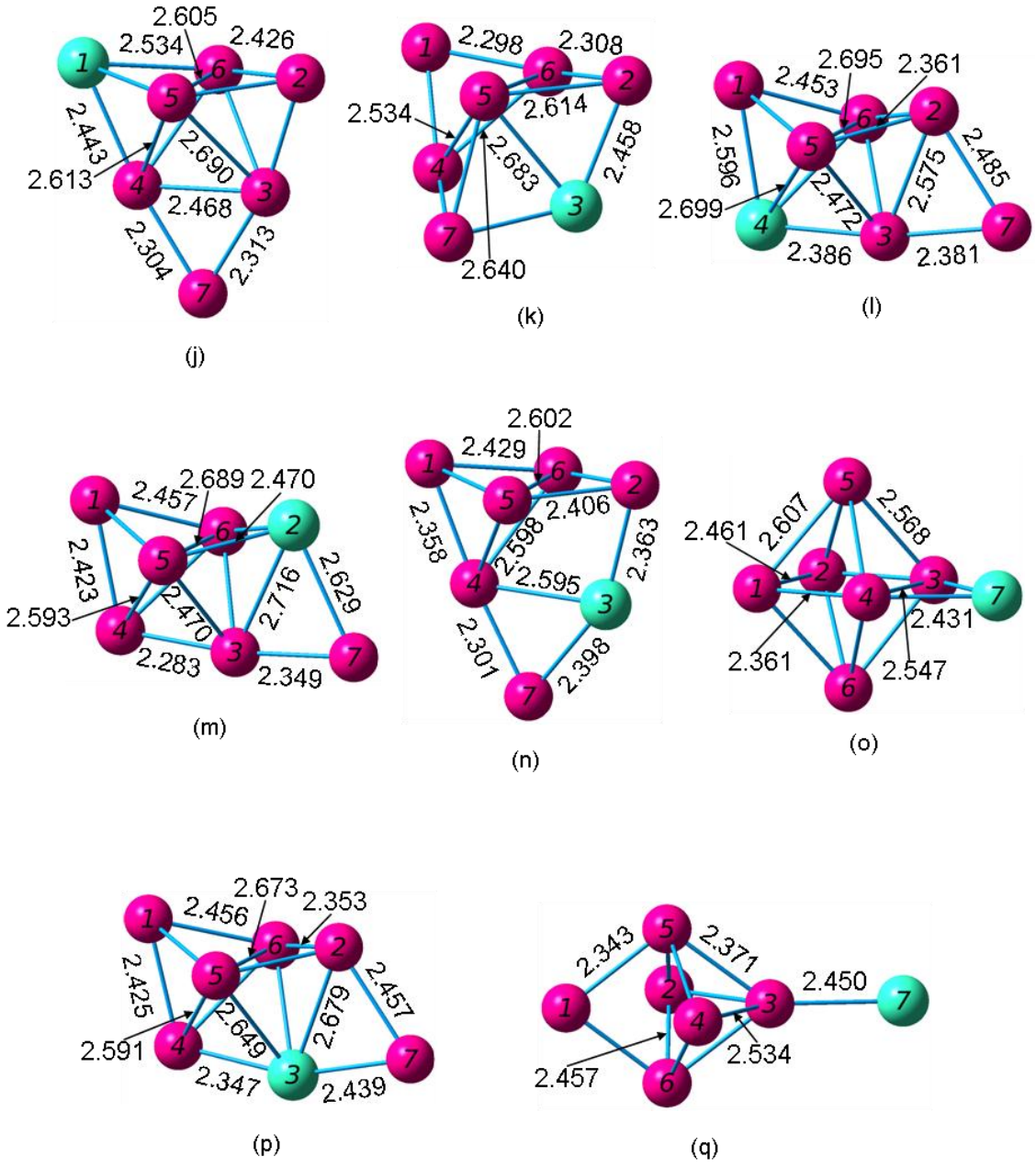

Figure 4.107 – *Continued*

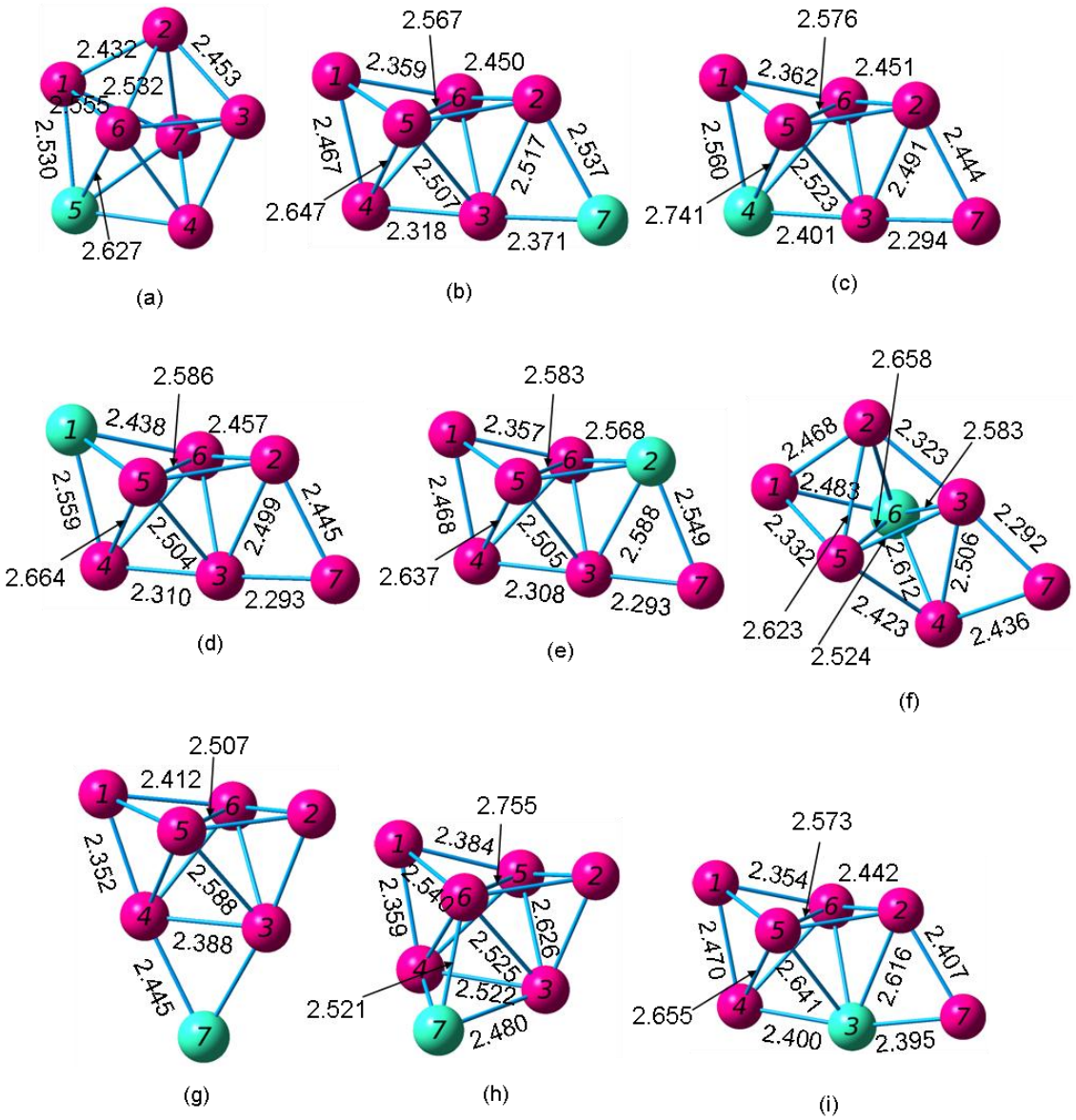

Figure 4.108 Geometries of the $(Si_6Ge)^-$ Anionic Septamers from (a) Most Stable through (q) Least Stable

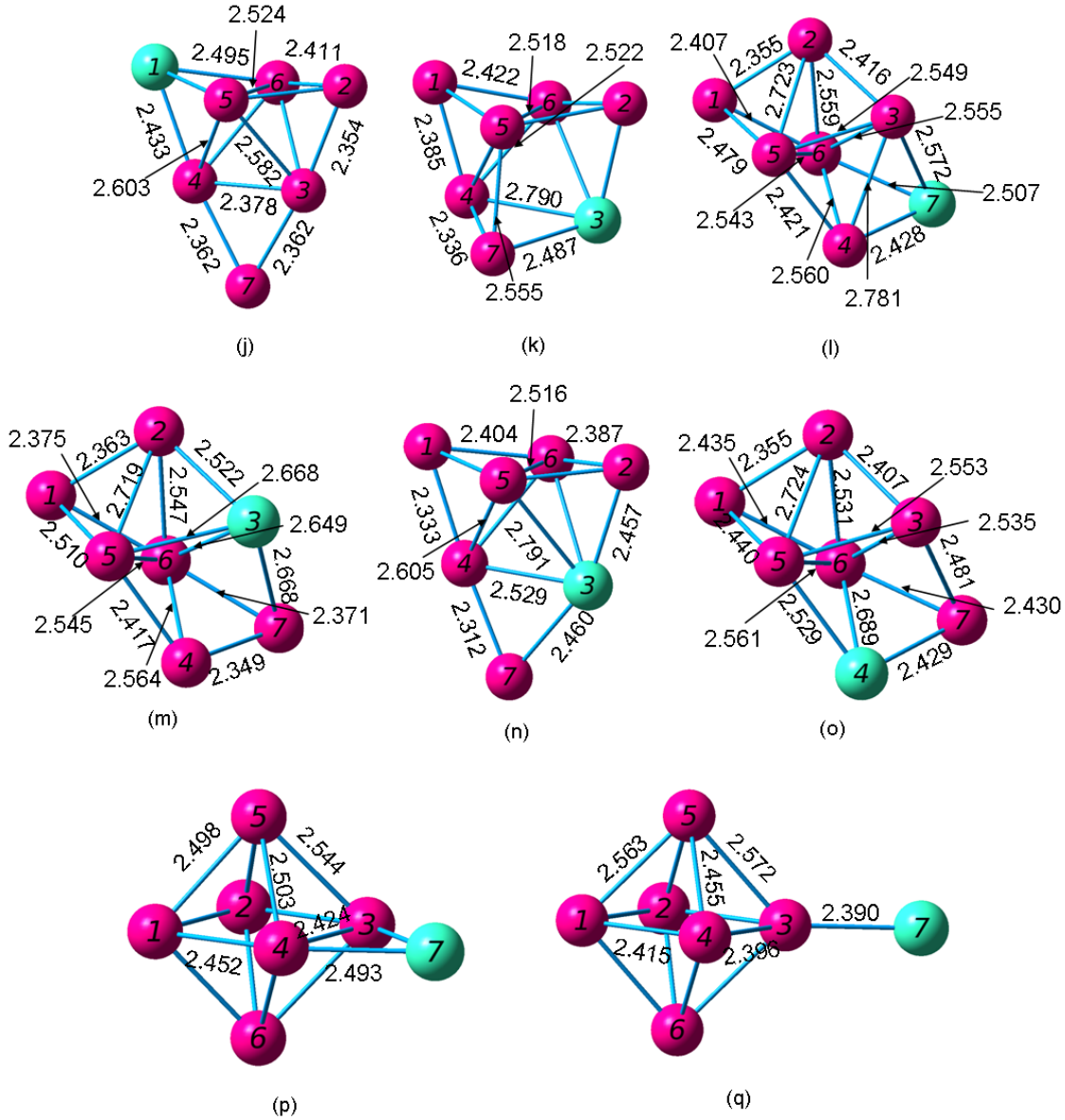

Figure 4.108 – *Continued*

4.17 Si_5Ge_2 Septamers

Marim *et al.* [49] reported their ground state cluster to be a pentagonal bipyramid. The base has three Si atoms and two Ge atoms. The base is composed of one Ge-Ge bond with a length of 2.66 Å, two Si-Ge bonds with lengths of 2.58 Å, and two Si-Si bonds with lengths of 2.49 Å. The bonds connecting the Ge atoms to the Si tips are 2.59 Å, and those connecting the Si atoms to the tips are 2.50 Å. They calculated a cohesive energy of 3.08 eV/atom for this cluster. Wang and Chao [51] reported that the most stable Si_5Ge_2 cluster has a ^1A electronic state, a dissociation energy of -28.4466 eV or -29.6067 eV, a HOMO-LUMO gap of 2.99 eV, and the following frequencies: 385(a), 369(a), and 413(a).

To form our input geometries for the Si_5Ge_2 clusters, we began with our optimized neutral Si_6Ge clusters. We only looked at the more stable clusters and abandoned those of the type pictured in figure 4.106 (j), 4.106 (p), and 4.106 (q). For the geometries that we did try, we investigated all the possible combinations of arrangements of atoms, and we ended up with twelve different stable neutral clusters. In turn, these led to twelve stable cations and anions.

Table 4.113 Properties of the Si_5Ge_2 Neutral Septamers

Figure	Symmetry Group	Electronic State	Binding E / Atom (eV)	HOMO-LUMO Gap (eV)	Dipole Moment (D)
4.109 (a)	C_s	$^1A'$	3.142	2.999	0.729
4.109 (b)	C_s	$^1A'$	3.138	3.066	0.277
4.109 (c)	C_s	$^1A'$	3.114	2.976	0.459
4.109 (d)	C_{2v}	$^1A_1$	3.068	2.908	0.002
4.109 (e)	C_1	^1A	3.060	3.203	0.567
4.109 (f)	C_s	$^1A'$	3.054	2.982	0.776
4.109 (g)	C_{2v}	$^1A_1$	3.028	2.701	0.064
4.109 (h)	C_s	$^1A'$	3.025	3.102	0.214
4.109 (i)	C_1	^1A	3.019	2.742	0.897
4.109 (j)	C_{2v}	$^1A_1$	3.002	2.425	0.169
4.109 (k)	C_{2v}	$^1A_1$	2.995	3.042	0.297
4.109 (l)	C_s	$^1A'$	2.978	2.586	0.699

Table 4.114 Properties of $(Si_5Ge_2)^+$ Septamers

Figure	Symmetry Group	Electronic State	Binding E / Atom (eV)	HOMO-LUMO Gap (eV)	Dipole Moment (D)
4.110 (a)	C_s	$^2A'$	3.198	1.679	1.653
4.110 (b)	C_s	$^2A'$	3.186	1.620	0.827
4.110 (c)	C_s	$^2A''$	3.155	1.616	1.435
4.110 (d)	C_s	$^2A''$	3.153	1.545	0.910
4.110 (e)	C_1	^2A	3.131	1.611	1.517
4.110 (f)	C_1	^2A	3.101	1.517	1.449
4.110 (g)	C_{2v}	$^2B_2$	3.101	1.520	0.434
4.110 (h)	C_1	^2A	3.100	1.499	1.937
4.110 (i)	C_{2v}	$^2A_1$	3.093	1.420	1.924
4.110 (j)	C_{2v}	$^2A_1$	3.093	1.476	1.945
4.110 (k)	C_1	^2A	3.071	1.509	1.083
4.110 (l)	C_{2v}	$^2A_1$	3.035	1.436	0.079

Table 4.115 Properties of the $(Si_5Ge_2)^-$ Septamers

Figure	Symmetry Group	Electronic State	Binding E / Atom (eV)	HOMO-LUMO Gap (eV)	Dipole Moment (D)
4.111 (a)	C_s	^2A"	3.238	1.595[a]	2.660
4.111 (b)	C_s	^2A"	3.233	1.597[a]	1.018
4.111 (c)	C_s	^2A'	3.228	1.612[a]	2.061
4.111 (d)	C_{2v}	$^2B_1$	3.206	1.512[a]	0.000
4.111 (e)	C_s	^2A'	3.143	1.431	1.599
4.111 (f)	C_{2v}	$^2B_1$	3.136	1.653[a]	3.177
4.111 (g)	C_1	^2A	3.131	1.456[a]	2.407
4.111 (h)	C_1	^2A	3.127	1.493	2.547
4.111 (i)	C_{2v}	$^2B_1$	3.120	1.552[a]	2.382
4.111 (j)	C_1	^2A	3.103	1.472	1.279
4.111 (k)	C_1	^2A	3.103	1.401	1.747
4.111 (l)	C_{2v}	$^2B_1$	3.086	1.658[a]	0.280

[a] HOMO and LUMO have opposite spins; this value includes the energy required to flip the spin of the electron.

Table 4.116 Ionization Potentials and Electron Affinities of the Si_5Ge_2 Septamers

Neutral Figure	VIP (eV)	Cationic Figure	AIP (eV)	VEA (eV)	Anionic Figure	AEA (eV)
4.109 (a)	7.758	4.110 (a)	7.513	1.535	4.111 (a)	1.810
4.109 (b)	7.813	4.110 (b)	7.562	1.531	4.111 (b)	1.806
4.109 (c)	7.815	4.110 (c)	7.612	1.613	4.111 (c)	1.937
4.109 (d)	7.920	4.110 (g)	7.670	1.789	4.111 (d)	2.103
4.109 (e)	7.481	4.110 (e)	7.405	1.131	4.111 (h)	1.607
4.109 (f)	7.575	4.110 (d)	7.206	1.413	4.111 (e)	1.762
4.109 (g)	7.512	4.110 (i)	7.448	1.751	4.111 (f)	1.890
4.109 (h)	7.671	4.110 (f)	7.367	1.299	4.111 (j)	1.684
4.109 (i)	7.489	4.110 (h)	7.332	1.604	4.111 (g)	1.922
4.109 (j)	7.342	4.110 (j)	7.266	1.847	4.111 (i)	1.966
4.109 (k)	7.768	4.110 (l)	7.616	1.633	4.111 (l)	1.779
4.109 (l)	7.435	4.110 (k)	7.248	1.684	4.111 (k)	2.010

Table 4.117 Fragmentation Energies of the Most Stable Si_5Ge_2 Neutral Septamer

Fragmented Clusters	Fragmentation Energy (eV)
$Si_5Ge + Ge$	3.415
$Si_4Ge_2 + Si$	3.688
$Si_3Ge + Si_2Ge$	4.198
$Si_4Ge + SiGe$	4.302
$Si_3Ge_2 + Si_2$	4.388
$Si_4Ge + Si + Ge$	7.363
$Si_3Ge_2 + 2Si$	7.611
$Si_3Ge + Si_2 + Ge$	7.726
$Si_3Ge + SiGe + Si$	7.887
$Si_2Ge_2 + Si_2 + Si$	7.994
$2Si_2Ge + Si$	8.495
$SiGe_2 + 2Si_2$	8.899
$Si_2Ge + Si_2 + SiGe$	8.962
$Si_3Ge + 2Si + Ge$	10.948
$Si_2Ge_2 + 3Si$	11.216
$Si_2Ge + Si_2 + Si + Ge$	12.023
$SiGe_2 + Si_2 + 2Si$	12.122
$Si_2Ge + SiGe + 2Si$	12.184
$2Si_2 + SiGe + Ge$	12.490
$2Si_2 + Ge_2 + Si$	12.623
$Si_2 + 2SiGe + Si$	12.651
$Si_2Ge + 3Si + Ge$	15.246
$SiGe_2 + 4Si$	15.344
$2Si_2 + Si + 2Ge$	15.551
$Si_2 + SiGe + 2Si + Ge$	15.712
$Si_2 + Ge_2 + 3Si$	15.845
$2SiGe + 3Si$	15.874
$Si_2 + 3Si + 2Ge$	18.774
$SiGe + 4Si + Ge$	18.935
$Ge_2 + 5Si$	19.068
$5Si + 2Ge$	21.997

Table 4.118 Fragmentation Energies of the Most Stable $(Si_5Ge_2)^+$ Cationic Septamer

Fragmented Clusters	Fragmentation Energy (eV)
$(Si_5Ge)^+ + Ge$	3.588
$(Si_4Ge_2)^+ + Si$	3.624
$Si_5Ge + Ge^+$	3.803
$(Si_3Ge)^+ + Si_2Ge$	4.452
$Si_4Ge + (SiGe)^+$	4.525
$Si_3Ge + (Si_2Ge)^+$	4.567
$(Si_4Ge)^+ + SiGe$	4.570
$(Si_3Ge_2)^+ + Si_2$	4.592
$(Si_4Ge)^+ + Si + Ge$	7.631
$Si_4Ge + Si + Ge^+$	7.751
$(Si_3Ge_2)^+ + 2Si$	7.815
$(Si_3Ge)^+ + Si_2 + Ge$	7.980
$Si_3Ge + (SiGe)^+ + Si$	8.110
$Si_3Ge + Si_2 + Ge^+$	8.113
$(Si_3Ge)^+ + SiGe + Si$	8.141
$(Si_2Ge_2)^+ + Si_2 + Si$	8.268
$(Si_2Ge)^+ + Si_2Ge + Si$	8.865
$Si_2Ge + Si_2 + (SiGe)^+$	9.185
$(Si_2Ge)^+ + Si_2 + SiGe$	9.331
$(SiGe_2)^+ + 2Si_2$	9.335
$(Si_3Ge)^+ + 2Si + Ge$	11.203
$Si_3Ge + 2Si + Ge^+$	11.336
$(Si_2Ge_2)^+ + 3Si$	11.490
$(Si_2Ge)^+ + Si_2 + Si + Ge$	12.393
$Si_2Ge + (SiGe)^+ + 2Si$	12.407
$Si_2Ge + Si_2 + Si + Ge^+$	12.411
$(Si_2Ge)^+ + SiGe + 2Si$	12.554
$(SiGe_2)^+ + Si_2 + 2Si$	12.558
$2Si_2 + (SiGe)^+ + Ge$	12.713
$Si_2 + (SiGe)^+ + Si_2 + Ge$	12.713
$2Si_2 + (Ge_2)^+ + Si$	12.730

Table 4.118 – *Continued*

Fragmented Clusters	Fragmentation Energy (eV)
$2Si_2 + (Ge_2)^+ + Si$	12.730
$Si_2 + (SiGe)^+ + SiGe + Si$	12.874
$2Si_2 + SiGe + Ge^+$	12.877
$(Si_2Ge)^+ + 3Si + Ge$	15.615
$Si_2Ge + 3Si + Ge^+$	15.633
$(SiGe_2)^+ + 4Si$	15.780
$Si_2 + (SiGe)^+ + 2Si + Ge$	15.936
$2Si_2 + Si + Ge^+ + Ge$	15.939
$Si_2 + (Ge_2)^+ + 3Si$	15.953
$(SiGe)^+ + SiGe + 3Si$	16.097
$Si_2 + SiGe + 2Si + Ge^+$	16.100
$(SiGe)^+ + 4Si + Ge$	19.158
$Si_2 + 3Si + Ge^+ + Ge$	19.161
$(Ge_2)^+ + 5Si$	19.175
$SiGe + 4Si + Ge^+$	19.323
$5Si + Ge^+ + Ge$	22.384

Table 4.119 Fragmentation Energies of the Most Stable $(Si_5Ge_2)^-$ Anionic Septamer

Fragmented Clusters	Fragmentation Energy (eV)
$(Si_5Ge)^- + Ge$	3.459
$(Si_4Ge_2)^- + Si$	3.614
$Si_3Ge + (Si_2Ge)^-$	3.829
$(Si_4Ge)^- + SiGe$	3.870
$(Si_3Ge)^- + Si_2Ge$	4.019
$(Si_3Ge_2)^- + Si_2$	4.019
$Si_5Ge + Ge^-$	4.087
$Si_4Ge + (SiGe)^-$	4.267
$(Si_4Ge)^- + Si + Ge$	6.931
$(Si_3Ge_2)^- + 2Si$	7.242
$(Si_3Ge)^- + Si_2 + Ge$	7.547
$(Si_3Ge)^- + SiGe + Si$	7.709
$(Si_2Ge_2)^- + Si_2 + Si$	7.838
$Si_3Ge + (SiGe)^- + Si$	7.852
$Si_4Ge + Si + Ge^-$	8.036
$(Si_2Ge)^- + Si_2Ge + Si$	8.126
$Si_3Ge + Si_2 + Ge^-$	8.398
$(Si_2Ge)^- + Si_2 + SiGe$	8.593
$(SiGe_2)^- + 2Si_2$	8.676
$Si_2Ge + Si_2 + (SiGe)^-$	8.927
$(Si_3Ge)^- + 2Si + Ge$	10.770
$(Si_2Ge_2)^- + 3Si$	11.061
$Si_3Ge + 2Si + Ge^-$	11.621
$(Si_2Ge)^- + Si_2 + Si + Ge$	11.654
$(Si_2Ge)^- + SiGe + 2Si$	11.815
$(SiGe_2)^- + Si_2 + 2Si$	11.898
$Si_2Ge + (SiGe)^- + 2Si$	12.150
$2Si_2 + (SiGe)^- + Ge$	12.455
$2Si_2 + (SiGe)^- + Ge$	12.455
$Si_2 + (SiGe)^- + SiGe + Si$	12.616
$2Si_2 + Si + (Ge_2)^-$	12.617

Table 4.119 – *Continued*

Fragmented Clusters	Fragmentation Energy (eV)
$2Si_2 + (Ge_2)^- + Si$	12.617
$Si_2Ge + Si_2 + Si + Ge^-$	12.695
$2Si_2 + SiGe + Ge^-$	13.162
$2Si_2 + SiGe + Ge^-$	13.162
$(Si_2Ge)^- + 3Si + Ge$	14.877
$(SiGe_2)^- + 4Si$	15.121
$Si_2 + (SiGe)^- + 2Si + Ge$	15.678
$(SiGe)^- + SiGe + 3Si$	15.839
$Si_2 + (Ge_2)^- + 3Si$	15.840
$Si_2Ge + 3Si + Ge^-$	15.918
$2Si_2 + Si + Ge^- + Ge$	16.223
$Si_2 + SiGe + 2Si + Ge^-$	16.385
$(SiGe)^- + 4Si + Ge$	18.900
$(Ge_2)^- + 5Si$	19.063
$Si_2 + 3Si + Ge^- + Ge$	19.446
$SiGe + 4Si + Ge^-$	19.608
$5Si + Ge^- + Ge$	22.669

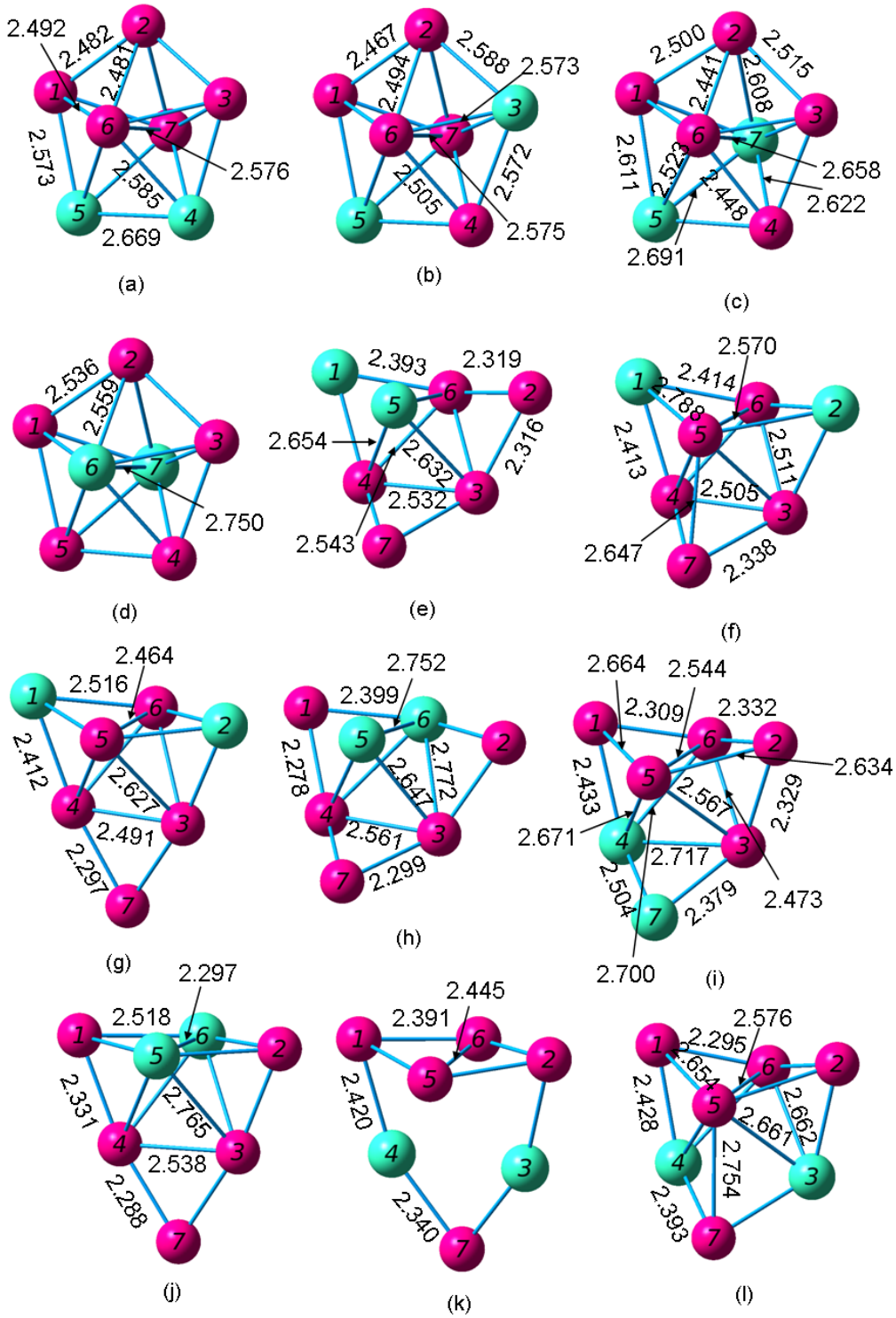

Figure 4.109 Geometries of the Si_5Ge_2 Neutral Septamers from (a) Most Stable through (l) Least Stable

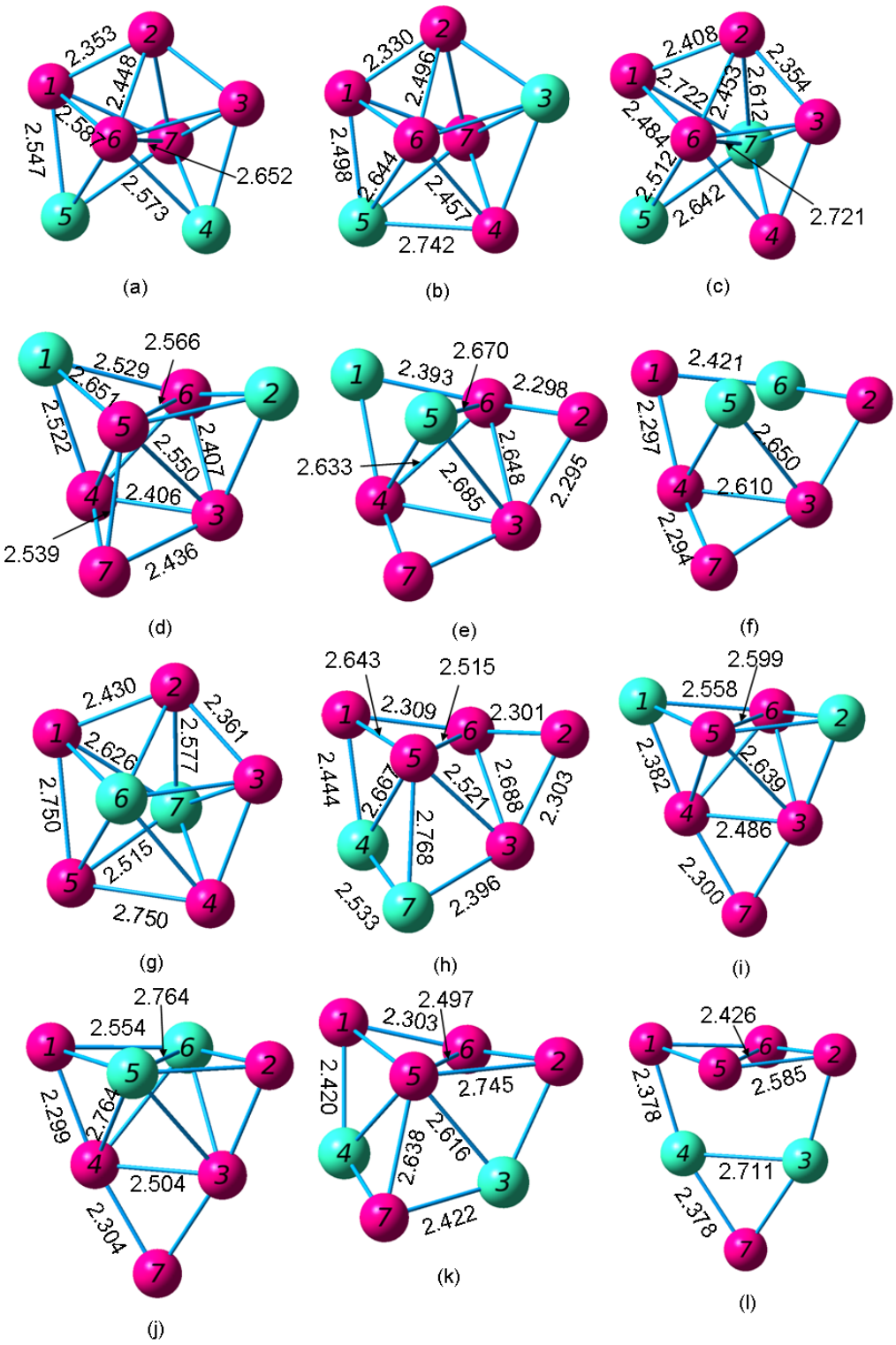

Figure 4.110 Geometries of the $(Si_5Ge_2)^+$ Cationic Septamers from (a) Most Stable through (l) Least Stable

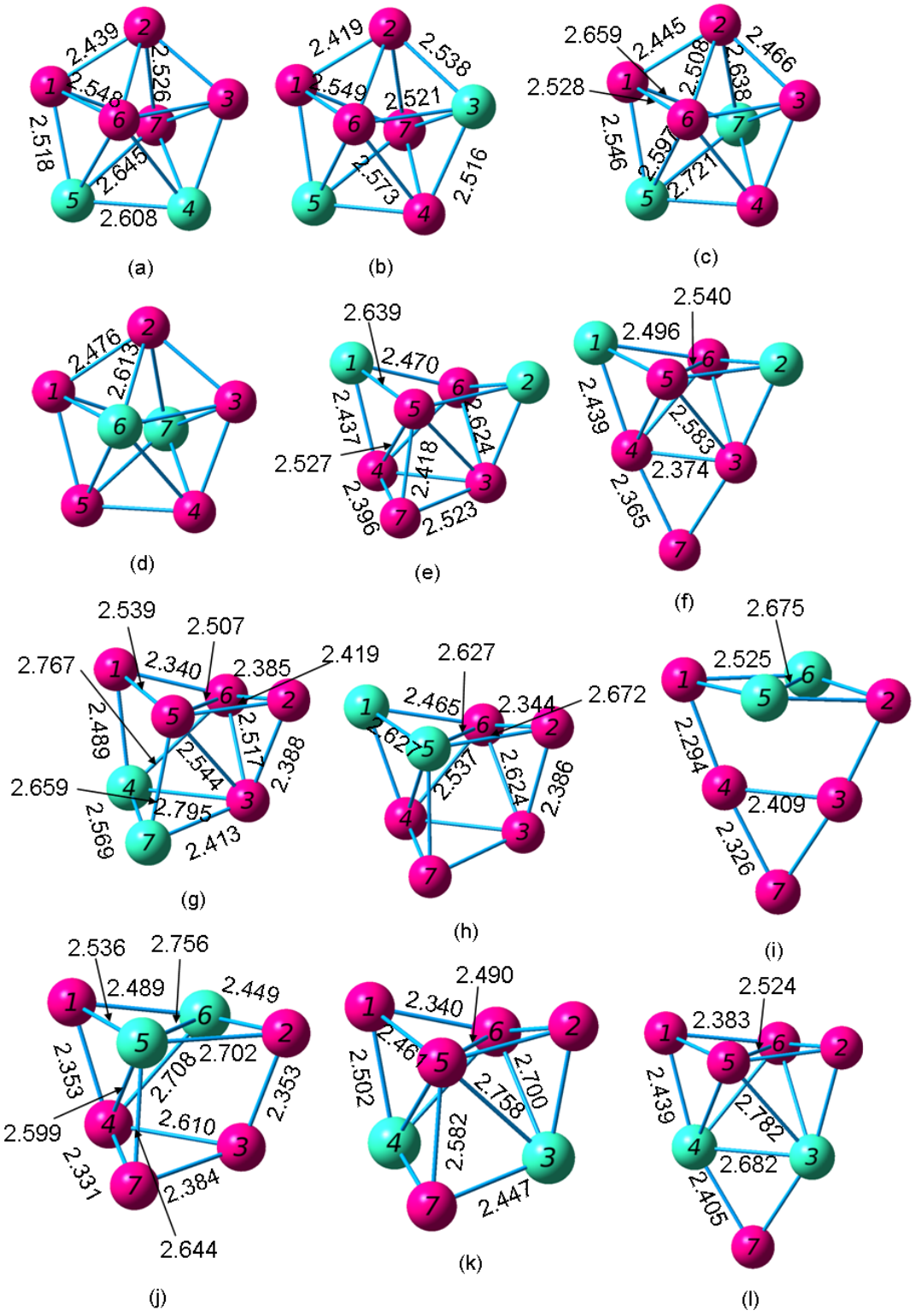

Figure 4.111 Geometries of the $(Si_5Ge_2)^-$ Anionic Septamers from (a) Most Stable through (l) Least Stable

4.18 Si_4Ge_3 Septamers

Marim *et al.* [49] reported their ground state cluster to be a pentagonal bipyramid. The base has two Si atoms and three Ge atoms. The base is composed of two Ge-Ge bonds with lengths of 2.65 Å, two Si-Ge bonds with lengths of 2.58 Å, and one Si-Si bond with a length of 2.48 Å. The bonds connecting the Ge atoms to the Si tips are 2.61 Å, and those connecting the Si atoms to the tips are 2.50 Å. They calculated a cohesive energy of 3.06 eV/atom for this cluster. Wang and Chao [51] reported that the most stable Si_4Ge_3 cluster has a ^1A electronic state, a dissociation energy of -29.0237 eV or -29.2701 eV, a HOMO-LUMO gap of 3.01 eV, and the following frequencies: 372(a), 300(a), and 338(a). They reported a second cluster with a ^1A electronic state, a dissociation energy of -29.0188 eV or -29.2496 eV, a HOMO-LUMO gap of 2.98 eV, and the following frequencies: 357(a), 405(a), and 366(a).

To find input geometries for the Si_4Ge_3 clusters, we used the same approach as we did for the Si_5Ge_2 clusters. We used the Si_6Ge neutral clusters as a basis and replace some of the silicon atoms with germanium atoms. This gave us sixteen neutral, cation, and anion isomers.

Table 4.120 Properties of the Si_4Ge_3 Neutral Septamers

Figure	Symmetry Group	Electronic State	Binding E / Atom (eV)	HOMO-LUMO Gap (eV)	Dipole Moment (D)
4.112 (a)	C_s	$^1A'$	3.098	2.979	0.704
4.112 (b)	C_s	$^1A'$	3.093	3.085	0.270
4.112 (c)	C_1	^1A	3.075	2.911	0.714
4.112 (d)	C_1	^1A	3.070	2.976	0.273
4.112 (e)	C_s	$^1A'$	3.030	2.798	0.457
4.112 (f)	C_s	$^1A'$	3.018	3.237	0.540
4.112 (g)	C_s	$^1A'$	3.011	2.898	0.440
4.112 (h)	C_{2v}	$^1A_1$	2.989	2.641	0.570
4.112 (i)	C_s	$^1A'$	2.981	3.060	0.530
4.112 (j)	C_s	$^1A'$	2.979	2.773	0.790
4.112 (k)	C_1	^1A	2.974	2.766	0.744
4.112 (l)	C_{2v}	$^1A_1$	2.961	2.368	0.798
4.112 (m)	C_{2v}	$^1A_1$	2.960	2.958	0.798
4.112 (n)	C_s	$^1A'$	2.954	3.164	0.180
4.112 (o)	C_s	$^1A'$	2.943	2.679	0.829
4.112 (p)	C_s	$^1A'$	2.901	2.950	0.549

Table 4.121 Properties of the $(Si_4Ge_3)^+$ Cationic Septamers

Figure	Symmetry Group	Electronic State	Binding E / Atom (eV)	HOMO-LUMO Gap (eV)	Dipole Moment (D)
4.113 (a)	C_s	$^2A'$	3.157	1.588[a]	1.299
4.113 (b)	C_s	$^2A'$	3.150	1.762[a]	0.705
4.113 (c)	C_1	^2A	3.142	1.678[a]	1.606
4.113 (d)	C_1	^2A	3.134	1.719[a]	1.054
4.113 (e)	C_s	$^2A''$	3.127	1.507[a]	0.467
4.113 (f)	C_s	$^2A'$	3.098	1.744[a]	1.122
4.113 (g)	C_s	$^2A'$	3.090	1.650[a]	1.312
4.113 (h)	C_s	$^2A'$	3.065	1.519[a]	1.836
4.113 (i)	C_s	$^2A'$	3.063	1.517[a]	0.656
4.113 (j)	C_1	^2A	3.062	1.503[a]	1.036
4.113 (k)	C_{2v}	$^2A_1$	3.058	1.487[a]	0.848
4.113 (l)	C_{2v}	$^2A_1$	3.057	1.306	0.789
4.113 (m)	C_s	$^2A'$	3.042	1.512[a]	1.744
4.113 (n)	C_s	$^2A'$	3.033	1.491[a]	0.985
4.113 (o)	C_{2v}	$^2A_1$	3.012	1.432	0.851
4.113 (p)	C_s	$^2A'$	3.012	1.512[a]	0.152

[a] HOMO and LUMO have opposite spins; this value includes the energy required to flip the spin of the electron.

Table 4.122 Properties of the $(Si_4Ge_3)^-$ Septamers

Figure	Symmetry Group	Electronic State	Binding E / Atom (eV)	HOMO-LUMO Gap (eV)	Dipole Moment (D)
4.114 (a)	C_s	^2A”	3.190	1.554[a]	2.371
4.114 (b)	C_1	^2A	3.185	1.573[a]	2.619
4.114 (c)	C_s	^2A”	3.185	1.555[a]	0.902
4.114 (d)	C_1	^2A	3.180	1.574[a]	1.424
4.114 (e)	C_s	^2A”	3.163	1.478[a]	1.488
4.114 (f)	C_{2v}	$^2B_1$	3.101	1.664[a]	1.018
4.114 (g)	C_s	^2A”	3.090	1.222	0.543
4.114 (h)	C_s	^2A’	3.087	1.430[a]	2.312
4.114 (i)	C_s	^2A’	3.085	1.505	1.671
4.114 (j)	C_{2v}	$^2B_1$	3.081	1.564[a]	0.356
4.114 (k)	C_1	^2A	3.080	1.429[a]	1.413
4.114 (l)	C_s	^2A’	3.064	1.463[a]	1.148
4.114 (m)	C_{2v}	$^2B_1$	3.055	1.647[a]	2.093
4.114 (n)	C_s	^2A’	3.051	1.355	2.825
4.114 (o)	C_s	^2A”	3.041	1.409	0.664
4.114 (p)	C_s	^2A’	3.030	1.463	1.802

[a] HOMO and LUMO have opposite spins; this value includes the energy required to flip the spin of the electron.

Table 4.123 Ionization Potentials and Electron Affinities of the Si_4Ge_3 Septamers

Neutral Figure	VIP (eV)	Cationic Figure	AIP (eV)	VEA (eV)	Anionic Figure	AEA (eV)
4.112 (a)	7.726	4.113 (a)	7.484	1.533	4.114 (a)	1.786
4.112 (b)	7.823	4.113 (b)	7.499	1.530	4.114 (c)	1.781
4.112 (c)	7.739	4.113 (c)	7.430	1.595	4.114 (b)	1.908
4.112 (d)	7.778	4.113 (d)	7.455	1.605	4.114 (d)	1.904
4.112 (e)	7.794	4.113 (f)	7.429	1.774	4.114 (e)	2.065
4.112 (f)	7.500	4.113 (g)	7.395	1.158	4.114 (i)	1.604
4.112 (g)	7.434	4.113 (e)	7.088	1.385	4.114 (g)	1.696
4.112 (h)	7.481	4.113 (l)	7.421	1.798	4.114 (f)	1.925
4.112 (i)	7.405	4.113 (i)	7.326	1.226	4.114 (l)	1.716
4.112 (j)	7.490	4.113 (h)	7.297	1.588	4.114 (h)	1.895
4.112 (k)	7.485	4.113 (j)	7.288	1.560	4.114 (k)	1.882
4.112 (l)	7.312	4.113 (k)	7.221	1.858	4.114 (j)	1.979
4.112 (m)	7.688	4.113 (o)	7.538	1.639	4.114 (m)	1.802
4.112 (n)	7.447	4.113 (n)	7.346	1.178	4.114 (o)	1.747
4.112 (o)	7.420	4.113 (m)	7.207	1.593	4.114 (n)	1.893
4.112 (p)	7.333	4.113 (p)	7.126	1.293	4.114 (p)	2.043

Table 4.124 Fragmentation Energies of the Most Stable Si_4Ge_3 Neutral Septamer

Fragmented Clusters	Fragmentation Energy (eV)
Si_4Ge_2 + Ge	3.375
Si_3Ge_3 + Si	3.673
Si_3Ge + $SiGe_2$	3.984
Si_4Ge + Ge_2	4.123
Si_2Ge_2 + Si_2Ge	4.153
Si_3Ge_2 + SiGe	4.237
Si_2Ge_3+ Si_2	4.325
Si_4Ge + 2Ge	7.051
Si_3Ge_2 + Si +Ge	7.299
Si_2Ge_3 + 2Si	7.548
Si_3Ge + SiGe + Ge	7.575
Si_2Ge_2 + Si_2 + Ge	7.681
Si_3Ge + Ge_2 + Si	7.708
Si_2Ge_2 + SiGe + Si	7.843
$SiGe_3$ + Si_2 + Si	8.025
$2Si_2Ge$ + Ge	8.183
Si_2Ge + $SiGe_2$ + Si	8.281
$SiGe_2$ + Si_2 + SiGe	8.748
Si_2Ge + Si_2 + Ge_2	8.782
Si_2Ge + 2SiGe	8.811
Si_3Ge + Si + 2Ge	10.636
Si_2Ge_2 + 2Si + Ge	10.904
$SiGe_3$ + 3Si	11.248
Si_2Ge + Si_2 + 2Ge	11.711
$SiGe_2$ + Si_2 + Si + Ge	11.810
Si_2Ge + SiGe + Si + Ge	11.872
$SiGe_2$ + SiGe + 2Si	11.971
Si_2Ge + Ge_2 + 2Si	12.005
$2Si_2$ + Ge_2 + Ge	12.311
Si_2 + 2SiGe + Ge	12.339
Si_2 + SiGe + Ge_2 + Si	12.472

Table 4.124 – *Continued*

Fragmented Clusters	Fragmentation Energy (eV)
SiGe + 2SiGe + Si	12.500
Si_2Ge + 2Si + 2Ge	14.934
$SiGe_2$ + 3Si + Ge	15.032
$2Si_2$ + 3Ge	15.239
Si_2 + SiGe + Si + 2Ge	15.400
Si_2 + Ge_2 + 2Si + Ge	15.533
2SiGe + 2Si + Ge	15.562
Ge_2 + SiGe + 3Si	15.695
Si_2 + 2Si + 3Ge	18.462
SiGe + 3Si + 2Ge	18.623
Ge_2 + 4Si + Ge	18.756
4Si + 3Ge	21.684

Table 4.125 Fragmentation Energies of the Most Stable $(Si_4Ge_3)^+$ Cationic Septamer

Fragmented Clusters	Fragmentation Energy (eV)
$(Si_4Ge_2)^+ + Ge$	3.341
$(Si_3Ge_3)^+ + Si$	3.658
$Si_4Ge_2 + Ge^+$	3.792
$Si_4Ge + (Ge_2)^+$	4.259
$(Si_3Ge)^+ + SiGe_2$	4.268
$(Si_4Ge)^+ + Ge_2$	4.420
$Si_3Ge + (SiGe_2)^+$	4.449
$(Si_2Ge_2)^+ + Si_2Ge$	4.457
$(Si_3Ge_2)^+ + SiGe$	4.471
$Si_3Ge_2 + (SiGe)^+$	4.490
$Si_2Ge_2 + (Si_2Ge)^+$	4.552
$(Si_2Ge_3)^+ + Si_2$	4.673
$(Si_4Ge)^+ + 2Ge$	7.348
$Si_4Ge + Ge^+ + Ge$	7.468
$(Si_3Ge_2)^+ + Si + Ge$	7.532
$Si_3Ge_2 + Si + Ge^+$	7.715
$Si_3Ge + (SiGe)^+ + Ge$	7.827
$Si_3Ge + (Ge_2)^+ + Si$	7.844
$(Si_3Ge)^+ + SiGe + Ge$	7.858
$(Si_2Ge_3)^+ + 2Si$	7.896
$(Si_2Ge_2)^+ + Si_2 + Ge$	7.985
$(Si_3Ge)^+ + Ge_2 + Si$	7.991
$Si_3Ge + SiGe + Ge^+$	7.992
$Si_2Ge_2 + (SiGe)^+ + Si$	8.095
$Si_2Ge_2 + Si_2 + Ge^+$	8.098
$(Si_2Ge_2)^+ + SiGe + Si$	8.146
$(SiGe_3)^+ + Si_2 + Si$	8.205
$(Si_2Ge)^+ + Si_2Ge + Ge$	8.582
$2Si_2Ge + Ge^+$	8.599
$(Si_2Ge)^+ + SiGe_2 + Si$	8.680
$Si_2Ge + (SiGe_2)^+ + Si$	8.747

Table 4.125 – *Continued*

Fragmented Clusters	Fragmentation Energy (eV)
$Si_2Ge + Si_2 + (Ge_2)^+$	8.919
$SiGe_2 + Si_2 + (SiGe)^+$	9.000
$Si_2Ge + (SiGe)^+ + SiGe$	9.063
$(Si_2Ge)^+ + Si_2 + Ge_2$	9.181
$(Si_2Ge)^+ + 2SiGe$	9.210
$(SiGe_2)^+ + Si_2 + SiGe$	9.213
$(Si_3Ge)^+ + Si + 2Ge$	10.920
$Si_3Ge + Si + Ge^+ + Ge$	11.053
$(Si_2Ge_2)^+ + 2Si + Ge$	11.207
$Si_2Ge_2 + 2Si + Ge^+$	11.321
$(SiGe_3)^+ + 3Si$	11.428
$(Si_2Ge)^+ + Si_2 + 2Ge$	12.110
$Si_2Ge + (SiGe)^+ + Si + Ge$	12.124
$Si_2Ge + Si_2 + Ge^+ + Ge$	12.128
$Si_2Ge + (Ge_2)^+ + 2Si$	12.141
$SiGe_2 + (SiGe)^+ + 2Si$	12.223
$SiGe_2 + Si_2 + Si + Ge^+$	12.226
$(Si_2Ge)^+ + SiGe + Si + Ge$	12.271
$(SiGe_2)^+ + Si_2 + Si + Ge$	12.275
$Si_2Ge + SiGe + Si + Ge^+$	12.289
$(Si_2Ge)^+ + Ge_2 + 2Si$	12.404
$(SiGe_2)^+ + SiGe + 2Si$	12.436
$Si_2 + Si_2 + (Ge_2)^+ + Ge$	12.447
$Si_2 + (SiGe)^+ + SiGe + Ge$	12.591
$Si_2 + SiGe + (Ge_2)^+ + Si$	12.608
$Si_2 + (SiGe)^+ + Ge_2 + Si$	12.724
$2Si_2 + Ge_2 + Ge^+$	12.727
$(SiGe)^+ + 2SiGe + Si$	12.752
$Si_2 + 2SiGe + Ge^+$	12.756
$(Si_2Ge)^+ + 2Si + 2Ge$	15.332
$Si_2Ge + 2Si + Ge^+ + Ge$	15.350

Table 4.125 – *Continued*

Fragmented Clusters	Fragmentation Energy (eV)
$SiGe_2 + 3Si + Ge^+$	15.449
$(SiGe_2)^+ + 3Si + Ge$	15.497
$Si_2 + (SiGe)^+ + Si + 2Ge$	15.653
$2Si_2 + Ge^+ + 2Ge$	15.656
$Si_2 + (Ge_2)^+ + 2Si + Ge$	15.670
$(SiGe)^+ + SiGe + 2Si + Ge$	15.814
$Si_2 + SiGe + Si + Ge^+ + Ge$	15.817
$(Ge_2)^+ + SiGe + 3Si$	15.831
$Ge_2 + (SiGe)^+ + 3Si$	15.947
$Si_2 + Ge_2 + 2Si + Ge^+$	15.950
$2SiGe + 2Si + Ge^+$	15.978
$(SiGe)^+ + 3Si + 2Ge$	18.875
$Si_2 + 2Si + Ge^+ + 2Ge$	18.878
$(Ge_2)^+ + 4Si + Ge$	18.892
$SiGe + 3Si + Ge^+ + Ge$	19.040
$Ge_2 + 4Si + Ge^+$	19.173
$4Si + Ge^+ + 2Ge$	22.101

Table 4.126 Fragmentation Energies of the Most Stable $(Si_4Ge_3)^-$ Anionic Septamer

Fragmented Clusters	Fragmentation Energy (eV)
$(Si_4Ge_2)^- + Ge$	3.278
$(Si_3Ge_3)^- + Si$	3.613
$(Si_4Ge)^- + Ge_2$	3.667
$Si_3Ge + (SiGe_2)^-$	3.737
$Si_2Ge_2 + (Si_2Ge)^-$	3.761
$(Si_3Ge)^- + SiGe_2$	3.782
$(Si_3Ge_2)^- + SiGe$	3.845
$(Si_2Ge_2)^- + Si_2Ge$	3.974
$(Si_2Ge_3)^- + Si_2$	3.986
$Si_4Ge_2 + Ge^-$	4.024
$Si_4Ge + (Ge_2)^-$	4.094
$Si_3Ge_2 + (SiGe)^-$	4.179
$(Si_4Ge)^- + 2Ge$	6.596
$(Si_3Ge_2)^- + Si + Ge$	6.906
$(Si_2Ge_3)^- + 2Si$	7.209
$(Si_3Ge)^- + SiGe + Ge$	7.373
$(Si_2Ge_2)^- + Si_2 + Ge$	7.503
$(Si_3Ge)^- + Ge_2 + Si$	7.506
$Si_3Ge + (SiGe)^- + Ge$	7.516
$(Si_2Ge_2)^- + SiGe + Si$	7.664
$Si_3Ge + (Ge_2)^- + Si$	7.679
$Si_4Ge + Ge^- + Ge$	7.700
$Si_2Ge_2 + (SiGe)^- + Si$	7.784
$(Si_2Ge)^- + Si_2Ge + Ge$	7.790
$(SiGe_3)^- + Si_2 + Si$	7.878
$(Si_2Ge)^- + SiGe_2 + Si$	7.889
$Si_3Ge_2 + Si + Ge^-$	7.947
$Si_2Ge + (SiGe_2)^- + Si$	8.034
$Si_3Ge + SiGe + Ge^-$	8.223
$Si_2Ge_2 + Si_2 + Ge^-$	8.330
$(Si_2Ge)^- + Si_2 + Ge_2$	8.390

Table 4.126 – *Continued*

Fragmented Clusters	Fragmentation Energy (eV)
$(Si_2Ge)^-$ + 2SiGe	8.418
$(SiGe_2)^-$ + Si_2 + SiGe	8.501
$SiGe_2$ + Si_2 + $(SiGe)^-$	8.690
Si_2Ge + $(SiGe)^-$ + SiGe	8.752
Si_2Ge + Si_2 + $(Ge_2)^-$	8.753
Si_2Ge + Si_2Ge + Ge^-	8.831
$(Si_3Ge)^-$ + Si + 2Ge	10.434
$(Si_2Ge_2)^-$ + 2Si + Ge	10.725
$(SiGe_3)^-$ + 3Si	11.100
Si_3Ge + Si + Ge^- + Ge	11.285
$(Si_2Ge)^-$ + Si_2 + 2Ge	11.318
$(Si_2Ge)^-$ + SiGe + Si + Ge	11.479
Si_2Ge_2 + 2Si + Ge^-	11.553
$(SiGe_2)^-$ + Si_2 + Si + Ge	11.562
$(Si_2Ge)^-$ + Ge_2 + 2Si	11.612
$(SiGe_2)^-$ + SiGe + 2Si	11.724
Si_2Ge + $(SiGe)^-$ + Si + Ge	11.814
$SiGe_2$ + $(SiGe)^-$ + 2Si	11.912
Si_2Ge + $(Ge_2)^-$ + 2Si	11.976
Si_2 + $(SiGe)^-$ + SiGe + Ge	12.280
2Si_2 + $(Ge_2)^-$ + Ge	12.281
Si_2Ge + Si_2 + Ge^- + Ge	12.359
Si_2 + $(SiGe)^-$ + Ge_2 + Si	12.413
$(SiGe)^-$ + 2SiGe + Si	12.442
Si_2 + SiGe + $(Ge_2)^-$ + Si	12.443
$SiGe_2$ + Si_2 + Si + Ge^-	12.458
Si_2Ge + SiGe + Si + Ge^-	12.521
2Si_2 + Ge_2 + Ge^-	12.959
Si_2 + 2SiGe + Ge^-	12.987
$(Si_2Ge)^-$ + 2Si + 2Ge	14.541
$(SiGe_2)^-$ + 3Si + Ge	14.785

Table 4.126 – *Continued*

Fragmented Clusters	Fragmentation Energy (eV)
$Si_2 + (SiGe)^- + Si + 2Ge$	15.342
$(SiGe)^- + SiGe + 2Si + Ge$	15.503
$Si_2 + (Ge_2)^- + 2Si + Ge$	15.504
$Si_2Ge + 2Si + Ge^- + Ge$	15.582
$Ge_2 + (SiGe)^- + 3Si$	15.636
$(Ge_2)^- + SiGe + 3Si$	15.665
$SiGe_2 + 3Si + Ge^-$	15.681
$2Si_2 + Ge^- + 2Ge$	15.888
$Si_2 + SiGe + Si + Ge^- + Ge$	16.049
$Si_2 + Ge_2 + 2Si + Ge^-$	16.182
$2SiGe + 2Si + Ge^-$	16.210
$(SiGe)^- + 3Si + 2Ge$	18.564
$(Ge_2)^- + 4Si + Ge$	18.727
$Si_2 + 2Si + Ge^- + 2Ge$	19.110
$SiGe + 3Si + Ge^- + Ge$	19.272
$Ge_2 + 4Si + Ge^-$	19.405
$4Si + Ge^- + 2Ge$	22.333

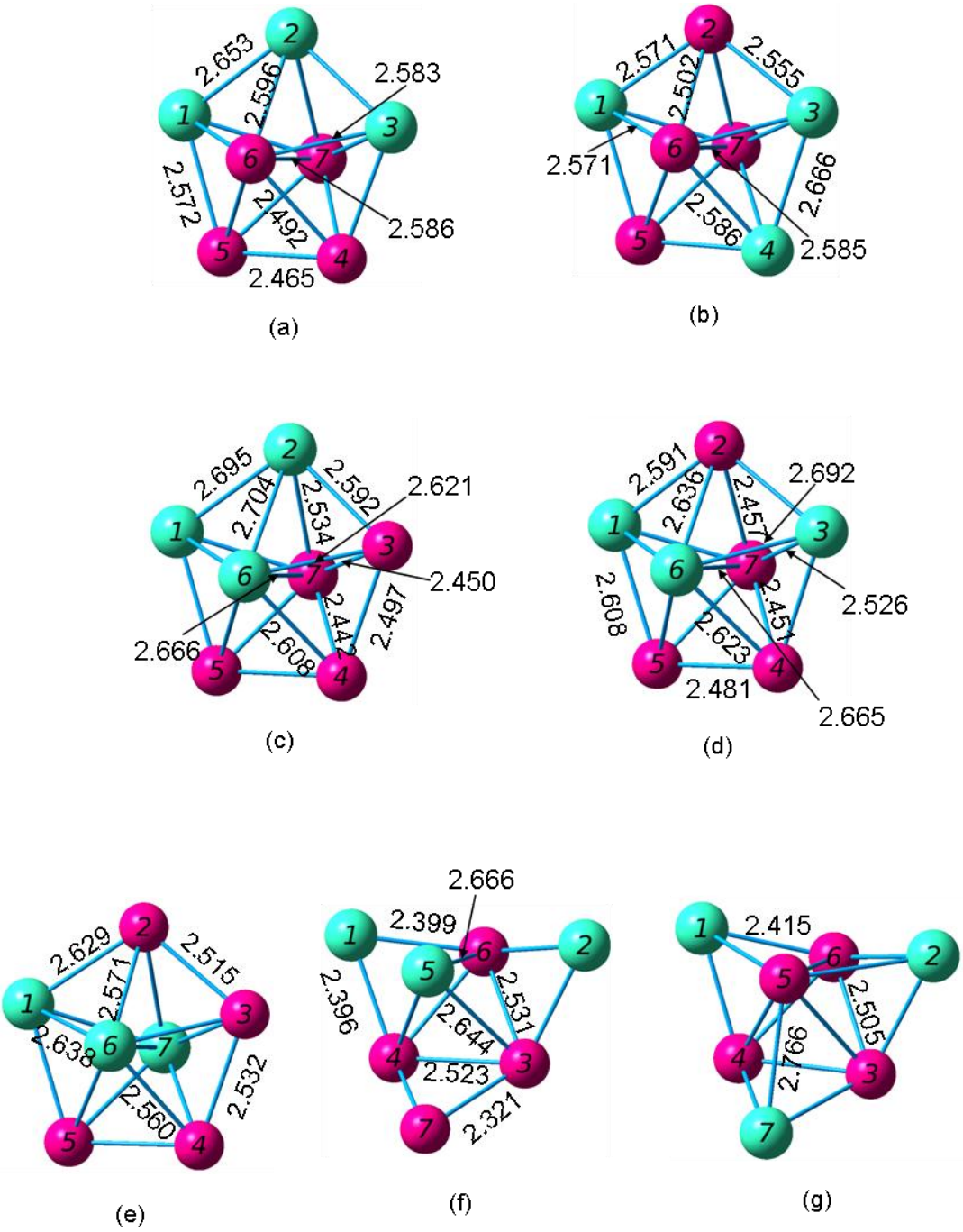

Figure 4.112 Geometries of the Si_4Ge_3 Neutral Septamers from (a) Most Stable through (p) Least Stable

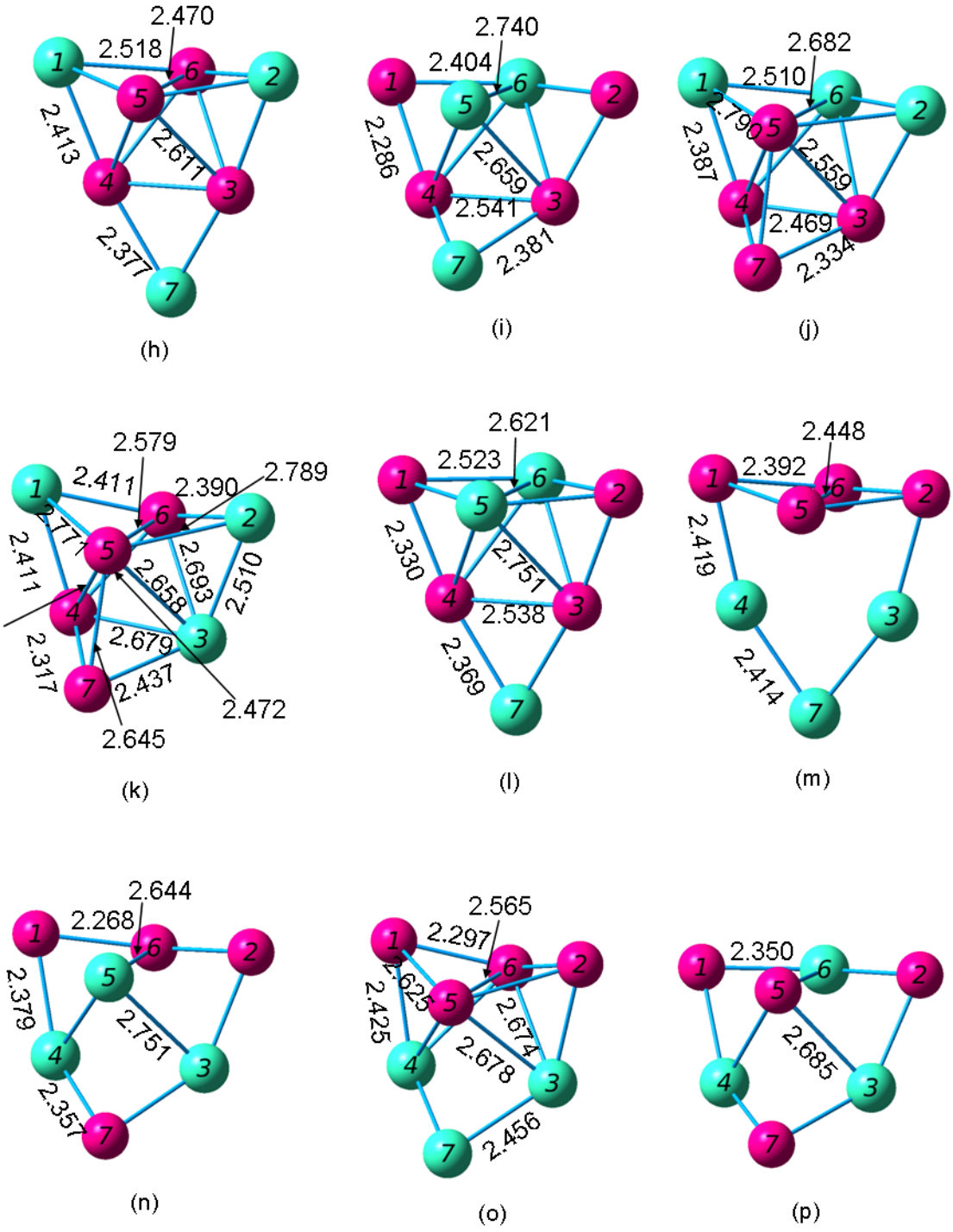

Figure 4.112 – *Continued*

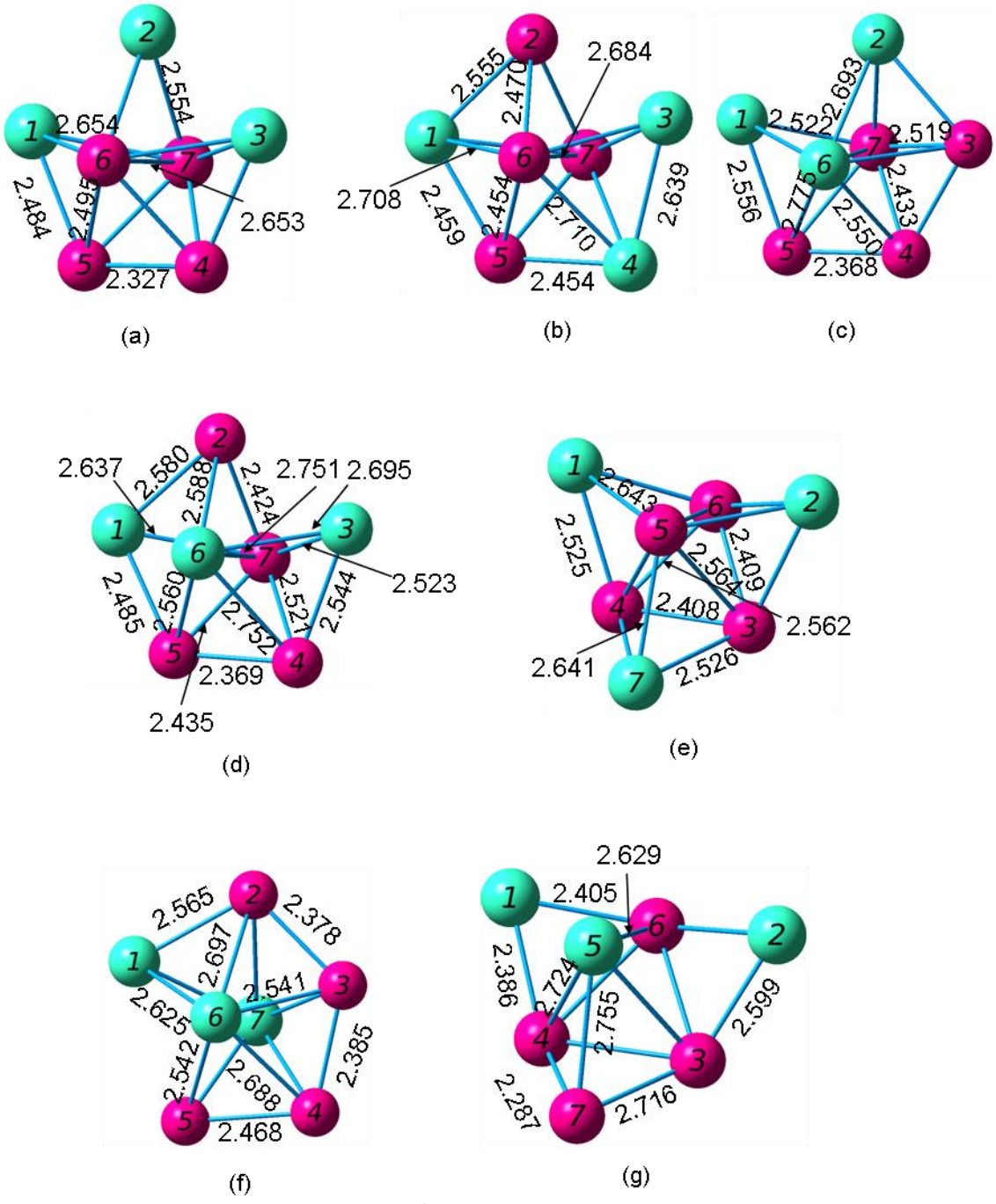

Figure 4.113 Geometries of the $(Si_4Ge_3)^+$ Cationic Septamers from (a) Most Stable through (p) Least Stable

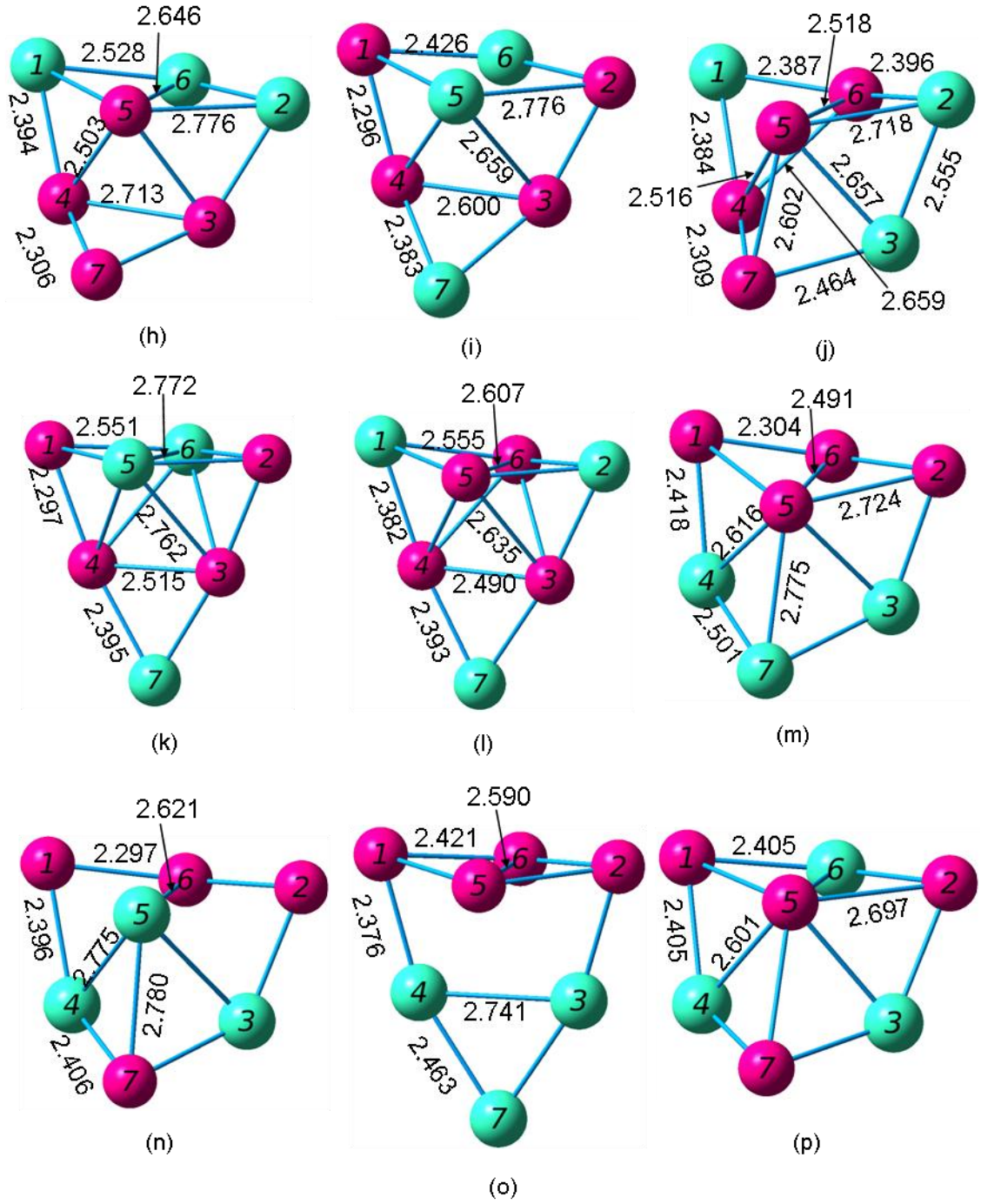

Figure 4.113 – *Continued*

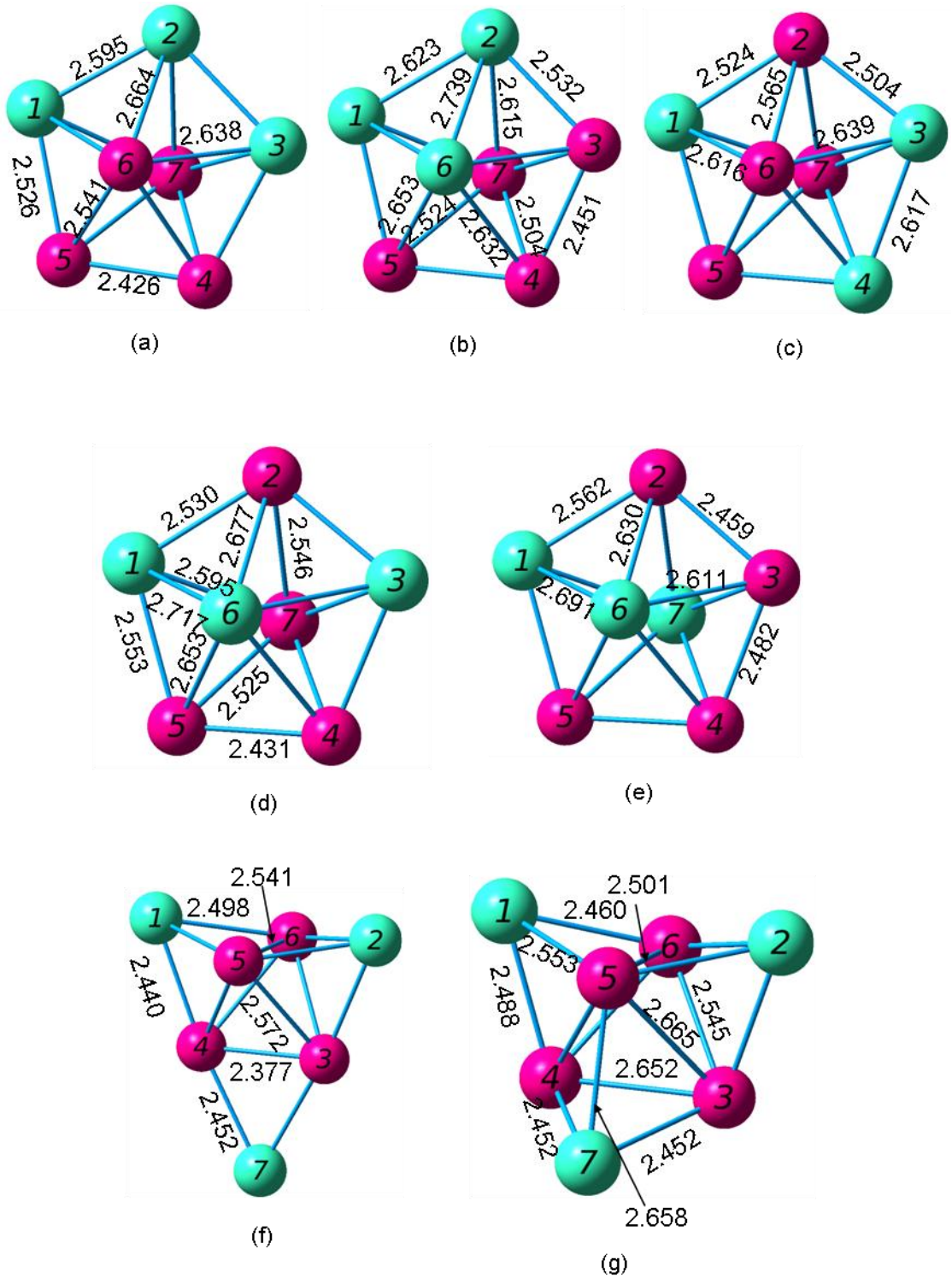

Figure 4.114 Geometries of the $(Si_4Ge_3)^-$ Anionic Septamers from (a) Most Stable through (p) Least Stable

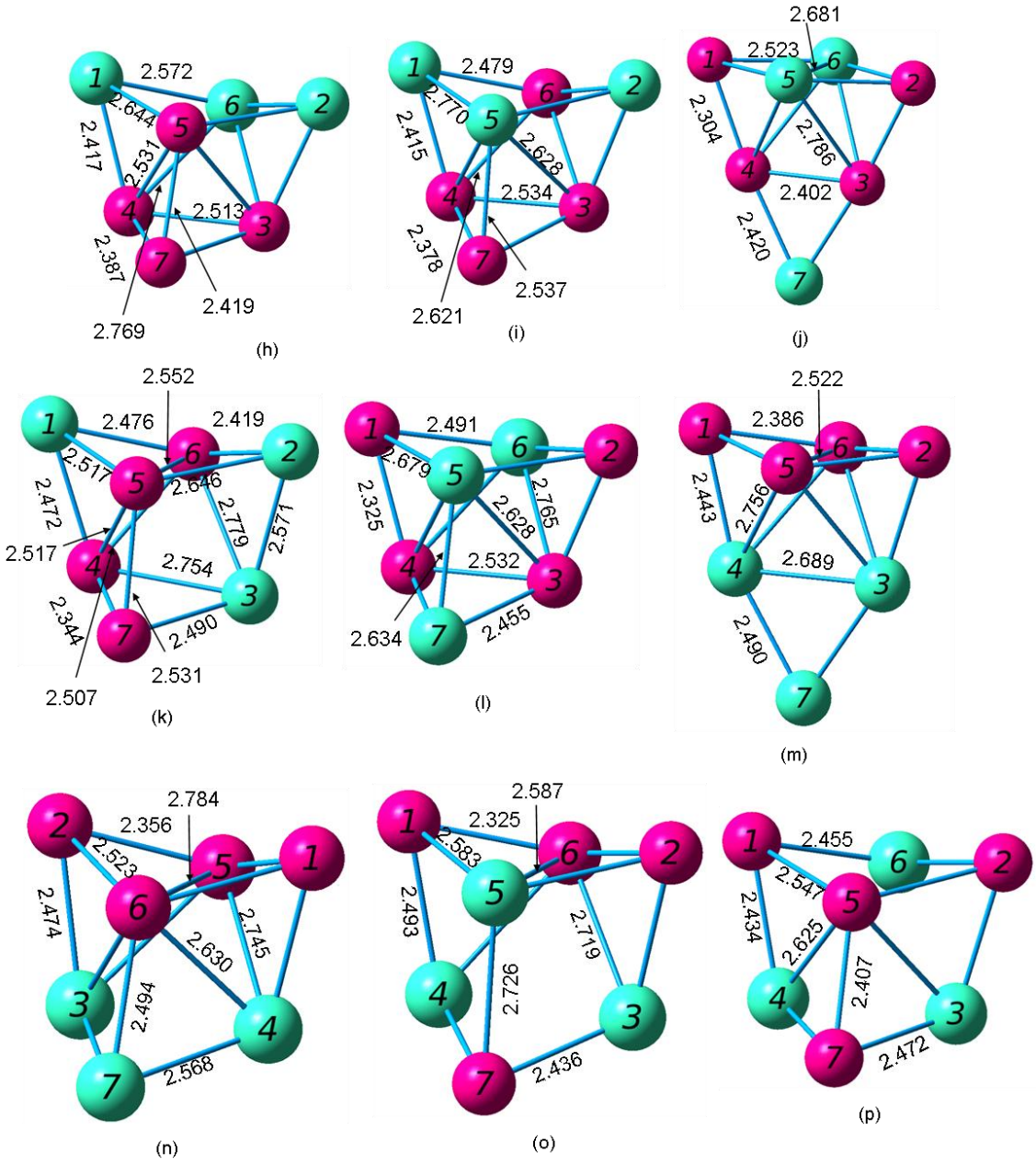

Figure 4.114 – *Continued*

4.19 Si_3Ge_4 Septamers

Li *et al.* [48] reported a pentagonal bipyramid with C_{2v} symmetry. The base has four Ge atoms and one Si atom. This cluster has a $^1A_1$ electronic state, a 2.79 eV HOMO-LUMO gap, and 325(A_1), 246(B_2), and 321 (B_2) frequencies. Marim *et al.* [49] reported the same Si_3Ge_4 cluster. The base is composed of one Ge-Ge bond with a length of 2.65 Å, two Ge-Ge bonds with lengths of 2.66 Å, and two Si-Ge bonds with lengths of 2.57 Å. The bonds connecting the Ge atoms to the Si tips are 2.61 Å, and those connecting the Si atoms to the tips are 2.59 Å. They calculated a cohesive energy of 3.04 eV/atom for this cluster. Wang and Chao [51] reported that the most stable Si_3Ge_4 cluster has a ^1A electronic state, a dissociation energy of -28.6982 eV or -28.8949 eV, a HOMO-LUMO gap of 3.03 eV, and the following frequencies: 305(a), 353(a), and 253(a).

To create the input geometries for the septamers, we started with the optimized neutral Si_4Ge_3 geometries and simply switched the silicon and germanium atoms. We also tried three geometries from Pradhan and Ray's paper on silicon carbon clusters [6]. As before, we exchanged their silicon atoms with our germanium atoms and their carbon atoms with our silicon atoms. We did not pursue this approach as input structures for the other septamers because they led to the five least stable clusters (figures 4.115 (r) through 4.115 (v)). Totally, we report results for twenty-one neutrals, cations, and anions.

Table 4.127 Properties of the Si_3Ge_4 Septamers

Figure	Symmetry Group	Electronic State	Binding E / Atom (eV)	HOMO-LUMO Gap (eV)	Dipole Moment (D)
4.115 (a)	C_s	$^1A'$	3.052	3.033	0.425
4.115 (b)	C_1	^1A	3.035	2.888	0.691
4.115 (c)	C_1	^1A	3.030	2.998	0.267
4.115 (d)	C_s	$^1A'$	2.996	2.730	0.715
4.115 (e)	C_s	$^1A'$	2.991	2.785	0.273
4.115 (f)	C_s	$^1A'$	2.976	3.286	0.074
4.115 (g)	C_s	$^1A'$	2.948	3.071	0.485
4.115 (h)	C_1	^1A	2.943	3.075	0.525
4.115 (i)	C_1	^1A	2.934	2.730	0.427
4.115 (j)	C_1	^1A	2.927	2.342	0.498
4.115 (k)	C_{2v}	$^1A_1$	2.920	2.490	0.302
4.115 (l)	C_s	$^1A'$	2.919	3.173	0.402
4.115 (m)	C_1	^1A	2.913	3.121	0.535
4.115 (n)	C_{2v}	$^1A_1$	2.898	3.060	0.189
4.115 (o)	C_s	$^1A'$	2.896	2.580	0.739
4.115 (p)	C_s	$^1A'$	2.887	3.243	0.144
4.115 (q)	C_{2v}	$^1A_1$	2.883	2.828	0.037
4.115 (r)	C_{2v}	$^1A_1$	2.781	1.860	0.549
4.115 (s)	Cs	1A'	2.779	2.118	0.530
4.115 (t)	C_{2v}	$^1A_1$	2.661	2.269	0.788
4.115 (u)	$D_{\infty h}$	$^1\Sigma_g$	2.038	1.386	0.000

Table 4.128 Properties of the $(Si_3Ge_4)^+$ Septamers

Figure	Symmetry Group	Electronic State	3.119	HOMO-LUMO Gap (eV)	Dipole Moment (D)
4.116 (a)	C_s	$^2A'$	3.108	1.710[a]	0.908
4.116 (b)	C_1	^2A	3.098	1.669[a]	1.342
4.116 (c)	C_1	^2A	3.077	1.746[a]	0.883
4.116 (d)	C_s	$^2A''$	3.073	1.509[a]	0.830
4.116 (e)	C_s	$^2A'$	3.065	1.693[a]	1.261
4.116 (f)	C_s	$^2A'$	3.057	1.726[a]	0.717
4.116 (g)	C_1	^2A	3.057	1.517[a]	1.219
4.116 (h)	C_1	^2A	3.031	1.487[a]	0.630
4.116 (i)	C_s	$^2A'$	3.028	1.508[a]	1.754
4.116 (j)	C_1	^2A	3.017	1.533[a]	1.080
4.116 (k)	C_{2v}	$^2A_1$	3.005	1.454[a]	2.247
4.116 (l)	C_s	$^2A'$	3.003	1.470[a]	1.541
4.116 (m)	C_s	$^2A'$	3.000	1.533[a]	0.167
4.116 (n)	C_1	^2A	2.984	1.499[a]	0.801
4.116 (o)	C_{2v}	$^2A_1$	2.970	1.382[a]	0.891
4.116 (p)	C_s	$^2A'$	2.953	1.435[a]	0.267
4.116 (q)	C_{2v}	$^2A_1$	2.952	1.469[a]	0.833
4.116 (r)	C_s	$^2A''$	2.946	1.555[a]	1.361
4.116 (s)	C_{2v}	$^2A_1$	2.803	1.450	0.653
4.116 (t)	C_{2v}	$^2B_1$	2.214	1.590[a]	0.569
4.116 (u)	$D_{\infty h}$	--	3.119	0.921	0.000

[a] HOMO and LUMO have opposite spins; this value includes the energy required to flip the spin of the electron.

Table 4.129 Properties of the $(Si_3Ge_4)^-$ Septamers

Figure	Symmetry Group	Electronic State	Binding E / Atom (eV)	HOMO-LUMO Gap (eV)	Dipole Moment (D)
4.117 (a)	C_s	^2A"	3.141	1.515[a]	1.320
4.117 (b)	C_1	^2A	3.141	1.535[a]	2.362
4.117 (c)	C_1	^2A	3.135	1.537[a]	1.279
4.117 (d)	C_s	^2A"	3.123	1.444[a]	2.172
4.117 (e)	C_s	^2A"	3.119	1.446[a]	0.834
4.117 (f)	C_1	^2A	3.092	1.647[a]	1.733
4.117 (g)	C_s	^2A'	3.038	1.450	1.375
4.117 (h)	C_1	^2A	3.037	1.405[a]	0.642
4.117 (i)	C_s	^2A'	3.030	1.434[a]	1.870
4.117 (j)	C_{2v}	$^2B_1$	3.026	1.485[a]	3.696
4.117 (k)	C_1	^2A	3.017	1.418	1.185
4.117 (l)	C_s	^2A"	3.010	1.303	1.209
4.117 (m)	C_1	^2A	3.000	1.430[a]	0.934
4.117 (n)	C_s	^2A'	2.993	1.383	2.624
4.117 (o)	C_{2v}	$^2B_1$	2.985	1.567[a]	1.736
4.117 (p)	C_{2v}	$^2B_1$	2.981	1.506[a]	0.969
4.117 (q)	C_s	^2A"	2.969	1.322	0.659
4.117 (r)	C_s	^2A'	2.906	1.521[a]	1.861
4.117 (s)	C_{2v}	$^2A_2$	2.900	1.137	0.923
4.117 (t)	C_{2v}	$^2B_2$	2.805	1.417[a]	1.036
4.117 (u)	$D_{\infty h}$	--	2.295	1.044[a]	0.000

[a] HOMO and LUMO have opposite spins; this value includes the energy required to flip the spin of the electron.

Table 4.130 Ionization Potentials and Electron Affinities of the Si_3Ge_4 Septamers

Neutral Figure	VIP (eV)	Cationic Figure	AIP (eV)	VEA (eV)	Anionic Figure	AEA (eV)
4.115 (a)	7.788	4.116 (a)	7.429	1.532	4.117 (a)	1.763
4.115 (b)	7.693	4.116 (b)	7.387	1.589	4.117 (b)	1.880
4.115 (c)	7.793	4.116 (c)	7.425	1.596	4.117 (c)	1.876
4.115 (d)	7.710	4.116 (e)	7.359	1.767	4.117 (d)	2.032
4.115 (e)	7.733	4.116 (f)	7.384	1.764	4.117 (e)	2.029
4.115 (f)	7.564	4.116 (d)	7.193	1.146	4.117 (g)	1.570
4.115 (g)	7.414	4.116 (i)	7.319	1.215	4.117 (i)	1.715
4.115 (h)	7.418	4.116 (j)	7.301	1.237	4.117 (k)	1.660
4.115 (i)	7.467	4.116 (h)	7.044	1.573	4.117 (h)	1.854
4.115 (j)	7.102	4.116 (g)	6.992	1.617	4.117 (f)	2.295
4.115 (k)	7.309	4.116 (k)	7.223	1.753	4.117 (j)	1.878
4.115 (l)	7.389	4.116 (l)	7.302	1.139	4.117 (n)	1.658
4.115 (m)	7.395	4.116 (n)	7.295	1.192	4.117 (m)	1.747
4.115 (n)	7.659	4.116 (s)	7.558	1.574	4.117 (o)	1.750
4.115 (o)	7.378	4.116 (m)	7.147	1.682	4.117 (l)	1.940
4.115 (p)	7.451	4.116 (p)	7.321	1.131	4.117 (q)	1.708
4.115 (q)	7.544	4.116 (q)	7.406	1.663	4.117 (p)	1.829
4.115 (r)	6.822	4.116 (o)	6.480	1.911	4.117 (s)	1.974
4.115 (s)	6.879	4.116 (r)	6.688	1.780	4.117 (r)	2.027
4.115 (t)	7.052	4.116 (t)	6.903	1.811	4.117 (t)	2.148
4.115 (u)	6.712	4.116 (u)	6.664	2.912	4.117 (u)	2.942

Table 4.131 Fragmentation Energies of the Most Stable Si_3Ge_4 Neutral Septamer

Fragmented Clusters	Fragmentation Energy (eV)
Si_3Ge_3 + Ge	3.352
Si_2Ge_4 + Si	3.640
Si_2Ge_2 + $SiGe_2$	3.930
Si_2Ge_3 + SiGe	4.165
$SiGe_3$ + Si_2Ge	4.176
$SiGe_4$+ Si_2	4.403
Si_3Ge_2+ Ge_2	6.977
Si_3Ge_2 + 2Ge	6.977
Si_2Ge_3 + Si + Ge	7.226
Si_3Ge + Ge_2 + Ge	7.386
Si_2Ge_2 + SiGe + Ge	7.521
$SiGe_4$ + 2Si	7.626
Si_2Ge_2 + Ge_2 + Si	7.654
$SiGe_3$ + Si_2 + Ge	7.704
$SiGe_3$ + SiGe + Si	7.865
$SiGe_2$ + Si_2Ge + Ge	7.960
2$SiGe_2$ + Si	8.058
$SiGe_2$ + Si_2 + Ge_2	8.559
$SiGe_2$ + 2SiGe	8.588
Si_2Ge + SiGe + Ge_2	8.622
Si_3Ge + 3Ge	10.314
Si_2Ge_2 + 2Ge + Si	10.582
$SiGe_3$ + Ge + 2Si	10.926
$SiGe_2$ + Si_2 + 2Ge	11.488
Si_2Ge + SiGe + 2Ge	11.550
$SiGe_2$ + SiGe + Si + Ge	11.649
Si_2Ge + Ge_2 + Si + Ge	11.683
$SiGe_2$ + Ge_2 + 2Si	11.782
Si_2 + SiGe + Ge_2 + Ge	12.150
3SiGe + Ge	12.178
Si_2 + 2Ge_2 + Si	12.283

Table 4.131 – *Continued*

Fragmented Clusters	Fragmentation Energy (eV)
$2SiGe + Ge_2 + Si$	12.311
$Si_2Ge + Si + 3Ge$	14.612
$SiGe_2 + 2Ge + 2Si$	14.710
$Si_2 + SiGe + 3Ge$	15.078
$Si_2 + Ge_2 + 2Ge + Si$	15.211
$2SiGe + Si + 2Ge$	15.240
$SiGe + Ge_2 + Ge + 2Si$	15.373
$2Ge_2 + 3Si$	15.506
$Si_2 + Si + 4Ge$	18.140
$SiGe + 2Si + 3Ge$	18.301
$Ge_2 + 3Si + 2Ge$	18.434
$4Ge + 3Si$	21.363

Table 4.132 Fragmentation Energies of the Most Stable $(Si_3Ge_4)^+$ Cationic Septamer

Fragmented Clusters	Fragmentation Energy (eV)
$(Si_3Ge_3)^+ + Ge$	3.391
$(Si_2Ge_4)^+ + Si$	3.792
$Si_3Ge_3 + Ge^+$	3.823
$Si_3Ge_2 + (Ge_2)^+$	4.240
$(Si_2Ge_2)^+ + SiGe_2$	4.288
$(Si_3Ge_2)^+ + Ge_2$	4.337
$(SiGe_3)^+ + Si_2Ge$	4.411
$Si_2Ge_2 + (SiGe_2)^+$	4.450
$Si_2Ge_3 + (SiGe)^+$	4.472
$(Si_2Ge_3)^+ + SiGe$	4.567
$SiGe_3 + (Si_2Ge)^+$	4.629
$(SiGe_4)^+ + Si_2$	4.752
$(Si_3Ge_2)^+ + 2Ge$	7.265
$Si_3Ge_2 + Ge^+ + Ge$	7.449
$Si_3Ge + (Ge_2)^+ + Ge$	7.577
$(Si_2Ge_3)^+ + Ge + Si$	7.629
$Si_2Ge_3 + Ge^+ + Si$	7.698
$(Si_3Ge)^+ + Ge_2 + Ge$	7.725
$Si_2Ge_2 + (SiGe)^+ + Ge$	7.828
$Si_2Ge_2 + (Ge_2)^+ + Si$	7.845
$Si_3Ge + Ge_2 + Ge^+$	7.858
$(Si_2Ge_2)^+ + SiGe + Ge$	7.879
$(SiGe_3)^+ + Si_2 + Ge$	7.939
$(SiGe_4)^+ + 2Si$	7.975
$Si_2Ge_2 + SiGe + Ge^+$	7.993
$(Si_2Ge_2)^+ + Ge_2 + Si$	8.012
$(SiGe_3)^+ + SiGe + Si$	8.100
$SiGe_3 + (SiGe)^+ + Si$	8.172
$SiGe_3 + Si_2 + Ge^+$	8.175
$SiGe_2 + (Si_2Ge)^+ + Ge$	8.413
$SiGe_2 + Si_2Ge^+ Ge+$	8.431

Table 4.132 – *Continued*

Fragmented Clusters	Fragmentation Energy (eV)
$(SiGe_2)^+ + Si_2Ge + Ge$	8.480
$(SiGe_2)^+ + SiGe_2 + Si$	8.578
$SiGe_2 + (Ge_2)^+ + Si_2$	8.750
$Si_2Ge + (Ge_2)^+ + SiGe$	8.813
$SiGe_2 + SiGe^+ + SiGe$	8.895
$Si_2Ge + Ge_2 + (SiGe)^+$	8.929
$(Si_2Ge)^+ + Ge_2 + SiGe$	9.076
$(SiGe_2)^+ + Ge_2 + Si_2$	9.079
$(SiGe_2)^+ + 2SiGe$	9.108
$(Si_3Ge)^+ + 3Ge$	10.653
$Si_3Ge + Ge^+ + 2Ge$	10.786
$(Si_2Ge_2)^+ + 2Ge + Si$	10.941
$Si_2Ge_2 + Ge^+ + Si + Ge$	11.054
$(SiGe_3)^+ + 2Si + Ge$	11.161
$SiGe_3 + 2Si + Ge^+$	11.398
$GeSi_2 + (GeSi)^+ + 2Ge$	11.858
$Si_2Ge + (Ge_2)^+ + Si + Ge$	11.875
$SiGe_2 + (SiGe)^+ + Si + Ge$	11.956
$SiGe_2 + Si_2 + Ge^+ + Ge$	11.959
$SiGe_2 + (Ge_2)^+ + 2Si$	11.973
$(Si_2Ge)^+ + SiGe + 2Ge$	12.004
$(SiGe_2)^+ + Si_2 + 2Ge$	12.008
$Si_2Ge + SiGe + Ge^+ + Ge$	12.022
$SiGe_2 + SiGe + Si + Ge^+$	12.121
$(Si_2Ge)^+ + Ge_2 + Si + Ge$	12.137
$Si_2Ge + Ge_2 + Si + Ge^+$	12.155
$(SiGe_2)^+ + SiGe + Si + Ge$	12.169
$(SiGe_2)^+ + Ge_2 + 2Si$	12.302
$(Ge_2)^+ + SiGe + Si_2 + Ge$	12.341
$Ge_2 + (SiGe)^+ + Si_2 + Ge$	12.457
$Si_2 + (Ge_2)^+ + Ge_2 + Si$	12.474

Table 4.132 – *Continued*

Fragmented Clusters	Fragmentation Energy (eV)
$(SiGe)^+ + 2SiGe + Ge$	12.486
$(Ge_2)^+ + 2SiGe + Si$	12.503
$(SiGe)^+ + SiGe + Ge_2 + Si$	12.619
$Si_2 + SiGe + Ge_2 + Ge^+$	12.622
$3SiGe + Ge^+$	12.650
$(Si_2Ge)^+ + Si + 3Ge$	15.066
$Si_2Ge + Si + Ge^+ + 2Ge$	15.083
$SiGe_2 + Ge^+ + Ge + 2Si$	15.182
$(SiGe_2)^+ + 2Ge + 2Si$	15.231
$Si_2 + (SiGe)^+ + 3Ge$	15.386
$(Ge_2)^+ + Si_2 + Si + 2Ge$	15.403
$(SiGe)^+ + SiGe + Si + 2Ge$	15.547
$Si_2 + SiGe + Ge^+ + 2Ge$	15.550
$SiGe + (Ge_2)^+ + Ge + 2Si$	15.564
$(SiGe)^+ + Ge_2 + 2Si + Ge$	15.680
$Si_2 + Ge_2 + Si + Ge^+ + Ge$	15.683
$(Ge_2)^+ + Ge_2 + 3Si$	15.697
$2SiGe + Si + Ge^+ + Ge$	15.711
$SiGe + Ge_2 + Ge^+ + 2Si$	15.844
$(SiGe)^+ + 2Si + 3Ge$	18.609
$Si_2 + Ge^+ + 3Ge + Si$	18.612
$(Ge_2)^+ + 2Ge + 3Si$	18.625
$SiGe + Ge^+ + 2Si + 2Ge$	18.773
$Ge_2 + Ge^+ + Ge + 3Si$	18.906
$3Si + Ge^+ + 2Ge$	21.834

Table 4.133 Fragmentation Energies of the Most Stable $(Si_3Ge_4)^-$ Anionic Septamer

Fragmented Clusters	Fragmentation Energy (eV)
$(Si_3Ge_3)^- + Ge$	3.268
$(Si_2Ge_4)^- + Si$	3.579
$(Si_3Ge_2)^- + Ge_2$	3.633
$Si_2Ge_2 + (SiGe_2)^-$	3.660
$(Si_2Ge_2)^- + SiGe_2$	3.728
$SiGe_3 + (Si_2Ge)^-$	3.760
$(Si_2Ge_3)^- + SiGe$	3.802
$Si_3Ge_3 + Ge^-$	3.977
$Si_3Ge_2 + (Ge_2)^-$	3.996
$(SiGe_3)^- + Si_2Ge$	4.005
$(SiGe_4)^- + Si_2$	4.011
$Si_2Ge_3 + (SiGe)^-$	4.083
$(Si_3Ge_2)^- + 2Ge$	6.561
$(Si_2Ge_3)^- + Si + Ge$	6.864
$(Si_3Ge)^- + Ge_2 + Ge$	7.161
$(SiGe_4)^- + 2Si$	7.233
$(Si_2Ge_2)^- + SiGe + Ge$	7.319
$Si_3Ge + (Ge_2)^- + Ge$	7.334
$Si_2Ge_2 + (SiGe)^- + Ge$	7.439
$(Si_2Ge_2)^- + Ge_2 + Si$	7.452
$(SiGe_3)^- + Si_2 + Ge$	7.533
$(Si_2Ge)^- + SiGe_2 + Ge$	7.544
$Si_2Ge_2 + (Ge_2)^- + Si$	7.602
$Si_3Ge_2 + Ge^- + Ge$	7.602
$Si_2Ge + (SiGe_2)^- + Ge$	7.689
$(SiGe_3)^- + SiGe + Si$	7.694
$SiGe_3 + (SiGe)^- + Si$	7.783
$(SiGe_2)^- + SiGe_2 + Si$	7.788
$Si_2Ge_3 + Si + Ge^-$	7.852
$Si_3Ge + Ge_2 + Ge^-$	8.012
$Si_2Ge_2 + SiGe + Ge^-$	8.146

Table 4.133 – *Continued*

Fragmented Clusters	Fragmentation Energy (eV)
$(Si_2Ge)^- + SiGe + Ge_2$	8.206
$(SiGe_2)^- + Si_2 + Ge_2$	8.289
$(SiGe_2)^- + 2SiGe$	8.317
$SiGe_3 + Si_2 + Ge^-$	8.329
$SiGe_2 + SiGe^- + SiGe$	8.506
$SiGe_2 + Si_2 + (Ge_2)^-$	8.507
$Si_2Ge + (SiGe)^- + Ge_2$	8.540
$Si_2Ge + SiGe + (Ge_2)^-$	8.570
$Si_2Ge + SiGe_2 + Ge^-$	8.585
$(Si_3Ge)^- + 3Ge$	10.089
$(Si_2Ge_2)^- + Si + 2Ge$	10.380
$(SiGe_3)^- + 2Si + Ge$	10.756
$Si_3Ge + Ge^- + 2Ge$	10.940
$(Si_2Ge)^- + SiGe + 2Ge$	11.135
$Si_2Ge_2 + Si + Ge^- + Ge$	11.208
$(SiGe_2)^- + Si_2 + 2Ge$	11.218
$(Si_2Ge)^- + Ge_2 + Si + Ge$	11.268
$(SiGe_2)^- + SiGe + Si + Ge$	11.379
$GeSi_2 + (SiGe)^- + 2Ge$	11.469
$(SiGe_2)^- + Ge_2 + 2Si$	11.512
$SiGe_3 + Ge^- + 2Si$	11.552
$SiGe_2 + (SiGe)^- + Si + Ge$	11.567
$Si_2Ge + (Ge_2)^- + Si + Ge$	11.631
$SiGe_2 + (Ge_2)^- + 2Si$	11.730
$Si_2 + (SiGe)^- + Ge_2 + Ge$	12.068
$(SiGe)^- + 2SiGe + Ge$	12.097
$Si_2 + SiGe + (Ge_2)^- + Ge$	12.098
$SiGe_2 + Si_2 + Ge^- + Ge$	12.113
$Si_2Ge + SiGe + Ge^- + Ge$	12.176
$(SiGe)^- + SiGe + Ge_2 + Si$	12.230
$Si_2 + (Ge_2)^- + Ge_2 + Si$	12.231

Table 4.133 – *Continued*

Fragmented Clusters	Fragmentation Energy (eV)
$2SiGe + (Ge_2)^- + Si$	12.259
$SiGe_2 + SiGe + Si + Ge^-$	12.275
$Si_2Ge + Ge_2 + Si + Ge^-$	12.309
$Si_2 + SiGe + Ge_2 + Ge^-$	12.776
$3SiGe + Ge^-$	12.804
$(Si_2Ge)^- + 3Ge + Si$	14.196
$(SiGe_2)^- + 2Si + 2Ge$	14.440
$Si_2 + (SiGe)^- + 3Ge$	14.997
$(SiGe)^- + SiGe + Si + 2Ge$	15.158
$Si_2 + (Ge_2)^- + Si + 2Ge + Ge$	15.159
$Si_2Ge + Si + Ge^- + 2Ge$	15.237
$(SiGe)^- + Ge_2 + 2Si + Ge$	15.291
$SiGe + (Ge_2)^- + 2Si + Ge$	15.321
$SiGe_2 + 2Si + Ge^- + Ge$	15.336
$(Ge_2)^- + Ge_2 + 3Si$	15.453
$Si_2 + SiGe + Ge^- + 2Ge$	15.704
$Si_2 + Ge_2 + Si + Ge^- + Ge$	15.837
$2SiGe + Si + Ge^- + Ge$	15.865
$SiGe + Ge_2 + 2Si + Ge^-$	15.998
$(SiGe)^- + 2Si + 3Ge$	18.220
$(Ge_2)^- + 3Si + 2Ge$	18.382
$Si_2 + Si + Ge^- + 3Ge$	18.765
$SiGe + Ge^- + 2Si + 2Ge$	18.927
$Ge_2 + 3Si + Ge^- + Ge$	19.060
$3Si + Ge^- + 3Ge$	21.988

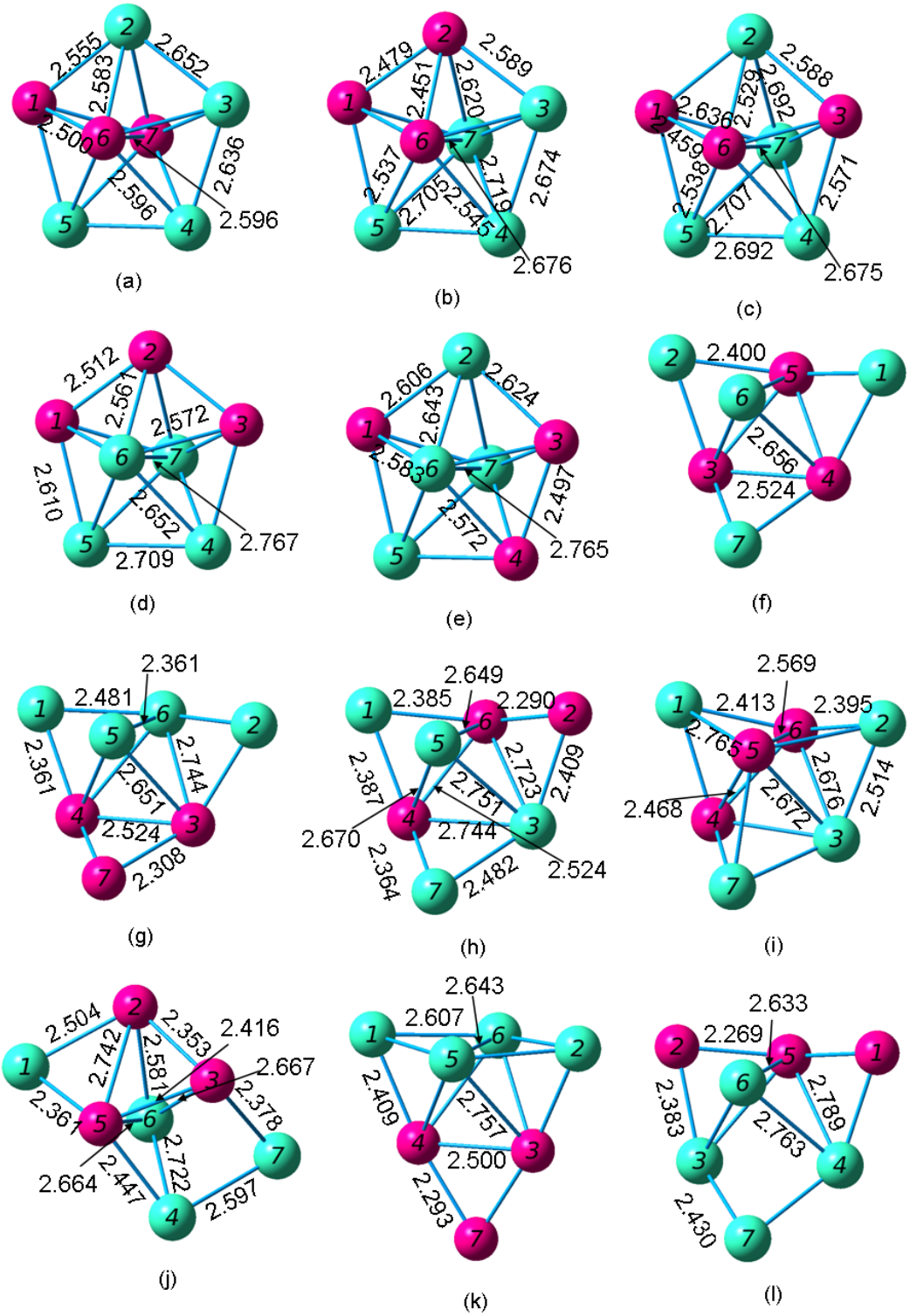

Figure 4.115 Geometries of the Si_3Ge_4 Neutral Septamersfrom (a) Most Stable through (u) Least Stable

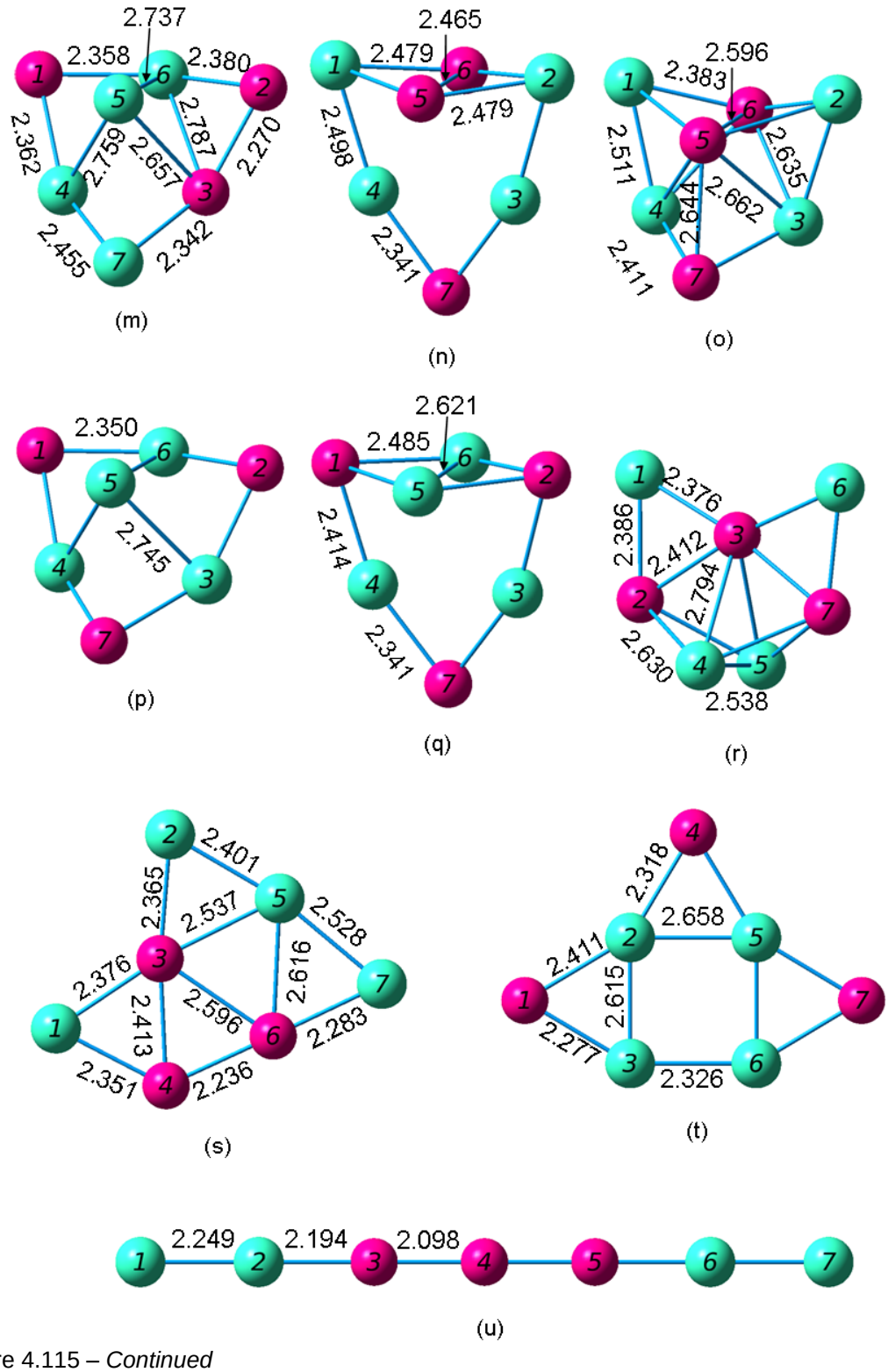

Figure 4.115 – *Continued*

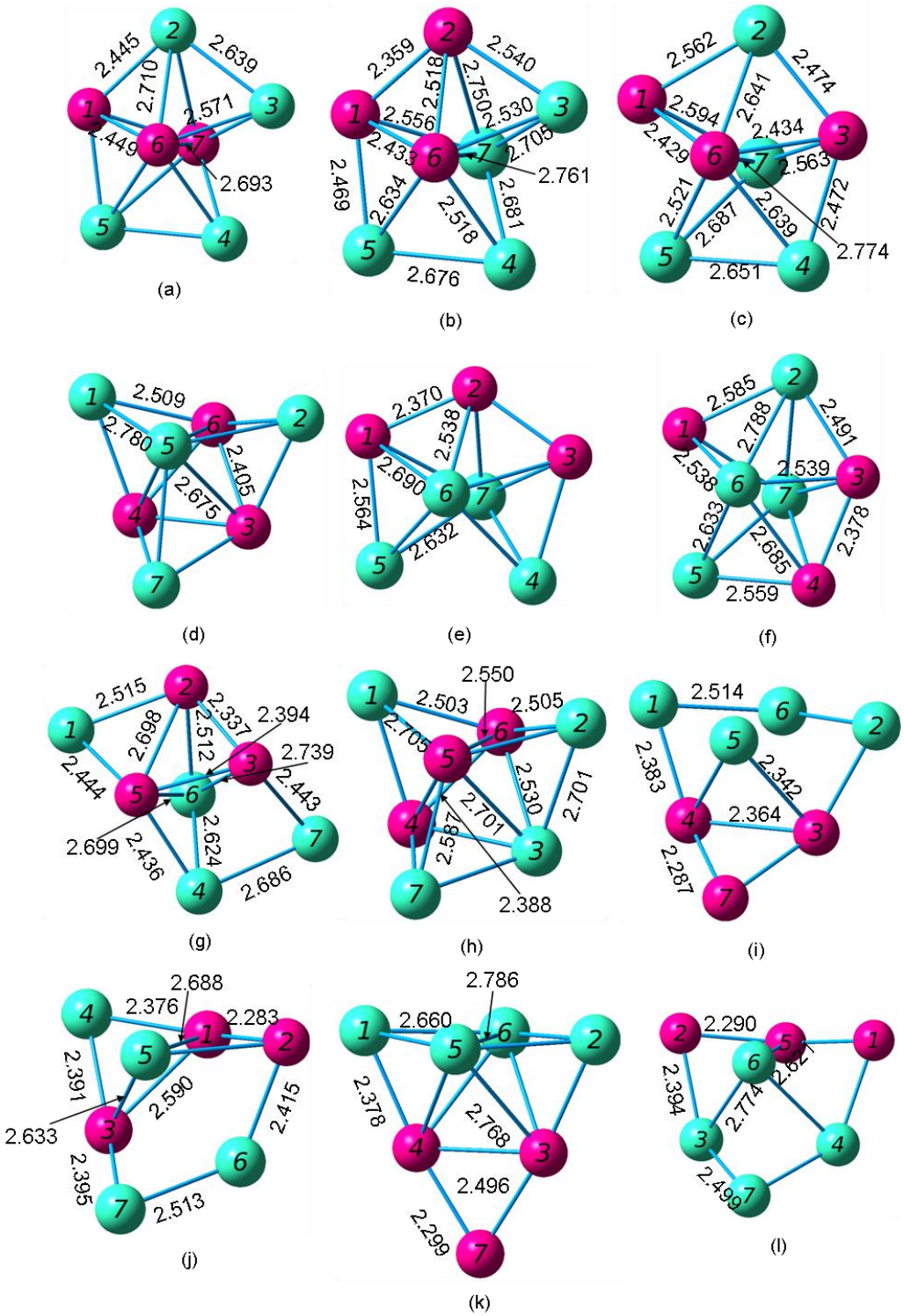

Figure 4.116 Geometries of the $(Si_3Ge_4)^+$ Cationic Septamers from (a) Most Stable through (u) Least Stable

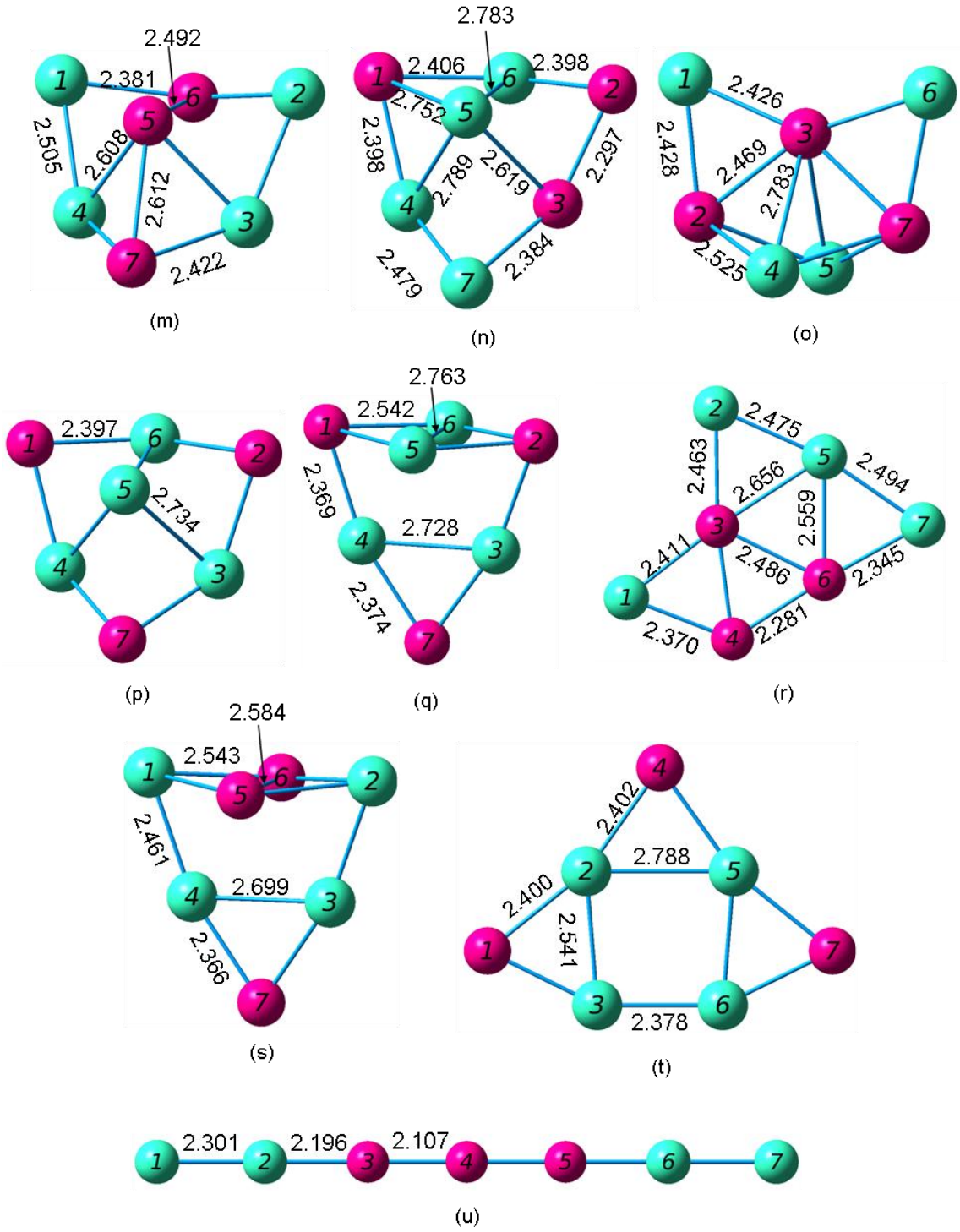

Figure 4.116 – *Continued*

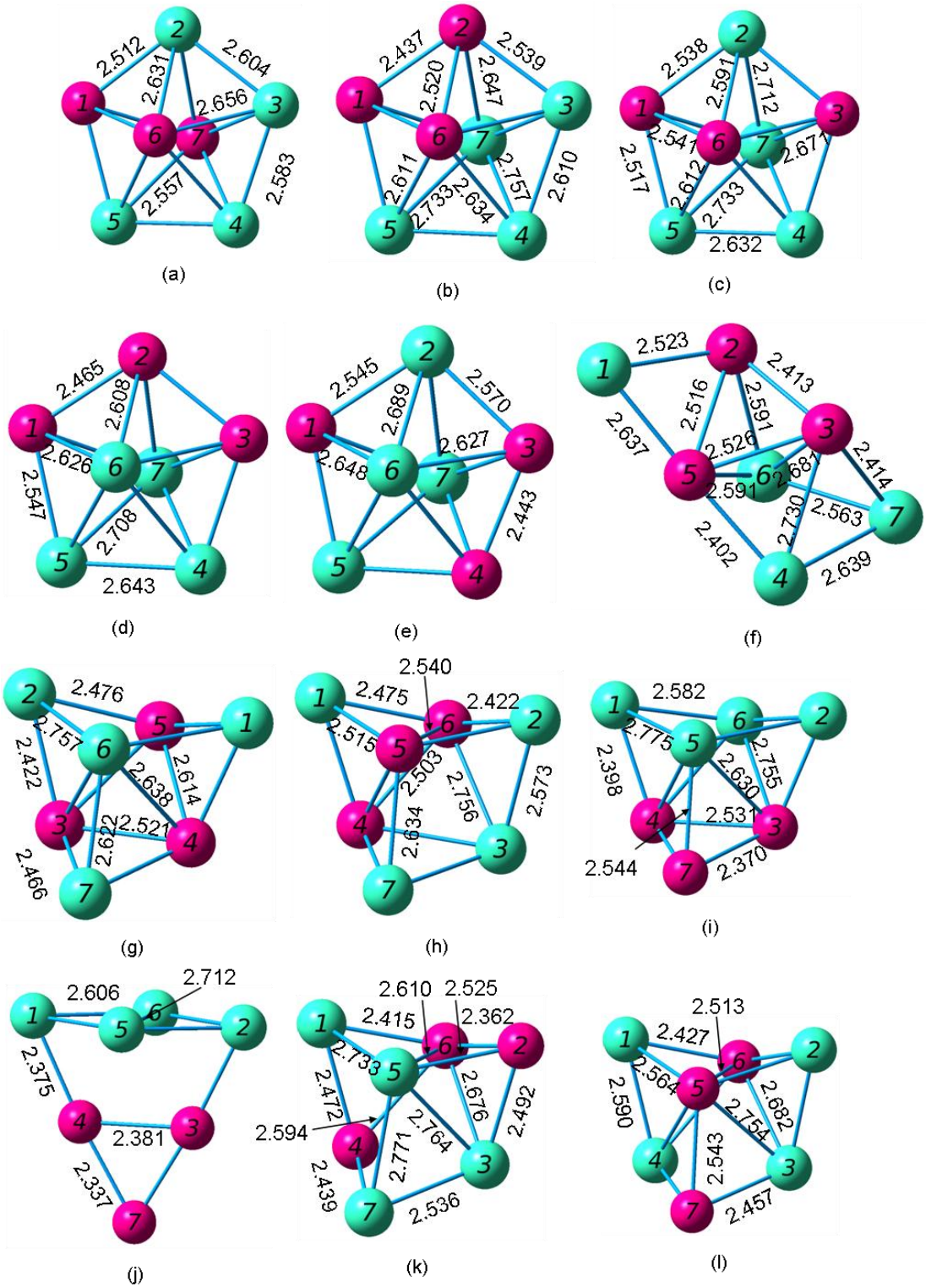

Figure 4.117 Geometries of the $(Si_3Ge_4)^-$ Anionic Septamers from (a) Most Stable through (u) Least Stable

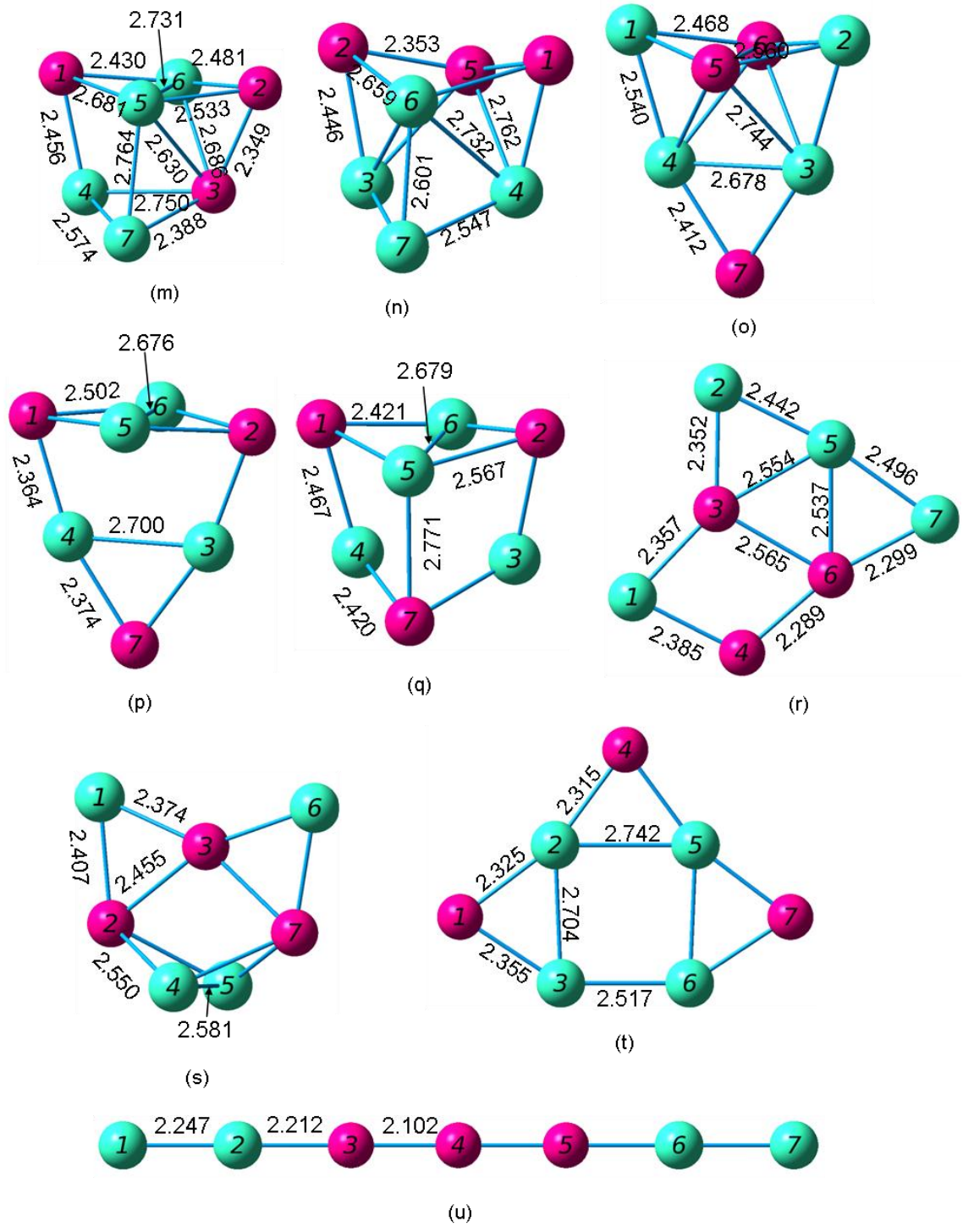

Figure 4.117 – *Continued*

4.20 Si_2Ge_5 Septamers

Li et al. [48] reported a pentagonal bipyramid with D_{5h} symmetry and an all Ge base. Within this cluster there are five Ge-Ge bonds with lengths of 2.64 Å, and ten Si-Ge bonds with lengths of 2.59 Å. This cluster has a ^1A_g electronic state, a 3.16 eV HOMO-LUMO gap, and 298(E'_1), 171(A''_2), and 149 (E'_1) frequencies. Marim *et al.* [49] reported the same Si_2Ge_5 cluster. They also found that the Ge-Ge bonds are 2.64 Å, and their Si-Ge bonds are 2.60 Å. They calculated a cohesive energy of 3.02 eV/atom for this cluster. Wang and Chao [51] reported that the most stable Si_2Ge_5 cluster has a ^1A electronic state, a dissociation energy of -28.5800 eV or -29.6142 eV, a HOMO-LUMO gap of 3.15 eV, and the following frequencies: 297(a), 297(a), and 170(a).

Our Si_2Ge_5 clusters originated from the Si_5Ge_2 clusters. We switched the silicon and germanium atoms and re-optimized them. This led to eleven different Si_2Ge_5 isomers.

Table 4.134 Properties of the Si_2Ge_5 Septamers

Figure	Symmetry Group	Electronic State	Binding E / Atom (eV)	HOMO-LUMO Gap (eV)	Dipole Moment (D)
4.118 (a)	C_{2v}	$^1A_1$	3.009	3.153	0.000
4.118 (b)	C_s	$^1A'$	2.993	2.943	0.415
4.118 (c)	C_s	$^1A'$	2.960	2.703	0.691
4.118 (d)	C_s	$^1A'$	2.904	3.079	0.020
4.118 (e)	C_{2v}	$^1A_1$	2.880	2.440	0.321
4.118 (f)	C_1	^1A	2.878	3.143	0.424
4.118 (g)	C_{2v}	$^1A_1$	2.863	2.985	0.328
4.118 (h)	C_s	$^1A'$	2.860	2.626	0.372
4.118 (i)	C_s	$^1A'$	2.851	3.195	0.443
4.118 (j)	C_{2v}	$^1A_1$	2.848	2.768	0.532
4.118 (k)	C_1	^1A	2.826	2.927	0.650

Table 4.135 Properties of the $(Si_2Ge_5)^+$ Septamers

Figure	Symmetry Group	Electronic State	Binding E / Atom (eV)	HOMO-LUMO Gap (eV)	Dipole Moment (D)
4.119 (a)	C_s	$^2A'$	3.070	1.695[a]	0.963
4.119 (b)	C_{2v}	$^2B_2$	3.036	1.500[a]	0.143
4.119 (c)	C_s	$^2A'$	3.035	1.559[a]	0.919
4.119 (d)	C_s	$^2A'$	2.990	1.496[a]	1.015
4.119 (e)	C_s	$^2A''$	2.989	1.448[a]	0.580
4.119 (f)	C_{2v}	$^2A_1$	2.981	1.444	1.390
4.119 (g)	C_1	^2A	2.970	1.471[a]	1.152
4.119 (h)	C_1	^2A	2.953	1.515[a]	0.535
4.119 (i)	C_s	$^2A'$	2.942	1.426[a]	0.649
4.119 (j)	C_{2v}	$^2A_1$	2.929	1.468[a]	0.206
4.119 (k)	C_{2v}	$^2A_1$	2.920	1.379	0.036

[a] HOMO and LUMO have opposite spins; this value includes the energy required to flip the spin of the electron.

Table 4.136 Properties of the $(Si_2Ge_5)^-$ Septamers

Figure	Symmetry Group	Electronic State	Binding E / Atom (eV)	HOMO-LUMO Gap (eV)	Dipole Moment (D)
4.120 (a)	C_{2v}	$^2B_1$	3.096	1.475[a]	0.000
4.120 (b)	C_s	$^2A'$	3.095	1.499[a]	1.502
4.120 (c)	C_s	$^2A''$	3.083	1.413[a]	1.979
4.120 (d)	C_{2v}	$^2B_1$	2.989	1.493[a]	2.006
4.120 (e)	C_s	$^2A'$	2.983	1.412[a]	0.713
4.120 (f)	C_s	$^2A''$	2.971	1.304	0.717
4.120 (g)	C_1	^2A	2.964	1.404[a]	1.470
4.120 (h)	C_{2v}	$^2B_1$	2.955	1.566[a]	0.065
4.120 (i)	C_1	^2A	2.951	1.425[a]	1.647
4.120 (j)	C_{2v}	$^2B_1$	2.946	1.497[a]	0.580
4.120 (k)	C_s	$^2A'$	2.932	1.419	1.675

[a] HOMO and LUMO have opposite spins; this value includes the energy required to flip the spin of the electron.

Table 4.137 Ionization Potentials and Electron Affinities of the Si_2Ge_5 Septamers

Neutral Figure	VIP (eV)	Cationic Figure	AIP (eV)	VEA (eV)	Anionic Figure	AEA (eV)
4.118 (a)	7.867	4.119 (b)	7.711	1.534	4.120 (a)	1.746
4.118 (b)	7.736	4.119 (a)	7.356	1.590	4.120 (b)	1.855
4.118 (c)	7.666	4.119 (c)	7.375	1.758	4.120 (c)	2.002
4.118 (d)	7.412	4.119 (d)	7.298	1.234	4.120 (e)	1.687
4.118 (e)	7.265	4.119 (f)	7.193	1.788	4.120 (d)	1.899
4.118 (f)	7.359	4.119 (g)	7.259	1.147	4.120 (g)	1.738
4.118 (g)	7.605	4.119 (k)	7.500	1.601	4.120 (h)	1.780
4.118 (h)	7.374	4.119 (e)	6.994	1.652	4.120 (f)	1.918
4.118 (i)	7.399	4.119 (i)	7.264	1.147	4.120 (k)	1.703
4.118 (j)	7.482	4.119 (j)	7.335	1.647	4.120 (j)	1.825
4.118 (k)	7.254	4.119 (h)	7.016	1.260	4.120 (i)	2.007

Table 4.138 Fragmentation Energies of the Most Stable Si_2Ge_5 Neutral Septamer

Fragmented Clusters	Fragmentation Energy (eV)
Si_2Ge_4 + Ge	3.342
$SiGe_5$ + Si	3.803
$SiGe_3$ + $SiGe_2$	3.977
Si_2Ge_3 + Ge_2	4.000
$SiGe_4$ + SiGe	4.267
Si_2Ge_3 + 2Ge	6.929
$SiGe_4$ + Si + Ge	7.329
Si_2Ge_2 + Ge_2 + Ge	7.357
$SiGe_3$ + SiGe + Ge	7.568
$SiGe_3$ + Ge_2 + Si	7.701
$2SiGe_2$ + Ge	7.761
$SiGe_2$ + SiGe + Ge_2	8.423
Si_2Ge + $2Ge_2$	8.458
Si_2Ge_2 + 3Ge	10.285
$SiGe_3$ + Si + 2Ge	10.629
$SiGe_2$ + SiGe + 2Ge	11.352
Si_2Ge + Ge_2 + 2Ge	11.386
$SiGe_2$ + Ge_2 + Si + Ge	11.485
Si_2 + $2Ge_2$ + Ge	11.986
Si_2 + $2Ge_2$ + Ge	11.986
2SiGe + Ge_2 + Ge	12.014
Ge_2 + Ge_2 + SiGe + Si	12.147
Ge_2 + SiGe + Ge_2 + Si	12.147
Si_2Ge + 4Ge	14.314
$SiGe_2$ + Si + 3Ge	14.413
Si_2 + Ge_2 + 3Ge	14.914
2SiGe + 3Ge	14.942
Ge_2 + SiGe + Si + 2Ge	15.075
$2Ge_2$ + Ge + 2Si	15.208
Si_2 + 5Ge	17.843
SiGe + Si + 4Ge	18.004
Ge_2 + 2Si + 3Ge	18.137
2Si + 5Ge	21.065

Table 4.139 Fragmentation Energies of the Most Stable $(Si_2Ge_5)^+$ Cationic Septamer

Fragmented Clusters	Fragmentation Energy (eV)
$(Si_2Ge_4)^+ + Ge$	3.451
$Si_2Ge_4 + Ge^+$	3.770
$(SiGe_5)^+ + Si$	3.819
$Si_2Ge_3 + (Ge_2)^+$	4.148
$(SiGe_3)^+ + SiGe_2$	4.168
$(Si_2Ge_3)^+ + Ge_2$	4.359
$SiGe_3 + (SiGe_2)^+$	4.453
$SiGe_4 + (SiGe)^+$	4.531
$(SiGe_4)^+ + SiGe$	4.573
$(Si_2Ge_3)^+ + 2Ge$	7.288
$Si_2Ge_3 + Ge^+ + Ge$	7.357
$Si_2Ge_2 + (Ge_2)^+ + Ge$	7.504
$(SiGe_4)^+ + Si + Ge$	7.634
$(Si_2Ge_2)^+ + Ge_2 + Ge$	7.671
$SiGe_4 + Si + Ge^+$	7.757
$(SiGe_3)^+ + SiGe + Ge$	7.759
$Si_2Ge_2 + Ge_2 + Ge^+$	7.784
$SiGe_3 + (SiGe)^+ + Ge$	7.831
$SiGe_3 + (Ge_2)^+ + Si$	7.848
$(SiGe_3)^+ + Ge_2 + Si$	7.892
$SiGe_3 + SiGe + Ge^+$	7.996
$2SiGe_2 + Ge^+$	8.189
$(SiGe_2)^+ + SiGe_2 + Ge$	8.237
$SiGe_2 + (Ge_2)^+ + SiGe$	8.571
$Si_2Ge + (Ge_2)^+ + Ge_2$	8.605
$SiGe_2{}^+ Ge_2 + (SiGe)^+$	8.687
$(Si_2Ge)^+ + 2Ge_2$	8.868
$(SiGe_2)^+ + SiGe + Ge_2$	8.900
$(Si_2Ge_2)^+ + 3Ge$	10.599
$Si_2Ge_2 + Ge^+ + 2Ge$	10.713
$(SiGe_3)^+ + Si + 2Ge$	10.820

Table 4.139 – *Continued*

Fragmented Clusters	Fragmentation Energy (eV)
$SiGe_3 + Si + Ge^+ + Ge$	11.057
$Si_2Ge + (Ge_2)^+ + 2Ge$	11.533
$SiGe_2 + (SiGe)^+ + 2Ge$	11.615
$SiGe_2 + (Ge_2)^+ + Si + Ge$	11.632
$SiGe_2 + SiGe + Ge^+ + Ge$	11.780
$(Si_2Ge)^+ + Ge_2 + 2Ge$	11.796
$Si_2Ge + Ge_2 + Ge^+ + Ge$	11.814
$(SiGe_2)^+ + SiGe + 2Ge$	11.828
$SiGe_2 + Ge_2 + Si + Ge^+$	11.913
$(SiGe_2)^+ + Ge_2 + Si + Ge$	11.961
$Si_2 + (Ge_2)^+ + Ge_2 + Ge$	12.133
$Si_2 + (Ge_2)^+ + Ge_2 + Ge$	12.133
$2SiGe + (Ge_2)^+ + Ge$	12.162
$2Ge_2 + (SiGe)^+ + SiGe + Ge$	12.278
$SiGe + (Ge_2)^+ + Ge_2 + Si$	12.294
$SiGe + (Ge_2)^+ + Ge_2 + Si$	12.294
$(SiGe)^+ + 2Ge_2 + Si$	12.410
$(SiGe)^+ + 2Ge_2 + Si$	12.410
$Si_2 + 2Ge_2 + Ge^+$	12.414
$Si_2 + 2Ge_2 + Ge^+$	12.414
$2SiGe + Ge_2 + Ge^+$	12.442
$(Si_2Ge)^+ + 4Ge$	14.724
$Si_2Ge + Ge^+ + 3Ge$	14.742
$SiGe_2 + Si + Ge^+ + 2Ge$	14.841
$(SiGe_2)^+ + Si + 3Ge$	14.890
$Si_2 + (Ge_2)^+ + 3Ge$	15.062
$(SiGe)^+ + SiGe + 3Ge$	15.206
$SiGe + (Ge_2)^+ + Si + 2Ge$	15.223
$(SiGe)^+ + Ge_2 + Si + 2Ge$	15.339
$Si_2 + Ge_2 + Ge^+ + 2Ge$	15.342
$(Ge_2)^+ + Ge_2 + Ge + 2Si$	15.356

Table 4.139 – *Continued*

Fragmented Clusters	Fragmentation Energy (eV)
$2SiGe + Ge^{+} + 2Ge$	15.370
$SiGe + Ge_2 + Si + Ge^{+} + Ge$	15.503
$2Ge_2 + Ge^{+} + 2Si$	15.636
$(SiGe)^{+} + Si + 4Ge$	18.267
$Si_2 + Ge^{+} + 4Ge$	18.270
$(Ge_2)^{+} + 2Si + 3Ge$	18.284
$SiGe + Si + Ge^{+} + 3Ge$	18.432
$Ge_2 + 2Si + Ge^{+} + 2Ge$	18.565
$2Si + Ge^{+} + 4Ge$	21.493

Table 4.140 Fragmentation Energies of the Most Stable $(Si_2Ge_5)^-$ Anionic Septamer

Fragmented Clusters	Fragmentation Energy (eV)
$(Si_2Ge_4)^- + Ge$	3.264
$(Si_2Ge_3)^- + Ge_2$	3.621
$(SiGe_5)^- + Si$	3.646
$SiGe_3 + (SiGe_2)^-$	3.690
$(SiGe_3)^- + SiGe_2$	3.789
$(SiGe_4)^- + SiGe$	3.857
$Si_2Ge_3 + (Ge_2)^-$	3.931
$Si_2Ge_4 + Ge^-$	3.951
$SiGe_4 + (SiGe)^-$	4.168
$(Si_2Ge_3)^- + 2Ge$	6.549
$(SiGe_4)^- + Si + Ge$	6.919
$(Si_2Ge_2)^- + Ge_2 + Ge$	7.137
$Si_2Ge_2 + (Ge_2)^- + Ge$	7.287
$(SiGe_3)^- + SiGe + Ge$	7.380
$SiGe_3 + (SiGe)^- + Ge$	7.469
$(SiGe_2)^- + SiGe_2 + Ge$	7.474
$(SiGe_3)^- + Ge_2 + Si$	7.513
$Si_2Ge_3 + Ge^- + Ge$	7.537
$SiGe_3 + (Ge_2)^- + Si$	7.631
$SiGe_4 + Si + Ge^-$	7.937
$Si_2Ge_2 + Ge_2 + Ge^-$	7.965
$(Si_2Ge)^- + 2Ge_2$	8.025
$(SiGe_2)^- + SiGe + Ge_2$	8.136
$SiGe_3 + SiGe + Ge^-$	8.176
$SiGe_2 + (SiGe)^- + Ge_2$	8.324
$SiGe_2 + SiGe + (Ge_2)^-$	8.354
$2SiGe_2 + Ge^-$	8.369
$Si_2Ge + (Ge_2)^- + Ge_2$	8.388
$(Si_2Ge_2)^- + 3Ge$	10.066
$(SiGe_3)^- + Si + 2Ge$	10.441
$Si_2Ge_2 + Ge^- + 2Ge$	10.893

Table 4.140 – *Continued*

Fragmented Clusters	Fragmentation Energy (eV)
$(Si_2Ge)^- + Ge_2 + 2Ge$	10.953
$(SiGe_2)^- + SiGe + 2Ge$	11.064
$(SiGe_2)^- + Ge_2 + Si + Ge$	11.197
$SiGe_3 + Si + Ge^- + Ge$	11.237
$SiGe_2 + (SiGe)^- + 2Ge$	11.253
$Si_2Ge + (Ge_2)^- + 2Ge$	11.317
$SiGe_2 + (Ge_2)^- + Si + Ge$	11.415
$(SiGe)^- + SiGe + Ge_2 + Ge$	11.915
$Si_2 + (Ge_2)^- + Ge_2 + Ge$	11.916
$Si_2 + (Ge_2)^- + Ge_2 + Ge$	11.916
$2SiGe + (Ge_2)^- + Ge$	11.945
$SiGe_2 + SiGe + Ge^- + Ge$	11.960
$Si_2Ge + Ge_2 + Ge^- + Ge$	11.994
$(SiGe)^- + 2Ge_2 + Si$	12.048
$(SiGe)^- + 2Ge_2 + Si$	12.048
$SiGe + (Ge_2)^- + Ge_2 + Si$	12.078
$SiGe_2 + Ge_2 + Si + Ge^-$	12.093
$Si_2 + 2Ge_2 + Ge^-$	12.594
$Si_2 + 2Ge_2 + Ge^-$	12.594
$Ge_2 + 2SiGe + Ge^-$	12.622
$(Si_2Ge)^- + 4Ge$	13.882
$(SiGe_2)^- + Si + 3Ge$	14.126
$(SiGe)^- + SiGe + 3Ge$	14.844
$Si_2 + (Ge_2)^- + 3Ge$	14.845
$Si_2Ge + Ge^- + 3Ge$	14.923
$(SiGe)^- + Ge_2 + Si + 2Ge$	14.977
$SiGe + (Ge_2)^- + Si + 2Ge$	15.006
$SiGe_2 + Si + Ge^- + 2Ge$	15.021
$(Ge_2)^- + Ge_2 + 2Si + Ge$	15.139
$Si_2 + Ge_2 + Ge^- + 2Ge$	15.522
$2SiGe + Ge^- + 2Ge$	15.551

Table 4.140 – *Continued*

Fragmented Clusters	Fragmentation Energy (eV)
$SiGe + Ge_2 + Si + Ge^- + Ge$	15.684
$2Ge_2 + 2Si + Ge^-$	15.817
$(SiGe)^- + Si + 4Ge$	17.905
$(Ge_2)^- + 2Si + 3Ge$	18.067
$Si_2 + Ge^- + 4Ge$	18.451
$SiGe + Si + Ge^- + 3Ge$	18.612
$Ge_2 + 2Si + Ge^- + 2Ge$	18.745
$2Si + Ge^- + 4Ge$	21.674

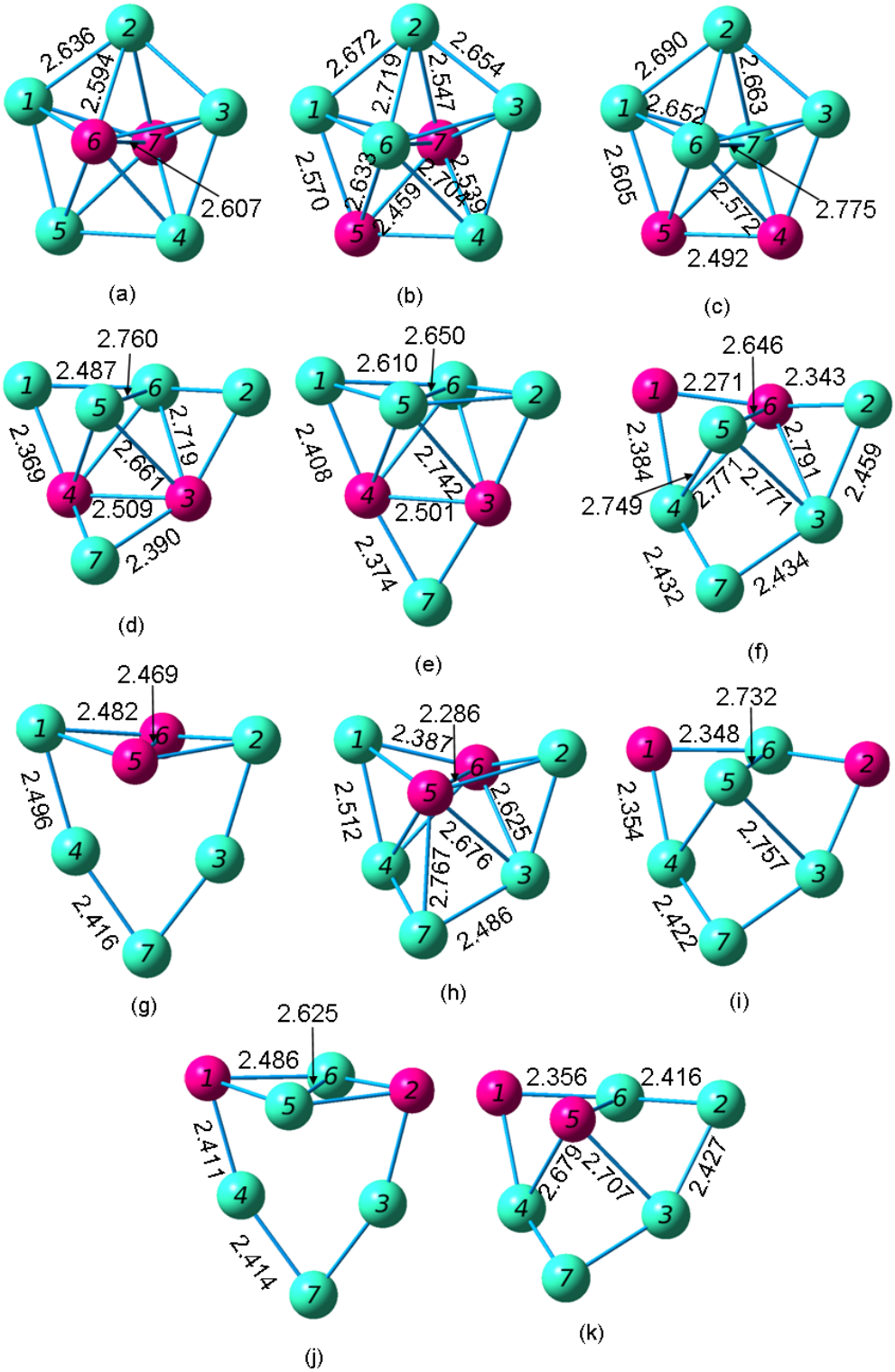

Figure 4.118 Geometries of the Si_2Ge_5 Neutral Septamers from (a) Most Stable through (k) Least Stable

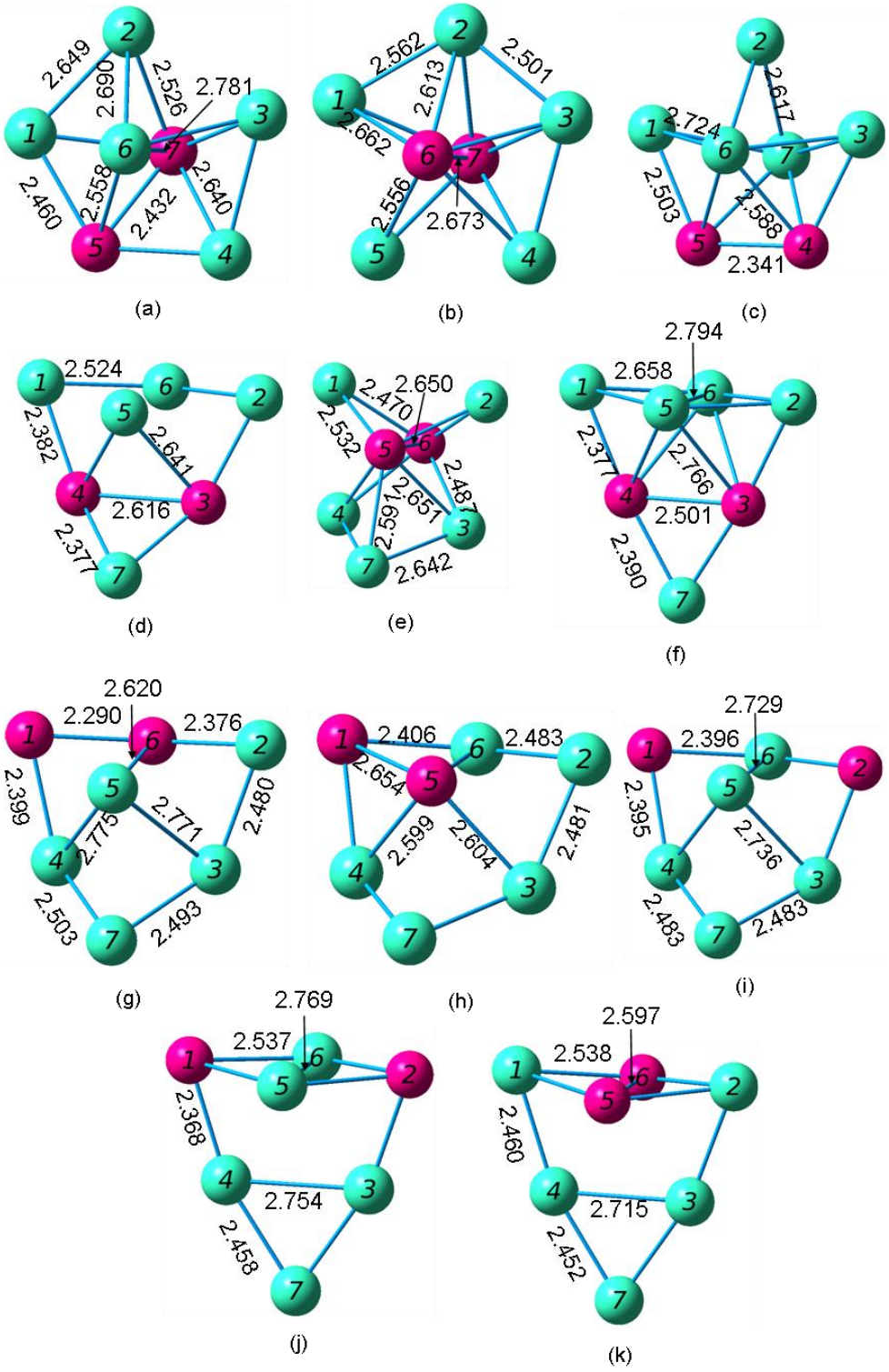

Figure 4.119 Geometries of the $(Si_2Ge_5)^+$ Cationic Septamers from (a) Most Stable through (k) Least Stable

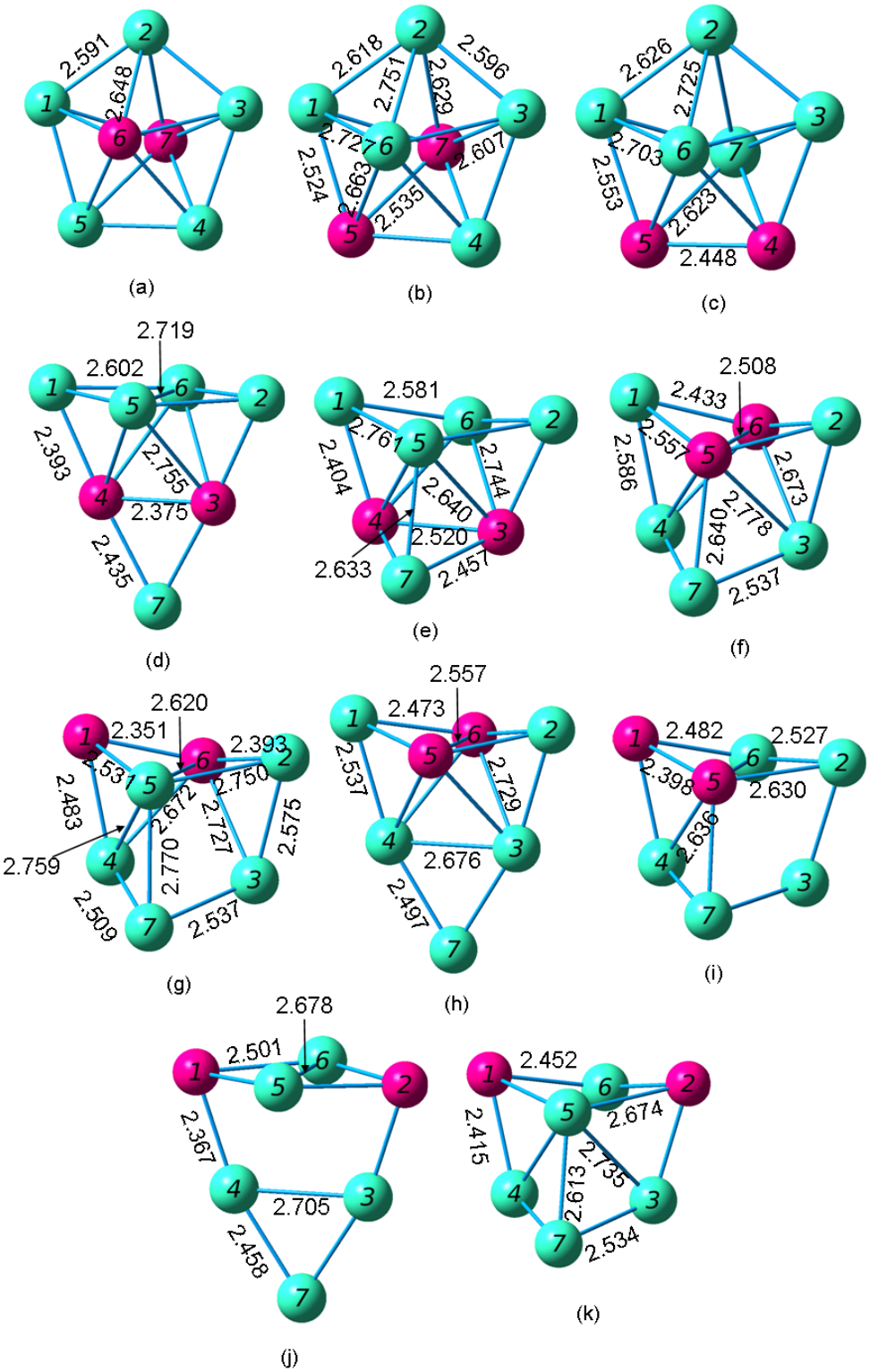

Figure 4.120 Geometries of the $(Si_2Ge_5)^-$ Anionic Septamers from (a) Most Stable through (k) Least Stable

4.21 $SiGe_6$ Septamers

Marim *et al.* [49] reported their one pentagonal bipyramid cluster. The base has five Ge atoms with Ge-Ge bonds of length 2.65 Å. The bonds connecting the Ge atoms to the Si tip are 2.56 Å, and those connecting the Ge atoms to the Ge tip are 2.71 Å. They calculated a cohesive energy of 3.00 eV/atom for this cluster. Wang and Chao [51] reported that the most stable $SiGe_6$ cluster has a ^1A electronic state, a dissociation energy of -28.0269 eV or -28.1417 eV, a HOMO-LUMO gap of 3.06 eV, and the following frequencies: 313(a), 313(a), and 188(a).

For the final group of clusters, the $SiGe_6$ septamers, we started with the optimized Si_6Ge clusters, and again switched the silicon and germanium atoms. Consistent with our other work on septamers, we omitted the less stable isomers. Totally, we investigated ten different neutral isomers. Our cation research again gave us ten isomers, but for the anions we only have nine isomers. Both the most stable and third most stable neutral clusters led to the most stable neutral cluster.

Table 4.141 Properties of the $SiGe_6$ Septamers

Figure	Symmetry Group	Electronic State	Binding E / Atom (eV)	HOMO-LUMO Gap (eV)	Dipole Moment (D)
4.121 (a)	C_{5v}	$^1A_1$	2.954	3.062	0.027
4.121 (b)	C_{2v}	$^1A_1$	2.922	2.758	0.414
4.121 (c)	C_1	^1A	2.837	3.133	0.124
4.121 (d)	C_s	$^1A'$	2.822	2.619	0.193
4.121 (e)	C_1	^1A	2.815	3.196	0.436
4.121 (f)	C_s	$^1A'$	2.808	2.773	0.482
4.121 (g)	C_{2v}	$^1A_1$	2.803	2.845	0.420
4.121 (h)	C_1	^1A	2.786	2.245	0.804
4.121 (i)	C_s	$^1A'$	2.785	2.536	0.260

Table 4.142 Properties of the $(SiGe_6)^+$ Septamers

Figure	Symmetry Group	Electronic State	Binding E / Atom (eV)	HOMO-LUMO Gap (eV)	Dipole Moment (D)
4.122 (a)	C_{2v}	$^2A_1$	3.010	1.697[a]	0.735
4.122 (b)	C_s	$^2A'$	3.007	1.555[a]	0.521
4.122 (c)	C_1	^2A	2.934	1.462[a]	0.704
4.122 (d)	C_s	$^2A'$	2.922	1.524[a]	0.010
4.122 (e)	C_s	$^2A'$	2.917	1.445	1.051
4.122 (f)	C_1	^2A	2.913	1.416[a]	0.574
4.122 (g)	C_1	^2A	2.913	1.530[a]	0.192
4.122 (h)	C_s	$^2A'$	2.898	1.534	0.896
4.122 (i)	C_{2v}	$^2A_1$	2.885	1.483[a]	1.144

[a] HOMO and LUMO have opposite spins; this value includes the energy required to flip the spin of the electron.

Table 4.143 Properties of the $(SiGe_6)^-$ Septamers

Figure	Symmetry Group	Electronic State	Binding E / Atom (eV)	HOMO-LUMO Gap (eV)	Dipole Moment (D)
4.123 (a)	C_{5v}	$^2A_1$	3.054	1.462[a]	0.816
4.123 (b)	C_{2v}	$^2B_1$	3.042	1.381[a]	1.122
4.123 (c)	C_s	$^2A''$	2.921	1.489[a]	1.531
4.123 (d)	C_1	^2A	2.909	1.327[a]	1.393
4.123 (e)	C_s	$^2A'$	2.907	1.371	0.711
4.123 (f)	C_s	$^2A''$	2.901	1.474[a]	1.156
4.123 (g)	C_1	^2A	2.897	1.423[a]	1.018
4.123 (h)	C_{2v}	$^2B_1$	2.891	1.446[a]	2.232

[a] HOMO and LUMO have opposite spins; this value includes the energy required to flip the spin of the electron.

Table 4.144 Ionization Potentials and Electron Affinities of the $SiGe_6$ Septamers

Neutral Figure	VIP (eV)	Cationic Figure	AIP (eV)	VEA (eV)	Anionic Figure	AEA (eV)
4.121 (a)	7.821	4.122 (b)	7.534	1.610	4.123 (a)	1.834
4.121 (b)	7.673	4.122 (a)	7.286	1.752	4.123 (b)	1.973
4.121 (c)	7.322	4.122 (c)	7.222	1.018	4.123 (a)	2.653
4.121 (d)	7.327	4.122 (e)	7.233	1.699	4.123 (c)	1.828
4.121 (e)	7.355	4.122 (f)	7.212	1.056	4.123 (g)	1.718
4.121 (f)	7.425	4.122 (h)	7.271	1.639	4.123 (f)	1.790
4.121 (g)	7.448	4.122 (i)	7.329	1.337	4.123 (h)	1.751
4.121 (h)	7.113	4.122 (g)	7.012	1.778	4.123 (d)	2.001
4.121 (i)	7.196	4.122 (d)	6.945	1.587	4.123 (e)	1.988

Table 4.145 Fragmentation Energies of the Most Stable $SiGe_6$ Neutral Septamer

Fragmented Clusters	Fragmentation Energy (eV)
$SiGe_5$ + Ge	3.417
$SiGe_4$ + Ge_2	4.015
$SiGe_4$ + 2Ge	6.943
$SiGe_3$ + Ge_2 + Ge	7.315
$SiGe_2$ + $2Ge_2$	8.171
$SiGe_3$ + 3Ge	10.243
$SiGe_2$ + Ge_2 + 2Ge	11.099
SiGe + $2Ge_2$ + Ge	11.761
SiGe + $2Ge_2$ + Ge	11.761
$3Ge_2$ +Si	11.894
$SiGe_2$ + 4Ge	14.028
SiGe + Ge_2 + 3Ge	14.690
SiGe + Ge_2 + 3Ge	14.690
$2Ge_2$ + 2Ge +Si	14.823
SiGe + 5Ge	17.618
Si + 6Ge	20.680

Table 4.146 Fragmentation Energies of the Most Stable $(SiGe_6)^+$ Cationic Septamer

Fragmented Clusters	Fragmentation Energy (eV)
$(SiGe_5)^+ + Ge$	3.397
$SiGe_5 + Ge^+$	3.809
$SiGe_4 + (Ge_2)^+$	4.126
$(SiGe_4)^+ + Ge_2$	4.284
$(SiGe_4)^+ + 2Ge$	7.212
$SiGe_4 + Ge^+ + Ge$	7.335
$SiGe_3 + (Ge_2)^+ + Ge$	7.426
$(SiGe_3)^+ + Ge_2 + Ge$	7.470
$SiGe_3 + Ge_2 + Ge^+$	7.707
$SiGe_2 + (Ge_2)^+ + Ge_2$	8.282
$(SiGe_2)^+ + 2Ge_2$	8.611
$(SiGe_3)^+ + 3Ge$	10.399
$SiGe_3 + Ge^+ + 2Ge$	10.635
$SiGe_2 + (Ge_2)^+ + 2Ge$	11.210
$SiGe_2 + Ge_2 + Ge^+ + Ge$	11.491
$(SiGe_2)^+ + Ge_2 + 2Ge$	11.539
$SiGe + (Ge_2)^+ + Ge_2 + Ge$	11.873
$(SiGe)^+ + 2Ge_2 + Ge$	11.989
$(Ge_2)^+ + 2Ge_2 + Si$	12.006
$SiGe + 2Ge_2 + Ge^+$	12.153
$SiGe + 2Ge_2 + Ge^+$	12.153
$SiGe_2 + Ge^+ + 3Ge$	14.419
$(SiGe_2)^+ + 4Ge$	14.468
$SiGe + (Ge_2)^+ + 3Ge$	14.801
$(SiGe)^+ + Ge_2 + 3Ge$	14.917
$(SiGe)^+ + Ge_2 + 3Ge$	14.917
$(Ge_2)^+ + Ge_2 + Si + 2Ge$	14.934
$SiGe + Ge_2 + Ge^+ + 2Ge$	15.082
$SiGe + Ge_2 + Ge^+ + 2Ge$	15.082
$2Ge_2 + Ge^+ + Si + Ge$	15.215
$(SiGe)^+ + 5Ge$	17.846
$SiGe + Ge^+ + 4Ge$	18.010
$Si + Ge^+ + 5Ge$	21.071

Table 4.147 Fragmentation Energies of the Most Stable $(SiGe_6)^-$ Anionic Septamer

Fragmented Clusters	Fragmentation Energy (eV)
$(SiGe_5)^- + Ge$	3.349
$(SiGe_4)^- + Ge_2$	3.693
$SiGe_4 + (Ge_2)^-$	4.033
$SiGe_5 + Ge^-$	4.114
$(SiGe_4)^- + 2Ge$	6.622
$(SiGe_3)^- + Ge_2 + Ge$	7.215
$SiGe_3 + (Ge_2)^- + Ge$	7.334
$SiGe_4 + Ge^- + Ge$	7.640
$(SiGe_2)^- + 2Ge_2$	7.972
$SiGe_3 + Ge_2 + Ge^-$	8.012
$SiGe_2 + (Ge_2)^- + Ge_2$	8.189
$(SiGe_3)^- + 3Ge$	10.144
$(SiGe_2)^- + Ge_2 + 2Ge$	10.900
$SiGe_3 + Ge^- + 2Ge$	10.940
$SiGe_2 + (Ge_2)^- + 2Ge$	11.118
$(SiGe)^- + 2Ge_2 + Ge$	11.751
$(SiGe)^- + 2Ge_2 + Ge$	11.751
$SiGe + (Ge_2)^- + Ge_2 + Ge$	11.780
$SiGe + (Ge_2)^- + Ge_2 + Ge$	11.780
$SiGe_2 + Ge_2 + Ge^- + Ge$	11.796
$(Ge_2)^- + 2Ge_2 + Si$	11.913
$SiGe + 2Ge_2 + Ge^-$	12.458
$(SiGe_2)^- + 4Ge$	13.829
$(SiGe)^- + Ge_2 + 3Ge$	14.679
$(SiGe)^- + Ge_2 + 3Ge$	14.679
$SiGe + (Ge_2)^- + 3Ge$	14.709
$SiGe + (Ge_2)^- + 3Ge$	14.709
$SiGe_2 + Ge^- + 3Ge$	14.724
$(Ge_2)^- + Ge_2 + Si + 2Ge$	14.842
$SiGe + Ge_2 + Ge^- + 2Ge$	15.387
$2Ge_2 + Si + Ge^- + Ge$	15.519
$(SiGe)^- + 5Ge$	17.608
$SiGe + Ge^- + 4Ge$	18.315
$Si + Ge^- + 5Ge$	21.376

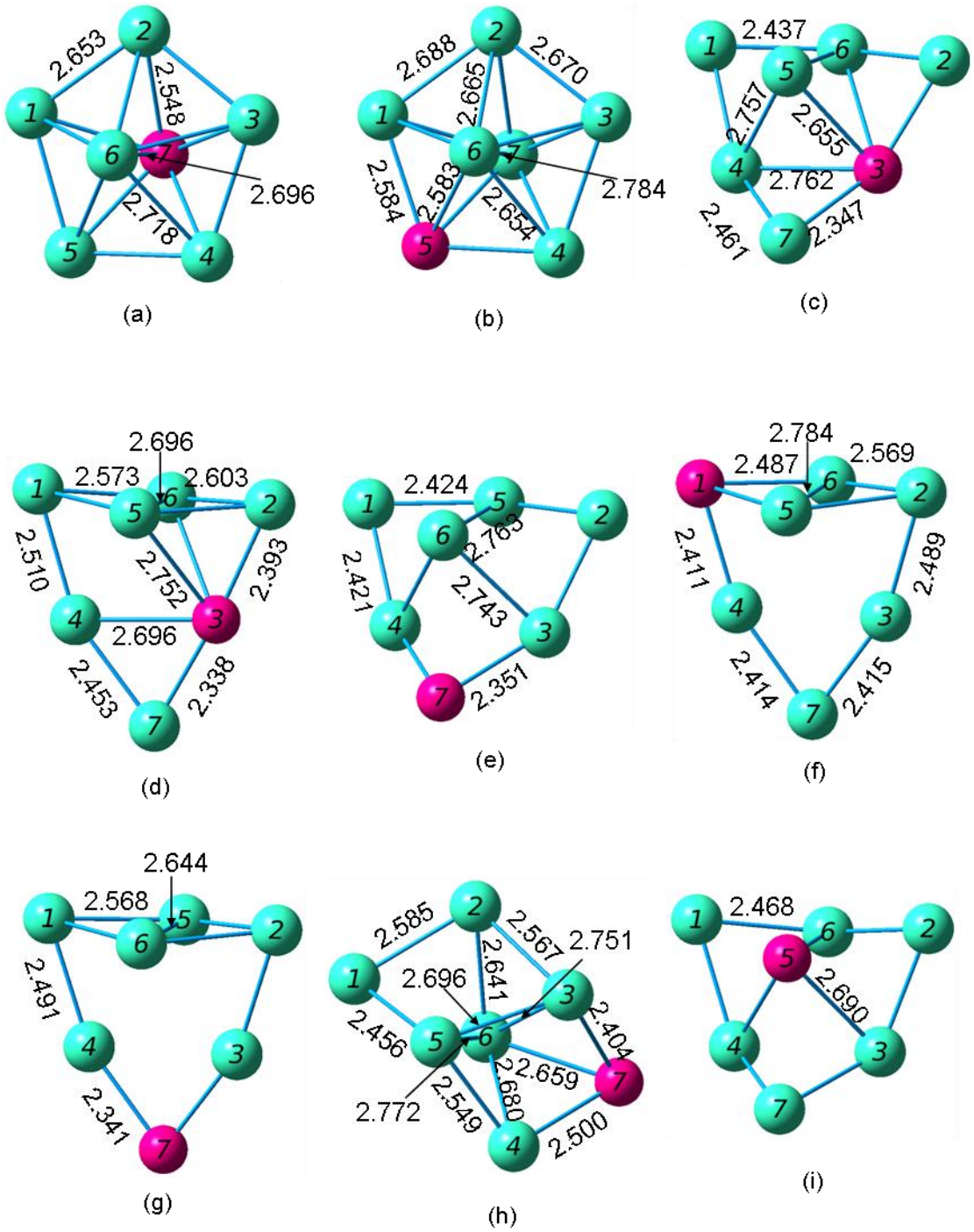

Figure 4.121 Geometries of the $SiGe_6$ Neutral Septamers from (a) Most Stable through (i) Least Stable

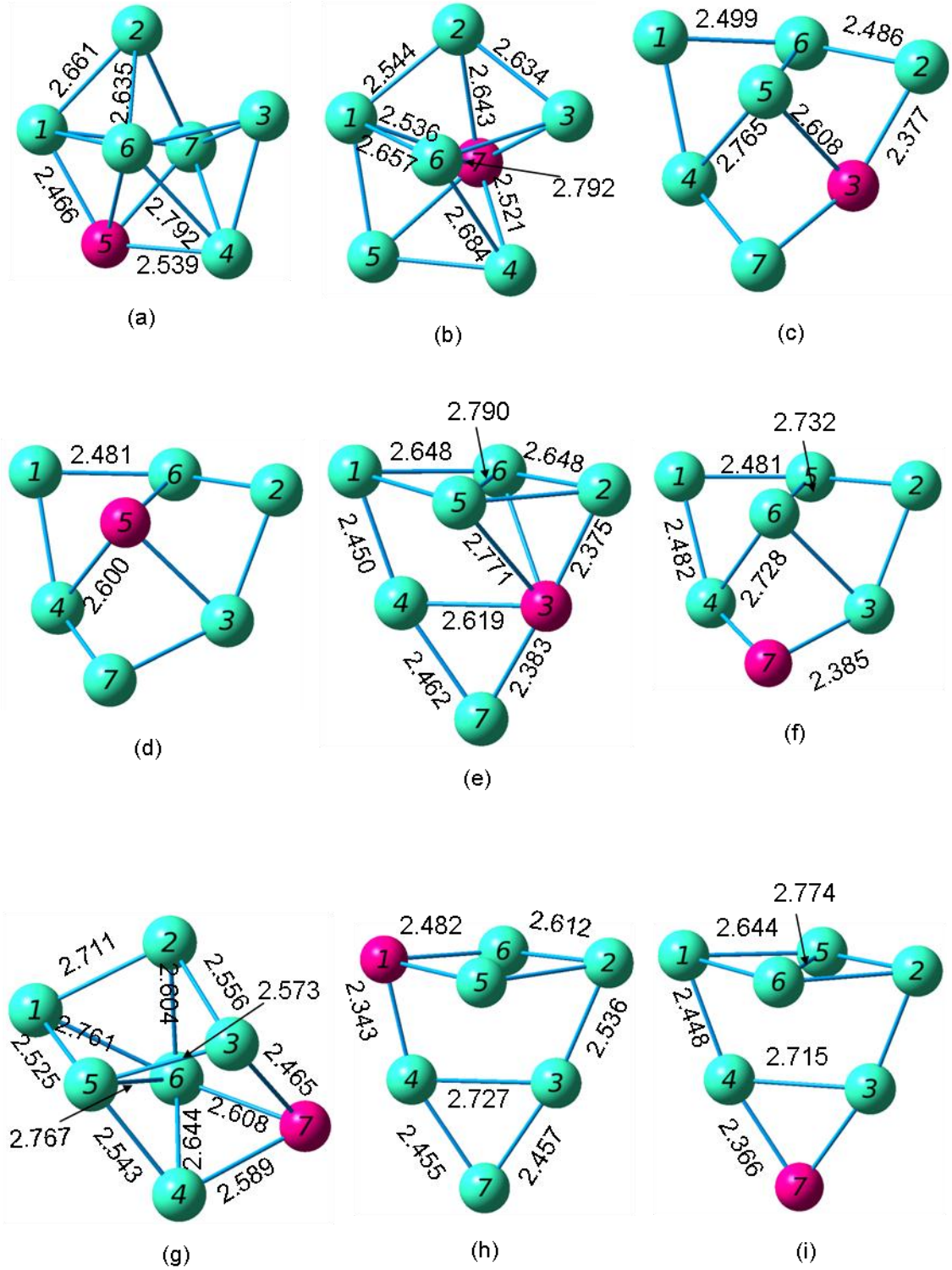

Figure 4.122 Geometries of the $(SiGe_6)^+$ Cationic Septamers from (a) Most Stable through (i) Least Stable

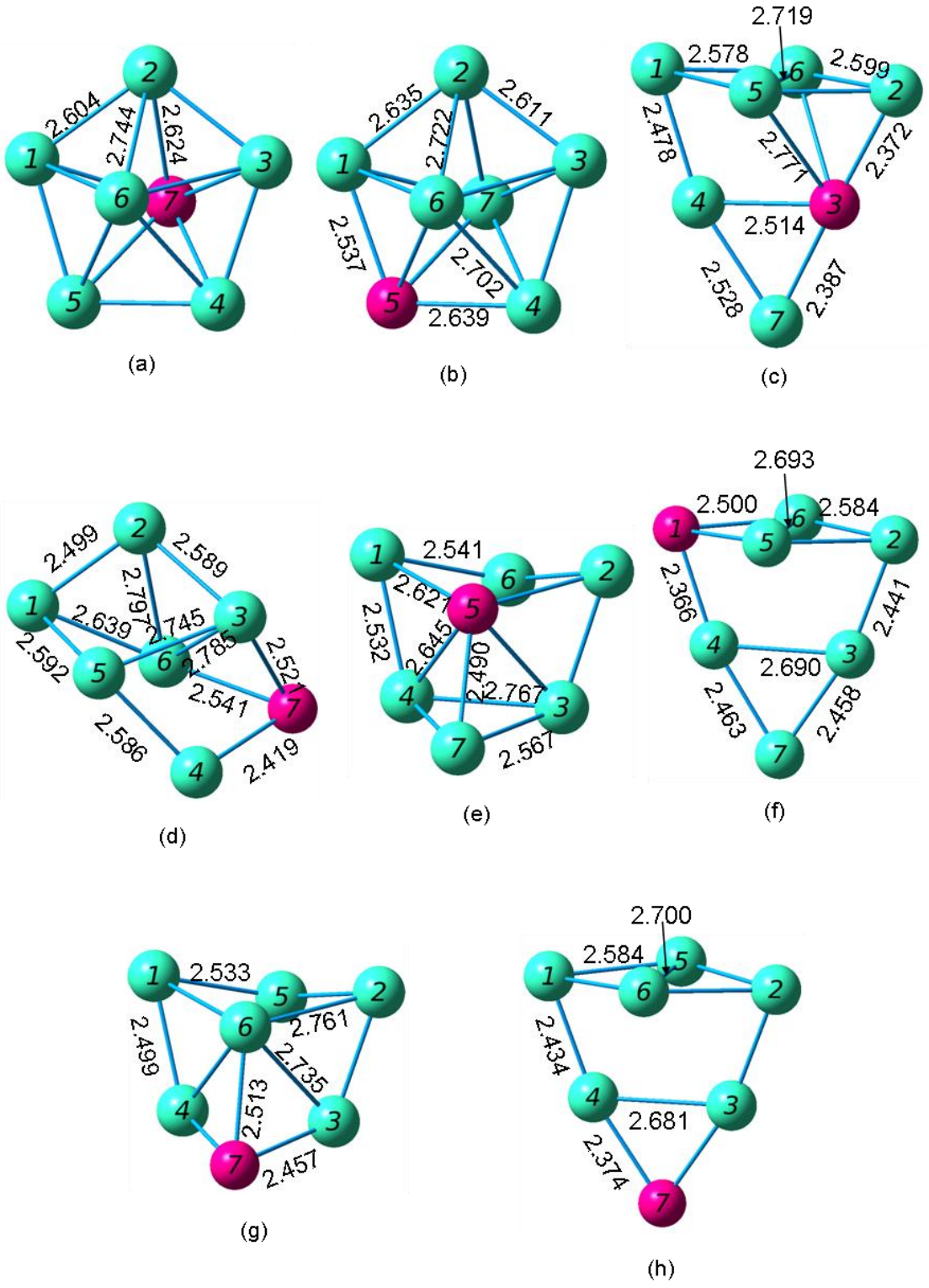

Figure 4.123 Geometries of the $(SiGe_6)^-$ Anionic Septamers from (a) Most Stable through (h) Least Stable

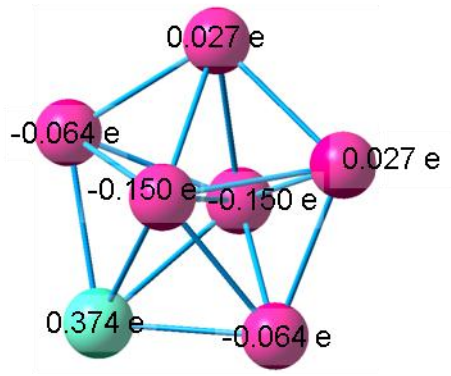

(a)

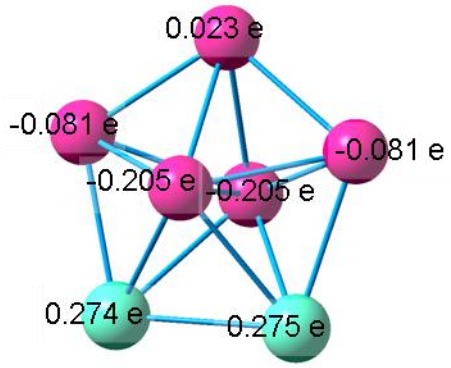

(b)

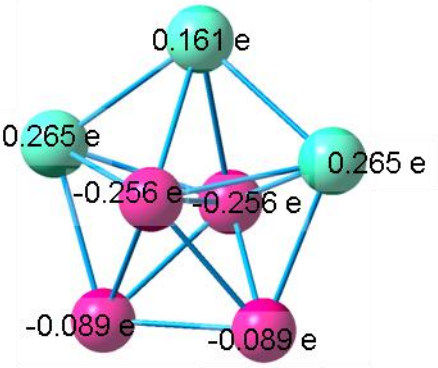

(c)

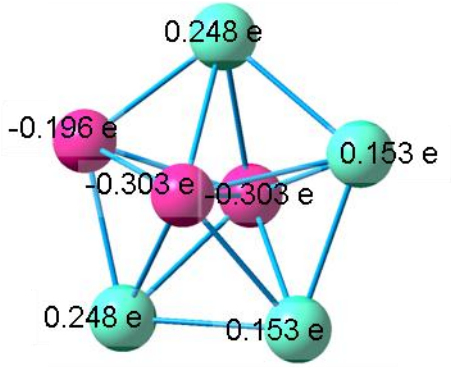

(d)

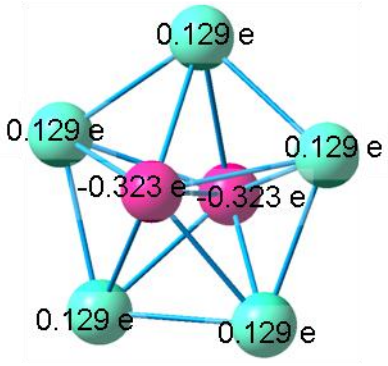

(e)

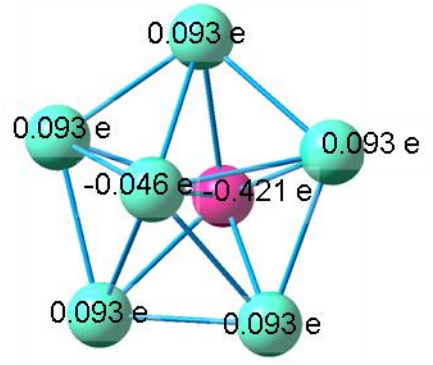

(f)

Figure 4.124 Atomic Charges of the Most Stable (a) Si_6Ge (b) Si_5Ge_2 (c) Si_4Ge_3 (d) Si_3Ge_4 (e) Si_2Ge_5 and (f) $SiGe_6$ Neutral Septamer

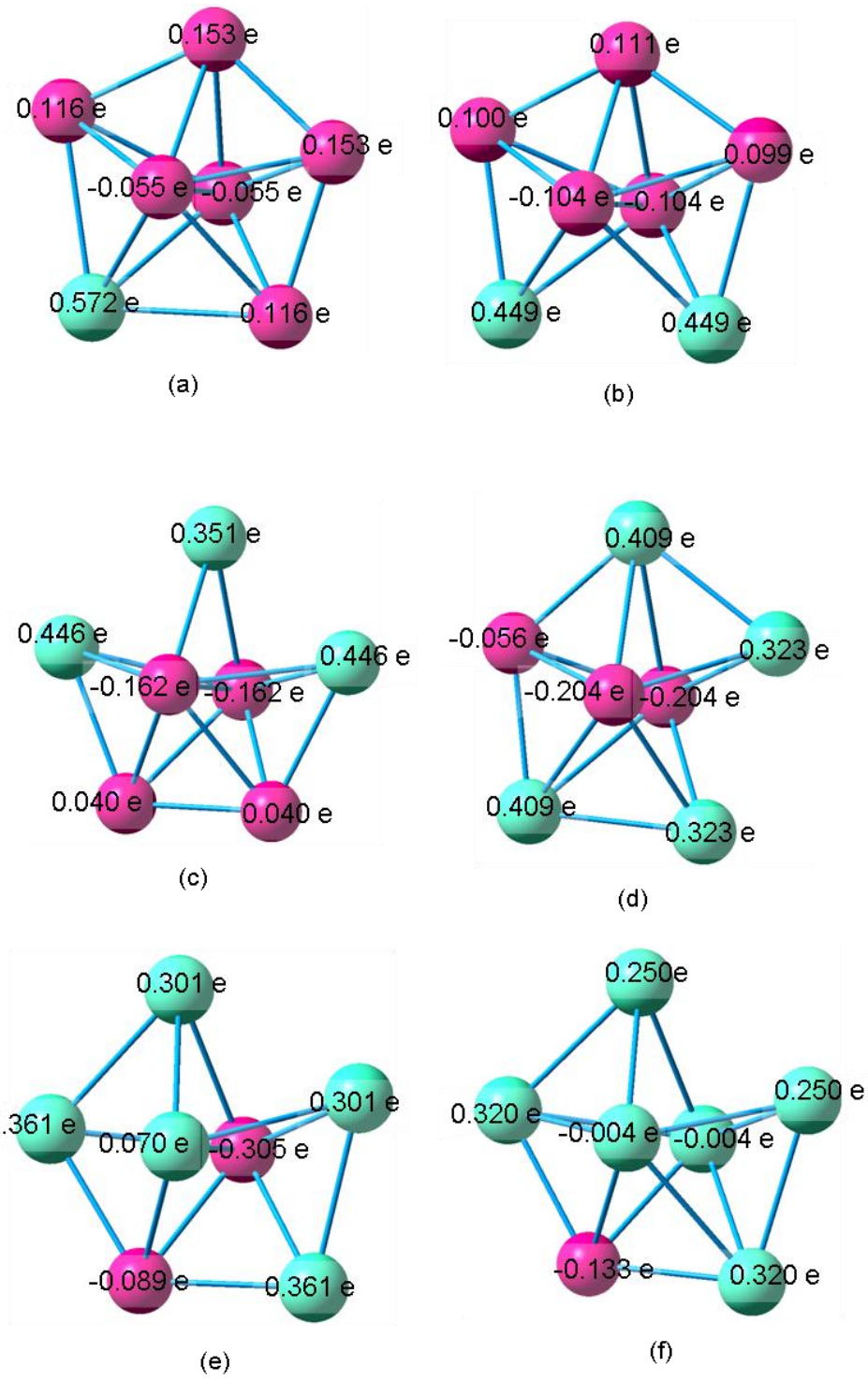

Figure 4.125 Atomic Charges of the Most Stable (a) $(Si_6Ge)^+$ (b) $(Si_5Ge_2)^+$ (c) $(Si_4Ge_3)^+$ (d) $(Si_3Ge_4)^+$ (e) $(Si_2Ge_5)^+$ and (f) $(SiGe_6)^+$ Cationic Septamer

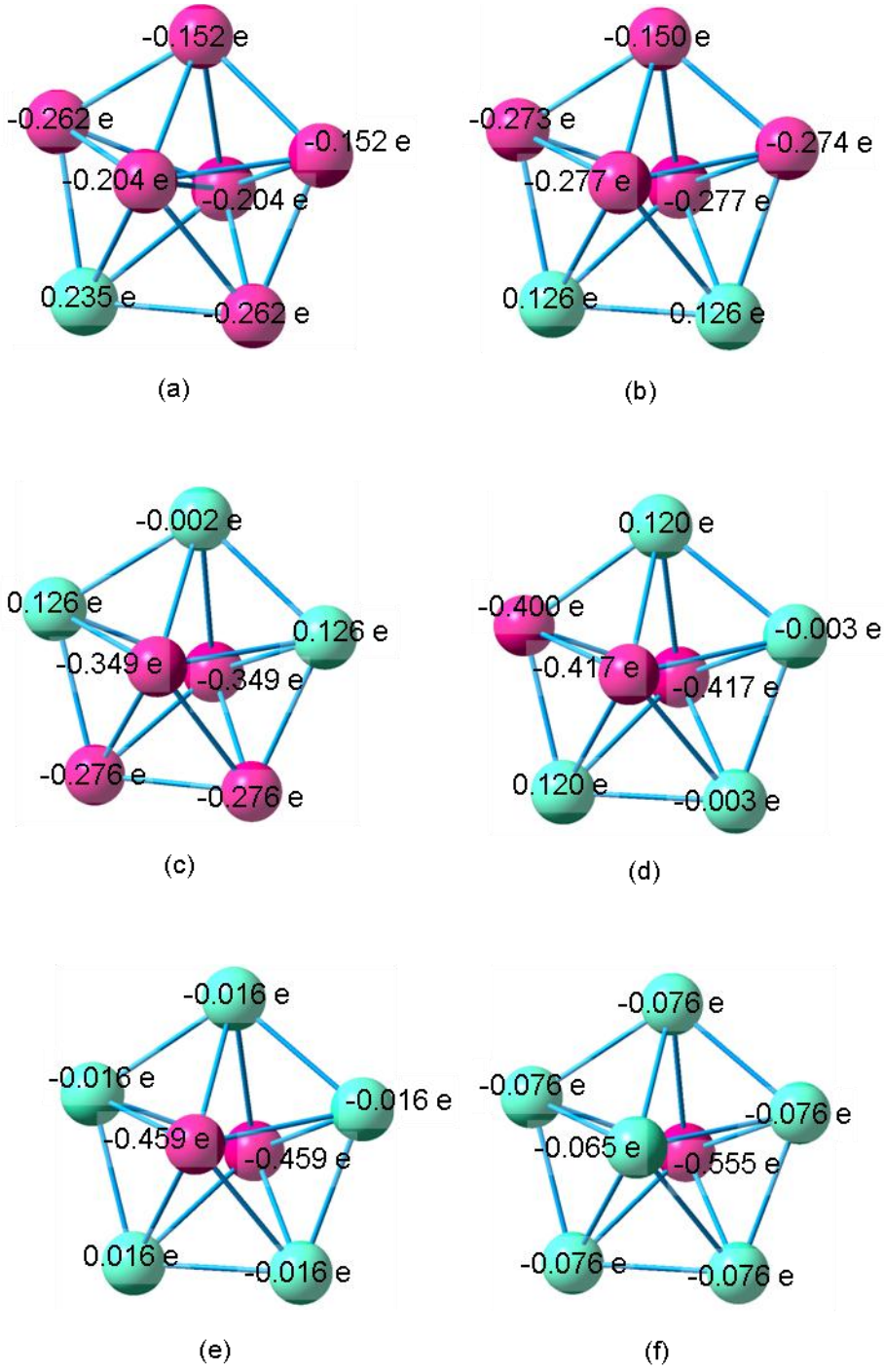

Figure 4.126 Atomic Charges of the Most Stable (a) $(Si_6Ge)^-$ (b) $(Si_5Ge_2)^-$ (c) $(Si_4Ge_3)^-$ (d) $(Si_3Ge_4)^-$ (e) $(Si_2Ge_5)^-$ and (f) $(SiGe_6)^-$ Anionic Septamer

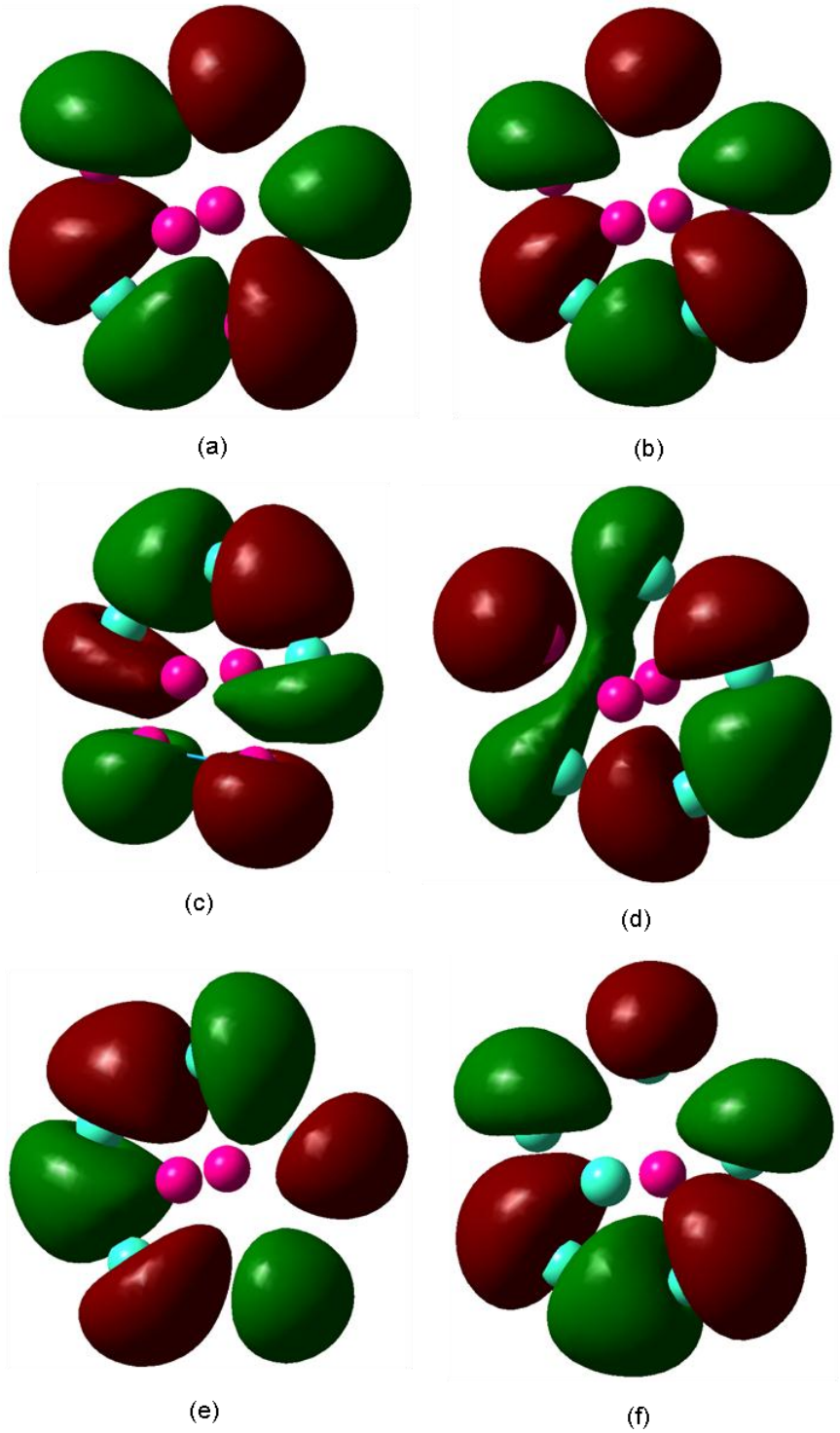

Figure 4.127 HOMO of the Most Stable (a) Si_6Ge (b) Si_5Ge_2 (c) Si_4Ge_3 (d) Si_3Ge_4 (e) Si_2Ge_5 and (f) $SiGe_6$ Neutral Septamer

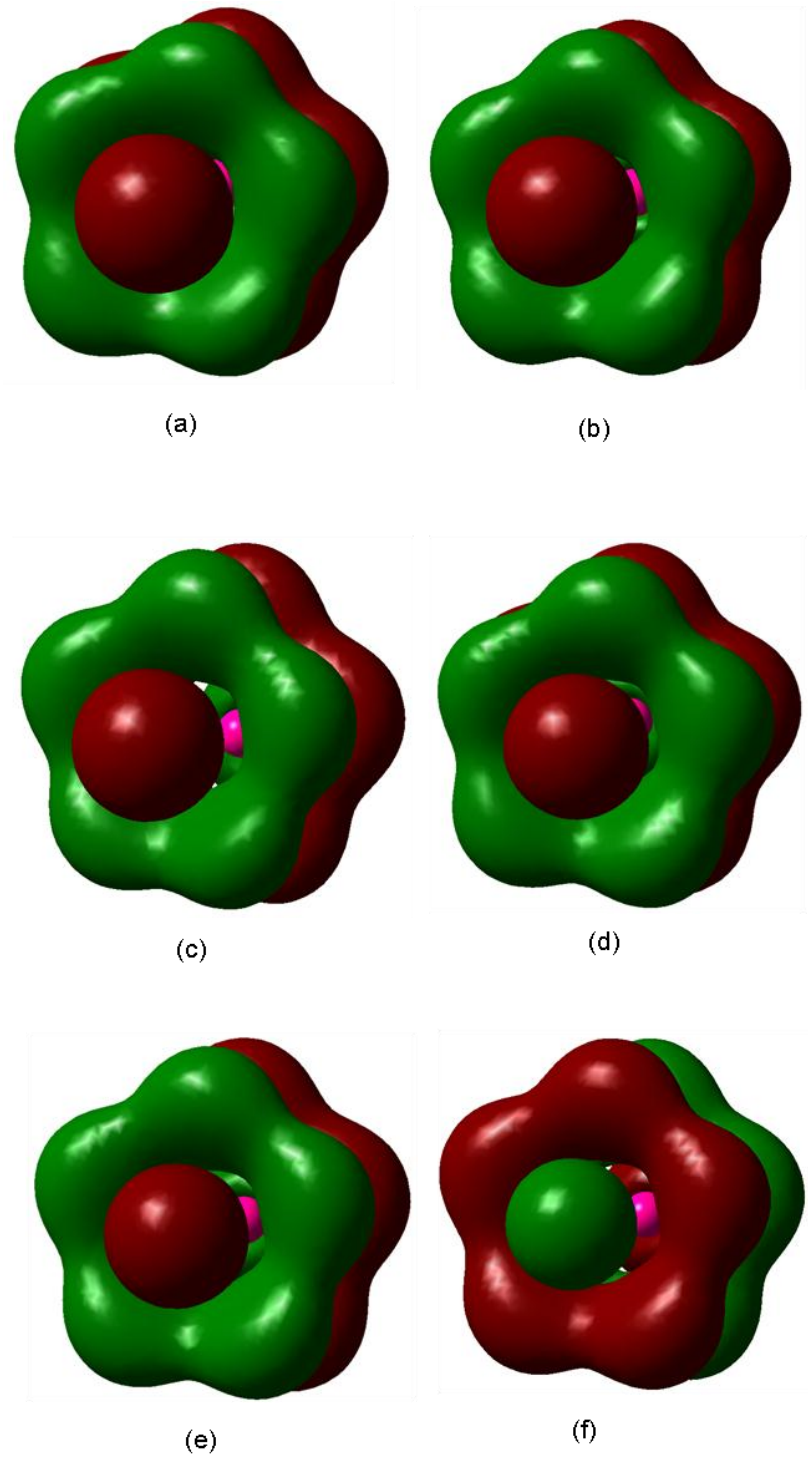

Figure 4.128 LUMO of the Most Stable (a) Si_6Ge (b) Si_5Ge_2 (c) Si_4Ge_3 (d) Si_3Ge_4 (e) Si_2Ge_5 and (f) $SiGe_6$ Neutral Septamer

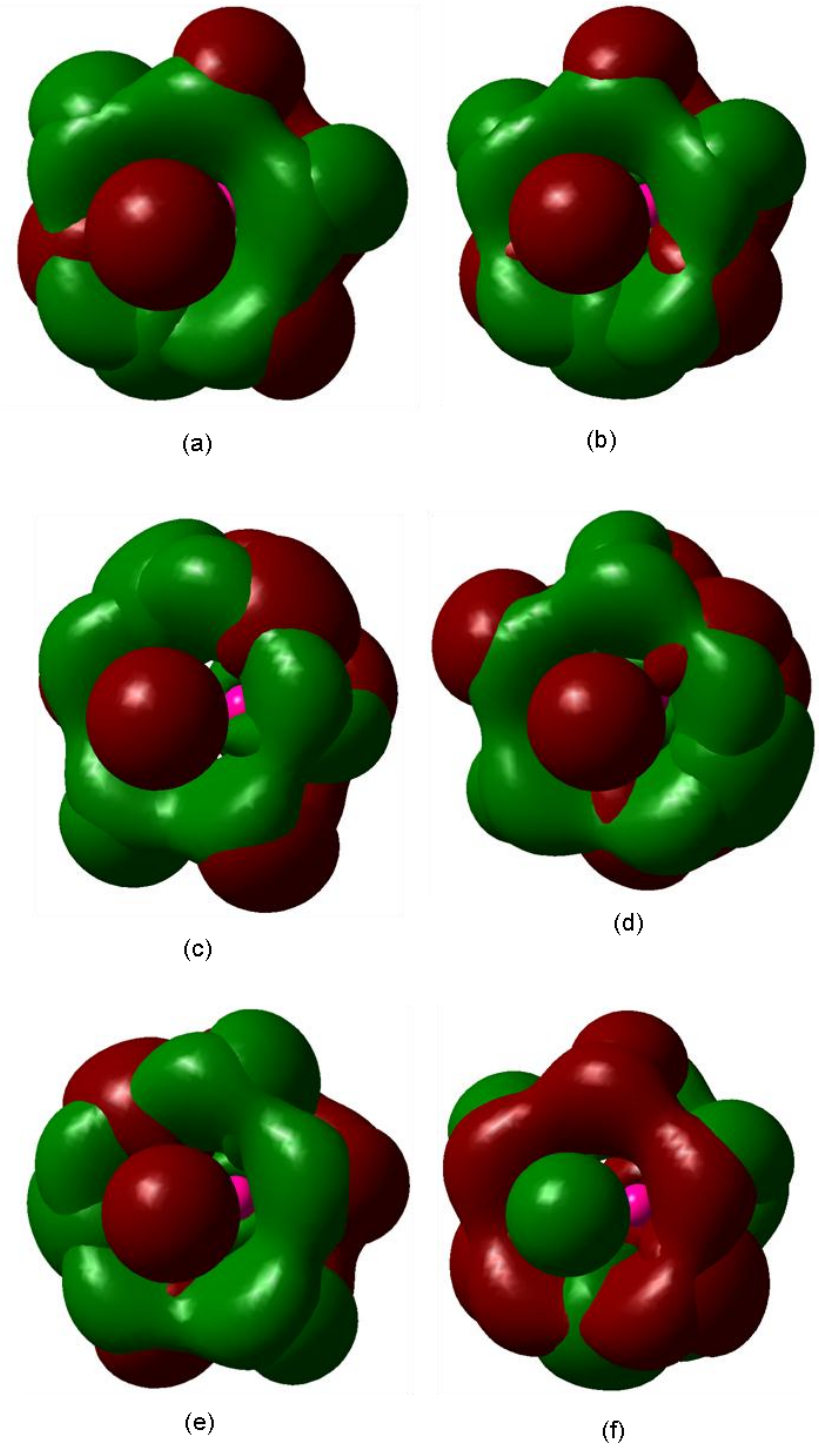

Figure 4.129 HOMO and LUMO of the Most Stable (a) Si_6Ge (b) Si_5Ge_2 (c) Si_4Ge_3 (d) Si_3Ge_4 (e) Si_2Ge_5 and (f) $SiGe_6$ Neutral Septamer

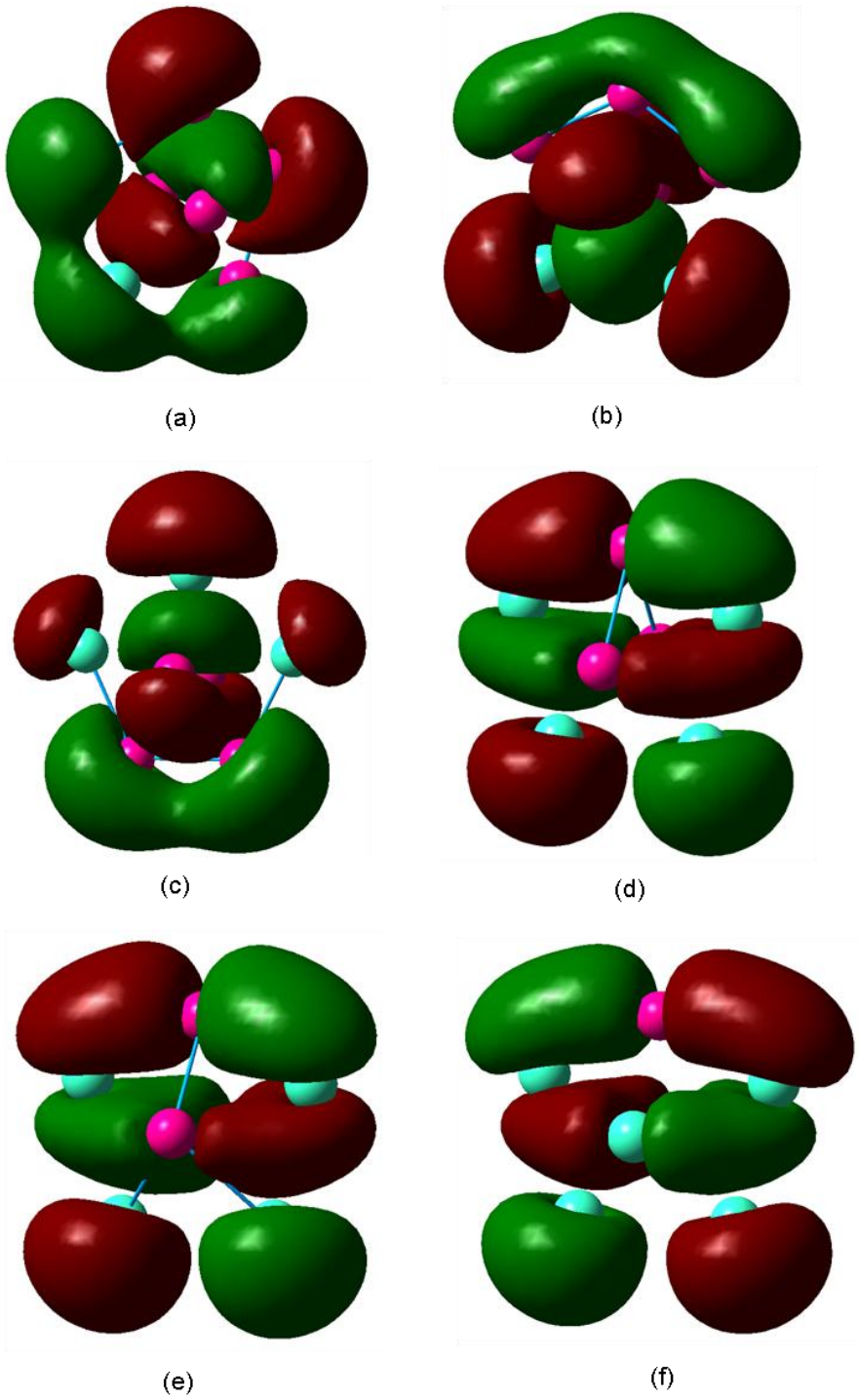

Figure 4.130 HOMO of the Most Stable (a) $(Si_6Ge)^+$ (b) $(Si_5Ge_2)^+$ (c) $(Si_4Ge_3)^+$ (d) $(Si_3Ge_4)^+$ (e) $(Si_2Ge_5)^+$ and (f) $(SiGe_6)^+$ Cationic Septamer

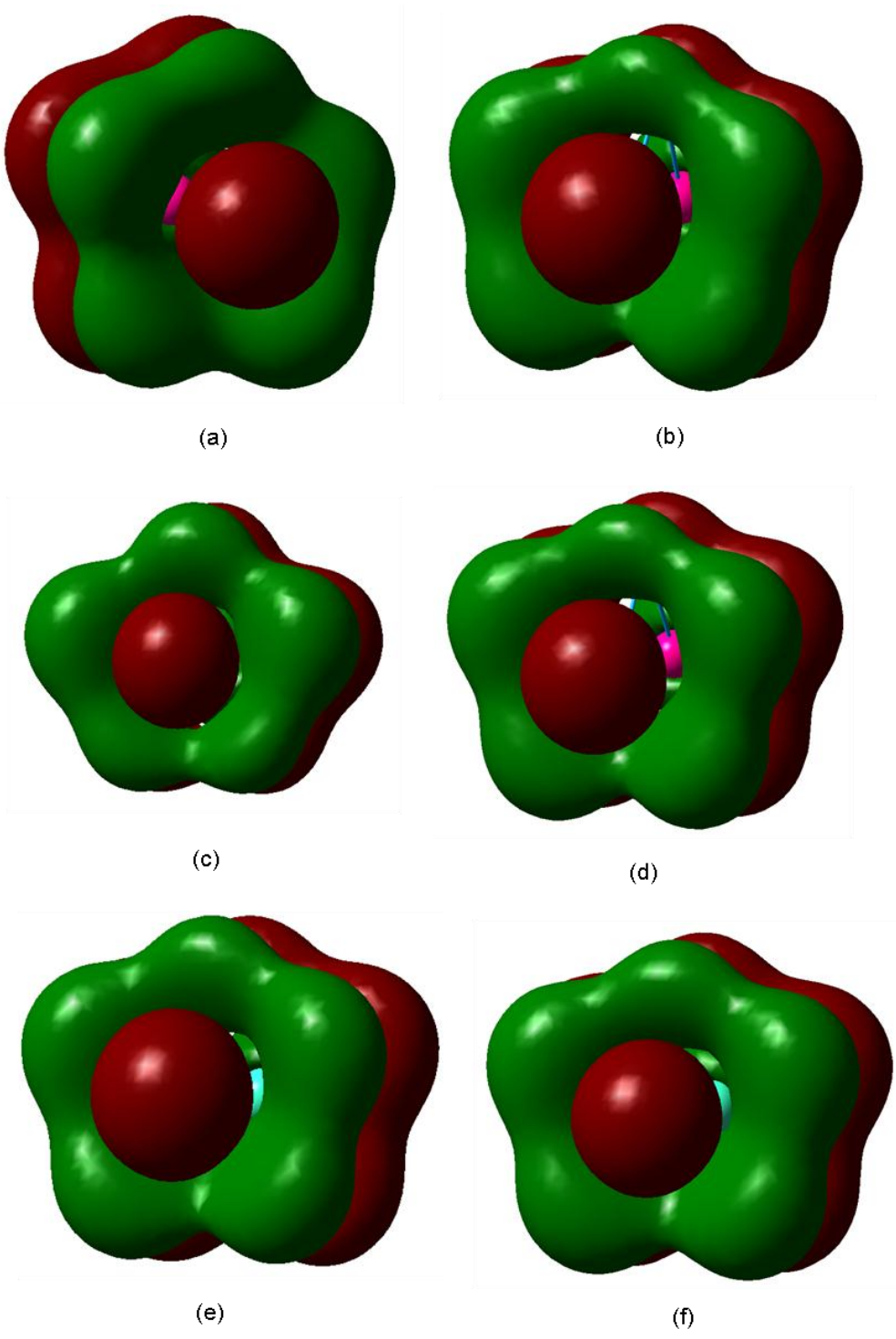

Figure 4.131 LUMO of the Most Stable (a) $(Si_6Ge)^+$ (b) $(Si_5Ge_2)^+$ (c) $(Si_4Ge_3)^+$ (d) $(Si_3Ge_4)^+$ (e) $(Si_2Ge_5)^+$ and (f) $(SiGe_6)^+$ Cationic Septamer

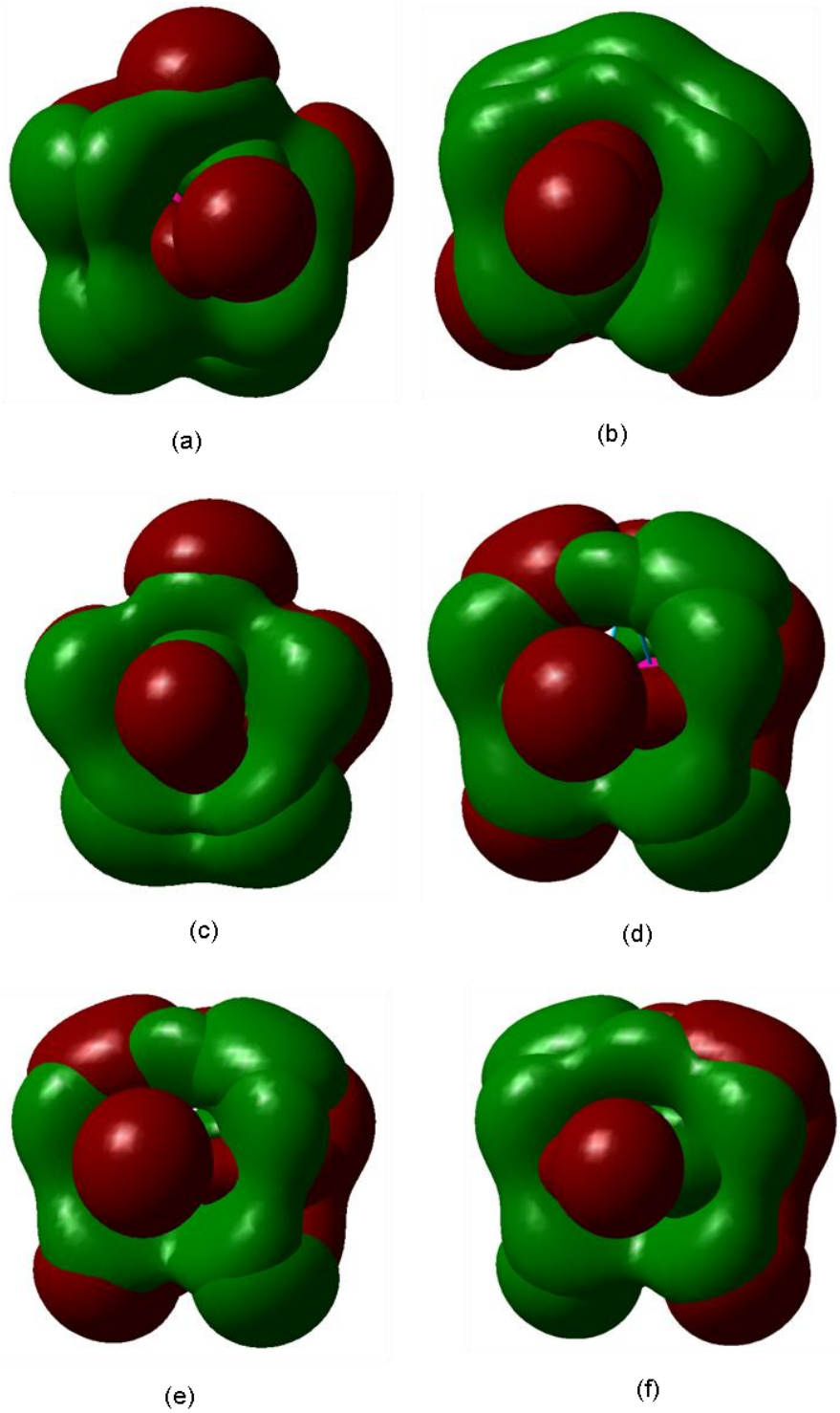

Figure 4.132 HOMO and LUMO of the Most Stable (a) $(Si_6Ge)^+$ (b) $(Si_5Ge_2)^+$ (c) $(Si_4Ge_3)^+$ (d) $(Si_3Ge_4)^+$ (e) $(Si_2Ge_5)^+$ and (f) $(SiGe_6)^+$ Cationic Septamer

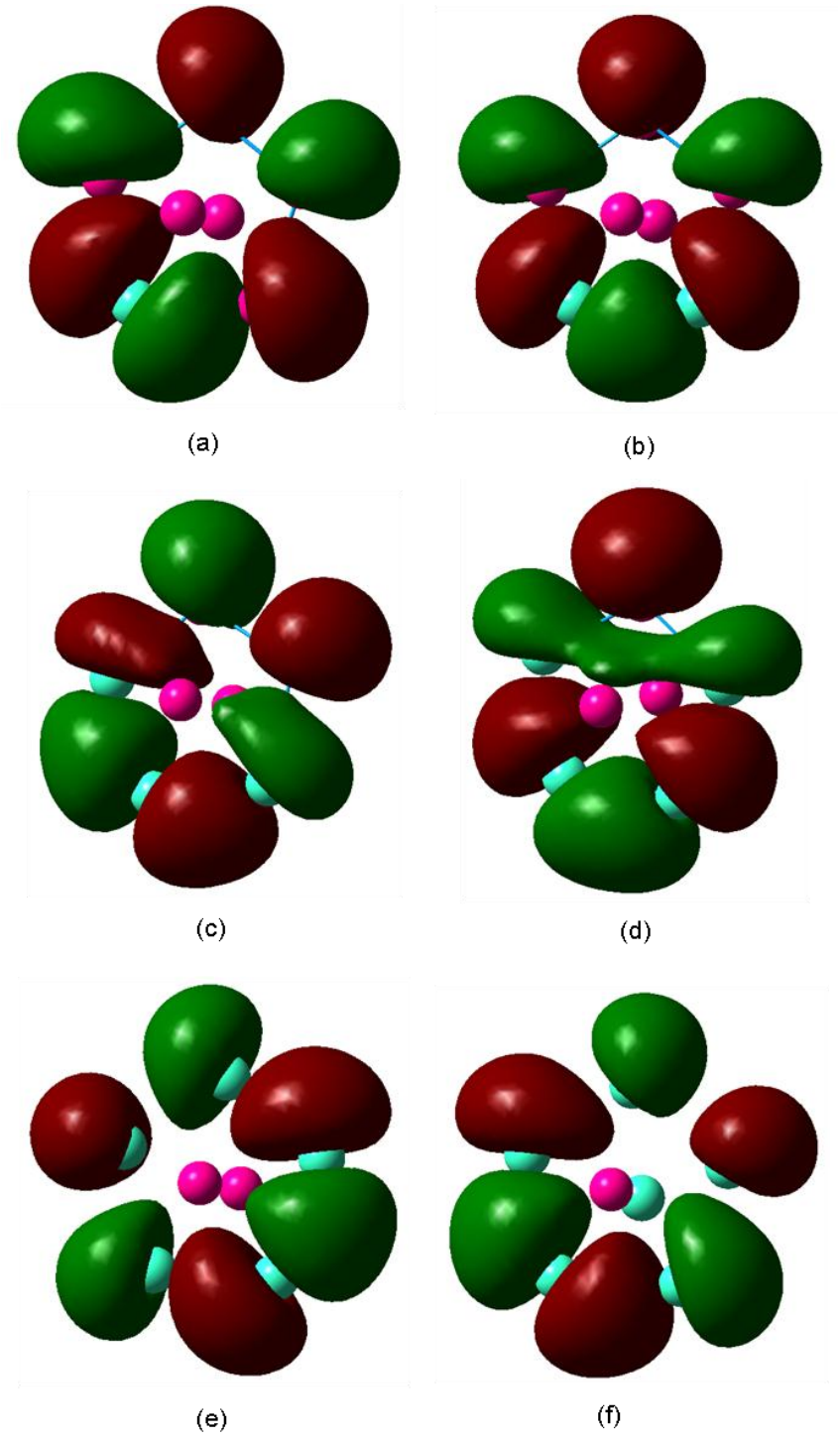

Figure 4.133 HOMO of the Most Stable (a) $(Si_6Ge)^-$ (b) $(Si_5Ge_2)^-$ (c) $(Si_4Ge_3)^-$ (d) $(Si_3Ge_4)^-$ (e) $(Si_2Ge_5)^-$ and (f) $(SiGe_6)^-$ Anionic Septamer

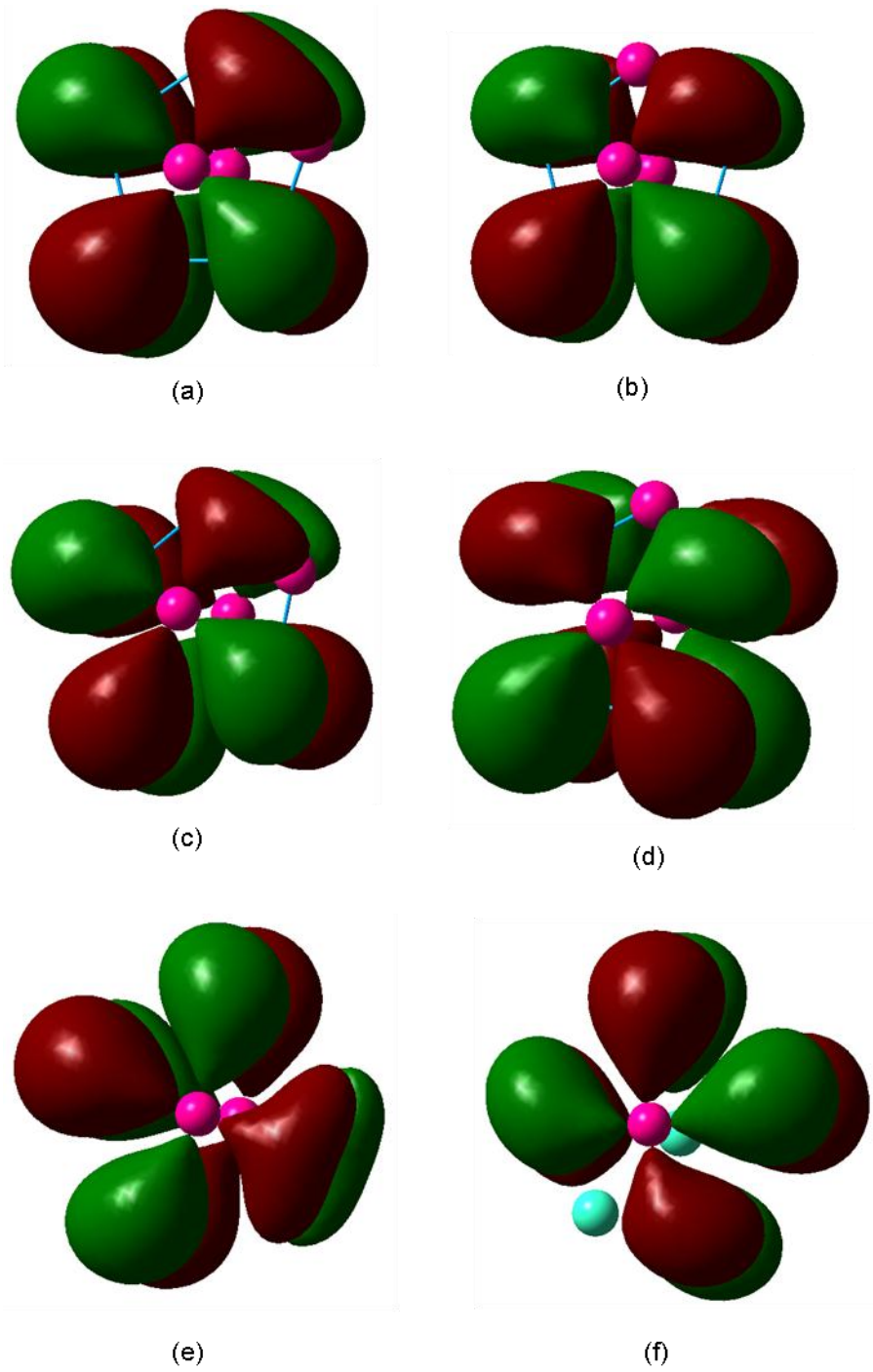

Figure 4.134 LUMO of the Most Stable (a) $(Si_6Ge)^-$ (b) $(Si_5Ge_2)^-$ (c) $(Si_4Ge_3)^-$ (d) $(Si_3Ge_4)^-$ (e) $(Si_2Ge_5)^-$ and (f) $(SiGe_6)^-$ Anionic Septamer

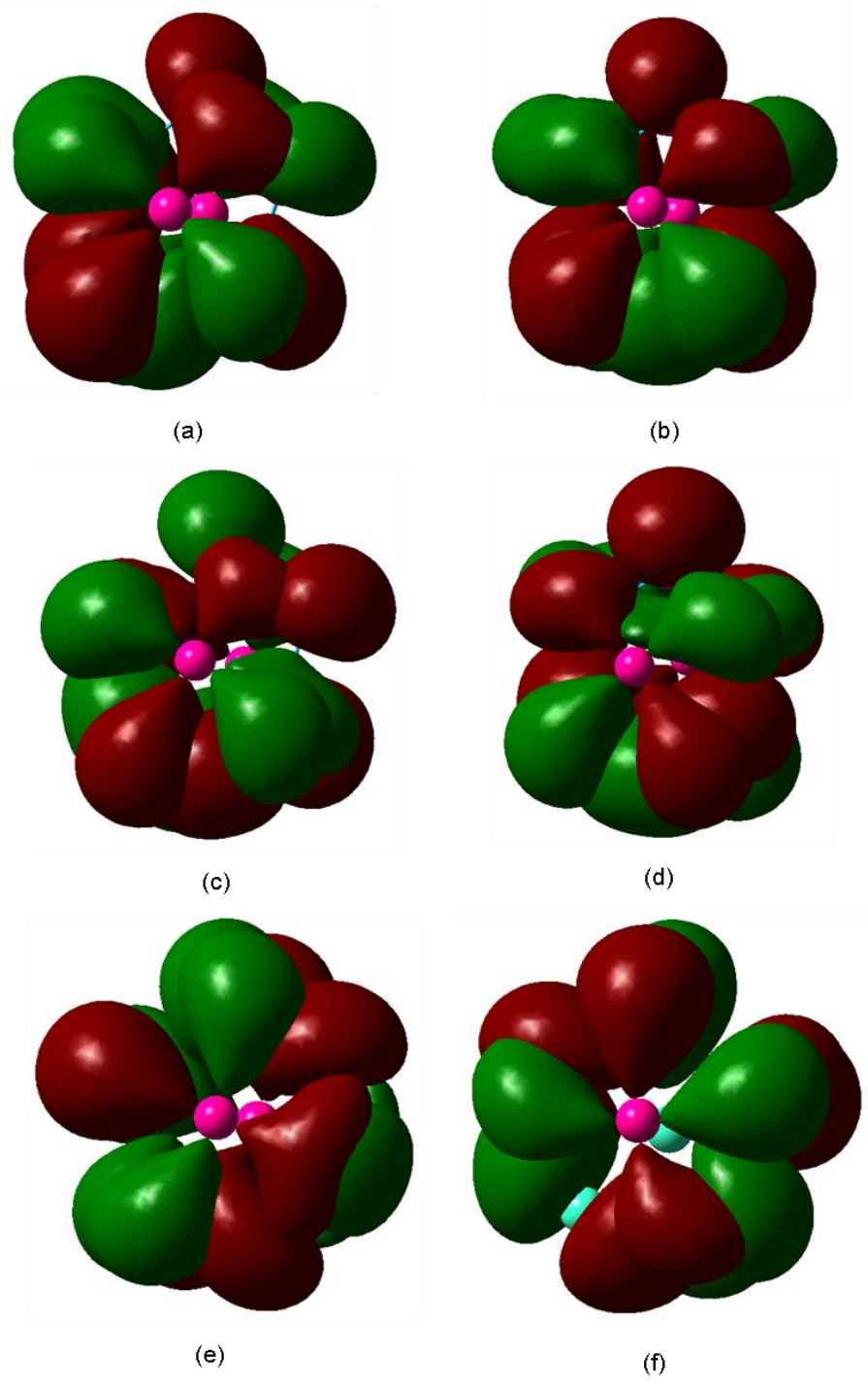

Figure 4.135 HOMO and LUMO of the Most Stable (a) $(Si_6Ge)^-$ (b) $(Si_5Ge_2)^-$ (c) $(Si_4Ge_3)^-$ (d) $(Si_3Ge_4)^-$ (e) $(Si_2Ge_5)^-$ and (f) $(SiGe_6)^-$ Anionic Septamer

4.22 Si_7Ge Octamers

To our knowledge, only two other papers have reported details about the silicon-germanium heteronuclear octamers – Li *et al.* and Wang and Chao. Li et al only investigated the Si_4Ge_4 nanocluster. For the neutral Si_7Ge cluster, Wang and Chao [51] reported a prism-shaped cluster with a ^1A electronic state, a dissociation energy of -33.7564 eV or -35.6338 eV, a HOMO-LUMO gap of 2.56 eV, and the following frequencies: 498(a), 347(a), and 381(a). For the cation they found the most stable cluster to be a silicon pentagonal bipyramid with an addition germanium atom attached to one of the faces. Their anion cluster is similar to our most stable anion.

Totally, we investigated twenty-four Si_7Ge clusters, but for the sake of brevity, we only include the data for the ten most stable clusters. It needs to be emphasized that these octamers are all extremely close in energy. The difference in binding energy per atom between our most stable Si_7Ge cluster and our twenty-fourth most stable cluster was only 0.093 eV. When investigating the octamers, we began with the Si_7Ge clusters. To find adequate input geometries, we again turned to the paper by Raghavachari and Rohlfing [20] on pure silicon nanoclusters. From their paper, we borrowed the following structures: a rectangular bipyramid with two opposite capped faces, half of a pentagonal bipyramid with two additional atoms attached to the base, a 7-atom arrangement as in figure 4.122 (c) with an eighth atom attached below, a pentagonal bipyramid with an eight atom attached to one face, and a pentagonal bipyramid with the eighth atom attached to only two atoms. In this work, we report the data for ten neutrals, nine cations, and ten anions.

Table 4.148 Properties of the Si_7Ge Octamers

Figure	Symmetry Group	Electronic State	Binding E / Atom (eV)	HOMO-LUMO Gap (eV)	Dipole Moment (D)
4.136 (a)	C_s	$^1A'$	3.089	2.171	0.793
4.136 (b)	C_s	$^1A'$	3.080	1.766	0.433
4.136 (c)	C_s	$^1A'$	3.070	1.684	0.451
4.136 (d)	C_1	^1A	3.067	2.350	0.791
4.136 (e)	C_s	$^1A'$	3.066	2.213	0.352
4.136 (f)	C_s	$^1A'$	3.064	1.757	0.970
4.136 (g)	C_s	$^1A'$	3.064	1.725	0.313
4.136 (h)	C_s	$^1A'$	3.059	1.792	1.064
4.136 (i)	C_1	^1A	3.059	2.112	0.790
4.136 (j)	C_1	^1A	3.052	1.869	0.226

Table 4.149 Properties of the $(Si_7Ge)^+$ Octamers

Figure	Symmetry Group	Electronic State	Binding E / Atom (eV)	HOMO-LUMO Gap (eV)	Dipole Moment (D)
4.137 (a)	C_s	$^2A''$	3.265	1.682[a]	1.089
4.137 (b)	C_s	$^2A''$	3.252	1.731[a]	1.177
4.137 (c)	C_1	^2A	3.216	1.537	0.950
4.137 (d)	C_s	$^2A'$	3.213	1.462[a]	0.853
4.137 (e)	C_s	$^2A'$	3.210	1.384[a]	1.305
4.137 (f)	C_1	^2A	3.201	1.480[a]	1.060
4.137 (g)	C_s	$^2A'$	3.190	1.520[a]	1.062
4.137 (h)	C_s	$^2A''$	3.170	1.491[a]	0.677
4.137 (i)	C_s	$^2A''$	3.150	1.491[a]	0.984

[a] HOMO and LUMO have opposite spins; this value includes the energy required to flip the spin of the electron.

Table 4.150 Properties of the $(Si_7Ge)^-$ Octamers

Figure	Symmetry Group	Electronic State	Binding E / Atom (eV)	HOMO-LUMO Gap (eV)	Dipole Moment (D)
4.138 (a)	C_s	^2A"	3.281	1.500[a]	1.929
4.138 (b)	C_s	^2A'	3.281	1.467[a]	1.918
4.138 (c)	C_s	^2A'	3.258	1.483[a]	1.179
4.138 (d)	C_s	^2A"	3.233	1.341[a]	1.570
4.138 (e)	C_s	^2A"	3.225	1.349[a]	2.162
4.138 (f)	C_1	^2A	3.216	1.519[a]	1.249
4.138 (g)	C_1	^2A	3.210	1.418[a]	1.183
4.138 (h)	C_1	^2A	3.205	1.666[a]	1.595
4.138 (i)	C_s	^2A"	3.187	1.553[a]	2.226
4.138 (j)	C_s	^2A"	3.175	1.560[a]	2.069

[a] HOMO and LUMO have opposite spins; this value includes the energy required to flip the spin of the electron.

Table 4.151 Ionization Potentials and Electron Affinities of the Si_7Ge Octamers

Neutral Figure	VIP (eV)	Cationic Figure	AIP (eV)	VEA (eV)	Anionic Figure	AEA (eV)
4.136 (a)	7.493	4.137 (h)	7.254	2.192	4.138 (b)	2.666
4.136 (b)	6.945	4.137 (d)	6.840	2.157	4.138 (d)	2.356
4.136 (c)	6.869	4.137 (e)	6.780	2.184	4.138 (e)	2.378
4.136 (d)	7.162	4.137 (c)	6.703	1.761	4.138 (h)	2.248
4.136 (e)	7.529	4.137 (i)	7.226	2.236	4.138 (c)	2.679
4.136 (f)	7.383	4.137 (g)	6.896	2.546	4.138 (a)	2.868
4.136 (g)	6.480	4.137 (a)	6.298	1.809	4.138 (i)	2.122
4.136 (h)	6.549	4.137 (b)	6.355	1.773	4.138 (j)	2.065
4.136 (i)	7.146	4.137 (c)	6.640	1.976	4.138 (f)	2.398
4.136 (j)	7.024	4.137 (f)	6.707	2.098	4.138 (g)	2.397

Table 4.152 Fragmentation Energies for the Most Stable Si_7Ge Octamers

Fragmented Cluster	Fragmentation Energy (eV)
$Si_6Ge + Si$	2.416
$Si_5Ge + Si_2$	2.912
$Si_5Ge + 2Si$	6.134
$Si_4Ge + Si_2 + Si$	6.860
$Si_3Ge + 2Si_2$	7.222
$Si_4Ge + 3Si$	10.083
$Si_3Ge + Si_2 + 2Si$	10.445
$Si_2Ge + 2Si_2 + Si$	11.520
$3Si_2 + SiGe$	11.986
$Si_3Ge + 4Si$	13.668
$Si_2Ge + Si_2 + 3Si$	14.742
$3Si_2 + Si + Ge$	15.048
$2Si_2 + SiGe + 2Si$	15.209
$Si_2Ge + 5Si$	17.965
$2Si_2 + 3Si + Ge$	18.270
$Si_2 + SiGe + 4Si$	18.432
$Si_2 + 5Si + Ge$	21.493
$SiGe + 6Si$	21.655
$7Si + Ge$	24.716

Table 4.153 Fragmentation Energies for the Most Stable $(Si_7Ge)^+$ Octamer

Fragmented Cluster	Fragmentation Energy (eV)
$(Si_6Ge)^+ + Si$	3.590
$(Si_5Ge)^+ + Si_2$	4.097
$(Si_5Ge)^+ + 2Si$	7.320
$(Si_4Ge)^+ + Si_2 + Si$	8.141
$(Si_3Ge)^+ + 2Si_2$	8.490
$(Si_4Ge)^+ + 3Si$	11.364
$(Si_3Ge)^+ + Si_2 + 2Si$	11.712
$(Si_2Ge)^+ + 2Si_2 + Si$	12.902
$3Si_2 + (SiGe)^+$	13.222
$(Si_3Ge)^+ + 4Si$	14.935
$(Si_2Ge)^+ + Si_2 + 3Si$	16.125
$2Si_2 + (SiGe)^+ + 2Si$	16.445
$3Si_2 + Si + (Ge)^+$	16.448
$(Si_2Ge)^+ + 5Si$	19.348
$Si_2 + (SiGe)^+ + 4Si$	19.668
$2Si_2 + 3Si + (Ge)^+$	19.671
$(SiGe)^+ + 6Si$	22.891
$Si_2 + 5Si + (Ge)^+$	22.894
$7Si + (Ge)^+$	26.116

Table 4.154 Fragmentation Energies for the Most Stable $(Si_7Ge)^-$ Octamer

Fragmented Cluster	Fragmentation Energy (eV)
$(Si_6Ge)^- + Si$	3.247
$(Si_5Ge)^- + Si_2$	3.813
$(Si_5Ge)^- + 2Si$	7.035
$(Si_4Ge)^- + Si_2 + Si$	7.285
$(Si_3Ge)^+ + 2Si_2$	7.901
$(Si_4Ge)^- + 3Si$	10.508
$(Si_3Ge)^- + Si_2 + 2Si$	11.124
$(Si_2Ge)^- + 2Si_2 + Si$	12.008
$3Si_2 + (SiGe)^-$	12.809
$(Si_3Ge)^- + 4Si$	14.347
$(Si_2Ge)^- + Si_2 + 3Si$	15.231
$2Si_2 + (SiGe)^- + 2Si$	16.031
$3Si_2 + Si + Ge^-$	16.577
$(Si_2Ge)^- + 5Si$	18.453
$Si_2 + (SiGe)^- + 4Si$	19.254
$2Si_2 + 3Si + Ge^-$	19.800
$(SiGe)^- + 6Si$	22.477
$Si_2 + 5Si + Ge^-$	23.023
$7Si + Ge^-$	26.246

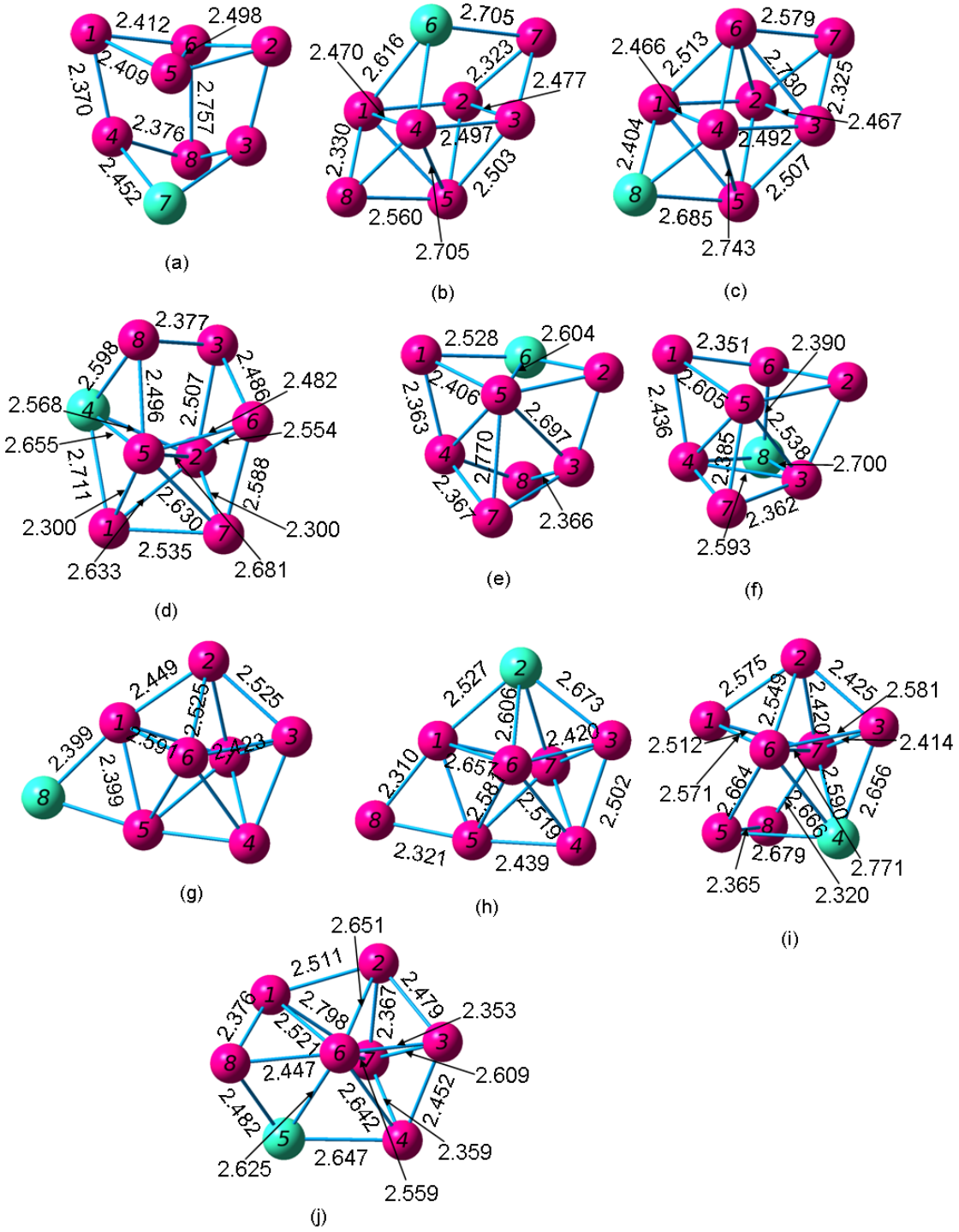

Figure 4.136 Geometries of the Si_7Ge Neutral Septamers from (a) Most Stable through (j) Least Stable

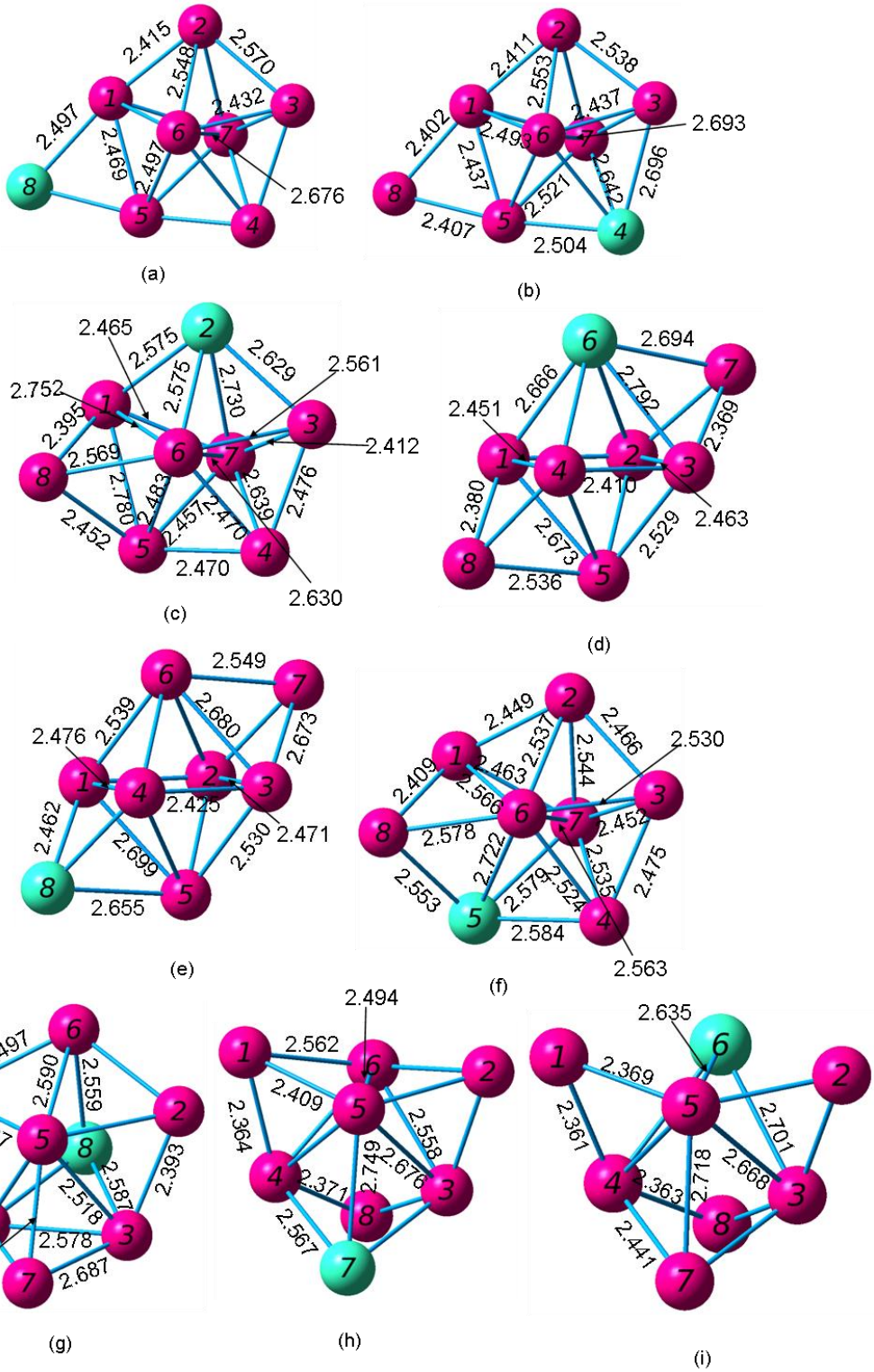

Figure 4.137 Geometries of the $(Si_7Ge)^+$ Cationic Septamers from (a) Most Stable through (i) Least Stable

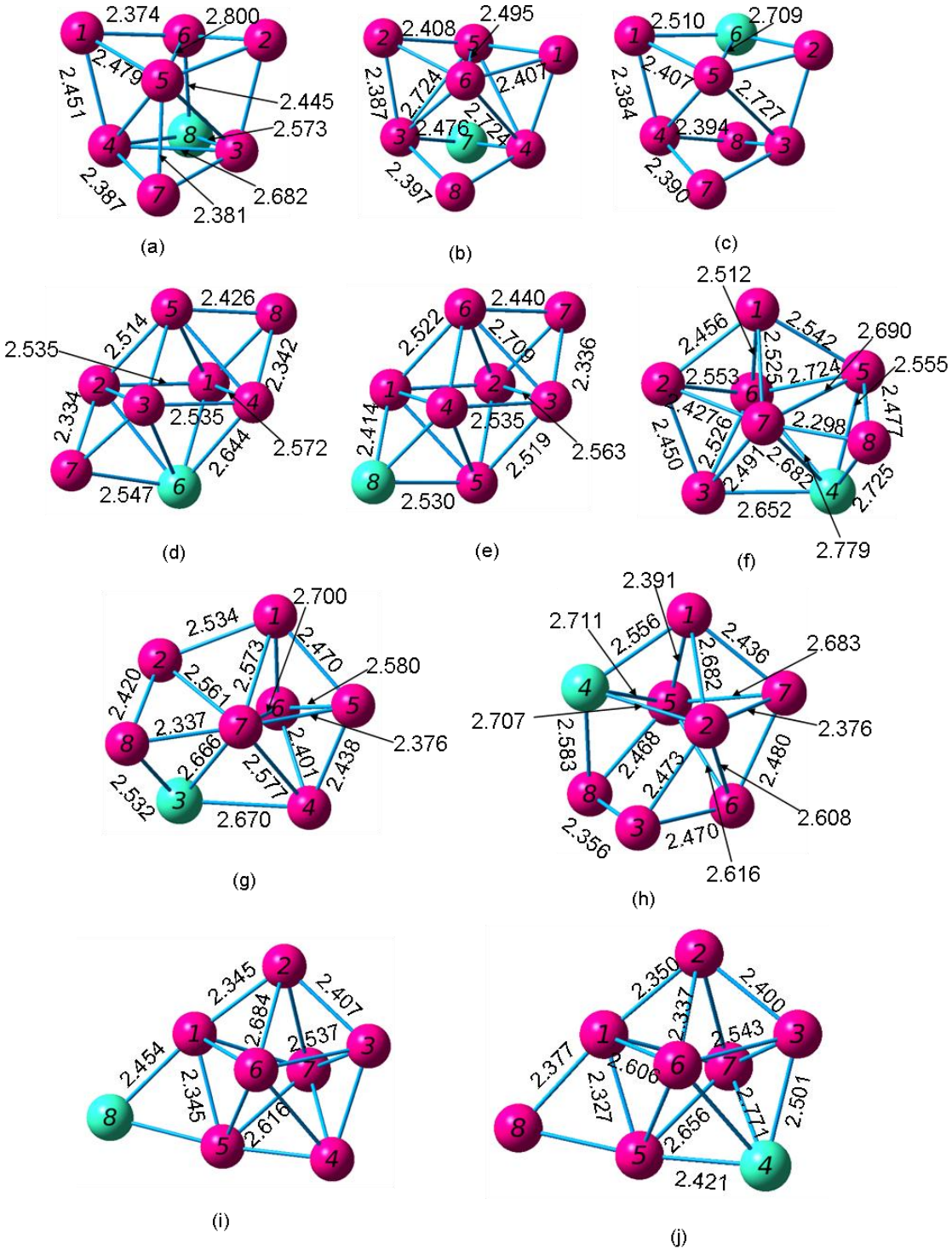

Figure 4.138 Geometries of the $(Si_7Ge)^-$ Anion Septamers from (a) Most Stable through (j) Least Stable

4.23 Si_6Ge_2 Octamers

Wang and Chao [51] reported a prism-shaped cluster for the neutral and cation Si_6Ge_2 octamers. The neutral cluster has a ^1A electronic state, a dissociation energy of -33.4421 eV or -35.7532 eV, a HOMO-LUMO gap of 2.60 eV, and the following frequencies: 491(a), 293(a), and 303(a). Their anion cluster is again similar to our most stable anion.

Totally, we investigated thirty-eight Si_6Ge_2 clusters. This was our largest group of isomers. The difference in binding energy per atom between our most stable cluster and our thirty-eighth most stable cluster was 0.1356 eV. Our most stable neutral cluster resembles two trigonal bipyramids attached by one of their sides. Other clusters include a half-pentagonal bipyramid with two atoms at the bottom and a rectangular bipyramid with atoms attached at opposite faces. Here, we report the properties of ten neutrals and cations and nine anions.

Table 4.155 Properties of the Si_6Ge_2 Octamers

Figure	Symmetry Group	Electronic State	Binding E / Atom (eV)	HOMO-LUMO Gap (eV)	Dipole Moment (D)
4.139 (a)	C_1	^1A	3.092	2.601	0.845
4.139 (b)	C_1	^1A	3.088	2.619	0.501
4.139 (c)	C_s	$^1A'$	3.058	2.144	0.923
4.139 (d)	C_1	^1A	3.048	2.115	0.699
4.139 (e)	C_s	$^1A'$	3.046	1.858	0.003
4.139 (f)	C_s	$^1A'$	3.041	1.757	0.671
4.139 (g)	C_s	$^1A'$	3.038	1.765	0.527
4.139 (h)	C_s	$^1A'$	3.037	2.092	0.002
4.139 (i)	C_s	$^1A'$	3.036	2.170	0.763
4.139 (j)	C_1	^1A	3.034	2.290	0.128

Table 4.156 Properties of the $(Si_6Ge_2)^+$ Octamers

Figure	Symmetry Group	Electronic State	Binding E / Atom (eV)	HOMO-LUMO Gap (eV)	Dipole Moment (D)
4.140 (a)	C_s	$^2A'$	3.184	1.439[a]	1.581
4.140 (b)	C_1	^2A	3.183	1.366[a]	0.953
4.140 (c)	C_s	$^2A'$	3.182	1.516[a]	0.000
4.140 (d)	C_1	^2A	3.182	1.454[a]	1.535
4.140 (e)	C_1	^2A	3.181	1.374[a]	1.105
4.140 (f)	C_s	$^2A'$	3.181	1.448[a]	0.845
4.140 (g)	C_s	$^2A''$	3.145	1.472[a]	0.762
4.140 (h)	C_1	^2A	3.141	1.460[a]	0.853
4.140 (i)	C_s	$^2A''$	3.126	1.402[a]	1.320
4.140 (j)	C_s	$^2A''$	3.125	1.476[a]	1.057

[a] HOMO and LUMO have opposite spins; this value includes the energy required to flip the spin of the electron.

Table 4.157 Properties of the $(Si_6Ge_2)^-$ Octamers

Figure	Symmetry Group	Electronic State	Binding E / Atom (eV)	HOMO-LUMO Gap (eV)	Dipole Moment (D)
4.141 (a)	C_s	$^2A'$	3.242	1.607[a]	2.139
4.141 (b)	C_s	$^2A'$	3.229	1.485[a]	1.631
4.141 (c)	C_s	$^2A'$	3.224	1.443	2.185
4.141 (d)	C_1	^2A	3.211	1.435[a]	1.765
4.141 (e)	C_1	^2A	3.195	1.483[a]	1.834
4.141 (f)	C_s	$^2A''$	3.187	1.320	0.000
4.141 (g)	C_s	$^2A''$	3.186	1.328[a]	2.808
4.141 (h)	C_s	$^2A''$	3.182	1.329[a]	1.787
4.141 (i)	C_1	^2A	3.161	1.678[a]	2.336

[a] HOMO and LUMO have opposite spins; this value includes the energy required to flip the spin of the electron.

Table 4.158 Ionization Potentials and Electron Affinities of the Si_6Ge_2 Octamers

Neutral Figure	VIP (eV)	Cationic Figure	AIP (eV)	VEA (eV)	Anionic Figure	AEA (eV)
4.139 (a)	7.290	4.140 (b)	7.169	1.678	4.141 (d)	2.089
4.139 (b)	7.282	4.140 (e)	7.155	1.640	4.141 (e)	1.991
4.139 (c)	7.394	4.140 (g)	7.201	2.172	4.141 (a)	2.611
4.139 (d)	7.398	4.140 (h)	7.158	2.198	4.141 (a)	2.690
4.139 (e)	6.931	4.140 (c)	6.814	2.079	4.141 (f)	2.268
4.139 (f)	6.869	4.140 (a)	6.755	2.075	4.141 (g)	2.299
4.139 (g)	6.866	4.140 (f)	6.756	2.081	4.141 (h)	2.292
4.139 (h)	7.352	4.140 (i)	7.183	2.205	4.141 (b)	2.673
4.139 (i)	7.470	4.140 (j)	7.185	2.197	4.141 (c)	2.639
4.139 (j)	7.071	4.140 (d)	6.717	1.747	4.141 (i)	2.157

Table 4.159 Fragmentation Energies for the Most Stable Si_6Ge_2 Octamer

Fragmented Cluster	Fragmentation Energy (eV)
$Si_6Ge + Ge$	2.437
$2Si_3Ge$	2.640
$Si_5Ge_2 + Si$	2.740
$Si_5Ge + SiGe$	3.093
$Si_4Ge_2 + Si_2$	3.204
$Si_4Ge + Si_2Ge$	3.352
$Si_5Ge + Si + Ge$	6.155
$Si_4Ge_2 + 2Si$	6.427
$Si_4Ge + Si_2 + Ge$	6.880
$Si_4Ge + SiGe + Si$	7.042
$Si_3Ge_2 + Si_2 + Si$	7.128
$Si_3Ge + SiGe + Si_2$	7.404
$Si_2Ge_2 + 2Si_2$	7.511
$2Si_2Ge + Si_2$	8.012
$Si_4Ge + 2Si + Ge$	10.103
$Si_3Ge_2 + 3Si$	10.351
$Si_3Ge + Si_2 + Si + Ge$	10.465
$Si_3Ge + SiGe + 2Si$	10.627
$Si_2Ge_2 + Si_2 + 2Si$	10.733
$2Si_2Ge + 2Si$	11.235
$Si_2Ge + 2Si_2 + Ge$	11.540
$SiGe_2 + 2Si_2 + Si$	11.639
$Si_2Ge + Si_2 + SiGe + Si$	11.701
$3Si_2 + Ge_2$	12.140
$2Si_2 + 2SiGe$	12.168
$Si_3Ge + 3Si + Ge$	13.688
$Si_2Ge_2 + 4Si$	13.956
$Si_2Ge + Si_2 + 2Si + Ge$	14.763
$SiGe_2 + Si_2 + 3Si$	14.861
$Si_2Ge + SiGe + 3Si$	14.924

Table 4.159 – *Continued*

Fragmented Cluster	Fragmentation Energy (eV)
$3Si_2 + 2Ge$	15.068
$2Si_2 + SiGe + Si + Ge$	15.229
$2Si_2 + 2Si + Ge_2$	15.362
$Si_2 + 2SiGe + 2Si$	15.391
$Si_2Ge + 4Si + Ge$	17.985
$SiGe_2 + 5Si$	18.084
$2Si_2 + 2Si + 2Ge$	18.291
$Si_2 + SiGe + 3Si + Ge$	18.452
$Si_2 + 4Si + 2Ge$	21.514
$Ge_2 + 6Si$	21.808
$6Si + 2Ge$	24.736

Table 4.160 Fragmentation Energies for the Most Stable $(Si_6Ge_2)^+$ Octamer

Fragmented Cluster	Fragmentation Energy (eV)
$(Si_6Ge)^+ + Ge$	2.944
$(Si_5Ge_2)^+ + Si$	3.085
$Si_6Ge + Ge^+$	3.170
$(Si_3Ge)^+ + Si_3Ge$	3.240
$(Si_4Ge_2)^+ + Si_2$	3.487
$(Si_5Ge)^+ + SiGe$	3.612
$Si_5Ge + (SiGe)^+$	3.662
$(Si_4Ge)^+ + Si_2Ge$	3.966
$Si_4Ge + (Si_2Ge)^+$	4.068
$(Si_5Ge)^+ + Si + Ge$	6.673
$(Si_4Ge_2)^+ + 2Si$	6.709
$Si_5Ge + Si + Ge^+$	6.888
$(Si_4Ge)^+ + Si_2 + Ge$	7.494
$Si_4Ge + (SiGe)^+ + Si$	7.611
$Si_4Ge + Si_2 + Ge^+$	7.614
$(Si_4Ge)^+ + SiGe + Si$	7.655
$(Si_3Ge_2)^+ + Si_2 + Si$	7.678
$Si_3Ge + (SiGe)^+ + Si_2$	7.973
$(Si_3Ge)^+ + SiGe + Si_2$	8.004
$(Si_2Ge_2)^+ + 2Si_2$	8.130
$(Si_2Ge)^+ + Si_2Ge + Si_2$	8.727
$(Si_4Ge)^+ + 2Si + Ge$	10.717
$Si_4Ge + 2Si + Ge^+$	10.836
$(Si_3Ge_2)^+ + 3Si$	10.900
$(Si_3Ge)^+ + Si_2 + Si + Ge$	11.065
$Si_3Ge + (SiGe)^+ + 2Si$	11.195
$Si_3Ge + Si_2 + Si + Ge^+$	11.199
$(Si_3Ge)^+ + SiGe + 2Si$	11.227
$(Si_2Ge_2)^+ + Si_2 + 2Si$	11.353
$(Si_2Ge)^+ + Si_2Ge + 2Si$	11.950

Table 4.160 – *Continued*

Fragmented Cluster	Fragmentation Energy (eV)
$(Si_2Ge)^+ + 2Si_2 + Ge$	12.255
$Si_2Ge + Si_2 + (SiGe)^+ + Si$	12.270
$Si_2Ge + 2Si_2 + Ge^+$	12.273
$(Si_2Ge)^+ + Si_2 + SiGe + Si$	12.417
$(SiGe_2)^+ + 2Si_2 + Si$	12.420
$3Si_2 + (Ge_2)^+$	12.592
$2Si_2 + (SiGe)^+ + SiGe$	12.737
$(Si_3Ge)^+ + 3Si + Ge$	14.288
$Si_3Ge + 3Si + Ge^+$	14.421
$(Si_2Ge_2)^+ + 4Si$	14.576
$(Si_2Ge)^+ + Si_2 + 2Si + Ge$	15.478
$Si_2Ge + (SiGe)^+ + 3Si$	15.493
$Si_2Ge + Si_2 + 2Si + Ge^+$	15.496
$(Si_2Ge)^+ + SiGe + 3Si$	15.639
$(SiGe_2)^+ + Si_2 + 3Si$	15.643
$2Si_2 + (SiGe)^+ + Si + Ge$	15.798
$3Si_2 + Ge^+ + Ge$	15.801
$2Si_2 + 2Si + (Ge_2)^+$	15.815
$Si_2 + (SiGe)^+ + SiGe + 2Si$	15.959
$2Si_2 + SiGe + Si + Ge^+$	15.963
$(Si_2Ge)^+ + 4Si + Ge$	18.701
$Si_2Ge + 4Si + Ge^+$	18.719
$(SiGe_2)^+ + 5Si$	18.866
$Si_2 + (SiGe)^+ + 3Si + Ge$	19.021
$2Si_2 + 2Si + Ge^+ + Ge$	19.024
$Si_2 + SiGe + 3Si + Ge^+$	19.185
$Si_2 + 4Si + Ge^+ + Ge$	22.247
$(Ge_2)^+ + 6Si$	22.261
$6Si + Ge^+ + Ge$	25.469

Table 4.161 Fragmentation Energies for the Most Stable $(Si_6Ge_2)^-$ Octamer

Fragmented Cluster	Fragmentation Energy (eV)
$(Si_6Ge)^-$ + Ge	2.938
$(Si_3Ge)^-$ +Si_3Ge	2.989
$(Si_5Ge_2)^-$ + Si	3.267
$(Si_4Ge)^-$ + Si_2Ge	3.448
Si_4Ge + $(Si_2Ge)^-$	3.511
Si_5Ge + $(SiGe)^-$	3.586
Si_6Ge + Ge^-	3.636
$(Si_4Ge_2)^-$ + Si_2	3.658
$(Si_5Ge)^-$ + SiGe	3.664
$(Si_5Ge)^-$ +Si + Ge	6.726
$(Si_4Ge_2)^-$ + 2Si	6.880
$(Si_4Ge)^-$ + Si_2 + Ge	6.976
$(Si_4Ge)^-$ + SiGe + Si	7.137
$(Si_3Ge_2)^-$ + Si_2 + Si	7.286
Si_5Ge +Si + Ge^-	7.354
Si_4Ge + $(SiGe)^-$ + Si	7.534
$(Si_3Ge)^-$ + SiGe + Si_2	7.753
$(Si_2Ge_2)^-$ + $2Si_2$	7.883
Si_3Ge + $(SiGe)^-$ + Si_2	7.896
Si_4Ge + Si_2 + Ge^-	8.080
$(Si_2Ge)^-$ + Si_2Ge + Si_2	8.170
$(Si_4Ge)^-$ + 2Si + Ge	10.198
$(Si_3Ge_2)^-$+ 3Si	10.509
$(Si_3Ge)^-$ + Si_2 + Si + Ge	10.814
$(Si_3Ge)^-$ + SiGe + 2Si	10.975
$(Si_2Ge_2)^-$ + Si_2 + 2Si	11.105
Si_3Ge + $(SiGe)^-$ + 2Si	11.119
Si_4Ge + 2Si + Ge^-	11.303
$(Si_2Ge)^-$ + Si_2Ge + 2Si	11.393
Si_3Ge + Si_2 + Si + Ge^-	11.665

Table 4.161 – *Continued*

Fragmented Cluster	Fragmentation Energy (eV)
$(Si_2Ge)^- + 2Si_2 + Ge$	11.698
$(Si_2Ge)^- + Si_2 + SiGe + Si$	11.860
$(SiGe_2)^- + 2Si_2 + Si$	11.943
$Si_2Ge + Si_2 + (SiGe)^- + Si$	12.194
$2Si_2 + (SiGe)^- + SiGe$	12.660
$3Si_2 + (Ge_2)^-$	12.661
$Si_2Ge + 2Si_2 + Ge^-$	12.740
$(Si_3Ge)^- + 3Si + Ge$	14.037
$(Si_2Ge_2)^- + 4Si$	14.328
$Si_3Ge + 3Si + Ge^-$	14.888
$(Si_2Ge)^- + Si_2 + 2Si + Ge$	14.921
$(Si_2Ge)^- + SiGe + 3Si$	15.082
$(SiGe_2)^- + Si_2 + 3Si$	15.165
$Si_2Ge + (SiGe)^- + 3Si$	15.416
$2Si_2 + (SiGe)^- + Si + Ge$	15.722
$Si_2 + (SiGe)^- + SiGe + 2Si$	15.883
$2Si_2 + 2Si + (Ge_2)^-$	15.884
$Si_2Ge + Si_2 + 2Si + Ge^-$	15.962
$3Si_2 + Ge^- + Ge$	16.268
$2Si_2 + SiGe + Si + Ge^-$	16.429
$(Si_2Ge)^- + 4Si + Ge$	18.144
$(SiGe_2)^- + 5Si$	18.388
$Si_2 + (SiGe)^- + 3Si + Ge$	18.945
$Si_2Ge + 4Si + Ge^-$	19.185
$2Si_2 + 2Si + Ge^- + Ge$	19.490
$Si_2 + SiGe + 3Si + Ge^-$	19.652
$(Ge_2)^- + 6Si$	22.330
$Si_2 + 4Si + Ge^- + Ge$	22.713
$6Si + Ge^- + Ge$	25.936

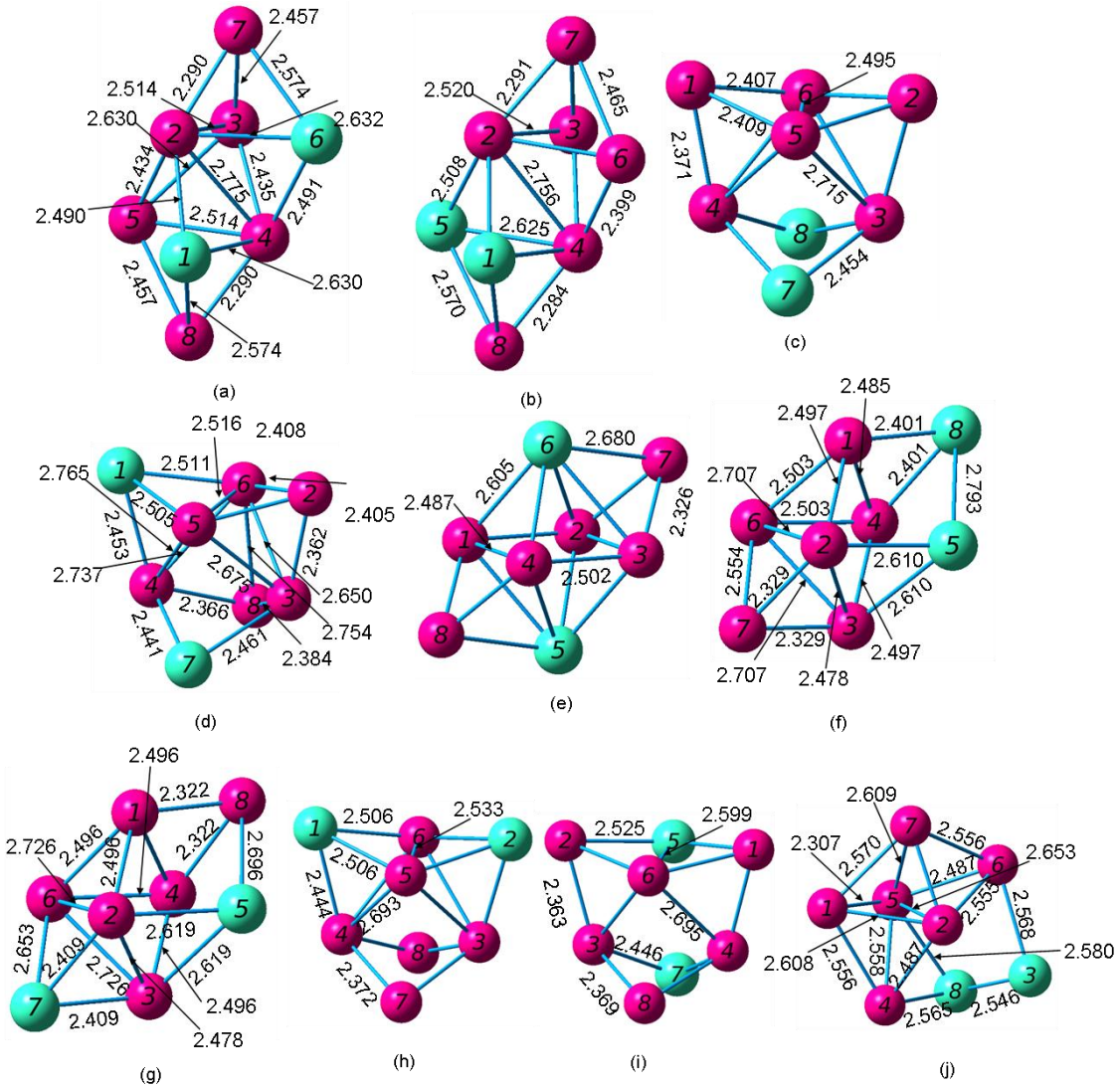

Figure 4.139 Geometries of the Si_6Ge_2 Neutral Septamers from (a) Most Stable through (j) Least Stable

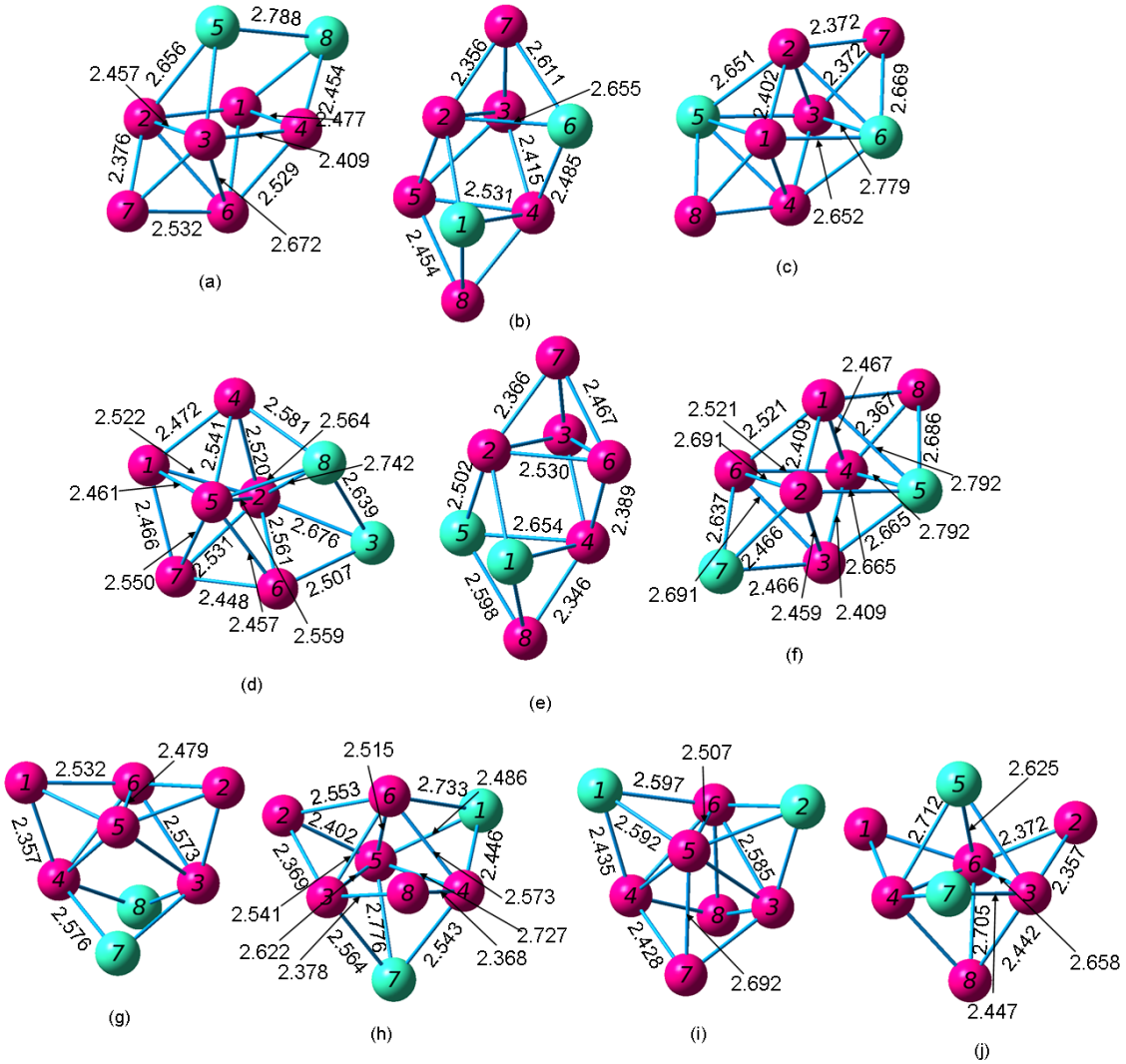

Figure 4.140 Geometries of the $(Si_6Ge_2)^+$ Cationic Septamers from (a) Most Stable through (j) Least Stable

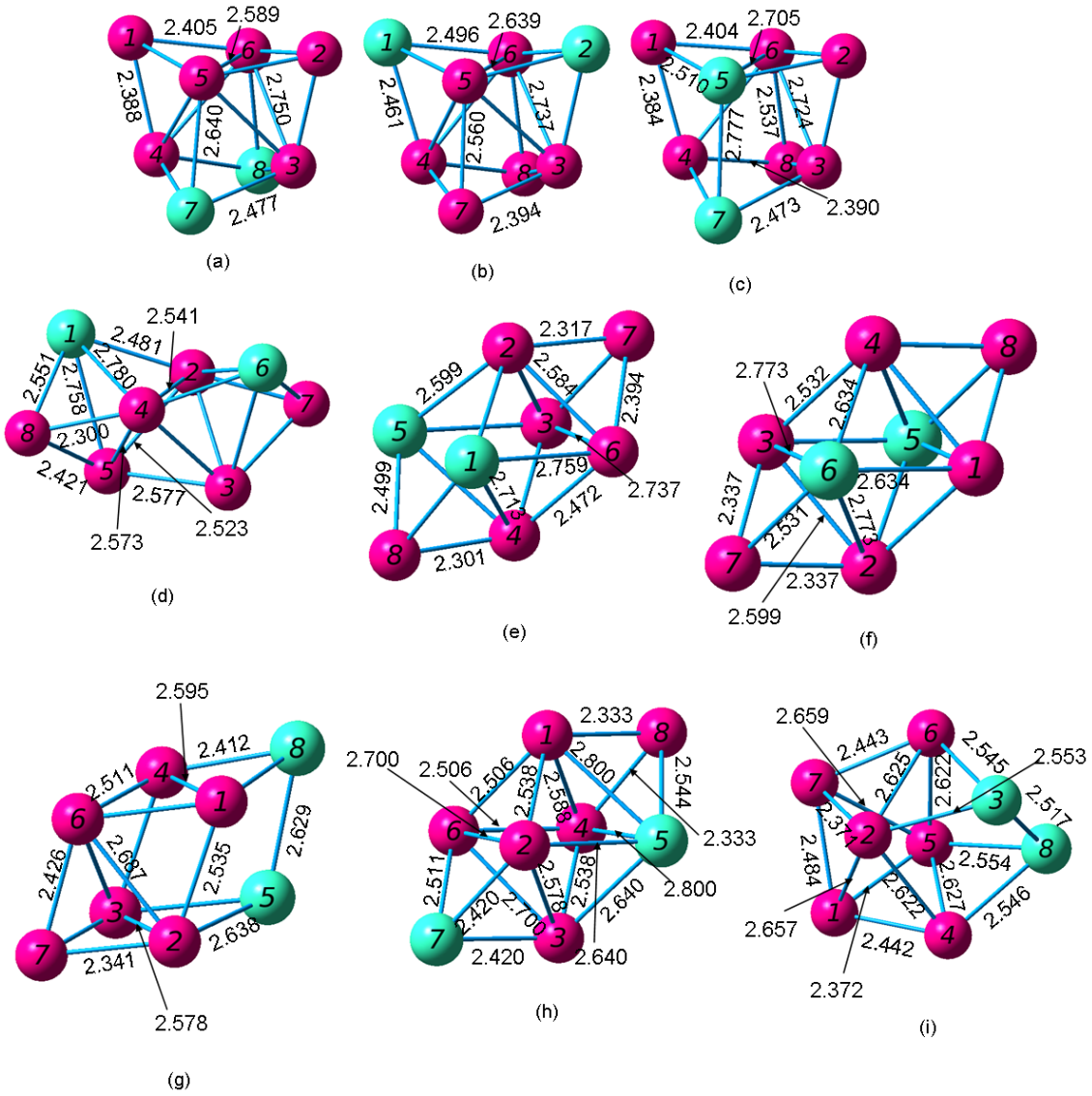

Figure 4.141 Geometries of the $(Si_6Ge_2)^-$ Anionic Septamers from (a) Most Stable through (i) Least Stable

4.24 Si_5Ge_3 Octamers

Wang and Chao [51] reported a rhombic cube for the neutral and cation Si_5Ge_3 octamers. The neutral cluster has a ^1A electronic state, a dissociation energy of -33.1222 eV or -34.9896 eV, a HOMO-LUMO gap of 2.58 eV, and the following frequencies: 485(a), 490(a), and 420(a). Their anion cluster is again similar to our most stable anion.

Totally, we investigated twenty Si_6Ge_2 clusters. The difference in binding energy per atom between our most stable cluster and our thirty-eighth most stable cluster was 0.0592 eV. Our clusters were the result of rearranging the input clusters for the Si_7Ge octamers with two additional germanium atoms. Our most stable neutral cluster resembles two trigonal bipyramids attached by one of their sides. Here, we report the properties of ten neutrals, cations, and anions.

Table 4.162 Properties of the Si_5Ge_3 Octamers

Figure	Symmetry Group	Electronic State	Binding E / Atom (eV)	HOMO-LUMO Gap (eV)	Dipole Moment (D)
4.142 (a)	C_1	^1A	3.052	2.638	0.472
4.142 (b)	C_1	^1A	3.052	2.600	0.772
4.142 (c)	C_1	^1A	3.047	2.578	0.406
4.142 (d)	C_1	^1A	3.045	2.616	0.466
4.142 (e)	C_1	^1A	3.016	2.093	0.785
4.142 (f)	C_s	$^1A'$	3.006	1.850	0.428
4.142 (g)	C_s	$^1A'$	3.005	2.054	0.449
4.142 (h)	C_s	$^1A'$	3.003	2.125	0.768
4.142 (i)	C_1	^1A	3.001	2.334	0.353
4.142 (j)	C_1	^1A	2.999	2.339	0.336

Table 4.163 Properties of the $(Si_5Ge_3)^+$ Octamers

Figure	Symmetry Group	Electronic State	Binding E / Atom (eV)	HOMO-LUMO Gap (eV)	Dipole Moment (D)
4.143 (a)	C_1	^2A	3.161	1.502[a]	0.888
4.143 (b)	C_1	^2A	3.157	1.352[a]	1.704
4.143 (c)	C_s	$^2A'$	3.152	1.497[a]	0.889
4.143 (d)	C_1	^2A	3.151	1.477[a]	1.427
4.143 (e)	C_1	^2A	3.150	1.358[a]	0.610
4.143 (f)	C_1	^2A	3.149	1.611[a]	0.842
4.143 (g)	C_1	^2A	3.147	1.410	0.549
4.143 (h)	C_1	^2A	3.112	1.383[a]	0.592
4.143 (i)	C_s	$^2A''$	3.110	1.420[a]	0.805
4.143 (j)	C_s	$^2A''$	3.106	1.450[a]	0.669

[a] HOMO and LUMO have opposite spins; this value includes the energy required to flip the spin of the electron.

Table 4.164 Properties of the $(Si_5Ge_3)^-$ Octamers

Figure	Symmetry Group	Electronic State	Binding E / Atom (eV)	HOMO-LUMO Gap (eV)	Dipole Moment (D)
4.144 (a)	C_1	^2A	3.201	1.441[a]	1.816
4.144 (b)	C_s	$^2A'$	3.190	1.444[a]	1.253
4.144 (c)	C_s	$^2A'$	3.184	1.409[a]	1.528
4.144 (d)	C_1	^2A	3.167	1.414[a]	1.043
4.144 (e)	C_1	^2A	3.159	1.454[a]	1.543
4.144 (f)	C_1	^2A	3.142	1.405[a]	3.246
4.144 (g)	C_s	$^2A''$	3.140	1.307[a]	1.730
4.144 (h)	C_1	^2A	3.135	1.404[a]	1.265
4.144 (i)	C_1	^2A	3.128	1.627[a]	1.626
4.144 (j)	C_1	^2A	3.127	1.653[a]	2.685

[a] HOMO and LUMO have opposite spins; this value includes the energy required to flip the spin of the electron.

Table 4.165 Ionization Potentials and Electron Affinities of the Si_5Ge_3 Octamers

Neutral Figure	VIP (eV)	Cationic Figure	AIP (eV)	VEA (eV)	Anionic Figure	AEA (eV)
4.142 (a)	7.286	4.143 (g)	7.141	1.627	4.144 (d)	2.054
4.142 (b)	7.190	4.143 (b)	7.060	1.567	4.144 (f)	1.862
4.142 (c)	7.155	4.143 (a)	6.985	1.580	4.144 (e)	2.034
4.142 (d)	7.200	4.143 (e)	7.067	1.572	4.144 (h)	1.857
4.142 (e)	7.319	4.143 (h)	7.128	2.137	4.144 (a)	2.622
4.142 (f)	6.860	4.143 (c)	6.729	2.011	4.144 (g)	2.211
4.142 (g)	7.271	4.143 (i)	7.055	2.161	4.144 (b)	2.621
4.142 (h)	7.382	4.143 (j)	7.081	2.146	4.144 (c)	2.581
4.142 (i)	7.062	4.143 (d)	6.699	1.696	4.144 (j)	2.139
4.142 (j)	7.068	4.143 (f)	6.700	1.662	4.144 (i)	2.175

Table 4.166 Fragmentation Energies for the Most Stable Si_5Ge_3 Octamer

Fragmented Cluster	Fragmentation Energy (eV)
$Si_5Ge_2 + Ge$	2.420
$Si_3Ge + Si_2Ge_2$	2.588
$Si_4Ge_3 + Si$	2.732
$Si_5Ge + Ge_2$	2.907
$Si_4Ge_2 + SiGe$	3.046
$Si_4Ge + SiGe_2$	3.131
$Si_3Ge_3 + Si_2$	3.183
$Si_3Ge_2 + Si_2Ge$	3.280
$Si_5Ge + 2Ge$	5.835
$Si_4Ge_2 + Si + Ge$	6.108
$Si_3Ge_3 + 2Si$	6.406
$Si_3Ge + Si_2Ge + Ge$	6.618
$Si_3Ge + SiGe_2 + Si$	6.716
$Si_4Ge + SiGe + Ge$	6.722
$Si_3Ge_2 + Si_2 + Ge$	6.808
$Si_4Ge + Si + Ge_2$	6.855
$Si_2Ge_2 + Si_2Ge + Si$	6.886
$Si_3Ge_2 + SiGe + Si$	6.970
$Si_2Ge_3 + Si_2 + Si$	7.058
$Si_3Ge + Si_2 + Ge_2$	7.217
$Si_3Ge + 2SiGe$	7.246
$Si_2Ge_2 + Si_2 + SiGe$	7.352
$SiGe_3 + 2Si_2$	7.535
$Si_2Ge + SiGe_2 + Si_2$	7.791
$Si_4Ge + Si + 2Ge$	9.784
$Si_3Ge_2 + 2Si + Ge$	10.031
$Si_3Ge + Si_2 + 2Ge$	10.146
$Si_2Ge_3 + 3Si$	10.280
$Si_3Ge + SiGe + Si + Ge$	10.307
$Si_2Ge_2 + Si_2 + Si + Ge$	10.414
$Si_3Ge + Ge_2 + 2Si$	10.440
$SiGe_3 + Si_2 + 2Si$	10.758

Table 4.166 – *Continued*

Fragmented Cluster	Fragmentation Energy (eV)
$Si_2Ge + SiGe_2 + 2Si$	11.014
$SiGe_2 + 2Si_2 + Ge$	11.319
$Si_2Ge + Si_2 + SiGe + Ge$	11.382
$SiGe_2 + Si_2 + SiGe + Si$	11.480
$Si_2Ge + Si_2 + Ge_2 + Si$	11.515
$Si_2Ge + 2SiGe + Si$	11.543
$2Si_2 + SiGe + Ge_2$	11.981
$Si_2 + 3SiGe$	12.010
$Si_3Ge + 2Si + 2Ge$	13.369
$Si_2Ge_2 + 3Si + Ge$	13.637
$SiGe_3 + 4Si$	13.981
$Si_2Ge + Si_2 + Si + 2Ge$	14.443
$SiGe_2 + Si_2 + 2Si + Ge$	14.542
$Si_2Ge + SiGe + 2Si + Ge$	14.605
$SiGe_2 + SiGe + 3Si$	14.703
$Si_2Ge + Ge_2 + 3Si$	14.737
$2Si_2 + SiGe + 2Ge$	14.910
$2Si_2 + Ge_2 + Si + Ge$	15.043
$Si_2 + 2SiGe + Si + Ge$	15.071
$Si_2 + SiGe + Ge_2 + 2Si$	15.204
$3SiGe + 2Si$	15.233
$SiGe_2 + 4Si + Ge$	17.765
$2Si_2 + Si + 3Ge$	17.971
$Si_2 + SiGe + 2Si + 2Ge$	18.133
$Si_2 + Ge_2 + 3Si + Ge$	18.266
$2SiGe + 3Si + Ge$	18.294
$Ge_2 + SiGe + 4Si$	18.427
$Si_2 + 3Si + 3Ge$	21.194
$SiGe + 4Si + 2Ge$	21.355
$Ge_2 + 5Si + Ge$	21.488
$5Si + 3Ge$	24.417

Table 4.167 Fragmentation Energies for the Most Stable $(Si_5Ge_3)^+$ Octamer

Fragmented Cluster	Fragmentation Energy (eV)
$(Si_5Ge_2)^+ + Ge$	2.904
$(Si_4Ge_3)^+ + Si$	3.187
$Si_5Ge_2 + Ge^+$	3.292
$(Si_3Ge)^+ + Si_2Ge_2$	3.327
$Si_3Ge + (Si_2Ge_2)^+$	3.347
$(Si_4Ge_2)^+ + SiGe$	3.467
$Si_5Ge + (Ge_2)^+$	3.498
$(Si_5Ge)^+ + Ge_2$	3.564
$(Si_3Ge_3)^+ + Si_2$	3.623
$Si_4Ge_2 + (SiGe)^+$	3.754
$(Si_4Ge)^+ + SiGe_2$	3.884
$(Si_3Ge_2)^+ + Si_2Ge$	3.969
$Si_4Ge + (SiGe_2)^+$	4.052
$Si_3Ge_2 + (Si_2Ge)^+$	4.134
$(Si_5Ge)^+ + 2Ge$	6.492
$(Si_4Ge_2)^+ + Si + Ge$	6.528
$Si_5Ge + Ge^+ + Ge$	6.707
$(Si_3Ge_3)^+ + 2Si$	6.846
$Si_4Ge_2 + Si + Ge^+$	6.980
$(Si_3Ge)^+ + Si_2Ge + Ge$	7.356
$Si_4Ge + (SiGe)^+ + Ge$	7.430
$Si_4Ge + Si + (Ge_2)^+$	7.447
$(Si_3Ge)^+ + SiGe_2 + Si$	7.455
$Si_3Ge + (Si_2Ge)^+ + Ge$	7.472
$(Si_4Ge)^+ + SiGe + Ge$	7.474
$Si_3Ge + Si_2Ge + Ge^+$	7.490
$(Si_3Ge_2)^+ + Si_2 + Ge$	7.497
$Si_4Ge + SiGe + Ge^+$	7.594
$(Si_4Ge)^+ + Si + Ge_2$	7.607

Table 4.167 – *Continued*

Fragmented Cluster	Fragmentation Energy (eV)
$Si_3Ge + (SiGe_2)^+ + Si$	7.637
$(Si_2Ge_2)^+ + Si_2Ge + Si$	7.644
$(Si_3Ge_2)^+ + SiGe + Si$	7.658
$Si_3Ge_2 + (SiGe)^+ + Si$	7.677
$Si_3Ge_2 + Si_2 + Ge^+$	7.680
$Si_2Ge_2 + (Si_2Ge)^+ + Si$	7.740
$Si_3Ge + Si_2 + (Ge_2)^+$	7.809
$(Si_2Ge_3)^+ + Si_2 + Si$	7.860
$Si_3Ge + (SiGe)^+ + SiGe$	7.953
$(Si_3Ge)^+ + Si_2 + Ge_2$	7.956
$(Si_3Ge)^+ + 2SiGe$	7.984
$Si_2Ge_2 + Si_2 + (SiGe)^+$	8.060
$(Si_2Ge_2)^+ + Si_2 + SiGe$	8.111
$(SiGe_3)^+ + 2Si_2$	8.170
$(Si_2Ge)^+ + SiGe_2 + Si_2$	8.645
$Si_2Ge + (SiGe_2)^+ + Si_2$	8.711
$(Si_4Ge)^+ + Si + 2Ge$	10.536
$Si_4Ge + Si + Ge^+ + Ge$	10.655
$(Si_3Ge_2)^+ + 2Si + Ge$	10.719
$(Si_3Ge)^+ + Si_2 + 2Ge$	10.885
$Si_3Ge_2 + 2Si + Ge^+$	10.903
$Si_3Ge + (SiGe)^+ + Si + Ge$	11.015
$Si_3Ge + Si_2 + Ge^+ + Ge$	11.018
$Si_3Ge + (Ge_2)^+ + 2Si$	11.032
$(Si_3Ge)^+ + SiGe + Si + Ge$	11.046
$(Si_2Ge_3)^+ + 3Si$	11.083
$(Si_2Ge_2)^+ + Si_2 + Si + Ge$	11.172
$(Si_3Ge)^+ + Ge_2 + 2Si$	11.179
$Si_3Ge + SiGe + Si + Ge^+$	11.179

Table 4.167 – *Continued*

Fragmented Cluster	Fragmentation Energy (eV)
$Si_2Ge_2 + Si_2 + Si + Ge^+$	11.286
$(SiGe_3)^+ + Si_2 + 2Si$	11.393
$(Si_2Ge)^+ + SiGe_2 + 2Si$	11.868
$Si_2Ge + (SiGe_2)^+ + 2Si$	11.934
$Si_2Ge + Si_2 + (SiGe)^+ + Ge$	12.089
$Si_2Ge + Si_2 + (Ge_2)^+ + Si$	12.106
$SiGe_2 + Si_2 + (SiGe)^+ + Si$	12.188
$SiGe_2 + 2Si_2 + Ge^+$	12.191
$(Si_2Ge)^+ + Si_2 + SiGe + Ge$	12.236
$(SiGe_2)^+ + 2Si_2 + Ge$	12.239
$Si_2Ge + (SiGe)^+ + SiGe + Si$	12.251
$Si_2Ge + Si_2 + SiGe + Ge^+$	12.254
$(Si_2Ge)^+ + Si_2 + Ge_2 + Si$	12.369
$(Si_2Ge)^+ + 2SiGe + Si$	12.397
$(SiGe_2)^+ + Si_2 + SiGe + Si$	12.401
$2Si_2 + SiGe + (Ge_2)^+$	12.573
$2Si_2 + (SiGe)^+ + Ge_2$	12.689
$Si_2 + (SiGe)^+ + 2SiGe$	12.717
$(Si_3Ge)^+ + 2Si + 2Ge$	14.107
$Si_3Ge + 2Si + Ge^+ + Ge$	14.240
$(Si_2Ge_2)^+ + 3Si + Ge$	14.395
$Si_2Ge_2 + 3Si + Ge^+$	14.508
$(SiGe_3)^+ + 4Si$	14.616
$(Si_2Ge)^+ + Si_2 + Si + 2Ge$	15.297
$Si_2Ge + (SiGe)^+ + 2Si + Ge$	15.312
$Si_2Ge + Si_2 + Si + Ge^+ + Ge$	15.315
$Si_2Ge + (Ge_2)^+ + 3Si$	15.329
$SiGe_2 + (SiGe)^+ + 3Si$	15.411
$SiGe_2 + Si_2 + 2Si + Ge^+$	15.414

Table 4.167 – *Continued*

Fragmented Cluster	Fragmentation Energy (eV)
$(Si_2Ge)^+ + SiGe + 2Si + Ge$	15.458
$(SiGe_2)^+ + Si_2 + 2Si + Ge$	15.462
$Si_2Ge + SiGe + 2Si + Ge^+$	15.476
$(Si_2Ge)^+ + Ge_2 + 3Si$	15.591
$2Si_2 + (SiGe)^+ + 2Ge$	15.617
$(SiGe_2)^+ + SiGe + 3Si$	15.624
$2Si_2 + (Ge_2)^+ + Si + Ge$	15.634
$Si_2 + (SiGe)^+ + SiGe + Si + Ge$	15.779
$2Si_2 + SiGe + Ge^+ + Ge$	15.782
$Si_2 + SiGe + (Ge_2)^+ + 2Si$	15.796
$Si_2 + (SiGe)^+ + Ge_2 + 2Si$	15.912
$2Si_2 + Ge_2 + Si + Ge^+$	15.915
$(SiGe)^+ + 2SiGe + 2Si$	15.940
$Si_2 + 2SiGe + Si + Ge^+$	15.943
$SiGe_2 + 4Si + Ge^+$	18.636
$(SiGe_2)^+ + 4Si + Ge$	18.685
$Si_2 + (SiGe)^+ + 2Si + 2Ge$	18.840
$2Si_2 + Si + Ge^+ + 2Ge$	18.843
$Si_2 + (Ge_2)^+ + 3Si + Ge$	18.857
$(SiGe)^+ + SiGe + 3Si + Ge$	19.001
$Si_2 + SiGe + 2Si + Ge^+ + Ge$	19.004
$(Ge_2)^+ + SiGe + 4Si$	19.018
$Ge_2 + (SiGe)^+ + 4Si$	19.134
$Si_2 + Ge_2 + 3Si + Ge^+$	19.137
$2SiGe + 3Si + Ge^+$	19.166
$(SiGe)^+ + 4Si + 2Ge$	22.063
$Si_2 + 3Si + Ge^+ + 2Ge$	22.066
$(Ge_2)^+ + 5Si + Ge$	22.080
$SiGe + 4Si + Ge^+ + Ge$	22.227
$Ge_2 + 5Si + Ge^+$	22.360
$5Si + Ge^+ + 2Ge$	25.289

Table 4.168 Fragmentation Energies for the Most Stable $(Si_5Ge_3)^-$ Octamer

Fragmented Cluster	Fragmentation Energy (eV)
$(Si_3Ge)^- + Si_2Ge_2$	2.930
$(Si_5Ge_2)^- + Ge$	2.940
$Si_3Ge + (Si_2Ge_2)^-$	2.953
$(Si_4Ge)^- + SiGe_2$	3.220
$(Si_4Ge_3)^- + Si$	3.276
$Si_5Ge + (Ge_2)^-$	3.421
$Si_4Ge + (SiGe_2)^-$	3.428
$Si_3Ge_2 + (Si_2Ge)^-$	3.431
$(Si_3Ge_2)^- + Si_2Ge$	3.432
$(Si_5Ge)^- + Ge_2$	3.471
$(Si_4Ge_2)^- + SiGe$	3.493
$Si_4Ge_2 + (SiGe)^-$	3.532
$Si_5Ge_2 + Ge^-$	3.613
$(Si_3Ge_3)^- + Si_2$	3.666
$(Si_5Ge)^- + 2Ge$	6.399
$(Si_4Ge_2)^- + Si + Ge$	6.554
$Si_3Ge + (Si_2Ge)^- + Ge$	6.769
$(Si_4Ge)^- + SiGe + Ge$	6.810
$(Si_3Ge_3)^- + 2Si$	6.889
$(Si_4Ge)^- + Si + Ge_2$	6.943
$(Si_3Ge)^- + Si_2Ge + Ge$	6.959
$(Si_3Ge_2)^- + Si_2 + Ge$	6.960
$Si_3Ge + (SiGe_2)^- + Si$	7.013
$Si_5Ge + Ge^- + Ge$	7.028
$Si_2Ge_2 + (Si_2Ge)^- + Si$	7.037
$(Si_3Ge)^- + SiGe_2 + Si$	7.058
$(Si_3Ge_2)^- + SiGe + Si$	7.121
$Si_4Ge + (SiGe)^- + Ge$	7.208
$(Si_2Ge_2)^- + Si_2Ge + Si$	7.251

Table 4.168 – *Continued*

Fragmented Cluster	Fragmentation Energy (eV)
$(Si_2Ge_3)^- + Si_2 + Si$	7.262
$Si_4Ge_2 + Si + Ge^-$	7.300
$Si_4Ge + Si + (Ge_2)^-$	7.370
$Si_3Ge_2 + (SiGe)^- + Si$	7.455
$(Si_3Ge)^- + Si_2 + Ge_2$	7.559
$(Si_3Ge)^- + 2SiGe$	7.587
$(Si_2Ge_2)^- + Si_2 + SiGe$	7.717
$Si_3Ge + (SiGe)^- + SiGe$	7.731
$Si_3Ge + Si_2 + (Ge_2)^-$	7.732
$Si_3Ge + Si_2Ge + Ge^-$	7.810
$Si_2Ge_2 + Si_2 + (SiGe)^-$	7.838
$Si_4Ge + SiGe + Ge^-$	7.915
$(SiGe_3)^- + 2Si_2$	7.931
$(Si_2Ge)^- + SiGe_2 + Si_2$	7.942
$Si_3Ge_2 + Si_2 + Ge^-$	8.001
$Si_2Ge + (SiGe_2)^- + Si_2$	8.088
$(Si_4Ge)^- + Si + 2Ge$	9.872
$(Si_3Ge_2)^- + 2Si + Ge$	10.182
$(Si_2Ge_3)^- + 3Si$	10.485
$(Si_3Ge)^- + Si_2 + 2Ge$	10.488
$(Si_3Ge)^- + SiGe + Si + Ge$	10.649
$(Si_2Ge_2)^- + Si_2 + Si + Ge$	10.779
$(Si_3Ge)^- + Ge_2 + 2Si$	10.782
$Si_3Ge + (SiGe)^- + Si + Ge$	10.793
$Si_3Ge + (Ge_2)^- + 2Si$	10.955
$Si_4Ge + Si + Ge^- + Ge$	10.976
$(SiGe_3)^- + Si_2 + 2Si$	11.154
$(Si_2Ge)^- + SiGe_2 + 2Si$	11.165
$Si_3Ge_2 + 2Si + Ge^-$	11.224

Table 4.168 – *Continued*

Fragmented Cluster	Fragmentation Energy (eV)
$Si_2Ge + (SiGe_2)^- + 2Si$	11.311
$Si_3Ge + Si_2 + Ge^- + Ge$	11.338
$Si_3Ge + SiGe + Si + Ge^-$	11.500
$(Si_2Ge)^- + Si_2 + SiGe + Ge$	11.533
$Si_2Ge_2 + Si_2 + Si + Ge^-$	11.606
$(SiGe_2)^- + 2Si_2 + Ge$	11.616
$(Si_2Ge)^- + Si_2 + Ge_2 + Si$	11.666
$(Si_2Ge)^- + 2SiGe + Si$	11.694
$(SiGe_2)^- + Si_2 + SiGe + Si$	11.777
$Si_2Ge + Si_2 + (SiGe)^- + Ge$	11.867
$SiGe_2 + Si_2 + (SiGe)^- + Si$	11.966
$Si_2Ge + (SiGe)^- + SiGe + Si$	12.029
$Si_2Ge + Si_2 + (Ge_2)^- + Si$	12.029
$2Si_2 + (SiGe)^- + Ge_2$	12.467
$Si_2 + (SiGe)^- + 2SiGe$	12.495
$2Si_2 + SiGe + (Ge_2)^-$	12.496
$SiGe_2 + 2Si_2 + Ge^-$	12.512
$Si_2Ge + Si_2 + SiGe + Ge^-$	12.574
$(Si_3Ge)^- + 2Si + 2Ge$	13.710
$(Si_2Ge_2)^- + 3Si + Ge$	14.002
$(SiGe_3)^- + 4Si$	14.377
$Si_3Ge + 2Si + Ge^- + Ge$	14.561
$(Si_2Ge)^- + Si_2 + Si + 2Ge$	14.594
$(Si_2Ge)^- + SiGe + 2Si + Ge$	14.756
$Si_2Ge_2 + 3Si + Ge^-$	14.829
$(SiGe_2)^- + Si_2 + 2Si + Ge$	14.839
$(Si_2Ge)^- + Ge_2 + 3Si$	14.889
$(SiGe_2)^- + SiGe + 3Si$	15.000
$Si_2Ge + (SiGe)^- + 2Si + Ge$	15.090

Table 4.168 – *Continued*

Fragmented Cluster	Fragmentation Energy (eV)
$SiGe_2 + (SiGe)^- + 3Si$	15.189
$Si_2Ge + (Ge_2)^- + 3Si$	15.252
$2Si_2 + (SiGe)^- + 2Ge$	15.395
$Si_2 + (SiGe)^- + SiGe + Si + Ge$	15.557
$2Si_2 + (Ge_2)^- + Si + Ge$	15.558
$Si_2Ge + Si_2 + Si + Ge^- + Ge$	15.636
$Si_2 + (SiGe)^- + Ge_2 + 2Si$	15.690
$(SiGe)^- + 2SiGe + 2Si$	15.718
$Si_2 + SiGe + (Ge_2)^- + 2Si$	15.719
$SiGe_2 + Si_2 + 2Si + Ge^-$	15.734
$Si_2Ge + SiGe + 2Si + Ge^-$	15.797
$2Si_2 + SiGe + Ge^- + Ge$	16.102
$2Si_2 + Ge_2 + Si + Ge^-$	16.235
$Si_2 + 2SiGe + Si + Ge^-$	16.264
$(SiGe_2)^- + 4Si + Ge$	18.061
$Si_2 + (SiGe)^- + 2Si + 2Ge$	18.618
$(SiGe)^- + SiGe + 3Si + Ge$	18.779
$Si_2 + (Ge_2)^- + 3Si + Ge$	18.780
$Ge_2 + (SiGe)^- + 4Si$	18.912
$(Ge_2)^- + SiGe + 4Si$	18.942
$SiGe_2 + 4Si + Ge^-$	18.957
$2Si_2 + Si + Ge^- + 2Ge$	19.164
$Si_2 + SiGe + 2Si + Ge^- + Ge$	19.325
$Si_2 + Ge_2 + 3Si + Ge^-$	19.458
$2SiGe + 3Si + Ge^-$	19.487
$(SiGe)^- + 4Si + 2Ge$	21.841
$(Ge_2)^- + 5Si + Ge$	22.003
$Si_2 + 3Si + Ge^- + 2Ge$	22.387
$SiGe + 4Si + Ge^- + Ge$	22.548
$Ge_2 + 5Si + Ge^-$	22.681
$5Si + Ge^- + 2Ge$	25.609

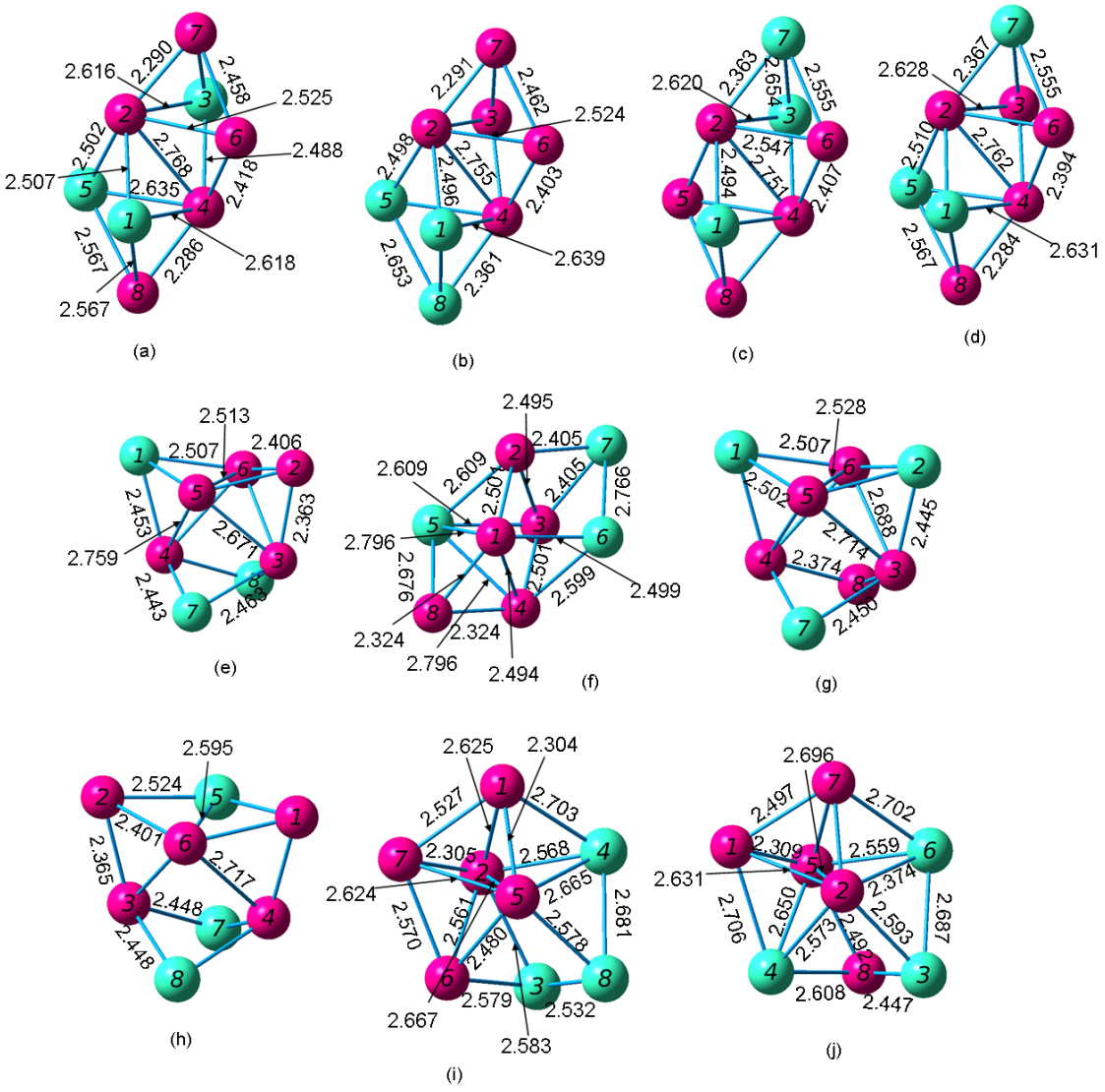

Figure 4.142 Geometries of the Si_5Ge_3 Neutral Septamers from (a) Most Stable through (j) Least Stable

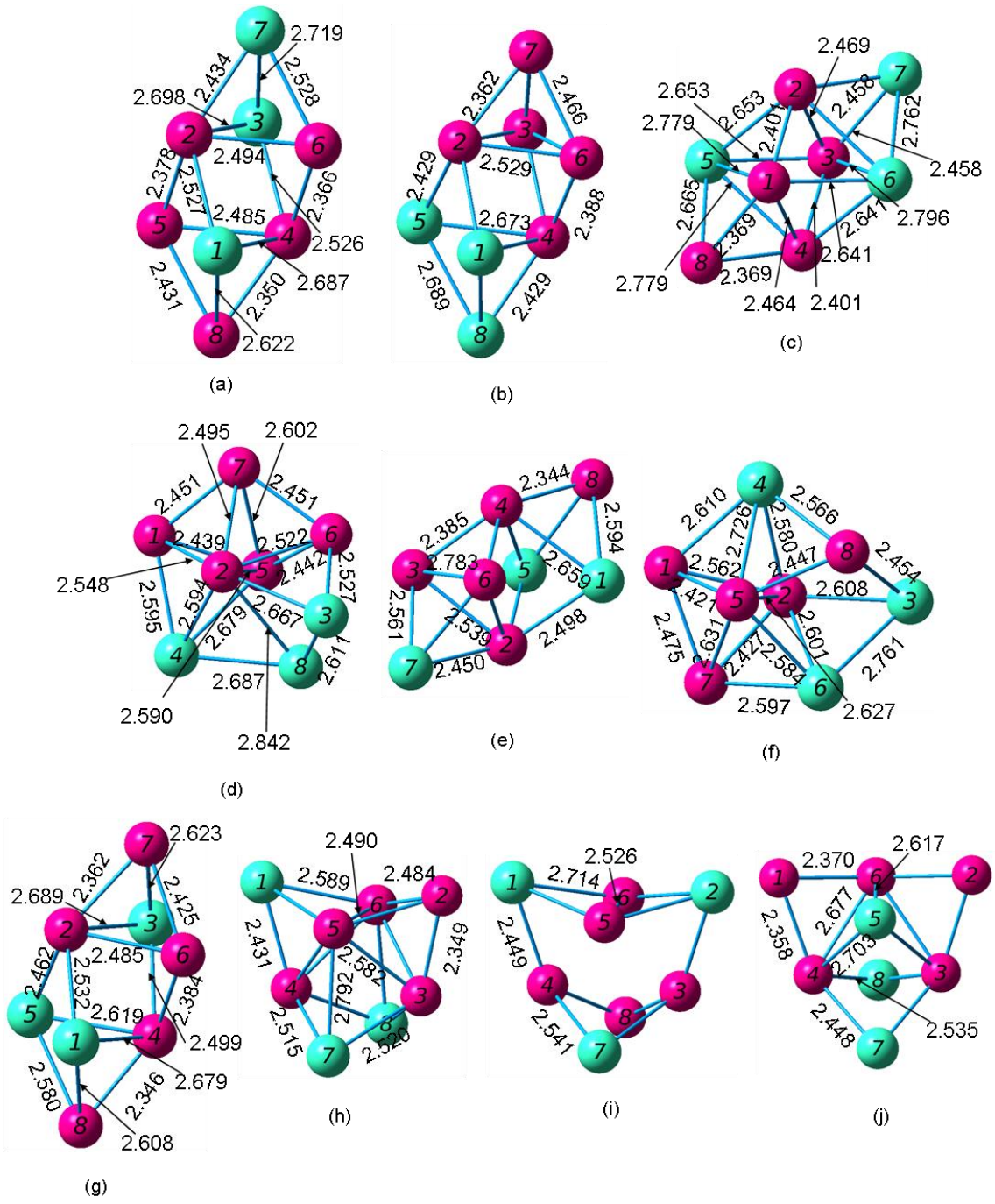

Figure 4.143 Geometries of the $(Si_5Ge_3)^+$ Cationic Septamers from (a) Most Stable through (j) Least Stable

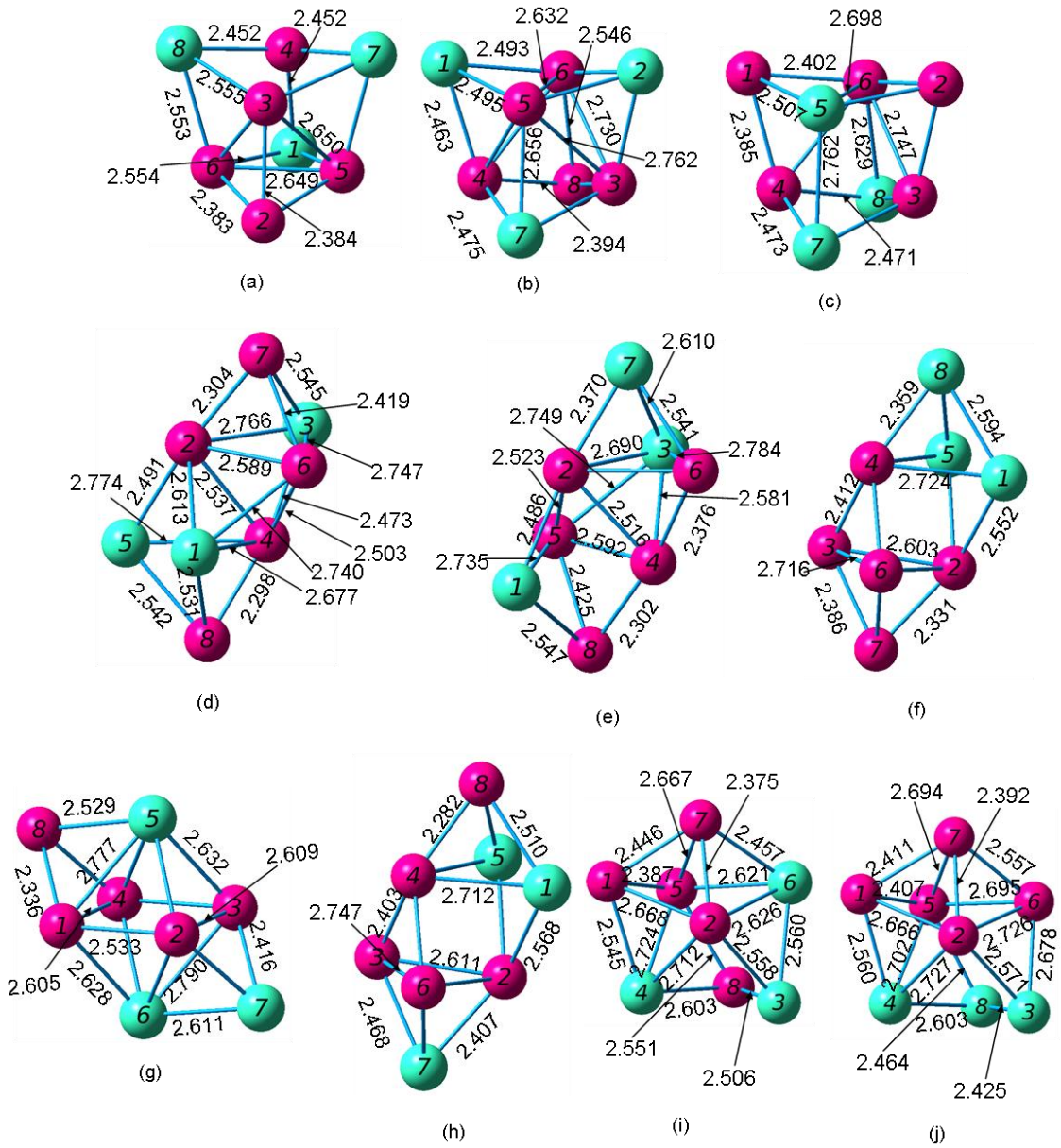

Figure 4.144 Geometries of the $(Si_5Ge_3)^-$ Anionic Septamers from (a) Most Stable through (j) Least Stable

4.25 Si_4Ge_4 Octamers

Li et al. [48] reported a rhombic cube and a distorted pentagonal bipyramid Si_4Ge_4 octamers. The first cluster has C_s symmetry, a ^1A electronic state, a HOMO-LUMO gap of 2.44 eV, and the following frequencies: 426 (A'), 341 (A"), and 278 (A'). Their less stable cluster has C_s symmetry, a $^1A_1$ electronic state, a HOMO-LUMO gap of 1.73 eV, and the following frequencies: 270 (A"), 296 (A'), and 447 (A'). Wang and Chao [51] reported a rhombic cube for the neutral and cation Si_5Ge_3 octamers. The neutral cluster has a ^1A electronic state, a dissociation energy of -33.7567 eV or -34.1688 eV, a HOMO-LUMO gap of 2.67 eV, and the following frequencies: 488(a), 293(a), and 229(a). Their anion cluster is again similar to our most stable anion.

Totally, we investigated twenty-seven Si_4Ge_4 clusters. The difference in binding energy per atom between our most stable cluster and our thirty-eighth most stable cluster was 0.1329 eV. Here, we report the properties of ten neutrals and cations and nine anions.

Table 4.169 Properties of the Si_4Ge_4 Octamers

Figure	Symmetry Group	Electronic State	Binding E / Atom (eV)	HOMO-LUMO Gap (eV)	Dipole Moment (D)
4.145 (a)	C_1	^1A	3.007	2.562	0.003
4.145 (b)	C_s	$^1A'$	2.972	2.029	0.487
4.145 (c)	C_1	^1A	2.965	2.079	0.670
4.145 (d)	C_1	^1A	2.964	2.751	0.362
4.145 (e)	C_s	$^1A'$	2.961	2.435	0.356
4.145 (f)	C_1	^1A	2.958	2.062	0.833
4.145 (g)	C_1	^1A	2.953	2.050	0.841
4.145 (h)	C_s	$^1A'$	2.951	2.185	0.568
4.145 (i)	C_s	$^1A'$	2.943	2.166	0.352
4.145 (j)	C_1	^1A	2.942	2.098	0.850

Table 4.170 Properties of the $(Si_4Ge_4)^+$ Octamers

Figure	Symmetry Group	Electronic State	Binding E / Atom (eV)	HOMO-LUMO Gap (eV)	Dipole Moment (D)
4.146 (a)	C_1	^2A	3.132	1.472[a]	0.002
4.146 (b)	C_1	^2A	3.118	1.382[a]	0.628
4.146 (c)	C_1	^2A	3.087	1.590[a]	0.515
4.146 (d)	C_s	^2A”	3.082	1.356[a]	0.234
4.146 (e)	C_s	^2A”	3.078	1.353[a]	0.134
4.146 (f)	C_1	^2A	3.066	1.582[a]	1.341
4.146 (g)	C_1	^2A	3.059	1.372[a]	1.145
4.146 (h)	C_1	^2A	3.054	1.381[a]	0.535
4.146 (i)	C_s	^2A”	3.041	1.377[a]	0.325
4.146 (j)	C_s	^2A”	3.035	1.363[a]	1.661

[a] HOMO and LUMO have opposite spins; this value includes the energy required to flip the spin of the electron.

Table 4.171 Properties of the $(Si_4Ge_4)^-$ Octamers

Figure	Symmetry Group	Electronic State	Binding E / Atom (eV)	HOMO-LUMO Gap (eV)	Dipole Moment (D)
4.147 (a)	C_s	^2A’	3.151	1.408[a]	0.301
4.147 (b)	C_1	^2A	3.146	1.421[a]	1.574
4.147 (c)	C_1	^2A	3.143	1.442[a]	2.506
4.147 (d)	C_1	^2A	3.129	1.434[a]	1.899
4.147 (e)	C_s	^2A’	3.127	1.393[a]	0.559
4.147 (f)	C_s	^2A’	3.125	1.447[a]	2.512
4.147 (g)	C_1	^2A	3.104	1.451[a]	1.467
4.147 (h)	C_1	^2A	3.097	1.381[a]	0.013
4.147 (i)	C_s	^2A’	3.081	1.385[a]	0.291

[a] HOMO and LUMO have opposite spins; this value includes the energy required to flip the spin of the electron.

Table 4.172 Ionization Potentials and Electron Affinities of the Si_4Ge_4 Octamers

Neutral Figure	VIP (eV)	Cationic Figure	AIP (eV)	VEA (eV)	Anionic Figure	AEA (eV)
4.145 (a)	7.061	4.146 (a)	6.902	1.527	4.147 (h)	1.860
4.145 (b)	7.198	4.146 (d)	7.025	2.132	4.147 (a)	2.565
4.145 (c)	7.317	4.146 (c)	6.925	2.126	4.147 (b)	2.583
4.145 (d)	7.070	4.146 (b)	6.673	1.688	4.147 (g)	2.254
4.145 (e)	7.096	4.146 (e)	6.968	1.657	4.147 (i)	2.096
4.145 (f)	7.284	4.146 (g)	7.096	2.151	4.147 (c)	2.617
4.145 (g)	7.285	4.146 (h)	7.094	2.174	4.147 (b)	2.680
4.145 (h)	7.357	4.146 (i)	7.184	2.127	4.147 (e)	2.544
4.145 (i)	7.363	4.146 (j)	7.171	2.148	4.147 (f)	2.594
4.145 (j)	7.382	4.146 (f)	6.911	2.171	4.147 (d)	2.633

Table 4.173 Fragmentation Energies for the Most Stable Si_4Ge_4 Octamer

Fragmented Cluster	Fragmentation Energy (eV)
$Si_4Ge_3 + Ge$	2.369
$2Si_2Ge_2$	2.493
$Si_3Ge + SiGe_3$	2.569
$Si_3Ge_4 + Si$	2.691
$Si_4Ge_2 + Ge_2$	2.816
$Si_3Ge_3 + SiGe$	2.981
$Si_3Ge_2 + SiGe_2$	3.016
$Si_2Ge_4 + Si_2$	3.108
$Si_2Ge_3 + Si_2Ge$	3.167
$Si_4Ge_2 + 2Ge$	5.745
$Si_3Ge_3 + Si + Ge$	6.043
$Si_2Ge_4 + 2Si$	6.331
$Si_3Ge + SiGe_2 + Ge$	6.354
$Si_4Ge + Ge_2 + Ge$	6.492
$Si_2Ge_2 + Si_2Ge + Ge$	6.523
$Si_3Ge_2 + SiGe + Ge$	6.607
$Si_2Ge_2 + SiGe_2 + Si$	6.621
$Si_2Ge_3 + Si_2 + Ge$	6.695
$Si_3Ge_2 + Ge_2 + Si$	6.740
$Si_2Ge_3 + SiGe + Si$	6.856
$SiGe_3 + Si_2Ge + Si$	6.867
$Si_3Ge + SiGe + Ge_2$	7.016
$SiGe_4 + Si_2 + Si$	7.094
$Si_2Ge_2 + Si_2 + Ge_2$	7.122
$Si_2Ge_2 + 2SiGe$	7.151
SiGe3 + Si_2 + SiGe	7.333
$2SiGe_2 + Si_2$	7.527
$Si_2Ge + SiGe_2 + SiGe$	7.589
$2Si_2Ge + Ge_2$	7.624
$Si_4Ge + 3Ge$	9.421

Table 4.173 – *Continued*

Fragmented Cluster	Fragmentation Energy (eV)
Si_3Ge_2 + Si + 2Ge	9.668
Si_2Ge_3 + 2Si + Ge	9.917
Si_3Ge + SiGe + 2Ge	9.944
Si_2Ge_2 + Si_2 + 2Ge	10.051
Si_3Ge + Ge_2 + Si + Ge	10.077
Si_2Ge_2 + SiGe + Si + Ge	10.212
$SiGe_4$ + 3Si	10.317
Si_2Ge_2 + Ge_2 + 2Si	10.345
$SiGe_3$ + Si_2 + Si + Ge	10.395
$2Si_2Ge$ +2Ge	10.552
$SiGe_3$ + SiGe + 2Si	10.556
Si_2Ge + $SiGe_2$ + Si + Ge	10.651
$2SiGe_2$ + 2Si	10.749
$SiGe_2$ + Si_2 + SiGe + Ge	11.118
Si_2Ge + Si_2 + Ge_2 + Ge	11.152
$SiGe_2$ + Si_2 + Ge_2 + Si	11.250
$SiGe_2$ + 2SiGe + Si	11.279
Si_2Ge + SiGe + Si + Ge_2	11.313
$2Si_2$ + $2Ge_2$	11.751
Si_2 + 2SiGe + Ge_2	11.780
4SiGe	11.808
Si_3Ge + Si + 3Ge	13.006
Si_2Ge_2 + 2Si + 2Ge	13.274
$SiGe_3$ + 3Si + Ge	13.618
Si_2Ge + Si_2 + 3Ge	14.080
$SiGe_2$ + Si_2 + Si + 2Ge	14.179
Si_2Ge + SiGe + Si + 2Ge	14.242
$SiGe_2$ + SiGe + 2Si + Ge	14.340
Si_2Ge + Ge_2 + 2Si + Ge	14.375

Table 4.173 – *Continued*

Fragmented Cluster	Fragmentation Energy (eV)
$SiGe_2 + Ge_2 + 3Si$	14.473
$2Si_2 + Ge_2 + 2Ge$	14.680
$Si_2 + 2SiGe + 2Ge$	14.708
$Si_2 + SiGe + Ge_2 + Si + Ge$	14.841
$3SiGe + Si + Ge$	14.870
$Si_2 + Ge_2 + 2Si + Ge_2$	14.974
$2SiGe + Ge_2 + 2Si$	15.003
$Si_2Ge + 2Si + 3Ge$	17.303
$SiGe_2 + 3Si + 2Ge$	17.402
$2Si_2 + 4Ge$	17.608
$Si_2 + SiGe + Si + 3Ge$	17.770
$Si_2 + Ge_2 + 2Si + 2Ge$	17.903
$2SiGe + 2Si + 2Ge$	17.931
$SiGe + Ge_2 + 3Si + Ge$	18.064
$2Ge_2 + 4Si$	18.197
$Ge_2 + 4Si + 2Ge$	21.125
$4Si + 4Ge$	24.054

Table 4.174 Fragmentation Energies for the Most Stable $(Si_4Ge_4)^+$ Octamer

Fragmented Cluster	Fragmentation Energy (eV)
$(Si_4Ge_3)^+ + Ge$	2.951
$(Si_3Ge_4)^+ + Si$	3.218
$Si_3Ge + (SiGe_3)^+$	3.331
$(Si_4Ge_2)^+ + Ge_2$	3.364
$Si_4Ge_3 + Ge^+$	3.368
$(Si_2Ge_2)^+ + Si_2Ge_2$	3.378
$(Si_3Ge)^+ + SiGe_3$	3.435
$Si_4Ge_2 + (Ge_2)^+$	3.534
$(Si_3Ge_3)^+ + SiGe$	3.548
$(Si_2Ge_4)^+ + Si_2$	3.787
$Si_3Ge_3 + (SiGe)^+$	3.815
$(Si_3Ge_2)^+ + SiGe_2$	3.831
$Si_3Ge_2 + (SiGe_2)^+$	4.063
$(Si_2Ge_3)^+ + Si_2Ge$	4.096
$Si_2Ge_3 + (Si_2Ge)^+$	4.147
$(Si_4Ge_2)^+ + 2Ge$	6.292
$(Si_3Ge_3)^+ + Si + Ge$	6.609
$Si_4Ge_2 + Ge^+ + Ge$	6.743
$(Si_2Ge_4)^+ + 2Si$	7.010
$Si_3Ge_3 + Si + Ge^+$	7.041
$Si_4Ge + (Ge_2)^+ + Ge$	7.210
$(Si_3Ge)^+ + SiGe_2 + Ge$	7.219
$Si_3Ge + SiGe_2 + Ge^+$	7.352
$(Si_4Ge)^+ + Ge_2 + Ge$	7.371
$Si_3Ge + (SiGe_2)^+ + Ge$	7.400
$(Si_2Ge_2)^+ + Si_2Ge + Ge$	7.408
$(Si_3Ge_2)^+ + SiGe + Ge$	7.422
$Si_3Ge_2 + (SiGe)^+ + Ge$	7.441
$Si_3Ge_2 + (Ge_2)^+ + Si$	7.458

Table 4.174 – *Continued*

Fragmented Cluster	Fragmentation Energy (eV)
$Si_4Ge + Ge_2 + Ge^+$	7.491
$Si_2Ge_2 + (Si_2Ge)^+ + Ge$	7.503
$(Si_2Ge_2)^+ + SiGe_2 + Si$	7.506
$Si_2Ge_2 + Si_2Ge + Ge^+$	7.521
$(Si_3Ge_2)^+ + Ge_2 + Si$	7.555
$Si_3Ge_2 + SiGe + Ge^+$	7.605
$(Si_2Ge_3)^+ + Si_2 + Ge$	7.624
$(SiGe_3)^+ + Si_2Ge + Si$	7.628
$Si_2Ge_2 + (SiGe_2)^+ + Si$	7.668
$Si_2Ge_3 + (SiGe)^+ + Si$	7.690
$Si_2Ge_3 + Si_2 + Ge^+$	7.693
$Si_3Ge + SiGe + (Ge_2)^+$	7.734
$(Si_2Ge_3)^+ + SiGe + Si$	7.785
$Si_2Ge_2 + Si_2 + (Ge_2)^+$	7.840
$SiGe_3 + (Si_2Ge)^+ + Si$	7.847
$Si_3Ge + (SiGe)^+ + Ge_2$	7.850
$(Si_3Ge)^+ + SiGe + Ge_2$	7.881
$(SiGe_4)^+ + Si_2 + Si$	7.970
$Si_2Ge_2 + (SiGe)^+ + SiGe$	7.985
$(Si_2Ge_2)^+ + Si_2 + Ge_2$	8.007
$(Si_2Ge_2)^+ + 2SiGe$	8.036
$(SiGe3)^+ + Si_2 + SiGe$	8.095
$SiGe3 + Si_2 + (SiGe)^+$	8.167
$2Si_2Ge + (Ge_2)^+$	8.342
$Si_2Ge + SiGe_2 + (SiGe)^+$	8.423
$(Si_2Ge)^+ + SiGe_2 + SiGe$	8.570
$(SiGe_2)^+ + SiGe_2 + Si_2$	8.574
$(Si_2Ge)^+ + Si_2Ge + Ge_2$	8.604
$Si_2Ge + (SiGe_2)^+ + SiGe$	8.636

Table 4.174 – *Continued*

Fragmented Cluster	Fragmentation Energy (eV)
$(Si_4Ge)^+ + 3Ge$	10.299
$Si_4Ge + Ge^+ + 2Ge$	10.419
$(Si_3Ge_2)^+ + Si + 2Ge$	10.483
$Si_3Ge_2 + Si + Ge^+ + Ge$	10.666
$Si_3Ge + (SiGe)^+ + 2Ge$	10.778
$Si_3Ge + (Ge_2)^+ + Si + Ge$	10.795
$(Si_3Ge)^+ + SiGe + 2Ge$	10.809
$(Si_2Ge_3)^+ + 2Si + Ge$	10.847
$Si_2Ge_3 + 2Si + Ge^+$	10.916
$(Si_2Ge_2)^+ + Si_2 + 2Ge$	10.936
$(Si_3Ge)^+ + Ge_2 + Si + Ge$	10.942
$Si_3Ge + SiGe + Ge^+ + Ge$	10.943
$Si_2Ge_2 + (SiGe)^+ + Si + Ge$	11.046
$Si_2Ge_2 + Si_2 + Ge^+ + Ge$	11.049
$Si_2Ge_2 + (Ge_2)^+ + 2Si$	11.063
$Si_3Ge + Ge_2 + Si + Ge^+$	11.076
$(Si_2Ge_2)^+ + SiGe + Si + Ge$	11.097
$(SiGe_3)^+ + Si_2 + Si + Ge$	11.156
$Si_2Ge_2 + SiGe + Si + Ge^+$	11.210
$(Si_2Ge_2)^+ + Ge_2 + 2Si$	11.230
$(SiGe_3)^+ + SiGe + 2Si$	11.318
$SiGe_3 + (SiGe)^+ + 2Si$	11.390
$SiGe_3 + Si_2 + Si + Ge^+$	11.393
$(Si_2Ge)^+ + Si_2Ge + 2Ge$	11.533
$2Si_2Ge + Ge^+ + Ge$	11.550
$(Si_2Ge)^+ + SiGe_2 + Si + Ge$	11.631
$Si_2Ge + SiGe_2 + Si + Ge^+$	11.649
$Si_2Ge + (SiGe_2)^+ + Si + Ge$	11.698
$(SiGe_2)^+ + SiGe_2 + 2Si$	11.796

Table 4.174 – *Continued*

Fragmented Cluster	Fragmentation Energy (eV)
$Si_2Ge + Si_2 + (Ge_2)^+ + Ge$	11.870
$SiGe_2 + Si_2 + (SiGe)^+ + Ge$	11.951
$SiGe_2 + Si_2 + (Ge_2)^+ + Si$	11.968
$Si_2Ge + SiGe + Si + (Ge_2)^+$	12.031
$SiGe_2 + (SiGe)^+ + SiGe + Si$	12.113
$SiGe_2 + Si_2 + SiGe + Ge^+$	12.116
$(Si_2Ge)^+ + Si_2 + Ge_2 + Ge$	12.132
$Si_2Ge + (SiGe)^+ + Si + Ge_2$	12.147
$Si_2Ge + Si_2 + Ge_2 + Ge^+$	12.150
$(SiGe_2)^+ + Si_2 + SiGe + Ge$	12.164
$(Si_2Ge)^+ + SiGe + Si + Ge_2$	12.294
$(SiGe_2)^+ + Si_2 + Ge_2 + Si$	12.297
$(SiGe_2)^+ + 2SiGe + Si$	12.326
$2Si_2 + (Ge_2)^+ + Ge_2$	12.469
$Si_2 + 2SiGe + (Ge_2)^+$	12.498
$Si_2 + (SiGe)^+ + SiGe + Ge_2$	12.614
$(SiGe)^+ + 3SiGe$	12.642
$(Si_3Ge)^+ + Si + 3Ge$	13.871
$Si_3Ge + Si + Ge^+ + 2Ge$	14.004
$(Si_2Ge_2)^+ + 2Si + 2Ge$	14.158
$Si_2Ge_2 + 2Si + Ge^+ + Ge$	14.272
$(SiGe_3)^+ + 3Si + Ge$	14.379
$SiGe_3 + 3Si + Ge^+$	14.616
$(Si_2Ge)^+ + Si_2 + 3Ge$	15.061
$Si_2Ge + (SiGe)^+ + Si + 2Ge$	15.075
$Si_2Ge + Si_2 + Ge^+ + 2Ge$	15.079
$Si_2Ge + (Ge_2)^+ + 2Si + Ge$	15.092
$SiGe_2 + (SiGe)^+ + 2Si + Ge$	15.174
$SiGe_2 + Si_2 + Si + Ge^+ + Ge$	15.177

Table 4.174 – *Continued*

Fragmented Cluster	Fragmentation Energy (eV)
$SiGe_2 + (Ge_2)^+ + 3Si$	15.191
$(Si_2Ge)^+ + SiGe + Si + 2Ge$	15.222
$(SiGe_2)^+ + Si_2 + Si + 2Ge$	15.226
$Si_2Ge + SiGe + Si + Ge^+ + Ge$	15.240
$SiGe_2 + SiGe + 2Si + Ge^+$	15.339
$(Si_2Ge)^+ + Ge_2 + 2Si + Ge$	15.355
$Si_2Ge + Ge_2 + 2Si + Ge^+$	15.373
$(SiGe_2)^+ + SiGe + 2Si + Ge$	15.387
$2Si_2 + (Ge_2)^+ + 2Ge$	15.398
$(SiGe_2)^+ + Ge_2 + 3Si$	15.520
$Si_2 + (SiGe)^+ + SiGe + 2Ge$	15.542
$Si_2 + SiGe + (Ge_2)^+ + Si + Ge$	15.559
$Si_2 + (SiGe)^+ + Ge_2 + Si + Ge$	15.675
$2Si_2 + Ge_2 + Ge^+ + Ge$	15.678
$Si_2 + (Ge_2)^+ + Ge_2 + 2Si$	15.692
$(SiGe)^+ + 2SiGe + Si + Ge$	15.704
$Si_2 + 2SiGe + Ge^+ + Ge$	15.707
$2SiGe + (Ge_2)^+ + 2Si$	15.720
$(SiGe)^+ + SiGe + Ge_2 + 2Si$	15.836
$Si_2 + SiGe + Ge_2 + Si + Ge^+$	15.840
$3SiGe + Si + Ge^+$	15.868
$(Si_2Ge)^+ + 2Si + 3Ge$	18.283
$Si_2Ge + 2Si + Ge^+ + 2Ge$	18.301
$SiGe_2 + 3Si + Ge^+ + Ge$	18.400
$(SiGe_2)^+ + 3Si + 2Ge$	18.448
$Si_2 + (SiGe)^+ + Si + 3Ge$	18.604
$2Si_2 + Ge^+ + 3Ge$	18.607
$Si_2 + (Ge_2)^+ + 2Si + 2Ge$	18.621
$(SiGe)^+ + SiGe + 2Si + 2Ge$	18.765
$Si_2 + SiGe + Si + Ge^+ + 2Ge$	18.768

Table 4.174 – *Continued*

Fragmented Cluster	Fragmentation Energy (eV)
$SiGe + (Ge_2)^+ + 3Si + Ge$	18.782
$(SiGe)^+ + Ge_2 + 3Si + Ge$	18.898
$Si_2 + Ge_2 + 2Si + Ge^+ + Ge$	18.901
$(Ge_2)^+ + Ge_2 + 4Si$	18.915
$2SiGe + 2Si + Ge^+ + Ge$	18.929
$SiGe + Ge_2 + 3Si + Ge^+$	19.062
$(Ge_2)^+ + 4Si + 2Ge$	21.843
$Ge_2 + 4Si + Ge^+ + Ge$	22.124
$4Si + Ge^+ + 3Ge$	25.052

Table 4.175 Fragmentation Energies for the Most Stable $(Si_4Ge_4)^-$ Octamer

Fragmented Cluster	Fragmentation Energy (eV)
$(Si_2Ge_2)^- + Si_2Ge_2$	2.817
$(Si_3Ge)^- + SiGe_3$	2.870
$(Si_4Ge_3)^- + Ge$	2.872
$Si_3Ge + (SiGe_3)^-$	2.925
$(Si_3Ge_2)^- + SiGe_2$	3.126
$(Si_3Ge_4)^- + Si$	3.217
$(Si_4Ge_2)^- + Ge_2$	3.222
$Si_3Ge_2 + (SiGe_2)^-$	3.272
$Si_2Ge_3 + (Si_2Ge)^-$	3.277
$Si_4Ge_2 + (Ge_2)^-$	3.290
$(Si_2Ge_3)^- + Si_2Ge$	3.330
$(Si_3Ge_3)^- + SiGe$	3.424
$Si_3Ge_3 + (SiGe)^-$	3.426
$Si_4Ge_3 + Ge^-$	3.521
$(Si_2Ge_4)^- + Si_2$	3.573
$(Si_4Ge_2)^- + 2Ge$	6.150
$(Si_3Ge_3)^- + Si + Ge$	6.485
$(Si_4Ge)^- + Ge_2 + Ge$	6.540
$Si_3Ge + (SiGe_2)^- + Ge$	6.609
$Si_2Ge_2 + (Si_2Ge)^- + Ge$	6.633
$(Si_3Ge)^- + SiGe_2 + Ge$	6.654
$(Si_3Ge_2)^- + SiGe + Ge$	6.717
$(Si_2Ge_4)^- + 2Si$	6.796
$(Si_2Ge_2)^- + Si_2Ge + Ge$	6.847
$(Si_3Ge_2)^- + Ge_2 + Si$	6.850
$(Si_2Ge_3)^- + Si_2 + Ge$	6.858
$Si_2Ge_2 + (SiGe_2)^- + Si$	6.877
$Si_4Ge_2 + Ge^- + Ge$	6.896
$(Si_2Ge_2)^- + SiGe_2 + Si$	6.946
$Si_4Ge + (Ge_2)^- + Ge$	6.966

Table 4.175 – *Continued*

Fragmented Cluster	Fragmentation Energy (eV)
$SiGe_3 + (Si_2Ge)^- + Si$	6.977
$(Si_2Ge_3)^- + SiGe + Si$	7.020
$Si_3Ge_2 + (SiGe)^- + Ge$	7.051
$Si_3Ge_3 + Si + Ge^-$	7.195
$Si_3Ge_2 + (Ge_2)^- + Si$	7.214
$(SiGe_3)^- + Si_2Ge + Si$	7.222
$(SiGe_4)^- + Si_2 + Si$	7.228
$Si_2Ge_3 + (SiGe)^- + Si$	7.301
$(Si_3Ge)^- + SiGe + Ge_2$	7.317
$(Si_2Ge_2)^- + Si_2 + Ge_2$	7.447
$Si_3Ge + (SiGe)^- + Ge_2$	7.460
$(Si_2Ge_2)^- + 2SiGe$	7.475
$Si_3Ge + SiGe + (Ge_2)^-$	7.490
$Si_3Ge + SiGe_2 + Ge^-$	7.505
$Si_2Ge_2 + (SiGe)^- + SiGe$	7.595
$Si_2Ge_2 + Si_2 + (Ge_2)^-$	7.596
$Si_4Ge + Ge_2 + Ge^-$	7.644
$Si_2Ge_2 + Si_2Ge + Ge^-$	7.674
$(SiGe3)^- + Si_2 + SiGe$	7.689
$(Si_2Ge)^- + SiGe_2 + SiGe$	7.700
$(Si_2Ge)^- + Si_2Ge + Ge_2$	7.734
$Si_3Ge_2 + SiGe + Ge^-$	7.758
$SiGe3 + Si_2 + (SiGe)^-$	7.778
$(SiGe_2)^- + SiGe_2 + Si_2$	7.783
$Si_2Ge + (SiGe_2)^- + SiGe$	7.845
$Si_2Ge_3 + Si_2 + Ge^-$	7.846
$Si_2Ge + SiGe_2 + (SiGe)^-$	8.034
$2Si_2Ge + (Ge_2)^-$	8.098
$(Si_4Ge)^- + 3Ge$	9.468

Table 4.175 – *Continued*

Fragmented Cluster	Fragmentation Energy (eV)
$(Si_3Ge_2)^-$ + Si + 2Ge	9.779
$(Si_2Ge_3)^-$ + 2Si + Ge	10.081
$(Si_3Ge)^-$ + SiGe + 2Ge	10.245
$(Si_2Ge_2)^-$ + Si_2 + 2Ge	10.375
$(Si_3Ge)^-$ + Ge_2 + Si + Ge	10.378
Si_3Ge + $(SiGe)^-$ + 2Ge	10.389
$(Si_2Ge_2)^-$ + SiGe + Si + Ge	10.536
Si_3Ge + $(Ge_2)^-$ + Si + Ge	10.551
Si_4Ge + Ge^- +2Ge	10.572
Si_2Ge_2 + $(SiGe)^-$ + Si + Ge	10.657
$(Si_2Ge)^-$ + Si_2Ge +2Ge	10.663
$(Si_2Ge_2)^-$ + Ge_2 + 2Si	10.669
$(SiGe_3)^-$ + Si_2 + Si + Ge	10.750
$(Si_2Ge)^-$ + $SiGe_2$ + Si + Ge	10.761
Si_2Ge_2 + $(Ge_2)^-$ + 2Si	10.819
Si_3Ge_2 + Si + Ge^- + Ge	10.820
Si_2Ge + $(SiGe_2)^-$ + Si + Ge	10.907
$(SiGe_3)^-$ + SiGe + 2Si	10.911
$SiGe_3$ + $(SiGe)^-$ + 2Si	11.001
$(SiGe_2)^-$ + $SiGe_2$ + 2Si	11.005
Si_2Ge_3 + 2Si + Ge^-	11.069
Si_3Ge + SiGe + Ge^- + Ge	11.096
Si_2Ge_2 + Si_2 + Ge^- + Ge	11.202
Si_3Ge + Ge_2 + Si + Ge^-	11.229
$(Si_2Ge)^-$ + Si_2 + Ge_2 + Ge	11.262
Si_2Ge_2 + SiGe + Si + Ge^-	11.364
$(SiGe_2)^-$ + Si_2 + SiGe + Ge	11.373
$(Si_2Ge)^-$ + SiGe + Ge_2 + Si	11.423
$(SiGe_2)^-$ + Si_2 + Ge_2 + Si	11.506

Table 4.175 – *Continued*

Fragmented Cluster	Fragmentation Energy (eV)
$(SiGe_2)^-$ + 2SiGe + Si	11.535
$SiGe_3$ + Si_2 + Si + Ge^-	11.546
$SiGe_2$ + Si_2 + $(SiGe)^-$ + Ge	11.562
Si_2Ge + Si_2 + $(Ge_2)^-$ + Ge	11.626
$2Si_2Ge$ +Ge^- + Ge	11.704
$SiGe_2$ + $(SiGe)^-$ + SiGe + Si	11.723
$SiGe_2$ + Si_2 + $(Ge_2)^-$ + Si	11.724
Si_2Ge + $(SiGe)^-$ + Ge_2 + Si	11.758
Si_2Ge + SiGe + Si + $(Ge_2)^-$	11.787
Si_2Ge + $SiGe_2$ + Si + Ge^-	11.802
Si_2 + $(SiGe)^-$ + SiGe + Ge_2	12.224
$2Si_2$ + $(Ge_2)^-$ + Ge_2	12.225
$(SiGe)^-$ + 3SiGe	12.253
Si_2 + 2SiGe + $(Ge_2)^-$	12.254
$SiGe_2$ + Si_2 + SiGe + Ge^-	12.269
Si_2Ge + Si_2 + Ge_2 + Ge^-	12.303
$(Si_3Ge)^-$ + Si + 3Ge	13.306
$(Si_2Ge_2)^-$ + 2Si + 2Ge	13.598
$(SiGe_3)^-$ + 3Si + Ge	13.973
Si_3Ge + Si + Ge^- + 2Ge	14.157
$(Si_2Ge)^-$ + Si_2 + 3Ge	14.191
$(Si_2Ge)^-$ + SiGe + Si + 2Ge	14.352
Si_2Ge_2 + 2Si + Ge^- + Ge	14.425
$(SiGe_2)^-$ + Si_2 + Si + 2Ge	14.435
$(Si_2Ge)^-$ + Ge_2 + 2Si + Ge	14.485
$(SiGe_2)^-$ + SiGe + 2Si + Ge	14.596
Si_2Ge + $(SiGe)^-$ + Si + 2Ge	14.686
$(SiGe_2)^-$ + Ge_2 + 3Si	14.729
$SiGe_3$ + 3Si + Ge^-	14.769

Table 4.175 – *Continued*

Fragmented Cluster	Fragmentation Energy (eV)
$SiGe_2 + (SiGe)^- + 2Si + Ge$	14.785
$Si_2Ge + (Ge_2)^- + 2Si + Ge$	14.848
$SiGe_2 + (Ge_2)^- + 3Si$	14.947
$Si_2 + (SiGe)^- + SiGe + 2Ge$	15.153
$2Si_2 + (Ge_2)^- + 2Ge$	15.154
$Si_2Ge + Si_2 + Ge^- + 2Ge$	15.232
$Si_2 + (SiGe)^- + Ge_2 + Si + Ge$	15.286
$(SiGe)^- + 2SiGe + Si + Ge$	15.314
$Si_2 + SiGe + (Ge_2)^- + Si + Ge$	15.315
$SiGe_2 + Si_2 + Si + Ge^- + Ge$	15.331
$Si_2Ge + SiGe + Si + Ge^- + Ge$	15.393
$(SiGe)^- + SiGe + Ge_2 + 2Si$	15.447
$Si_2 + (Ge_2)^- + Ge_2 + 2Si$	15.448
$2SiGe + (Ge_2)^- + 2Si$	15.476
$SiGe_2 + SiGe + 2Si + Ge^-$	15.492
$Si_2Ge + Ge_2 + 2Si + Ge^-$	15.526
$2Si_2 + Ge_2 + Ge^- + Ge$	15.832
$Si_2 + 2SiGe + Ge^- + Ge$	15.860
$Si_2 + SiGe + Ge_2 + Si + Ge^-$	15.993
$3SiGe + Si + Ge^-$	16.021
$(Si_2Ge)^- + 2Si + 3Ge$	17.413
$(SiGe_2)^- + 3Si + 2Ge$	17.658
$Si_2 + (SiGe)^- + Si + 3Ge$	18.214
$(SiGe)^- + SiGe + 2Si + 2Ge$	18.376
$Si_2 + (Ge_2)^- + 2Si + 2Ge$	18.377
$Si_2Ge + 2Si + Ge^- + 2Ge$	18.455
$(SiGe)^- + Ge_2 + 3Si + Ge$	18.509
$SiGe + (Ge_2)^- + 3Si + Ge$	18.538
$SiGe_2 + 3Si + Ge^- + Ge$	18.553
$(Ge_2)^- + Ge_2 + 4Si$	18.671

Table 4.175 – *Continued*

Fragmented Cluster	Fragmentation Energy (eV)
$2Si_2 + Ge^- + 3Ge$	18.760
$Si_2 + SiGe + Si + Ge^- + 2Ge$	18.921
$Si_2 + Ge_2 + 2Si + Ge^- + Ge$	19.054
$2SiGe + 2Si + Ge^- + Ge$	19.083
$SiGe + Ge_2 + 3Si + Ge^-$	19.216
$(Ge_2)^- + 4Si + 2Ge$	21.599
$Ge_2 + 4Si + Ge^- + Ge$	22.277
$4Si + Ge^- + 3Ge$	25.206

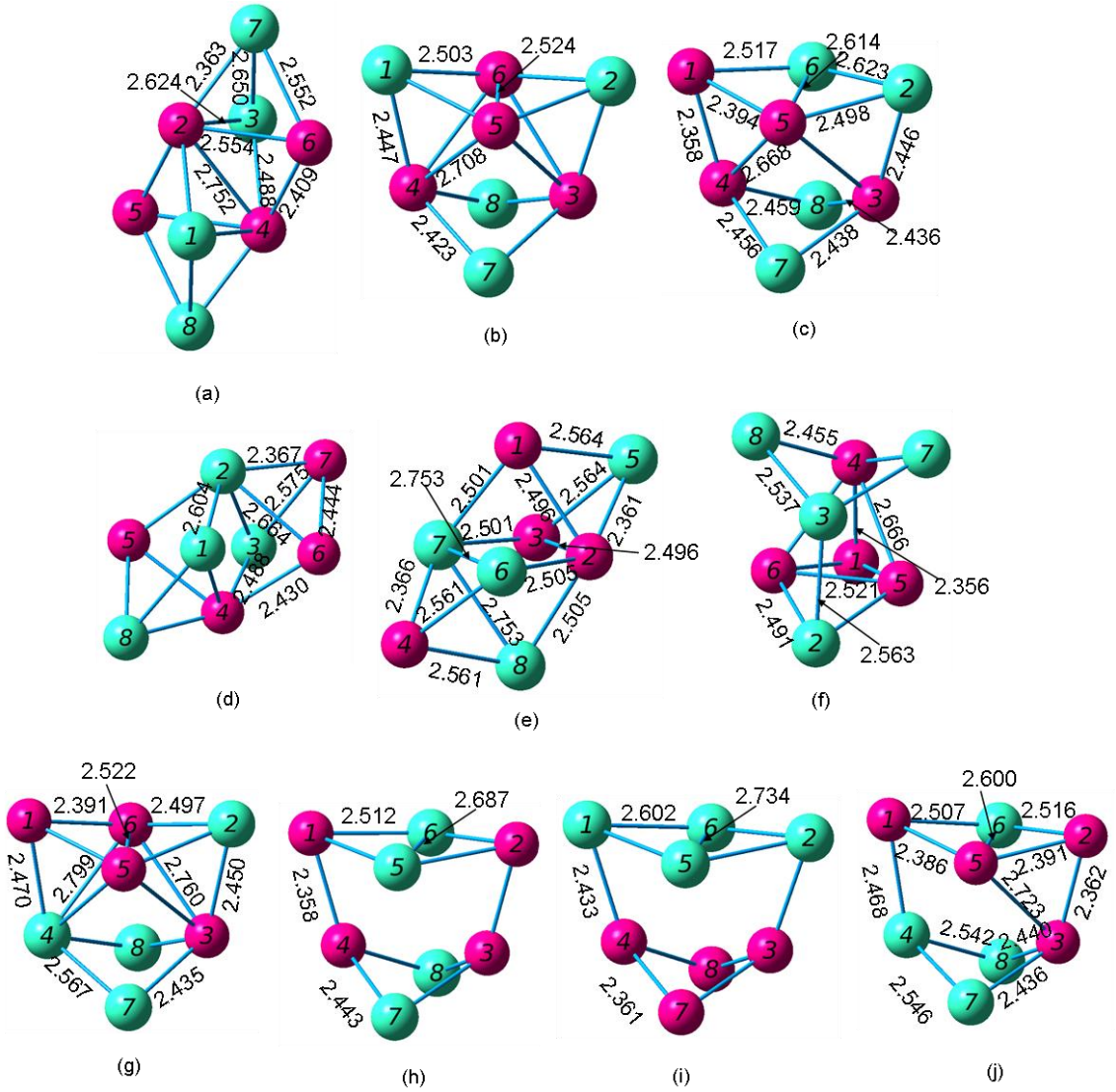

Figure 4.145 Geometries of the Si_4Ge_4 Neutral Septamers from (a) Most Stable through (j) Least Stable

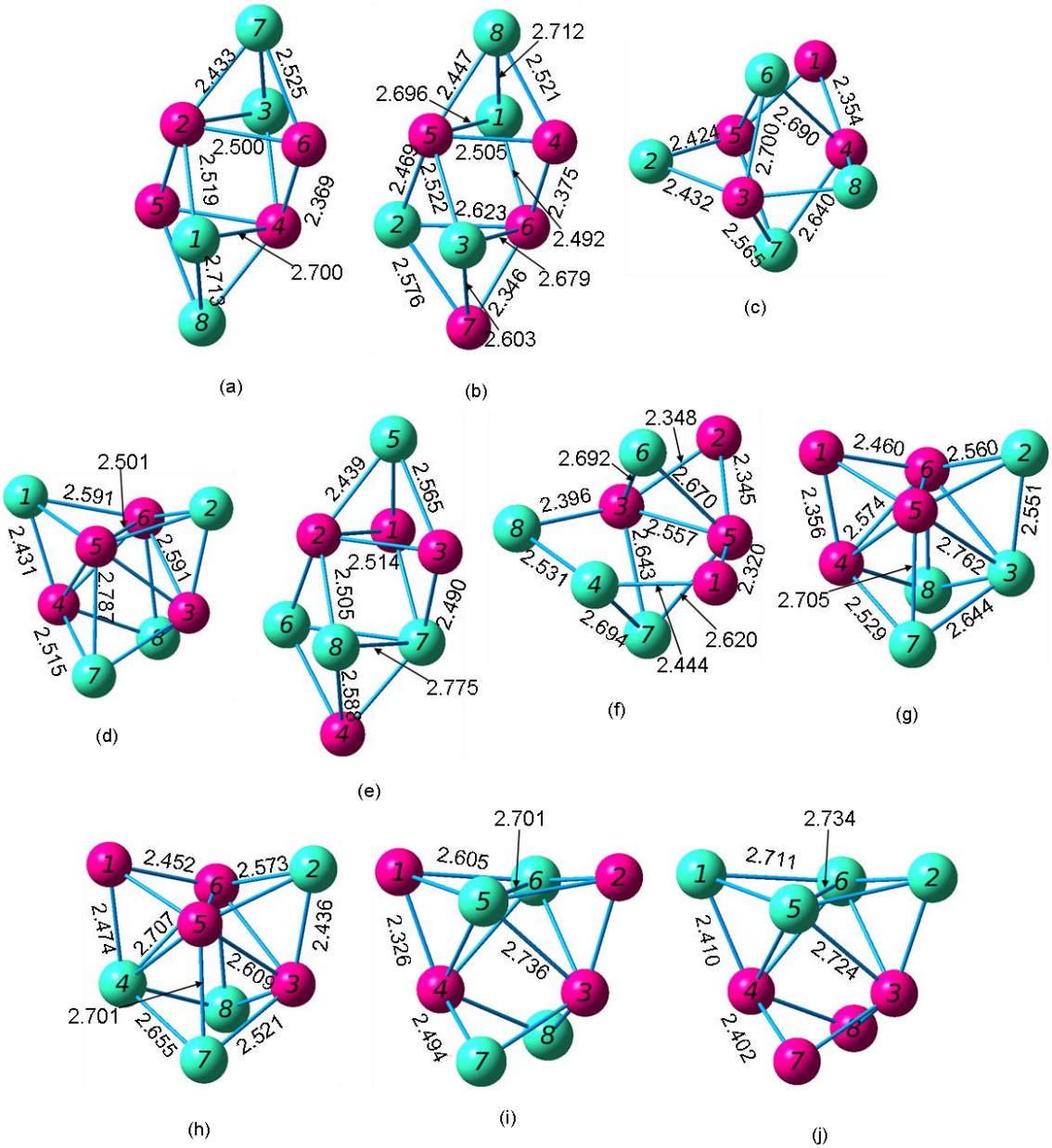

Figure 4.146 Geometries of the $(Si_4Ge_4)^+$ Cationic Septamers from (a) Most Stable through (j) Least Stable

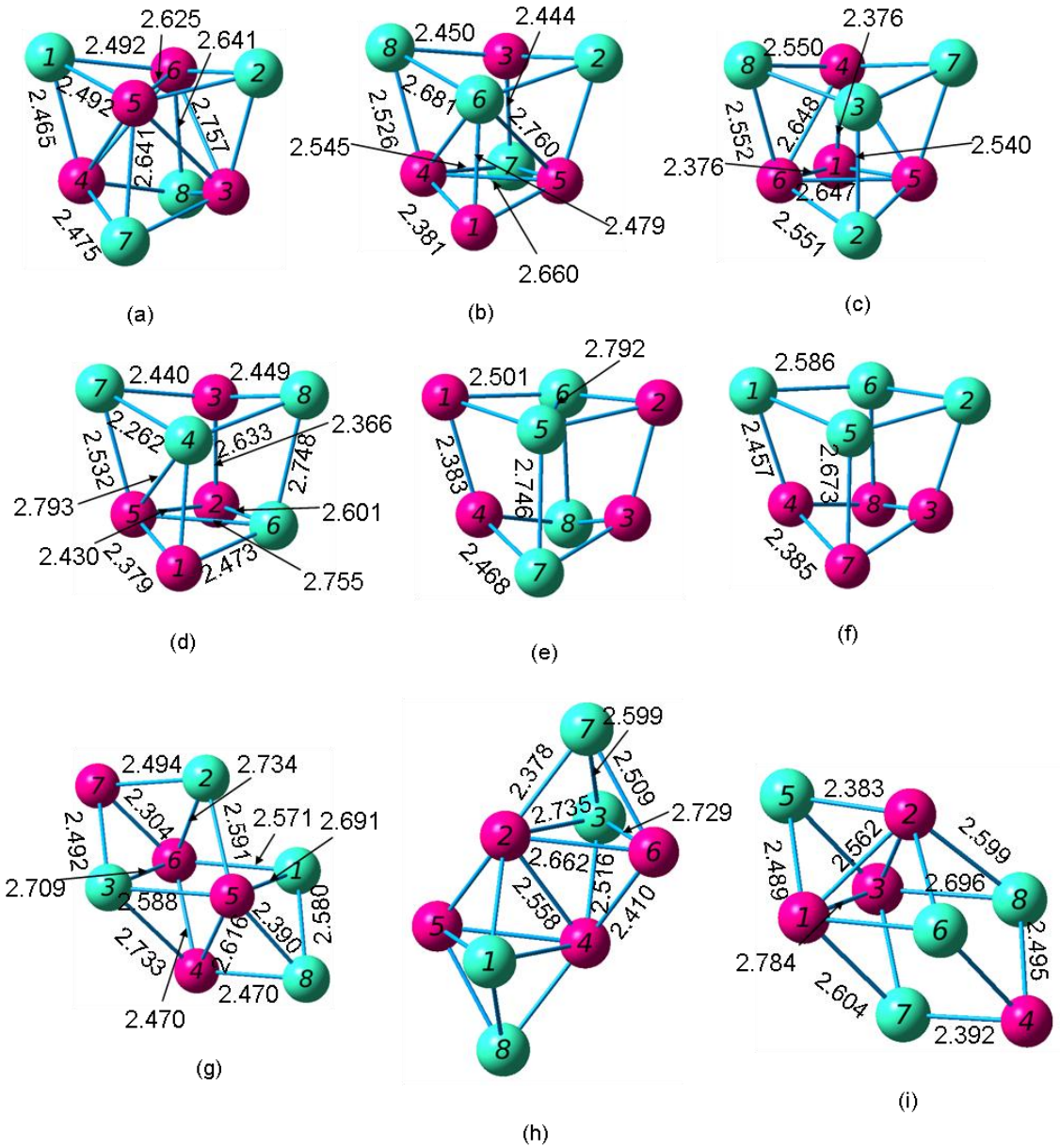

Figure 4.147 Geometries of the $(Si_4Ge_4)^-$ Anionic Septamers from (a) Most Stable through (i) Least Stable

4.26 Si_3Ge_5 Octamers

Wang and Chao [51] reported a rhombic cube for the neutral Si_3Ge_5 octamers. The cation is a pentagonal bipyramid with a germanium atom attached to a face. The neutral cluster has a ^1A electronic state, a dissociation energy of -33.1183 eV or -32.6810 eV, a HOMO-LUMO gap of 2.42 eV, and the following frequencies: 490(a), 478(a), and 406(a). Their anion cluster is again similar to our most stable anion.

Totally, we investigated twenty-six Si_3Ge_5 clusters. The difference in binding energy per atom between our most stable cluster and our thirty-eighth most stable cluster was 0.1367 eV. Here, we report the properties of ten neutrals and cations and nine anions.

Table 4.176 Properties of the Si_3Ge_5 Octamers

Figure	Symmetry Group	Electronic State	Binding E / Atom (eV)	HOMO-LUMO Gap (eV)	Dipole Moment (D)
4.148 (a)	C_1	^1A	2.979	2.650	0.402
4.148 (b)	C_1	^1A	2.976	2.595	0.438
4.148 (c)	C_1	^1A	2.940	2.493	0.088
4.148 (d)	C_1	^1A	2.940	2.399	0.635
4.148 (e)	C_1	^1A	2.933	2.441	0.540
4.148 (f)	C_1	^1A	2.929	2.418	0.435
4.148 (g)	C_s	$^1A'$	2.925	2.019	0.345
4.148 (h)	C_1	^1A	2.916	2.139	0.522
4.148 (i)	C_1	^1A	2.913	1.999	0.568
4.148 (j)	C_s	$^1A'$	2.912	2.115	0.343

Table 4.177 Properties of the $(Si_3Ge_5)^+$ Octamers

Figure	Symmetry Group	Electronic State	Binding E / Atom (eV)	HOMO-LUMO Gap (eV)	Dipole Moment (D)
4.149 (a)	C_1	^2A	3.093	1.355[a]	0.402
4.149 (b)	C_1	^2A	3.081	1.315[a]	0.610
4.149 (c)	C_1	^2A	3.057	1.327[a]	0.751
4.149 (d)	C_1	^2A	3.057	1.357[a]	0.920
4.149 (e)	C_s	$^2A''$	3.050	1.386[a]	0.405
4.149 (f)	C_1	^2A	3.050	1.368[a]	0.345
4.149 (g)	C_1	^2A	3.042	1.318[a]	0.457
4.149 (h)	C_s	$^2A''$	3.026	1.390[a]	1.060
4.149 (i)	C_1	^2A	3.026	1.352[a]	0.504
4.149 (j)	C_1	^2A	3.016	1.355[a]	0.698

[a] HOMO and LUMO have opposite spins; this value includes the energy required to flip the spin of the electron.

Table 4.178 Properties of the $(Si_3Ge_5)^-$ Octamers

Figure	Symmetry Group	Electronic State	Binding E / Atom (eV)	HOMO-LUMO Gap (eV)	Dipole Moment (D)
4.150 (a)	C_s	$^2A'$	3.100	1.387[a]	0.697
4.150 (b)	C_1	^2A	3.091	1.400[a]	1.214
4.150 (c)	C_s	$^2A'$	3.089	1.409[a]	1.814
4.150 (d)	C_1	^2A	3.082	1.418[a]	0.742
4.150 (e)	C_1	^2A	3.071	1.337[a]	1.479
4.150 (f)	C_1	^2A	3.058	1.391[a]	1.852
4.150 (g)	C_1	^2A	3.053	1.369[a]	0.759
4.150 (h)	C_1	^2A	3.048	1.405[a]	0.957
4.150 (i)	C_1	^2A	3.042	1.361[a]	1.240

[a] HOMO and LUMO have opposite spins; this value includes the energy required to flip the spin of the electron.

Table 4.179 Ionization Potentials and Electron Affinities of the Si_3Ge_5 Octamers

Neutral Figure	VIP (eV)	Cationic Figure	AIP (eV)	VEA (eV)	Anionic Figure	AEA (eV)
4.148 (a)	7.183	4.149 (b)	7.087	1.554	4.150 (e)	1.875
4.148 (b)	7.117	4.149 (a)	6.964	1.512	4.150 (d)	1.989
4.148 (c)	7.197	4.149 (g)	7.086	1.713	4.150 (g)	2.040
4.148 (d)	7.117	4.149 (d)	6.963	1.726	4.150 (f)	2.088
4.148 (e)	7.129	4.149 (f)	6.964	1.683	4.150 (h)	2.062
4.148 (f)	7.008	4.149 (c)	6.876	1.633	4.150 (i)	2.042
4.148 (g)	7.182	4.149 (e)	6.896	2.122	4.150 (a)	2.539
4.148 (h)	7.289	4.149 (j)	7.102	2.104	4.150 (b)	2.536
4.148 (i)	7.212	4.149 (i)	6.995	2.116	4.150 (a)	2.639
4.148 (j)	7.286	4.149 (h)	6.985	2.125	4.150 (c)	2.550

Table 4.180 Fragmentation Energies for the Most Stable Si_3Ge_5 Octamer

Fragmented Cluster	Fragmentation Energy (eV)
$Si_3Ge_4 + Ge$	2.470
$SiGe_3 + Si_2Ge_2$	2.617
$Si_2Ge_5 + Si$	2.768
$Si_3Ge_3 + Ge_2$	2.894
$Si_2Ge_3 + SiGe_2$	3.044
$Si_2Ge_4 + SiGe$	3.049
$SiGe_4 + Si_2Ge$	3.346
$SiGe_5 + Si_2$	3.348
$Si_3Ge_3 + 2Ge$	5.822
$Si_2Ge_4 + Si + Ge$	6.110
$Si_2Ge_2 + SiGe_2 + Ge$	6.401
$Si_3Ge_2 + Ge_2 + Ge$	6.519
$SiGe_5 + 2Si$	6.571
$Si_2Ge_3 + SiGe + Ge$	6.635
$SiGe_3 + Si_2Ge + Ge$	6.646
$SiGe_3 + SiGe_2 + Si$	6.745
$Si_2Ge_3 + Ge_2 + Si$	6.768
$SiGe_4 + Si_2 + Ge$	6.874
$Si_3Ge + 2Ge_2$	6.928
$SiGe_4 + SiGe + Si$	7.035
$Si_2Ge_2 + SiGe + Ge_2$	7.063
$SiGe_3 + Si_2 + Ge_2$	7.246
$SiGe_3 + 2SiGe$	7.274
$Si_2Ge + SiGe_2 + Ge_2$	7.502
$Si_3Ge_2 + 3Ge$	9.447
$Si_2Ge_3 + Si + 2Ge$	9.697
$Si_3Ge + Ge_2 + 2Ge$	9.857
$SiGe_4 + 2Si + Ge$	10.096
$Si_2Ge_2 + Ge_2 + Si + Ge$	10.124
$SiGe_3 + Si_2 + 2Ge$	10.174

Table 4.180 – *Continued*

Fragmented Cluster	Fragmentation Energy (eV)
$SiGe_3 + SiGe + Si + Ge$	10.335
$Si_2Ge + SiGe_2 + 2Ge$	10.430
$SiGe_3 + Ge_2 + 2Si$	10.468
$SiGe_2 + Si_2 + Ge_2 + Ge$	11.030
$SiGe_2 + 2SiGe + Ge$	11.058
$Si_2Ge + SiGe + Ge_2 + Ge$	11.092
$SiGe_2 + SiGe + Ge_2 + Si$	11.191
$Si_2Ge + 2Ge_2 + Si$	11.225
$Si_2 + SiGe + 2Ge_2$	11.692
$3SiGe + Ge_2$	11.720
$Si_3Ge + 4Ge$	12.785
$Si_2Ge_2 + Si + 3Ge$	13.053
$SiGe_3 + 2Si + 2Ge$	13.397
$SiGe_2 + Si_2 + 3Ge$	13.958
$Si_2Ge + SiGe + 3Ge$	14.021
$SiGe_2 + SiGe + Si + 2Ge$	14.120
$Si_2Ge + Ge_2 + Si + 2Ge$	14.154
$SiGe_2 + Ge_2 + 2Si + Ge$	14.252
$SiGe + Si_2 + Ge_2 + 2Ge$	14.621
$3SiGe + 2Ge$	14.649
$Si_2 + 2Ge_2 + Si + Ge$	14.753
$2SiGe + Ge_2 + Si + Ge$	14.782
$SiGe + 2Ge_2 + 2Si$	14.915
$Si_2Ge + Si + 4Ge$	17.082
$Si_2 + SiGe + 4Ge$	17.549
$Si_2 + Ge_2 + Si + 3Ge$	17.682
$2SiGe + Si + 3Ge$	17.710
$SiGe + Ge_2 + 2Si + 2Ge$	17.843
$2Ge_2 + 3Si + Ge$	17.976
$Si_2 + Si + 5Ge$	20.610

Table 4.180 – *Continued*

Fragmented Cluster	Fragmentation Energy (eV)
SiGe + 2Si + 4Ge	20.772
Ge_2 +3Si + 3Ge	20.905
3Si + 5Ge	23.833
$(Si_3Ge_4)^+$ + Ge	2.907
$(Si_2Ge_5)^+$ + Si	3.248
$(SiGe_3)^+$ + Si_2Ge_2	3.288
$(Si_3Ge_3)^+$ + Ge_2	3.370
Si_3Ge_4 + Ge^+	3.378
$SiGe_3$ + $(Si_2Ge_2)^+$	3.411
Si_3Ge_3 + $(Ge_2)^+$	3.521
$(Si_2Ge_4)^+$ + SiGe	3.638
Si_2Ge_4 + $(SiGe)^+$	3.792
$(SiGe_5)^+$ + Si_2	3.844
$(Si_2Ge_3)^+$ + $SiGe_2$	3.883
Si_2Ge_3 + $(SiGe_2)^+$	4.001
$(SiGe_4)^+$ + Si_2Ge	4.131
$SiGe_4$ + $(Si_2Ge)^+$	4.236
$(Si_3Ge_3)^+$ + 2Ge	6.298
$(Si_2Ge_4)^+$ + Si + Ge	6.699
Si_3Ge_3 + Ge^+ + Ge	6.730
Si_2Ge_4 + Si + Ge^+	7.018
$(SiGe_5)^+$ + 2Si	7.067
Si_3Ge_2 + $(Ge_2)^+$ + Ge	7.147
$(Si_2Ge_2)^+$ + $SiGe_2$ + Ge	7.195
$(Si_3Ge_2)^+$ + Ge_2 + Ge	7.243
Si_2Ge_2 + $SiGe_2$ + Ge^+	7.309
$(SiGe_3)^+$ + Si_2Ge + Ge	7.317
Si_2Ge_2 + $(SiGe_2)^+$ + Ge	7.357
Si_2Ge_3 + $(SiGe)^+$ + Ge	7.379
Si_2Ge_3 + $(Ge_2)^+$ + Si	7.396

Table 4.181 Fragmentation Energies for the Most Stable $(Si_3Ge_5)^+$ Octamer

Fragmented Cluster	Fragmentation Energy (eV)
$(Si_3Ge_4)^+ + Ge$	2.907
$(Si_2Ge_5)^+ + Si$	3.248
$(SiGe_3)^+ + Si_2Ge_2$	3.288
$(Si_3Ge_3)^+ + Ge_2$	3.370
$Si_3Ge_4 + Ge^+$	3.378
$SiGe_3 + (Si_2Ge_2)^+$	3.411
$Si_3Ge_3 + (Ge_2)^+$	3.521
$(Si_2Ge_4)^+ + SiGe$	3.638
$Si_2Ge_4 + (SiGe)^+$	3.792
$(SiGe_5)^+ + Si_2$	3.844
$(Si_2Ge_3)^+ + SiGe_2$	3.883
$Si_2Ge_3 + (SiGe_2)^+$	4.001
$(SiGe_4)^+ + Si_2Ge$	4.131
$SiGe_4 + (Si_2Ge)^+$	4.236
$(Si_3Ge_3)^+ + 2Ge$	6.298
$(Si_2Ge_4)^+ + Si + Ge$	6.699
$Si_3Ge_3 + Ge^+ + Ge$	6.730
$Si_2Ge_4 + Si + Ge^+$	7.018
$(SiGe_5)^+ + 2Si$	7.067
$Si_3Ge_2 + (Ge_2)^+ + Ge$	7.147
$(Si_2Ge_2)^+ + SiGe_2 + Ge$	7.195
$(Si_3Ge_2)^+ + Ge_2 + Ge$	7.243
$Si_2Ge_2 + SiGe_2 + Ge^+$	7.309
$(SiGe_3)^+ + Si_2Ge + Ge$	7.317
$Si_2Ge_2 + (SiGe_2)^+ + Ge$	7.357
$Si_2Ge_3 + (SiGe)^+ + Ge$	7.379
$Si_2Ge_3 + (Ge_2)^+ + Si$	7.396

Table 4.181 – *Continued*

Fragmented Cluster	Fragmentation Energy (eV)
$(SiGe_3)^+ + SiGe_2 + Si$	7.416
$Si_3Ge_2 + Ge_2 + Ge^+$	7.427
$(Si_2Ge_3)^+ + SiGe + Ge$	7.474
$SiGe_3 + (Si_2Ge)^+ + Ge$	7.536
$Si_2Ge_3 + SiGe + Ge^+$	7.543
$SiGe_3 + Si_2Ge + Ge^+$	7.554
$Si_3Ge + (Ge_2)^+ + Ge_2$	7.556
$(Si_2Ge_3)^+ + Ge_2 + Si$	7.607
$(SiGe_4)^+ + Si_2 + Ge$	7.659
$Si_2Ge_2 + SiGe + (Ge_2)^+$	7.690
$SiGe_3 + (SiGe_2)^+ + Si$	7.701
$(Si_3Ge)^+ + 2Ge_2$	7.703
$SiGe_4 + (SiGe)^+ + Si$	7.779
$SiGe_4 + Si_2 + Ge^+$	7.782
$Si_2Ge_2 + (SiGe)^+ + Ge_2$	7.807
$(SiGe_4)^+ + SiGe + Si$	7.821
$(Si_2Ge_2)^+ + SiGe + Ge_2$	7.857
$SiGe_3 + Si_2 + (Ge_2)^+$	7.873
$(SiGe_3)^+ + Si_2 + Ge_2$	7.917
$(SiGe_3)^+ + 2SiGe$	7.945
$SiGe_3 + (SiGe)^+ + SiGe$	8.018
$Si_2Ge + SiGe_2 + (Ge_2)^+$	8.129
$(Si_2Ge)^+ + SiGe_2 + Ge_2$	8.392
$Si_2Ge + (SiGe_2)^+ + Ge_2$	8.458
$(Si_3Ge_2)^+ + 3Ge$	10.172
$Si_3Ge_2 + Ge^+ + 2Ge$	10.355
$Si_3Ge + (Ge_2)^+ + 2Ge$	10.484
$(Si_2Ge_3)^+ + Si + 2Ge$	10.536
$Si_2Ge_3 + Si + Ge^+ + Ge$	10.605
$(Si_3Ge)^+ + Ge_2 + 2Ge$	10.631

Table 4.181 – *Continued*

Fragmented Cluster	Fragmentation Energy (eV)
$Si_2Ge_2 + (Ge_2)^+ + Si + Ge$	10.752
$Si_3Ge + Ge_2 + Ge^+ + Ge$	10.764
$(SiGe_3)^+ + Si_2 + 2Ge$	10.845
$(SiGe_4)^+ + 2Si + Ge$	10.882
$(Si_2Ge_2)^+ + Ge_2 + Si + Ge$	10.919
$SiGe_4 + 2Si + Ge^+$	11.004
$(SiGe_3)^+ + SiGe + Si + Ge$	11.007
$Si_2Ge_2 + Ge_2 + Si + Ge^+$	11.032
$SiGe_3 + (SiGe)^+ + Si + Ge$	11.079
$SiGe_3 + Si_2 + Ge^+ + Ge$	11.082
$SiGe_3 + (Ge_2)^+ + 2Si$	11.096
$(SiGe_3)^+ + Ge_2 + 2Si$	11.140
$SiGe_3 + SiGe + Si + Ge^+$	11.243
$(Si_2Ge)^+ + SiGe_2 + 2Ge$	11.320
$Si_2Ge + SiGe_2 + Ge^+ + Ge$	11.338
$Si_2Ge + (SiGe_2)^+ + 2Ge$	11.387
$SiGe_2 + Si_2 + (Ge_2)^+ + Ge$	11.657
$Si_2Ge + SiGe + (Ge_2)^+ + Ge$	11.720
$SiGe_2 + (SiGe)^+ + SiGe + Ge$	11.802
$SiGe_2 + SiGe + (Ge_2)^+ + Si$	11.819
$Si_2Ge + (SiGe)^+ + Ge_2 + Ge$	11.836
$Si_2Ge + (Ge_2)^+ + Ge_2 + Si$	11.853
$SiGe_2 + (SiGe)^+ + Ge_2 + Si$	11.935
$SiGe_2 + Si_2 + Ge_2 + Ge^+$	11.938
$SiGe_2 + 2SiGe + Ge^+$	11.966
$(Si_2Ge)^+ + SiGe + Ge_2 + Ge$	11.982
$(SiGe_2)^+ + Si_2 + Ge_2 + Ge$	11.986
$Si_2Ge + SiGe + Ge_2 + Ge^+$	12.000
$(SiGe_2)^+ + 2SiGe + Ge$	12.015
$(Si_2Ge)^+ + 2Ge_2 + Si$	12.115

Table 4.181 – *Continued*

Fragmented Cluster	Fragmentation Energy (eV)
$(SiGe_2)^+ + SiGe + Ge_2 + Si$	12.148
$Si_2 + SiGe + (Ge_2)^+ + Ge_2$	12.320
$3SiGe + (Ge_2)^+$	12.348
$Si_2 + (SiGe)^+ + 2Ge_2$	12.436
$(SiGe)^+ + 2SiGe + Ge_2$	12.464
$(Si_3Ge)^+ + 4Ge$	13.560
$Si_3Ge + Ge^+ + 3Ge$	13.693
$(Si_2Ge_2)^+ + Si + 3Ge$	13.847
$Si_2Ge_2 + Si + Ge^+ + 2Ge$	13.961
$(SiGe_3)^+ + 2Si + 2Ge$	14.068
$SiGe_3 + 2Si + Ge^+ + Ge$	14.305
$Si_2Ge + (SiGe)^+ + 3Ge$	14.764
$Si_2Ge + (Ge_2)^+ + Si + 2Ge$	14.781
$SiGe_2 + (SiGe)^+ + Si + 2Ge$	14.863
$SiGe_2 + Si_2 + Ge^+ + 2Ge$	14.866
$SiGe_2 + (Ge_2)^+ + 2Si + Ge$	14.880
$(Si_2Ge)^+ + SiGe + 3Ge$	14.911
$(SiGe_2)^+ + Si_2 + 3Ge$	14.915
$Si_2Ge + SiGe + Ge^+ + 2Ge$	14.929
$SiGe_2 + SiGe + Si + Ge^+ + Ge$	15.027
$(Si_2Ge)^+ + Ge_2 + Si + 2Ge$	15.044
$Si_2Ge + Ge_2 + Si + Ge^+ + Ge$	15.062
$(SiGe_2)^+ + SiGe + Si + 2Ge$	15.076
$SiGe_2 + Ge_2 + 2Si + Ge^+$	15.160
$(SiGe_2)^+ + Ge_2 + 2Si + Ge$	15.209
$SiGe + Si_2 + (Ge_2)^+ + 2Ge$	15.248
$(SiGe)^+ + Si_2 + Ge_2 + 2Ge$	15.364
$Si_2 + (Ge_2)^+ + Ge_2 + Si + Ge$	15.381
$(SiGe)^+ + 2SiGe + 2Ge$	15.392
$2SiGe + (Ge_2)^+ + Si + Ge$	15.409

Table 4.181 – *Continued*

Fragmented Cluster	Fragmentation Energy (eV)
$(SiGe)^+ + SiGe + Ge_2 + Si + Ge$	15.525
$SiGe + Si_2 + Ge_2 + Ge^+ + Ge$	15.528
$SiGe + (Ge_2)^+ + Ge_2 + 2Si$	15.542
$3SiGe + Ge^+ + Ge$	15.557
$(SiGe)^+ + 2Ge_2 + 2Si$	15.658
$Si_2 + 2Ge_2 + Si + Ge^+$	15.661
$2SiGe + Ge_2 + Si + Ge^+$	15.690
$(Si_2Ge)^+ + Si + 4Ge$	17.972
$Si_2Ge + Si + Ge^+ + 3Ge$	17.990
$Si_2 + (SiGe)^+ + 4Ge$	18.293
$Si_2 + (Ge_2)^+ + Si + 3Ge$	18.309
$(SiGe)^+ + SiGe + Si + 3Ge$	18.454
$Si_2 + SiGe + Ge^+ + 3Ge$	18.457
$SiGe + (Ge_2)^+ + 2Si + 2Ge$	18.471
$(SiGe)^+ + Ge_2 + 2Si + 2Ge$	18.587
$Si_2 + Ge_2 + Si + Ge^+ + 2Ge$	18.590
$(Ge_2)^+ + Ge_2 + 3Si + Ge$	18.604
$2SiGe + Si + Ge^+ + 2Ge$	18.618
$SiGe + Ge_2 + 2Si + Ge^+ + Ge$	18.751
$2Ge_2 + 3Si + Ge^+$	18.884
$(SiGe)^+ + 2Si + 4Ge$	21.515
$Si_2 + Si + Ge^+ + 4Ge$	21.518
$(Ge_2)^+ + 3Si + 3Ge$	21.532
$SiGe + 2Si + Ge^+ + 3Ge$	21.680
$Ge_2 + 3Si + Ge^+ + 2Ge$	21.813
$3Si + Ge^+ + 4Ge$	24.741

Table 4.182 Fragmentation Energies for the Most Stable $(Si_3Ge_5)^-$ Octamer

Fragmented Cluster	Fragmentation Energy (eV)
$SiGe_3 + (Si_2Ge_2)^-$	2.756
$(SiGe_3)^- + Si_2Ge_2$	2.787
$(Si_3Ge_4)^- + Ge$	2.812
$(Si_2Ge_3)^- + SiGe_2$	3.024
$Si_2Ge_3 + (SiGe_2)^-$	3.116
$(Si_2Ge_5)^- + Si$	3.127
$(Si_3Ge_3)^- + Ge_2$	3.152
$Si_3Ge_3 + (Ge_2)^-$	3.183
$SiGe_4 + (Si_2Ge)^-$	3.271
$(SiGe_4)^- + Si_2Ge$	3.295
$Si_2Ge_4 + (SiGe)^-$	3.309
$(Si_2Ge_4)^- + SiGe$	3.329
$Si_3Ge_4 + Ge^-$	3.438
$(SiGe_5)^- + Si_2$	3.550
$(Si_3Ge_3)^- + 2Ge$	6.080
$(Si_2Ge_4)^- + Si + Ge$	6.391
$(Si_3Ge_2)^- + Ge_2 + Ge$	6.445
$Si_2Ge_2 + (SiGe_2)^- + Ge$	6.472
$(Si_2Ge_2)^- + SiGe_2 + Ge$	6.540
$SiGe_3 + (Si_2Ge)^- + Ge$	6.572
$(Si_2Ge_3)^- + SiGe + Ge$	6.614
$(Si_2Ge_3)^- + Ge_2 + Si$	6.747
$(SiGe_5)^- + 2Si$	6.772
$Si_3Ge_3 + Ge^- + Ge$	6.789
$Si_3Ge_2 + (Ge_2)^- + Ge$	6.808
$SiGe_3 + (SiGe_2)^- + Si$	6.816
$(SiGe_3)^- + Si_2Ge + Ge$	6.817
$(SiGe_4)^- + Si_2 + Ge$	6.823
$Si_2Ge_3 + (SiGe)^- + Ge$	6.895
$(SiGe_3)^- + SiGe_2 + Si$	6.915

Table 4.181 – *Continued*

Fragmented Cluster	Fragmentation Energy (eV)
$(SiGe_4)^-$ + SiGe + Si	6.984
$(Si_3Ge)^-$ + $2Ge_2$	7.044
Si_2Ge_3 + $(Ge_2)^-$ + Si	7.057
Si_2Ge_4 + Si + Ge^-	7.077
$(Si_2Ge_2)^-$ + SiGe + Ge_2	7.203
Si_3Ge + $(Ge_2)^-$ + Ge_2	7.217
$SiGe_4$ + $(SiGe)^-$ + Si	7.295
Si_2Ge_2 + $(SiGe)^-$ + Ge_2	7.323
Si_2Ge_2 + SiGe + $(Ge_2)^-$	7.352
Si_2Ge_2 + $SiGe_2$ + Ge^-	7.368
$(SiGe_3)^-$ + Si_2 + Ge_2	7.416
$(Si_2Ge)^-$ + $SiGe_2$ + Ge_2	7.427
$(SiGe_3)^-$ + 2SiGe	7.445
Si_3Ge_2 + Ge_2 + Ge^-	7.486
$SiGe_3$ + $(SiGe)^-$ + SiGe	7.534
$SiGe_3$ + Si_2 + $(Ge_2)^-$	7.535
Si_2Ge + $(SiGe_2)^-$ + Ge_2	7.573
Si_2Ge_3 + SiGe + Ge^-	7.602
$SiGe_3$ + Si_2Ge + Ge^-	7.613
Si_2Ge + $SiGe_2$ + $(Ge_2)^-$	7.791
$SiGe_4$ + Si_2 + Ge^-	7.841
$(Si_3Ge_2)^-$ + 3Ge	9.373
$(Si_2Ge_3)^-$ + Si + 2Ge	9.676
$(Si_3Ge)^-$ + Ge_2 + 2Ge	9.973
$(SiGe_4)^-$ + 2Si + Ge	10.045
Si_3Ge + $(Ge_2)^-$ + 2Ge	10.146
$(Si_2Ge_2)^-$ + Ge_2 + Si + Ge	10.264
$(SiGe_3)^-$ + Si_2 + 2Ge	10.345
$(Si_2Ge)^-$ + $SiGe_2$ + 2Ge	10.356
Si_2Ge_2 + $(Ge_2)^-$ + Si + Ge	10.414

Table 4.181 – *Continued*

Fragmented Cluster	Fragmentation Energy (eV)
$Si_3Ge_2 + Ge^- + 2Ge$	10.414
$Si_2Ge + (SiGe_2)^- + 2Ge$	10.501
$(SiGe_3)^- + SiGe + Si + Ge$	10.506
$SiGe_3 + (SiGe)^- + Si + Ge$	10.595
$(SiGe_3)^- + Ge_2 + 2Si$	10.639
$Si_2Ge_3 + Si + Ge^- + Ge$	10.664
$SiGe_3 + (Ge_2)^- + 2Si$	10.758
$Si_3Ge + Ge_2 + Ge^- + Ge$	10.824
$(Si_2Ge)^- + SiGe + Ge_2 + Ge$	11.018
$SiGe_4 + 2Si + Ge^-$	11.063
$Si_2Ge_2 + Ge_2 + Si + Ge^-$	11.091
$(SiGe_2)^- + Si_2 + Ge_2 + Ge$	11.101
$(SiGe_2)^- + 2SiGe + Ge$	11.129
$SiGe_3 + Si_2 + Ge^- + Ge$	11.141
$(Si_2Ge)^- + 2Ge_2 + Si$	11.151
$(SiGe_2)^- + SiGe + Ge_2 + Si$	11.262
$SiGe_3 + SiGe + Si + Ge^-$	11.302
$SiGe_2 + (SiGe)^- + SiGe + Ge$	11.318
$SiGe_2 + Si_2 + (Ge_2)^- + Ge$	11.319
$Si_2Ge + (SiGe)^- + Ge_2 + Ge$	11.352
$Si_2Ge + SiGe + (Ge_2)^- + Ge$	11.382
$Si_2Ge + SiGe_2 + Ge^- + Ge$	11.397
$SiGe_2 + (SiGe)^- + Ge_2 + Si$	11.451
$SiGe_2 + SiGe + (Ge_2)^- + Si$	11.480
$Si_2Ge + (Ge_2)^- + Ge_2 + Si$	11.515
$Si_2 + (SiGe)^- + 2Ge_2$	11.952
$(SiGe)^- + 2SiGe + Ge_2$	11.980
$Si_2 + SiGe + (Ge_2)^- + Ge_2$	11.981
$SiGe_2 + Si_2 + Ge_2 + Ge^-$	11.997
$3SiGe + (Ge_2)^-$	12.010

Table 4.181 – *Continued*

Fragmented Cluster	Fragmentation Energy (eV)
$SiGe_2 + 2SiGe + Ge^-$	12.025
$Si_2Ge + SiGe + Ge_2 + Ge^-$	12.059
$(Si_3Ge)^- + 4Ge$	12.901
$(Si_2Ge_2)^- + Si + 3Ge$	13.192
$(SiGe_3)^- + 2Si + 2Ge$	13.568
$Si_3Ge + Ge^- + 3Ge$	13.752
$(Si_2Ge)^- + SiGe + 3Ge$	13.947
$Si_2Ge_2 + Si + Ge^- + 2Ge$	14.020
$(SiGe_2)^- + Si_2 + 3Ge$	14.030
$(Si_2Ge)^- + Ge_2 + Si + 2Ge$	14.080
$(SiGe_2)^- + SiGe + Si + 2Ge$	14.191
$Si_2Ge + (SiGe)^- + 3Ge$	14.281
$(SiGe_2)^- + Ge_2 + 2Si + Ge$	14.324
$SiGe_3 + 2Si + Ge^- + Ge$	14.364
$SiGe_2 + (SiGe)^- + Si + 2Ge$	14.379
$Si_2Ge + (Ge_2)^- + Si + 2Ge$	14.443
$SiGe_2 + (Ge_2)^- + 2Si + Ge$	14.542
$(SiGe)^- + Si_2 + Ge_2 + 2Ge$	14.880
$(SiGe)^- + 2SiGe + 2Ge$	14.909
$SiGe + Si_2 + (Ge_2)^- + 2Ge$	14.910
$SiGe_2 + Si_2 + Ge^- + 2Ge$	14.925
$Si_2Ge + SiGe + Ge^- + 2Ge$	14.988
$(SiGe)^- + SiGe + Ge_2 + Si + Ge$	15.042
$Si_2 + (Ge_2)^- + Ge_2 + Si + Ge$	15.043
$2SiGe + (Ge_2)^- + Si + Ge$	15.071
$SiGe_2 + SiGe + Si + Ge^- + Ge$	15.087
$Si_2Ge + Ge_2 + Si + Ge^- + Ge$	15.121
$(SiGe)^- + 2Ge_2 + 2Si$	15.175
$SiGe + (Ge_2)^- + Ge_2 + 2Si$	15.204
$SiGe_2 + Ge_2 + 2Si + Ge^-$	15.220

Table 4.181 – *Continued*

Fragmented Cluster	Fragmentation Energy (eV)
$SiGe + Si_2 + Ge_2 + Ge^- + Ge$	15.588
$3SiGe + Ge^- + Ge$	15.616
$Si_2 + 2Ge_2 + Si + Ge^-$	15.721
$2SiGe + Ge_2 + Si + Ge^-$	15.749
$(Si_2Ge)^- + Si + 4Ge$	17.008
$Si_2 + (SiGe)^- + 4Ge$	17.809
$(SiGe)^- + SiGe + Si + 3Ge$	17.970
$Si_2 + (Ge_2)^- + Si + 3Ge$	17.971
$Si_2Ge + Si + Ge^- + 3Ge$	18.049
$(SiGe)^- + Ge_2 + 2Si + 2Ge$	18.103
$SiGe + (Ge_2)^- + 2Si + 2Ge$	18.133
$(Ge_2)^- + Ge_2 + 3Si + Ge$	18.265
$Si_2 + SiGe + Ge^- + 3Ge$	18.516
$Si_2 + Ge_2 + Si + Ge^- + 2Ge$	18.649
$2SiGe + Si + Ge^- + 2Ge$	18.677
$SiGe + Ge_2 + 2Si + Ge^- + Ge$	18.810
$2Ge_2 + 3Si + Ge^-$	18.943
$(SiGe)^- + 2Si + 4Ge$	21.032
$(Ge_2)^- + 3Si + 3Ge$	21.194
$Si_2 + Si + Ge^- + 4Ge$	21.577
$SiGe + 2Si + Ge^- + 3Ge$	21.739
$Ge_2 + 3Si + Ge^- + 2Ge$	21.872
$3Si + Ge^- + 4Ge$	24.800

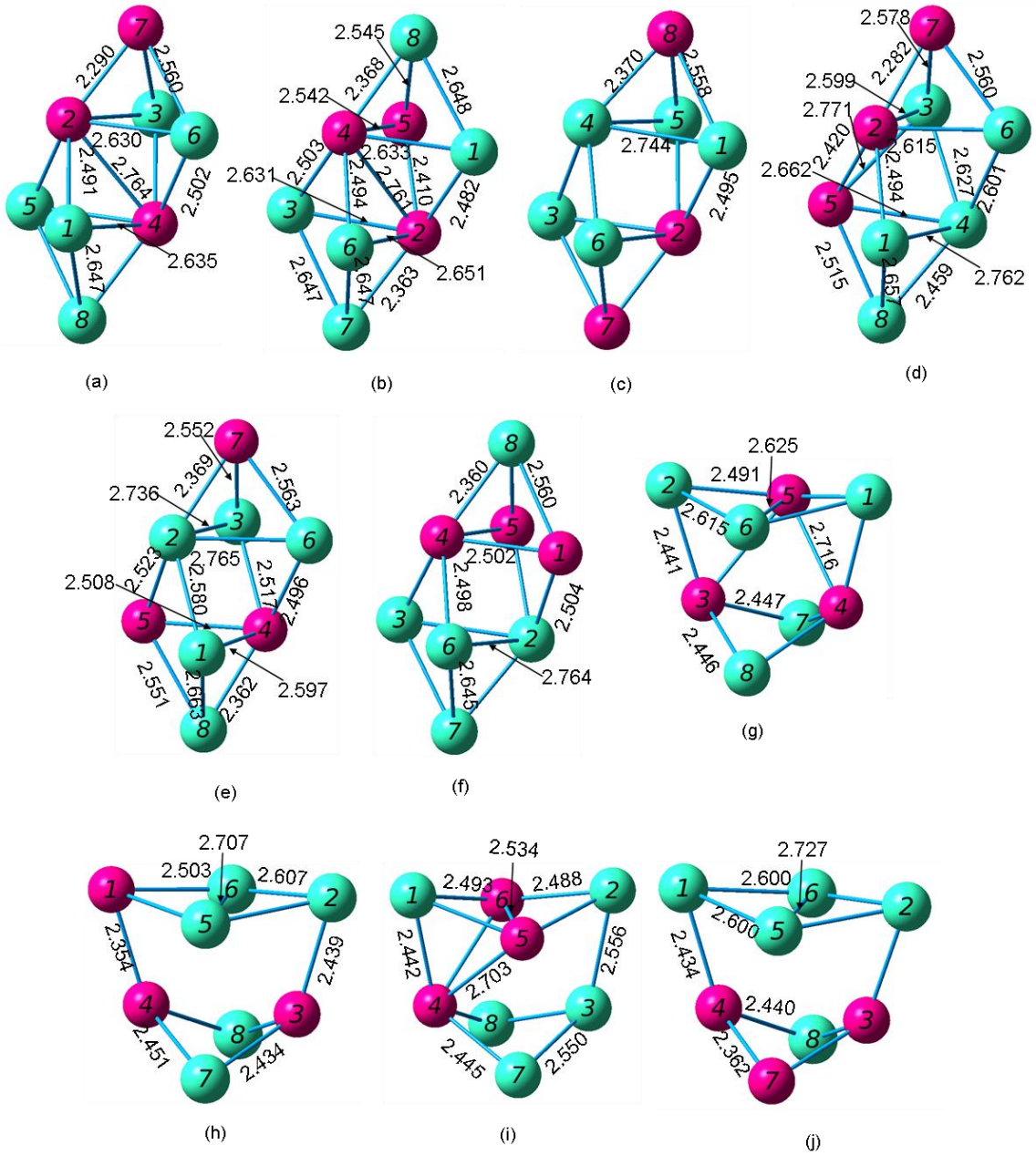

Figure 4.148 Geometries of the Si_3Ge_5 Neutral Septamers from (a) Most Stable through (j) Least Stable

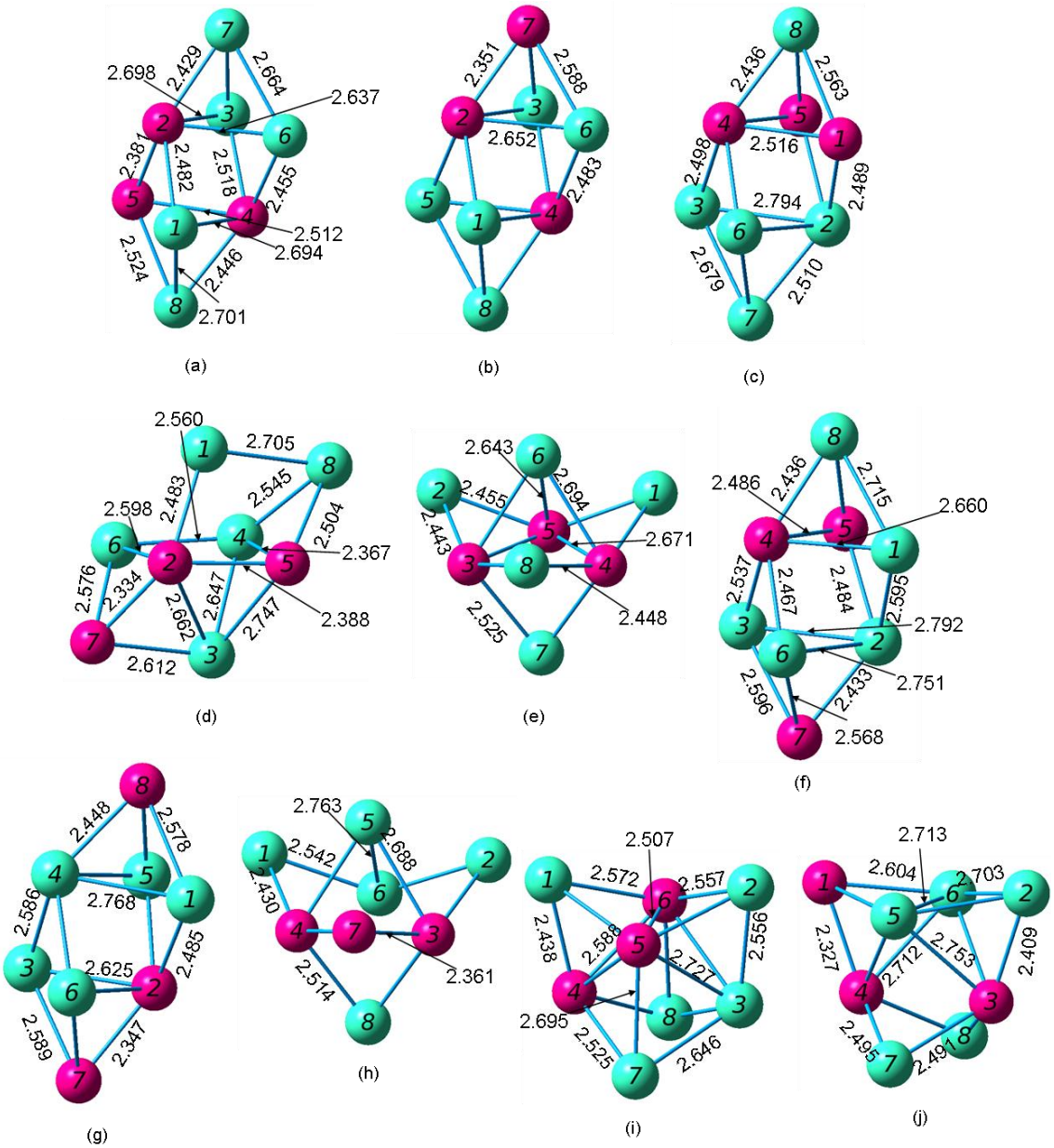

Figure 4.149 Geometries of the $(Si_3Ge_5)^+$ Cationic Septamers from (a) Most Stable through (j) Least Stable

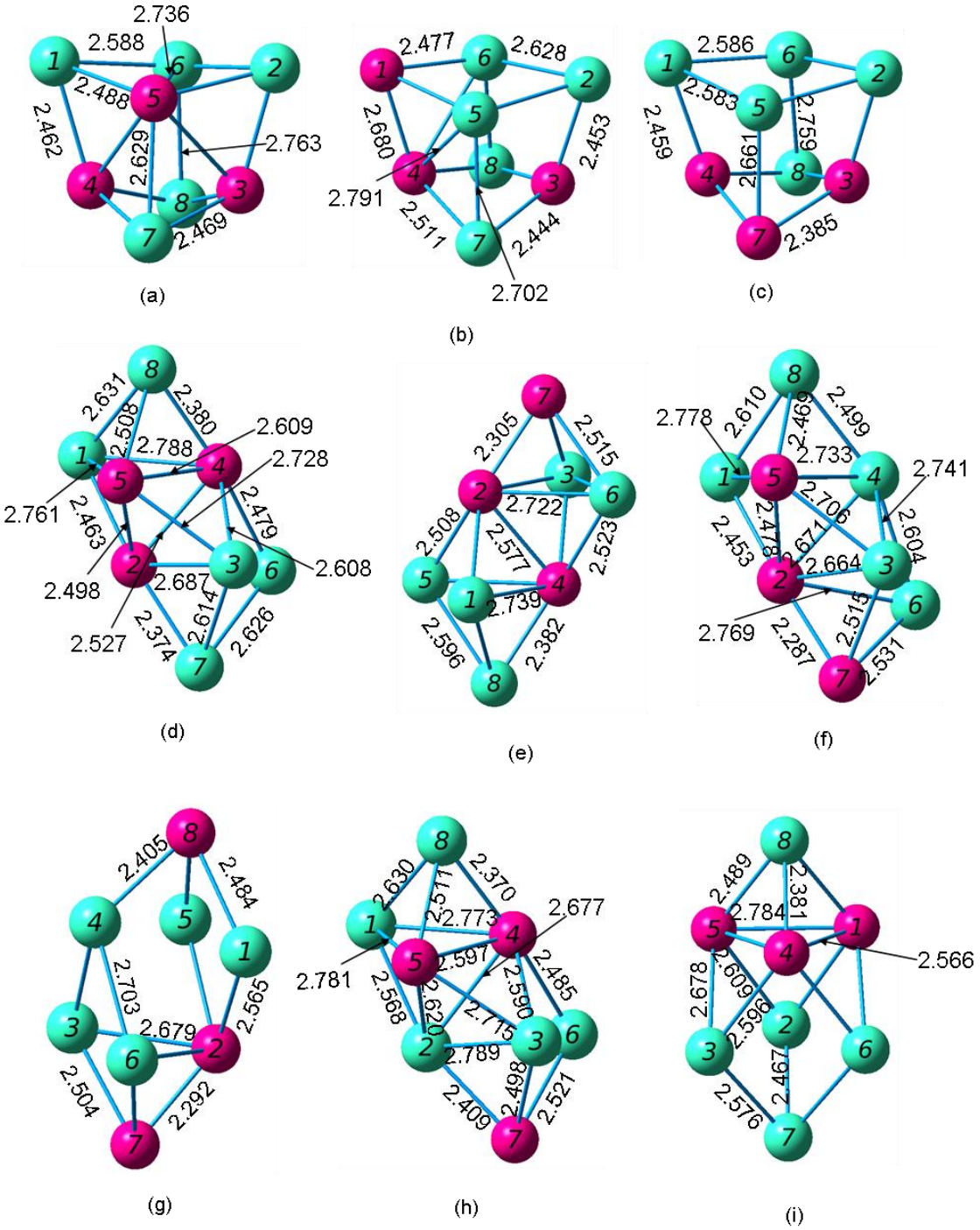

Figure 4.150 Geometries of the $(Si_3Ge_5)^-$ Anionic Septamers from (a) Most Stable through (i) Least Stable

4.27 Si_2Ge_6 Octamers

Wang and Chao [51] reported a rhombic cube for the neutral and cation Si_2Ge_6 octamers. The neutral cluster has a ^1A electronic state, a dissociation energy of -32.0791 eV or -32.2503 eV, a HOMO-LUMO gap of 2.62 eV, and the following frequencies: 415(a), 287(a), and 192(a). Their anion cluster is again similar to our most stable anion.

Totally, we investigated twenty-one Si_2Ge_6 clusters. The difference in binding energy per atom between our most stable cluster and our thirty-eighth most stable cluster was 0.1327 eV. Here, we report the properties of ten neutrals and cations and nine anions.

Table 4.183 Properties of the Si_2Ge_6 Octamers

Figure	Symmetry Group	Electronic State	Binding E / Atom (eV)	HOMO-LUMO Gap (eV)	Dipole Moment (D)
4.151 (a)	C_1	^1A	2.942	2.625	0.002
4.151 (b)	C_1	^1A	2.908	2.465	0.443
4.151 (c)	C_1	^1A	2.903	2.478	0.385
4.151 (d)	C_1	^1A	2.902	2.394	0.499
4.151 (e)	C_s	$^1A'$	2.880	2.083	0.118
4.151 (f)	C_1	^1A	2.866	1.988	0.417
4.151 (g)	C_s	$^1A'$	2.862	1.707	0.341
4.151 (h)	C_1	^1A	2.859	2.106	0.572
4.151 (i)	C_1	^1A	2.855	2.105	0.570
4.151 (j)	C_s	$^1A'$	2.853	1.958	0.643

Table 4.184 Properties of the $(Si_2Ge_6)^+$ Octamers

Figure	Symmetry Group	Electronic State	Binding E / Atom (eV)	HOMO-LUMO Gap (eV)	Dipole Moment (D)
4.152 (a)	C_1	^2A	3.056	1.296[a]	0.000
4.152 (b)	C_1	^2A	3.031	1.337[a]	0.576
4.152 (c)	C_1	^2A	3.022	1.297[a]	0.789
4.152 (d)	C_s	$^2A'$	3.019	1.340[a]	0.572
4.152 (e)	C_1	^2A	3.017	1.302[a]	0.456
4.152 (f)	C_1	^2A	3.013	1.529[a]	0.666
4.152 (g)	C_s	$^2A''$	2.991	1.327[a]	0.763
4.152 (h)	C_1	^2A	2.982	1.576[a]	0.897
4.152 (i)	C_s	$^2A''$	2.974	1.345[a]	0.432
4.152 (j)	C_1	^2A	2.955	1.346[a]	0.331

[a] HOMO and LUMO have opposite spins; this value includes the energy required to flip the spin of the electron.

Table 4.185 Properties of the $(Si_2Ge_6)^-$ Octamers

Figure	Symmetry Group	Electronic State	Binding E / Atom (eV)	HOMO-LUMO Gap (eV)	Dipole Moment (D)
4.153 (a)	C_s	$^2A'$	3.051	1.375[a]	0.764
4.153 (b)	C_1	^2A	3.037	1.391[a]	0.615
4.153 (c)	C_s	$^2A'$	3.036	1.388[a]	1.140
4.153 (d)	C_1	^2A	3.035	1.370[a]	1.585
4.153 (e)	C_1	^2A	3.029	1.336[a]	0.001
4.153 (f)	C_1	^2A	3.016	1.395[a]	0.953
4.153 (g)	C_1	^2A	3.014	1.350[a]	1.785
4.153 (h)	C_1	^2A	3.009	1.362[a]	1.180
4.153 (i)	C_s	$^2A''$	3.002	1.265[a]	1.018

[a] HOMO and LUMO have opposite spins; this value includes the energy required to flip the spin of the electron.

Table 4.186 Ionization Potentials and Electron Affinities of the Si_2Ge_6 Octamers

Neutral Figure	VIP (eV)	Cationic Figure	AIP (eV)	VEA (eV)	Anionic Figure	AEA (eV)
4.151 (a)	7.083	4.152 (a)	6.992	1.503	4.153 (e)	1.835
4.151 (b)	7.113	4.152 (c)	6.993	1.628	4.153 (g)	1.981
4.151 (c)	7.104	4.152 (e)	6.993	1.647	4.153 (h)	1.985
4.151 (d)	7.023	4.152 (b)	6.875	1.619	4.153 (f)	2.049
4.151 (e)	7.188	4.152 (g)	7.012	2.061	4.153 (a)	2.504
4.151 (f)	7.207	4.152 (f)	6.722	2.135	4.153 (a)	2.619
4.151 (g)	6.745	4.152 (d)	6.641	2.032	4.153 (i)	2.261
4.151 (h)	7.303	4.152 (h)	6.916	2.143	4.153 (d)	2.547
4.151 (i)	7.278	4.152 (j)	7.101	2.154	4.153 (b)	2.597
4.151 (j)	7.179	4.152 (i)	6.931	2.186	4.153 (c)	2.605

Table 4.187 Fragmentation Energies for the Most Stable Si_2Ge_6 Octamer

Fragmented Cluster	Fragmentation Energy (eV)
$Si_2Ge_5 + Ge$	2.473
$2SiGe_3$	2.665
$SiGe_6 + Si$	2.858
$Si_2Ge_4 + Ge_2$	2.886
$SiGe_4 + SiGe_2$	3.149
$SiGe_5 + SiGe$	3.214
$Si_2Ge_4 + 2Ge$	5.815
$SiGe_5 + Si + Ge$	6.276
$Si_2Ge_3 + Ge_2 + Ge$	6.473
$SiGe_4 + SiGe + Ge$	6.740
$SiGe_4 + Ge_2 + Si$	6.873
$Si_2Ge_2 + 2Ge_2$	6.901
$SiGe_3 + SiGe + Ge_2$	7.112
$2SiGe_2 + Ge_2$	7.305
$Si_2Ge_3 + 3Ge$	9.401
$SiGe_4 + Si + 2Ge$	9.801
$Si_2Ge_2 + Ge_2 + 2Ge$	9.829
$SiGe_3 + SiGe + 2Ge$	10.040
$SiGe_3 + Ge_2 + Si + Ge$	10.173
$2SiGe_2 + 2Ge$	10.233
$SiGe_2 + SiGe + Ge_2 + Ge$	10.896
$Si_2Ge + 2Ge_2 + Ge$	10.930
$SiGe_2 + 2Ge_2 + Si$	11.029
$Si_2 + 3Ge_2$	11.530
$2SiGe + 2Ge_2$	11.558
$Si_2Ge_2 + 4Ge$	12.758
$SiGe_3 + Si + 3Ge$	13.102
$SiGe_2 + SiGe + 3Ge$	13.824
$Si_2Ge + Ge_2 + 3Ge$	13.859
$SiGe_2 + Ge_2 + Si + 2Ge$	13.957

Table 4.187 – *Continued*

Fragmented Cluster	Fragmentation Energy (eV)
$Si_2 + 2Ge_2 + 2Ge$	14.458
$2SiGe + Ge_2 + 2Ge$	14.487
$SiGe + 2Ge_2 + Si + Ge$	14.620
$3Ge_2 + 2Si$	14.752
$Si_2Ge + 5Ge$	16.787
$SiGe_2 + Si + 4Ge$	16.886
$SiGe + Ge_2 + Si + 3Ge$	17.548
$2Ge_2 + 2Si + 2Ge$	17.681
$Si_2 + 6Ge$	20.315
$Ge_2 + 2Si + 4Ge$	20.609
$2Si + 6Ge$	23.538

Table 4.188 Fragmentation Energies for the Most Stable $(Si_2Ge_6)^+$ Octamer

Fragmented Cluster	Fragmentation Energy (eV)
$(Si_2Ge_5)^+ + Ge$	2.953
$(SiGe_3)^+ + SiGe_3$	3.337
$(SiGe_6)^+ + Si$	3.374
$Si_2Ge_5 + Ge^+$	3.380
$(Si_2Ge_4)^+ + Ge_2$	3.475
$Si_2Ge_4 + (Ge_2)^+$	3.514
$(SiGe_5)^+ + SiGe$	3.710
$(SiGe_4)^+ + SiGe_2$	3.934
$SiGe_5 + (SiGe)^+$	3.958
$SiGe_4 + (SiGe_2)^+$	4.105
$(Si_2Ge_4)^+ + 2Ge$	6.404
$Si_2Ge_4 + Ge^+ + Ge$	6.723
$(SiGe_5)^+ + Si + Ge$	6.771
$Si_2Ge_3 + (Ge_2)^+ + Ge$	7.100
$SiGe_5 + Si + Ge^+$	7.183
$(Si_2Ge_3)^+ + Ge_2 + Ge$	7.312
$Si_2Ge_3 + Ge_2 + Ge^+$	7.381
$SiGe_4 + (SiGe)^+ + Ge$	7.483
$SiGe_4 + (Ge_2)^+ + Si$	7.500
$(SiGe_4)^+ + SiGe + Ge$	7.525
$Si_2Ge_2 + (Ge_2)^+ + Ge_2$	7.528
$SiGe_4 + SiGe + Ge^+$	7.648
$(SiGe_4)^+ + Ge_2 + Si$	7.658
$(Si_2Ge_2)^+ + 2Ge_2$	7.695
$SiGe_3 + SiGe + (Ge_2)^+$	7.739
$(SiGe_3)^+ + SiGe + Ge_2$	7.783
$SiGe_3 + (SiGe)^+ + Ge_2$	7.855
$2SiGe_2 + (Ge_2)^+$	7.932
$(SiGe_2)^+ + SiGe_2 + Ge_2$	8.261
$(Si_2Ge_3)^+ + 3Ge$	10.240

Table 4.188 – *Continued*

Fragmented Cluster	Fragmentation Energy (eV)
$Si_2Ge_3 + Ge^+ + 2Ge$	10.309
$Si_2Ge_2 + (Ge_2)^+ + 2Ge$	10.457
$(SiGe_4)^+ + Si + 2Ge$	10.587
$(Si_2Ge_2)^+ + Ge_2 + 2Ge$	10.624
$SiGe_4 + Si + Ge^+ + Ge$	10.709
$(SiGe_3)^+ + SiGe + 2Ge$	10.711
$Si_2Ge_2 + Ge_2 + Ge^+ + Ge$	10.737
$SiGe_3 + (SiGe)^+ + 2Ge$	10.784
$SiGe_3 + (Ge_2)^+ + Si + Ge$	10.801
$(SiGe_3)^+ + Ge_2 + Si + Ge$	10.844
$SiGe_3 + SiGe + Ge^+ + Ge$	10.948
$SiGe_3 + Ge_2 + Si + Ge^+$	11.081
$2SiGe_2 + Ge^+ + Ge$	11.141
$(SiGe_2)^+ + SiGe_2 + 2Ge$	11.190
$SiGe_2 + SiGe + (Ge_2)^+ + Ge$	11.523
$Si_2Ge + (Ge_2)^+ + Ge_2 + Ge$	11.558
$SiGe_2 + (SiGe)^+ + Ge_2 + Ge$	11.639
$SiGe_2 + (Ge_2)^+ + Ge_2 + Si$	11.656
$SiGe_2 + SiGe + Ge_2 + Ge^+$	11.804
$(Si_2Ge)^+ + 2Ge_2 + Ge$	11.820
$Si_2Ge + 2Ge_2 + Ge^+$	11.838
$(SiGe_2)^+ + SiGe + Ge_2 + Ge$	11.852
$(SiGe_2)^+ + 2Ge_2 + Si$	11.985
$Si_2 + (Ge_2)^+ + 2Ge_2$	12.157
$2SiGe + (Ge_2)^+ + Ge_2$	12.186
$(SiGe)^+ + SiGe + 2Ge_2$	12.302
$(Si_2Ge_2)^+ + 4Ge$	13.552
$Si_2Ge_2 + Ge^+ + 3Ge$	13.665
$(SiGe_3)^+ + Si + 3Ge$	13.773
$SiGe_3 + Si + Ge^+ + 2Ge$	14.010

Table 4.188 – *Continued*

Fragmented Cluster	Fragmentation Energy (eV)
$Si_2Ge + (Ge_2)^+ + 3Ge$	14.486
$SiGe_2 + (SiGe)^+ + 3Ge$	14.568
$SiGe_2 + (Ge_2)^+ + Si + 2Ge$	14.585
$SiGe_2 + SiGe + Ge^+ + 2Ge$	14.732
$(Si_2Ge)^+ + Ge_2 + 3Ge$	14.749
$Si_2Ge + Ge_2 + Ge^+ + 2Ge$	14.766
$(SiGe_2)^+ + SiGe + 3Ge$	14.781
$SiGe_2 + Ge_2 + Si + Ge^+ + Ge$	14.865
$(SiGe_2)^+ + Ge_2 + Si + 2Ge$	14.914
$Si_2 + (Ge_2)^+ + Ge_2 + 2Ge$	15.086
$2SiGe + (Ge_2)^+ + 2Ge$	15.114
$(SiGe)^+ + SiGe + Ge_2 + 2Ge$	15.230
$SiGe + (Ge_2)^+ + Ge_2 + Si + Ge$	15.247
$(SiGe)^+ + 2Ge_2 + Si + Ge$	15.363
$Si_2 + 2Ge_2 + Ge^+ + Ge$	15.366
$(Ge_2)^+ + 2Ge_2 + 2Si$	15.380
$2SiGe + Ge_2 + Ge^+ + Ge$	15.394
$SiGe + 2Ge_2 + Si + Ge^+$	15.527
$(Si_2Ge)^+ + 5Ge$	17.677
$Si_2Ge + Ge^+ + 4Ge$	17.695
$SiGe_2 + Si + Ge^+ + 3Ge$	17.794
$(SiGe_2)^+ + Si + 4Ge$	17.842
$SiGe + (Ge_2)^+ + Si + 3Ge$	18.175
$(SiGe)^+ + Ge_2 + Si + 3Ge$	18.292
$(Ge_2)^+ + Ge_2 + 2Si + 2Ge$	18.308
$SiGe + Ge_2 + Si + Ge^+ + 2Ge$	18.456
$2Ge_2 + 2Si + Ge^+ + Ge$	18.589
$Si_2 + Ge^+ + 5Ge$	21.223
$(Ge_2)^+ + 2Si + 4Ge$	21.237
$Ge_2 + 2Si + Ge^+ + 3Ge$	21.517
$2Si + Ge^+ + 5Ge$	24.446

Table 4.189 Fragmentation Energies for the Most Stable $(Si_2Ge_6)^-$ Octamer

Fragmented Cluster	Fragmentation Energy (eV)
$(Si_2Ge_5)^- + Ge$	2.734
$(SiGe_3)^- + SiGe_3$	2.739
$(SiGe_4)^- + SiGe_2$	3.000
$(SiGe_6)^- + Si$	3.031
$(Si_2Ge_4)^- + Ge_2$	3.069
$Si_2Ge_4 + (Ge_2)^-$	3.078
$SiGe_4 + (SiGe_2)^-$	3.123
$(SiGe_5)^- + SiGe$	3.318
$Si_2Ge_5 + Ge^-$	3.342
$SiGe_5 + (SiGe)^-$	3.377
$(Si_2Ge_4)^- + 2Ge$	5.998
$(Si_2Ge_3)^- + Ge_2 + Ge$	6.355
$(SiGe_5)^- + Si + Ge$	6.380
$(SiGe_4)^- + SiGe + Ge$	6.591
$Si_2Ge_3 + (Ge_2)^- + Ge$	6.665
$Si_2Ge_4 + Ge^- + Ge$	6.685
$(SiGe_4)^- + Ge_2 + Si$	6.724
$SiGe_4 + (SiGe)^- + Ge$	6.902
$(Si_2Ge_2)^- + 2Ge_2$	6.943
$SiGe_4 + (Ge_2)^- + Si$	7.065
$Si_2Ge_2 + (Ge_2)^- + Ge_2$	7.092
$SiGe_5 + Si + Ge^-$	7.145
$(SiGe_3)^- + SiGe + Ge_2$	7.185
$SiGe_3 + (SiGe)^- + Ge_2$	7.274
$(SiGe_2)^- + SiGe_2 + Ge_2$	7.279
$SiGe_3 + SiGe + (Ge_2)^-$	7.304
$Si_2Ge_3 + Ge_2 + Ge^-$	7.343
$2SiGe_2 + (Ge_2)^-$	7.497
$SiGe_4 + SiGe + Ge^-$	7.609
$(Si_2Ge_3)^- + 3Ge$	9.283

Table 4.189 – *Continued*

Fragmented Cluster	Fragmentation Energy (eV)
$(SiGe_4)^-$ + Si + 2Ge	9.653
$(Si_2Ge_2)^-$ + Ge_2 + 2Ge	9.871
Si_2Ge_2 + $(Ge_2)^-$ + 2Ge	10.021
$(SiGe_3)^-$ + SiGe + 2Ge	10.113
$SiGe_3$ + $(SiGe)^-$ + 2Ge	10.203
$(SiGe_2)^-$ + $SiGe_2$ + 2Ge	10.207
$(SiGe_3)^-$ + Ge_2 + Si + Ge	10.246
Si_2Ge_3 + Ge^- + 2Ge	10.271
$SiGe_3$ + $(Ge_2)^-$ + Si + Ge	10.365
$SiGe_4$ + Si + Ge^- + Ge	10.671
Si_2Ge_2 + Ge_2 + Ge^- + Ge	10.699
$(Si_2Ge)^-$ + $2Ge_2$ + Ge	10.758
$(SiGe_2)^-$ + SiGe + Ge_2 + Ge	10.870
$SiGe_3$ + SiGe + Ge^- + Ge	10.910
$(SiGe_2)^-$ + $2Ge_2$ + Si	11.003
$SiGe_3$ + Ge_2 + Si + Ge^-	11.043
$SiGe_2$ + $(SiGe)^-$ + Ge_2 + Ge	11.058
$SiGe_2$ + SiGe + $(Ge_2)^-$ + Ge	11.088
$2SiGe_2$ + Ge^- + Ge	11.103
Si_2Ge + $(Ge_2)^-$ + Ge_2 + Ge	11.122
$SiGe_2$ + $(Ge_2)^-$ + Ge_2 + Si	11.221
$(SiGe)^-$ + SiGe + $2Ge_2$	11.721
Si_2 + $(Ge_2)^-$ + $2Ge_2$	11.722
2SiGe + $(Ge_2)^-$ + Ge_2	11.750
$SiGe_2$ + SiGe + Ge_2 + Ge^-	11.765
Si_2Ge + $2Ge_2$ + Ge^-	11.800
$(Si_2Ge_2)^-$ + 4Ge	12.800
$(SiGe_3)^-$ + Si + 3Ge	13.175
Si_2Ge_2 + Ge^- + 3Ge	13.627
$(Si_2Ge)^-$ + Ge_2 + 3Ge	13.687

Table 4.189 – *Continued*

Fragmented Cluster	Fragmentation Energy (eV)
$(SiGe_2)^-$ + SiGe + 3Ge	13.798
$(SiGe_2)^-$ + Ge_2 + Si + 2Ge	13.931
$SiGe_3$ + Si + Ge^- + 2Ge	13.971
$SiGe_2$ + $(SiGe)^-$ + 3Ge	13.987
Si_2Ge + $(Ge_2)^-$ + 3Ge	14.050
$SiGe_2$ + $(Ge_2)^-$ + Si + 2Ge	14.149
$(SiGe)^-$ + SiGe + Ge_2 + 2Ge	14.649
Si_2 + $(Ge_2)^-$ + Ge_2 + 2Ge	14.650
2SiGe + $(Ge_2)^-$ + 2Ge	14.678
$SiGe_2$ + SiGe + Ge^- + 2Ge	14.694
Si_2Ge + Ge_2 + Ge^- + 2Ge	14.728
$(SiGe)^-$ + $2Ge_2$ + Si + Ge	14.782
SiGe + $(Ge_2)^-$ + Ge_2 + Si + Ge	14.811
$SiGe_2$ + Ge_2 + Si + Ge^- + Ge	14.827
$(Ge_2)^-$ + $2Ge_2$ + 2Si	14.944
Si_2 + $2Ge_2$ + Ge^- + Ge	15.328
2SiGe + Ge_2 + Ge^- + Ge	15.356
SiGe + $2Ge_2$ + Si + Ge^-	15.489
$(Si_2Ge)^-$ + 5Ge	16.615
$(SiGe_2)^-$ + Si + 4Ge	16.860
Si_2Ge + Ge^- + 4Ge	17.657
$(SiGe)^-$ + Ge_2 + Si + 3Ge	17.711
SiGe + $(Ge_2)^-$ + Si + 3Ge	17.740
$SiGe_2$ + Si + Ge^- + 3Ge	17.755
$(Ge_2)^-$ + Ge_2 + 2Si + 2Ge	17.873
SiGe + Ge_2 + Si + Ge^- + 2Ge	18.418
$2Ge_2$ + 2Si + Ge^- + Ge	18.551
$(Ge_2)^-$ + 2Si + 4Ge	20.801
Si_2 + Ge^- + 5Ge	21.185
Ge_2 + 2Si + Ge^- + 3Ge	21.479
2Si + Ge^- + 5Ge	24.408

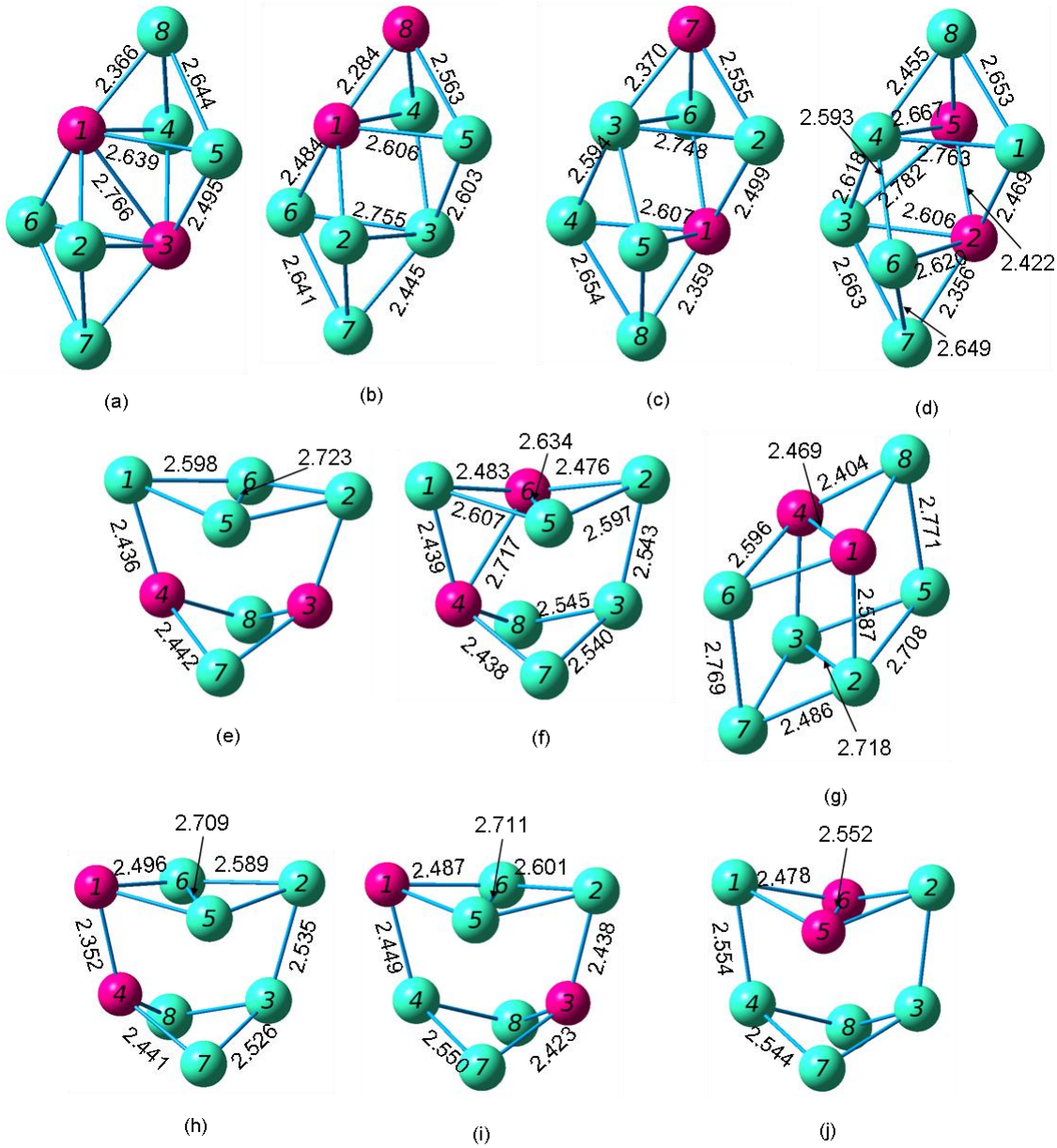

Figure 4.151 Geometries of the Si_2Ge_6 Neutral Septamers from (a) Most Stable through (j) Least Stable

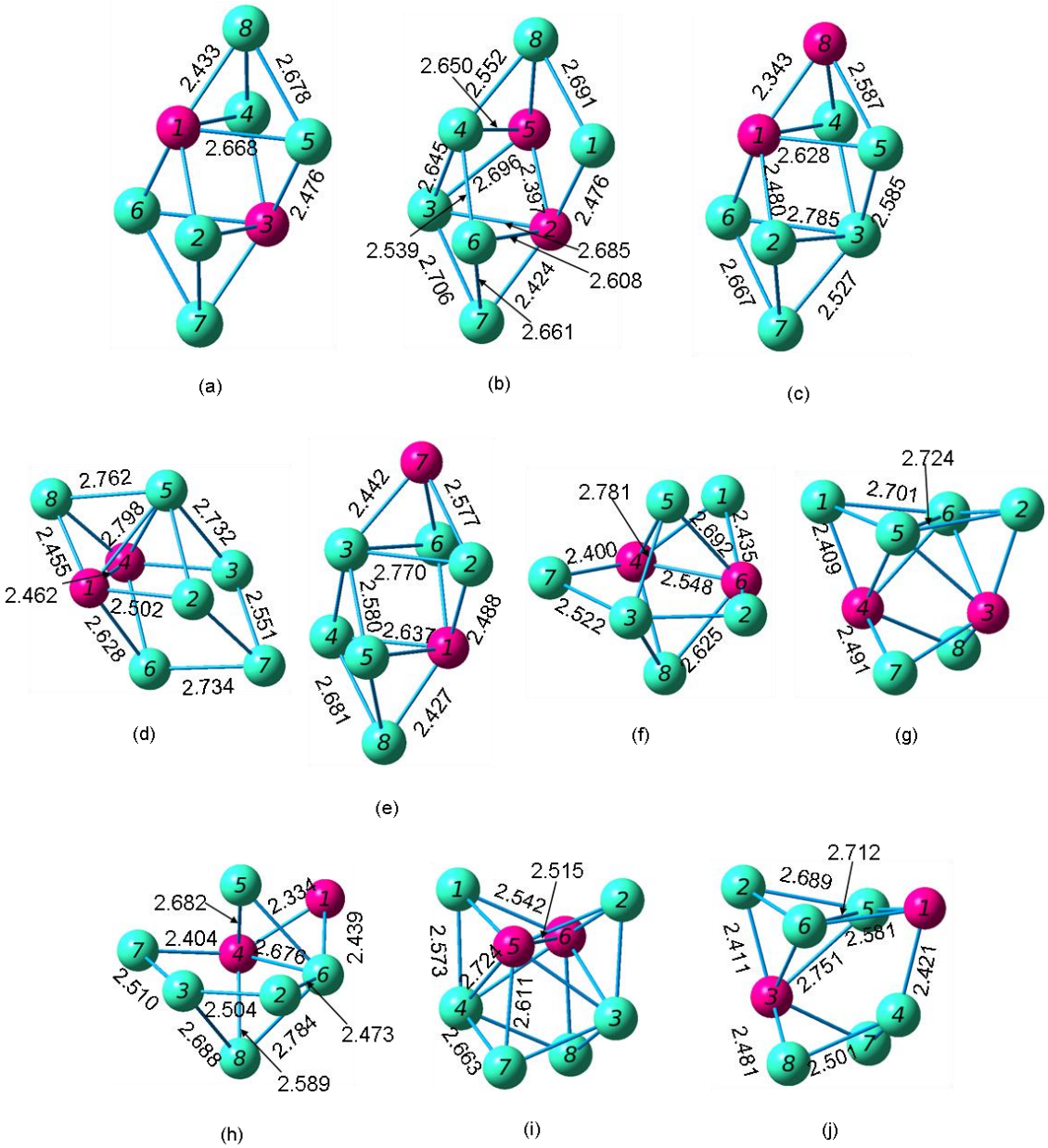

Figure 4.152 Geometries of the $(Si_2Ge_6)^+$ Cationic Septamers from (a) Most Stable through (j) Least Stable

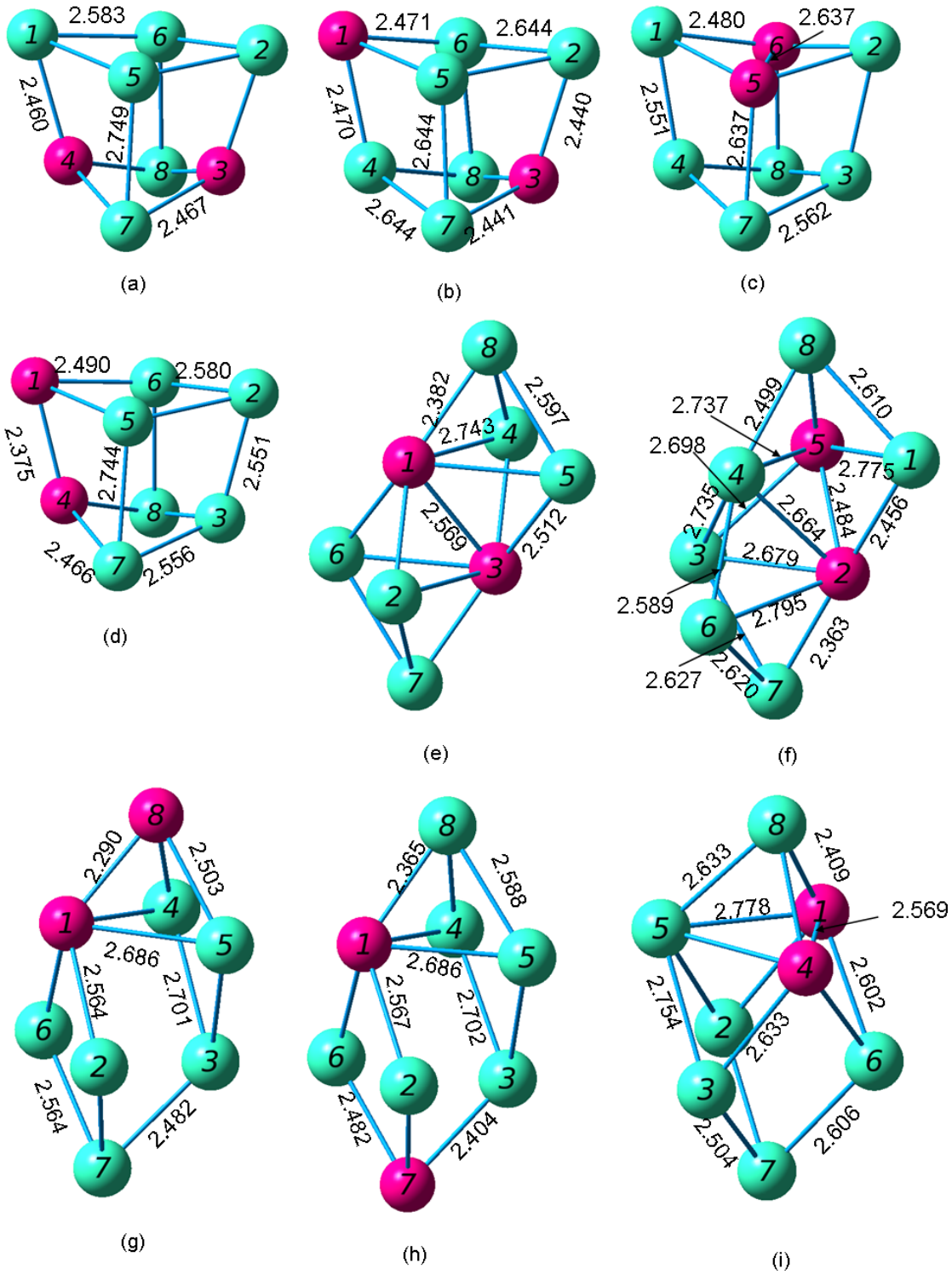

Figure 4.153 Geometries of the $(Si_2Ge_6)^-$ Anionic Septamers from (a) Most Stable through (i) Least Stable

4.28 $SiGe_7$ Octamers

Wang and Chao [51] reported a rhombic cube for the neutral $SiGe_7$ octamer, and a pentagonal bipyramid with germanium atom attached to one face for the cation. The neutral cluster has a ^1A electronic state, a dissociation energy of -31.4674 eV or -31.7475 eV, a HOMO-LUMO gap of 2.45 eV, and the following frequencies: 277(a), 415(a), and 272(a). Their anion cluster is again similar to our most stable anion.

Totally, we investigated five $SiGe_7$ clusters. The difference in binding energy per atom between our most stable cluster and our thirty-eighth most stable cluster was 0.0436 eV. As with the other octamers, the most stable neutral and cation are two joined trigonal bipyramids while the most stable anion has a completely different geometry.

Table 4.190 Properties of the $SiGe_7$ Octamers

Figure	Symmetry Group	Electronic State	Binding E / Atom (eV)	HOMO-LUMO Gap (eV)	Dipole Moment (D)
4.154 (a)	C_1	^1A	2.830	2.285	0.416
4.154 (b)	C_1	^1A	2.822	2.047	0.207
4.154 (c)	C_s	$^1A'$	2.806	1.951	0.517
4.154 (d)	C_1	^1A	2.797	2.069	0.647
4.154 (e)	C_s	$^1A'$	2.786	2.032	0.324

Table 4.191 Properties of the $(SiGe_7)^+$ Octamers

Figure	Symmetry Group	Electronic State	Binding E / Atom (eV)	HOMO-LUMO Gap (eV)	Dipole Moment (D)
4.155 (a)	C_1	^2A	2.956	1.281[a]	0.424
4.155 (b)	C_s	$^2A''$	2.935	1.379[a]	0.308
4.155 (c)	C_1	^2A	2.933	1.316[a]	0.576
4.155 (d)	C_1	^2A	2.921	1.568[a]	0.420
4.155 (e)	C_s	$^2A''$	2.905	1.377[a]	0.442

[a] HOMO and LUMO have opposite spins; this value includes the energy required to flip the spin of the electron.

Table 4.192 Properties of the $(SiGe_7)^-$ Octamers

Figure	Symmetry Group	Electronic State	Binding E / Atom (eV)	HOMO-LUMO Gap (eV)	Dipole Moment (D)
4.156 (a)	C_1	^2A	3.000	1.392[a]	0.470
4.156 (b)	C_s	$^2A'$	2.987	1.367[a]	0.838
4.156 (c)	C_1	^2A	2.980	1.392[a]	1.267
4.156 (d)	C_s	$^2A'$	2.970	1.384[a]	0.987
4.156 (e)	C_1	^2A	2.954	1.282[a]	1.279

[a] HOMO and LUMO have opposite spins; this value includes the energy required to flip the spin of the electron.

Table 4.193 Ionization Potentials and Electron Affinities of the $SiGe_7$ Octamers

Neutral Figure	VIP (eV)	Cationic Figure	AIP (eV)	VEA (eV)	Anionic Figure	AEA (eV)
4.154 (a)	7.016	4.155 (a)	6.893	1.768	4.156 (e)	2.132
4.154 (b)	7.186	4.155 (c)	7.007	2.134	4.156 (a)	2.561
4.154 (c)	7.176	4.155 (b)	6.872	2.153	4.156 (b)	2.588
4.154 (d)	7.259	4.155 (d)	6.904	2.174	4.156 (c)	2.602
4.154 (e)	7.238	4.155 (e)	6.953	2.201	4.156 (d)	2.606

Table 4.194 Fragmentation Energies for the Most Stable $SiGe_7$ Octamer

Fragmented Cluster	Fragmentation Energy (eV)
$SiGe_6$ + Ge	1.959
$SiGe_5$ + Ge_2	2.448
$SiGe_5$ + 2Ge	5.377
$SiGe_4$ + Ge_2 + Ge	5.974
$SiGe_3$ + 2Ge_2	6.346
$SiGe_4$ + 3Ge	8.903
$SiGe_3$ + Ge_2 + 2Ge	9.274
$SiGe_2$ + 2Ge_2 + Ge	10.130
SiGe + 3Ge_2	10.792
$SiGe_3$ + 4Ge	12.203
$SiGe_2$ + Ge_2+ 3Ge	13.059
SiGe + 2Ge_2 + 2Ge	13.721
3Ge_2 + Si + Ge	13.854
$SiGe_2$ + 5Ge	15.987
SiGe + Ge_2 + 4Ge	16.649
2Ge_2 + Si + 3Ge	16.782
SiGe + 6Ge	19.578
Ge_2 + Si + 5Ge	19.711
Si + 7Ge	22.639

Table 4.195 Fragmentation Energies for the Most Stable $(SiGe_7)^+$ Octamer

Fragmented Cluster	Fragmentation Energy (eV)
$(SiGe_6)^+ + Ge$	2.575
$SiGe_6 + Ge^+$	2.966
$(SiGe_5)^+ + Ge_2$	3.043
$SiGe_5 + (Ge_2)^+$	3.175
$(SiGe_5)^+ + 2Ge$	5.972
$SiGe_5 + Ge^+ + Ge$	6.384
$SiGe_4 + (Ge_2)^+ + Ge$	6.701
$(SiGe_4)^+ + Ge_2 + Ge$	6.859
$SiGe_4 + Ge_2 + Ge^+$	6.981
$SiGe_3 + (Ge_2)^+ + Ge_2$	7.073
$(SiGe_3)^+ + 2Ge_2$	7.116
$(SiGe_4)^+ + 3Ge$	9.787
$SiGe_4 + Ge^+ + 2Ge$	9.909
$SiGe_3 + (Ge_2)^+ + 2Ge$	10.001
$(SiGe_3)^+ + Ge_2 + 2Ge$	10.045
$SiGe_3 + Ge_2 + Ge^+ + Ge$	10.281
$SiGe_2 + (Ge_2)^+ + Ge_2 + Ge$	10.857
$SiGe_2 + 2Ge_2 + Ge^+$	11.137
$(SiGe_2)^+ + 2Ge_2 + Ge$	11.186
$SiGe + (Ge_2)^+ + 2Ge_2$	11.519
$(SiGe)^+ + 3Ge_2$	11.635
$(SiGe_3)^+ + 4Ge$	12.973
$SiGe_3 + Ge^+ + 3Ge$	13.210
$SiGe_2 + (Ge_2)^+ + 3Ge$	13.785
$SiGe_2 + Ge_2 + Ge^+ + 2Ge$	14.066
$(SiGe_2)^+ + Ge_2 + 3Ge$	14.114
$SiGe + (Ge_2)^+ + Ge_2 + 2Ge$	14.447
$(SiGe)^+ + 2Ge_2 + 2Ge$	14.563
$(Ge_2)^+ + 2Ge_2 + Si + Ge$	14.580

Table 4.195 – *Continued*

Fragmented Cluster	Fragmentation Energy (eV)
$SiGe + 2Ge_2 + Ge^+ + Ge$	14.728
$3Ge_2 + Si + Ge^+$	14.861
$SiGe_2 + Ge^+ + 4Ge$	16.994
$(SiGe_2)^+ + 5Ge$	17.043
$SiGe + (Ge_2)^+ + 4Ge$	17.376
$(SiGe)^+ + Ge_2 + 4Ge$	17.492
$(Ge_2)^+ + Ge_2 + Si + 3Ge$	17.509
$SiGe + Ge_2 + Ge^+ + 3Ge$	17.656
$2Ge_2 + Si + Ge^+ + 2Ge$	17.789
$(SiGe)^+ + 6Ge$	20.420
$(Ge_2)^+ + Si + 5Ge$	20.437
$SiGe + Ge^+ + 5Ge$	20.585
$Ge_2 + Si + Ge^+ + 4Ge$	20.718
$Si + Ge^+ + 6Ge$	23.646

Table 4.196 Fragmentation Energies for the Most Stable $(SiGe_7)^-$ Octamer

Fragmented Cluster	Fragmentation Energy (eV)
$(SiGe_6)^- + Ge$	2.621
$(SiGe_5)^- + Ge_2$	3.041
$SiGe_5 + (Ge_2)^-$	3.129
$SiGe_6 + Ge^-$	3.317
$(SiGe_5)^- + 2Ge$	5.969
$(SiGe_4)^- + Ge_2 + Ge$	6.314
$SiGe_4 + (Ge_2)^- + Ge$	6.654
$SiGe_5 + Ge^- + Ge$	6.735
$(SiGe_3)^+ + 2Ge_2$	6.908
$SiGe_3 + (Ge_2)^+ + Ge_2$	7.026
$SiGe_4 + Ge_2 + Ge^-$	7.332
$(SiGe_4)^- + 3Ge$	9.242
$(SiGe_3)^- + Ge_2 + 2Ge$	9.836
$SiGe_3 + (Ge_2)^- + 2Ge$	9.955
$SiGe_4 + Ge^- + 2Ge$	10.261
$(SiGe_2)^- + 2Ge_2 + Ge$	10.592
$SiGe_3 + Ge_2 + Ge^- + Ge$	10.633
$SiGe_2 + (Ge_2)^- + Ge_2 + Ge$	10.810
$(SiGe)^- + 3Ge_2$	11.443
$SiGe + (Ge_2)^- + 2Ge_2$	11.473
$SiGe_2 + 2Ge_2 + Ge^-$	11.488
$(SiGe_3)^- + 4Ge$	12.765
$(SiGe_2)^- + Ge_2 + 3Ge$	13.521
$SiGe_3 + Ge^- + 3Ge$	13.561
$SiGe_2 + (Ge_2)^- + 3Ge$	13.739
$(SiGe)^- + 2Ge_2 + 2Ge$	14.372
$SiGe + (Ge_2)^- + Ge_2 + 2Ge$	14.401
$SiGe_2 + Ge_2 + Ge^- + 2Ge$	14.417
$(Ge_2)^- + 2Ge_2 + Si + Ge$	14.534

Table 4.196 – *Continued*

Fragmented Cluster	Fragmentation Energy (eV)
$SiGe + 2Ge_2 + Ge^- + Ge$	15.079
$3Ge_2 + Si + Ge^-$	15.212
$(SiGe_2)^- + 5Ge$	16.449
$(SiGe)^- + Ge_2 + 4Ge$	17.300
$SiGe + (Ge_2)^- + 4Ge$	17.330
$SiGe_2 + Ge^- + 4Ge$	17.345
$(Ge_2)^- + Ge_2 + Si + 3Ge$	17.463
$SiGe + Ge_2 + Ge^- + 3Ge$	18.007
$2Ge_2 + Si + Ge^- + 2Ge$	18.140
$(SiGe)^- + 6Ge$	20.229
$(Ge_2)^- + Si + 5Ge$	20.391
$SiGe + Ge^- + 5Ge$	20.936
$Ge_2 + Si + Ge^- + 4Ge$	21.069
$Si + Ge^- + 6Ge$	23.997

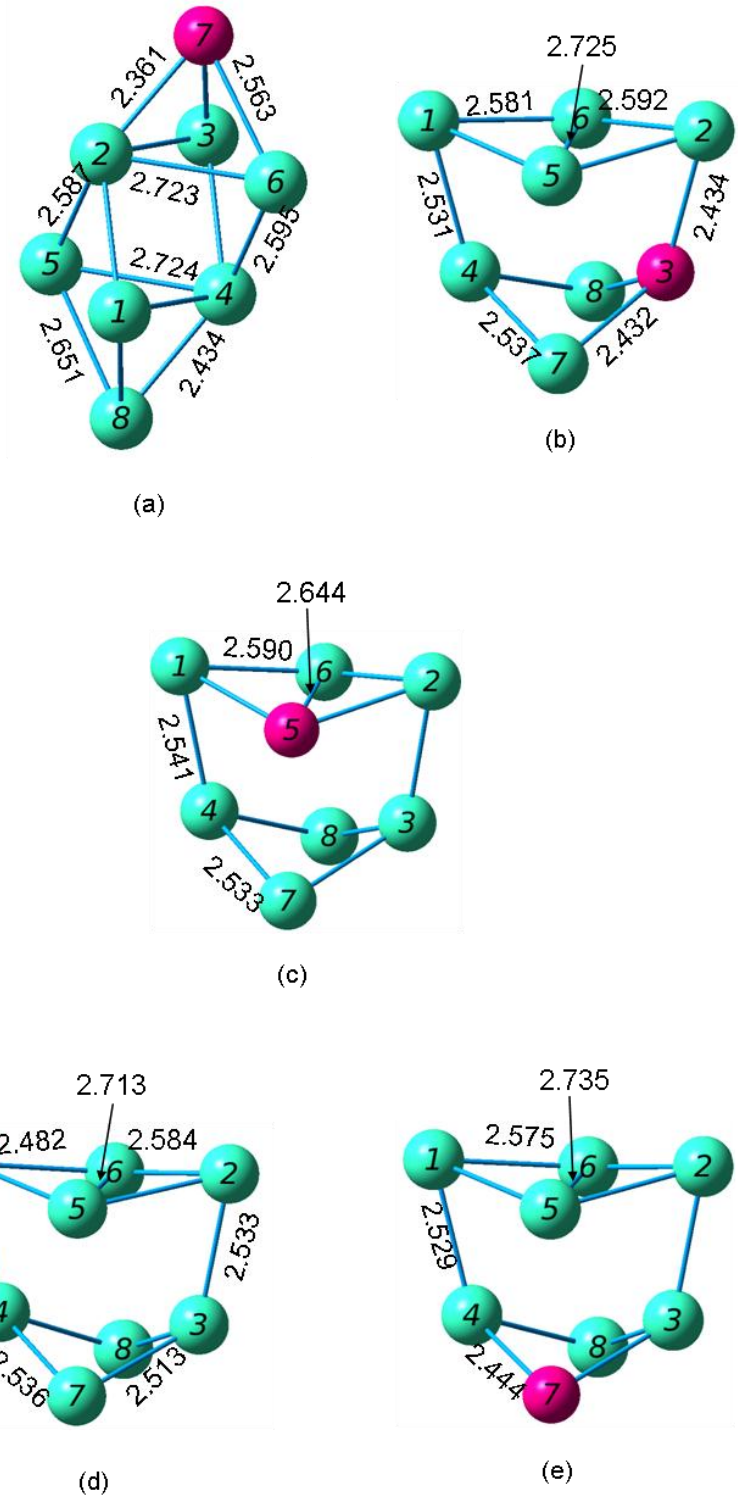

Figure 4.154 Geometries of the $SiGe_7$ Neutral Septamers from (a) Most Stable through (e) Least Stable

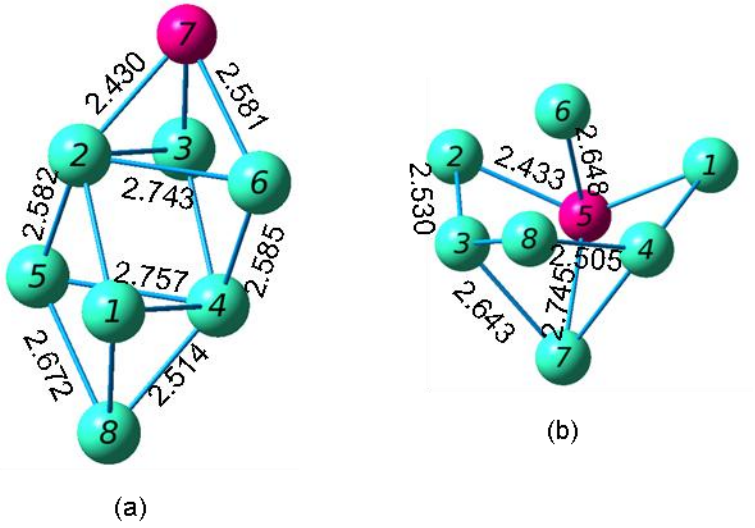

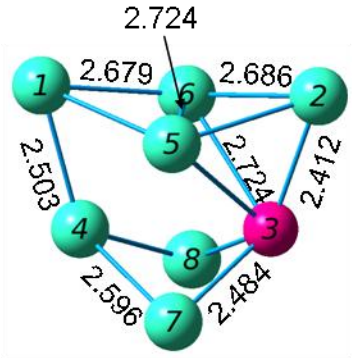

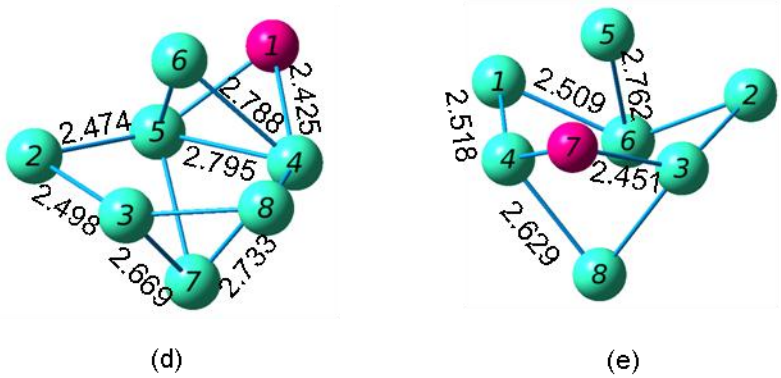

Figure 4.155 Geometries of the $(SiGe_7)^+$ Cationic Septamers (a) Most Stable through (e) Least Stable

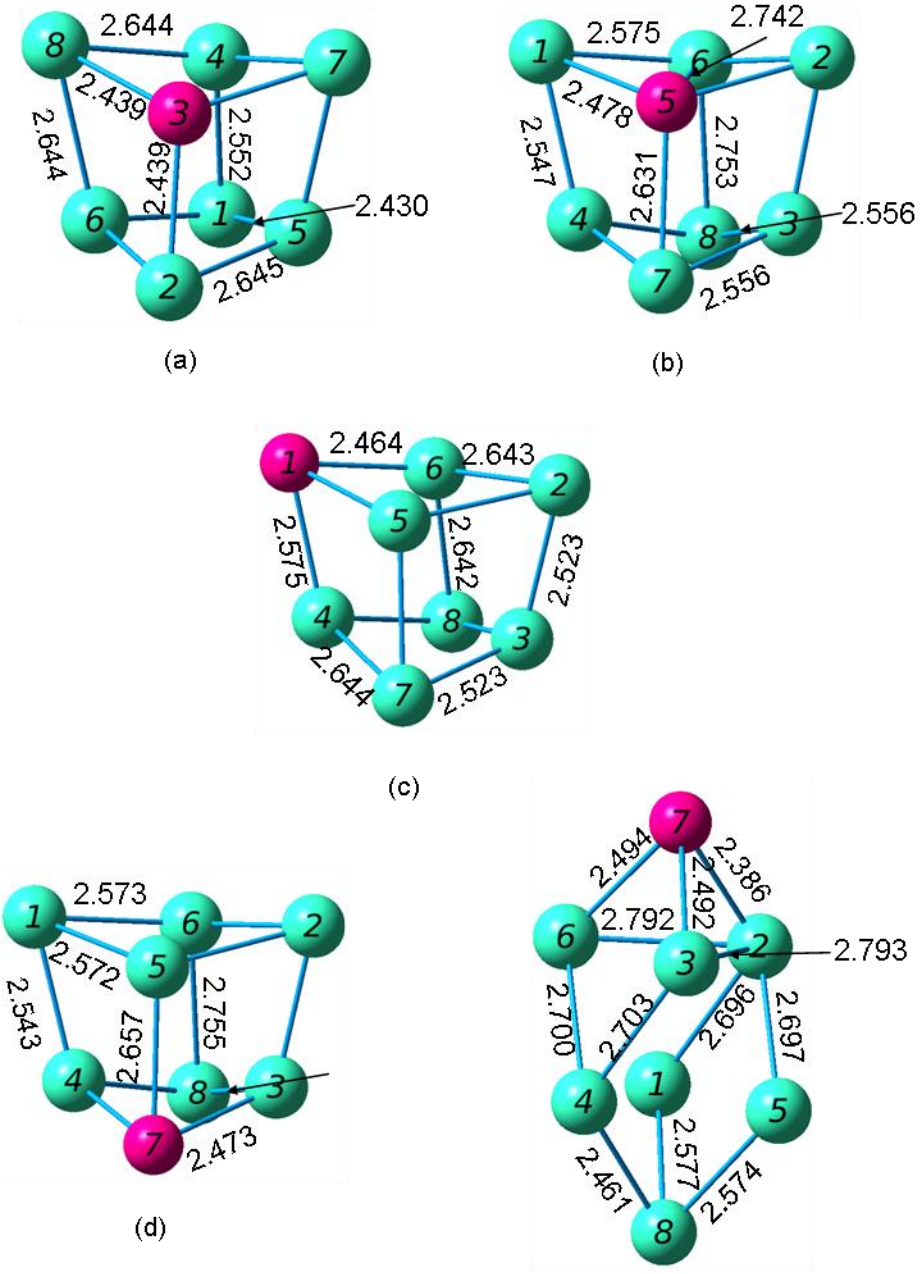

Figure 4.156 Geometries of the $(SiGe_7)^-$ Anionic Septamers (a) Most Stable through (e) Least Stable

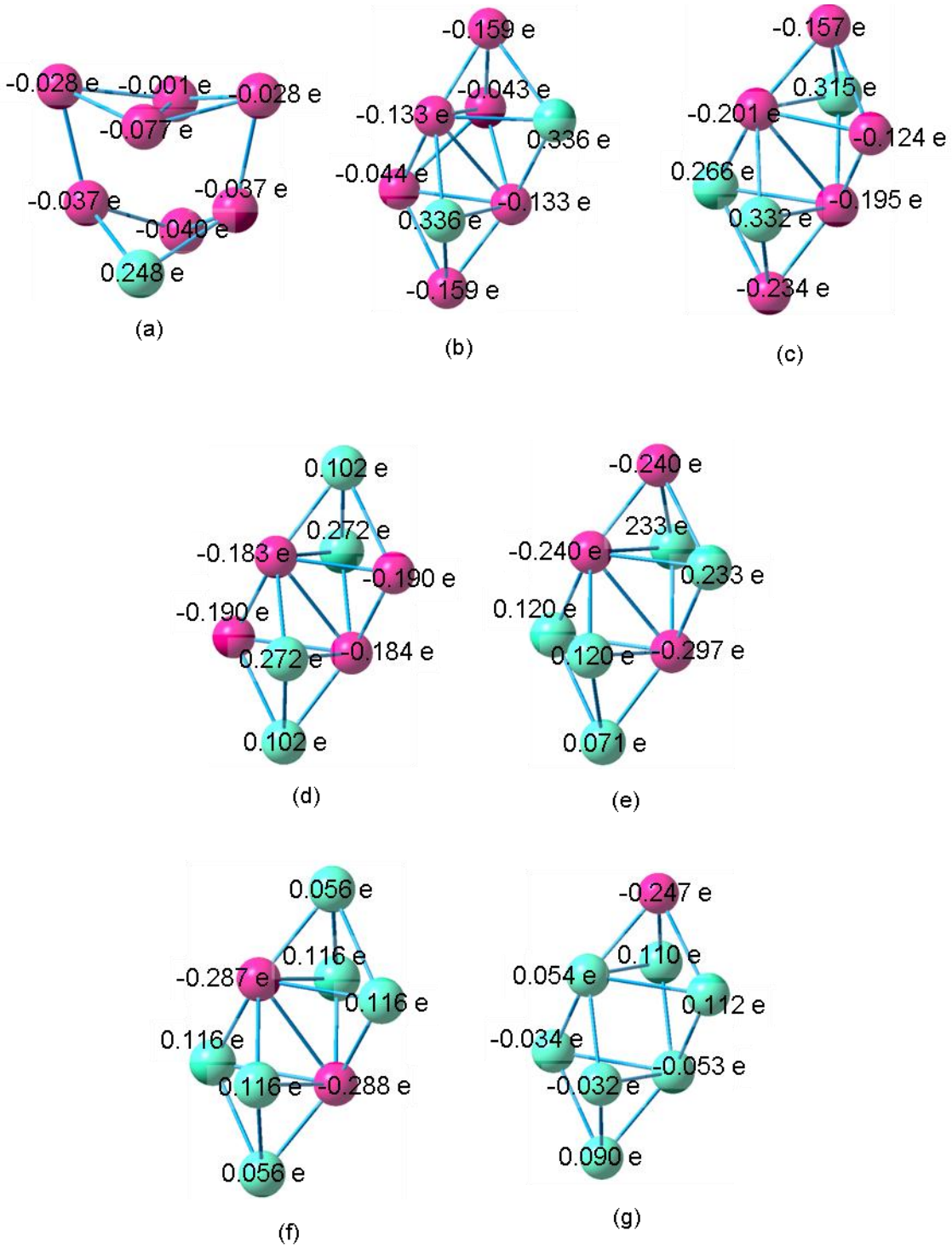

Figure 4.157 Atomic Charges of the Most Stable (a) Si_7Ge (b) Si_6Ge_2 (c) Si_5Ge_3 (d) Si_4Ge_4 (e) Si_3Ge_5 (f) Si_2Ge_6 and (g) $SiGe_7$ Neutral Octamer

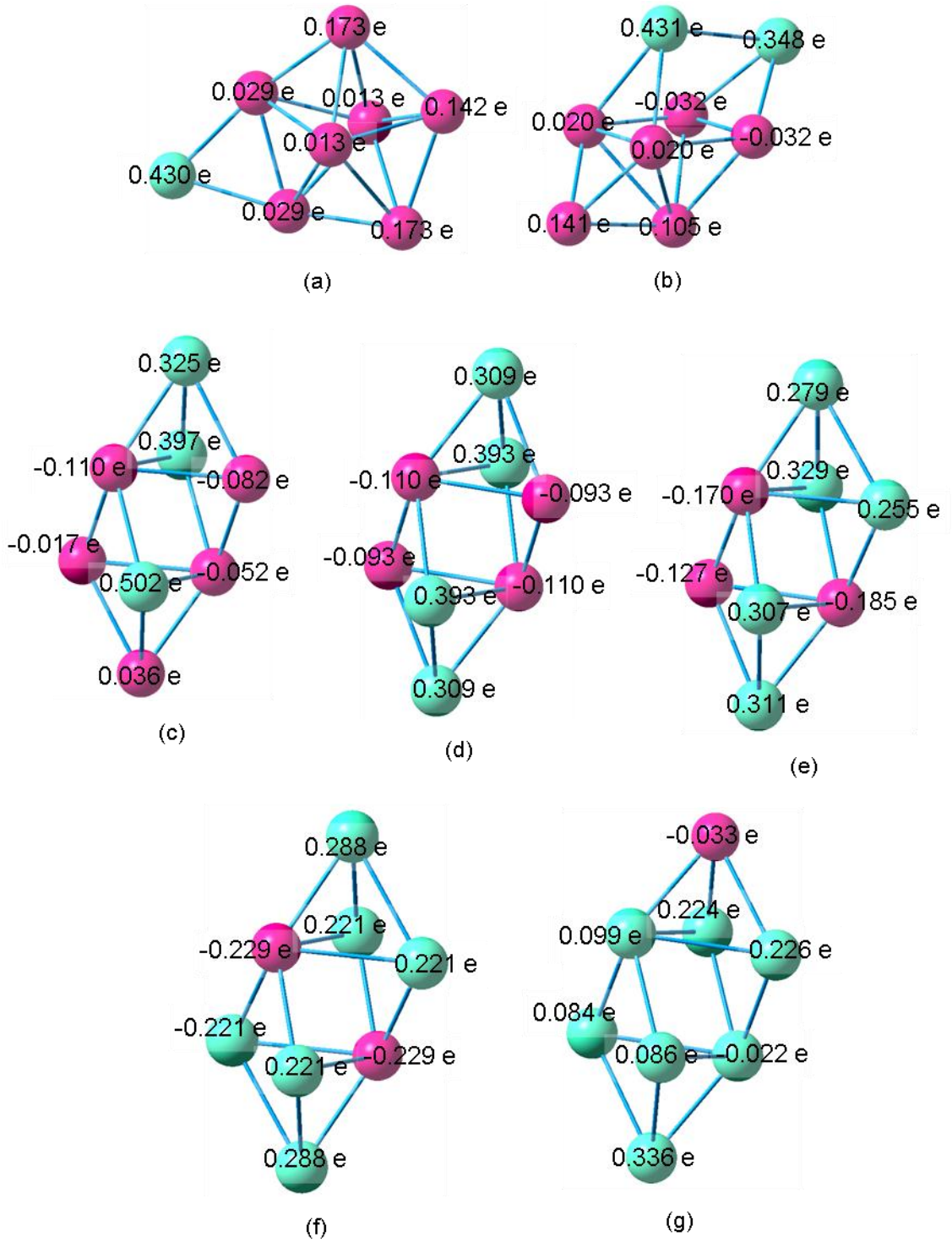

Figure 4.158 Atomic Charges of the Most Stable (a) $(Si_7Ge)^+$ (b) $(Si_6Ge_2)^+$ (c) $(Si_5Ge_3)^+$ (d) $(Si_4Ge_4)^+$ (e) $(Si_3Ge_5)^+$ (f) $(Si_2Ge_6)^+$ and (g) $(SiGe_7)^+$ Cationic Octamer

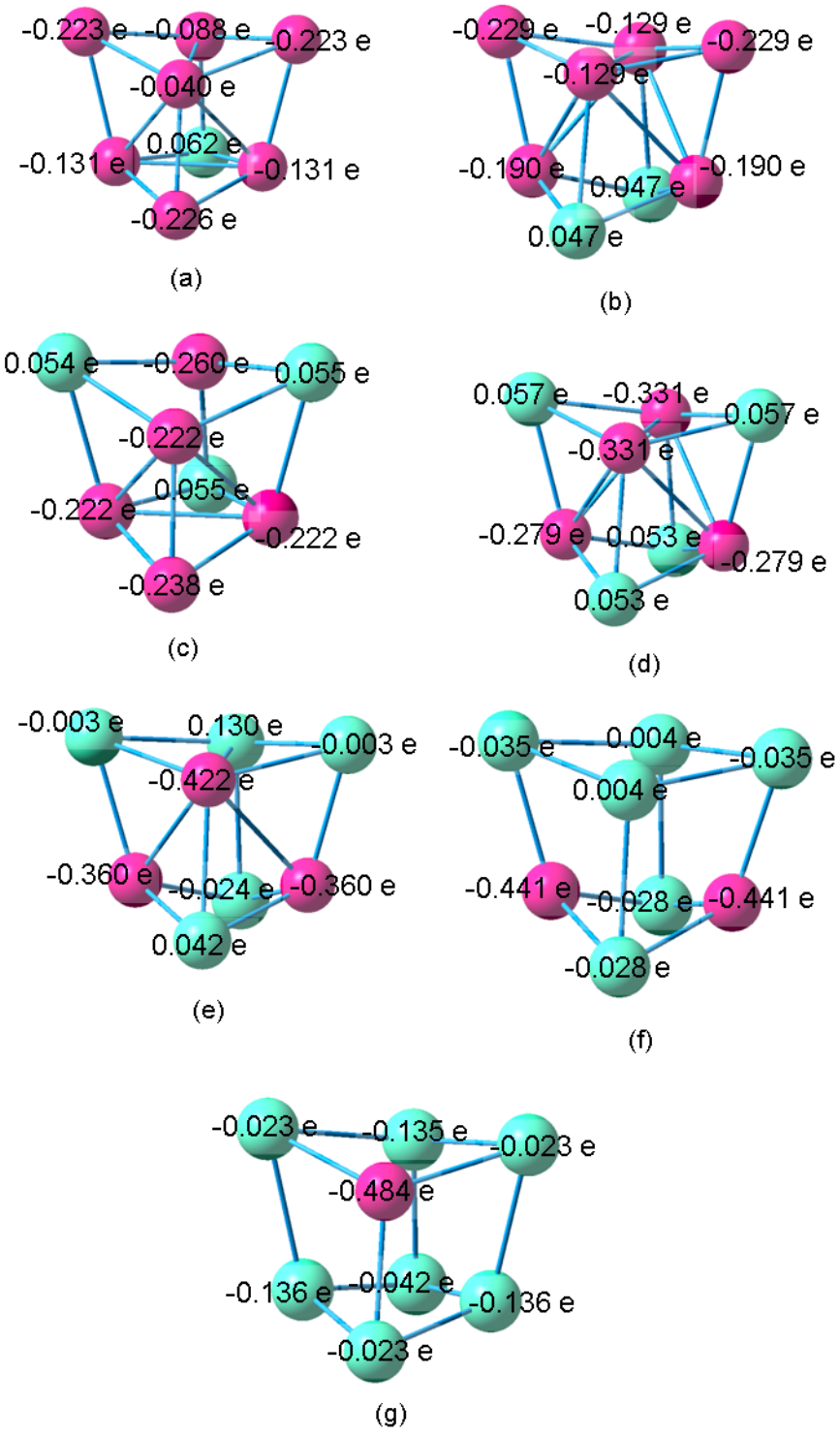

Figure 4.159 Atomic Charges of the Most Stable (a) $(Si_7Ge)^-$ (b) $(Si_6Ge_2)^-$ (c) $(Si_5Ge_3)^-$ (d) $(Si_4Ge_4)^-$ (e) $(Si_3Ge_5)^-$ (f) $(Si_2Ge_6)^-$ and (g) $(SiGe_7)^-$ Anionic Octamer

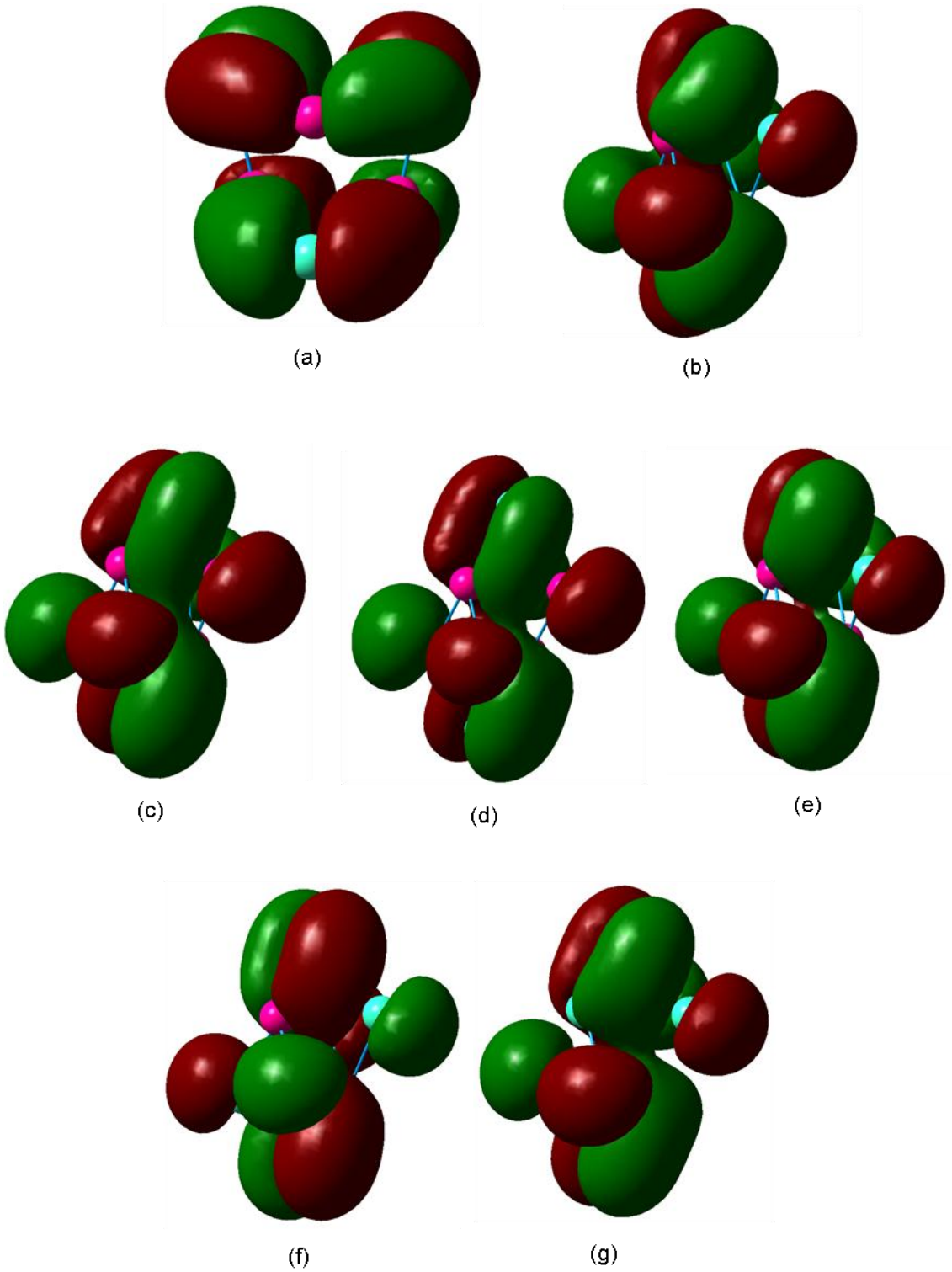

Figure 4.160 HOMO of the Most Stable (a) Si_7Ge (b) Si_6Ge_2 (c) Si_5Ge_3 (d) Si_4Ge_4 (e) Si_3Ge_5 (f) Si_2Ge_6 and (g) $SiGe_7$ Neutral Octamer

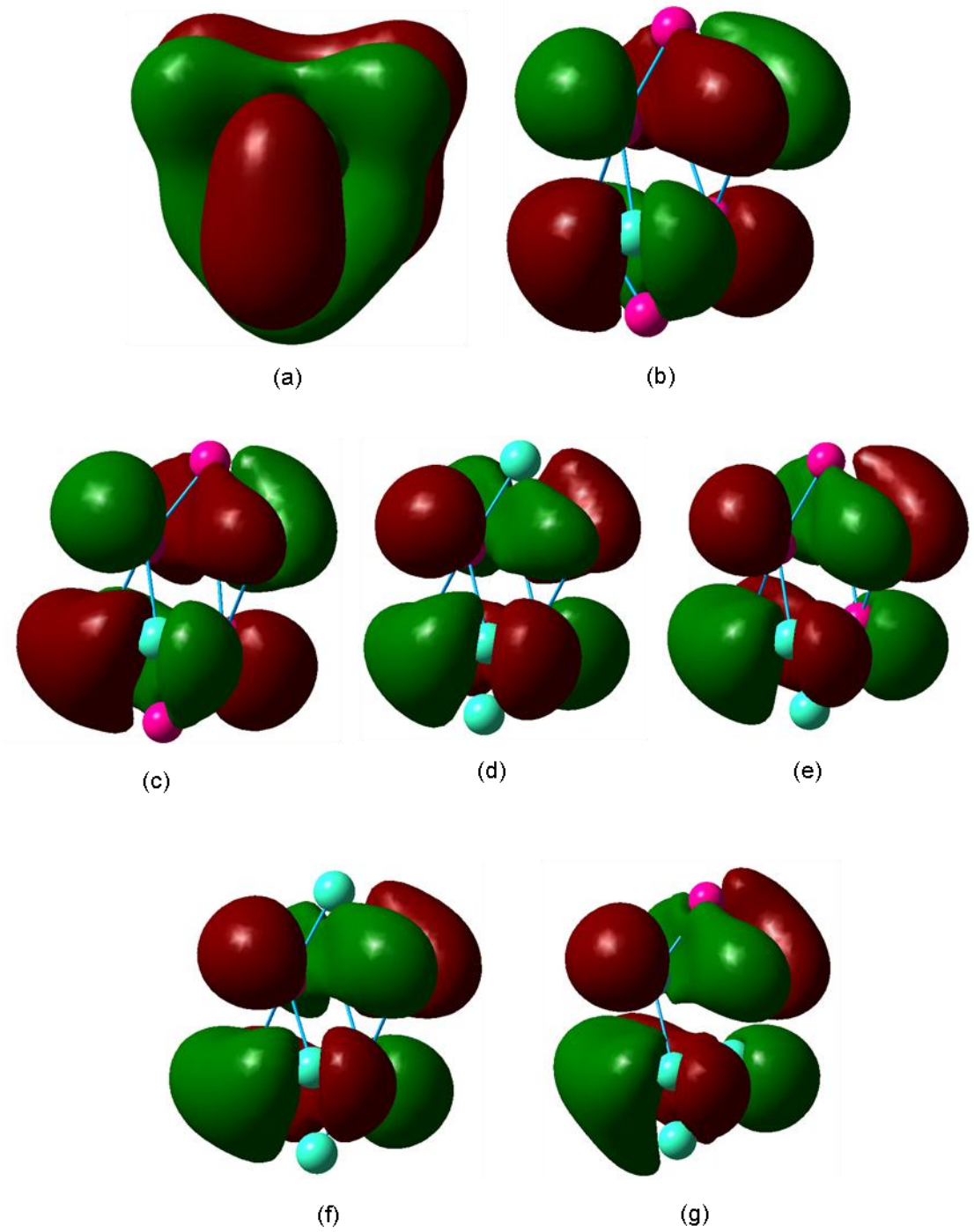

Figure 4.161 LUMO of the Most Stable (a) Si_7Ge (b) Si_6Ge_2 (c) Si_5Ge_3 (d) Si_4Ge_4 (e) Si_3Ge_5 (f) Si_2Ge_6 and (g) $SiGe_7$ Neutral Octamer

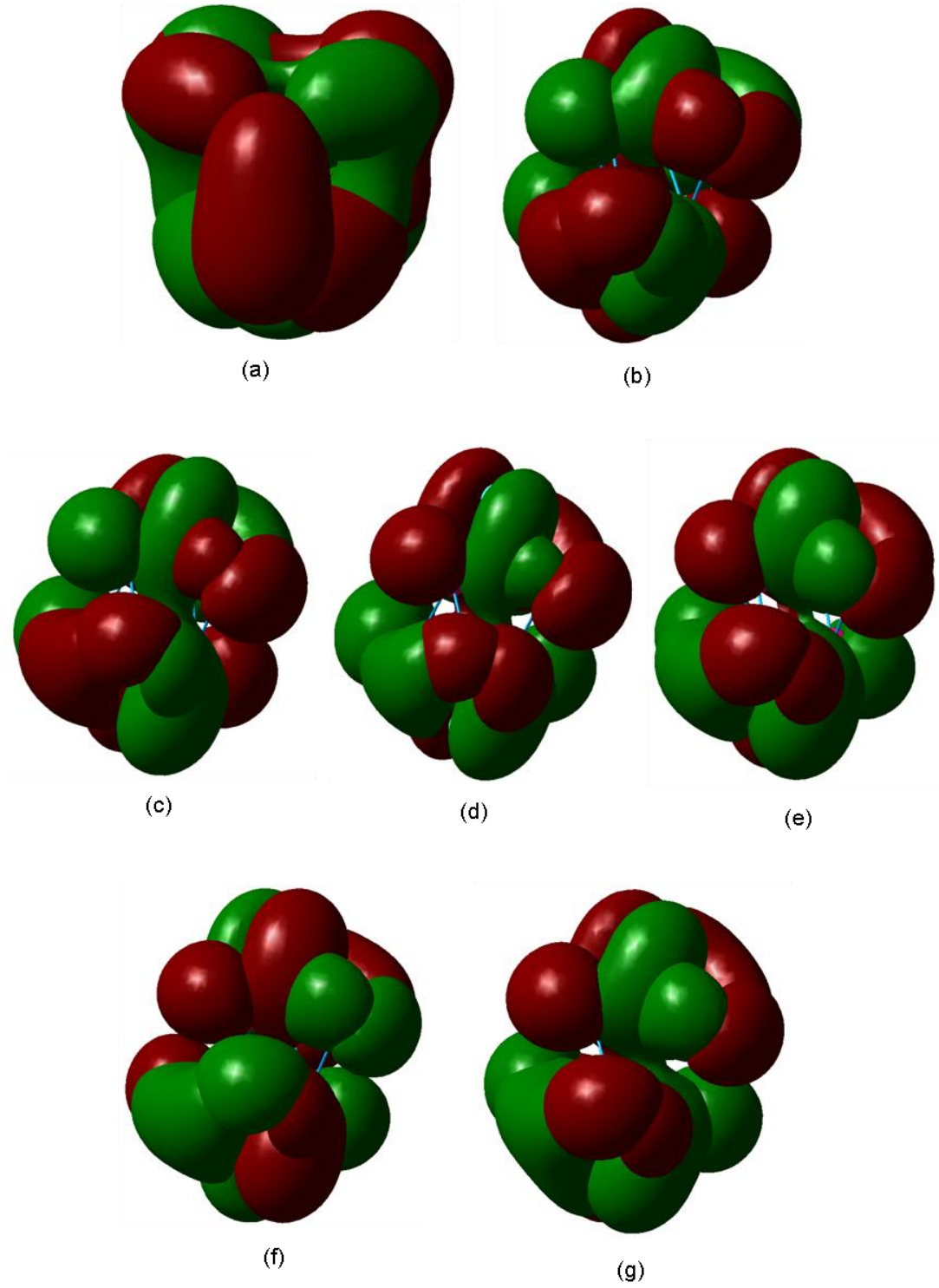

Figure 4.162 HOMO and LUMO of the Most Stable (a) Si_7Ge (b) Si_6Ge_2 (c) Si_5Ge_3 (d) Si_4Ge_4 (e) Si_3Ge_5 (f) Si_2Ge_6 and (g) $SiGe_7$ Neutral Octamer

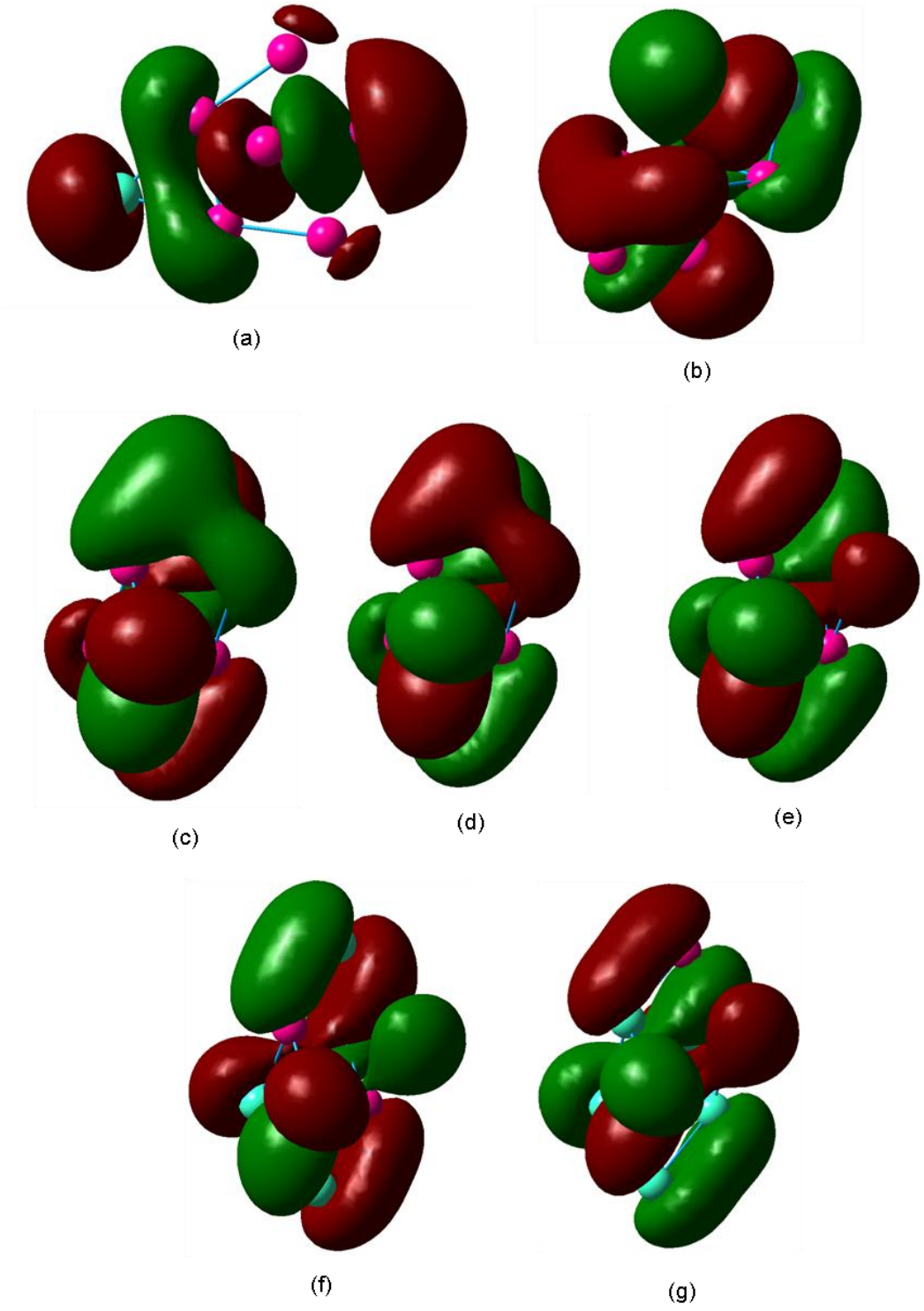

Figure 4.163 HOMO of the Most Stable (a) $(Si_7Ge)^+$ (b) $(Si_6Ge_2)^+$ (c) $(Si_5Ge_3)^+$ (d) $(Si_4Ge_4)^+$ (e) $(Si_3Ge_5)^+$ (f) $(Si_2Ge_6)^+$ and (g) $(SiGe_7)^+$ Cationic Octamer

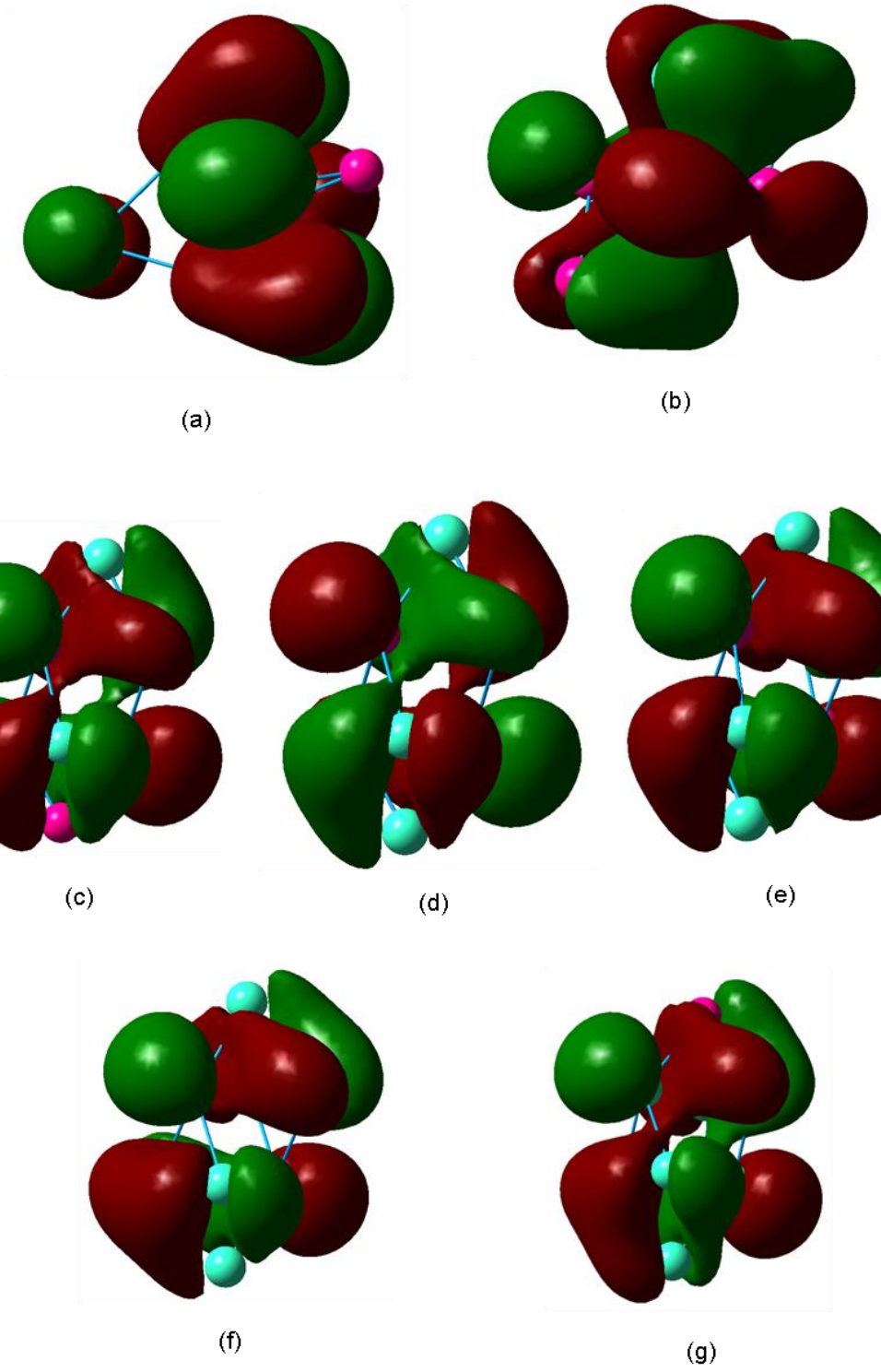

Figure 4.164 LUMO of the Most Stable (a) $(Si_7Ge)^+$ (b) $(Si_6Ge_2)^+$ (c) $(Si_5Ge_3)^+$ (d) $(Si_4Ge_4)^+$ (e) $(Si_3Ge_5)^+$ (f) $(Si_2Ge_6)^+$ and (g) $(SiGe_7)^+$ Cationic Octamer

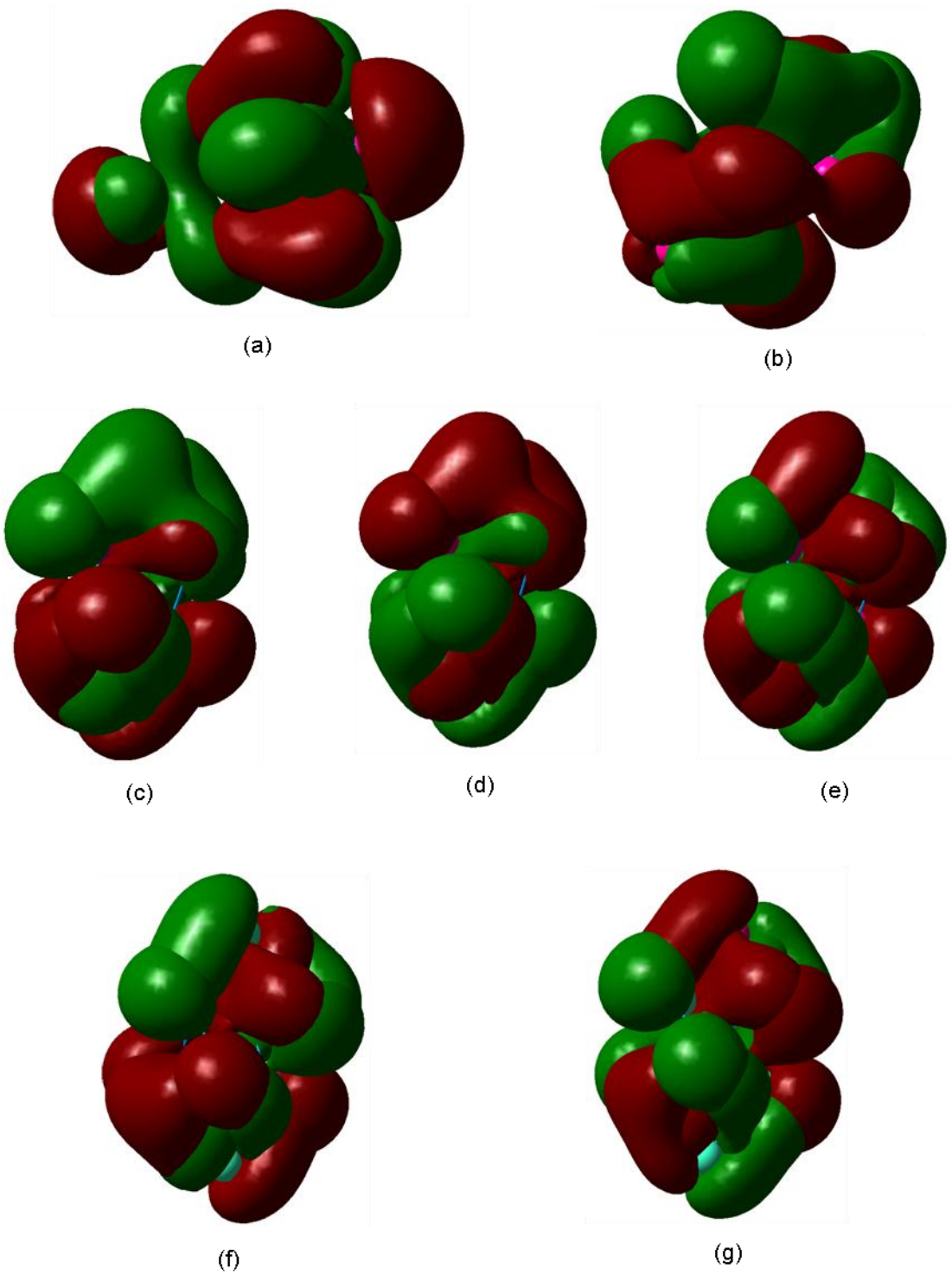

Figure 4.165 HOMO and LUMO of the Most Stable (a) $(Si_7Ge)^+$ (b) $(Si_6Ge_2)^+$ (c) $(Si_5Ge_3)^+$ (d) $(Si_4Ge_4)^+$ (e) $(Si_3Ge_5)^+$ (f) $(Si_2Ge_6)^+$ and (g) $(SiGe_7)^+$ Cationic Octamer

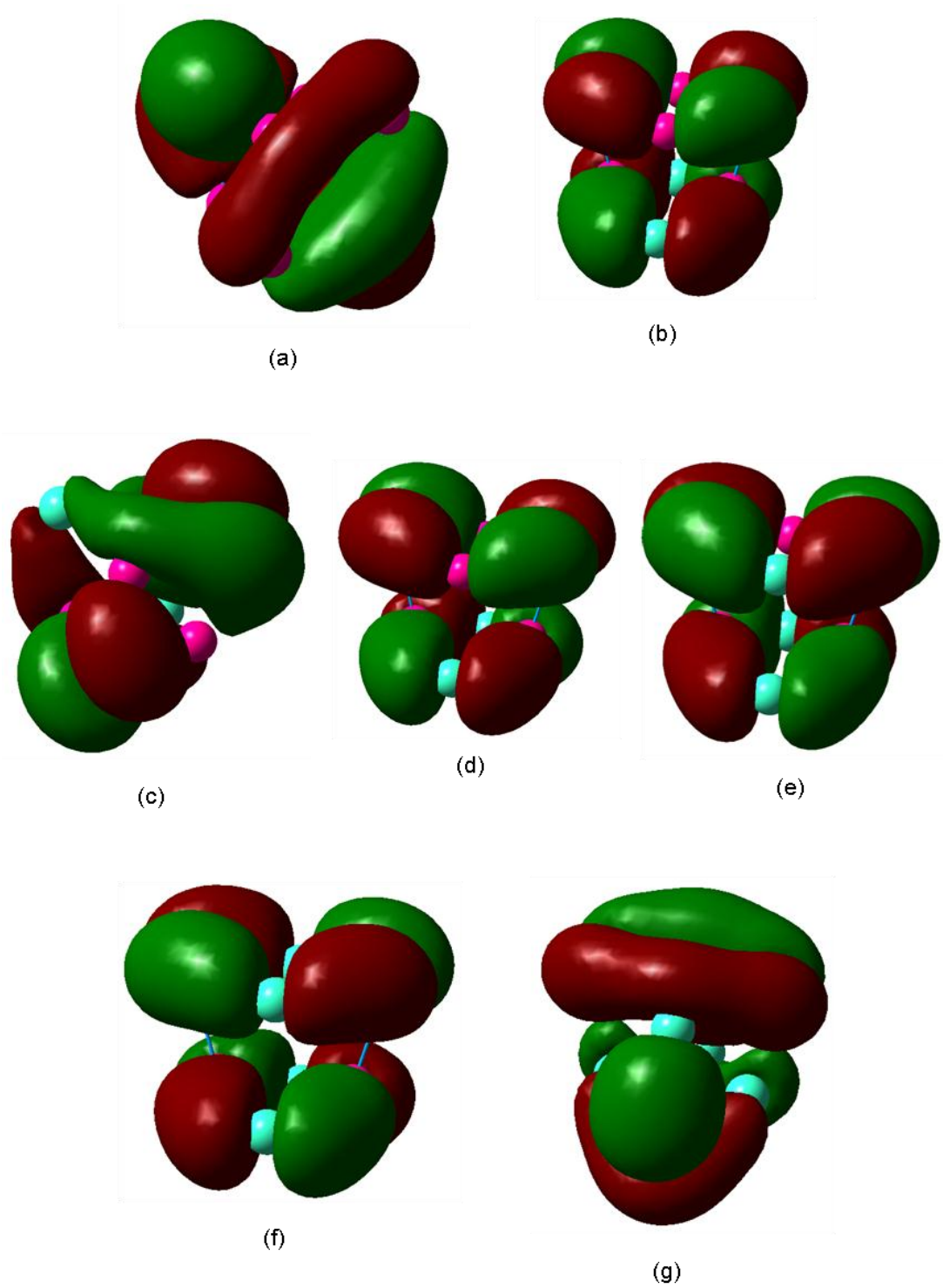

Figure 4.166 HOMO of the Most Stable (a) $(Si_7Ge)^-$ (b) $(Si_6Ge_2)^-$ (c) $(Si_5Ge_3)^-$ (d) $(Si_4Ge_4)^-$ (e) $(Si_3Ge_5)^-$ (f) $(Si_2Ge_6)^-$ and (g) $(SiGe_7)^-$ Anionic Octamer

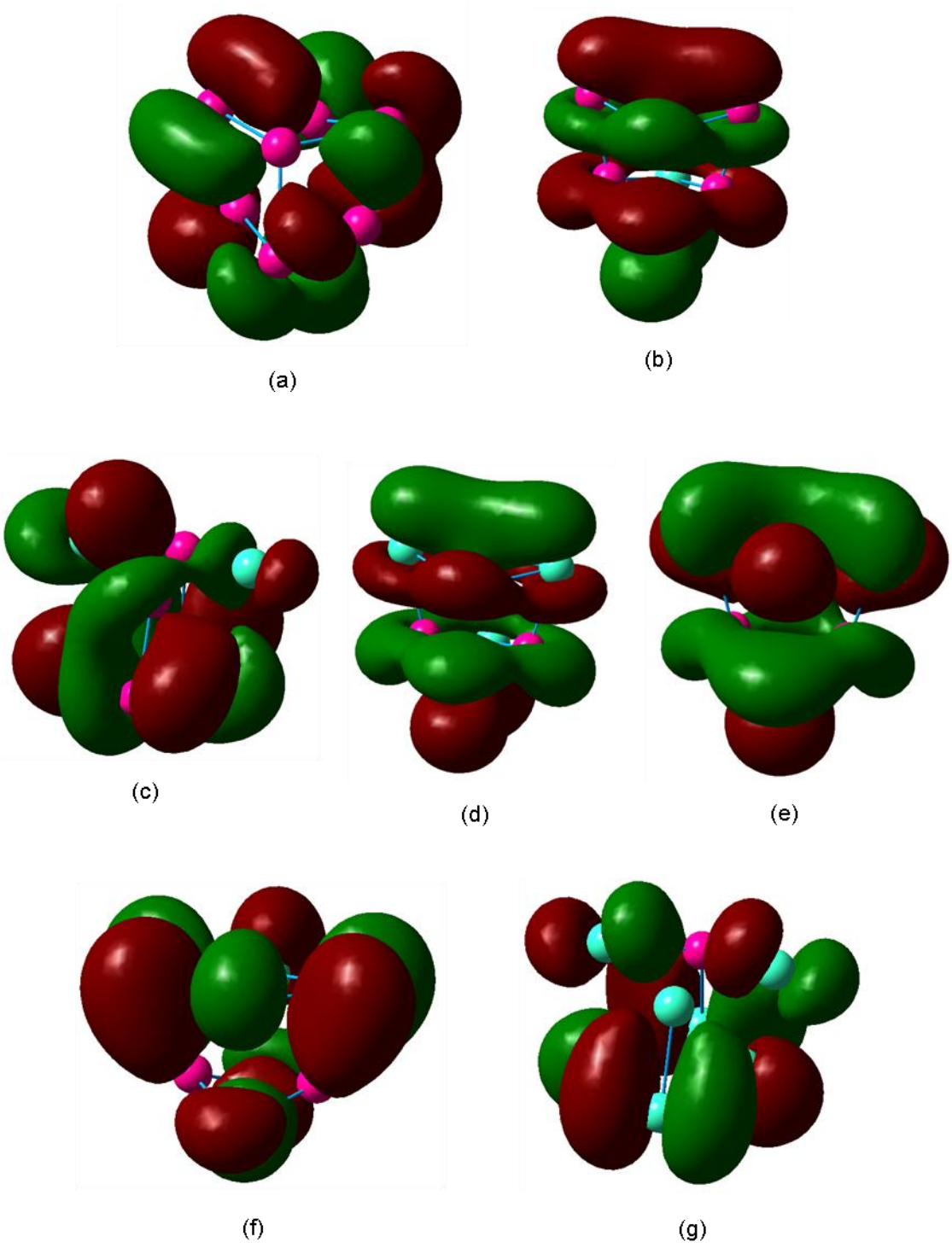

Figure 4.167 LUMO of the Most Stable (a) $(Si_7Ge)^-$ (b) $(Si_6Ge_2)^-$ (c) $(Si_5Ge_3)^-$ (d) $(Si_4Ge_4)^-$ (e) $(Si_3Ge_5)^-$ (f) $(Si_2Ge_6)^-$ and (g) $(SiGe_7)^-$ Anionic Octamer

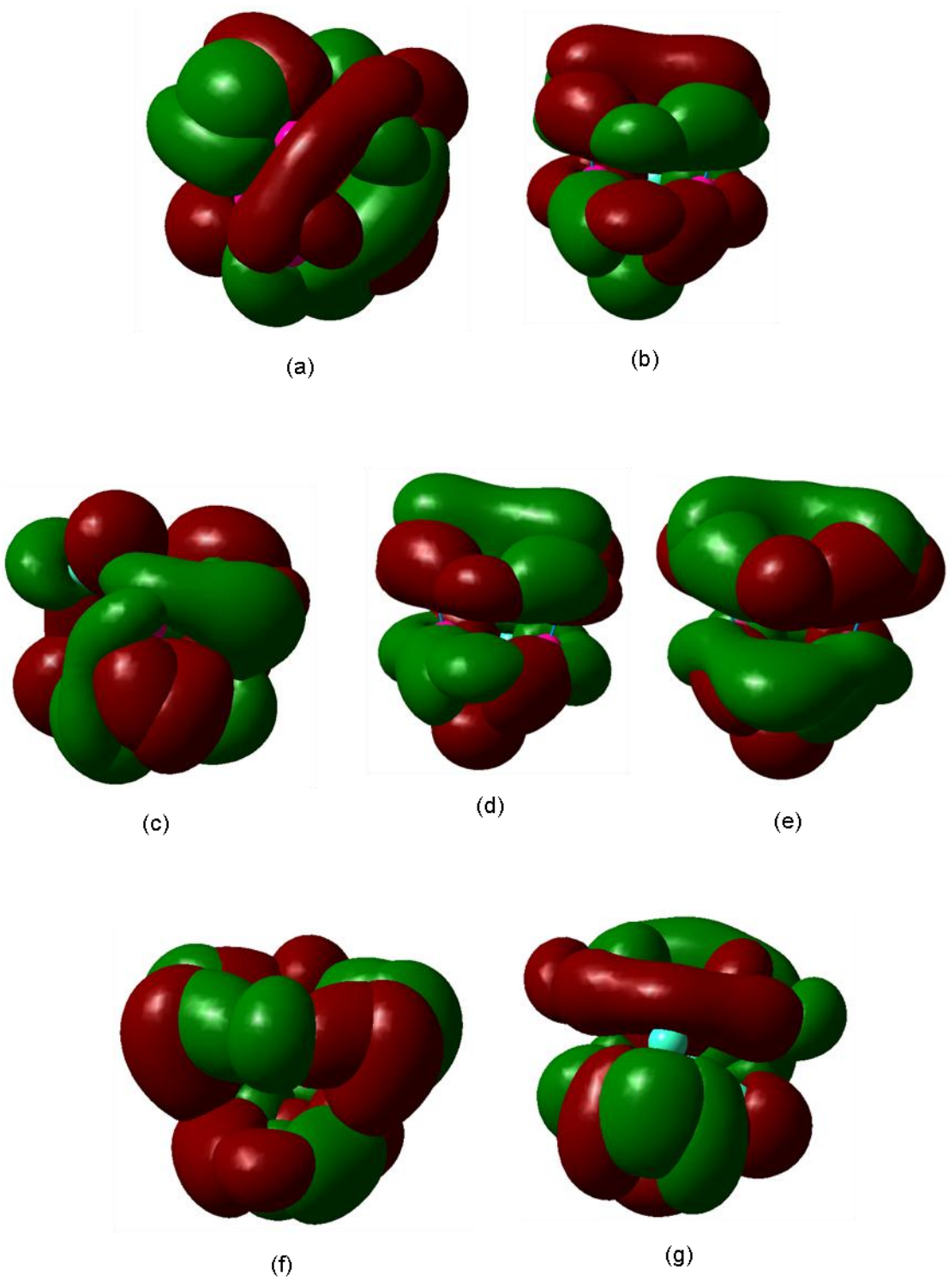

Figure 4.168 HOMO and LUMO of the Most Stable (a) $(Si_7Ge)^-$ (b) $(Si_6Ge_2)^-$ (c) $(Si_5Ge_3)^-$ (d) $(Si_4Ge_4)^-$ (e) $(Si_3Ge_5)^-$ (f) $(Si_2Ge_6)^-$ and (g) $(SiGe_7)^-$ Anionic Octamer

CHAPTER 5

DISCUSSIONS

In this section, we present data that summarizes the results section. Tables 5.1 through 5.3 list the frequencies of the most stable isomers in each category. For the neutral clusters, all frequencies are positive, indicating that we have indeed found the most stable clusters. Table 5.4 lists the average coordination number for each of the most stable isomers. These values are the average number of bonds per atom. Figure 5.1 is a plot of binding energy per atom versus number of atoms. In general, the binding energy per atom increases with the number of atoms, although the curve does dip down slightly at eight atoms. Figure 5.2 illustrates the relationship between fragmentation energy and number of atoms. It shows peaks at four, six, and seven atoms. Lastly, figure 5.3 plots the second order difference in binding energy against number of atoms. These values are computed by

2^{nd} order E Difference for $E_n = 2E_n - (E_{n+1} - E_{n-1})$

where E_n is the binding energy of the most stable cluster with n atoms, and E_{n+1} and E_{n-1} are the binding energy of the most stable cluster with $n+1$ and $n-1$ atoms. For the neutrals and cations, this plot also shows peaks for the four-, six-, and seven- atom clusters.

Table 5.1 Harmonic Frequencies of the Most Stable Neutral Isomers

Clusters	Frequencies (cm^{-1})
SiGe	395.768 (Σ)
Si_2Ge	243.566 (A_1), 274.753 (B_2), 440.752 (A_1)
$SiGe_2$	111.735 (A_1), 424.086 (B_2), 426.746 (A_1)
Si_3Ge	74.752 (B_1), 204.509 (B_2), 269.968 (A_1), 405.499 (B_2), 414.053 (A_1), 479.723 (A_1)
Si_2Ge_2	66.979 (B_{3u}), 180.269 (B_{2u}), 214.175 (A_g), 372.991 (B_{3g}), 395.600 (B_{1u}), 410.582 (A_g)
$SiGe_3$	61.597 (B_1), 140.678 (A_1), 203.860 (A_1), 240.974 (B_2), 341.843 (A_1), 402.728 (B_2)
Si_4Ge	146.539 (A”), 167.789 (A’), 204.055 (A’), 284.284 (A’), 341.980 (A”), 357.614 (A’), 376.157 (A’), 435.034 (A”), 455.267 (A’)
Si_3Ge_2	122.047 (A_1), 154.850 (B_1), 179.642 (A_1), 274.796 (A_2), 290.821 (B_2), 339.082 (B_1), 364.014 (B_2), 371.052 (A_1), 446.563 (A_1)
Si_2Ge_3	117.299 (B_1), 117.534 (A_1), 154.199 (A_1), 271.855 (A_2), 272.058 (B_2), 310.558 (B_2), 336.673 (A_1), 336.675 (B_1), 386.967 (A_1)
$SiGe_4$	107.644 (A”), 107.947 (A’), 143.398 (A’), 201.531 (A’), 201.770 (A”), 227.387 (A’), 320.787 (A’), 321.960 (A”), 356.852 (A’)
Si_5Ge	37.853 (B_2), 93.381 (A_1), 111.664 (B_1), 264.689 (B_2), 270.726 (A_1), 276.470 (B_1), 344.502 (A_1), 351.856 (A_2), 368.735 (B_1), 400.733 (A_1), 435.809 (B_2), 439.356 (A_1),
Si_4Ge_2	24.376 (A’), 59.030 (A’), 94.524 (A”), 231.108 (A’), 259.133 (A”), 268.705 (A’), 283.736 (A’), 345.391 (A”), 351.939 (A”), 379.052 (A’), 401.308 (A’), 437.952 (A’)
Si_3Ge_3	52.991 (B_2), 55.680 (A_1), 76.441 (B_1), 208.479 (A_1), 212.861 (B_2), 253.185 (B_1), 267.858 (A_1), 311.375 (A_2), 338.624 (B_2), 348.068 (B_1), 375.635 (A_1), 407.926 (A_1)
Si_2Ge_4	35.586 (E_u), 35.586 (E_u), 55.967 (B_{2u}), 149.715 (B_{2g}), 199.681 (A_{1g}), 214.686 (B_{1g}), 250.334 (A_{2u}), 320.662 (E_g), 320.662 (E_g), 332.864 (E_u), 332.684 (E_u), 372.478 (A_{1g})
$SiGe_5$	18.658 (A”), 18.700 (A’), 60.821 (A’), 144.285 (A”), 179.126 (A’), 200.315 (A’), 211.355 (A’), 219.996 (A’), 220.163 (A”), 331.179 (A’), 339.679 (A”), 340.026 (A’)
Si_6Ge	128.413 (B_1), 155.834 (A_2), 176.677 (B_2), 205.007 (B_1), 207.176 (A_1), 234.762 (A_1), 254.758 (B_2), 289.936 (A_1), 309.154 (B_1), 317.107 (A_2), 326.268 (B_2), 345.033 (A_1), 381.623 (A_1), 400.041 (B_2), 417.164 (A_1)
Si_5Ge_2	105.954 (A”), 145.352 (A”), 153.847 (A’), 184.232 (A’), 193.473 (A”), 210.350 (A’), 232.809 (A’), 256.945 (A’), 293.019 (A’), 304.426 (A”), 306.598 (A”), 328.129 (A’), 370.423 (A’), 385.727 (A’), 413.310 (A’)

Table 5.1 – *Continued*

Clusters	Frequencies (cm^{-1})
Si_4Ge_3	89.894 (A"), 129.880 (A"), 155.398 (A'), 160.165 (A'), 183.837 (A"), 186.589 (A'), 193.163 (A'), 252.857 (A'), 256.236 (A'), 284.730 (A'), 290.097 (A"), 300.722 (A"), 357.733 (A'), 365.881 (A'), 405.454 (A')
Si_3Ge_4	82.696 (A"), 105.847 (A"), 148.851 (A') 152.390 (A'), 166.193 (A'), 178.073 (A"), 181.869 (A'), 204.109 (A'), 251.189 (A'), 253.243 (A'), 275.839 (A"), 290.439 (A"), 305.967 (A'), 354.465 (A'), 384.885 (A')
Si_2Ge_5	80.103 (A_2), 80.256 (B_1), 148.828 (A_1), 148.972 (B_2), 161.165 (A_1), 161.338 (B_2), 170.367 (B_1), 193.783 (A_1), 193.899 (B_2), 215.059 (A_1), 271.884 (B_1), 271.894 (A_2) 297.426 (A_1), 297.588 (B_2), 369.479 (A_1)
$SiGe_6$	84.144 (E_2), 84.144 (E_2), 127.231 (E_1), 127.231 (E_1), 135.384 (A_1), 156.349 (E_2), 156.349 (E_2), 188.477 (E_1), 188.477 (E_1), 190.806 (E_2), 190.806 (E_2), 208.027 (A_1), 311.489 (A_1), 313.651 (E_1), 313.653 (E_1)

Table 5.2 Harmonic Frequencies of the Most Stable Cations

Clusters	Frequencies (cm^{-1})
$(SiGe)^+$	350.906 (Σ)
$(Si_2Ge)^+$	111.574 (B_2), 250.839 (A_1), 530.116 (A_1)
$(SiGe_2)^+$	118.377 (A_1), 173.117 (B_2), 364.384 (A_1)
$(Si_3Ge)^+$	85.291 (B_1), 221.032 (A_1), 242.005 (B_2), 351.774 (A_1), 431.326 (B_2), 447.641 (A_1)
$(Si_2Ge_2)^+$	81.279 (A"), 179.914 (A'), 197.003 (A'), 292.955 (A'), 350.512 (A'), 453.333 (A')
$(SiGe_3)^+$	71.565 (B_1), 161.021 (A_1), 171.373 (A_1), 230.500 (B_2), 315.137 (A_1), 383.843 (B_2)
$(Si_4Ge)^+$	30.345 (B_2), 177.005 (A_1), 199.466 (B_1), 210.589 (A_1), 257.577 (B_2), 299.516 (A_1), 356.324 (A_2), 406.777 (B_1), 458.144 (A_1)
$(Si_3Ge_2)^+$	101.388 (A_1), 176.670 (A_1), 177.547 (B_1), 225.238 (B_2), 228.033 (A_2), 230.200 (B_1), 323.705 (A_1), 435.747 (B_2), 470.166 (A_1)
$(Si_2Ge_3)^+$	91.704 (A'), 143.002 (A"), 159.328 (A'), 168.918 (A'), 173.226 (A"), 250.746 (A"), 294.912 (A'), 348.802 (A'), 455.537 (A')
$(SiGe_4)^+$	-79.944 (A"), 113.592 (A'), 118.142 (A"), 142.818 (A'), 145.657 (A'), 223.275 (A'), 250.299 (A"), 268.170 (A'), 358.264 (A')
$(Si_5Ge)^+$	-92.620 (B_2), 98.527 (B_1), 100.0509 (A_1), 224.456 (B_2), 249.696 (A_1), 295.177 (B_1), 313.414 (A_2), 337.324 (A_1), 371.872 (A_1), 377.411 (B_2), 409.405 (B_1), 439.077 (A_1)
$(Si_4Ge_2)^+$	-107.910 (B_{3u}), 29.967 (B_{2u}), 79.070 (B_{1u}), 199.738 (A_g), 218.595 (B_{1g}), 284.033 (B_{3u}), 295.095 (B_{2g}), 303.446 (A_g), 324.659 (B_{1u}), 408.497 (B_{2u}), 415.250 (B_{3g}), 435.676 (A_g)
$(Si_3Ge_3)^+$	-82.909 (B_2), 65.286 (A_1), 69.374 (B_1), 180.300 (B_2), 199.794 (A_1), 246.532 (A_1), 278.691 (A_2), 282.132 (B_1), 291.339 (B_2), 352.733 (A_1), 391.176 (B_1), 421.375 (A_1)
$(Si_2Ge_4)^+$	-74.567 (A"), 60.119 (A'), 74.968 (A'), 155.141 (A"), 190.262 (A'), 204.726 (A'), 217.726 (A"), 221.678 (A'), 306.711 (A'), 308.969 (A"), 338.486 (A'), 409.558 (A')
$(SiGe_5)^+$	-77.117 (A'), 41.803 (A"), 60.965 (A'), 148.910 (A"), 176.156 (A'), 177.142 (A'), 195.174 (A'), 208.402 (A'), 228.183 (A"), 300.546 (A'), 330.403 (A'), 333.629 (A")
$(Si_6Ge)^+$	-187.772 (B_2), 67.119 (B_1), 107.140 (A_2), 182.658 (A_1), 188.003 (B_2), 194.764 (B_1), 211.971 (A_1), 289.475 (B_2), 312.402 (A_2), 313.338 (A_1), 317.368 (B_1), 362.445 (A_1), 380.673 (B_2), 396.504 (A_1), 425.577 (A_1)
$(Si_5Ge_2)^+$	69.999 (A"), 97.304 (A"), 101.842 (A'), 168.415 (A'), 187.819 (A'), 188.245 (A"), 205.957 (A'), 271.147 (A'), 289.156 (A'), 293.450 (A"), 312.808 (A"), 318.879 (A'), 357.414 (A'), 412.201 (A'), 415.575 (A')

Table 5.2 – *Continued*

Clusters	Frequencies (cm^{-1})
$(Si_4Ge_3)^+$	-108.977 (A'), 44.373 (A"), 91.731 (A"), 132.723 (A'), 162.440 (A'), 172.718 (A'), 183.949 (A"), 240.309 (A'), 251.914 (A'), 288.163 (A"), 307.230 (A'), 309.552 (A"), 340.009 (A'), 368.778 (A'), 432.799 (A')
$(Si_3Ge_4)^+$	54.310 (A"), 75.601 (A"), 116.673 (A'), 134.958 (A'), 155.163 (A'), 162.342 (A'), 183.562 (A'), 193.547 (A"), 240.418 (A'), 263.459 (A"), 267.116 (A'), 305.059 (A"), 336.118 (A'), 337.213 (A'), 381.880(A')
$(Si_2Ge_5)^+$	62.024 (A"), 82.363 (A'), 104.406 (A'), 130.282 (A"), 138.658 (A"), 149.204 (A'), 160.796, 178.360 (A'), 181.737 (A"), 201.714 (A'), 258.823 (A'), 294.412 (A"), 303.652 (A'), 327.004 (A"), 370.017 (A')
$(SiGe_6)^+$	65.655 (A_2), 80.552 (B_1), 90.788 (A_1), 124.392 (B_2), 137.719 (B_2), 142.404 (B_1), 153.068 (A_1), 171.006 (A_2), 173.443 (A_1), 190.173 (A_1), 212.791 (B_2), 213.957 (B_1), 226.9949 (A_1), 319.873 (B_2), 327.334 (A_1)

Table 5.3 Harmonic Frequencies of the Most Stable Anions

Clusters	Frequencies (cm^{-1})
$(SiGe)^-$	434.160 (Σ)
$(Si_2Ge)^-$	-157.664 (B_2), 296.817 (A_1), 512.768 (A_1)
$(SiGe_2)^-$	173.318 (A_1), 281.193 (B_2), 410.467 (A_1)
$(Si_3Ge)^-$	129.282 (B_1), 196.136 (B_2), 267.173 (A_1), 317.634 (B_2), 416.470 (A_1), 467.981 (A_1)
$(Si_2Ge_2)^-$	111.303 (B_{3u}), 176.384 (B_{2u}), 214.317 (A_g), 288.094 (B_{3g}), 360.224 (B_{1u}), 435.680 (A_g)
$(SiGe_3)^-$	99.845 (B_1), 139.814 (A_1), 187.124 (B_2), 205.666 (A_1), 348.169 (B_2), 356.202 (A_1)
$(Si_4Ge)^-$	162.228 (B_2), 189.079 (A_1), 242.575 (A_1), 264.849 (B_1), 313.557 (A_1), 333.353 (A_2), 361.266 (B_2), 420.064 (B_1), 443.255 (A_1)
$(Si_3Ge_2)^-$	138.082 (A_1), 175.485 (B_1), 218.195 (A_1), 244.928 (A_2), 271.582 (B_1), 282.588 (B_2), 326.867 (A_1), 395.906 (B_2), 422.040 (A_1)
$(Si_2Ge_3)^-$	134.466 (A_1), 134.649 (B_1), 192.612 (A_1), 241.228 (B_2), 241.571 (A_2), 268.393 (A_1), 268.936 (B_1), 347.752 (B_2), 389.162 (A_1)
$(SiGe_4)^-$	119.613 (A'), 119.918 (A"), 177.346 (A'), 186.614 (A"), 186.918 (A'), 247.213 (A'), 263.683 (A'), 264.0851 (A"), 372.006 (A')
$(Si_5Ge)^-$	90.873 (A'), 90.882 (A"), 158.402 (A'), 236.662 (A'), 278.250 (A"), 297.221 (A'), 297.501 (A"), 325.051 (A'), 363.326 (A'), 391.835 (A"), 392.260 (A'), 411.204 (A')
$(Si_4Ge_2)^-$	91.120 (A'), 100.669 (A'), 110.042 (A"), 239.184 (A'), 249.807 (A'), 253.757 (A'), 289.853 (A"), 324.493 (A"), 345.987 (A"), 346.841 (A'), 373.721 (A'), 409.520 (A')
$(Si_3Ge_3)^-$	79.975 (A_1), 89.841 (B_1), 98.353 (B_2), 207.183 (A_1), 213.283 (B_2), 242.104 (A_1), 283.829 (B_1), 293.485 (A_2), 298.042 (B_2), 326.149 (B_1), 341.952 (A_1), 388.668 (A_1)
$(Si_2Ge_4)^-$	72.408 (B_{2u}), 84.208 (E_u), 84.208 (E_u), 172.190 (B_{2g}), 203.316 (A_{1g}), 204.598 (B_{1g}), 282.862 (A_{2u}), 283.806 (E_g), 283.806 (E_g), 284.550 (E_u), 284.550 (E_u), 356.767 (A_{1g})
$(SiGe_5)^-$	70.709 (A'), 70.714 (A"), 76.281 (A'), 166.640 (A"), 182.693 (A'), 200.943 (A'), 204.182 (A'), 204.245 (A"), 217.171 (A'), 291.491 (A"), 291.588 (A'), 328.720 (A')
$(Si_6Ge)^-$	149.736 (B_1), 180.444 (B_2), 180.058 (A_2), 212.160 (A_1), 214.969 (A_1), 245.259 (B_1), 249.020 (B_2), 274.027 (A_1), 286.153 (B_1), 289.302 (A_2), 310.290 (A_1), 316.583 (B_2), 355.217 (A_1), 375.948 (B_2), 393.348 (A_1)
$(Si_5Ge_2)^-$	124.935 (A"), 157.928 (A'), 169.784 (A"), 190.288 (A'), 191.026 (A'), 226.005 (A'), 230.933 (A"), 231.037 (A'), 280.339 (A"), 285.094 (A"), 290.397 (A'), 292.558 (A'), 335.502 (A'), 361.184 (A'), 389.486 (A')

Table 5.3 – *Continued*

Clusters	Frequencies (cm^{-1})
$(Si_4Ge_3)^-$	108.310 (A"), 153.037 (A"), 156.643 (A'), 160.201 (A'), 176.890 (A'), 194.637 (A'), 218.292 (A'), 220.528 (A"), 238.140 (A'), 265.893 (A"), 269.123 (A'), 280.480 (A"), 313.472 (A'), 336.292 (A'), 381.913 (A')
$(Si_3Ge_4)^-$	101.169 (A"), 128.473 (A"), 146.602 (A'), 151.404 (A'), 161.646 (A'), 174.473 (A'), 189.257 (A'), 217.714 (A"), 225.994 (A'), 239.737 (A'), 249.787 (A"), 266.022 (A"), 283.684 (A'), 299.093 (A'), 348.955 (A')
$(Si_2Ge_5)^-$	99.465 (B_1), 99.508 (A_2), 145.147 (A_1), 145.389 (B_2), 153.691 (A_1), 153.924 (B_2), 184.981 (A_1), 193.897 (A_1), 193.927 (B_2), 213.342 (B_1), 244.821 (B_1), 245.173 (A_2), 261.483 (A_1), 261.664 (B_2), 310.199 (A_1)
$(SiGe_6)^-$	102.472 (E_2), 102.472 (E_2), 126.642 (E_1), 126.642 (E_1), 144.194 (E_2), 144.194 (E_2), 153.754 (A_1), 188.906 (?A), 189.834 (?A), 189.835 (?A), 190.551 (E_2), 190.551 (E_2), 266.796 (E_1), 266.797 (E_1), 282.329 (A_1)

Table 5.4 Average Coordination Number of the Most Stable Neutrals, Cations, and Anions

Clusters	Average Coordination Number		
	Neutral	Cation	Anion
SiGe	1.000	1.000	1.000
Si_2Ge	2.000	2.000	2.000
$SiGe_2$	1.333	1.333	1.333
Si_3Ge	2.500	2.500	2.500
Si_2Ge_2	2.500	2.500	2.500
$SiGe_3$	2.500	2.000	2.500
Si_4Ge	2.400	2.400	2.800
Si_3Ge_2	2.400	2.400	2.400
Si_2Ge_3	2.400	2.400	2.400
$SiGe_4$	2.400	2.400	2.400
Si_5Ge	3.667	3.333	4.000
Si_4Ge_2	3.333	4.000	3.667
Si_3Ge_3	3.667	3.333	4.000
Si_2Ge_4	3.000	3.333	4.000
$SiGe_5$	2.667	2.667	4.000
Si_6Ge	4.571	4.571	4.286
Si_5Ge_2	4.571	4.286	4.286
Si_4Ge_3	4.571	4.000	4.286
Si_3Ge_4	4.571	4.286	4.286
Si_2Ge_5	4.571	3.857	4.286
$SiGe_6$	4.571	4.000	4.286
Si_7Ge	3.000	4.500	4.000
Si_6Ge_2	3.750	4.000	4.250
Si_5Ge_3	3.750	3.375	3.750
Si_4Ge_4	3.625	3.500	4.250
Si_3Ge_5	3.750	3.500	3.750
Si_2Ge_6	3.750	3.500	3.000
$SiGe_7$	3.500	3.500	3.000

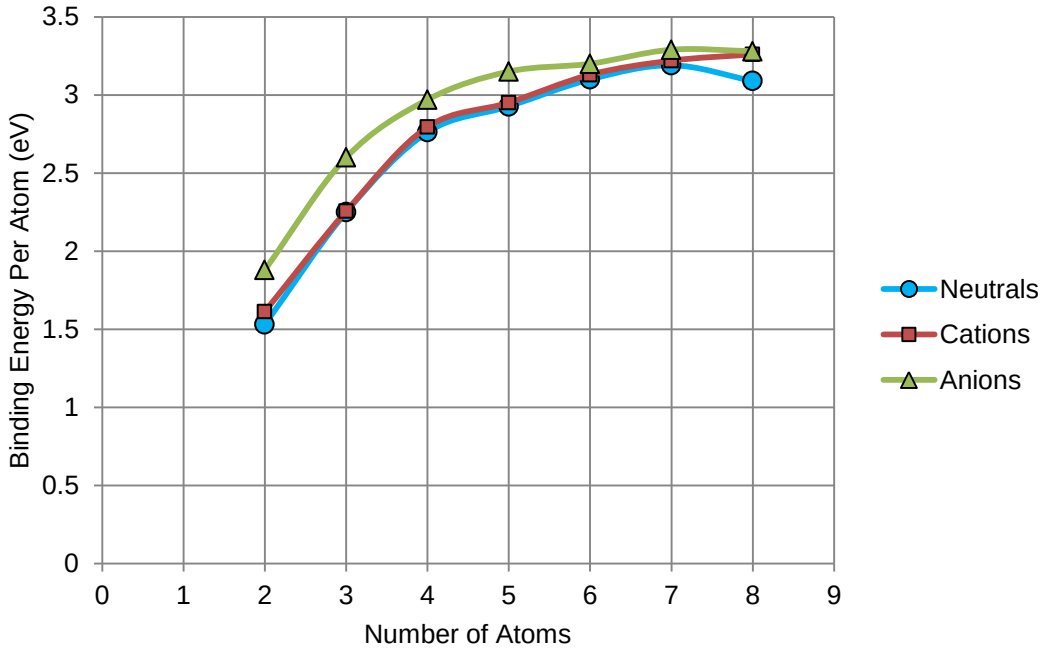

Figure 5.1 Binding Energy per Atom (eV) Versus Number of Atoms for the Most Stable Neutral, Cationic, and Anionic Clusters

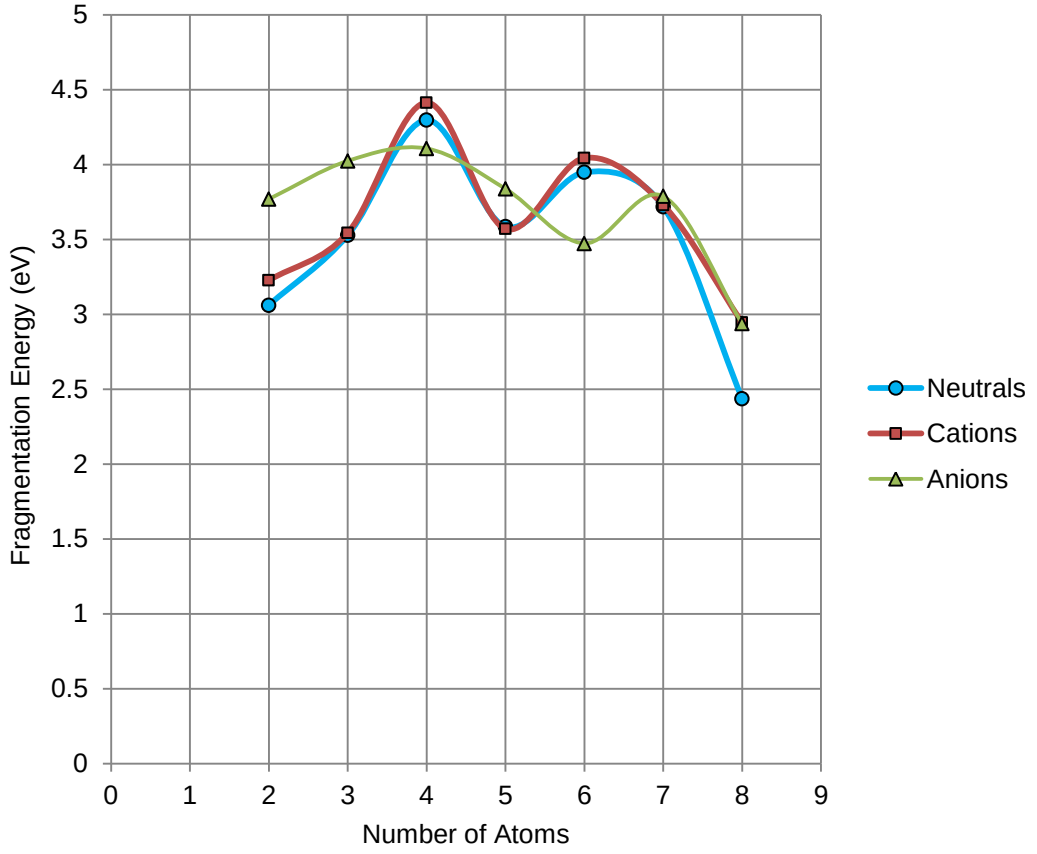

Figure 5.2 Lowest Fragmentation Energy (eV) Versus Number of Atoms for the Most Stable Neutral, Cationic, and Anionic Clusters

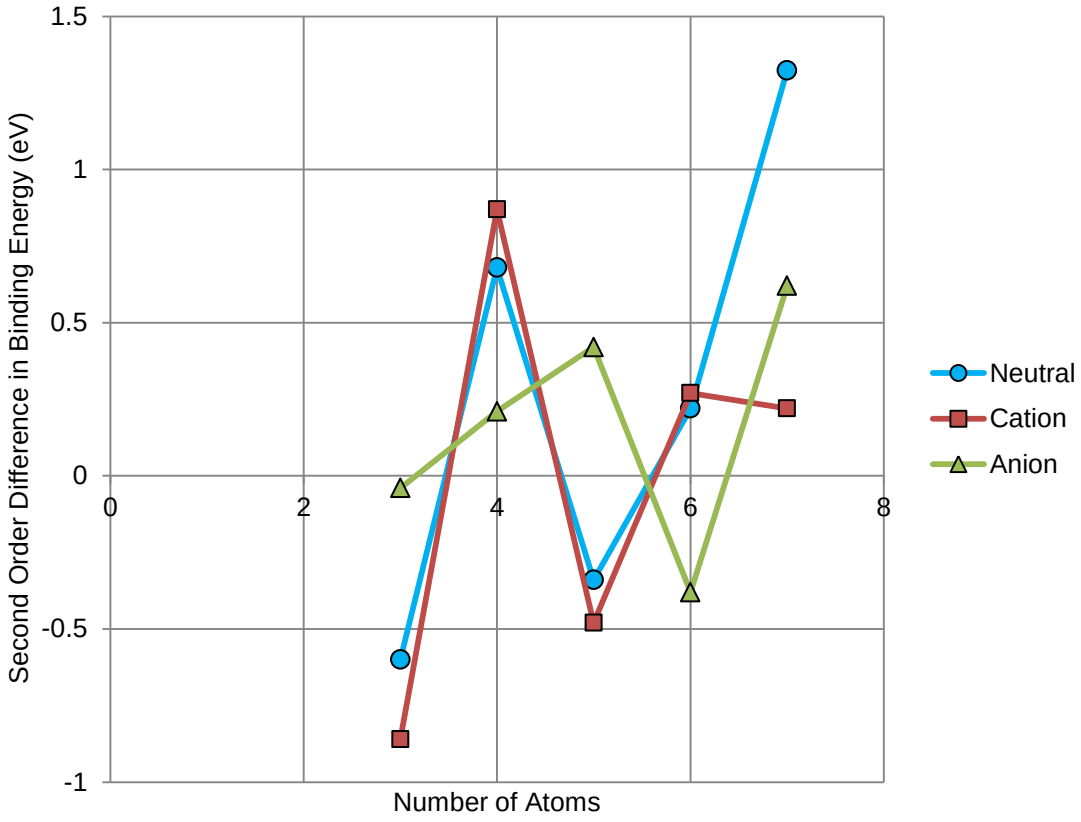

Figure 5.3 Second Order Difference in Binding Energy (eV) Versus Number of Atoms for the Most Stable Neutral, Cationic, and Anionic Clusters

CHAPTER 6

CONCLUSIONS

After studying these nanoclusters, certain trends become apparent. We have already discussed the single dimer in detail. Out of all the trimers, the Si_2Ge cluster that is nearly an equilateral triangle is the most stable. Comparing all the tetramers, the Si_3Ge tetramer with a Si-Si bond through the middle has the lowest energy. For the pentamers, the most stable is the Si_4Ge trigonal bipyramid with Si atoms at each tip. In the case of hexamers, the most stable cluster is a rhombic bipyramid, and for the septamers it is a pentagonal bipyramid. Finally, for the octamers the most stable isomer resembles two adjoined trigonal bipyramid. The data supports the general trend that clusters with more silicon atoms are more stable, except in the case of the octamers where a Si_6Ge_2 cluster is most stable. However, the difference in binding energy per atom between the most stable Si_7Ge cluster and Si_6Ge_2 cluster is only 0.003 eV. Because some of the charged clusters converged to the same geometry, there are fewer stable cation and anion clusters than neutral clusters. However, in general, the cations, anions, and neutrals have similar geometric structures.

The relationship between binding energy and structure adheres to a noticeable pattern for the neutral clusters. For the trimers, the triangular structures are more stable than the linear structures. For the tetramers, the rhomboidal structures are the most stable, followed by the triangles with an extra atom, followed by the linear structures. Extra clusters, like the tetragons and the square clusters, fall somewhere in the middle. The pentamers all have singlet trigonal bipyramids for their most stable structure, followed by triplet trigonal bipyramids. Any more three dimensional structures will be more stable than the two dimensional clusters. In the two dimensional structures, a fan-shaped structure is more stable than clusters formed fro rhombus

with an extra atom attached. The least stable states are triangles with two linear atoms attached and completely linear clusters. The most stable hexamers are always rhombic bipyramids. Other, less stable clusters include trigonal bipyramid with two atoms attached to a single atom and a tetragonal pyramid with an atom attached to one of the triangular faces. Sometimes one of these clusters is more stable than a rhombic bipyramid, but they are never the most stable cluster. For completeness, we look at a few two-dimensional hexamers, but they are always the least stable. (Linear clusters are the least stable of all.) The most stable septamers are all pentagonal bipyramids. The other isomers are combinations of trigonal pyramids with atoms attached to three faces and half-pentagonal bipyramids with an atom attached with two or three bonds. For octamers, there is a little discrepancy in the geometry of the most stable isomers. For Si_7Ge, the most stable cluster resembles two stacked rhombuses. However for all other octamer categories the most stable cluster are trigonal bipyramids that share two atoms.

The charged clusters follow these same trends except in the pentamers and octamers. In the case of cationic pentamers, we found some two-dimensional structures to be more stable than the least stable three-dimensional ones. In the octamers, the most stable $(Si_7Ge)^+$ cluster is a pentagonal bipyramid with an atom attached with two bonds, while the most stabe clusters in the other categories remain joined trigonal bipyramids. The anion $(Si_7Ge)^-$ octamer resembles the neutral cluster, but the most stale isomers in all the other categories becomes a stacked rhombuses.

Across the range of clusters we studied, we found that binding energy per atom increases as number of atoms increases. Furthermore, the VIP and AIP are significantly higher than the VEA and AIP, meaning that the molecules are more apt to gain an electron than to lose one. From the figures listing the Mulliken atomic charges, we note that within each cluster the germanium atoms usually have a more positive charge than the silicon atoms. This indicates

that if an electron is removed from a cluster, giving it a net positive charge, the electron will most likely come from one of the germanium atoms.

The fragmentation energies show trends determining how a cluster will most likely break up. The most probable channel always involves a single atom and a cluster with one fewer atoms than the original cluster. When we graphed the lowest fragmentation energies against the number of atoms, we found peaks at four, six, and seven atoms. Finally, in all cases except the neutral octamers, the graph of binding energy per atom increases with number of atoms and the most stable isomer always contains a single germanium atom.

REFERENCES

[1] K. Raghavachari, V. Logovinsky, *Structure and bonding in small silicon clusters*, Phys. Rev. Lett. 55 (1985) 2853-2856.

[2] K. Raghavachari, *Theoretical study of small silicon clusters: equilibrium geometries and electronic structures of Si_n (n = 2-7, 10)*, J. Chem. Phys. 84 (1986) 5672–5686.

[3] D. Tomańek, M. A. Schluter, *Structure and bonding of small semiconductor clusters*, Phys. Rev. B 36 (1987) 1208-1217.

[4] K. Raghavachari and C. Rohlfing, *Bonding and stabilities of small silicon clusters: A theoretical study of Si_7-Si_{10}*, J. Chem. Phys. 89 (1988) 2219-2234.

[5] P. Ballone, W. Andreoni, R. Car, M. Parrinello, *Equilibrium structures and finite temperature properties of silicon microclusters from* ab initio *molecular-dynamics calculations*, Phys Rev. Lett. 60 (1988) 271-275.

[6] W. Andreoni, G. Pastore, *Transferability of bulk empirical potentials to silicon microclusters: a critical study*, Phys. Rev. B 41 (1990) 10243-10246.

[7] C. H. Patterson, R. P. Messmer, *Bonding and structures in silicon clusters: A valence-bond interpretation*, Phys. Rev. B 42 (1990) 7530-7555.

[8] L. A. Curtiss, P. W. Deutsch, K. Raghavachari, *Binding energies and electron affinities of small silicon clusters (n=2-5)*, J. Chem. Phys. 96 (1992) 6868–6872.

[9] R. Fournier, S. B. Sinnott, A. E. DePristo, *Density functional study of the bonding in small silicon clusters*, J. Chem. Phys. 97 (1992) 4149–4161.

[10] N. Binggeli, J. R. Chelikowsky, *Langevin molecular dynamics with quantum forces: application to silicon clusters*, Phys. Rev. B 50 (1994) 11764–11770.

[11] X. Jing, N. Troullier, D. Dean, N. Binggeli, J. R. Chelikowsky, K. Wu, Y. Saad, Ab initio *molecular-dynamics simulations of Si clusters using the higher-order-finite-difference-pseudopotential method*, Phys. Rev. B 50 (1994) 12234-12237.

[12] J. C. Grossman, L. Mitás, *Quantum Monte Carlo determination of electronic and structural properties of Si_n clusters ($n \leq 20$)*, Phys. Rev. Lett. 74 (1995) 1323-1326.

[13] A. M. Mazzone, *Bond hybridization and structural properties of clusters of group-IV elements*, Phys. Rev. B 56 (1997) 15926-15937.

[14] B. Liu, Z.-Y. Lu, B. Pan, C.-Z. Wang, K.-M. Ho, A. A. Shvartsburg, M. F. Jarrold, *Ionization of medium-sized silicon clusters and the geometries of the cations*, J. Chem. Phys 109 (1998) 9401-9409.

[15] A. A. Shvartsburg, M. F. Jarrold, B. Liu, Z.-Y. Lu, C.-Z. Wang, K.-M. Ho, *Dissociation energies of silicon clusters: a depth gauge for the global minimum on the potential energy surface*, Phys. Rev. Lett. 81 (1998) 4616-4619.

[16] C. Jo, K. Lee, *Semiempirical tight binding method study of small Ge and Sn clusters*, J. ChemPhys, 113 (2000) 7268-7272.

[17] V. E. Bazterra, O. Oña, M. C. Caputo, M. B. Ferraro, P. Fuentealba, J. C. Facelli, *Modified genetic algorithms to model cluster structures in medium-size silicon clusters*, Phys. Rev. A 69 (2004) 053202-1-7.

[18] L. R. Marim, M. R. Lemes, A. Dal Pino Jr., *Investigation of prolate and near spherical geometries of mid-sized silicon clusters*, Phys. Stat. Sol. (b) 243 (2006) 449-458.

[19] P. W. Deutsch, L. A. Curtiss, J. P. Blaudeau, *Binding energies of germanium clusters, Ge_n (n=2-5)*, Chem. Phys. Lett. 270 (1997) 413-418.

[20] S. Ogut, J. R. Chelikowsky, *Structural changes induced upon charging Ge clusters*, Phys Rev. B 55 (1997) R4914–R4917.

[21] E. F. Archibong, A. St-Amant, *A study of Ge^-_n and Ge_n (n = 2–6) using B3LYP-DFT and CCSD(T) methods: the structures and electron affinities of small germanium clusters*, J. Chem. Phys. 109 (1998) 962-972.

[22] B. Li, P. Cao, *Structures of Ge_n clusters (n=3-10) and comparisons to Si_n clusters*, Phys. Rev. B 62 (2000) 15788-15796.

[23] S.-D. Li, Z.-G. Zhao, H.-S. Wu, Z.-H. Jin, *Ionization potentials, electron affinities, and vibrational frequencies of Ge_n (n=5-10) neutrals and charged ions from density functional theory*, J. Chem. Phys. 115 (2001) 9255-9259.

[24] J. Wang, G. Wang, J. Zhao, *Structure and electronic properties of Ge_n (n=2-25) clusters from density-functional theory*, Phys. Rev. B 64 (2001) 205411-1-5.

[25] N. Bernstein, M. J. Mehl, D. A. Papaconstantopoulos, *Nonorthogonal tight-binding model for germanium*, Phys. Rev. B 66 (2002) 075212-1-12.

[26] S. Li, R. J. Van Zee, W. Weltner Jr., K. Raghavachari, *Si_3-Si_7. Experimental and theoretical infared spectra*, Chem. Phys. Lett 243 (1995) 275-280.

[27] A. Kant, B. H. Strauss, *Atomization Energies of the Polymers of Germanium Ge_2 to Ge_7*, J. Chem. Phys. 45 (1966) 822-826.

[28] J. R. Chelikowsky, J. C. Phillips, *Chemical Reactivity and Covalent-Metallic Bonding of Si_n^+ (n=11-25) Clusters*, Phys Rev. Lett. 63 (1989) 1653-1656.

[29] E. C. Honea, A. Ogura, C. A. Murray, K. Raghavachari, W. O. Sprenger, M. F. Jarrold, W. L. Brown, *Raman spectra of size-selected silicon clusters and comparison with calculated structures*, Lett. To Nature 366 (1993) 42-44.

[30] J. M. Hunter, J. L. Fye, M. F. Jarrold, J. E. Bower, *Structural transitions in size-selected germanium cluster ions*, Phys. Rev. Lett. 73 (1994) 2063-2066.

[31] S. Yoshida, K. Fuke, *Photoionization studies of germanium and tin clusters in the energy region of 5.0-8.8 eV: ionization potentials for Ge_n (n=2-57) and Sn_n (n=2-41)*, J. Chem. Phys. 111 (1999) 3880-3890.

[32] A. A. Shvartsburg, R. R. Hudgins, P. Dugourd, M. F. Jarrold, *Structural information from ion mobility measurements: applications to semiconductor clusters*, Chem. Soc. Rev. 30 (2001) 26-35.

[33] A. N. Andriotis, M. Menon, G. E. Froudakis, Z. Fthenakis, J. E. Lowther, *A tight-binding molecular dynamics study of Ni_mSi_n binary clusters*, Chem. Phys Lett. 292 (1988) 487-492.

[34] J. R. Chelikowsky, *Structural and electronic properties of neutral and charged silicalike clusters*, Phys Rev. B 57 (1998) 3333-3339.

[35] P. Pradhan, A. K. Ray, *A density functional study of the structures and energetic of small hetero-atomic silicon-carbon nanoclusters*, J. Mol. Struc.: THEOCHEM 716 (2005) 109–130.

[36] P. Pradhan, A. K. Ray, *An* ab initio *study of the electronic and geometric structures of $Si_mC_n^+$ cationic nanoclusters*, Eur. Phys. J. D 37 (2006) 393–407.

[37] S. Ogut, *First principles modeling of nanostructures*, Turk. J. Phys. 27 (2003) 443–458.

[38] G. Pacchioni, J. Koutecký, *Silicon and germanium clusters. a theoretical study of their electronic structures and properties*, J. Chem. Phys 84 (1986) 3301-3310.

[39] Z.-Y. Lu, C.-Z. Wang, K.-M. Ho, *Structures and dynamical properties of C_n, Si_n, Ge_n, and Sn_n clusters with n up to 13*, Phys. Rev. B 61 (2000) 2329-2334.

[40] A. A. Shvartsburg, M. F. Jarrold, *Tin clusters adopt prolate geometries*, Phys. Rev. A 60 (1999) 1235-1239.

[41] A. A. Shvartsburg, B. Liu, Z.-Y. Lu, C.-Z. Wang, M. F. Jarrold, K.-M. Ho, *Structures of germanium clusters: where the growth patterns of silicon and germanium clusters diverge*, 83 (1999) 2167-2170.

[42] C. Tzoumanekas, P. C. Kelires, *Theory of bond-length variations in relaxed, strained, and amorphous silicon-germanium alloys*, Phys. Rev. B 66 (2002) 195209-1-11.

[43] P. Venezuela, G. M. Dalpian, A. J. R. da Silva, A. Fazzio, Ab initio *determination of the atomistic structure of Si_xGe_{1-x} alloy*, Phys. Rev. B 64 (2001) 193202-1-4.

[44] J. Tarus, M. Tantarimaki, K. Nordlund, *Segregation in SiGe clusters*, Nucl. Instr. and Meth. in Phys. Res. B 228 (2005) 51-56.

[45] H. ur Rehman, M. Springborg, Y. Dong, *Structural, energetic, and electronic properties of Si_n, Ge_n, and Si_nGe_n clusters*, Eur. Phys. J. D 52 (2009) 39-42.

[46] A. Harjunmaa, K. Nordlund, *Molecular dynamics simulations of Si/Ge cluster condensation*, Comp. Mat. Sci. 47 (2009) 456-459.

[47] A. N. Andriotis, M. Menon, G. E. Froudakis, *Tight-binding molecular dynamics study of heteronuclear systems: application to Si_mGe_n clusters*, J. Cluster Sci. 10 (1999) 549-556.

[48] S.-D. Li, Z.-G. Zhao, X.-F. Zhao, H.-S. Wu, Z.-H. Jin, *Structural and electronic properties of semiconductor binary microclusters A_mB_n (A,B=Si,Ge,C): a B3LYP-DFT study*, Phys. Rev. B 64 (2001) 195312-1–195312-5.

[49] L. R. Marim, L. T. Ueno, F. B. C. Machado, A. D. Pino Jr., *Investigation of strain relaxation mechanism in small SiGe clusters*, Phys. Stat. Sol. (b) 244 (2007) 3601–3611.

[50] P. Wielgus, S. Roszak, D. Majumdar, J. Saloni, J. Leszczynski, *Theoretical studies on the bonding and thermodynamic properties of Ge_nSi_m (m+n=5) clusters: the precursors of germanium/silicon nanomaterials*, J. Chem. Phys. 128 (2008) 144305-1–144305-10.

[51] Y.-S. Wang, S. D. Chao, *Structures and energetics of neutral and ionic silicon-germanium clusters: density functional theory and coupled cluster studies*, J. Phys. Chem. A 115 (2011) 1472-1485.

[52] R. G. Parr and W. Yang, *Density Functional Theory of Atoms and Molecules*, Oxford University Press, New York, (1989).

[53] P. Hohenberg and W. Kohn, *Inhomogeneous electron gas*, Phys. Rev. 136 (1964) B864-B871.

[54] W. Kohn and L. J. Sham, *Self-consisten equations including exchange and correlation effects*, Phys Rev. 140 (1965) A1133-A1138.

[55] D. M. Ceperley and B. J. Adler, *Ground state of the electron gas by a stochastic method*, Phys. Rev. Lett. 45 (1980) 566-569.

[56] W. Kohn, A.D. Becke and R. G. Parr, *Density functional theory of electronic structure*, J. Phys. Chem. 100 (1996) 12974-12980.

[57] R. O. Jones and O. Gunnarsson, *The density functional formalism, its applications and prospects*, Rev. Mod. Phys. 61 (1989) 689-746.

[58] G. Sentore and N. H. March, *Recent progress in the field of electron correlation*, Rev. Mod. Phys. 66 (1996) 445-479.

[59] J. F. Dobson, G. Vignale, and M. P. Das (Eds.), *Electronic Density Functional Theory: Recent Progress and New Directions*, Plenum Press, New York and London (1998).

[60] D. R. Hartree, *The wave mechanics of an atom with a non-coulomb central field. Part I. Theory and methods*, Proc. Cambridge Philos. Soc. 24 (1928) 89-110.

[61] V. Fock, *Näherungsmethode zur Lösung des quantenmechanischen Mehrkörperproblems*, Z. Phys. 61 (1930) 126-148.

[62] J. C. Slater, *Note on Hartree's method*, Phys. Rev. 35 (1930) 210-211.

[63] C. Coulson, *Present state of molecular structure calculations*, Rev. Mod. Phys. 32 (1960) 170-177.

[64] L. H. Thomas, *The calculation of atomic fields*, Proc. Cambridge Philos. Soc. 23 (1927) 542-548.

[65] E. Fermi, *Eine statistische Methode zur Bestimmung einiger Eigenschaften des Atoms und ihre Anwendung auf die Theorie des periodischen Systems der Elemente*, Z. Phys. 48 (1928) 73-79.

[66] P. A. M. Dirac, *Note on exchange phenomena in the Thomas atom*, Proc. Cambridge Plilos. Soc. 26 (1930) 376-385.

[67] P. Hohenberg and W. Kohn, *Inhomogeneous electron gas*, Phys. Rev. 136 (1964) B864-B871.

[68] U. von Barth and L. Hedin, *A local exchange-correlation potential for the spin polarized case*, J. Phys. C: Solid State Phys. 5 (1972) 1629-1644.

[69] O. Gunnarsson and B. I. Lundqvist, *Exchange and correlation in atoms, molecules, and solids by the spin-density-functional formalism*, Phys. Rev. B 13 (1976) 4274-4298.

[70] S. H. Vosko, L. Wilk, and M. Nusair, *Accurate spin-dependent electron liquid correlation energies for local spin density calculations: a critical analysis*, Can. J. Phys. 58 (1980) 1200-1211.

[71] M. Rasolt and D. J.W. Geldart, *Exchange and correlation energy in a nonuniform fermion fluid*, Phys. Rev. B 34 (1986) 1325-1328.

[72] J. P. Perdew, *Density-funcional approximation for the correlation energy of the inhomogeneous electron gas*, Phys. Rev. B 33, (1986) 8822-8824; erratum, 34 (1984) 7406.

[73] A. D. Becke, *Density-functional thermochemistry. III. The role of exact exchange*, J. Chem. Phys. 98 (1993) 5648-5652.

[74] C. Lee, W. Yang, and R. G. Parr, *Development of the Colle-Salvetti correlation-energy formula into a functional of the electron density*, Phys. Rev. B 37 (1988) 785-789.

[75] J. P. Perdew, J. A. Chevary, S. H. Vosko, K. A. Jackson, M. R. Pederson, D. J. Singh, and C. Fiolhais, *Erratum: Atoms, molecules, solids, and surfaces: applications of the generalized gradient approximation for exchange and correlation*, Phys. Rev. B 48 (1993) 4978; K. Burke, J. P. Perdew, and Y. Wang, in *Electronic Density Functional Theory: Recent Progress and New Directions,* Ed. J. F. Dobson, G. Vignale, and M. P. Das, Plenum, New York (1998).

[76] J. P. Perdew, K. Burke, and M. Ernzerhof, *Generalized gradient approximation made simple*, Phys. Rev. Lett. 77 (1996) 3865-3868; *Generalized gradient approximation made simple*, Phys. Rev. Lett. 78 (1997) 1396.

[77] J. P. Perdew, *Electronic Structure of Solids '91*, edited by P. Ziesche and H. Eschig, Akademie Verlag, Berlin (1991); J. P. Perdew and Y. Wang, *Pair-distribution function and its coupling-constant average for the spin-polarized electron gas*, Phys. Rev. B 46 (1992) 12947-12954; J. P. Perdew, J. A. Chevary, S. H.Vosko, K. A. Jackson, M. R. Pederson, D. J. Singh, C. Fiolhais, *Atoms, molecules, solids, and surfaces: applications of the generalized gradient approximation for exchange and correlation*, Phys. Rev. B 46 (1992) 6671-6687.

[78] D. C. Langreth and M. Mehl, *Beyond the local-density approximation in calculations of ground-state electronic properties*, Phys. Rev. B 28 (1983) 1809-1834.

[79] A.D. Becke, *Density-functional thermochemistry. III. The role of exact exchange*, J. Chem. Phys. 98 (1993) 5648-5652.

[80] C.Lee, W. Yang, R.G.Parr, *Development of the Colle-Salvetti correlation-energy formula into a functional of the electron density*, Phys. Rev. B 37 (1988) 785–789.

[81] M.J. Frisch *et al.*, GAUSSIAN'03 (revision D.02), Gaussian, Inc., Wallingford, CT, 2004.

[82] M.J. Frisch *et al.*, GAUSSIAN'09 (revision A.02), Gaussian, Inc., Wallingford, CT, 2009.

[83] W. J. Hehre, L. Radom, P. v. R. Schleyer, J. A. Pople, *Ab initio Molecular Orbital Theory*, Wiley, New York, 1986.

[84] D. R. Lide (editor). *CRC Handbook of Chemistry and Physics, 76th edition*. CRC Press, Boca Raton, 1995.

BIOGRAPHICAL INFORMATION

Sarah Duesman earned a Bachelors of Science degree in physics from Texas Christian University. While at the University of Texas at Arlington, she has worked with Dr. Asok Ray conducting computational research on semiconducting nanoclusters. She will continue working with Dr. Ray to publish her research in a scientific journal. After graduation she intends to begin a career in industry or education.